

2010-01-01

Categorization of Functional Impairments in Human Locomotion using the Methods of the Fusion of Multiple Sensors and Computational Intelligence

Huiying Yu

University of Texas at El Paso, hyu@miners.utep.edu

Follow this and additional works at: https://digitalcommons.utep.edu/open_etd



Part of the [Biomedical Commons](#), and the [Electrical and Electronics Commons](#)

Recommended Citation

Yu, Huiying, "Categorization of Functional Impairments in Human Locomotion using the Methods of the Fusion of Multiple Sensors and Computational Intelligence" (2010). *Open Access Theses & Dissertations*. 2814.
https://digitalcommons.utep.edu/open_etd/2814

This is brought to you for free and open access by DigitalCommons@UTEP. It has been accepted for inclusion in Open Access Theses & Dissertations by an authorized administrator of DigitalCommons@UTEP. For more information, please contact lweber@utep.edu.

CATEGORIZATION OF FUNCTIONAL IMPAIRMENTS IN HUMAN
LOCOMOTION USING THE METHODS OF THE FUSION OF MULTIPLE
SENSORS AND COMPUTATIONAL INTELLIGENCE

HUIYING YU

Department of Electrical and Computer Engineering

APPROVED:

Thompson Sarkodie-Gyan, Ph.D., Chair

Scott Starks, Ph.D.

Richard Brower, M.D.

Bill Tseng, Ph.D.

Eric Spier, M.D.

Patricia D. Witherspoon, Ph.D.
Dean of the Graduate School

Copyright ©

by

Huiying Yu

2010

CATEGORIZATION OF FUNCTIONAL IMPAIRMENTS IN HUMAN
LOCOMOTION USING THE METHODS OF THE FUSION OF MULTIPLE
SENSORS AND COMPUTATIONAL INTELLIGENCE

by

HUIYING YU, MPHIL

DISSERTATION

Presented to the Faculty of the Graduate School of

The University of Texas at El Paso

in Partial Fulfillment

of the Requirements

for the Degree of

DOCTOR OF PHILOSOPHY

Department of Electrical and Computer Engineering

THE UNIVERSITY OF TEXAS AT EL PASO

August 2010

Acknowledgements

I would never have been able to finish my dissertation without the guidance of my committee members, help from friends and colleagues, and support from my family.

First and foremost I would like to express the deepest appreciation to my committee chair, Dr. Thompson Sarkodie-Gyan, who has the attitude and the substance of a genius: he continually and convincingly conveyed a spirit of adventure in regard to research and scholarship, and an excitement in regard to teaching. Without his guidance and persistent help this dissertation would not have been possible. One simply could not wish for a better or friendlier supervisor.

I would like to thank one of my committee members, Dr. Richard Brower, who always gave the greatest support: he provided me funding which made it possible to attend one of the most important IEEE conferences in the area of rehabilitation (ICORR, 2009, Japan); he also provided Lab equipment, an electromyographic device (EMG) to support this research. Dr. Brower also introduced many participants including some of the neurological impaired subjects to me. I would further like to thank Dr. Amr Abdelgawad, Dr. Eric Spear, Dr Steven Glusman, and Mr. James Moody for providing mobility-related impaired subjects as participants to my research. I would also like to extend sincere thanks to Dr. Scott Starks and Dr. Bill Tseng for guiding my PhD research study over the past years. I would like to express my special thanks to them for their membership of my dissertation committee that always supported me from the beginning of the proposal to the final defense.

In my daily work I have been blessed with a friendly and cheerful group of student colleagues. Murad Alaqtash, Chad McDonald (graduated in December 2009), Oscar Espino, Luis Sagarnaga, Julio Torres, all helped me with the equipment set-up and data collection. Without their help, this dissertation could not contain the enriched information from so much data.

This dissertation was performed and accomplished six months ahead of time. Instead of completing the dissertation in December, it was finally done on June 29, 2010. This was possible through the financial support obtained from the Stern Foundation. I am deeply indebted to the Stern Foundation for this great cooperation and assistance.

Abstract

The main aim of this dissertation work was to develop an intelligent system to monitor, quantify and differentiate variances in human gait with high reliability and efficiency using the fusion of multiple sensor data and the methods of fuzzy inferential logic.

Gait disorders are heterogeneous and produce disabilities that vary substantially from individual to individual. The recognition, quantification and analysis of gait dysfunction is complex and, requires the integration of large amounts of data across multiple domains (kinetic, kinematic and electromyographic). Current systems for gait analysis generally require space and complex imaging equipment, as well as prolonged processing time, rendering them unsuitable for real-time applications. Quantitative gait analysis has been used to elucidate characteristic features of neurological gait disturbances. Although a number of studies have compared single patient groups with controls, there are only a few studies comparing gait parameters between patients with different neurological disorders.

This dissertation work is based on the hypothesis that functional rehabilitation can be most effectively achieved through the reduction of variances from normal patterns through training and other compensatory strategies, hence, efficient and reliable detection, quantification and differentiation of these variances is a critical link between diagnosis and optimal recovery. Current clinical methods of gait analysis are time and labor intensive and involve extensive post-hoc data analysis. These limitations reduce access to gait analysis and exclude direct application of the patient's gait data to rehabilitative interventions in real-time.

The goal of the dissertation work was to develop a novel intelligent system to monitor, quantify and differentiate variances in human gait with high reliability and efficiency using the fusion of multiple sensor data and the methods of fuzzy inferential logic.

Applications of this innovative technology will include improved recognition of complex patterns related to variable and combined pathophysiologic factors, and reliable quantitative monitoring of gait-related disability with recovery or therapeutic intervention over time.

Table of Contents

Acknowledgements	iv
Abstract	vi
Table of Contents	viii
List of Tables	xii
List of Figures	xiii
Chapter 1: Introduction	1
1.1 Background and Significance	5
1.2 Motivation	15
1.3 Specific Aims	16
1.4 Overview of this Dissertation	18
Chapter 2: Global Burden of Neurological Disorders	19
2.1 The Global Burden Awareness for Neurological Disorders	19
2.2 Stroke	20
2.2.1 Effects of the Stroke	21
2.2.2 Burden of the Stroke	21
2.2.3 Treatment and Rehabilitation of Stroke Survivors	22
2.3 Multiple Sclerosis	23
2.3.1 Effects of Multiple Sclerosis	24
2.3.2 Types of Multiple Sclerosis	25
2.3.3 Burden of Multiple Sclerosis	26
2.3.4 Treatment and Neurorehabilitation of Multiple Sclerosis	27
2.4 Spinal Cord Injury	28
2.4.1 Location and Effects of Spinal Cord Injury	30
2.4.2 Classification of Spinal Cord Injury	31
2.4.3 Incidence, Prevalence and Consequence of SCI	32
2.4.4 Treatment and Rehabilitation of Spinal Cord Injury	34
2.5 Cerebral Palsy	37
2.5.1 Classification of Cerebral Palsy	38
2.5.2 Prevalence and Incidence of Cerebral Palsy	39

2.5.3 Treatments and Rehabilitation of Cerebral Palsy	40
2.6 Summary	40
Chapter 3: Background of Neurological Rehabilitation	42
3.1 Principals of Neurological Rehabilitation.....	42
3.2 Mobility, Exercise Training, and Functional Recovery.....	43
3.2.1 Gait Rehabilitation	44
3.2.2 PWBTT and Conventional Gait Trainers	44
3.2.3 Gait Trainers with Robotic Devices.....	47
3.2.3.1 Robotic Gait Trainer Versions I and II	48
3.2.3.2 Lokomat and AutoAmulator	49
3.2.4 Other Therapeutic Interventions for Task-Specific Training.....	51
3.3 Rehabilitation Management and Rehab Cycle.....	53
3.4 Summary	56
Chapter 4: Biomechanical Model on Human Locomotion	57
4.1 Human Gait – Basic Concepts and Terminology	57
4.2 Gait Cycle and Gait Phases.....	57
4.3 Kinematics Approach.....	59
4.3.1 Spatial-Temporal Gait Parameters	59
4.3.2 Joint Kinematics.....	60
4.4 Dynamic Kinetics.....	61
4.4.1 Ground Reaction Forces	61
4.4.2 Foot Pressure Distribution	62
4.5 Surface Electromyography.....	63
4.6 Summary	65
Chapter 5: State-of-the-Art in Human Locomotion.....	66
5.1 Analytical Techniques for Automated Gait Assessment	66
5.2 Classification of Gait Abnormalities	66
5.3 Gait Variability Study	68
5.3.1 Spatial-Temporal Parameters Variability	68
5.3.2 Stride Variability with Elderly Fallers	69
5.3.3 Stride Variability in Neurodegenerative Disorders.....	69
5.4 Summary	71

Chapter 6: Current Devices for Diagnosis and Therapy	72
6.1 Importance of the Quantitative Measurement for Diagnosis	72
6.2 Motion Analysis Technologies	73
6.2.1 Optical Motion Capture System with Passive Relective Markers ...	74
6.2.1.1 Inverse Dynamics.....	77
6.2.1.2 Objective Gait Analysis and Quantitative Assessment of Rehabilitation.....	77
6.2.2 Markerless Motion Capture	78
6.2.3 Wearable Inrtial Sensors	79
6.2.3.1 Accelerometers	80
6.2.3.2 Gyroscopes.....	82
6.2.3.3 Electrogoniometers	82
6.2.4 Electromyography and Nerve Conduction Velocity (NCV).....	83
6.2.5 Measurement of Ground Reaction Force and Moments	85
6.3 Summary	87
Chapter 7: Limitations of Current Technology.....	88
7.1 Limitations of Optical/Video Motion Capture System.....	88
7.2 Weakness of the Wearable Sensor Detection	91
7.3 Limitation of Surface EMG	93
7.4 Limitation of GRF measurements.....	95
7.5 Summary	97
Chapter 8: Design of Research Activities	98
8.1 Fusion of Multiple Sensor Data	99
8.2 Fuzzy Inferential Logic.....	101
8.2.1 The Fuzzy Sets Theory	102
8.2.2 Fuzzy Set Definition	102
8.2.3 Fuzzy Relations.....	102
8.2.4 Fuzzy Relation Matrix	103
8.2.5 Fuzzy Similarity.....	105
8.3 Experimental Determination of Gait Dynamics	106
8.4 Participant Recruitment	109
8.5 Design Activities.....	109

8.5.1 Specific Aim-1	109
8.5.2 Specific Aim-2	112
Chapter 9: Data Acquisition.....	118
9.1 Ground Reaction Force Measurement	118
9.2 Elctromyographic Data Acquisition	120
9.3 Acceleration Measurement	120
9.4 Sensor Placements	121
9.5 Synchronization of Multi-Portable Sensors	124
9.6 Data Acquisition Procedures.....	125
9.7 Anthropometric Measurement	126
Chapter 10: Data Processing.....	127
10.1 Ground Reaction Force Data Processing	127
10.2 EMG Data Processing.....	128
10.3 Acceleration Data Processing	133
Chapter 11: Case Studies and Analysis	135
11.1 Healthy and Patient Participants	135
11.2 Data Acquisition	138
11.3 Results of Temporal Stride Variability	138
11.4 Study of Multiple Sclerosis.....	141
11.5 Study of Cerebral Palsy	158
Chapter 12: Comparative Analysis and Discussion.....	171
12.1 Multiple Sclerosis (MS3) vs Cerebral Palsy (CP3)	171
12.2 A Hemiparetic Stroke Subject (made two times visits for testing)....	176
Chapter 13: Conclusions, Outcomes and Claims of the Research.....	181
Chapter 14: Suggestions for Future Enhancements	183
References	186
Appendix.....	217
Curriculum Vita	368

List of Tables

Table 9-1: EMG Electrode Placement of Eight Muscles in the back and lower extremity.	121
Table 11-1: Anthropometric data of able-bodied subjects.....	136
Table 11-2: Anthropometric data of mobility-related impaired subjects.....	137
Table 11-3: Stride Variability of Able-bodied Subjects.	139
Table 11-4: Stride Variability of Mobility-related Impaired Subjects.....	140
Table 11-5: Characteristics of segment's accelerations in MS-1.....	151
Table 11-6: Characteristics of Multiple Sclerosis.....	155
Table 11-7: Description of EMG patterns of CP-2.....	165
Table 11-8: Characteristics of segment's accelerations of CP-2	167
Table 11-9: Characteristics of Cerebral Palsy.	169
Table 12-1: Comparative Analysis between MS and CP.....	175
Table 12-2: Comparative Analysis before and after two-month hydrotherapy in Stroke 1.....	180

List of Figures

Figure 2-1: Structure of Axon with Myelin Sheath wrapping.	24
Figure 2-2: Spinal Cord Cross-section.....	29
Figure 2-3: Location of the spinal cord injury and consequent effects.....	31
Figure 3-1: Therapist-assisted training using the parallel bar.....	45
Figure 3-2: Treadmill training with partial body-weight support.	46
Figure 3-3: Robotic Gait Trainer Version II.	49
Figure 3-4: Driven Gait Orthosis - Lokomat.	50
Figure 3-5: Driven Gait Orthosis - AutoAmbulator.	51
Figure 4-1: Functional Phases within the gait cycle.	58
Figure 4-2: Schematic diagram that reveals the stride length, step length, and step width.....	59
Figure 4-3: Typical joint rotation of the lower extremity on sagittal plane during a full gait cycle during free walking.	60
Figure 4-4: Ground Reaction Force.	62
Figure 4-5: 3D presentation of foot pressure distribution pattern while walking.....	63
Figure 6-1: Reflective markers are used to track the motion.....	75
Figure 6-2: High-speed cameras system with Infra-red LED's around, VICON motion capture system	75
Figure 6-3: SIMI motion system.....	76
Figure 6-4: F-Scan sensor inserted into patient's shoe	86
Figure 8-1: Sensor fusion driven computational intelligence scheme	98
Figure 8-2: Feature analysis.....	104
Figure 8-3: Differential pattern analysis scheme	107

Figure 8-4: Temporal Stride Variables	112
Figure 9-1: Ground Reaction Force (GRF) measurement	119
Figure 9-2: Surface EMG and Tri-axial accelerometer placements for Data Acquisition	124
Figure 10-1: Comparison before and after filtering on vertical GRF	127
Figure 10-2: Raw EMG data from Soleus muscle of an able-bodied subject.....	128
Figure 10-3: EMG data filtering	129
Figure 10-4: Full-wave rectified EMG data.....	130
Figure 10-5: Linear envelope of EMG data.....	131
Figure 10-6: Mean of soleus EMG signal.....	132
Figure 10-7: Normalized EMG signals within gait cycle	133
Figure 10-8: Acceleration signal processing.....	134
Figure 11-1: Stride variability of healthy subject and a multiple sclerosis patient case 1	142
Figure 11-2: Right and left ground reaction forces in 3-D in MS-1	143
Figure 11-3: Comparison of grade of similarity between right and left GRFs in MS-1.....	144
Figure 11-4: Average EMG activity of the eight muscles in a gait cycle in MS1 compared to averaged healthy female control group.....	145
Figure 11-5: Comparison of grade of similarity between right and left EMG in MS-1	146
Figure 11-6: Comparison of acceleration signal pattern in a gait cycle between healthy subjects and MS1	148
Figure 11-7: Comparison of grade of similarity between right and left acceleration in MS-1...	149
Figure 11-8: Stride variability of healthy subject and a male cerebral palsy case 2 (CP-2).....	158
Figure 11-9: Right and left ground reaction forces in 3-D in CP-2	159
Figure 11-10: Comparison of grade of similarity between right and left GRFs in CP-2.....	160

Figure 11-11: Average EMG activity of the eight muscles in a gait cycle in CP-2 compared to averaged healthy control group.....	160
Figure 11-12: Comparison of grade of similarity between right and left EMG in CP-2	161
Figure 11-13: Comparison of acceleration signal pattern in a gait cycle between healthy subjects and CP-2.....	163
Figure 11-14: Comparison of grade of similarity between right and left acceleration in CP-2..	164
Figure 12-1: Comparison of ground reaction force and grade of similarity between MS-3 and CP-3.....	171
Figure 12-2: Comparison of EMG patterns and grade of similarity between MS-3 and CP-3 ..	172
Figure 12-3: Comparison of segment's acceleration and similarity between MS-3 and CP-3 ...	174
Figure 12-4: GRF and similarity of a stroke subject with two visits in two months interval.....	176
Figure 12-5: Comparison of EMG patterns and similarity between two times of visits with two months interval.....	177
Figure 12-6: Comparison of segment's acceleration and similarity between two visits of a stroke subject	179

Chapter 1: Introduction

Locomotion disabilities are most commonly caused by neurological disorders to the central nervous system (CNS). Hemiplegic stroke, paraparesis from spinal cord injuries, and other upper motor neuron syndromes such as multiple sclerosis and cerebral palsy, cause serious neurological impairments and mobility-related disabilities. Each year, approximately 700,000 suffer stroke [203], 12,000 spinal cord injuries [180] and over 250,000 are disabled by multiple sclerosis [176] in the United States. Cerebral palsy is one of the most common chronic childhood disorders, occurring in approximately 1 in 500 children [44]. The mobility impairments can affect patients physically, mentally, emotionally, or a combination of the three. Moreover, the reduction in inpatient rehabilitation length of stay and the decline in outpatient care times covered by insurers, efficacious and cost-effective interventions for the recovery of walking have become critical. The associated reduction in the quality of life for the patient and the burden placed on the health care system and therapists have led to efforts to improve the rehabilitation strategies employed in a clinical setting (for example, partial weight bearing treadmill training, PWBTT, and functional electrical stimulation), according to [76-87, 200, 212, 243, 244, 245, 249, 263].

Neurological disorders are an important cause of mortality and constitute 12% of total deaths globally [177]. Within these, cerebrovascular diseases are responsible for 85% of the deaths due to neurological disorders [177]. Neurological disorders constitute 16.8% of the deaths in lower middle income countries compared with 13.2% of the total deaths in high income countries [177, 178]. Among the neurological disorders, Alzheimer and other dementias are estimated to constitute 2.84% of the total deaths in high income countries in 2005. Cerebrovascular disease constitutes 15.8%, 9.6%, 9.5% and 6.4% of the total deaths in lower

middle, upper middle, high and low income countries respectively [177, 178]. Thus neurological disorders constitute 6.3% of the global burden of disease [178].

The disabling consequences of neurological disease present a great challenge. Many neurological diseases are age-related and populations in the developed world are aging. In the USA today some 65 to 80 million citizens are disabled or elderly and the population is growing older, with people living longer and the numbers of younger people falling. The proportion of people with disability and/or frailty due to age in the population will continue to climb across the community. Both the incidence of disability and the capital cost of care rise steeply with advancing age. Today, it is estimated that nearly 70% of persons with disabilities are aged 60 or over. The number of people over 60 is projected to rise to one in four of the population by the year 2020. The cost of health care will rise even more steeply. The burden of caring will fall, both physically and financially on an ever smaller proportion of the population. Ways of reducing the burden of care and improving the quality of life for the elderly and disabled people through independent living are urgently needed.

Most recent studies depict that stroke is the second most common cause of mortality world-wide and the third most common disease in more developed countries [178]. According to the World Health Organization (WHO), stroke causes about 5.54 million deaths worldwide each year, with two thirds of these deaths occurring in less developed countries. Stroke is a major cause of long-term disability. About half of the patients surviving for three months after stroke will be alive for five years later, and one third will survive for 10 years. Approximately 60% of survivors are expected to recover independence with self-care, and 75% are expected to walk independently. It is estimated that 20% will require institutional care. The remainder will need assistance either by family, a close friend, or paid attendant. It is noteworthy that psychosocial

disabilities (such as difficulties in socialization and vocational functions) are more common than physical disabilities (such as problems with mobility or activities of daily living). According to WHO in 2006 [178], further increase in stroke is expected, with the majority of deaths from stroke to occur in less developed countries. By 2015, over 50 million healthy life years will be lost from stroke, with 90% of this burden in low and middle income countries. While some progress has been made in preventing conditions such as stroke and in attenuating symptoms in progressive conditions such as Parkinson's disease (PD), it has been slow and so major focus has been on neurorehabilitation.

Our society is, therefore, faced with the challenge to improve the quality of life for our citizens who experience disabilities and handicaps by virtue of impairment or ageing. This challenge may involve the facilitation of independent living of these citizens through promotion of greater community/societal integration, and also through the enhancement of opportunities for education and training, communication, employment, transportation and leisure. Neurorehabilitation seeks to lessen the disabling impact of neurological diseases when there is limited potential for reversing the underlying pathological process. There is evidence of its effectiveness in many conditions but the degree of disability carried by many patients remains high. Though a simplification, it is useful to divide neurorehabilitation into measures primarily aimed at assisting adaptation to impairment and those primarily aimed at reducing impairments. The latter addresses underlying neurological deficits more directly but are relatively poorly developed.

Rehabilitation technology not only provides means for independent living but can help reduce the cost of care. Rehabilitation technology is applied technology provided to elderly and disabled people to enable them to live independently and participate in the everyday social and

economic activities of the community. The use of technology to enable people with disabilities to gain access to education and to contribute through working is both cost-effective and socially desirable.

This research project is prompted by the belief that recent advances in neuroscience should benefit individuals with neurological disability by reducing impairment and that such advances are not being exploited clinically as fast as they might. One reason for this may be a lack of efficient transfer of knowledge between basic neuroscience and clinical neurorehabilitation, a lack this research is designed to address.

An area where rehabilitation strategies could be improved may involve the application of automated diagnostic and therapeutic algorithms. Currently, clinical interpretation of neurological data is solely performed manually and requires long-term experience of highly specialized clinical experts [84]. Current concepts employed for gait analysis using human experts have failed to acquire data and properly use these data as a tool for diagnosis with respect to the variability of each patient's gait pattern. The variability between the diagnoses by experts and even between diagnoses by the same expert at different times provides a motivation for designing intelligent systems that are capable of emulating the human reasoning process in a consistent and repeatable manner.

1.1 Background and Significance

Chronic diseases, such as arrhythmias, stroke, multiple sclerosis, congestive heart failure, cancer, arthritis, chronic respiratory diseases and diabetes, are leading causes of morbidity and mortality in the world, representing 60% of all deaths. Stroke survivors, for example, show marked decreases in their ability to ambulate 6 months post-insult, with 20% of them unable to walk without physical assistance and half of them walking at less than 50% of normal casual speed. These changes in mobility translate into a significant reduction in the patients' quality of life, and increase the burden of therapists and the health care system in treating these patients. Following a stroke, patients often suffer from impairments of motor and sensory functions of the body contralateral to the site of lesion. Other common symptoms include speech disturbances, perception disorders and cognitive disturbances. Efforts to improve walking ability and efficiency have been undertaken using rehabilitative strategies such as partial weight bearing treadmill training (PWBTT) to establish or re-initiate normal gait patterns in human subjects following injury [40, 76-77, 158, 198, 212, 226, 249, 254, 255].

Recovery of locomotor activity following spinal cord injury has been extensively studied in animal models. Rats and cats that have undergone complete low-thoracic spinal cord transection can be trained to walk on a treadmill, and have been shown to accomplish full weight-bearing stepping at normal speeds [12, 42, 110, 116, 143]. Other data suggest, however, that this type of training induces a motor task-specific kind of learning. For example, Hodgson et al. showed that spinalized cats trained to step were less able to stand and bear weight without the motion of walking, whereas animals trained to stand were deficient in their ability to walk on a moving treadmill [84, 144]. The re-establishment of ambulation following treadmill training may be due to the activation of central pattern generator (CPG) neurons in the spinal cord, in

which locomotor-associated motor neuron pools are activated in response to sensory input coming from the limbs [142, 165, 174, 191, 235-236]. An important aspect of this behavior is that it occurs in the absence of supraspinal input. Crucial to the success of this training, therefore, is the coordination of sensory input to the spinal cord. The ability to step in both human and animal subjects is highly influenced by the pattern of loading placed on the legs and by the kinematics of the gait cycle [40, 42].

Animal studies have led to the development of measures to assist human patients following spinal cord injury (SCI). Wernig et al. [254, 255] demonstrated a significant increase in the ability to ambulate independently or semi-independently following intensive PWBTT in people with incomplete spinal cord transections. Moreover, the positive effects of this intervention persisted for more than 6 years following training. In patients with complete SCI, Dietz et al. [36] showed improved gait patterns as a result of treadmill training, possibly due to the normalization of muscle activation patterns. In support of this idea, Harkema et al. recorded electromyographic (EMG) data in lower limb muscles during stepping in complete SCI patients and showed that their ambulatory patterns were, in fact, regulated by sensory input to the lumbosacral spinal cord [67]. Results from both human and animal experiments, therefore, provide evidence that spinal cord CPGs can control locomotion, and that their activity is largely a function of proprioceptive and other sensory inputs from the limbs [116, 117, 139]. Step-related cues can thus alter CPG activity somewhat independently of higher central nervous system activation.

In addition to SCI, patients with brain injury or disease also have been shown to respond positively to PWBTT. One problematic variable in patients learning to walk after a neurological insult is that of maintaining balance during locomotion. The trunk stability provided by PWBTT

allows for gait training, through the performance of repetitive and complicated motor activities, without the interference of vestibular reflexes. For example, adult hemiplegic stroke patients who failed to respond to traditional physical therapy interventions showed a 123% improvement in swing symmetry, with a 24% improvement in stance symmetry, after PWBTT [76]. These results were obtained in 25 training sessions carried out over 5 weeks, with the amount of body weight support provided decreasing from 31% to 0% (full weight-bearing) in 7 out of 9 patients. Further comparisons between subjects walking under different levels of body weight support versus normal overground ambulation showed that partial weight support provided the most efficacious circumstance for reducing spasticity, limiting co-contraction of antagonistic muscle groups, and producing appropriate gait patterns [78, 226]. In another controlled study of partial compared to no body weight support in 100 patients, increased performance, as evidenced by positive outcomes in balance, speed, endurance and recovery was seen in the partially supported group following a 6-week treadmill training intervention [249]. Other investigations have resulted in rehabilitative success following PWBTT in stroke [31] and Parkinson's [169] patients.

Several studies have suggested that plastic processes taking place in brain areas contralateral to the injury might be of importance for functional recovery [15, 19-20, 102-104, 179]. Stimulation of axonal outgrowth from the intact hemisphere and re-innervation of denervated regions in the midbrain and spinal cord correlated with functional improvement after stroke [23]. Synchronous neuronal depolarization activity in the perilesional area appears to constitute a signal for axonal sprouting from the non-lesional hemisphere [20]. Other studies have, however, indicated that contralesional activation is accompanied by worsened outcome and shown that re-organization of ipsilateral regions might be involved in functional recovery after stroke, findings that are in agreement with current clinical data [37, 50, 192].

The concept of neural plasticity includes not only synaptogenesis and dendritic branching, but also neurogenesis, a relatively novel aspect of structural regeneration [142]. Neurogenesis occurs in the adult mammalian central nervous system (CNS) following the migration and differentiation of neural stem/progenitor cells (NSPCs). The majority of these cells reside in one of two germinal zones; the subventricular zone in the wall of the lateral ventricles (SVZ) and the subgranular zone of the hippocampus (SGZ) [236].

Evidence of neuronal self-repair following insults to the adult brain has been scarce until very recently [19, 107, 183]. Ischemic insults have now been shown to trigger neurogenesis from neural stem cells or progenitor cells located in the dentate subgranular zone, the subventricular zone lining the lateral ventricle, and the posterior periventricle adjacent to the hippocampus. New neurons migrate to the granule cell layer or to the damaged CA1 region and striatum, where they express morphological markers characteristic of those neurons that have died. Some evidence indicates that these neurons can re-establish connections and contribute to functional recovery [96, 120, 142]. Neural stem cells undergo symmetric or asymmetric cell divisions. In a symmetric division, both progeny will be stem cells. In contrast, an asymmetric division produces one new stem cell that is identical to the mother cell and one cell that is more determined for a certain lineage of differentiation. These daughter cells have less stem cell properties and are termed progenitor cells.

It has been unambiguously demonstrated that persistent neurogenesis occurs in two regions of the brain, i.e. in the subventricular zone (SVZ) lining the lateral ventricles, and in the subgranular zone (SGZ) of the dentate gyrus [215]. In these areas, populations of neural stem cells have been identified in rodents [100], monkeys [119] and humans [13]. Proliferating SVZ cells normally migrate along the rostral migratory stream into the olfactory bulb and are finally

incorporated as olfactory interneurons, whereas newborn neurons in the SGZ migrate into the granular cell layer and establish synaptic contacts with the hippocampal CA3 region [153]. Although the physiological function of persistent neurogenesis is poorly understood, it has been shown that hippocampal neurogenesis is important for spatial learning and memory [218]. In addition, recent studies have demonstrated that focal cerebral ischemia induces SVZ and SGZ cell proliferation, and that these cells differentiate into mature region-specific neurons, and replace damaged neurons [8, 188]. These findings suggest the possibility of a restorative method that aids stroke recovery.

Physical therapy has been widely used to promote stroke recovery, and its favorable effects have been repeatedly confirmed by many clinical stroke trials [24]. Moreover, although the biochemical mechanism is not fully understood, neural reorganization and plasticity are likely to be important aspects of the recovery mechanism [202]. Furthermore, it has been reported that voluntary exercise increases SGZ cell proliferation and neurogenesis [148]. These data importantly suggest an association between physical exercise and neurogenesis. However, clinically applied physical therapy for stroke patients is an enforced, scheduled, non-voluntary form of exercise that is fundamentally different from the proposed experimental voluntary exercise protocols. Thus, it is necessary to investigate the effects of clinically relevant exercise with respect to its association with neurogenesis after stroke. Because previous studies have been restricted to SGZ neurogenesis, SVZ and SGZ neurogenesis should be compared after physical activity. In the study, the authors sought to evaluate effects of enforced physical training (EPT) on neurogenesis in the SVZ and SGZ regions after stroke. To find evidence of cell proliferation and neurogenesis, the authors [235] used some specific markers such as 5-bromo-2'-deoxyuridine (BrdU), double cortin (Dcx), neuronal nuclei (NeuN), and glial fibrillary acidic

protein (GFAP), because despite some limitations, these antibodies are currently the most widely used techniques for studying adult neurogenesis in situ despite some limitations.

The restoration of healthy locomotion (gait) after stroke, traumatic brain injury, and spinal cord injury, is a major task in neurological rehabilitation. Motor-learning and control research clearly favors task-specific repetitive training [39]. The complexity of the interactions of the various components of human gait has been researched and documented extensively, and to date it is the experienced clinician who continues to perform functional gait assessment and training in the absence of virtually any technological assistance.

There have been many attempts to elucidate the mechanisms underlying the intelligent adaptive behavior in the complex human locomotor system. These attempts involve directly capturing the activities of the neuronal system in human locomotion [93, 97-99]. They do not, however, clarify how the nervous system adaptively functions as a dynamic system and how it effectively coordinates adaptive interactions with the musculo-skeletal system during locomotion [93, 99]. Other studies have tried to artificially emulate locomotion by using mathematical models and robots based on control theory. Here again, the successful locomotor control of a simulation model or robot does not lead to an understanding of biological locomotor mechanisms, as the control laws are artificially constructed solely based on an engineering perspective independent of actual biological mechanisms. Innovations in the quantitative analysis of gait physiology and biomechanics are essential to truly understand the principles of adaptive behavior in human locomotion and locomotion rehabilitation. Quantitative gait analysis has been used to elucidate characteristic features of neurological gait disturbances. Although a number of studies compared single patient groups with controls, there are only a few studies comparing gait

parameters between patients with different neurological disorders affecting gait [12, 93, 99, 158, 254].

Robotic assistive devices have become the focus of clinical research due to the physical demands therapists face when manually assisting the trunk and legs of subjects at treadmill speeds greater than 0.8 mph. There are constraints on therapists' ability to optimize sensory inputs associated with the step cycle such as kinematics, temporal symmetries during the stance and swing cycles due to the tasks therapists must perform and monitor simultaneously as they sit by the subject's legs. Current commercial robotic assistive devices automatically drive a subject's legs passively through the gait cycle and do not take into account the torques that a subject can generate or incorporate the subject's potential ability to step. Despite some evidence of the benefit of partial weight bearing treadmill training after stroke [226] passive step training would not seem to be an optimal method for retraining a complex motor skill such as walking. Step training would more likely drive basic mechanisms of motor learning and representational plasticity for the lower extremities [249] if it included the following: incorporate the subject's intentions and abilities, is based on subject-specific locomotor feedback, and proceeds at walking speeds typical of overground ambulation.

There are other significant limitations in the current systems. The absence of objective measures of essential gait parameters is a major shortcoming of commercially available robotic assistive devices. No reported study has outlined a training method that can be reproduced by others. Additionally, application of single sensors in the analysis of biomechanical/physiologic states may offer only marginal results [12, 158, 198, 212, 254, 255]. These single-sensor single-algorithm systems work well in situations where the environment is structured and the objects are well known, but are severely limited in their ability to resolve ambiguities in complex

systems like the human locomotor system involving multi-body dynamics, biomechanics, physiology and other factors that obscure the interactions between the vestibular, somatosensory and visual inputs for postural control [89, 143, 144, 174]. Murad et al in [102] have applied the wearable sensors for human gait analysis using fuzzy inferential reasoning. However, this method only recognized gait-related mobility but failed to characterize and differentiate the subtle variances inherent in making decisions about outcome measures. Accelerometers and gyroscopes are fixed to the body as sensing devices to measure motion of body segments, and the orientation of the body segments, respectively, of human movement in free-living subjects. They are used in several applications including the monitoring of activities of daily living [36, 42, 67], assessment of internal mechanical working load in ergonomics studies [15, 20, 31, 169], measurement of neurological disorders [102, 104, 179] and mixed and augmented reality [23, 37, 50]. These inertial sensors were used as single sensors to monitor gait-related mobility. Relatively small offset errors due to temperature effects on the gyroscope signals and noise do introduce large integration errors. Sensor validation and fusion schemes enable high sensitivity and resolution in measured data especially for therapy and rehabilitation of human.

This dissertation work has developed a novel technology to link the physiological and biomechanical responses underlying human gait, to quantify and to differentiate the functional components of normal and impaired locomotion. The dissertation work has developed an array of wearable sensors that are unobtrusively attached to the body for real-time quantitative analysis of human locomotion under any circumstances. This system allows the recording and manipulation of locomotor-related parameters during different styles of training in order to determine which features are most important for an individual patient. One of the expected

outcomes is a reproducible methodology for helping therapists make reliable and differentiable diagnosis and follow-ups on patients' functional recovery.

This system derives intelligence through the fusion of data from the multiple sensors, and the fuzzy inferential logic is correlated with each subject's physiological states, including gender, age, health conditions, and underlying mechanisms of disability, if any. The fuzzy inferential logic allows perturbations during the step cycle to be incorporated into a control scheme that can test postural adjustments and evaluate mechanisms of motor control.

Ultimately it is expected that the integration of multiple sensor data coupled with analysis technologies based on fuzzy inferential logic will lead to a new gait rehabilitation paradigm based on a thorough and rapidly-derived understanding of individual kinematic variations from normal. More specifically, the overarching goal of this research is the development of an intelligent system for rehabilitative therapies and/or compensatory interventions that are driven by subject-specific locomotor data in real-time.

The World Health Organization (WHO) defines rehabilitation as an active process by which those affected by injury or disease achieve a full recovery or, if a full recovery is not possible, realize their optimal physical, mental and social potential and are integrated into their most appropriate environment. Rehabilitation involves a coordinated and iterative problem-solving process along the continuum of care from the acute hospital to the home and community. It is based on four key approaches integrating a wide spectrum of interventions: 1) biomedical and engineering-based compensatory strategies; 2) strengthening of the individual's personal resources and residual capabilities; 3) adaptive modification of the affected individual's environment; and 4) coordination of care across services, sectors and payers.

This dissertation work introduces technological innovations that will enable clinicians and investigators to flexibly and efficiently quantify and differentiate the effects of disease, aging, therapy and compensatory interventions on human gait, essential contributions to rehabilitative and performance enhancements and a direct challenge to established systems for clinical gait analysis. Existing systems are generally fixed, complex, expensive, and they require prolonged data processing, characteristics that render them unsuitable for real-time applications. There are other inertial-based sensing of activities of the human daily living. Single-sensor single algorithms have been applied in these instances, and therefore are severely limited in their ability to resolve ambiguities in a complex system like the human locomotor system [12, 102, 103, 158, 212, 254, 255]. Innovations in the quantitative analysis of gait physiology and biomechanics are essential to truly understand the principles of adaptive behavior in human locomotion and locomotion rehabilitation. New directions for research efforts are needed to improve the effectiveness of rehabilitation treatments for sensorimotor disabilities, especially for ambulation, balance, and maintenance of physical fitness across neurologic diagnoses. In recent years, there has been a growing interest in the use of miniature inertial sensors and systems [23, 37, 42, 50, 96, 102-104, 120, 179, 192, 251].

This research project directly challenges current research and clinical practice by providing a platform for relatively low cost, portable and rapid gait analysis that can function in almost any rehabilitative setting and performance-enhancing technology based on subject-specific locomotor feedback in real-time.

1.2 Motivation

In recognition of the demographic time bomb facing the developed world, this research work seeks to contribute to, and respond to the needs of aging populations with research into aging and disabling diseases, coupled with technologies for maintaining independence and reasonable quality of life. This calls for the utilization of technologies to compensate for the growing inadequacies in traditional medical intervention.

There are very hard problems to be tackled in this area which demand much more basic science and technology: these include supporting frail people and people with dementia, aphasia following a stroke, memory loss within the community, and transportation and care for those with failing senses and slowing reaction times. The unfilled needs and wants of elderly and disabled people will lead directly to the need for new basic and strategic science and technology: this will include new materials, new sensors, a greater understanding of degenerating cognitive, and physical processes and methodologies for modeling and supporting these processes using technology.

Through the use of engineering, mathematical and computational techniques in an interdisciplinary field, this research work tries to apply optimally and newly developed technologies to further our understanding of neuro-(patho-) physiology and improve the quality of diagnosis, prognosis and follow-up for individual patients suffering from neurological and other mobility-related disorders.

1.3 Specific Aims

Gait disorders are heterogeneous and produce disabilities that vary substantially from individual to individual. The quantification, differentiation and analysis of gait dysfunction are complex and, more specifically, require the integration of large amounts of data across multiple domains (kinetic, kinematic and electromyographic). Quantitative gait analysis has been used to elucidate characteristic features of neurological gait disturbances. Although a number of studies compared single patient groups with controls, there are only a few studies comparing gait parameters between patients with different neurological disorders. Current systems for gait analysis generally require space and complex imaging equipment. Additionally, these systems generally require prolonged processing time, rendering them unsuitable for real-time applications affecting gait. The overarching goal of this dissertation work is to develop an intelligent system for rehabilitative therapies and/or compensatory interventions that are driven by subject-specific locomotor data in real-time. The goal of the research is to develop an intelligent system to monitor, quantify and differentiate variances in human gait with high reliability and efficiency using the fusion of multiple sensor data, and the methods of fuzzy inferential logic. Sensor fusion will be used to solve the problem of integrating information from different sensory sources. The effort includes organizing the distributed sensing systems, integrating the sensors' diverse observations, coordinating and guiding the decisions based on each sensor's observation, and controlling devices with the goal of improving sensor system performance. The fusion of multiple sensor data will use a fuzzy rule-based algorithm.

The hypothesis of this dissertation is that since functional rehabilitation can be most effectively achieved through the reduction of variances from normal patterns through training and other compensatory strategies, efficient and reliable differentiation and quantification of these variances is a critical link between diagnosis and optimal recovery. Therefore, the main goals or specific aims of this research project are:

- 1) To investigate stride-to-stride fluctuations in gait to increase our understanding of the neural control of locomotion.
- 2) To gain knowledge of gait dynamics to increase our understanding of the neurophysiology/biomechanics of gait, and augment objective measurements of mobility and functional status.

The knowledge acquired through this research work will enable the development of novel ways to link physiological and biomechanical responses and quantify the functional attributes of impairment. Therefore, the expected outcome of this research project will be the development of a low-cost, real-time, compact and portable intelligent system for the assessment and evaluation of functional impairments.

The expected outcomes of the dissertation work are the integration of multiple sensor data and analysis technologies based on fuzzy inferential logic that will lead to a new gait rehabilitation paradigm and an understanding of individual kinematic variations. In particular, the work will improve our understanding of the neurophysiology and biomechanics of gait through innovative technologies that provide more rapid and accurate measurements and analysis of gait dynamics and functional mobility.

1.4 Overview of this Dissertation

Chapter 2 presents the neurological disorders such as stroke, multiple sclerosis, spinal cord injury, and cerebral palsy. In this chapter, WHO has realized that the burden on disability adjusted life years (DALYs) for these common disorders, estimated according to prevalence, duration and mortality rates, is higher than other global burdens of diseases.

Chapter 3 reviews the background of the neurological rehabilitation. This chapter introduces the traditional gait training such as parallel bar training and PWBTT (partial body weight support treadmill training), and a number of the modern robotic devices for gait training.

Chapter 4 reviews the basic concepts of human locomotion. It defines the gait parameters, the joint kinematics, the kinetics and EMG activity.

Chapters 5 and 6 introduce the state-of-the-art in human locomotion, and the most recent technologies including optical motion capture systems, inertial sensors, surface EMG, and ground reaction force (GRF), to monitor the human locomotor for objective and quantitative measurement and/or assessment of the recovery. In chapter 7, the limitations of the recent technologies (as introduced in chapter 6) are discussed in detail.

The experimental design, data acquisition and data processing are presented in chapters 8, 9, and 10, respectively. Sensor fusion was used to augment the data acquisition, and the fuzzy inferential logic (FIL) serves as the engine to make decisions. Subjects, both able-bodied and neurological impaired were recruited. The ground reaction forces (GRF), electrical activities of the muscle (EMG), and the segmental accelerations data were carefully processed.

Case studies are presented, explained and discussed in detail in chapters 11, 12, and appendix. Chapter 13 highlights the contributions that have been made in this research. Finally, the limitations and suggestions for future enhancement of this research are given in chapter 14.

Chapter 2: Global Burden of Neurological Disorders

2.1 The Global Burden Awareness for Neurological Disorders

Neurological disorders are a significant and increasing public health problem. The Global Burden of Disease (GBD) study found that the burden of neurological disorders was seriously underestimated by traditional epidemiological and health statistical methods that take into account only mortality rates but not disability (physically and mentally) rates [178]. A large body of evidence shows that policy-makers and health-care providers may be unprepared to cope with the predicted rise in the prevalence of neurological and other chronic disorders and the disability resulting from the extension of life expectancy and ageing of populations globally [65, 209].

Most of the neurological disorders result in long-term disability, and pain is a significant symptom in several neurological disorders and adds significantly to emotional suffering and disability. Furthermore, even the burden estimates combining mortality and disability do not take into account the suffering from social and economic losses affecting patients, their families and the community. The World Health Organization (WHO) has brought a clear message that unless immediate action is taken globally, the neurological burden is expected to become an even more serious and unmanageable threat to public health.

This chapter addresses a number of important neurological disorders including stroke, multiple sclerosis (MS), spinal cord injury (SCI), and cerebral palsy (CP). These neurological disorders are studied significantly in this research and will be discussed with case studies in later chapters.

2.2 Stroke

A stroke is a cardiovascular disease that affects the supply of blood to the brain. It occurs when an artery supplying blood to the brain either becomes blocked or bursts. The brain cells lose their supply of oxygen and nutrients, which in a matter of a few minutes the cells can die. Cell death results in areas of localized cerebral infarct, and the parts of the body that they control are unable to function. The overwhelming effects caused by stroke can often be permanent if the person is not properly treated or rehabilitated after he/she has had a stroke.

There are two types of stroke: ischemic (occlusion of the cerebral blood vessel) and hemorrhagic (rupture of a blood vessel). Ischemic stroke is more prevalent, and account for more than 80% of all stroke insults. Ischemic stroke can be divided into two types: cerebral thrombosis and cerebral embolism. Cerebral thrombosis is a blockage in an artery of the brain caused by a blood clot or thrombus that forms within the blood vessel system; while cerebral embolism is a blockage caused by a detached fragment of thrombus or other material that has formed somewhere else (usually in the heart and large arteries of the upper chest and neck) and is carried by the bloodstream to the brain. Hemorrhagic stroke can also be divided into two types: subarachnoid and intracerebral. Subarachnoid hemorrhage occurs when a blood vessel on the surface of the brain ruptures and bleeds into the cavity between the brain and the skull, but not inside the brain itself. An intracerebral hemorrhage transpires when an artery in the brain bursts, flooding the surrounding brain tissue with blood.

There are a number of risk factors for stroke including hypertension, high cholesterol, cardiovascular disease, brain tumors, obesity, diabetes, smoking, and other miscellaneous conditions.

2.2.1 Effects of Stroke

The effects of stroke vary from person to person based on the type, severity, and location of the stroke. The brain is divided into three regions: cerebrum (including left and right hemispheres), cerebellum, and brain stem. Since each hemisphere of the brain controls the activity of the opposite side of the body, any damage of one side of hemisphere will lead to a disability to the opposite side of the body. The following body functions may be impaired by someone who has had a stroke:

- Loss of normal motor control: muscle weakness (hemiparesis) or paralysis (hemiplegia due to abnormal muscle tone e.g. spasticity) on one side of the body.
- Sensory and proprioceptive loss: causing problems with speech, hearing, touch, sight, smell and balance.
- Problems with understanding of spatial concepts: affected depth perception and directions such as up/down and front/back.
- Learning, memory, and concentration may be affected.
- Psychological and emotional problems: behavioral changes, e.g. depression which may also lead to the social consequences.

2.2.2 Burden of Stroke

According to the most recent estimates, stroke is the second most common cause of mortality worldwide [177, 208]. In report of the World Health Organization [2004], stroke causes about 5.54 million deaths worldwide each year, with two thirds of these deaths occurring in less developed countries. Without urgent action, deaths from stroke will increase over the next decade by 12% globally and 20% in developing countries.

Stroke is a major cause of long-term disability. About half of the patients surviving for three months after their stroke will be alive five years later, and one third will survive for ten years. Approximately 60% of survivors are expected to live independence with self-care, and 75% of these survivors are expected to walk independently. About 20% of the survivors will require institutional care, and the remainder will need assistance either by family or other communities. The long-term disability with dependent activities of daily living consequently causes psychosocial disabilities such as difficulties in socialization and vocational functions. Furthermore, the long-term disability has potentially enormous emotional and socioeconomic impact on patients, families, and public health services (world health report, 2004).

2.2.3 Treatment and Rehabilitation of Stroke Survivors

Treatment of acute stroke may vary with respect to the type and subtype, severity and the location of the disease. In the past decade, treatment of acute stroke improved dramatically in the majority of developed countries. The development of specialized stroke services (e.g. stroke units) plays a key role in the provision of effective therapies and in improving the overall outcome after stroke. Evidence shows that treatment in stroke units is very effective, especially when compared with treatment in general medical wards, geriatric wards or any other of hospital department in which no specialized staff and equipments are exclusively dedicated to stroke care [106].

Stroke rehabilitation is the restoration of patients to their previous physical, mental and social capability. Rehabilitation starts as soon as possible after stroke onset (often within 24 to 48 hours after the stroke) in the stroke units. It is followed by short-term rehabilitation in the rehabilitation centers or outpatient settings. It is of extreme importance to reacquire the ability to

carry out the basic activities of daily living such as bathing, dressing, using a toilet in the first stage for a stroke survivor's return to functional independence. The scientific basis for rehabilitation and neural repair has increased considerably, and reorganization of activation patterns in the brain after injury may be monitored by functional imaging studies (fMRI and PET).

2.3 Multiple Sclerosis

Nerve cells communicate by sending action potentials along the axons, which are wrapped in an insulating protective substance called myelin sheaths, shown in figure 2-1. Myelin sheath provides insulation for nerves, and improves the conduction of impulses along the nerves and also is important for maintaining the normal function of the nerves. Multiple sclerosis (MS) is generally considered to be autoimmune inflammatory condition in which the myelin sheaths around the axons of the brain and spinal cord are damaged, leading to demyelination. Demyelination causes scarring and sclerosis of the nerve tissue in the brain, spinal cord, and optic nerves. In regions of inflammation, breakdown of the blood brain barrier occurs and destruction of myelin ensues, with axonal damage, gliosis and the formation of sclerotic plaques. Consequently, the electrical impulses that travel along the nerves decelerate or can no longer effectively be conducted, which results in weakness, numbness, pain, and vision loss. Plaques may form in the central nervous system (CNS) white matter in any location; thus clinical presentations may vary from people to people, and from time to time.

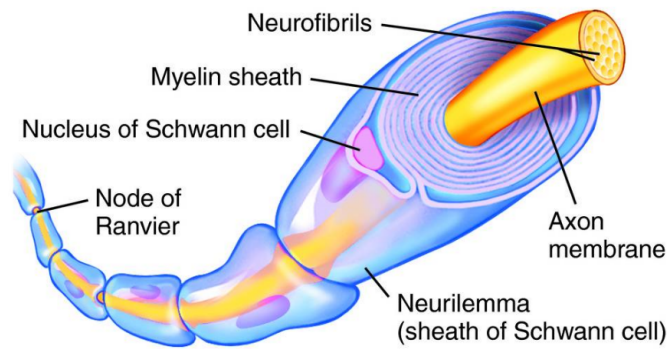


Figure 2-1: Structure of Axon with Myelin Sheath wrapping

To date no clear risk factor for the MS has been unequivocally identified. In the last two decades, researchers have focused on disorders of the immune system and genetics for explanations. It is now generally accepted that the etiology of MS involves some interplay of genetic and environmental factors. Researchers also suspect that a foreign agent such as a virus alters the immune system so that the immune system perceives myelin as an intruder and attacks it.

2.3.1 Effects of Multiple Sclerosis

Because different nerves are affected at different times, MS symptoms may be single or multiple, and may range from mild to severe in intensity and short to long in duration.

- Early symptoms of the disorder may include vision changes (e.g. blurred vision, blind spots, and color desaturation), numbness, and dizziness.
- Heat sensitivity.
- Muscle weakness, coordination and balance problems.

- Spasticity of the muscle, speech impediment, tremors.
- Mental changes such as decreased concentration, attention deficits, loss of memory, depression or paranoia.

2.3.2 Types of Multiple Sclerosis

MS is a complex condition, and often no two people experience the same thing. In order to develop a common language for evaluating and researching MS, an international survey was conducted among scientists who specialize in MS research and patient care. Analysis of responses resulted in defining the four typical categories of MS, which were introduced in 1996 [145]:

- Relapsing Remitting MS (RRMS) – most common type, around 80-85% of MS patients

A relapse is defined as an appearance of new symptoms or existing symptoms become more severe. The relapse can last for varying periods (days or months) and there is partial or total recovery (remission). In RRMS relapses occur with full or partial recovery and there is disease/symptom stability between attacks.

- Primary Progressive MS (PPMS) – affects around 10-15% of all MS patients

PPMS are characterized by a lack of distinct attacks, but with slow onset and then steadily worsening symptoms. There is no relapses or remissions period. However, there are variations in rates of progression over time, occasional plateaus and temporary minor improvements.

- Secondary Progressive MS (SPMS) – most of RRMS convert to SPMS

Patients with SPMS experience an initial period of RRMS, followed by a steadily worsening disease course with or without occasional flare-ups, minor recoveries (remissions), or plateaus.

Approximately 50% of patients with RRMS will develop SPMS within 10 years, and 80% will have developed SPMS within 20 years of disease onset.

- Progressive Relapsing MS (PRMS) – approximately 5% of MS patients

Patients with PRMS experience a steadily worsening disease from the onset but subsequently also have clear acute relapses, with or without recovery. In contrast to RRMS, the periods between relapses are characterized by continuing disease progression.

2.3.3 Burden of Multiple Sclerosis

MS affects around 2.5 million people worldwide each year. It is one of the most common neurological disorders and cause of disability of young adults (between 18 to 38 years old), especially in Europe and North America. The frequency of MS varies by geographical region throughout the world, apparently increasing with distance from the equator in both hemispheres. MS is more common among women than men, is less common among non-white individuals than whites.

Several studies have evaluated that maintaining mobility is ranked as one of the highest priorities among patients with MS, regardless of disease duration or disability level [227]. The loss of mobility contributes to a substantial patient burden. The statistical techniques of path analysis has shown how difficult walking significantly affects physical activity in patients with MS. Impaired mobility is associated with reductions in quality of life and activities of daily living.

MS has a profound impact on patient's social roles and the well-being of their families. MS is frequently diagnosed during a person's most productive years (the onset is usually at about 30 years of age), and because life expectancy for patients with MS approaches that of the general

population, MS is associated with a considerable economic burden from medical costs and lost productivity. Physical disability complicated by depression and possibly cognitive impairment contributes to a high rate of unemployment. Together with their family members, they may bear a financial burden related to home and transport modifications and the need for additional personal services.

2.3.4 Treatment and Neurorehabilitation of Multiple Sclerosis

There are no curative treatments available for MS. Drugs that are common to MS symptoms such as urinary dysfunction, spasticity and neuropathic pain, are relatively well established and widely used. To date, studies on MS prevention and curative treatments focus on neuro-protection and neuro-repair.

Even though drug treatment options are relatively limited, significant improvements in the quality of life of people with MS can be supported by improved rehabilitation approaches. Neurorehabilitation has been defined by WHO as “an active process by which those disabled by injury or disease achieve a full recovery or, if a full recovery is not possible, realize their optimal physical, mental and social potential and are integrated into their most appropriate environment”. The essential components of successful neurorehabilitation include expert multidisciplinary assessment, goal-oriented programs and evaluation of impact on patient and goal achievement through the use of clinically appropriate, scientifically sound outcome measures incorporating the patient’s perspective [197].

2.4 Spinal Cord Injury

The spinal cord is an extension of the brain and together with the brain forms the central nervous system (CNS). The spinal cord is the main pathway for information connecting the brain and peripheral nervous system (PNS). The human spinal cord extends from the medulla oblongata and continues through the conus medullaris near the first or second lumbar vertebra (L1 or L2), terminating in the cauda equina. It consists of 31 pairs of spinal nerves containing both sensory and motor fibers, which transmit electrical information to and from the limbs, trunk, and other parts of the body, back to and from the brain. The spinal nerves are grouped together in different bundles called ascending and descending tracts, forming white matter neuron pathways, shown in Figure 2-2. Ascending tracts (bundles of afferent/sensory neurons) within the spinal cord carry impulses, such as touch, temperature, pain and joint position, from the body upwards to the brain. Descending tracts (bundles of efferent/motor neurons) carry impulses from the brain downwards to the effectors to initiate movement and control body functions.

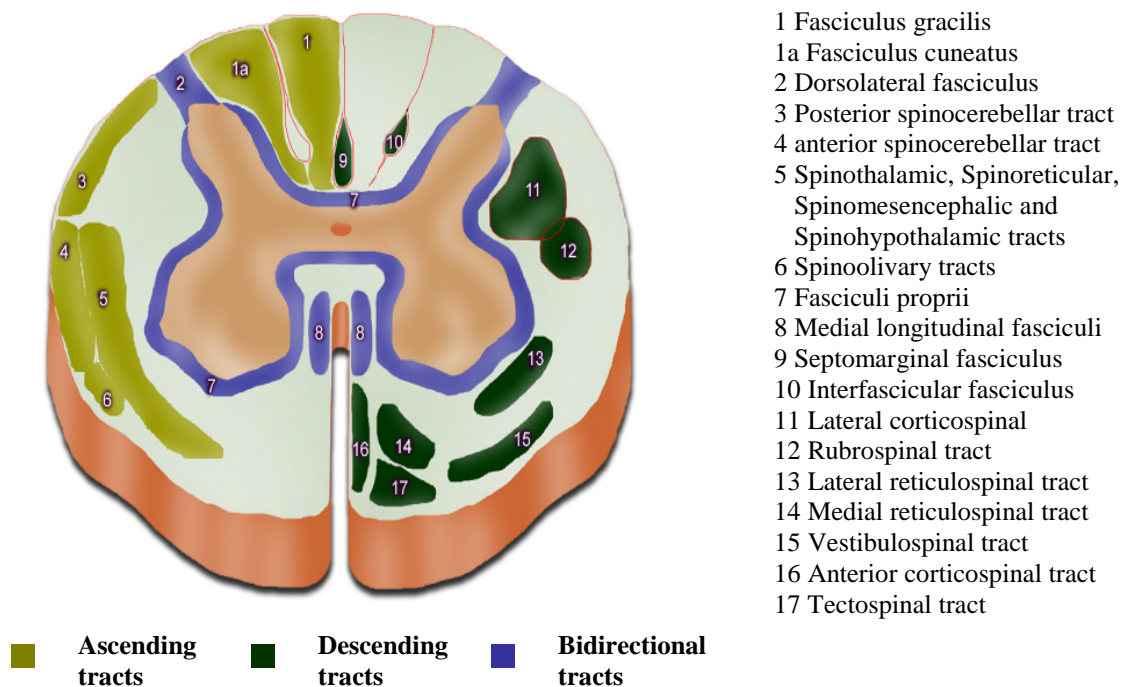


Figure 2-2: Spinal Cord Cross-section

The major ascending and descending spinal cord pathways

(<http://emedicine.medscape.com/article/1148570-overview>)

The diagram of the cross-section of the spinal cord of Figure 2-2, the center of the cord consists of gray matter shaped like *H* or a butterfly. The anterior or motor horns contain nerve cells that carry signals from the CNS through the motor root to muscles; the posterior or sensory horns contains nerve cells that receive sensory information through the sensory root from peripheral nerve cells outside the spinal cord.

A spinal cord injury (SCI) is damage of spinal nerves (nerve roots) or myelinated fiber tracts that carry signals to and from the brain [114, 140]. Spinal cord injury can occur from many causes, including trauma from falls or accidents, tumor, developmental disorders, ischemia of

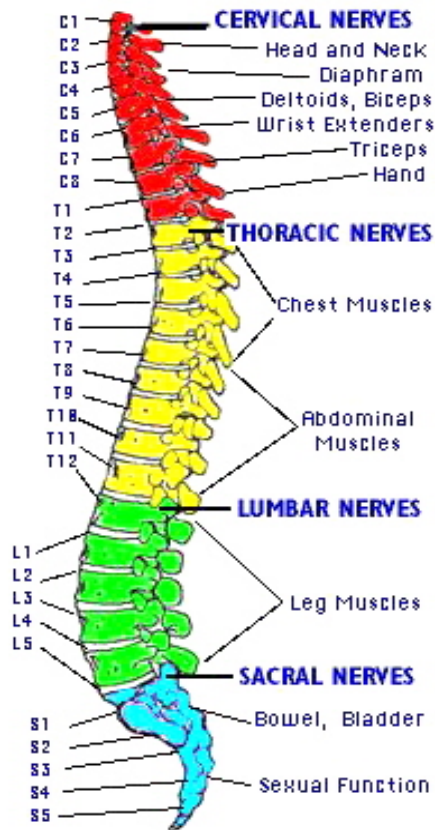
spinal blood vessels, meningitis and myelitis, inflammation, multiple sclerosis and vascular malformations. Spinal cord injury results in loss of communication between the brain and other parts of the body and cause paralysis, loss of sensation, or weakness in the parts of the body below the injured region.

2.4.1 Location and Effects of the Injury

There are 31 pairs of spinal nerves which branch off from the spinal cord. There are four main groups of spinal nerves which exit different levels of the spinal cord. Figure 2-3 illustrates the four groups in descending order down the vertebral column: cervical, thoracic, lumbar, and sacral. Each group is referred to by the letters C, T, L, or S respectively. Cervical (neck) nerves supply movement and sense to the arms, neck and upper trunk; thoracic (chest) nerves supply the chest and abdomen; lumbar (lower back) and sacral (Pelvis) nerves supply the legs, bladder, bowel and sexual organs.

The symptoms after a spinal cord injury differ by location of the injury. In general, the higher location in the spinal column the injury occurs, the more severe symptoms a person will experience. For example, injury between C1 and C2 can result in a loss of many involuntary functions that are controlled by sympathetic and parasympathetic nervous systems, including the ventilation control mechanisms for breathing, and the mechanisms to maintain blood pressure and to control body temperature.

Since each spinal nerve runs from a specific vertebra in the spinal cord to a specific area of the body, the skin's surface has been divided into areas called dermatomes. A dermatome is an area of skin whose sensory nerves all come from a single spinal nerve root. Loss of sensation in a particular dermatome enables doctors to locate where the spinal cord is injured.



Cervical Injuries

Between C1 and C5: paralysis of the muscle used for breathing (more likely causing fetal), and all arms and legs (quadriplegia).

Between C5 and T1: paralysis of the legs, trunk, hands and wrist. Weakness of the muscles that move the shoulder, elbow, hands and fingers.

Thoracic Injuries

Between T1 and T8: instability of the trunk above the waist due to poor abdominal muscle control.

Between T8 and L1: loss of trunk and abdominal muscle control, loss of sensation between the rib cage and hips and legs.

Lumbar and Sacral Injuries

Between L1 and S5: muscle weakness of the hips, legs and feet, decreasing control of the flexors and extensors of the lower extremity, decreased control of urinary system and anus.

Figure 2-3: Location of the spinal cord injury and consequent effects

(<http://www.spinalinjury.net/>)

2.4.2 Classification of Spinal Cord Injury

SCI can be divided into two major types of injury: complete and incomplete. A complete injury means that there is no function below the level of the injury, no sensation and no voluntary movement. Both sides of the body are equally affected. An incomplete injury means that there is some functioning below the primary level of the injury. However, the clinicians found this traditional classification was difficult to apply. The American Spinal Injury Association (ASIA) considered the difficulty and formulated the classification system for spinal cord injury in 1992.

ASIA impairment scale classified [5, 38] the SCI into five categories from the most severe to normal:

- A = Complete, no motor or sensory function is preserved in the sacral segments S4-S5;
- B = Incomplete, sensory but not motor function is preserved below the neurological level and includes the sacral segments S4-S5;
- C = Incomplete, motor function is preserved below the neurological level, and more than half of key muscles below the neurological level have a muscle grade less than 3, which indicates active movement with full range of motion against gravity;
- D = incomplete, motor function is preserved below the neurological level, and at least half of key muscles below the neurological level have a muscle grade of 3 or more;
- E = Normal, motor and sensory function are normal.

2.4.3 Incidence, Prevalence, and Consequence of SCI

The latest statistical report from the National Spinal Cord Injury Statistical Center (NSCISC), Birmingham, Alabama, shows that the number of people in the United States who are alive in 2008 who have SCI has been estimated to be within a range of 229,000 to 306,000 persons, and there are about 12,000 new injuries occurring each year. More than 80% of the victims are male (partially due to males being more likely to engage in risk taking behavior), and average age at time of injury is 40.2 years. The majority of all new injuries reported are the result of auto accidents (42%), falls (27%), violence (15%), sports injuries (8%) and other or unknown (8%). The most common cause of death is respiratory ailment such as pneumonia and pulmonary embolism. Mortality rates are significantly higher during the first year after injury than during subsequent years [180].

Persons with quadriplegia have sustained injuries to one of the eight cervical segments of the spinal cord; those with paraplegia have lesions in the thoracic, lumbar, or sacral regions of the spinal cord. The most frequent neurologic category at discharge of persons reported to the database is incomplete quadriplegia (30.1%), followed by complete paraplegia (25.6%), complete quadriplegia (20.4%), and incomplete paraplegia (18.5%). Less than 1% of persons experienced complete neurologic recovery by hospital discharge. Over the last 15 years, the percentage of persons with incomplete quadriplegia has increased slightly while complete paraplegia has decreased slightly [180].

Overall, median day hospitalization in the acute care unit following injury have declined from 24 days in 1979 to 12 days in 2008. Similar downward trends are noted for days in the rehab unit from 98 to 37 days. Median day hospitalization were greater for patients with neurologically complete injuries [180].

The psychological impact of spinal cord injuries presents patients with the difficult task of grieving for their lost mobility, adjusting a new dependency on others, and learning to create different goals for their lives. Their family members must also learn to adjust to the patient's injury and changes in relationship dynamics.

Treatment at hospitals and rehabilitation centers can be expensive, and when combined with costs of purchasing equipment (such as a motorized wheelchair), modifying housing and transportation for accessibility, continuing medical visits, and personal assistance services, the result is a large financial burden for spinal cord injury patients. This burden is made worse by the lost earnings that spinal cord injury patients experience during treatment and beyond.

2.4.4 Treatment and Rehabilitation of Spinal Cord Injury

In the acute stage of spinal cord injury, doctors focus on rescuing victim's life: maintaining the ability to breathe, preventing shock, immobilizing the neck and back to prevent further damage, and avoiding complications, such as respiratory or cardiovascular conditions. After the disease stabilizes, doctors turn their attention to preventing secondary damage, such as restricted blood flow, excitotoxicity, inflammation, free radical release, and apoptosis.

- Restriction of blood flow

Immediately after the injury, there is a major reduction in blood flow to the site, which can last for as long as 24 hours and becomes progressively worse if untreated. The combination of leaking, swelling, and sluggish blood flow prevents the normal delivery of oxygen and nutrients to neurons, causing further damage. Reduction of the blood flow also causes the drop in blood pressure and heart rate.

- Excessive release of neurotransmitters and excitotoxicity

The crushing and tearing of axons is just the beginning of the devastation that occurs in the injured spinal cord and continues for days. The initial physical injury sets off a cascade of biochemical and cellular events that kills neurons and their myelin insulation, and triggers an inflammatory immune system response. For example, after the injury, an excessive release of neurotransmitters (Glutamate) flood the area of the injury for reasons that are not yet well understood. These excessive glutamate triggers a process called excitotoxicity, which disrupts normal processes and kills neurons and other cells such as oligodendrocytes that surround and protect axons.

- Autoimmune system cells creates inflammation

Under normal conditions, the blood brain barrier keeps immune system cells from entering the brain or spinal cord. When the blood brain barrier is broken by blood vessels bursting and leaking into spinal cord tissue, immune system cells such as *neutrophils*, *T-cells*, *macrophages* and *monocytes*, can invade the surrounding tissue and trigger an inflammatory response.

- Free radical attack nerve cells

In spinal cord injury, the inflammation of the spinal cord tissue signals particular cells to overproduce free radicals. Free radicals then attack and disable molecules that are crucial for normal cell function.

- Nerve cells apoptosis

Apoptosis can help the body get rid of old and unhealthy cells by causing them to shrink and implode. In normal condition, apoptosis seems to be regulated by specific molecules that have the ability to either start or stop the process. For reasons that are not clear, spinal cord injury sets off apoptosis, which kills oligodendrocytes in damaged area, and this damage in turn causes the damage of the myelin sheath.

Treatment for a spinal cord injury is complex. Repairing it has to take into account all of the different kinds of damage that occur during and after the injury. Because the molecular and cellular environment of the spinal cord is constantly changing from the moment of injury until several weeks or even months later, combination therapies will have to be designed to address specific types of damage at different points in time.

The rehabilitation must begin in the early stages of recovery. During the initial stages of rehabilitation, therapists usually emphasize maintenance and strengthening of existing muscle function, redeveloping fine motor skills and learning adaptive techniques to accomplish everyday

living tasks. The rehabilitation team includes physical therapist, occupational therapist, rehabilitation nurse, psychologist, social worker, dietitian, recreation therapist, who work together to participate in therapies and treatment.

Research on understanding the cellular and molecular mechanisms in both the healthy and damaged spinal cord could point the way to therapies that encourage axons to grow in injured areas, and reconnect vital neural circuits within the spinal cord and CNS. Researchers, many of whom are supported by the National Institute of Neurological Disorders and Stroke (NINDS), are focused on advancing our understanding of the four key principles of spinal cord repair:

- Protecting surviving nerve cells from further damage
- Replacing damaged nerve cells
- Stimulating the regrowth of axons and targeting their connections appropriately
- Retraining neural circuits to restore body functions

Advances in basic research are also being matched by progress in clinical research, especially in understanding the kinds of physical rehabilitation that work best to restore function. Some of the more promising rehabilitation techniques are helping spinal cord injury patients become more mobile. For example, modern rehabilitation therapies that retrain neural circuits through forced motion and electrical stimulation of muscle groups are helping injured patients regain lost function.

2.5 Cerebral Palsy

Cerebral Palsy (CP) is caused by damage to the motor control of the developing brain early in life before or after birth. CP describes a group of neurological disorders that appear in infancy or early childhood and permanently affect body movement and muscle coordination. The motor disorders of CP are often accompanied by disturbances of sensation, perception, cognition, behavior, by epilepsy, and by secondary musculoskeletal problems [204].

The most common symptoms of CP with motor control deficits are stiff or tight muscles and exaggerated reflexes (muscle spasticity), a crouched or “scissor” gait, a lack of muscle coordination and balance when performing voluntary movements (ataxia), walking with one or both legs dragging, and foot drops.

A large number of factors can damage the developing brain, such as infection (meningitis), bleeding into the brain (intraventricular hemorrhage), damage caused by lack of oxygen, and developmental brain malformation. The severity of the brain damage generally depends on the type and timing of the injury.

Researchers are investigating the risk of CP occurrence in early brain development, including genetic defects, which may be responsible for the brain malformations and abnormalities that result in CP. Scientists are also looking at traumatic events in newborn babies' brains, such as bleeding, epileptic seizures, and breathing and circulation problems, which can cause the abnormal release of chemicals that trigger the kind of damage that causes CP.

2.5.1 Classification of Cerebral Palsy

Cerebral palsy is classified into four broad categories – spastic, athetoid, ataxic, and mixed forms. Spastic CP affects around 70 to 80 percent of patients. In spastic CP, the muscles are stiffly and permanently contracted. Athetoid or dyskinetic CP is characterized by uncontrolled, slow, and writhing movements, caused by damage to the cerebellum or basal ganglia which are responsible for processing the signals that enable coordinated movements as well as maintaining body posture. About 10 percent of children with cerebral palsy have athetoid CP. Ataxic CP is described as low muscle tone and poor coordination of movements. Damage affects the sense of balance and depth perception. About five percent of children are diagnosed with this form of CP. Children with ataxic CP look very unsteady and have a lot of shakiness like a tremor, especially when they are trying to handle small objects such as a pen. Mixed CP is the form that the children with CP have more than one type of cerebral palsy mentioned above. For example, some patients have spastic CP with athetoid movements. About five to ten percent of children with CP have the mixed type cerebral palsy.

Spastic CP is the most common type of cerebral palsy. This abnormally high muscle tone creates difficulty with voluntary and passive movement, and generally creates stress over time, depending on the severity of the condition in the individual, the constant spasticity ultimately produces pain, muscle/joint inflammation including tendinitis and arthritis, contractures, spasms, and progressively worse deformities misalignments of bone structure around areas of the tightened musculature as the time progress.

Generally, spastic CP is sub-classified into three types: hemiplegia (affects limbs on one side of the body), diplegia (affects both sides, either arms or legs), and quadriplegia (affects all

limbs). Spastic diplegia is the most common of all CP cases, with the lower limbs affected. A typical sign of spastic diplegia is “scissor” gait.

2.5.2 Prevalence and Incidence of Cerebral Palsy

Cerebral palsy is one of the leading causes of childhood disability with the greatest burden found worldwide. The incidence of cerebral palsy is about two per 1,000 live births [3]. In the United States, approximately 10,000 infants and babies are diagnosed with CP each year, and 1,200 are diagnosed at preschool age [246]. Furthermore, there is a high default rate with majority of children lacking ready access to medical care and education in developing countries [128]. The major reasons for default were financial constraints.

The ability to live independently with CP varies widely depending on the severity of each case. Some individuals with CP will require personal assistance for all activities of daily living. Others can lead semi-independent lives, needing support only for certain activities. A few can live in complete independence. In most cases persons with CP can expect to have a normal life expectancy and reproductive function.

Because of the physical disability, CP children or adults have usually difficulties to achieve the normal role in society commensurate with age and socio-cultural milieu. There is an urgent need for improvement in medical services and social support for children with CP and their families.

Last but not the least, there is an incredible financial burden on CP patients and their families. In 2003, the Center for Disease Control [CDC] estimated that the average lifetime cost of caring for a child with cerebral palsy totals over \$921,000. This is much more than the cost of caring for a healthy individual.

2.5.3 Treatments and Rehabilitation of Cerebral Palsy

To date, there is no cure for cerebral palsy. It is only that life can be made more bearable, more meaningful for the child. Early diagnosis and an immediate therapy regimen will help reduce the impact of the disabilities and discomfort caused by CP. For example, seizures and spasticity are the most common discomforts of cerebral palsy. Drug therapy can reduce these discomforts. For seizures, anti-convulsants work well, while muscle relaxants are prescribed for spasticity. Surgery may be recommended to handle extreme contractures, which can inhibit movement, balance and coordination.

Physical rehabilitation must start as soon as a diagnosis is made, and need to be adjusted to suit the changing needs of the child. In addition to physical therapy, psychological rehabilitation also assumes great significance in CP patients. The behavioral therapy helps to reduce destructive behavior, and increase self-reliance through motivation. The occupational therapy works at improving the child's simple physical skills, which make him/her more independent, while speech therapy helps improve the social life. The professionals are faced with a diversity of problems in the child and family (physical, psychological, communicative, and social), so a multidisciplinary approach for treatment is needed.

2.6 Summary

This chapter addresses the most important neurological disorders: stroke, multiple sclerosis, spinal cord injury, and cerebral palsy. These common disorders were discussed with respect to causes, symptoms, classifications, treatment and rehabilitation. The WHO has realized that the burden on disability adjusted life years (DALYs) for these common disorders, estimated according to prevalence, duration and mortality rates, is higher than other diseases. And physical,

emotional, social and economic burden of these neurological disorders in patients, their families, and the public health services has gained awareness by the professionals and public health organizations.

Chapter 3: Background of Neurological Rehabilitation

3.1 Principals of Neurological Rehabilitation

Rehabilitation has been defined by WHO in 1980 as an active process by which those disabled by injury or disease achieve a full recovery or, if a full recovery is not possible, realize their physical, mental and social potential and are integrated into their most appropriate environment. The American Society of Neurorehabilitation (ASNR) announced the mission of the rehabilitation as to: 1) promote the medical and social well-being of persons with disabling neurological disorders; 2) advance training and research in the basic and clinical sciences that can lead to functional recovery of neurologically impaired persons; and 3) disseminate the knowledge of rehabilitation research among professionals and the general public.

Rehabilitation requires the active collaboration of professionals and patients to achieve desired outcomes. An outcome may be improvement or it may be prevention of deterioration. Rehabilitation is not only focused on the person with the impairment, but also dependants, relatives, friends and colleagues are involved in collaboration with a number of professionals. Medical rehabilitation usually involves a professional team based on a specialized rehabilitation unit or center [108]. The professional team provides physical, behavioral, cognitive and social rehabilitation.

A number of inpatients within typical comprehensive rehabilitation hospitals are those with neurologic injuries such as stroke, spinal cord injury, and traumatic brain injury. It is evident that neurological rehabilitation helps to rebuild lives. Rehabilitation helps the patient regain muscle strength, joint rang-of-motion (ROM), balance, coordination endurance, and functional mobility.

3.2 Mobility, Exercise Training, and Functional Recovery

Studies in animals have demonstrated that exercise training enhanced brain functional recovery by increasing neurogenesis, neurotrophic factors, and neuronal survival. Some human studies have indirectly supported this notion with observations of improved neuromuscular and cognitive function and attention in people who participate in regular physical activity and who have higher cardiovascular fitness.

Meeteren et al. (1997) investigated that exercise training enhanced the return of sensorimotor function in the early phases of recovery after sciatic nerve crush lesions in rats, and the effects persisted in the late phase of peripheral nerve regeneration. The research group further studied the effects of different exercise trainings on functional recovery after the nerve lesion in rats. They found out that treadmill training after the lesion significantly deteriorated the gradual return of motor function [160, 161].

The task-specific training improves functional outcomes after stroke. Additional, clinical trials have provided insights into methods such as trunk-restraint that promote adaptations within the nervous system that correlate with improved walking and upper extremity function after stroke. Exercise training paradigms, such as constraint-induced movement therapy, have also been shown to be effective in the management of cerebral palsy [43]. CP patients typically have lower cardiopulmonary fitness levels and abnormal muscle strength. It is especially important for them to maintain normal muscle strength into adulthood since the functional consequences of even a small loss can lead to loss of mobility and independence. Patients with spastic diplegic CP were able to increase their strength through isokinetic and repetitive exercise [155]. With exercise, quadriceps strength may increase to normal levels, which may also improve gait abnormalities, such as ‘scissor’ gait.

3.2.1 Gait Rehabilitation

Gait rehabilitation is a major aspect of neurological rehabilitation since neurologic impairment often causes severe disability that produces a wide variety of deficits on the lower extremity. Modern concepts of motor learning favor a task specific training, i.e. to relearn walking. The restoration of gait for patients with impairments of the CNS, e.g. stroke, spinal cord injury, and traumatic brain injury, is integral part of rehabilitation and often influences whether a patient can return to daily life or work. Current rehabilitation concepts have aimed at the restoration of physiological gait pattern [205]; and rehabilitation devices such as the partial body weight support treadmill training and the gait trainer (GT1). These devices have been designed to enable the patients train pre-programmed trajectories during all phases of gait.

3.2.2 PWBTT and Conventional Gait Trainers

One of the primary goals of patients that suffer a mobility-related disability is to achieve some kind of independent ambulation. This may be partially achieved by enrolling into physical therapy programs, inpatient as or outpatient or a combination of both, to help achieve the Activities of daily living (ADL). The traditional intervention of physical therapies relies on the gait therapists and nurses as the means to deliver the desired training gait to the patients. This is accomplished through a “hands-on” method where the therapist holds the patient’s arms/legs/trunk and moves the limbs when walking between the parallel bars or overground corridors (see Figure 3-1). There are number of limitations and drawbacks to this therapist-assisted rehabilitation: 1) it is labor intensive and physically demanding; 2) it requires and relies on the best knowledge of expertise; 3) it is time inefficient; and 4) it is difficult to follow up the session-to-session repetition and consistency.



Figure 3-1: Therapist-assisted training using the parallel bar.

Therapy by treadmill training with partial body weight support (PWBTT) evolves as a very promising treatment concept over many years. It enables severely affected patients the repetitive practice of complex gait cycles and thus follows modern aspects of motor learning that favor a task-specific approach. Several studies have shown its potential in patients after stroke [76, 85, 166, 237, 249], spinal cord injury [46, 53, 55, 195, 256], multiple sclerosis [56], Parkinson [168] and cerebral palsy [158, 212], by improvement of range-of-motion (ROM), muscle strength, walking velocity, postural instability, coordination and balance.

The key capabilities needed in a PWBTT device to provide effective gait therapy include [206].

- A machine (harnesses) to support the patient and adjust the weight-load placed on the lower extremities during therapy, ranging from on load (the machine bears the full weight of the patient) to full load (the patient supports his/her full weight).
- A treadmill or similar device that allows the patient to walk in place.
- The ability to assist the patient's lower extremities to train in an effective overground gait pattern that is energy-efficient.

PWBTT makes gait training possible for people who are unable to have safety during overground gait training, and intervention may be initiated earlier than conventional methods. This method also has the advantage of eliminating the fear of falling that is common in the early stage of the therapy.

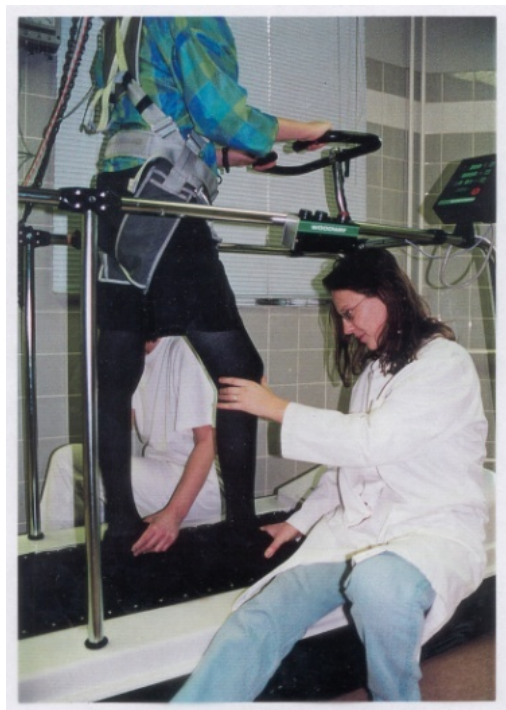


Figure 3-2: Treadmill training with partial body-weight support.

3.2.3 Gait Trainers with Robotic Devices

The PWBTT relieves the working load of the therapist, but it still requires the expertise and therapist(s) to assist the training, Figure 3-2. This also requires at least two therapists during the gait training. Two therapists sitting alongside the patient have to place the paretic limbs manually while sometimes a third therapist is needed to stand behind the patient to assist the lateral weight shifting and trunk erection. Despite these measures, accurate and repetitive gait motions still are unachievable through PWBTT. As the therapists fatigue, the patient's gait can become asymmetrical, therefore losing the benefit of sustained practice. With the provision of assistance of this nature the pattern of sensory input to the CNS may vary greatly between trainers and sessions. As a remedy to the problems associated with using therapists to provide the desired gait, some investigators attempted the robotic devices – gait trainer to help patient's replicate normal walking patterns. In addition, current research focuses on the different unloading systems for the patients partial body weight support at treadmill training, which enables non-ambulatory patients to practice complete gait cycles as soon as possible.

The first electromechanical gait trainer, the Gait Trainer Version I was built and patented in Germany in 1997 [206]. Using the gait trainer, GT1, the patient is supported with a harness and the feet are placed either on motor-driven footplates or on the treadmill. The patients walk according to a pre-programmed physiological gait pattern and/or an exoskeleton-type robot. A Cochrane Review of the electromechanical-assisted training for walking after stroke reported that the use of the gait trainer, GT1, could reduce dependency in walking by 25% [162].

3.2.3.1 Robotic Gait Trainer Versions I and II

Modern concepts of gait rehabilitation favor a task-specific repetitive approach. In practice, the required physical effort of the therapists limits the realization of this approach. Therefore, a mechanized gait trainer enabling non-ambulatory patients to have the repetitive practice of a gait-like movement without overstraining therapists was constructed at the Free University in Berlin, Germany, in 1997 [243, 244]. The gait trainer version I used a driven mechanism with an electric motor and a gear system to move footplates. The gait cadence was controlled by the speed of the drive mechanism. Stride length was adjusted and produced a 50/50 stance/swing phase of the gait cycle. A short time later, the second version of the gait trainer (Gait Trainer Version II, Figure 3-3) was built and patented in Germany with much improvement over the version I. The device consists of two footplates just like the version I, and connected to a double crank and rocker system. An induction motor drives the cranks via a planetary gear system. The rear ends of the footplates follow an ellipsoidal-like movement. Different gears can be incorporated to vary stride length and stride time. The planetary gear system also moves the patient harness in a gait-like trajectory through two cranks attached to suspension ropes. The torque generated by the motor is sensed and displayed on a monitor to provide a biofeedback to the patient. This advanced gait trainer provide a gait-like movement simulating stance and swing phases with an actual lifting of the foot during swing, and a ratio of 60/40 percent between the two phases, which characterized the actual human gait. In addition, it controls the center of mass (COM) in vertical and horizontal directions, and effectively reduced physical demands on the therapists.

Many studies have shown that the advanced gait trainer (Gait Trainer Version II) allowed more effective training sessions, where patients could train up to 1000 steps within a typical

training session of 15-20 minutes, whereas during conventional gait training only approximate 100 steps per session were performed [213].



Figure 3-3: Robotic Gait Trainer Version II.

3.2.3.2 Lokomat and AutoAmbulator

The Lokomat (Figure 3-4) is a motorized exoskeleton worn by the patients during treadmill walking; some literature called it the Driven Gait Orthosis (DGO). The major difference of the Lokomat from the Gait Trainer Version II, GT1, is that the patient's feet are placed on the treadmill instead of the two separate footplates. The exoskeleton device has four rotary joints that accommodate hip and knee flexion and extension for each leg movement. The weight of the exoskeleton is supported by a parallelogram mechanism that moves in the vertical direction and is counterbalanced by a gas spring. The hip and knee motions can be pre-programmed to drive the legs along gait-like trajectories. The device is fully instrumented,

allowing the trainers to track a patient's functional recovery and utilize biofeedback in the therapy sessions.

The other DGO robotic device is the AutoAmbulator. The device as illustrated in Figure 3-5, is intended to replicate a normal walking pattern. The patient is supported by a hoist, and the limbs are secured in a pair of aluminum rotating arms located above a treadmill. The motion of the joints, forces/torques of the segments, walking speed, body weight, and wiring voltage are automatically monitored during the treadmill training.



Figure 3-4: Driven Gait Orthosis - Lokomat

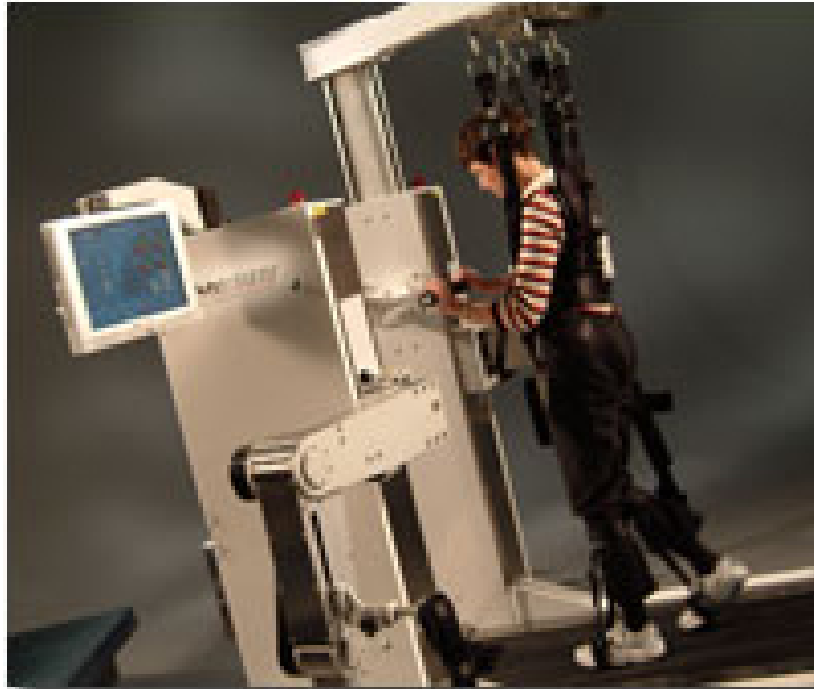


Figure 3-5: Driven Gait Orthosis - AutoAmbulator

The revolutionary new devices replicate the walking patterns by using advanced robotic designs and computer technology. They are, in essence, the highly specialized and instrumented treadmills with sophisticated features including: an overhead harness safety system to partially/fully support the patient; programmable exoskeleton/braces to move the patient's limbs; numerous sensor detected biofeedback by tracking important movement features; and most importantly the patient's progress of the treadmill training can be viewed from the computer monitor during the session, which will motivate the patients for rehabilitation.

3.2.4 Other Therapeutic Interventions for Task-Specific Training

Therapeutic interventions leading to functional improvement emphasize intensive task-specific practice to facilitate training induced neuroplasticity [92]. Task-specific means the best way to relearn a given task and to train specifically for that task. Repetitive task-specific training

is a treatment in which a series of specific movements are repeated over and over again to improve functional recovery. A recent systematic review specifically investigated the effects of exercise intensity as measured by time in therapy on ADL, walking, and dexterity in patients with stroke [123-126]. The results of this meta-analysis suggests that more intensive therapy that includes approximately 16 hours of additional task-specific training in the first six months post-brain injury particularly dedicated to lower limb and ADL activities is more effective than standard therapy programs.

Rehabilitation is directed to the restoration of motor control in gait and gait-related activities, improvement of upper extremity function and trunk muscle strength, teaching the patient to cope with existing deficits in ADL and enhancement of participation in general. It has been shown that there is some improvement in treadmill training with or without body weight support and also in use of the robotic training in gait-specific rehabilitation. Strong evidence was also found for therapies that administered functional training, such as constraint-induced movement therapy, aerobics for cardiovascular fitness, external auditory rhythms during gait and neuromuscular electrical stimulation for glenohumeral subluxation [189].

Constraint-induced movement therapy (CIMT) forces the use of the affected side by restraining the unaffected side. CIMT was developed by Dr. Edward Taub of the University of Alabama at Birmingham [230-234]. Taub argues that, after a stroke, the patient stops using the affected limb because they are discouraged by the difficulty. As a result, a process that Taub called “learned non-use” sets in, furthering the deterioration [230]. A number of studies have shown that the CIMT produced major and sustained improvement in motor function in neurologic injuries such as hemiplegic stroke [231], traumatic brain injury [216], and cerebral palsy in children with hemiparesis [233]. The American Stroke Association has written that

Taub's therapy is "at the forefront of a revolution" in what is regarded possible in terms of recovery for stroke survivors [Constraint-induced movement therapy].

Rhythmic behavior of movement such as gait results from complex, dynamic, inter-connections of the CNS. When an individual suffers a stroke for instance, the neural circuitry is damaged, and rhythmicity in motor skills is altered. The coupling between an external rhythm and rhythmic movement can be an effective tool for improving motor performance. There is enough evidence to show that gait training with an external auditory rhythm leads to improved rhythmic and reciprocal movement of the legs in persons who have suffered a cerebrovascular accident (CVA) or stroke. Spatial-temporal characteristics of walking have improved [239].

Neuromuscular electrical stimulation is commonly known as functional electrical stimulation (FES). It can be divided into two categories: (i) stimulation of muscles to treat muscle atrophy, and (ii) enhancement of functional activity in neurologically impaired individuals. FES devices use electrical impulses to activate paralyzed or weak muscles in precise sequence and have been utilized to provide spinal cord injury patients with the ability to walk. Klose, et al. [115] in 1997 showed that the FES enabled person with thoracic-level SCI to stand and ambulate short distances but with high degree of performance variability across individuals. In addition to the enhancement of walking abilities, FES has also had some success in improving ventilatory function in adult patients with SCI [58, 59].

3.3 Rehabilitation Management and Rehab Cycle

Rehabilitation management can be characterized by a coordinated and iterative problem-solving approach along the continuum of care from the hospital to the community. Such approach, based on the International Classification of Functioning, Disability and Health (ICF),

can be described as a rehabilitation cycle or Rehab Cycle [225], with its four steps: assessment, assignment, intervention and evaluation. The Rehab Cycle facilitates the structuring, organization and documentation of the rehabilitation process. It enables all professionals involved in patient care to coordinate their actions. Specific rehabilitation interventions include those related to physical medicine, orthopedic-reconstructive surgery, pharmacology and nutrition, psychology and behavior, education and counseling, occupational and vocational advice, social and supportive services, engineering and other interventions. Rehabilitation services are like a bridge between isolation and exclusion. They often the first step towards achieving fundamental rights.

The goals of a neurological rehabilitation program include helping the individual to return to the highest level of function and independence, and improve the overall quality of life for that individual – physically, emotionally, and socially. A typical neurological rehabilitation program helps to accomplish and/or may include the following:

- Assistance with ADLs such as eating, dressing, reaching, and manipulation, bathing, making bed, using the toilet, handwriting, cooking, basic housekeeping, and other activities critical to an independent and effective lifestyle
- Speech therapy to retrain the communication skills
- Counseling to deal with anxiety and depression
- Bladder and bowel retraining
- Improve control and muscle strength in the trunk, pelvis, and shoulder girdle
- Gait and balance retraining
- Social skills retraining
- Education regarding the disease and therapy

- Activities to improve cognitive impairments, such as attention, memory and difficulties with concentration and poor judgment.
- Short- and long-term goal setting involving the patient and family members

The Rehab-CYCLE is applied on two levels. The first refers to the guidance along the continuum of care and the second to the provision of a specific service [225]. From the first level, the assessment step includes the identification of the person's problems and needs, the evaluation of rehabilitation and prognosis and the definition of long-term service and goals of the intervention program. The assignment step refers to the assignment to a service and an intervention program. The evaluation step refers to service and the achievement of the intervention goal. From the second level, the assessment step includes the identification of a person's problems, the review and potential modification of the service or goals of the intervention program and the definition of the first Rehab-CYCLE goals and intervention targets. The assignment step refers to the assignment of health professionals and interventions to the intervention targets. The intervention step refers to the specification of the intervention techniques, the definition of indicator measures to follow the progress of the intervention, and the definition of target values to be achieved within a predetermined time period. The evaluation step refers to the evaluation of the achievement of the goal with respect to the specified target values of the indicator measures, the Rehab-CYCLE goals and ultimately the goals of the intervention program. It also includes the decision regarding the need for another intervention cycle based on a reassessment [225].

3.4 Summary

This chapter introduced the definition and principle of neurological rehabilitation from the World Health Organization, WHO. Neurorehabilitation is the nature of the adaptive system to perform the optimization of functional recovery. It indicates the importance for intensive task-specific training approach for functional recovery and neuroplasticity, and a number of devices have been introduced to illustrate the different therapeutic interventions for this approach. Finally, the Rehab Cycle for neurological rehabilitation management was introduced and recommended by WHO.

Chapter 4: Biomechanical Model on Human Locomotion

4.1 Human Gait – Basic Concepts and Terminology

The human gait is a pattern of locomotion, which is achieved using synchronization of the skeletal, neurological and muscular systems of the human body [47]. Over the past several decades, the evolution of gait science has produced an array of terms and concepts relating to observational and computational gait analysis. The terminology of human walking began with descriptive phrases obtained as a result of observational and kinematic analysis of normal subjects. These include terms such as “heel strike” and “toe off”. Many more contemporary terms described events and functions that were not apparent through observation but could be measured through instrumentation in gait laboratories [190]. The conceptual knowledge of human locomotion and related terminology will facilitate an optimal treatment plan for the patient, and enhance communication to the physician and relevant communities.

The term “normal gait” is used to present those patterns that have been generalized across sex, age, genetic predisposition and anthropometric variables. When the basic principles of normal walking are understood, a more penetrating grasp of pathological gait becomes possible.

4.2 Gait Cycle and Gait Phases

Walking is the rhythmic and repetitious movements of the limbs which result in the forward movement of the body. A number of events follow each other continuously and smoothly. A gait cycle or a gait stride is normally from the initial contact of one foot to the following contact of the same foot. Each gait cycle is divided into two periods, stance (from initial contact to toe-off) and swing (from toe-off to the initial contact again). For a typical

healthy subject, the stance phase approximately covers the first 60% of the gait cycle while the swing phase represents the remaining 40% [190]. Each of these periods is then subdivided for the functional phases of gait, as shown in figure (4-1) [41].

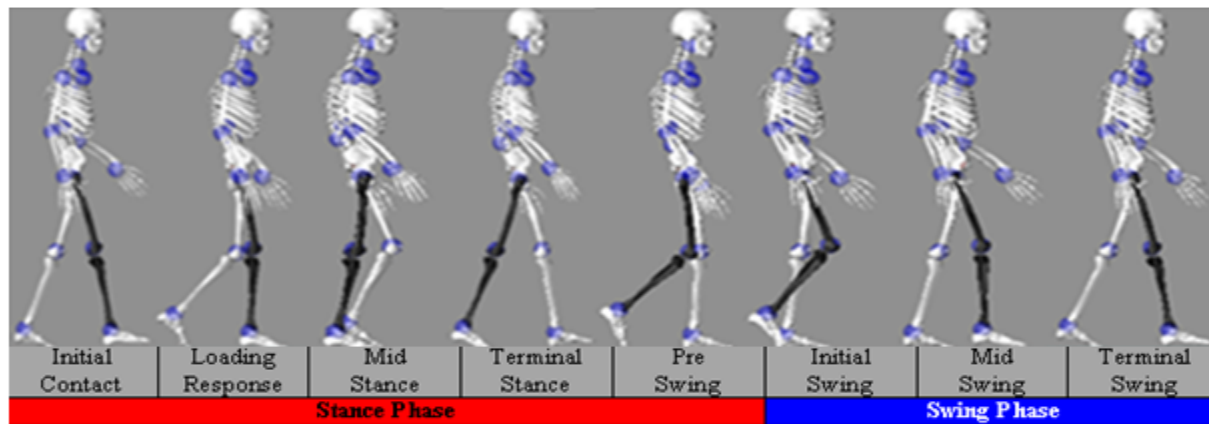


Figure4-1: Functional phases within the gait cycle. Consequence changing functional phases of a single gait cycle from right-foot contact to the next right-foot contact.

The functional phases of the stance period are described below with their associated typical gait cycle percentages [190]:

- Initial Contact (0~2%): the moment when the foot just touches the floor.
- Loading Response (0~10%): from the initial contact and continue until the other foot toe-off.
- Mid Stance (10~30%): from the other foot toes off until body weight is aligned over the forefoot.
- Terminal Stance (30~50%): from the end of the mid-stance until the opposite foot contact.
- Pre Swing (50~60%): begins with the initial contact of the opposite foot and ends with ipsilateral toe-off.

Similarly, the swing period components are [10]:

- Initial Swing (60~70%): from the toe-off even until the maximum knee flexion occurs.
- Mid Swing (70~85%): from the maximum knee flexion until the tibia is in a vertical position.
- Terminal Swing (85~100%): from the vertical tibia to the ipsilateral foot contact.

4.3 Kinematics Approach

4.3.1 Spatial-Temporal Gait Parameters

Apart from the gait cycle, the nature of walking may be expressed as spatial-temporal terms such as stride/step length, stride/step width, stride/step time, stance phase, swing phase, double-supported phase, walking speed, and cadence. Stride length can be defined as the linear distance between the initial contacts of the same foot, while the step length is usually defined as the distance between the opposite feet, as shown in figure (4-2). Cadence is number of steps per minute, and velocity is the product of cadence and step length, expressed in meters per second.

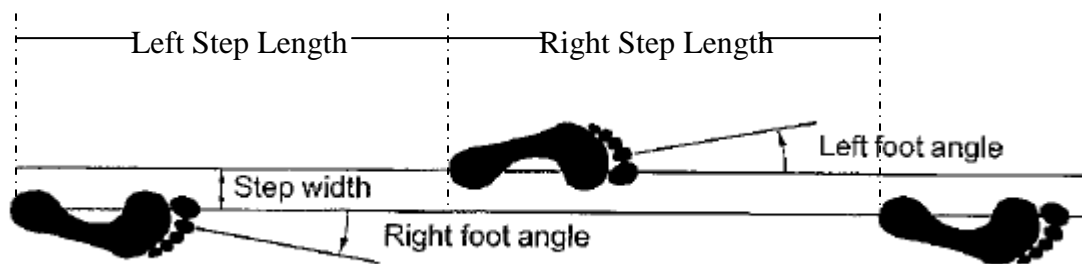


Figure 4-2: Schematic diagram that reveals the stride length, step length, and step width.

Numerous studies have shown that gait variability of spatial-temporal parameters was a quantifiable feature in clinically relevant gait disorders, such as age-related falling and neurodegenerative disease (e.g. Parkinson's and Huntington's disease) [71, 211, 217].

4.3.2 Joint Kinematics

Joint kinematics includes rotations/velocity/acceleration of the body joints in their sagittal, coronal, and transverse planes. Figure 4-3 illustrates a typical joint motion of the hip, knee, and ankle angle in a sagittal plane.

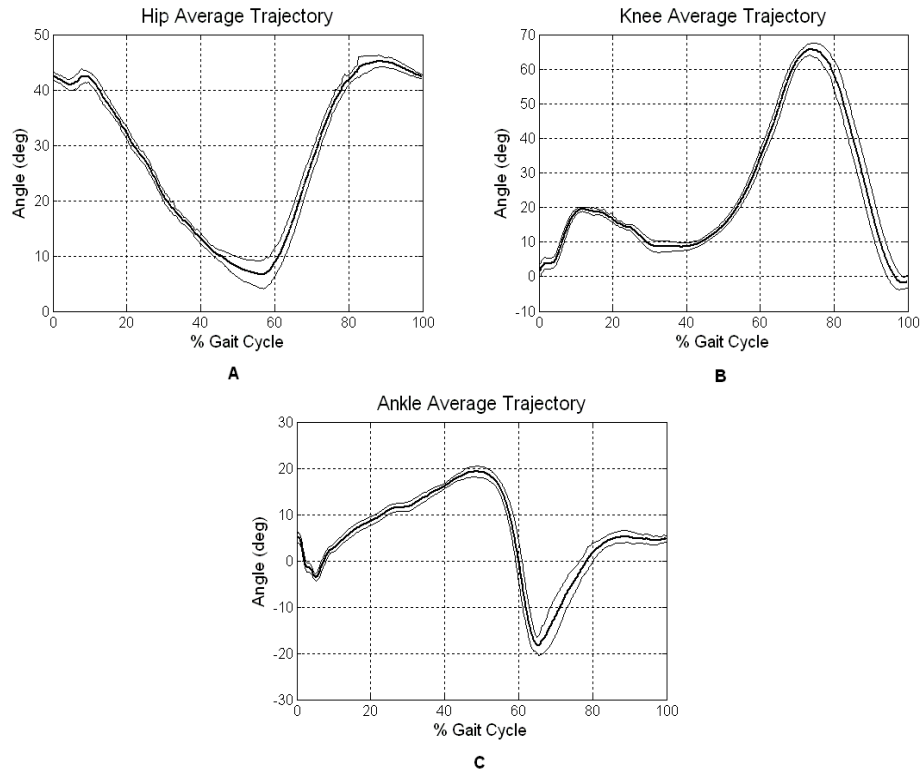


Figure 4-3: Typical joint rotation of the lower extremity on sagittal plane during a full gait cycle during free walking. A: hip flexion-extension; B: knee flexion-extension; C: ankle flexion-extension. Black line denotes the means from number of strides, and grey lines denote the upper and lower limit of the standard deviation.

4.4 Dynamic Kinetics

Gait kinetics involves the forces that produce movements including joint reaction forces, ground reaction forces (GRF) and muscles activities. The major tools for kinetic measurement are force plate or foot pressure distribution (FPD) plate, and electromyography (EMG).

4.4.1 Ground Reaction Forces

Kinetics is the study of forces that cause movement. Forces generated can be internal (such as muscle activity, friction in muscles and joints, or ligamentous constraint) and external such as ground-reaction forces (GRF) created from the external loads.

The rotational potential of the forces acting on a joint is called torque or moment (N-m). The internal joint moment is the net result of all of the internal forces acting about the joint. The moments usually are normalized to the subject's body mass, expressed as N-m/kg.

The ground-reaction force is the external force acting on joints during gait. GRF is obtained from a force platform or force plate, which is a transducer set into the floor or under the treadmill to measure the forces and torques applied by the foot to the ground. GRF is comprised of three-dimensional components (Fig. 4-4): 1) vertical, 2) mediolateral and 3) anterior-posterior.

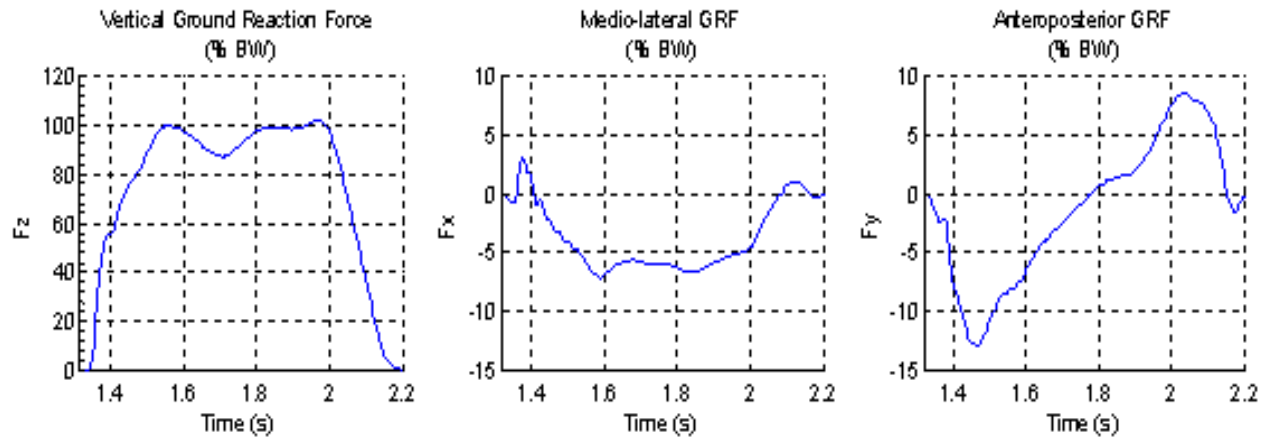


Figure 4-4: Ground Reaction Force. The typical ground reaction force during stance phase with its three components: F_z – Vertical force; F_x – Mediolateral shear; F_y – Anterior-posterior shear. All GRF values were normalized by body weight (88 kg in this example), and the data represented as % BW.

In normal dynamic kinetics, human muscles must be controlled to maintain the weight shifting during gait [262]. Force data will show variations with walking speed, shoe wear, and compensatory mechanisms of gait, such as the avoidance of weight bearing on a painful extremity. The components of the ground reaction force in gait can be an indication of dynamic aspects of gait. For examples, the vertical GRF tends to increase in magnitude and higher frequency content with increasing velocity and decrease with lower velocity or lower extremity pain; and changes in medial-lateral shear component is an indicator of balance control as in scoliosis [219].

4.4.2 Foot Pressure Distribution

Modern foot pressure distribution (FPD) plate and/or shoe insoles could be an alternative to traditional force plates for quantitative gait analysis, thereby providing the clinician with

objective data on the gait while unraveling the loading of different regions of the foot during the stance phase. Figure 4-5 shows a typical 3D distribution pattern during walking.

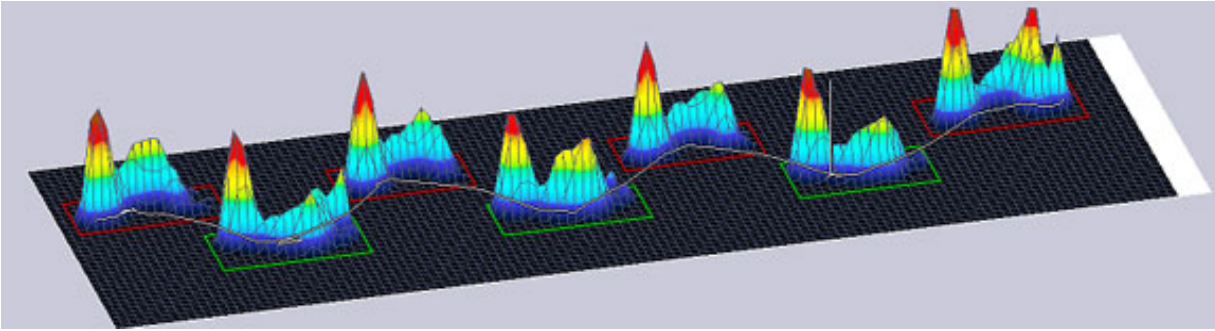


Figure 4-5: 3D presentation of foot pressure distribution pattern while walking.

Measurement of FPD is clinically useful because it can identify anatomical foot deformities, guide the diagnosis and treatment of gait disorders and falls, as well as lead to strategies for preventing pressure ulcers in diabetes with peripheral neuropathy. Age-related anatomical and physiological changes in foot bone and ligament structure affect FPD during gait [201]. Gait analysis in geriatric study has revealed decreased stride length and step force, and increased variability in gait parameters. Age was independently associated with lower pressure under the heel, mid-foot, and hallux in the multivariate analysis [172].

4.5 Surface Electromyography

Electromyography (EMG) is a technique for detecting the electrical potential generated by muscle cells (fibers) when these fibers are active or at rest. EMG signals have many clinical and biomedical applications, including identifying neuromuscular disease, assessing lower back pain, biofeedback of prosthetic devices, kinesiology and sports applications.

The surface EMG (SEMG) is a technique for detecting the neuromuscular activity in dynamic movement. The SEMG is noninvasive and easy to perform but exhibits some limitations based on its causative factors that affect the quality of the signals. De Luca (1997) categorized these causative factors into two groups: extrinsic and intrinsic. The extrinsic factors are electrode configuration, location of the electrodes and orientation of the detection surfaces; the intrinsic factors are the number of active motor units, fiber type composition, blood flow in the muscle, fiber diameter, depth and location of the active fibers and the amount of fatty tissue between the muscle and the electrode. The intrinsic factors cannot be controlled due to the limitation of current knowledge and technology [34].

EMG can be plagued with poor signal-to-noise ratios (SNR) and one result of this poor SNR is increased within- and between-subject variability of quantified EMG variables. Methods that can reduce within- and between-subject variability can increase the statistical power of an experimental design and aid in the functional interpretation of experimental results. Therefore, a proper method for EMG signal processing must be selected to reduce the signal artifacts [34]; and the EMG signals are recommended to be normalized for study of comparative diagnosis.

EMG signals during gait provide insight into muscle recruitment patterns and neuromuscular control of walking. Diagnostic assessment and treatment decisions may be based on the EMG behavior associated with the dynamics of gait [62]. Previous researches have shown that EMG activity was repeated consistently over a locomotion gait cycle during preferred walking speed in normal adults [7, 258] and children [62]. The muscles differ from the peak activity at each of the various phases of the gait cycle.

4.6 Summary

This chapter reviewed the terminology of gait cycle with its functional sub-phases, defining the spatial-temporal gait parameters, joint kinematics, dynamic kinetics, and EMG activity. These are very important parameters today for studying in neurological impairments and locomotor recovery.

Chapter 5: State-of-the-Art in Human Locomotion

5.1 Analytical Techniques for Automated Gait Assessment

Gait analysis commonly involves the measurement of the dynamic movement of the body expressed as the kinematics, kinetics, and muscle activity. Kinematics can be recorded using optical motion capture and reflective marker system, and/or variety inertial sensors (goniometers, gyroscopes, accelerometers). Dynamic kinetics can be measured using either force sensor platforms for overground walking or an instrumented treadmill [127]. Muscle activity as mentioned in section 2.6, can be measured using inner or surface EMG.

For the last two decades, gait analysis in healthy, geriatric, and impaired conditions has been studied widely from gait pattern classification to gait variability. Computer and mathematical expertise investigated different algorithms to classify the different abnormalities from normal gaits, and/or classify different stages within one disease. Classification of gait abnormality can be done by dynamic programming, neural networks, cluster statistical analysis, or by Hidden Markov Models (HMMs) for gait recognition. Study of gait variability will be discussed in details in section 5.3.

5.2 Classification of Gait Abnormalities

Gait pattern classification was studied particularly in the sagittal plane, the kinematic, because abnormalities of flexion or extension occur mostly in this plane and therefore, most therapeutic interventions address sagittal abnormalities. Gait abnormalities and their etiologies may be summarized for each of the three planes (sagittal, coronal, transverse) at each joint or segment level. Once all these parameters are considered, more precise solutions for classification

of the pathology can be offered [34]. Pathologic gait can range from temporary gait deviations in one plane to complex chronic deviations in all planes of motion. The primary reason for misinterpretation of gait disorder on assessment is “out of plane”, i.e. missing information on coronal and transverse planes. In many cases, pathologic gait is characterized by reduced motion in the sagittal plane and increased motion in the coronal and/or transverse planes [48]. In the coronal plane for example, the principal joint disturbances in cerebral palsy are adduction contracture, which causes a scissoring gait, and abductor insufficiency of the stance limb which results in a pelvic drop compounding foot clearance problems. Transverse plane abnormalities occur in patients with idiopathic femoral anteversion and tibial torsion with associated knee pain, and they also occur in many patients with cerebral palsy. In addition, mediolateral (coronal plane) postural instability has recently been identified as a risk factor for falls in the elderly community-dwelling population. However, few clinical tests involve challenges to stability limits in mediolateral direction.

At this time, exact technical parameters and gait analysis models have not been established. For example, O’Byrne (1998) has identified eight groups from 237 cerebral palsy patients using statistical cluster algorithm. However, the classification was made based on the kinematic abnormalities of flexion or extension in the sagittal plane. The more accurate description of the various patterns of gait is possible if the patterns of movement of the three dimensional planes and EMG also were evaluated. One prospective controlled study investigated whether computerized gait analysis could differentiate patients with dyskinetic CP from those with spastic CP and those with normal gait [32]. The study evaluated a diagnostic model based on three parameters: step width, step profile, and maximal lateral acceleration. Only step profile and maximal lateral acceleration differentiated CP types. The model accurately predicted 87% of

patients with dyskinetic CP and 71% of patients with spastic CP. The computerized classification of gait can distinguish between normal and spastic or dyskinetic gait depending on the gait parameters. Fuzzy logic classification system was used by Yardimci (2007) to discriminate healthy subjects from patients using kinematic three-axial acceleration inputs, but with the limitations imposed on the input he could not classify the patients with different stages of stroke [264].

It is evident that only by combining data obtained from clinical examination and kinematic/kinetic and EMG data can functional pathology be classified. Overall, with the single or limited number of input variables, classification of the gait abnormalities becomes difficult or unreliable.

5.3 Gait Variability Study

The study of gait variability involves the stride-to-stride fluctuations in walking, an important indicator of impaired mobility in adults. Previous work has suggested that measures of gait variability may be more closely related to falls, a serious consequence of many gait disorders, than are measures based on the mean values of other walking parameters [60, 63, 72, 238, 257].

5.3.1 Spatial-Temporal Parameters Variability

Gait variability is an index of how much gait parameters change from one to the next during walking. In healthy subjects, the variability is relatively small and the coefficient of variations of many gait variables (stride length, stride width, stride velocity, stride time, etc) is on the order of very small percentages. Any fine-tuned physiologic factors regulating gait such

as CNS/PNS control, muscle function and postural control, may be perturbed, motor control may be impaired leading to increased stride-to-stride fluctuations.

5.3.2 Stride Variability with Elderly Fallers

In studies of healthy young adults and healthy older adults, there was no age effect on stride variability, even though gait speed was reduced in the older adults while stride times were similar [52, 61, 70]. Another investigation demonstrated that whereas both healthy older controls and patients with a higher-level gait disorder walked more slowly in reduced lighting, only the latter's stride variability increased [112]. All those investigations suggested that any increases in variability of gait parameters must be due to pathology.

In one of the first quantitative studies of geriatric and rehabilitation research, Guimaraes and Isaacs [64] suggested that elderly fallers walked with increased gait variability, both in terms of step length and step time, compared to non-falling older adults. This age-related fall risk causing increased gait variability was further studied by Hausdorff and other researchers [70, 73, 164]. They investigated that stride-to-stride temporal variations were significantly increased in elderly fallers, and Hausdorff concluded that gait variability is an important marker for fall risk in the geriatric group [68].

5.3.3 Stride Variability in Neurodegenerative Disorders

The basal ganglia are thought to play an important role in regulating motor control programs involved in gait and sequencing of movement. Parkinson's disease (PD) and Huntington's disease (HD) are two major basal ganglia disorders.

Patients with PD often experience freezing of gait which the subject suddenly becomes unable to start walking or to continue to move forward. The pattern of subjects who experience freezing of gait was not different from those of other PD patients who do not experience the same episodes of freezing of gait. However, researchers found that although average stride time was similar in subjects with and without freezing, stride-to-stride variability was markedly increased among PD subjects with freezing of gait compared to those without freezing of gait [211]. Furthermore, stride time variability significantly improved in response to levodopa treatment in non-fallers of PD subjects, but remained increased in fallers [211].

Huntington's disease (HD) patients had a decreased gait velocity (bradykinesia) and a decreased stride length (hypokinesia). In addition, fallers with HD had increased stride length variability and a significantly greater trunk sway in medio-lateral direction compared to non-fallers [64]. From study of fMRI, greater variability of step length was associated with greater prevalence of infarcts in the basal ganglia.

Previous studies also found that there was an increase in stride length variability in Alzheimer's disease (AD) at all walking speeds (self-selected slow, natural, and fast) which may contribute to the increased incidence of falls in AD. The gait speed and average stride length were significantly related to fear of falling, but not to fall risk. In contrast, stride length variability was associated with fall risk, but not with fear of falling. This finding also applied in a study of the effects of dual tasking on the gait of subjects with Alzheimer's disease [217].

Amyotrophic lateral sclerosis (ALS) is a disorder marked by loss of motor neurons [6]. The gait of patients with ALS, HD, and PD shared common features of altered stride dynamics. The gait stability and the stride-to-stride control are also affected in ALS.

5.4 Summary

In recent approaches, pattern recognition of gait within a repeated cycle has been heavily studied in the sagittal plane. The analysis lacks the information on other two planes, which may consist of important signs for pathologic gait. Spatial-temporal gait kinematic parameters often used in gait variability approach. There is limitation on other parameters due to lack of complete knowledge of technologies of signal detection, data processing, and advanced analysis techniques.

Chapter 6: Current Devices for Diagnosis and Therapy

6.1 Importance of the Quantitative Measurement for Diagnosis

In general, the state of health or geriatric condition with aging can be recognizable by gait. For example, people generally walk more slowly when they are getting older and may start to shuffle. In pathological conditions, people who suffered a stroke for example, may drag one of their legs that making the asymmetrical gait. To date the observational gait analysis still plays an important role to characterize most gait impairments. It is still the experienced clinician who continues to perform functional gait assessment. The clinical research would recognized the importance of gait information many years ago and today there are numerous groups worldwide doing research and writing articles to discuss issues that relate gait profiles to medical conditions. However, the benefit of these research and development activities is not being received by clinical practitioners. Current modern technologies that involve sophisticated kinematic and kinetic analyses have not been applied widely in clinical assessments and diagnosis. Instead, a set of functional gait-related tests (such as usual and maximal gait speed, 6-Minute walk test, long-distance corridor walk, gait abnormality rating scale –GARS, timed up and go test, and performance-oriented mobility assessment - POMA) have been widely used as semi-quantitative assessments [68]. Compared to modern computerized assessments, these are easy to perform, do not require expensive equipment and long testing time. However, those semi-quantitative assessments could not accurately detect the optimal rehabilitation and evaluation of treatment effects.

There are numerous reasons why those modern technologies are not being applied. First, the improvement of the reliable and quantifiable method is required to monitor the gait

parameters in a normal environment. A second major limitation of the computerized assessment is lack of the knowledge to perform and analyze the acquired data from those instrumented equipment. With recent methods of assessment, the level of support for scientific evidence was usually insufficient to make very strong recommendations to the clinic. Finally, a good communication between scientific researches or engineering and clinical expertise is required to improve the quality of the diagnosis and/or assessment. Scientists, engineers, and doctors must merge their knowledge together to serve the public community. The scientific literature has to be intended as a communication format between doctors, scientists, and other health professionals.

The following will discuss the most recent motion analysis technologies that are applied to monitor the gait for objective and quantitative assessment of the treatment, and the devices that are used for neurological rehabilitation.

6.2 Motion Analysis Technologies

Gait analysis can provide significant information regarding the kinetic and kinematics of human motion. Such an analysis has become a standard collaboration of engineers and medical professionals determining force and motion characteristics of individuals coming to a gait analysis laboratory for evaluation. Current motion analysis technologies offer a variety of methods for recording movements of interest. Tools such as motion capture system or wearable/wireless sensors, force platforms or pressure sensor distribution devices, and EMG are necessary for a full analysis. Each method offers unique advantages for achieving these goals. In the past two decades advances in computers, electronics and opto-electronics have led to the development of many different systems for acquiring motion analysis data. Many of the

commercially available movement recording systems are complex, expensive and require technically trained operators. Software and hardware innovation in recent years are obviating the need for technical ability while reducing processing time. Human motion data is most often presented quantitatively as anatomic plane graphs showing relative joint rotation angles. Some current software packages now allow acquired motion data to be displayed as a moving 3D skeletal model permitting an enhanced physical appreciation for the motions being performed.

6.2.1 Optical Motion Capture System with Passive Reflective Markers

Motion construction has revolutionized computer animation in the last decade. The success is readily apparent in films such as Lord of the Rings, which transfer expressive performances of real actors onto digital characters both real and fantastic. Numerous commercial companies have merged and induced this technology into biomechanical research. Numbers of optical or video motion acquisition systems are used for motion analysis today (e.g., VICON: <http://www.vicon.com/> , SIMI: <http://www.simi.com/>, and Motion Analysis Corporation: <http://www.motionanalysis.com/>).

Optical/Video motion capture (MC) systems tend to utilize proprietary video cameras to track the motion of reflective markers (passive, Figure 6-1) attached to particular locations of the subject's body (Figure 6-3). Numbers of high-speed (up to 2000 frame per second) and high resolution (up to 16 megapixels) cameras (at least 2 or more) are used for full-body 3D capture. Reflective optical MC systems use typically Infra-red (IR) LED's mounted around the camera lens, along with IR pass filters placed over the camera lens. Figure 6-2 shows a typical cameras system with IR mounted around each from VICON motion capture system. The centers of the

marker images are matched from the various camera views using triangulation to compute their frame-to-frame positions in 3D space.

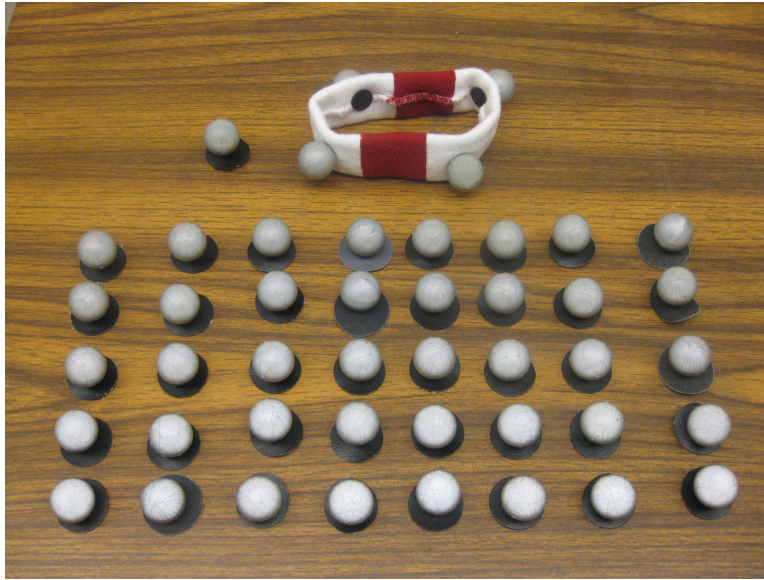
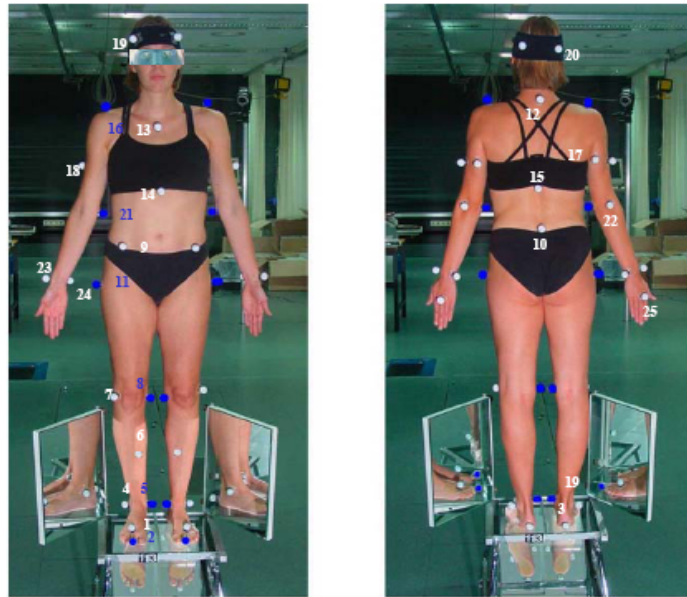


Figure 6-1: Reflective markers are used to track the motion. These markers are lightweight spheres covered with reflective Scotchlite tape (3M Corporation, St. Paul, MN). The tape is designed to reflect incident light directly back along its line of incidence.



Figure 6-2: High-speed cameras system with Infra-red LED's around, VICON motion capture system

(A)



(B)

(C)

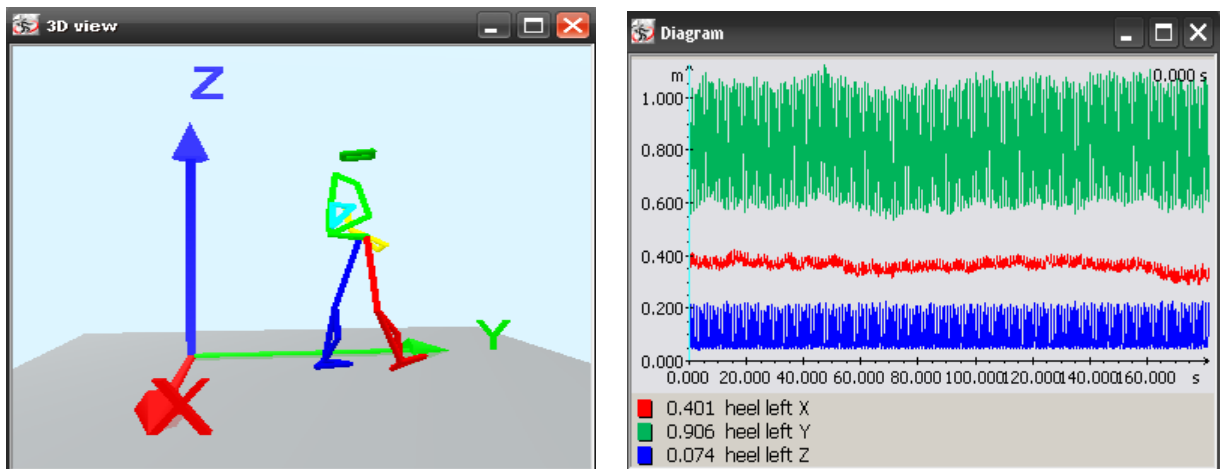


Figure 6-3: SIMI motion system. (A). Marker placement in SIMI Motion 3-D Capture System (www.simi.com). 12 blue markers are static markers, and will be removed before the dynamic trail are performed. (B). Schematic diagram of three-coordinate planes: X-coronal, Y-sagittal, Z-transverse. (C). Three coordinates plots throughout a three-minute walking trail.

6.2.1.1 Inverse Dynamics

In traditional kinematics analysis, the measured locations of the joint center and the end effectors are used to calculate the corresponding body joint angles locally and globally. This can be done using the commercial software packages such as VICON, Visual 3D, and/or SIMI 3D motion analysis.

An important aspect of human movement biomechanics involves the determination of net joint reaction forces and moments-of-force (torques). Inverse dynamic analysis is used to evaluate the reaction forces transmitted between adjacent segments and to calculate the net moments-of-force that result from the muscle activity about each biomechanical joint. Inverse dynamics is a method for computing forces and/or torques based on the motion kinematics, body segment parameters and the external forces such as ground reaction force (GRF) vectors. The process used to derive the joint moments involves differential calculations of the position and angle trajectories of the body segments in order to obtain the accelerations required for the applied forces.

6.2.1.2 Objective Gait Analysis and Quantitative Assessment of Rehabilitation

Motion capture (MC) system is among the first complete quantitative gait analysis technique used in objective documentation of normal gait as well as identifying the underlying causes for gait abnormalities in patients with cerebral palsy, stroke, brain injury and other neuromuscular disorders. MC system usually offers state-of-the-art, high resolution, accurate systems to acquire, analyze and display 3D dynamic data. The system is also integrated with analog data acquisition systems to enable simultaneous acquisition of force plate and

electromyographic data. Therefore, it can display and analyze kinematic, kinetic and electromyographic data in forms that are easy to interpret.

Quantitative assessment of function is important in determining the functional status of patients immediately after neurological injury to aid in the determination of a pharmaceutical or physical therapeutic treatment regimen. Optical motion capture offers unrestricted movements for determining a patient's function, allows us quickly and easily to measure performance and to determine the patient's functional outcome.

6.2.2 Markerless Motion Capture

The most popular technique for human motion capture uses markers placed on the skin, despite some important drawbacks including the impediment to the motion by the presence of skin markers and relative movement between the skin where the markers are placed and the underlying body segments. This makes it difficult to estimate the actual motion of the body segments and joints, which is the variable of interest for biomechanical and clinical applications.

The markerless motion capture is model-based natural motion of human body being captured and analyzed without attaching reflective markers or straps. Markerless motion capture is an active field of research in computer vision and graphics. In contrast to commonly used marker based approaches, the analysis for markerless methods is based on image data without special preparation of the subject. The goal is to determine the position and orientation as well as the joint angles of a human body from image data. Markerless motion capture offers an attractive solution to the problems associated with marker based methods. However, the use of markerless methods to capture human movement for biomechanical or clinical applications has been limited

by the complexity of acquiring accurate three-dimensional kinematics using a markerless approach.

The general problem of estimating the free motion of the human body without markers, from multiple camera views, is underconstrained without the spatial and temporal correspondence that tracked markers guarantee. Generic models typically lack accurate joint information and thus lack accuracy for movement analysis. However, biomechanical and, in particular, clinical applications typically require knowledge of detailed and accurate representation of 3D joint mechanics. Some of the most challenging issues in whole-body movement capture are due to the complexity and variability of the appearance of the human body, the nonlinear and non-rigid nature of human motion, a lack of sufficient image cues about 3D body pose, including self-occlusion as well as the presence of other occluding objects, and exploitation of multiple image streams.

6.2.3 Wearable Inertial Sensors

Over the years, the evolution of methods for the capture of human locomotion has been motivated by the need for new information on the characteristics of normal and pathological human movement. However, the majority of current acquisition systems including the optical motion capture system inhibit broader use of motion analysis by requiring data collection within restrictive lab-like environments. Furthermore, the acquisition using lab-based capture system normally takes about 1 to 3 minutes per trail, but with one or more hours for preparation; recording the activities, routines, and motions of a human for long time or even an entire day like 24-hour portable ECG monitoring detector, is still challenging. There is an emerging trend in biomechanics to measure outside of the laboratory setting, ideally in the everyday environments

as the subject, either for ambulation or for upper-limb motion. This has led to the recent development of several motion-measuring devices based on portable inertial sensing, combining accelerometers, gyroscopes, electrogoniometers and magnetometers.

Inertial sensing technology is widely spread in several application domains, which involve motion sensing of vehicles, planes, spacecrafts, cars and robots. In recent years, inertial sensing has also been regarded as a means to sense human movement with some advantages in comparison with well-established sensing technologies, e.g. optical/video motion sensing. Those inertial sensors are usually lightweight and small size often called micro-electromechanical systems (MEMS), the smallest sensors are less than 1g in mass and have dimensions smaller than $1\text{cm} \times 1\text{cm} \times 1\text{cm}$, and they are low costs compare with optical motion capture systems. The most important advantage is that they lead to direct measurements of kinematics such as angular velocity and segment acceleration using gyroscopes and accelerometer respectively. Moreover, temporal parameters of gait are also determined by classification of accelerations and angular velocities through these direct measurements [132].

6.2.3.1 Accelerometers

Accelerometers are attached to the object and measure the acceleration of the object directly at the point of attachment. A triaxial accelerometer measures three accelerations along three different axes at right angles to each other. The orientation of the accelerometer determines the direction of the acceleration measured.

Accelerometer systems have been pervasively evolving as a technology, with multiple industry applications such as the automotive industry for safety approach [175]. The use of accelerometers has a long tradition in biomechanics measurement. Accelerometer systems have

been demonstrated for gait evaluation in different environments [154, 170, 171, 181]. Accelerometer systems have also been used to measure metabolic energy expenditure, physical activity levels, balance and postural sway, and to detect falls [22]. The accelerometer and footswitch component synthesis enabled the device to contrast temporal attributes of gait. Some preliminary testing and evaluation of basic wireless accelerometer applications have already been conducted [133]. With the growing interest and increasing use, validation of the accuracy and reliability of the sensors needs to be more clearly established.

Advantages of accelerometers over other biomechanical devices primarily are expressed by their miniature size, they are generally small and would offer limited restrictions to their anatomical placement and provide minimal impediment to movement. Therefore, they can be used as wearable biosensors to measure gait parameters in real world situations without the limitations inherent to more immobile laboratory approaches such as camera systems. However, accelerometer signals alone do not contain information about the rotation around the vertical and therefore do not give a complete description of orientation. There are suggestions that the limitation can be recovered by integrating the angular velocity measured from gyroscope. Orientation can be estimated by combining the sensor signals from gyroscopes, accelerometers, and magnetometers [147]. However, an error in measured angular velocity and magnetometers will result in increasing inaccuracy in the estimated orientation. In particular, a relatively small offset on the gyroscope signal will give rise to large integration errors [147]. In addition, the use of magnetometers as a compass for stable orientation measurements could give large errors in the vicinity of ferromagnetic materials.

6.2.3.2 Gyroscopes

A gyroscope directly measures the angular velocity or joint rotational rate without the signal being affected by gravity as is the case with the accelerometers. If the drift or offset is compensated, the gyroscope signal can be used to measure rotational velocity (directly and precisely) or angular excursions (by integration of the gyroscope signal).

Gyroscopes are compact in size and can be easily fixed to the skin, and are therefore suitable for a portable gait analysis system. Data could be collected from these signals using either a portable computer or data logging device with appropriate interfacing. The signals from gyroscopes can provide a range of useful information for gait analysis and the signals are highly correlated with the signals from the motion analysis system.

In the past, gyroscopes have been used for several purposes in the field of biomedical rehabilitation. Henty et al., for example, placed a gyroscope on the foot above the metatarsals in order to distinguish two phases in the gait cycle, the swing and the stance phase. Further, he calculated the hip, knee and ankle flexion angles during the gait cycle by placing a gyroscope at the thigh, at the shank, and at the foot and by integrating the differences of gyroscope signals [75]. Gyroscopes together with accelerometers were used for even detailed gait event identification on person with dropped foot [132]. Gyroscopes could also be used on other body segments, in particular the pelvis and the trunk, to provide useful information on pathological gait patterns.

6.2.3.3 Electrogoniometers

Electrogoniometers are computerized versions of simple goniometers, which are commonly used in clinical practice to assess joint range of motion or angular displacement of a

joint. An electrogoniometer consists of one or more potentiometers placed between two bars, with one bar strapped to the proximal limb segment and the other strapped to the distal limb segment. The potentiometer, which is placed over the joint, provides a varying electrical impulse, depending on the instantaneous angle between the two limb segments. This electrical impulse information is then interfaced to an analog-to-digital converter in a PC to plot joint angle information over time. Despite the limitations (discussed in chapter 7), electrogoniometers remain the most convenient and least expensive means of measuring hip, knee and ankle angular motions during walking. Another significant advantage of electrogoniometers is the immediate availability of the data, which facilitates the functional interpretation in real-time.

Triaxial electrogoniometers are usually placed between two linear segments meeting at a joint e.g. hip, knee, and ankle, to measure the flexion/extension, abduction/adduction, and vertical rotation movements. The joint angle measurements have been identified as important feedback signals for both mechanical and functional electrical prostheses. Studies on range of angular motion of healthy individual for different walking speed can be used for developing prosthetic control algorithm to provide swing stance stability [122].

6.2.4 Electromyography and Nerve Conduction Velocity (NCV)

In section in 4.2, the technique of the electromyography for evaluation of the electrical activity of muscles was discussed. In fact, there are two types of electromyography: surface EMG (most commonly used for clinical research) and intramuscular (needle or fine-wire) EMG.

A needle EMG contains two fine-wire electrodes which are inserted through the skin into the muscle tissue. A trained EMG professional (physiatrist or neurologist) is required to perform and observe the electrical activity while testing. The electrical activity when the muscle is at rest

or static state can be studied using needle EMG. The presence, shape, size and frequency of the resulting action potentials produced on the oscilloscope provide information about the ability of the muscle to respond to nervous stimulation. Abnormal spontaneous activity might indicate some nerve and/or muscle damage. Needle EMG is an invasive process that most the patients find unpleasant and discomforting. Since skeletal muscles are often large, several needle electrodes may need to be placed at various locations to obtain an accurate electrical activity.

A nerve conduction velocity (NCV) test is often done at the same time as a needle EMG. The nerve is electrically stimulated while a second electrode detects the electrical impulse downstream from the first. Paired surface patch electrodes are placed on the skin over the nerve at specific locations. One electrode stimulates the nerve with a very mild electrical impulse. The resulting electrical activity is recorded by the other electrodes. The distance between electrodes and the time it takes for electrical impulses to travel between electrodes are used to calculate the speed of impulse transmission. A decrease speed of transmission indicates nerve disease. EMG and nerve conduction studies are done together to give more complete information.

Because of some drawbacks of the needle EMG, surface EMG (SEMG) is used more often as a diagnostic tool for neurologic disorders. SEMG measure muscle activity noninvasively using surface electrodes placed on the skin overlying the muscle. SEMG electrodes record from a wide area of muscle territory, have a relatively narrow frequency band (20 to 500 Hz), have low signal resolution, and are highly susceptible to movement artifact [196].

Recent commercial SEMG products (Delsys <http://www.delsys.com/> and BTS <http://www.zflomotion.com/>) contain preamplifier electronics that lessen the need for low skin resistance and improve the signal-to-noise ratio. SEMG can record both voluntary and involuntary muscle activity in addition to externally stimulated muscle action potentials such as

motor evoked potentials after central or peripheral nerve stimulation. SEMG signals are used as a diagnostic tool for identifying neuromuscular diseases, assessing low back pain and disorders of motor control [196]. In recent research, SEMG signals are used as a control signals for electronic bio-devices such as prosthetic hands, arms, and lower limbs.

6.2.5 Measurement of Ground Reaction Force and Moments

Ground reaction force (GRF) can be measured using instrumented treadmill or overground force plate(s), e.g. Kistler <http://www.kistler.com/> and Bertec <http://bertec.com/>. These devices can measure three components of the ground reaction force: vertical, mediolateral and lateral anterioposterior, as well as the force moments in three-dimensional orientation. The GRF is a “reflection of the total mass-times-acceleration product of all body segments and therefore represents the total of all net muscle and gravitational forces action at each instant of time over the stance phase” [258]. Therefore, accurate measurement on GRF can provide significant information for the study of normal and pathologic gait. Normally, joint reaction forces are relatively small in the lower extremity, at least during stance phase. Clinicians can use the GRF itself to understand the forces that human muscles must control during the stance phase in the gait cycle.

Over the past decade, a number of researchers have emphasized treadmill training to increase ambulatory ability for functional recovery of neurological disorders. There are a number of advantages of training and studying locomotion on treadmill. First, walking on a treadmill allows patients to walk over long distances without moving far in the real world. Second, multiple aspects of locomotor skills can be trained safely within a confined space. Many therapies use some degree of body-weight support through harness devices. The harness can be

easily mounted on the treadmill, so that patients can be partially supported with. Finally, the experimental walking speeds can be controlled accurately and the ground reaction forces and moments will be digitized for data-processing in this study.

GRF can also be measured using the pressure distribution devices such as In-shoe Foot-scan (*F-Scan*[®] system) or Floor mat (*Walkway*[™]) from Tekscan Inc. (<http://www.tekscan.com/>). The great advantage of the In-shoe Foot-scan measurement devices are evaluated for use in portable measurement system that will allow for the complete measurement of human gait outside of the laboratory settings. It is a cost-effective measurement of in-shoe plantar pressures. The In-shoe Foot-Scan captures foot pressure distribution during walking or running using an ultra thin, disposable sensor, which is placed inside the patient's shoes as an insole, shown in Figure 6- . Despite some limitations, In-shoe Foot-Scan is a tool for providing quantitative information to determine orthotic efficacy, identify areas of potential ulceration, screen diabetic and other neuropathic patients and observe gait abnormalities.



Figure 6-4: F-Scan sensor inserted into patient's shoe.

Takscan *Walkway*[™] as discussed in chapter 4, is a floor mat that captures barefoot plantar pressures distribution and vertical force during walking. It can be used in conjunction

with a force plate. It is a few meters long and contains over eight thousands sensing elements. Both Takscan Fscan and Walkaway softwares provide automated calculation of an array of gait parameters. Individual gait stance phase information such as foot strike and toe-off are detected and spatial-temporal parameters are calculated. In addition, the pressure maps of pressure distribution on plantar surface are displayed in a colored scheme graph both in 2D and 3D.

6.3 Summary

This chapter introduced the most recent technologies including optical motion capture system, markerless motion capture, different inertial sensors, EMG , and ground reaction force and foot pressure, to monitor the human locomotor for objective and quantitative measurement and/or assessment of the therapeutic treatment.

Chapter 7: Limitations of Current Technology

7.1 Limitations of Optical/Video Motion Capture System

The standard method for human analysis is the optical motion analysis using high-speed cameras to record human 3D motion, but there are number of limitation in this laboratory set-up.

- It requires expensive devices.

Most motion capture devices range from US\$100,000 to US\$350,000; this makes motion capture an option available only for some research labs with financial capabilities. During complicated motions, more cameras have to be used to increase the ability of a system to faithfully track a marker through a full motion path in three-dimensional space.

- It also requires large indoor space.

Motion capture system produces excellent indoor motion analysis, but offer no comparable solution for acquisition in everyday environments. The acquisition usually takes place in a motion analysis laboratory environment.

- It contains time-exhausted data processing.

Although the ability of track multiple markers has been remarkably improved (some systems now tracking over 100 markers simultaneously) in recent years, but in general, tracking process still remains time-extensive.

- The line of sight from camera to marker can be blocked, resulting in incomplete data.

Movement of limbs causes occlusion of data recorded, making the optical motion analysis unpractical. This marker occlusion becomes even worse in data acquisition on subjects with locomotion impairments using walkers, harness, or many other body-weight support equipments.

- It is light sensitive.

The CCD (charge-coupled device) is light-sensitive that use an array of pixels to capture light, and then measure the intensity of the light for each pixel, creating a digital representation of the image. The intensity of the light and the reflection from surrounding objects may affect the accuracy of the acquired data.

- It requires calibration process

The optical system must be calibrated by having all the cameras track an object with known dimensions the software is able to recognize. By combining the views from all cameras with the known dimensions of the object, the exact position of each camera in space can be calculated. If a camera is bumped even slightly, a new calibration must be performed. Ideally, the system should be calibrated every few minutes of capture since any kind of motion or vibration can shift the position of a camera, especially if the lab is located in a multi-storey building.

- It is sometimes difficult for pathological conditions.

Common motion capture systems acquire static/reference marker position, asking subjects to strengthen their body segments to enable the visibility of all markers at the same time. This, sometime become difficult for some patients such as stroke patients with constrained limb movement and joint extension.

- Optical motion analysis cannot be done in real-time for analysis.

Normally, optical motion capture system is not a real-time process. It requires most of the time to “fill-in” the missing data due to occlusion. Although some systems tout “real-time” data analysis, user intervention is required to ensure the accuracy of data collection.

- Low reliability due to noise introduced from differentiation.

The optical motion capture system measures the angular displacements of the anatomical body segments. In gait dynamics, the forces and torques a subject is able to generate is significant for rehabilitation. This stands to reason that the measured angles are then differentiated twice to obtain the accelerations required to determine the forces through inverse dynamics calculations. The differentiation, however, introduces unwanted distortions, noise and other parameters like the phase-shifts with respect to the angular displacements. These uncertainties corrupt the objectivity in the measured quantities, and affect the reliability of the system.

- The motion capture system with reflective markers leads to unnatural motion patterns.

Marker-based systems are designed to track the motion of the markers themselves and thus it must be assumed that the recorded motion of the markers is identical to the motion of the underlying human segments. Since human segments are not truly rigid, this assumption may cause problems, especially in highly dynamic movements in sporting activities and impaired movements of the patients. Cappozzo et al. [18] examined five subjects with external fixator device and compared the estimates of bone location and orientation between coordinate systems embedded in the bone and coordinate systems determined from skin-based marker systems for walking, cycling and flexion-extension activities. Comparisons of bone orientation from true bone embedded markers versus clusters of three skin-based markers indicate a worst-case root mean square artifact of 7° .

- Low sampling rates

With multiple cameras used for complicated motion analysis, one limitation is the relative slow sampling rate. The number of velocity measures per second between six and eight cameras is usually 70 frames or less.

- Impractical for certain conditions.

Some able-bodied subjects have certain skin conditions such as allergy from the double-sided tape, and wet/oily skin type and sweating while moving that cause the markers dropping during the experiment, making the marker-based motion capture impractical.

7.2 Weakness of the Wearable Sensor Detection

Since inertial sensors are compact and light, they have been a popular choice for application in human locomotor analysis. However, the highest quality inertial sensors also exhibit limitations. These include problems with drift from data integration, error introduced from improper body attachment of the sensors causing movement of sensors during data collection, and errors introduced from the assumption of rigid behavior of human limbs. Moreover, problems can become cumbersome and difficult to use if multiple sensors are required for accurate motion capture, subjects may feel uncomfortable wearing so many sensors.

- Bias of the inertial sensors cause output errors.

In inertial sensors the output is usually non-zero even in the absence of any input (zero acceleration or angular velocity ideally). This error is called sensor offset that is added to the actual measured signal. The most important problem with this offset is that it drifts depending on time, temperature and stochastic factors. The error is relatively small, the miniature measurement (measuring distance between sensors) and combination of inertial sensors with an extended Kalman Filter can be used to minimize the offset and sensor noise [147].

- Cumulative drift due to single or double integrations.

One common problem of the inertial sensors is cumulative drift through integrations. After the single integration (e.g. to find the angle from angular velocity) the error due to noise

grows proportionally to the square root of time. After double integrations (e.g. to find position from acceleration), the error due to noise grows proportionally to $t^{3/2}$.

- Physical, anatomical and physiological errors.

Inertial sensors with low sensitivity may fail to detect smaller movements such as in human tremors. A common error shared by accelerometers and other inertial sensors for motion measurement based on skin-mounted sensors is the movement of the soft tissues covering the bones. If the sensors are attached to the body segments using straps, the straps may lead to free motion of the sensors. Furthermore, sensors may be hit or vibrated during heel strike.

- Problems with inertial sensor placement.

Multiple inertial sensors (wearable or wireless) are often attached to various locations on the human body for gait analysis, especially at the hip, trunk, neck and head, for the best recognition of human movement. However, location of the sensor and attachment of multiple sensors become difficult in most of the data collection. Placement is often imprecise. Because of these difficulties, wearing multiple sensors is not an immediate and pragmatic solution for data collection in real-life. Furthermore, due to individual variations, exact orientations may not be consistent between individuals.

- Poor accuracy of Electrogoniometer

Cross talk is a potential limitation to triaxial electrogoniometers. If the axes of the potentiometers are not fully aligned with the axes of the joint motion, the cross talk becomes apparent and the potentiometers' readings do not correlate with clinical rotations. When the angle in the coronal or transverse plane equaled 10° or more there is a significant error in sagittal motion [17], based on the assumption that the three-dimensional dependency is consistent with computer corrections of the data have been formulated. Clinically, the cross talk would not be

significant in normal subject who has minimal coronal or transverse motion, but values obtained on patients with hypermobility require the added calculations.

A major disadvantage of current electrogoniometers is relatively poor accuracy because they are difficult to apply, particularly about the hip and ankle. Measurement of hip motion for example should be between the pelvis and thigh, but this rarely occurs with electrogoniometers. It is only possible with thin subjects to keep a strap around the pelvis. In the slender person with a normal gait, there is so little trunk motion that no significant error is introduced. Patients with incompetent hip musculature however, frequently use large arcs of trunk motion to substitute for their limitations. Hence, the electrogoniometer is not a useful instrument at the hip when pathological function leads to significant displacement of the trunk.

7.3 Limitations of Surface EMG

There is limited approach for gait studies based on SEMG analysis due to the noisy character and inconsistency of the signal. The reliability of the SEMG signal is mostly affected by movement artifacts in the study of the dynamics. Cross-talk from other muscles including antagonists also results in trial to trial variations. In addition, the inconsistency can be caused by electrode placement and skin/muscle interface impedance (particularly when the active muscle is 10 mm or more below the skin surface) [51]. Researchers tried to avoid this inconsistency by reporting EMG in percentages of a baseline maximal voluntary isometric contraction (MVC), and other researchers study the EMG “on and off” “peak-to-peak” time durations.

In normal subjects, normalized EMG is not always associated with changes in muscle force. The relationship is consistent and linear when muscle action is isometric [220], consistent with muscle length during rhythmic movement, and increased muscle forces by increasing their motor neuron firing rate, not by recruiting additional motor units.

These bring the doubt of validity of the EMG: do variations in EMG signal reflect real variations in on-and-off time, and muscle tension? The on and off times may be distorted by movement artifact which can be eliminated or reduced using smoothing and averaging techniques. However, the on-and-off times and muscle tension may also be distorted by electromechanical delay. Winter explains electromechanical delay in terms of muscular anatomy. Because the muscle's contractile proteins develop force in parallel with elastic and viscous elements, muscle force must elongate these elastic and viscous proteins in their fluid environment before tension is registered in tendon. Electromechanical delay may vary inversely with the velocity of muscle shortening.

So far, research and extensive efforts have been made in the area, developing better algorithms to cope with the noisy signals and hence make precise decisions, upgrading existing methodologies for data processing, improving detection techniques to reduce noise, and to acquire accurate EMG signals. Recent advances in technologies to signal processing and mathematical models have made it practical to develop advanced EMG detection and analysis techniques. Various mathematical techniques and Artificial Intelligence (AI) have received extensive attraction. Mathematical models include wavelet transform (WT), time-frequency approaches, Fast Fourier Transform (FFT), and multiple statistical approaches. AI towards signal recognition includes Artificial Neural Networks (ANNs), Dynamic Recurrent Neural Networks (DRNNs), Fuzzy Logic System (FLS), and Genetic Algorithm (GA).

The main reason for the interest in EMG signal analysis is in clinical diagnosis and biomedical applications. The patterns and firing rates of Motor Unit Action Potentials (MUAPs) in EMG signals provide an important source of information for the diagnosis of neuromuscular disorders. Once appropriate algorithms and methods for EMG signal analysis are readily

available, the nature and characteristics of the signal can be properly interpreted for various applications.

7.4 Limitation of GRF measurements

Ground reaction force measurement is important in the analysis of human locomotion. Drawbacks of the existing measurement systems discussed in chapter 6 are the restriction to a laboratory environment and poor accuracy of the measurement.

- Drawbacks of the overground force platform.

First, the subjects are required to place their feet completely on the force plates (each with maximum size of 60cm x 60cm) in order to perform a correct force measurement. However, successful trials are harder to achieve, making for a longer and more frustrating process. Some subjects try to adjust their gait before getting to the plate to obtain a successful trial, which leads to a restriction on the natural gait pattern. This becomes even more complicated with some neurologic patients such as cerebral palsy with scissoring gait. Second, only one or two steps can be measured during a trial, so cumbersome process of multiple successive trials are required to get an average gait pattern. The gait speed varies between trials. In addition, both left and right forces are often looked at individually, especially with pathologic conditions. Therefore, the process can be very tiring and fatigue affecting gait performance becomes an issue. Third, it could not record the force of each foot if both feet are standing on one plate. Finally, the force platform in the laboratory is time and financially expensive. The entire testing procedure, including patient preparation, commonly takes two hours at minimum to complete, limiting the lab in number of evaluations that can be run in a day. The force platform is normally expensive and requires engineers to mount force plates flush with the floor. The force plate is fixed on the

floor in the gait laboratory, which means a relative large space is required, and the measurements cannot be done in every life environment.

- Drawbacks of the instrumented treadmill.

The force measurement system is incorporated into treadmill, making so called instrumented treadmill with force platform(s) under the belt (or dual-belt) of the treadmill. The instrumented treadmill eliminates many limitations that the overground platform has. It allows a decrease in the data collection time and the space required, and to record GRF at constant gait speeds. Despite its numerous advantages, the instrumented treadmill however has several disadvantages. First, walking on a treadmill is more dangerous and some patients become overanxious. The patient has to be made familiar with the treadmill walking before the assessment. Second, a major error introduced into force data is the instrumental noise due to vibrations and the moving artifact during walking and running on the treadmill. Third, the single belt instrumented treadmill records the summed GRFs from both feet. Although a simple algorithm allows the separation of the individual foot vertical forces before computing joint moments, this is still unsuitable for the assessment of joint moments. One solution is to use split belts treadmill and force transducers. However, it compels the subject to walk with a wider base of support. Finally, walking on the treadmill does not realistically simulate everyday life conditions for most of the patients. Clinicians are sometimes suspicious of gait analyses results collected on a treadmill, arguing that treadmill gait is different from over ground gait.

- Poor accuracy of in-shoe Foot-scan

The in-shoe Foot-scan system lacks durability and suffers significant calibration error. Woodburn and Helliwell showed the creep (19%) and hysteresis (21%) properties of Foot-scan were poor [261]. Within- and between-sensor variability in output was demonstrated and overall

repeatability was poor. Furthermore, adjusting the sensor size adversely affected output. They concluded that Foot-scan has a limited capability for absolute accuracy but could still be used for quantitative studies outside the laboratory while its limitations are noted.

- Walkaway Floor Mat force distribution is time and space costing

The Floor Mat force distribution system is just a few meters in length, only two or three strides per trial can be captured. Therefore, numbers of trials are required to increase the statistical power for gait analysis studies. It also requires a large space just like the overground force platform that makes the measurement impractical a daily activity environment.

7.5 Summary

Computerized gait analysis provides the tools necessary to evaluate both normal and pathological gait. Through the study of normal gait, it is possible to understand pathological gait and to prescribe more effective treatments. Recent advances in technology have allowed the measurement of gait variables more precisely and in a timely manner. There is no single method of measurement, however, that provides a complete analysis of gait. And each device contains its own strengths and weaknesses. The usefulness of each device should be judged not solely on its own disadvantages or advantages but on the balance of the two. Sophisticated gait measurement is possible with a basic knowledge on which specific information collected, processed and calculated. These sophisticated gait measurement will be very useful information as the control tool to assist the design of the treatment devices.

Chapter 8: Design of Research Activities

This research included both theoretical and experimental analyses of the central and segmental interaction between motor and sensory control mechanisms and the biomechanical structures of the lower extremities in healthy, and motor and sensory impaired persons. A wearable miniature sensor array enables efficient, reliable, and real-time analysis of functional impairments in human locomotion.

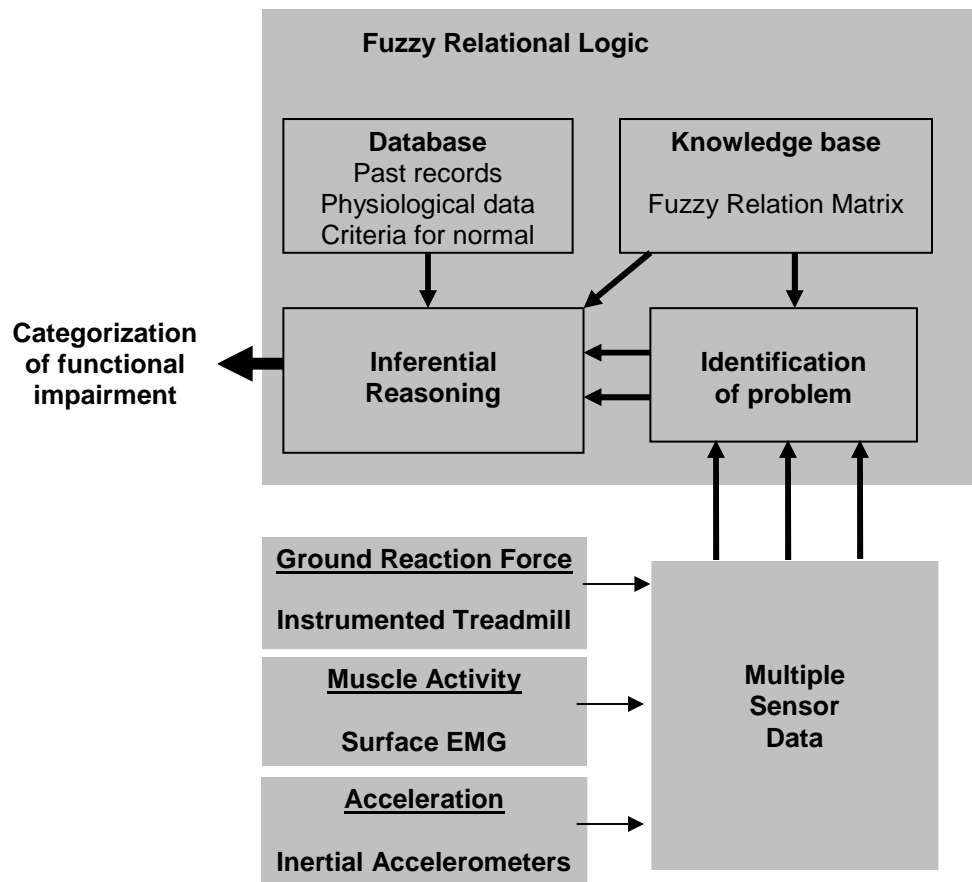


Figure 8-1: Sensor fusion driven computational intelligence scheme.

This dissertation work introduces three innovative technologies as illustrated in Figure 8-1: a) an unobtrusive combination of wearable sensors for the acquisition of locomotor data in multiple domains (kinetic, kinematic and electromyographic, b) a sensor data fusion scheme for

combining information from multiple sensors and sensor types in order to increase efficiency and reliability, reduce uncertainty and ambiguity inherent in making decisions based on a single information source, thus increasing accuracy and resolving ambiguities in the knowledge about the complexity of gait dynamics, and c) a rapid and reliable data analysis system based on fuzzy inferential logic algorithms-capable of identifying, differentiating and quantifying clinically relevant variations from morphometrically adjusted normal gait.

The final product of this research work is a sensor fusion driven computational intelligence scheme whose structure is illustrated in Figure 8-1. This final product enables the effective, reliable and differential monitoring and assessment of gait disorders.

8.1 Fusion of Multiple Sensor data

The application of the single-sensor single-algorithms, like the EMG device or the force plate sensor, in monitoring functional impairments in mobility-related behaviors of human subjects, may offer only marginal results. This is because the single-sensor single-algorithm systems may work well in situations where the environment is structured and the objects are well known, but are severely limited in their ability to resolve ambiguities in complex systems like the human locomotor system that involves multi-body dynamics, biomechanics, physiology and other factors that obscure the interactions between the vestibular, somatosensory and visual inputs for postural control.

Acquiring signals from multiple sensors and providing correlated data from multiple domains leads to dramatic and practical improvement over current methods for automated gait analysis. A novel analysis system utilizing principles of fuzzy inferential logic will integrate information from different sensory sources; coordinate and guide the observations made by each

sensor; and improve the reliability of automated assessment by reducing the uncertainty and ambiguity inherent in making decisions based on only a single type of information. This fusion of multiple sensor data is critical to the efficient recognition and differentiation of aberrations' in gait dynamics for the objective determination of functional impairment and fall risk due to disease severity, medication effect, and the like. This integration of inputs is also essential to the efficient monitoring of therapeutic interventions because it enables objective measurement of responses, and response variability.

This research work has developed a novel intelligent system that linked the physiological and biomechanical responses underlying human gait, to recognize, quantify and differentiate the functional components of normal and impaired locomotion. It has provided adequate knowledge of the patient and characteristics of the impairments that determined the functional outcome. This way, the system contributes to a better understanding of functional recovery in general and patient characteristics that may allow for an early reliable prediction of the final outcome in particular. It also enables individually tailored optimal treatment programs to be designed and implemented.

Whereas the current gait rehabilitation paradigm drives subjects' limbs through pre-determined interventions based on qualitative assessments, the new system in this dissertation work will generate tailored interventions responsive to each subject's immediate and objectively determined abilities and effort. Because this can be applied across all mechanisms of gait impairment, this research can benefit any person who has acquired gait-related disability but that retains a potential to stand and ambulate.

8.2 Fuzzy Inferential Logic

A goal of this dissertation work was to develop an innovative system to assist clinicians reliably assess, at an early post-insult stage, the degree of disability the patient will ultimately experience. Physician decision processes offered to date, especially those relative to diagnosis and patient treatment, suffer from the inability to incorporate all useful data on the patient. A fuzzy inferential logic has been developed to aid the physician to categorize the complete representation of information emanating from the measured kinetic, kinematics and electromyographic data from the patient.

One way of dealing with the functional impairments in locomotor systems may be qualitative, non-numerical and imprecise in nature. The ratings of the physician may be influenced by qualitative factors such as emotion, perception, shifting and imprecise knowledge states, etc. One way of unscrambling the data or partitioning the weighted evaluation points into subsets is via the approach of cluster analysis. The subsets can be distinct or fuzzy. However, in situations such as the foregoing, it is instructive to analyze the data via fuzzy clustering techniques. The application of cluster analysis is centered on the formulation of relationships for the variables (kinetics, kinematics and electromyographic data) under consideration, fuzzy relational mappings.

In this research work, a fuzzy rule-based system (relational mappings) for the categorization of different types of neurologic disorders was designed to cope with uncertainty and perform approximate reasoning. In the following sections, the fuzzy set theory, fuzzy inference system (FIS), and fuzzy rule-based matrix formation will be explained.

8.2.1 The Fuzzy Sets Theory

Fuzzy logic systems form a class of production systems that map $R^n \rightarrow R^p$ and that are based on an extension of classical logic, in which truth values are continuous between 0 and 1.

A fuzzy logic system is a rule-based system that maps an input domain $X \subset R^n$ to an output domain $Y \subset R^p$. The rule base is composed of fuzzy rules (or associations) that associate fuzzy conditions to fuzzy conclusions. Each condition fuzzy set A (resp. conclusion fuzzy set B) is defined as a "membership function" m_A (resp. m_B) over X (resp. Y) that assigns to every $x \in X$ (resp. $y \in Y$) a value between 0 and 1 representing the degree to which x belongs to A (resp. y belongs to B).

8.2.2 Fuzzy Set Definition

Let X be a space of points (objects), with a generic element of X denoted by x, [X is often referred to as the universe of discourse]. A fuzzy set (class) A in X is characterized by a membership (characteristic) function $m_A(x)$ which associates with each point in X a real number in the interval [0,1] with the value of $m_A(x)$ representing the "grade of membership" of x in A. Thus, the nearer the value of $m_A(x)$ to unity, the higher the grade of membership of x is in A.

8.2.3 Fuzzy Relations

Relations represent and quantify associations between objects. Let x in a fuzzy set **X** with its membership function $\mu_x(x)$, and y in a fuzzy set **Y** with its membership function $\mu_y(y)$, the fuzzy relation \mathfrak{R} from a set X and a set Y is a fuzzy set of the Cartesian product written as

$$\mathfrak{R} : X \times Y \rightarrow [0,1] \quad (8.1)$$

Where (x, y) , $x \in X$, $y \in Y$ is the collection of the ordered pairs. \mathfrak{R} is characterized by a membership function $\mu_R(x, y)$ and is expressed as

$$\mu_R(x, y) = \text{Min}\{\mu_x(x), \mu_y(y)\} \quad (8.2)$$

Or

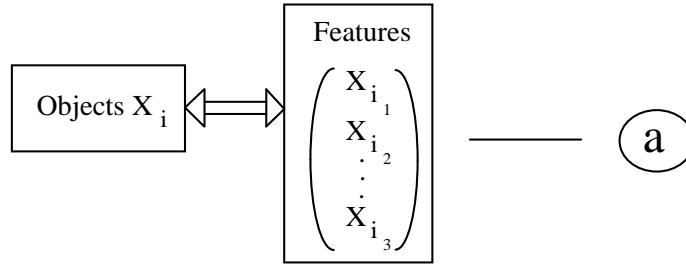
$$\mu_R(x, y) = \mu_x(x)\mu_y(y) \quad (8.3)$$

The membership function of \mathfrak{R} for pair (x, y) , $\mathfrak{R}(x, y) = 1$ denotes that the two elements x and y are fully related. On the other hand, $\mathfrak{R}(x, y) = 0$ means that these elements are unrelated while the values in between, $0 < \mathfrak{R}(x, y) < 1$ underline a partial association (a degree of belonging of a degree of similarity).

8.2.4 Fuzzy Relation Matrix

When determining the presence or absence of association, interaction or interconnection between the elements of the kinetic, kinematic and electromyographic data and gait phases, the mapping is usually non-fuzzy. But when the severity level of an element of the gait functions must be determined, fuzzy sets are often involved in the mapping. Comparison between mappings is a pattern analysis procedure. Figure 8-2 illustrates the feature extraction and classification for pattern analysis.

Feature Extraction



Classification

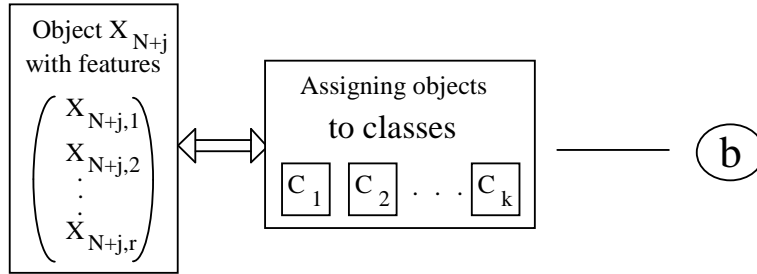


Figure 8-2: Feature Analysis.

Feature Extraction:

The extraction of features in this cluster analysis is centered on the formulation of relationships for the variables under consideration. Fuzzy clustering provides a richer description of the geometric structure of the data set in many cases, and has a lesser tendency to get stuck in local minima. The fuzzy relational matrix depicts the feature extraction, i.e. it establishes membership functions between the measured variables. It can be interpreted as degrees of typicality or degrees of sharing.

Classification:

The essential concept of pattern recognition may be expressed by a mapping from feature space to decision space. The design of a classifier consists of two parts: one part to collect data

samples from various classes and to find the boundaries which separate the classes. This process is called classifier training, or the learning. The other part is to test the designed classifier by feeding the samples the class identities of which are known.

The classification stage involves assigning the examining variables to the appropriate classes based on the properties of the variables.

Let $x \in X$, where $X = \{x_1, x_2, \Lambda, x_i\}$, and $y \in Y$, where $Y = \{y_1, y_2, \Lambda, y_j\}$, then a relation μ_R , also called the Cartesian Product, $X \times Y$, can assume the matrix form with the following entries and in a corresponding matrix notation as:

$$\mu_R(x, y) = \begin{bmatrix} \mu_R(x_1, y_1) & \Lambda & \mu_R(x_1, y_j) \\ \mathbf{M} & \mathbf{M} & \mathbf{M} \\ \mu_R(x_i, y_1) & \Lambda & \mu_R(x_i, y_j) \end{bmatrix} \quad (8.4)$$

in which the $(i, j)th$ element is the value of $\mu_R(x_i, y_j)$. For a finite universe of discourse, a matrix notation is useful. In this case, fuzzy relation \mathfrak{R} can be represented as a $(i \times j)$ matrix with the entries taking values between 0 and 1.

The matrix depicts a feature space (a rule base) that describes the association, interaction or interconnection between the elements of the x and y .

8.2.5 Fuzzy Similarity

The application of the fuzzy similarity measure enables the comparison between the relation matrices, as described by

$$\mu_{ref*test} = \frac{\min[\mu_R(x_i, y_j), \mu_T(x'_i, y'_j)]}{\max[\mu_R(x_i, y_j), \mu_T(x'_i, y'_j)]} = \textit{similarity} \quad (8.5)$$

where the symbol “*” represents the fuzzy cross-correlation operator, “Min” represents the fuzzy logic intersection, “Max” represents the fuzzy logic union and the $\mu_{ref*test}$ is the grade of similarity between the test-subject (x', y') , and the reference-subject (x, y) , whereby the grade of similarity ranges between 0 and 1. The application of the grade of similarity in this work enables the quantitative and differential comparison between various types of functional impairments.

8.3 Experimental Determination of Gait Dynamics

- **Dynamic approach in stride-to-stride fluctuation**

Quantitative studies of gait have typically focused on properties of a typical or average stride, ignoring the stride-to-stride fluctuations and considering these fluctuations to be noise. Work over the past two decades has demonstrated however, that the alleged noise actually conveys important information. The magnitude of the stride-to-stride fluctuations and their changes over time during a gait dynamics may be useful in understanding the physiology of gait, in quantifying age-related and pathologic alterations in the locomotor control system, and in augmenting objective measurement of mobility and functional status. Indeed, alterations in gait dynamics may help to determine disease severity, medication utility, and fall risk, and to objectively document improvements in response to therapeutic interventions, above and beyond what can be gleaned from measures based on the average pattern of stride [69].

To study the intrinsic stride-to-stride dynamics and its changes with neurologic impairment, the standard deviation of each time series and the coefficient of variation (CV), an index of variability normalized to each subject's mean cycle duration, are computed. Both the standard deviation and the CV provide a measure of overall variations in gait timing during the entire walking task, i.e., the amplitude of the fluctuations in the time series with respect to the mean.

- **Pattern Analysis Scheme**

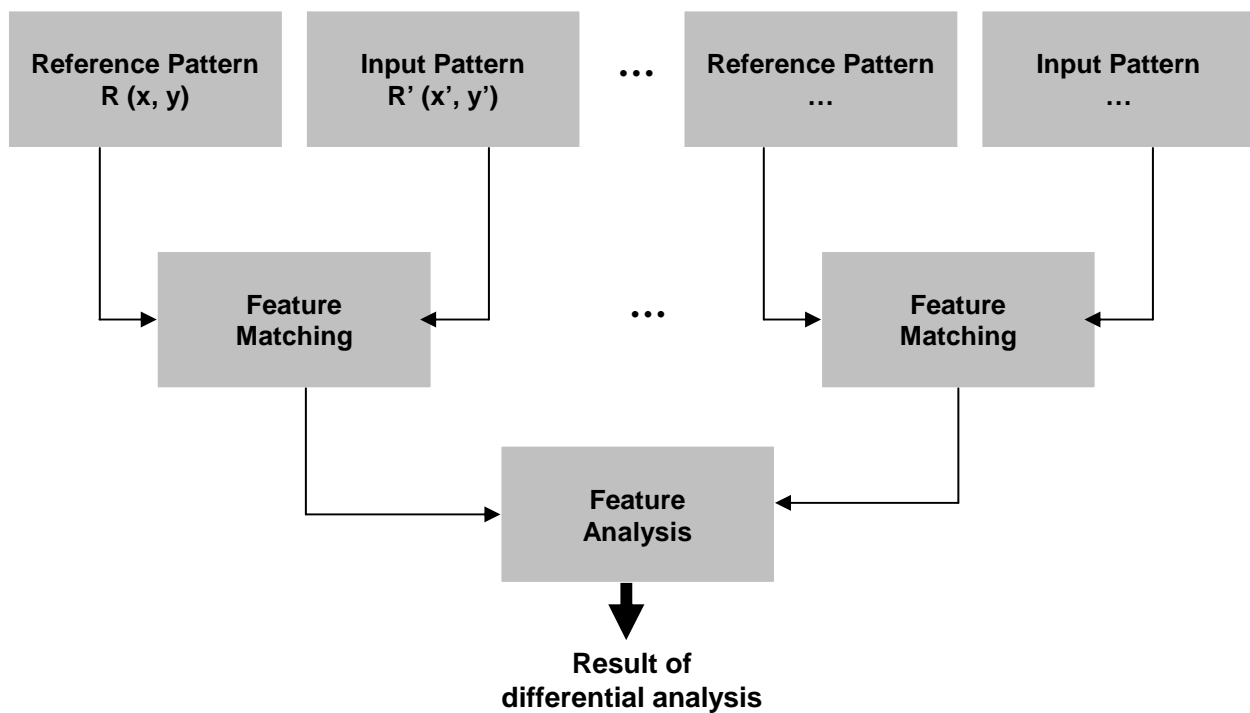


Figure 8-3: Differential pattern analysis scheme.

In Figure 8-3, a pattern analysis scheme for the differentiation of the gait patterns is illustrated. The reference pattern features are extracted from the averaged biomechanical data (ground reaction force, EMG, and acceleration) for all able-bodied subjects, and stored as the knowledge-base. The input patterns are obtained from the measurements of the mobility-related

impaired patients using the same feature extraction procedure. Through feature matching, the patterns are analyzed and may be used to: 1) differentiate gait patterns of the right and left limbs for establishing any level of symmetry within a patient; 2) differentiate the severity of the attributive features of the impairment between patients with the same disease; and 3) differentiate amongst different disease characteristics, and also amongst same diseases.

8.4 Participant Recruitment

This study was approved by the University of Texas at El Paso (UTEP) Institutional Review Boards (IRB), El Paso, Texas, USA. Twenty-two (twelve male and ten female) able-bodied subjects (18 years old and above) were recruited from the campus of UTEP. Patients with neurological disorders including cerebral palsy, multiple sclerosis, stroke, spinal cord injury, traumatic brain injury, idiopathic neurologic conditions were recruited from the local hospitals and rehabilitation clinics. In addition, injured subjects as well as elderly fallers were recruited from the community. All able-bodied subjects at the time of data collection declared no orthopedic or neurological pathology, injury or illness likely to affect locomotion or balance. Patients were fully or partial ambulatory which may or may not require partial body weight support (harness) during the experiment. All subjects provided informed consent prior to inclusion in the study according to institutional policy on human research.

8.5 Design Activities

8.5.1 Specific Aim – 1:

To investigate stride-to-stride fluctuations in gait to increase our understanding of the neural control of locomotion.

- **Objectives**

The measurement of the variability and fluctuations in the timing and length of gait phases could assist in providing more specific information regarding the type of impairment and, therefore, determine appropriate treatments. The study included:

1) How different control mechanisms produce the variability of gait, the magnitude of the stride-to-stride fluctuations, the stride dynamics, how stride fluctuates with time, independent of the magnitude.

2) How time between heel strikes, i.e. the stride interval or stride time, may function as a gait “clock” and reflect the internal rhythmicity of the locomotor system. Thus, examination of the fluctuations in the stride interval would theoretically provide insight into the organization, regulation, interactions and stability of the entire locomotor system.

- **Stride Variable Extraction Methods**

The stride-to-stride fluctuations present in twenty-two able-bodied subjects were evaluated in order to gain insight into normal locomotor function and its control mechanisms, in order to enhance our understanding of “pathological” deviations.

In this study, the temporal stride variables including stride time, stance ratio, swing ratio, and double-stance ratio were used. The purpose was to determine whether the impairment or disorders and/or individuals with the same disorder among different severity provoke significant gait changes with respect to the mean, standard deviation and coefficients of variation of these stride parameters.

Data from ground reaction forces were smoothened using second order Butterworth low pass filter to remove the noise above 20 Hz. The heel strike was then determined using a threshold-based criterion, i.e. the heel strike was defined as the period when the magnitude of the vertical force (F_z) exceeded the threshold [91]. In this case, the stride interval time (or gait cycle duration) series is obtained simply by taking the difference of the temporal data between the consequence heel strikes. Similar method was applied for extracting stance time (i.e. difference

of the temporal data from heel strike to toe-off of the same foot), swing time (i.e. difference of the temporal data from toe-off to the following heel strike of the same foot), and double-stance time (i.e. difference of the temporal data from heel-strike of one foot to toe-off of the other foot).

Figure 8-4 illustrates the examples of these temporal stride variables.

First, the 100 strides from the three-minute walking data were extracted from each able-bodied subject. The number of strides from patient's data varies and depends on their walking speeds. Second, the ratio of the stance phase/swing phase/double stance phase in each gait cycle was calculated. Finally, the mean and standard deviation of both healthy and patient subjects were calculated. The magnitude of the stride-to-stride fluctuations in the gait cycle duration/stance ratio/swing ratio/ double-stance ratio was also calculated, and the coefficient of variance (CV) of each subject was also calculated. The coefficient of variance is a normalized measure of dispersion of a probability distribution. It is defined as the ratio of the standard deviation σ to the mean μ , written as

$$CV (\%) = 100 \times \frac{Std (\sigma)}{Mean (\mu)} \quad (8.6)$$

The statistical results were reported as mean \pm standard deviation and CV (%).

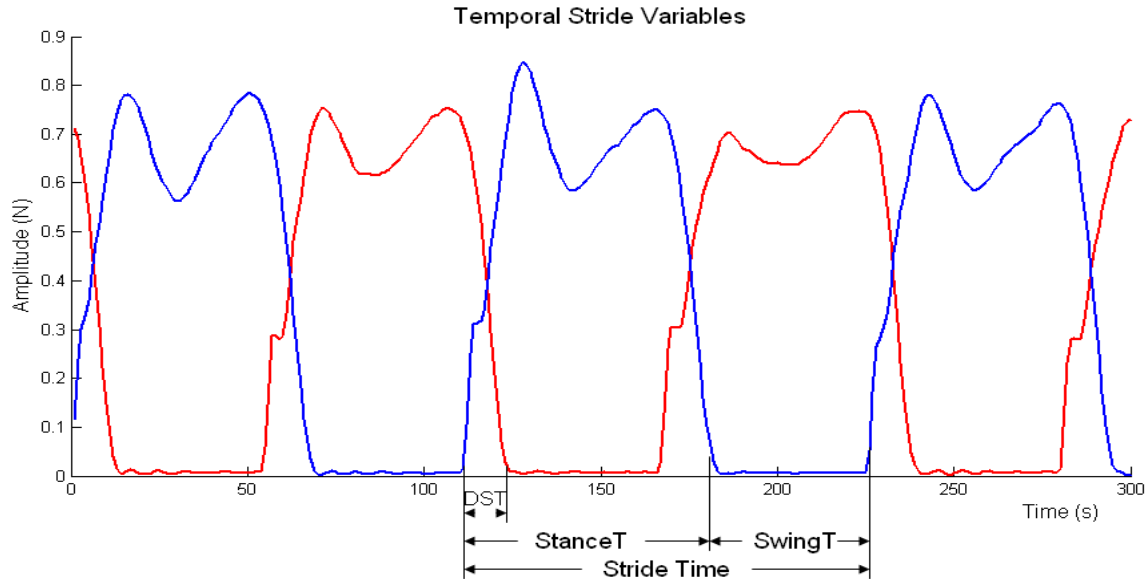


Figure 8-4: Temporal Stride Variables. (StanceT: Stance Time; SwingT: Swing Time; DST: Double Stance Time).

8.5.2 Specific Aim – 2:

To gain knowledge of gait dynamics in a specific pattern to increase our understanding of the neurophysiology/biomechanics of gait, and augment objective measurements of mobility and functional status.

- **Objective**

Perform studies to acquire and analyze complex and multidimensional motion-related physiologic data and use this to demonstrate specific effects of defined states of diseases, injuries, and aging. The acquisition and quantification of gait dynamics will augment objective measurement of mobility and functional status.

- **Pattern Analysis Methods**

Twenty-two able-bodied subjects were used to create the reference or normal gait pattern in ground reaction force (GRF), electromyography (EMG) and segmental acceleration. The

methods for feature extraction will be discussed in detail in the following sections, and the same methods will be applied on each patient.

Ground Reaction Force – (mediolateral F_x , anterior-posterior F_y , vertical F_z)

An instrumented treadmill was used to record the consecutive left and right forces in mediolateral (F_x), anterioposterior (F_y) and vertical (F_z) planes. Information about the characteristics of the normal force pattern within gait cycle (mean of 100 strides) was obtained from the able-bodied subjects (i.e. averaging GRF data within a gait cycle from ten healthy female subjects, and averaging GRF data within a gait cycle from twelve healthy male subjects), whereas the characteristics of the force pattern in a gait cycle (mean of number of strides, it may be noted that this number varied between patients) from each patient was also extracted. In order to allow comparison of the GRF among different subjects, the GRF values were normalized by body weight of individuals (i.e. the GRF data are represented as percentage of body weight - %BW).

The relationship between the GRF with respect to the seven gait phases defined in Figure 4-1 is established. Hence, fuzzy sets of the GRF of healthy subjects are described as the ground reaction forces in three planes x from a GRF collection, X , expressed as $x \in X$ with $X = \{ F_x, F_y, F_z \}$, where F_x indicates mediolateral GRF, F_y indicates anterioposterior GRF, and F_z indicates vertical GRF. The fuzzy sets for the seven gait phases are expressed as the gait phase, y out of a number of gait phases, Y , expressed as $y \in Y$, with $Y = \{ p_1 \ p_2 \ p_3 \ p_4 \ p_5 \ p_6 \ p_7 \}$; where $p(i)$ indicates gait phases from one to seven.

A fuzzy relation among healthy subjects, R , is established between the fuzzy sets X and Y using the Cartesian product. This relationship models the connectiveness of the two fuzzy sets into a fuzzy rule base. The Cartesian product $X \times Y$, a relational matrix, is then expressed as

$$R_{(x,y)} = \begin{bmatrix} \mu_r(x_1, y_1) & \Lambda & \mu_r(x_1, y_7) \\ M & M & M \\ \mu_r(x_3, y_1) & \Lambda & \mu_r(x_3, y_7) \end{bmatrix} \quad (8.7)$$

$\mu_r(x, y)$ is defined as a membership function (the grade of belonging), this means, the relationship between GRF with respect to the gait phase of an able-bodied subject. The membership function is expressed as

$$\mu_r(x, y) = \frac{1}{n} \sum_{i=1}^n \mu(i) \quad (8.8)$$

where x represents the GRF in the seven gait phases, and y is the seven gait phases, n is the number of data frames within a phase, $\mu(i)$ is the normalized GRF.

The actual measurements of an impaired subject can be compared with the reference data in the fuzzy rule-based system through inferencing. This procedure is called the fuzzy similarity analysis, and it provides an outcome measure in aggregation. The application of the fuzzy similarity measure enables the comparison between the rule base of GRF and a impaired subject's GRF, expressed as:

$$\mu_r * \mu_t = \frac{\text{Min} [\mu_r(x_i, y_j), \mu_t(x'_i, y'_j)]}{\text{Max} [\mu_r(x_i, y_j), \mu_t(x'_i, y'_j)]} = \text{similarity} \quad (8.9)$$

where the symbol “*” represents the fuzzy cross-correlation operator, “Min” represents the fuzzy logic intersection, “Max” represents the fuzzy logic union and the $\mu_r * \mu_t$ is the grade of similarity between a patient subject (x', y') , and the rule base or reference (x, y) , whereby the grade of similarity ranges between 0 and 1.

EMG data

Filtered EMG signals (eight on each side of the lower extremity) within a gait cycle were extracted from twenty-two healthy subjects, and the mean of the 100 strides were calculated. In order to compare the EMG signals among different subjects, the EMG signals were normalized by the maximum of the EMG values. The average of EMG data of ten healthy female subjects and the average of EMG of twelve male subjects were calculated to create the fuzzy rule base of healthy subject's EMG pattern. The same methods were used to extract the EMG data from each patient's data set (Note: the number of strides varied between patients).

The relationship between the electrical activities of the muscles with respect to the seven gait phases is established. Hence, fuzzy sets of the EMG signals are described as the muscle type x from a muscle collection, X , expressed as $x \in X$ with $X = \{Sol \quad TA \quad LG \quad VL \quad RF \quad BF \quad Gmed \quad ES\}$, where $\{\dots\}$ indicates muscles and *Sol* – soleus; *TA* – tibialis anterior; *LG* – gastrocnemius lateralis; *VL* – vastus lateralis; *RF* – rectus femoris; *BF* – biceps femoris; *Gmed* – gluteus medius; *ES* – erector spinae.

The fuzzy sets for the seven gait phases are expressed as the gait phase, y out of a number of gait phases, Y , expressed as $y \in Y$, with $Y = \{p1 \quad p2 \quad p3 \quad p4 \quad p5 \quad p6 \quad p7\}$; where $p(i)$ indicates gait phases from one to seven.

A fuzzy relation, R , is established between the fuzzy sets X and Y using the Cartesian product. The Cartesian product $X \times Y$, a relational matrix, is then expressed as

$$R_{(x,y)} = \begin{bmatrix} \mu_R(x_1, y_1) & \Lambda & \mu_R(x_1, y_7) \\ \text{M} & \text{M} & \text{M} \\ \mu_R(x_8, y_1) & \Lambda & \mu_R(x_8, y_7) \end{bmatrix} \quad (8.10)$$

Therefore, the fuzzy relational matrix represents the fuzzy rules or the fuzzy rule base. The actual EMG measurements of the impaired subject are compared with the reference data within the rule-base through inference engine (the similarity measure in Equation 8.5.).

Acceleration data

Acceleration data in a gait cycle were extracted from twenty-two healthy subjects, and the mean of the 100 strides were calculated. In order to compare the acceleration signals among different subjects, the accelerations were normalized by the maximum values. The average of acceleration of ten healthy female subjects and the average of acceleration of twelve male subjects were calculated to create the fuzzy rule base of healthy subject's acceleration pattern. The same methods were used to extract the acceleration pattern from each patient's data set (Note: the number of strides varied between patients).

The relationship between the acceleration with respect to the seven gait phases is established. Hence, fuzzy sets of the EMG signals are described as the muscle type x from a muscle collection, X , expressed as $x \in X$, with

$X = \{Ft_x, Ft_y, Ft_z, Sk_x, Sk_y, Sk_z, Th_x, Th_y, Th_z, Hip_x, Hip_y, Hip_z\}$ where $\{...\}$ indicates acceleration and Ft_x – mediolateral acceleration of foot; Ft_y – anteroposterior acceleration of foot; Ft_z – vertical acceleration of foot; Sk_x – mediolateral acceleration of shank; Sk_y – anteroposterior acceleration of shank; Sk_z – vertical acceleration of shank; Th_x – mediolateral acceleration of thigh; Th_y – anteroposterior acceleration of thigh; Th_z – vertical acceleration of thigh; Hip_x – mediolateral acceleration of hip; Hip_y – anteroposterior acceleration of hip; Hip_z – vertical acceleration of hip.

The fuzzy sets for the seven gait phases are expressed as the gait phase, y out of a number of gait phases, Y , expressed as $y \in Y$, with $Y = \{p1 \ p2 \ p3 \ p4 \ p5 \ p6 \ p7\}$; where $p(i)$ indicates gait phases from one to seven.

A fuzzy relation, R , is established between the fuzzy sets X and Y using the Cartesian product. The Cartesian product $X \times Y$, a relational matrix, is then expressed as

$$R_{(x,y)} = \begin{bmatrix} \mu_r(x_1, y_1) & \Lambda & \mu_r(x_1, y_7) \\ M & M & M \\ \mu_r(x_{12}, y_1) & \Lambda & \mu_r(x_{12}, y_7) \end{bmatrix} \quad (8.11)$$

Therefore, the fuzzy relational matrix represents the fuzzy rules or the fuzzy rule base. The actual acceleration measurements of a patient are compared with the reference data within the rule-base through inference, the similarity measure in Equation 8.5.

Chapter 9: Data Acquisition

9.1 Ground Reaction Force Measurement

Each subject walked on an instrumented treadmill (*Bertec Corporation, USA*) at free speeds (self-selected natural speed) for three minutes. The instrumented treadmill is a dual-belt type with two independent force plates mounted beneath the belts (see Figure in Appendix I). Each force plate independently measures six load components - the three orthogonal components of the resultant force and the three components of the resultant moment in the same orthogonal coordinate system. The point of application of the force and the couple acting can be readily calculated from the measured force and moment components independently for each half of the treadmill. Figure 9-1 shows example of force digital output from signal acquisition in 3-D.

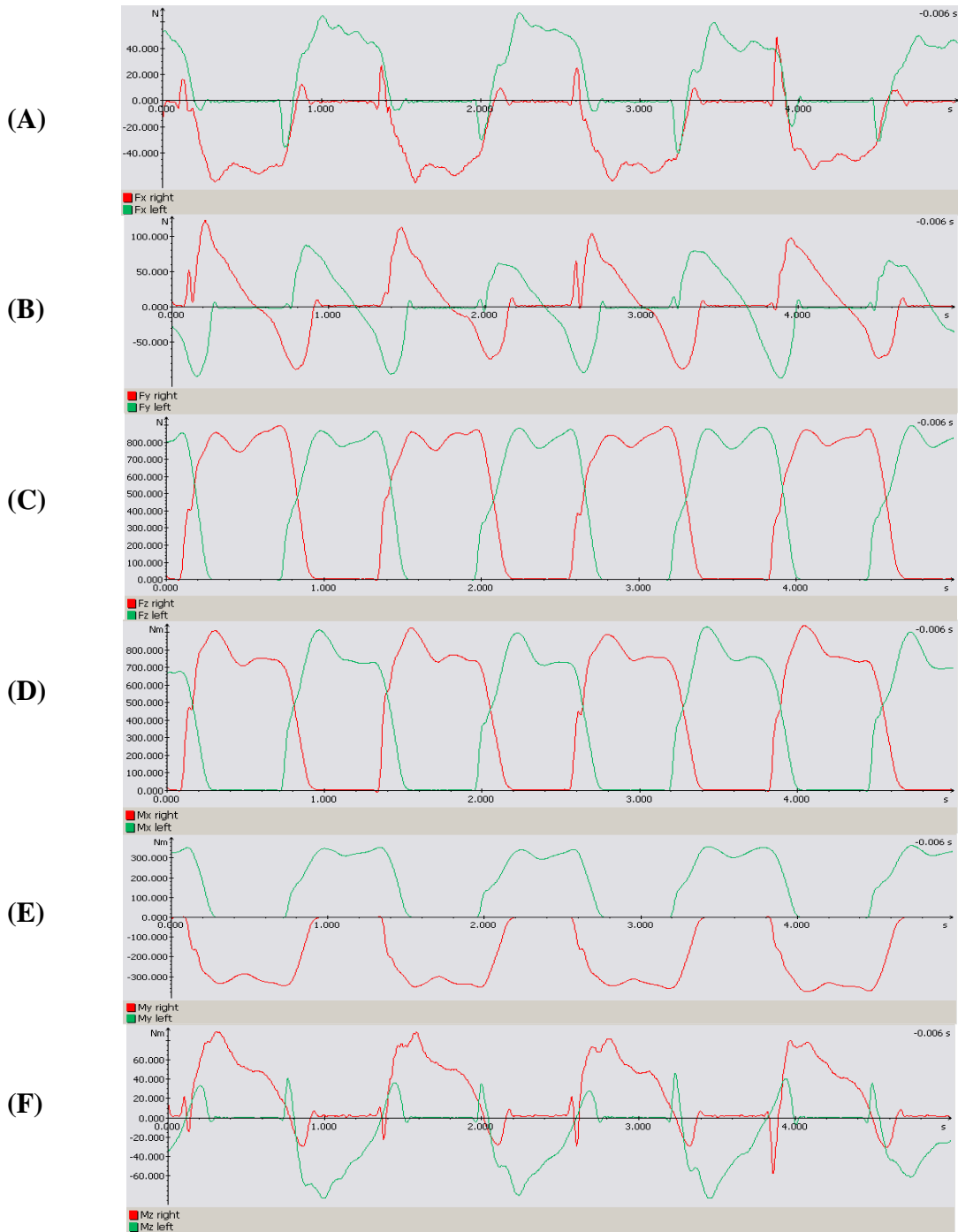


Figure 9-1: Ground Reaction Force (GRF) measurement. (A): Mediolateral force; (B): Anteroposterior force; (C): Vertical force; (D): Mediolateral moment; (E): Anteroposterior moment; (F): Vertical moment. Red and green colors represent right and left respectively.

9.2 Electromyographic Data Acquisition

Surface electromyographic data were recorded using Delsys Myomonitor[®] Wireless EMG systems (*Delsys Inc., Boston, MA, USA*). This EMG system consists of 16 channels, each channel has 41 x 20 x 5 mm electrode with two 10.0 x 1.0 mm contacts and -92 dB CMRR (Common Mode Rejection Ratio). All channel data are synchronized through a Tethered Trigger Module to the Myomonitor. As a wireless transmitter the Myomonitor sends EMG data over a wireless local area network (WLAN) to the host computer for real-time display and storage. The complete EMG system components can be found in Appendix II.

9.3 Acceleration Measurement

An important aim of biomechanical analysis of gait is to know the amount of force generated (or moment of force about a joint) from the muscles. This internal force can be calculated from accelerations. As mentioned before, acceleration can be measured directly using triaxial accelerometers. In this study, a triaxial accelerometer (ADXL330, 4×4×1.45 mm, Analog Devices, Inc.), was used to measure linear accelerations in three sensitive planes – X, Y, and Z. It measured acceleration with a minimum full-scale range of $\pm 3g$. The output signals are analog voltages that are proportional to acceleration and it measured the static acceleration of gravity in tilt-sensing applications, as well as dynamic acceleration resulting from motion or vibration. All acceleration sensors were orthogonally aligned. The sensor system also contained a data logger (NI-DAQ[™]mx) that simultaneously records the all tri-axial acceleration data at a sampling rate of 100Hz. Detailed information is shown in Appendix III.

9.4 Sensor Placements

The complete sensor placements including surface EMG and triaxial accelerometers are illustrated in Figure 9-2.

- Surface EMG electrode placements

The Delsys Myomonitor® wireless EMG system (Delsys Inc., Boston, MA, USA) was used for measuring the dynamic activities of the muscles on both sides of the lower extremity. The placement of the electrodes on the subjects was performed based on [Cram 1998] and the signals were tested before the data acquisition. The acquisition process was performed with the Delsys EMGworks® Software at a sampling frequency of 1000 Hz. The following eight muscles for each side were recorded: soleus (Sol), tibialis anterior (TA), gastrocnemius lateralis (LG), vastus lateralis (VL), rectus femoris (RF), biceps femoris (BF), gluteus medius (Gmed), and erector spinae (ES). Table 9-1 shows the detailed EMG electrode placement of each muscle.

The electrode-skin interface generates a D/C voltage potential, mainly caused by a large increase in impedance from the outermost layer of skin, including skin hair, dead skin material and oil secretions. Therefore, proper skin preparation is essential for collecting a quality EMG signal. This was explained in the informed consent form. Each subject was asked to shave the area where the electrode would be placed to. Alcohol swab was used to rub off the dead skin material and oil secretions.

Table 9-1: EMG Electrode Placement of Eight Muscles in the back and lower extremity.

Muscle	Placement
Soleus	The electrode is placed on the lateral, posterior side of lower leg. The electrode is placed in a near vertical plane relative to the ground so that they run parallel to the muscle fibers.
Tibialis anterior	The electrode is placed about a third of the distance from the knee to the ankle, lateral to the tibia on the anterior surface of the lower leg. The electrode is oriented in a vertical plane relative to the ground.
Gastrocnemius lateralis	The electrode is placed laterally, on the upper half of the posterior aspect of the calf. The electrode is placed in a vertical plane relative to the ground.
Vastus lateralis	The electrode is placed on the lateral surface of the lower third of the thigh, approximately 6cm above the kneecap. The electrode is oriented laterally at approximately a 20 degree angle from vertical.
Rectus femoris	The electrode is placed on the medial anterior surface of the thigh, approximately half the distance between the hip and the knee. The electrode is placed in a vertical plane from the ground.
Biceps femoris	Biceps femoris locates in posterior thigh. The electrode is placed half way between the ischial tuberosity and the lateral epicondyle of the tibia.
Gluteus medius	The electrode is placed in the proximal third of the distance between the iliac crest and the greater trochanter. The electrode is placed in a vertical plane to the ground.
Elector spinae	Elector spinae is originated in lumbar region of the spine. The electrode is placed at two finger width lateral from medial L1.

- **Accelerometer placements**

A custom array of accelerometer system was developed in the UTEP's Human Motion Analysis and Neurorehabilitation Laboratory for the detection of the acceleration of body segments during walking. The system's sensing device consists of ADXL330 iMEMS® Tri-axial accelerometers (Analog Devices Inc.) and 12-bits analog to digital (A/D) converters (National Instruments Inc.). The sensors measure the dynamic acceleration resulting from motion.

The placement of accelerometers on human subject is an issue of importance to accuracy and reliability of the devices and has received some attention in the literature. The location of the accelerometers for example is important for the accuracy of measurement. It is suggested that accelerometers should be attached to those parts of the body where they would register the most activity, i.e. the legs during walking [131, 252].

In fact, the output of a body-fixed accelerometer is the net measurement including the actual physical activities of the body and external distortions. The actual physical activity measurements from the accelerometer are acceleration due to body movement, and gravitational acceleration. The external distortions include external vibration especially from the instrumented treadmill, and acceleration not produced by the body itself (acceleration due to motion of the skin under the accelerometer or jolting of the sensor on the body due to loose attachment).

Further, due to individual variation, exact orientation may not be consistent between individuals or types of activities. For example, the hip placement becomes difficult since there is no flat surface for most of the subjects; the orientation varies dramatically between subjects.

The tri-axial accelerometers were placed on the surface of the body-segments from down to the top: foot, shank, thigh, and hip with 3M Corporation (Minnesota Mining and Manufacturing Company) double-sided tape. For hip acceleration measurement, the

accelerometer was attached to the belt, hence increased the flat surface area and unsure the constant measurement between subjects.

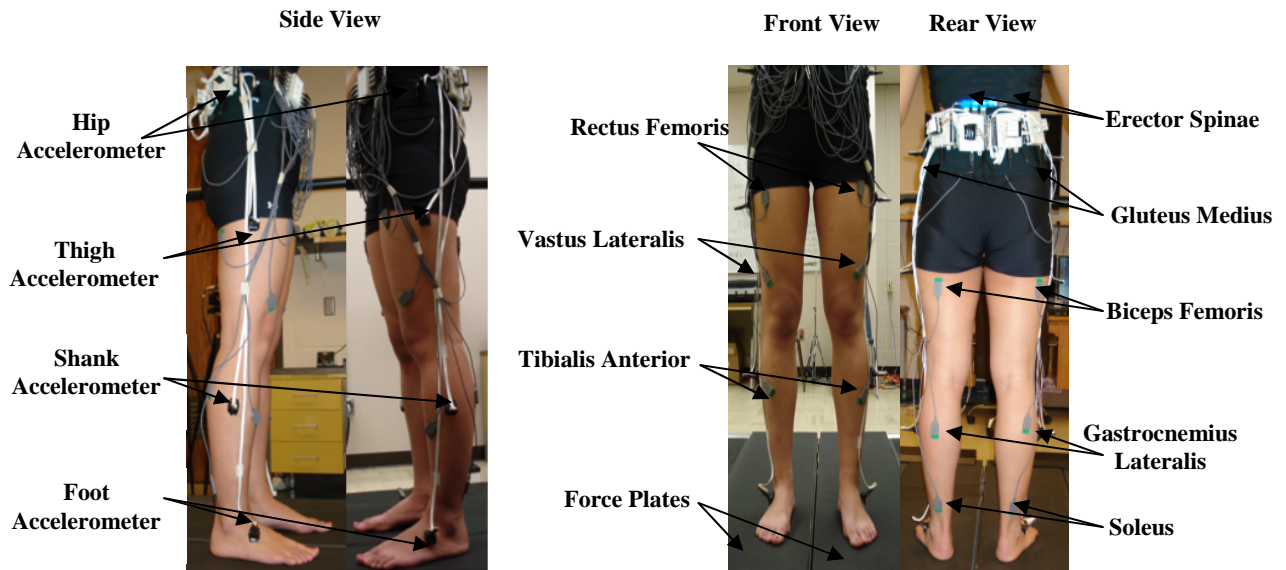


Figure 9-2: Surface EMG and Tri-axial accelerometer placements for Data Acquisition.

9.5 Synchronization of Multi-Portable Sensors

- **LabView Software synchronization for data acquisition**

Two tri-axial accelerometers were connected to one TI data logger. There were four data loggers connected through a USB hub, then to the PC with LabView software installed. The instrumented treadmill is also connected to the same PC through a USB cable. The LabView software was then used to synchronize the data acquisition of accelerometers and forces. The acceleration and force data have sampling frequency of 100 Hz.

- **Wireless network connection and EMG Triggering Module**

The wireless connection between the Myomonitor and the EMGworks Acquisition on host PC is enabled by the D-Link WUA-1340 Wireless USB Adapter. Delsys EMG trigger

Module was used to triggering with Start/Stop and Input/Output signals in order to synchronize the all acquired data including acceleration, force and EMG.

9.6 Data Acquisition Procedures

Each subject wore running shorts and comfortable T-shirt during the experiment. Subjects were allowed to become familiar with the walking track on the treadmill before running the experiment. For impaired subjects, partial body-weight support (harness) fixing on the instrumented treadmill could be applied if it was necessary throughout the experiment. Clinical doctors or nurses could attend the experiment if the patients had severe medical conditions such as diabetes. Two experimental-staffers stood on each side of the treadmill for safety. The patients rested for 20 to 30 minutes or more frequently when necessary depending on their physiological condition.

The self-selected natural speed is a subjective speed selection (comfortable speed via instruction to “walk at a comfortable pace”) by the subject. The speed of the treadmill was incrementally increased or decreased to determine the participant’s comfortable walking speed.

Sixteen surface EMG electrodes were placed on the prepared skin on the lower limbs and back of the subject. Each EMG signal was tested carefully before the walking trial. Eight tri-axial accelerometers were also placed carefully at the half-way of segments on both legs (feet, shank, thigh, and hip). Since an accelerometer measures the sum of acceleration of the movement and gravitational (the white noise component ignored), therefore, ten seconds of static acceleration was measured before walking. The real acceleration of the movement was defined by subtracting the mean static acceleration. Every subject was instructed to walk three minutes

on the instrumented treadmill continually. Therefore, the ground reaction force and moment, EMG and acceleration signals were collected simultaneously.

9.7 Anthropometric Measurement

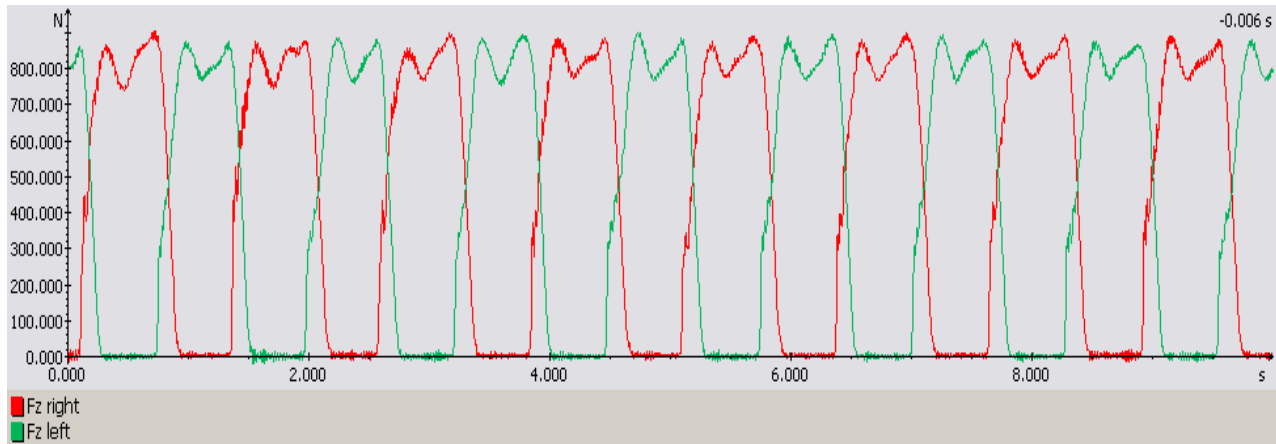
Anthropometric data of each subject were recorded including: age, height and weight (and/or Body Mass Index - BMI), body fat, lower extremity segment length and circumference, etc. (see Appendix IV). The anthropometric measurements allowed cross-sectional analysis of the relationship between the normal subjects and patients. Furthermore, mass of body segments could be determined from the anthropometric measurements [258] and hence force generated from each segment could be calculated.

Chapter 10: Data Processing

10.1 Ground Reaction Force Data Processing

There is white noise introduced into force data due to vibrations and the moving artifact during walking on the treadmill. Ground reaction force and moment data were smoothed using second order Butterworth low pass filter to remove the noise above 20 Hz. Figure 10-1 illustrates the right and left vertical ground reaction forces (F_z) before and after filtering process.

(A)



(B)

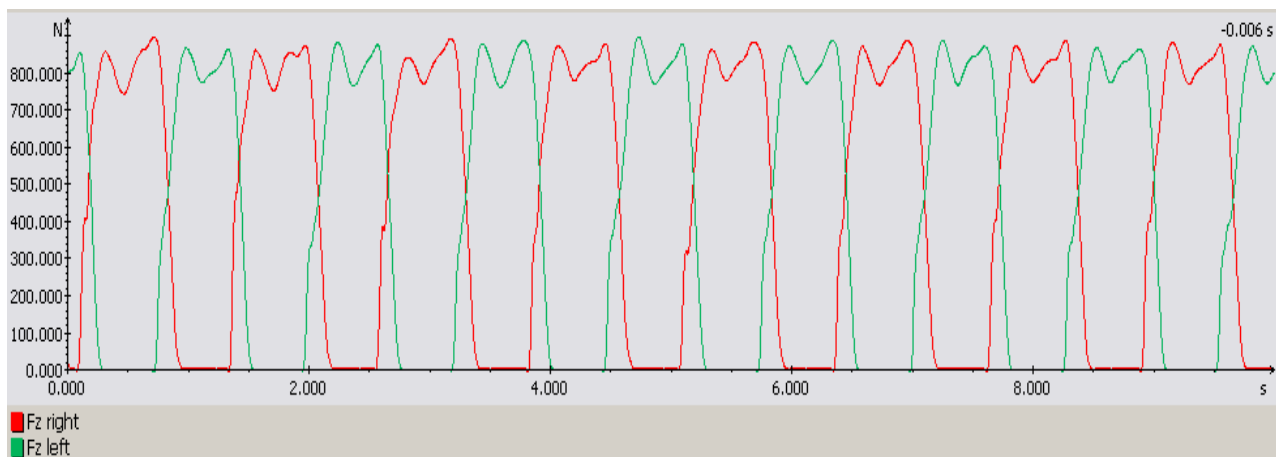


Figure 10-1: Comparison before (A) and after (B) filtering on vertical GRF.

10.2 EMG Data Processing

Surface EMG data of sixteen muscles were collected using Delsys EMGacquisition[®], and processed using Delsys EMGworks[®] Software. The following steps describe the manipulation of EMG data from an able-bodied subject's left soleus.

Step 1: Raw EMG data from acquisition

The raw EMG data were acquired at a sampling frequency of 1000 sample/sec. Figure 10-2 depicts a three-second EMG raw data without DC offset.

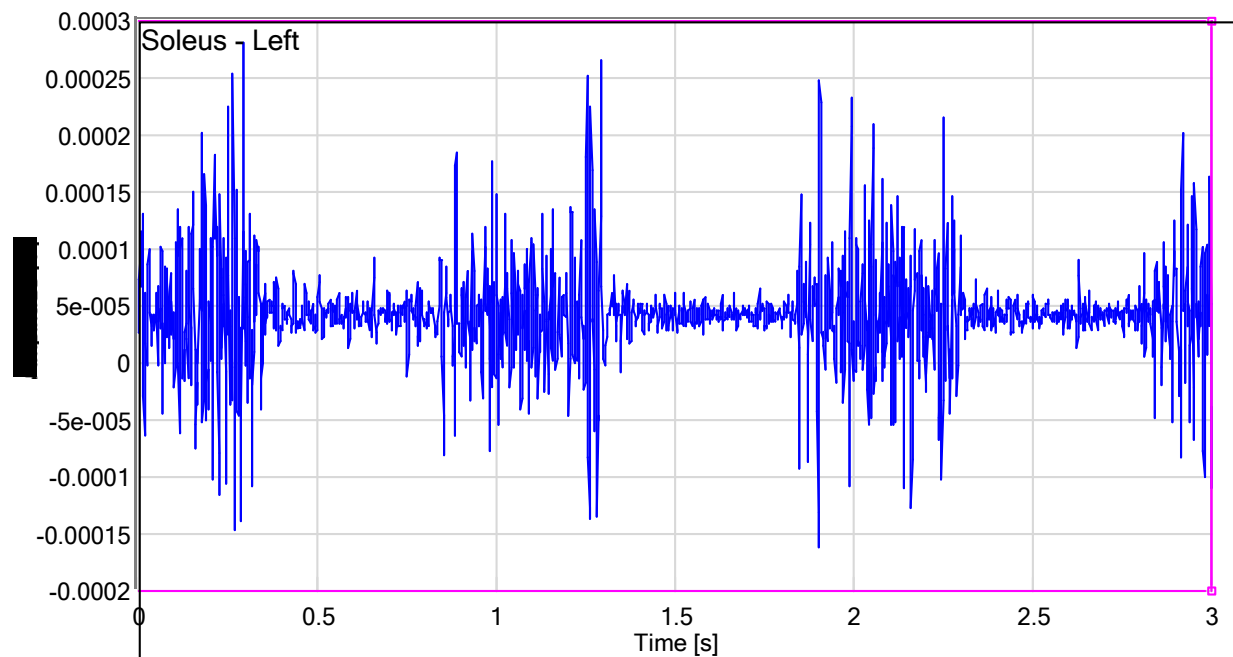


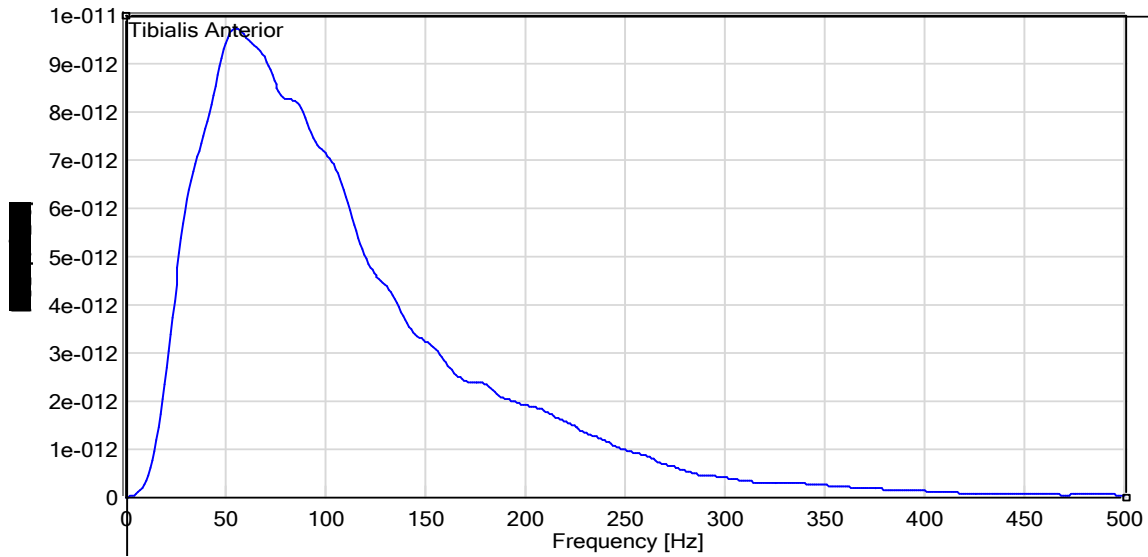
Figure 10-2: Raw EMG data from Soleus muscle of an able-bodied subject. The X axis represents the time in second and Y axis represents the amplitude in Volts.

Step 2: EMG filtering

In order to reduce the noise such as motion artifacts and treadmill vibration, a band pass filter process was used. De Luca in 1997 showed the most significant power of EMG was located between 20 and 400 Hz. In this experiment the power spectrum density (PSD) of the raw data shown in Figure 10-3 (A) clarify that the power of EMG was located between 20 and 200 Hz.

Second order Butterworth band-pass filter was applied to the raw EMG data between 20 and 200 Hz, shown in Figure 10-3 (B).

(A)



(B)

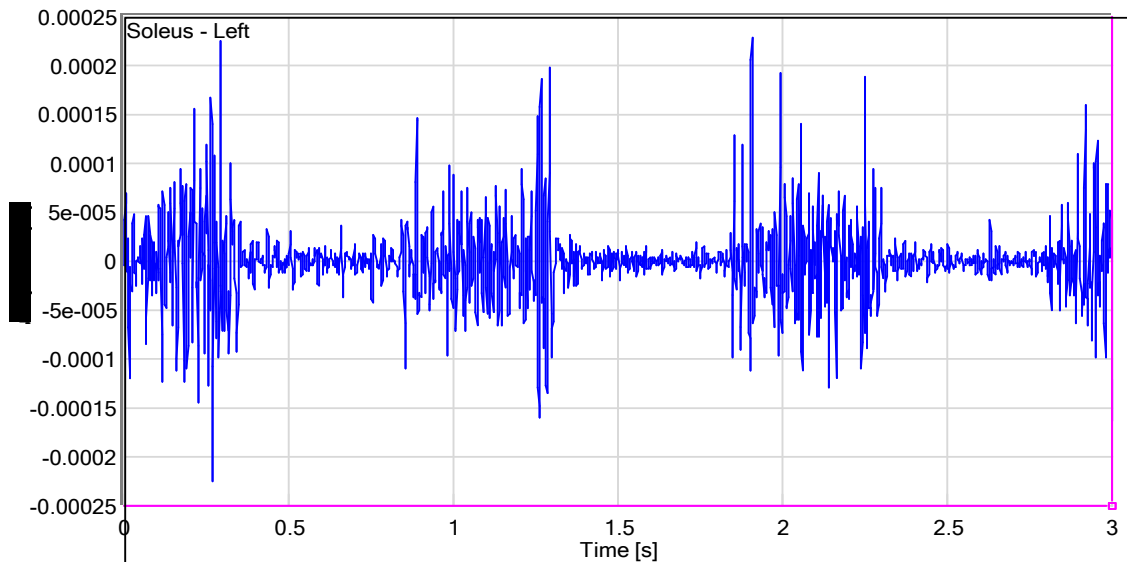


Figure 10-3: EMG data filtering. (A): Power spectrum density (PSD) for raw EMG data, the X axis represents the frequency in Hz and Y axis represents the PSD in $\text{Volts}^2 \cdot \text{sec}$; (B): Filtered EMG data, the X axis represents the time in seconds and Y axis represents the amplitude in Volts.

Step 3: Full-wave rectification

The filtered data were then full-wave rectified to generate the absolute value of the EMG as shown in Figure10-4.

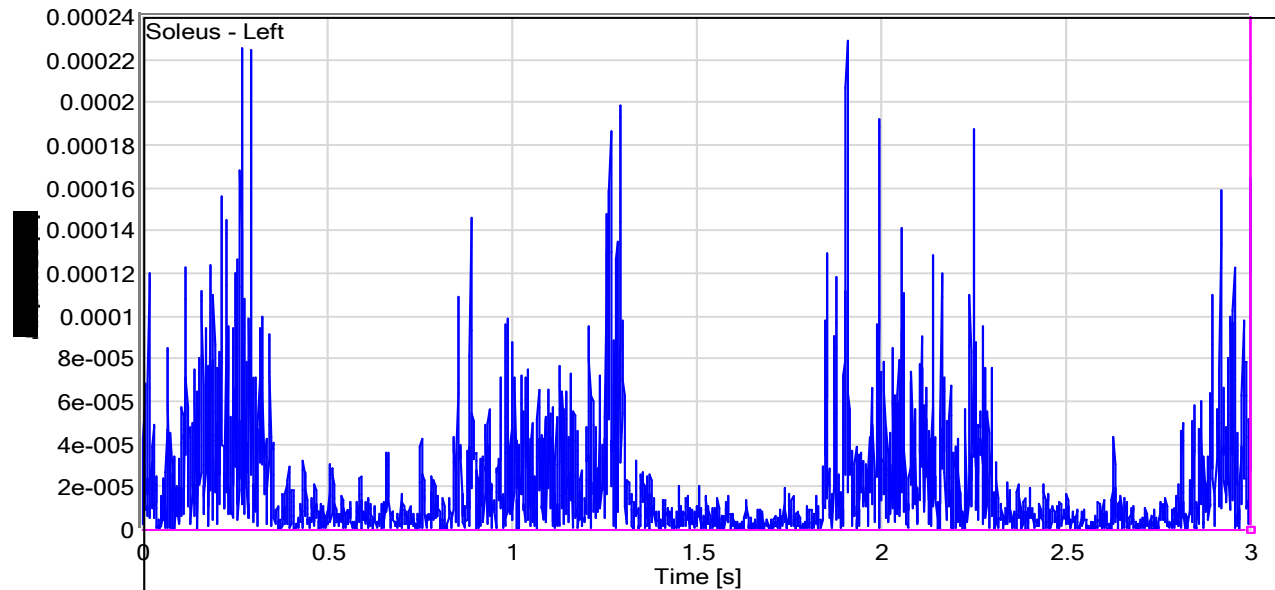


Figure 10-4: Full-wave rectified EMG data. The X axis is the time in seconds and Y axis is the amplitude in Volts.

Step 4: Linear envelope

Linear envelope is a common way to manipulate EMG signal [De Luca, 1997; De Luca, 2006]. It can be called also as moving average. The linear envelope was produced by using an FIR (finite impulse response) second order Butterworth low-pass digital filter with a cutoff frequency of 7 Hz to the full-wave rectified EMG signal, see Figure 10-5.

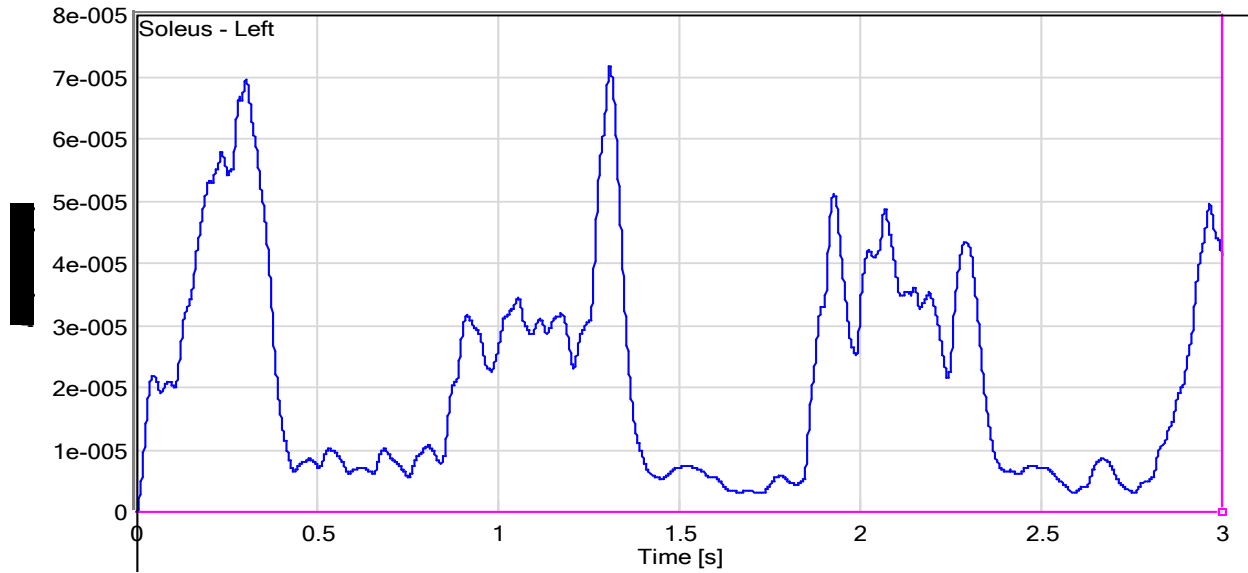


Figure 10-5: Linear envelope of EMG data. The X axis is the time in seconds and Y axis is the amplitude in volts.

Step 5: Averaging over strides

The strides were specified based on the GRF. 100 strides were selected from the three minutes walking [Arsenault et al. 2001]. The stride time varied among strides. Therefore, a re-sampling technique was used to unify the length of strides [De Stefano et al., 2003]. The EMG signals of 100 strides were extracted and re-sampled to 1000 samples per stride, and then the mean and the standard deviation (SD) of all strides were calculated during one gait cycle. Figure 10-6 depicts an example of EMG mean \pm SD over 100 strides.

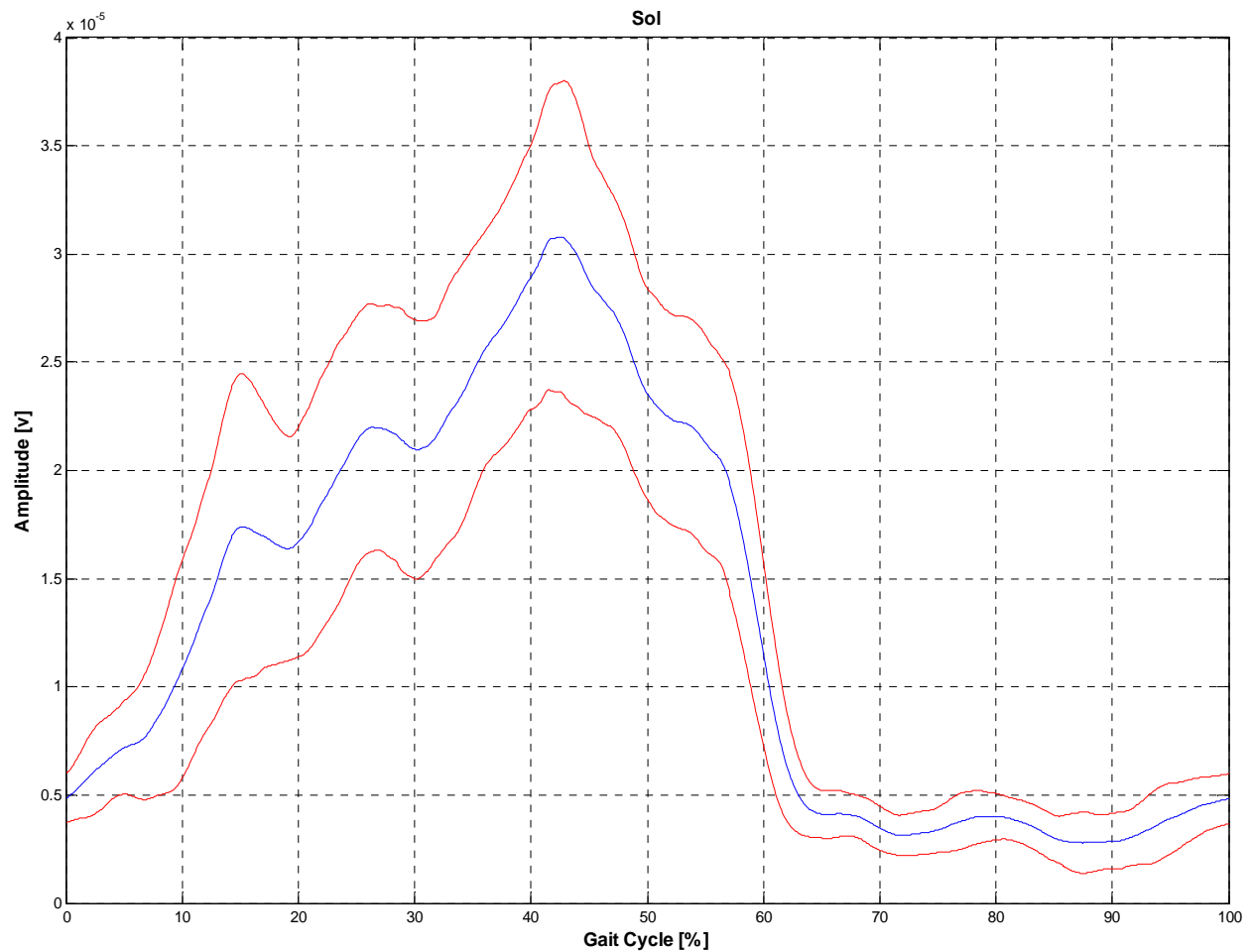


Figure 10-6: Mean of soleus EMG signal. The X-axis is one gait cycle, and the Y-axis is the amplitude in volts. Blue line represents mean of EMG in a gait cycle. Red line represents upper and lower standard deviation (SD) in a gait cycle.

Step 6: EMG normalization

In order to allow comparison of the EMG signal among different subjects, EMG data were normalized for each subject based on the maximum of EMG signal (mean of EMG signal), so that the EMG amplitude ranged between 0 and 1. Figure 10-7 shows eight normalized EMG signals of eight muscles for one gait cycle.

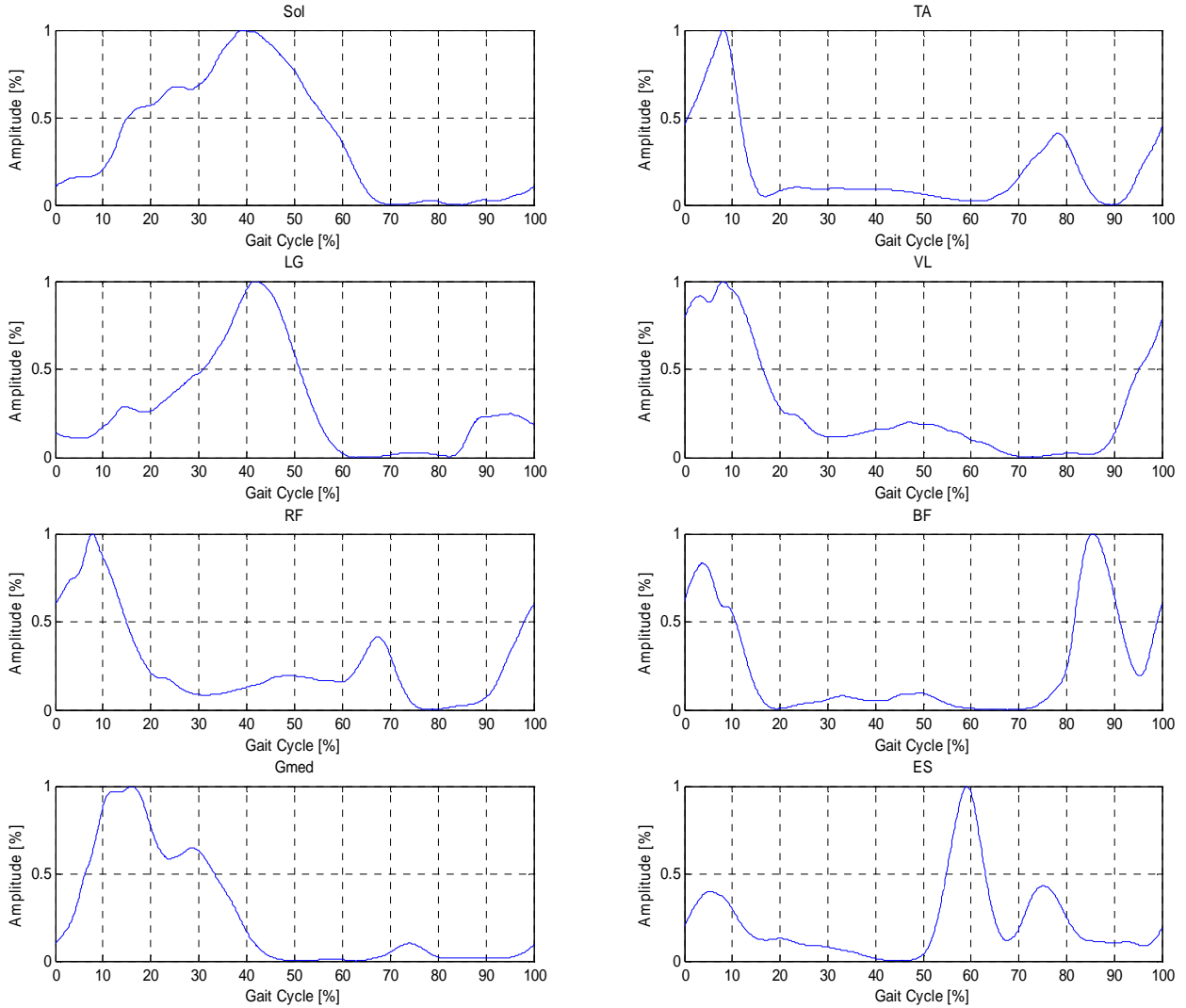


Figure 10-7: Normalized EMG signals within gait cycle. The X axis is one full gait cycle, and the Y axis is the normalized amplitude. Sol – Soleus; TA – Tibialis Anterior; LG – Gastrocnemius Lateralis; VL – Vastus Lateralis; RF – Rectus Femoris; BF – Biceps Femoris; Gmed – Gluteus Medius; ES – Erector Spinae.

10.3 Acceleration Data Processing

The gravitational baseline signal (zero g offset) was first subtracted from the dynamic raw data to make the signal offset at zero. Then, second order Butterworth low pass filter with

cutoff frequency of 6 Hz was applied to lower the noise and improve the resolution of the accelerometers [229, 258]. Figure10-8 describes the processing procedures of the acceleration.

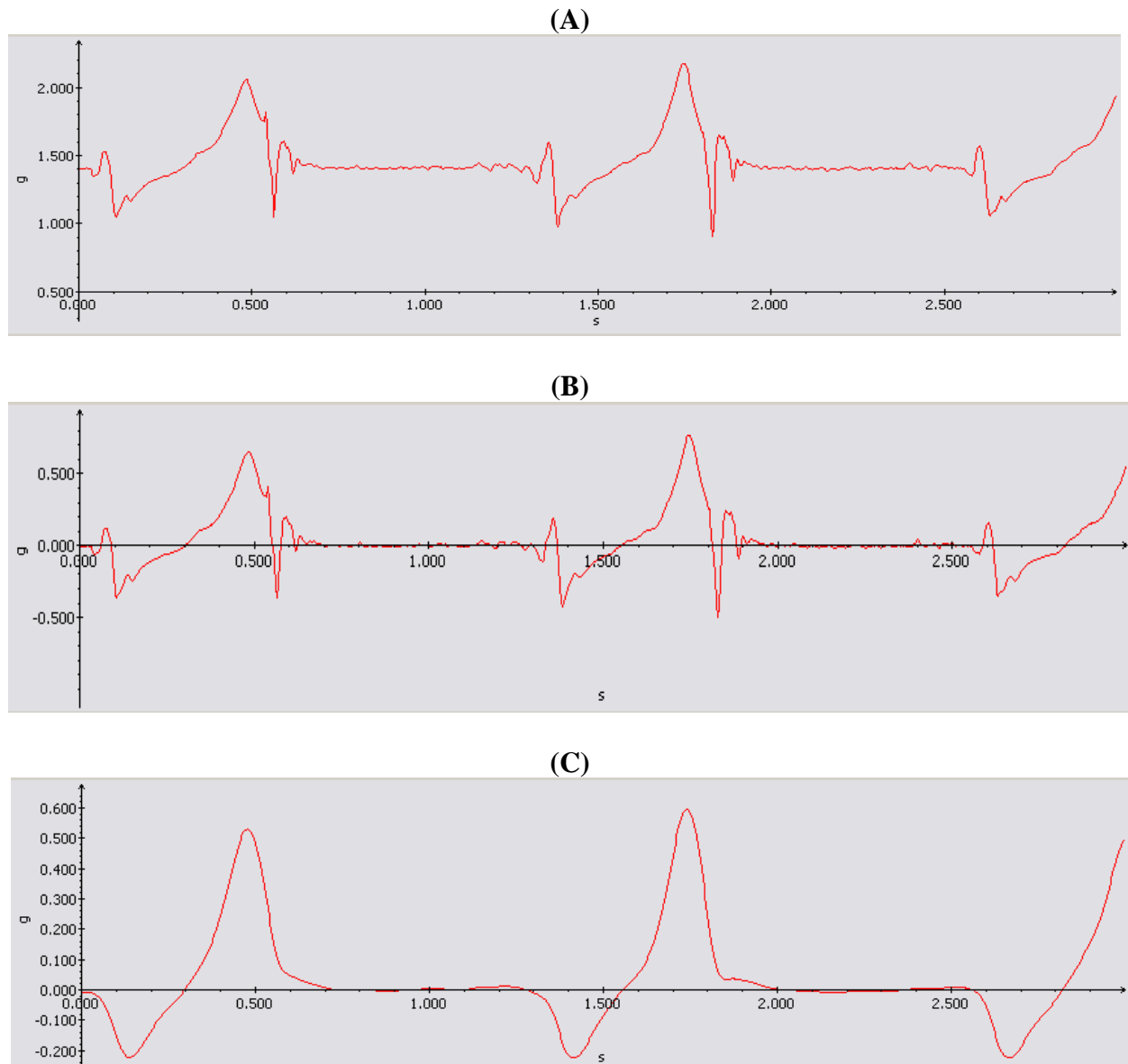


Figure 10-8: Acceleration signal processing. . The signal in the figure represents the sagittal acceleration of foot segment. The X axis is the time in seconds, and the Y axis is the amplitude in g. (A): Raw sagittal acceleration signal; (B): Raw signal after subtracting the baseline offset; (C): Filtering, 2nd Butterworth low pass filter with cutoff frequency of 6 Hz.

Chapter 11: Case Studies and Analysis

This chapter contains experimental case studies on both healthy and impaired subjects in relation to stride variability approach and pattern comparison methods. The experimental procedure and feature extraction were explained in Chapter 8. Experimental results of these impairments are presented and discussed.

11.1 Healthy and Patient Participants

Twenty two healthy adults (ten female subjects and twelve male subjects) were recruited from the campus of University of Texas at El Paso (UTEP) after having given their written informed consent. These adults reported no physical and mental disorders, and no medications at the time of data collection. Patients with different types of gait impairments were recruited, they included:

- six relapsing remission multiple sclerosis (RRMS) patients (two female and four male patients)
- four spastic diplegic cerebral palsy (SDCP) patients (one female and three male patients)
- two female hemiparetic stroke patients
- a male patient with spinal cord injury (SPI)
- a male patient with traumatic brain injury (TBI),
- a male elderly faller
- a female patient with idiopathic neurologic disorder.

The following chapter will discuss the case studies involving the subjects with Multiple sclerosis and cerebral palsy. The other case studies may be found in the Appendix III-Appendix XVII.

Table 11-1 shows the anthropometric data for all able-bodied subjects, and Table 11-2 shows the anthropometric data for all the impaired subjects.

Table 11-1: Anthropometric data of able-bodied subjects

Female	Age	Weight	Height	BMI	Male	Age	Weight	Height	BMI
	(yrs)	(kg)	(cm)	(kg/m ²)		(yrs)	(kg)	(cm)	(kg/m ²)
F_1	37	58.0	165.0	21.3	M_1	20	71.3	170.5	24.5
F_2	26	49.0	162.0	18.7	M_2	24	83.7	180.0	25.8
F_3	21	63.0	173.0	21.0	M_3	25	56.6	157.5	22.8
F_4	22	56.0	166.5	20.2	M_4	21	61.2	163.0	23.0
F_5	23	63.4	163.5	23.7	M_5	22	67.0	176.0	21.6
F_6	21	70.7	170.0	24.5	M_6	23	71.6	171.0	24.5
F_7	28	61.0	169.0	21.4	M_7	24	66.6	170.0	23.0
F_8	22	56.0	161.0	21.6	M_8	20	65.7	164.0	24.4
F_9	23	57.0	157.0	23.1	M_9	22	45.7	163.0	17.2
F_10	35	76.5	167.0	27.4	M_10	25	56.6	169	19.8
					M_11	24	78.3	185	22.9
					M_12	23	88.1	181	26.9

BMI (Body Mass Index) kg/m²; Note: Speed of female subjects has range from 0.85 to 1.5 m/s (1.12±.21), and speed of male subjects has range of 0.98 to 1.17 m/s (1.02±.07).

Table 11-2: Anthropometric data of mobility-related impaired subjects

Patient	Sex	Age (yrs)	Weight (kg)	Height (cm)	BMI (kg/m ²)	Speed (m/s)
MS_1	F	55	66.1	150.0	29.4	0.65
MS_2	F	40	61.2	165.0	22.5	0.65
MS_3	M	62	77.7	162.0	29.6	0.50
MS_4	M	37	130.7	181.0	39.9	0.35
MS_5	M	45	124.2	178.0	39.2	0.75
MS_6	M	28	82.5	194.5	21.8	0.50
CP_1	F	26	44.9	151.0	19.7	0.50
CP_2	M	17	69.5	162.0	26.5	0.15
CP_3	M	18	68.3	164.0	25.4	0.30
CP_4	M	55	88.9	172.0	30.1	0.45
Stroke_1	F	37	68.0	160.0	26.6	0.10/0.30*
Stroke_2	F	53	48.3	156.0	19.8	0.60
SCI	M	48	67.5	167.0	24.2	0.85
TBI	M	35	89.2	173.0	29.8	0.75
Elderly Faller	M	76	85.7	170.0	29.7	0.30
IND	F	58	83.5	158.0	33.4	0.10

MS = Multiple Sclerosis); CP = Cerebral Palsy; SPI = Spinal Cord Injury; TBI = Traumatic Brain Injury;

IND = Idiopathic Neurologic Disorder. * Speed of the first visit/speed of the second visit after two month.

11.2 Data Acquisition

The measurement of the kinematic, kinetic and electromyographic data was performed using the inertial sensor array (tri-axial accelerometers – ADXL330 iMEMS), the dual-belt instrumented treadmill (Bertec Corporation, USA), and a surface EMG system (Delsys Inc., Boston, USA), respectively.

Subjects wore running shorts and comfortable T-shirts. Since a number of subjects had never walked on the treadmill, each of them was allowed to become familiar with the walking track before running the experiment. In order to reduce the error of the EMG signals, the skin was shaved and cleaned with alcohol swabs on the area where the surface EMG electrodes would be placed on. Sixteen surface EMG electrodes were placed on the back and both side of the lower extremity, and eight tri-axial accelerometers were also placed on the body, refer to Table 9-1 and Figure 9-2.

11.3 Results of Temporal Stride Variability

Table 11-3 concludes the stride variability with stride time, stance phase, swing phase, and double-stance phase for all able-bodied subjects.

Table 11-3: Stride Variability of Able-bodied Subjects

Able-bodied subjects	Stride Time (sec.)		Stance Phase (%)		Swing Phase (%)		Double-stance Phase (%)	
	mean±SD	CV	mean±SD	CV	mean±SD	CV	mean±SD	CV
F_1	0.875±.015	1.71	58.06±1.13	1.95	41.94±1.12	2.67	10.29±0.80	7.78
F_2	1.060±.016	1.51	61.10±1.01	1.65	38.90±1.01	2.60	12.03±0.78	6.48
F_3	1.009±.011	1.09	58.58±1.22	2.08	41.42±1.22	2.95	10.24±1.31	12.79
F_4	1.160±.023	1.98	61.75±1.80	2.92	38.25±1.71	4.47	12.53±0.87	6.94
F_5	1.050±.016	1.52	61.64±0.96	1.56	38.36±0.96	2.50	12.83±0.75	5.85
F_6	1.140±.023	2.02	62.57±1.31	2.09	37.43±1.31	3.50	13.44±0.72	5.36
F_7	1.154±.019	1.65	63.51±1.13	1.78	36.49±1.13	3.10	14.03±1.12	7.98
F_8	1.093±.018	1.65	62.30±1.02	1.64	37.70±1.12	2.97	13.55±0.98	7.23
F_9	0.978±.020	2.05	61.57±1.34	2.18	38.43±1.34	3.49	11.95±0.72	6.03
F_10	0.977±.011	1.13	60.75±0.98	1.61	39.25±0.98	2.50	11.38±0.72	6.33
M_1	1.135±.022	1.94	62.01±1.06	1.71	37.99±1.06	2.79	12.58±0.73	5.80
M_2	1.158±.021	1.81	62.58±0.89	1.42	37.42±0.89	2.38	13.07±0.54	4.13
M_3	1.100±.021	1.91	62.27±1.48	2.38	37.73±1.48	3.92	11.42±0.76	6.66
M_4	0.993±.018	1.81	62.27±1.25	2.01	37.73±1.25	3.31	13.13±0.68	5.18
M_5	1.139±.026	2.28	62.24±1.86	2.99	37.76±1.86	4.93	13.65±0.82	6.01
M_6	1.071±.021	1.96	61.90±1.17	1.89	38.10±1.17	3.07	13.25±0.99	7.47
M_7	1.063±.018	1.69	61.38±0.91	1.48	38.62±0.91	2.36	12.12±0.70	5.78
M_8	1.074±.021	1.96	63.92±1.32	2.06	36.08±1.32	3.66	14.47±0.74	5.11
M_9	1.055±.014	1.33	62.79±0.88	1.40	37.21±0.88	2.37	13.74±0.56	4.08
M_10	1.000±.016	1.60	62.74±1.13	1.80	37.26±1.13	3.03	13.31±0.89	6.69
M_11	1.130±.020	1.77	61.54±1.17	1.90	38.46±1.17	3.04	12.16±0.92	7.57
M_12	1.142±.019	1.66	62.21±1.03	1.66	37.79±1.10	2.91	13.41±0.77	5.74

Note: The values of stride time/stance phase/swing phase in the table are the average of right and left for each able-bodied subject.

Table 11-4 concludes the stride variability with stride time, stance phase, swing phase, and double-stance phase for all patient subjects.

Table 11-4: Stride Variability of Mobility-related Impaired Subjects

Patient subjects		Stride Time (sec.)		Stance Phase (%)		Swing Phase (%)		Double-stance Phase (%)	
		Mean	CV	Mean	CV	Mean	CV	Mean	CV
		±SD		±SD		±SD		±SD	
MS_1	R	1.085±.032	2.95	67.33±2.48	3.68	32.67±2.48	7.59	15.97	6.89
	L	1.086±.036	3.32	61.99±1.92	3.10	38.01±1.92	5.05	(1.10)	
MS_2	R	1.181±.035	2.96	70.94±2.67	3.76	29.06±2.67	9.19	18.79	9.74
	L	1.181±.039	3.30	64.03±2.22	3.47	35.97±2.22	6.17	(1.83)	
MS_3	R	1.850±.092	4.97	84.79±3.63	4.28	15.21±3.63	23.87	36.89	17.27
	L	1.854±.113	6.10	82.81±4.14	5.00	17.19±4.14	24.08	(6.37)	
MS_4	R	2.103±.145	6.90	74.10±2.17	2.93	25.90±2.17	8.38	23.85	8.09
	L	2.104±.161	7.65	71.02±2.37	3.34	28.98±2.37	8.18	(1.93)	
MS_5	R	1.133±.032	2.84	64.78±2.62	4.04	35.22±2.62	7.44	14.78	7.38
	L	1.133±.034	3.00	63.57±2.12	3.34	36.43±2.12	5.82	(1.09)	
MS_6	R	1.427±.084	5.89	67.99±4.34	6.38	32.01±4.34	13.56	19.61	13.36
	L	1.426±.085	5.96	69.70±3.39	4.86	30.30±3.39	11.19	(2.62)	
CP_1	R	1.269±.060	4.73	63.78±2.10	3.29	36.22±2.10	5.80	13.97	8.66
	L	1.269±.059	4.65	66.58±2.48	3.73	33.42±2.18	6.52	(1.21)	
CP_2	R	2.654±.144	5.43	77.22±1.59	2.06	22.78±1.59	6.98	25.85	10.25
	L	2.658±.173	6.51	70.52±2.63	3.73	29.48±2.63	8.92	(2.65)	
CP_3	R	1.834±.059	3.22	78.52±1.51	1.92	21.48±1.51	7.03	27.64	4.99
	L	1.835±.056	3.06	77.16±1.63	2.11	22.84±1.26	5.52	(1.38)	
CP_4	R	1.632±.054	3.31	67.23±1.82	2.71	32.77±1.82	5.55	19.89	7.59

	L	1.632±.053	3.25	65.69±1.39	2.12	34.31±1.39	4.05	(1.51)	
Stroke1-1	R	2.975±.191	6.42	80.48±1.58	1.96	19.52±1.58	8.09	55.46	5.50
	L	2.975±.193	6.49	86.24±1.17	1.36	13.76±1.17	8.50	(3.05)	
Stroke1-2	R	1.636±.050	3.06	70.29±1.85	2.63	29.71±1.85	6.23	28.12	7.15
	L	1.636±.049	3.00	76.37±1.29	1.69	23.63±1.29	5.46	(2.01)	
Stroke2	R	1.227±.044	3.59	67.74±3.51	5.18	32.26±3.51	10.88	16.53	8.23
	L	1.227±.042	3.42	66.05±2.95	4.47	33.95±2.95	8.69	(1.36)	
SCI	R	1.079±.025	2.32	63.75±1.91	3.00	36.25±1.91	5.27	16.07	8.21
	L	1.079±.026	2.41	66.47±2.05	3.08	33.53±2.05	6.11	(1.32)	
TBI	R	1.186±.039	3.29	67.73±2.57	3.79	32.27±2.57	7.96	16.70	7.96
	L	1.187±.044	3.71	64.68±1.94	3.00	35.32±1.94	5.49	(1.33)	
Elderly	R	1.346±.064	4.76	76.31±1.79	2.35	23.69±1.79	7.56	29.60	7.16
Faller	L	1.346±.076	5.65	73.22±2.40	3.28	26.78±2.40	8.96	(2.12)	
IND	R	3.640±.502	13.79	90.83±2.94	3.24	9.17±2.94	32.06	42.71	49.24
	L	3.643±.448	12.30	85.93±5.10	5.94	14.07±5.10	36.25	(21.03)	

MS = Multiple Sclerosis); CP = Cerebral Palsy; SPI = Spinal Cord Injury;

TBI = Traumatic Brain Injury; IND = Idiopathic Neurologic Disorder.

11.4 Study of Multiple Sclerosis

- **Multiple Sclerosis Case #1 (MS1)**

Subject is a 55 year old female who was diagnosed with fairly mild multiple sclerosis four years ago (2006). From observation at this point of time, she had some amount of wobbliness in her gait. She received medical treatment for Relapsing-Remitting MS and secondary progressive MS with relapses, the *Beta interferon* injection for every other day. This

patient was tested with barefoot walking on the instrumented treadmill without any assistive devices or harness support at a speed of 0.65 m/s.

Figure 11-1 illustrates the stride-to-stride fluctuations over 100 strides of this MS subject (MS1), compared with a healthy female subject. In the figure, the stride variables change from one stride to the next.

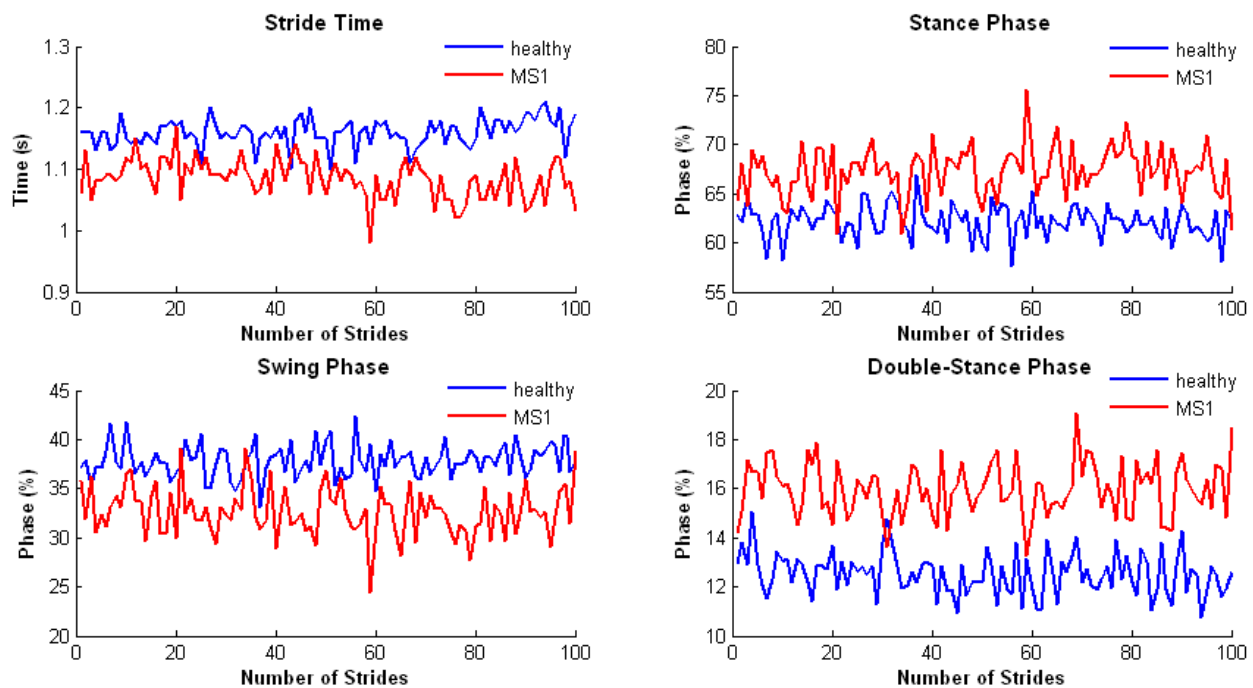


Figure 11-1: Stride variability of healthy subject and a multiple sclerosis case 1.

MS1- Multiple Sclerosis Case 1

Figure 11-2 shows the ground reaction force pattern (GRF) in a gait cycle of the MS1 subject, compared with the averaged GRF in ten healthy female subjects. The magnitudes of the GRF were normalized based on the body mass of each subject (%BW).

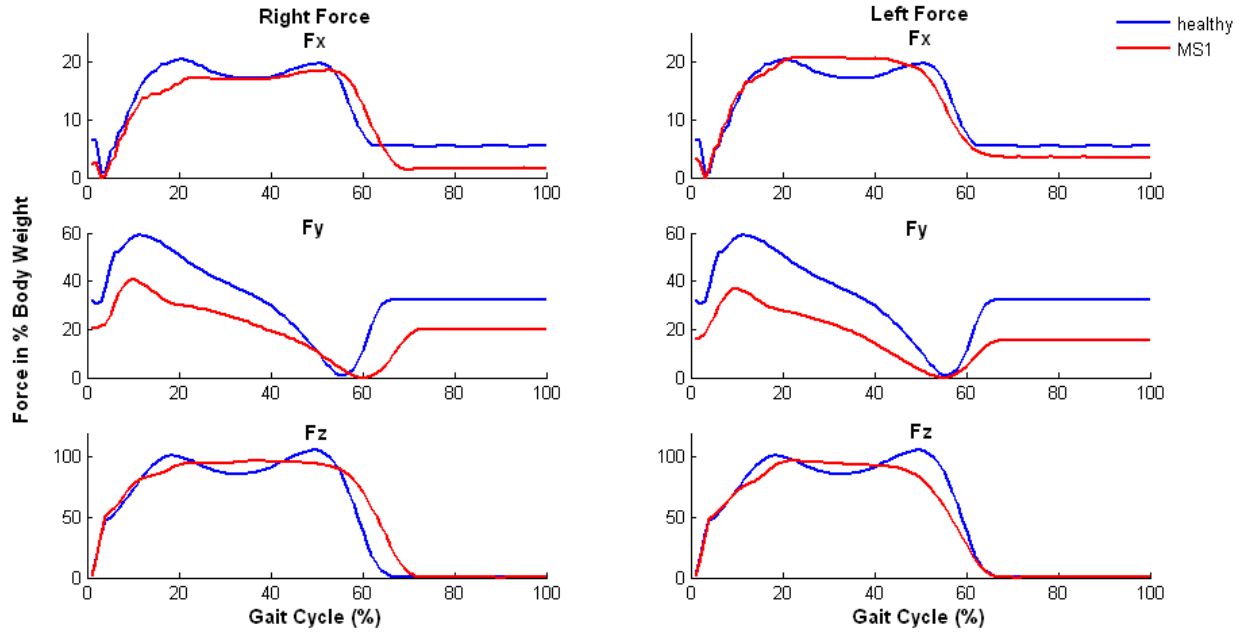


Figure 11-2: Right and left ground reaction forces in 3-D in MS1. Mediolateral (Fx)/anterioposterior (Fy)/vertical (Fz), compared between averaged healthy-female subjects and a female multiple sclerosis (MS-1). Note: the y axis is the normalization of the magnitudes of force values by body weight of the each subject (%BW), and the x axis is a full gait cycle in %.

Fuzzy similarity relationships are obtained from Equation 8.5 and illustrated in Figure 11-3, which shows the fuzzy similarity relationships (the mean values of the force signals during the seven gait phases of the gait cycle) of a female subject with Multiple Sclerosis (MS1), for comparison of left and right symmetrical approach.

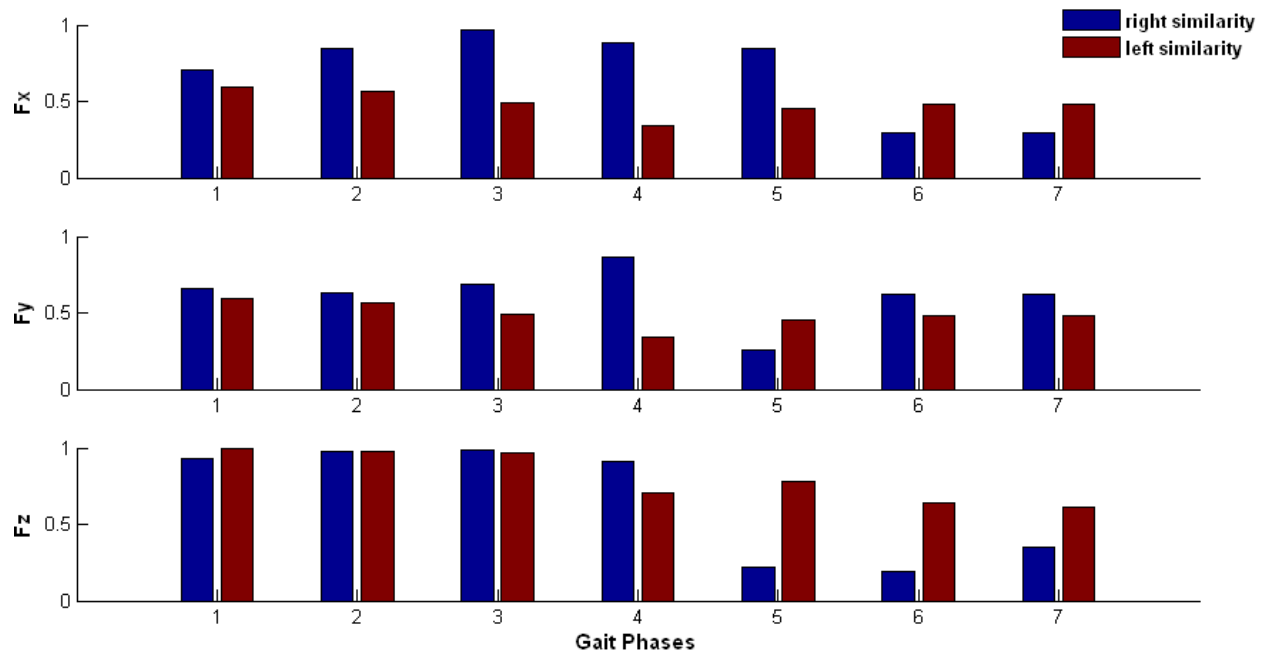


Figure 11-3: Comparison of grade of similarity between right and left GRFs in MS1.

Figure 11-4 shows the electrical muscle activity pattern in a gait cycle of the MS1, compared with the averaged muscle activity in ten healthy female subjects. Both right and left EMG signals of the MS1 subject are shown in this figure.

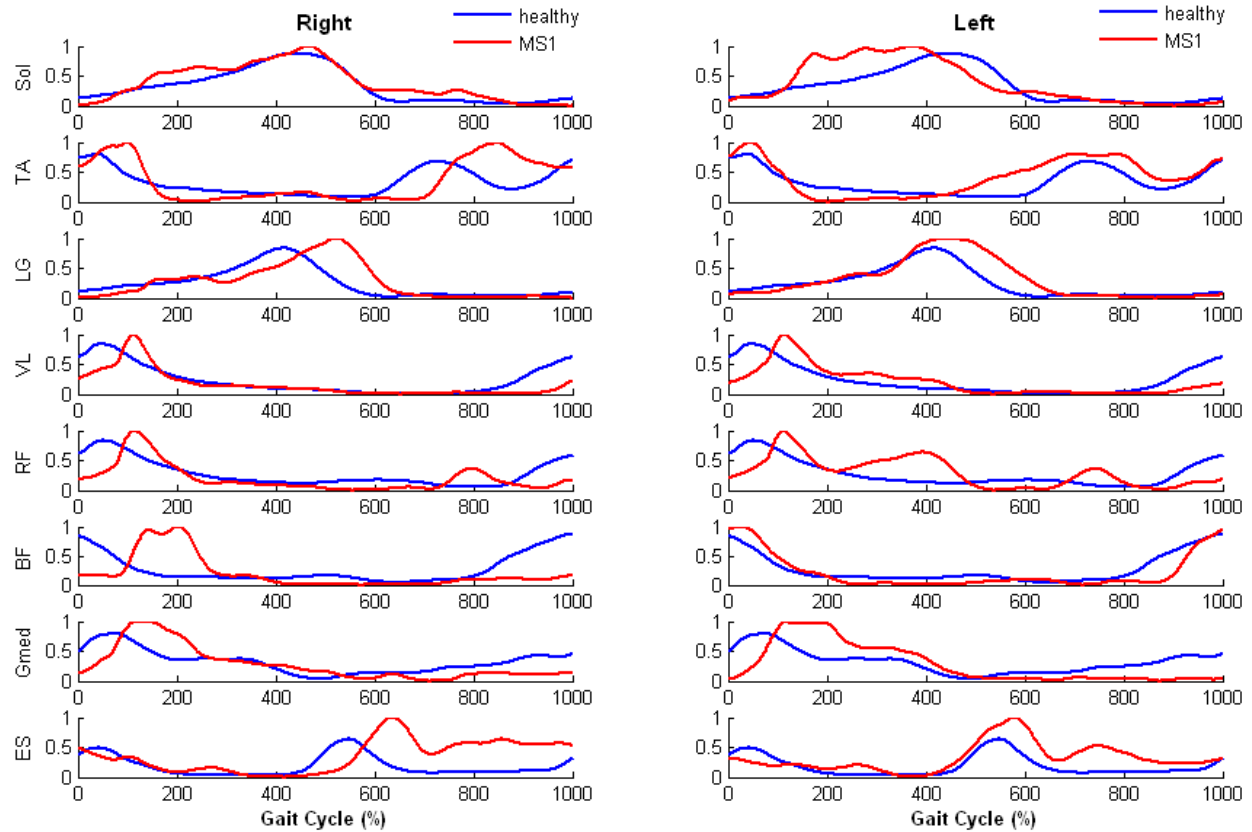


Figure 11-4: Average EMG activity of the eight muscles in a gait cycle in MS1 compared to averaged healthy female control group. (Note: the EMG sample frequency was 1000 Hz.)

Fuzzy similarity relationships are obtained from Equation 8.5 and illustrated in Figure 11-5, which shows the fuzzy similarity relationships (the mean values of the EMG signals during the seven gait phases of the gait cycle) of a this female subject with Multiple Sclerosis, for comparison of left and right symmetrical approach.

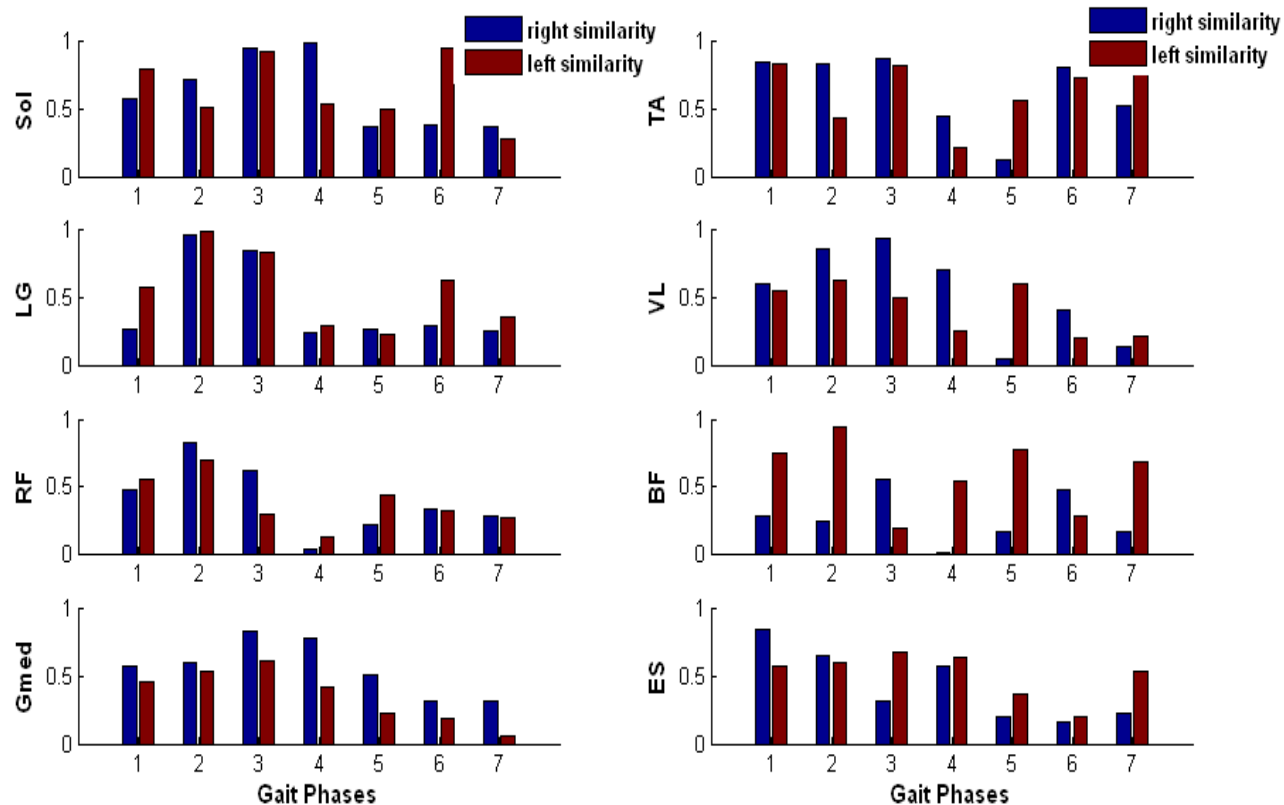
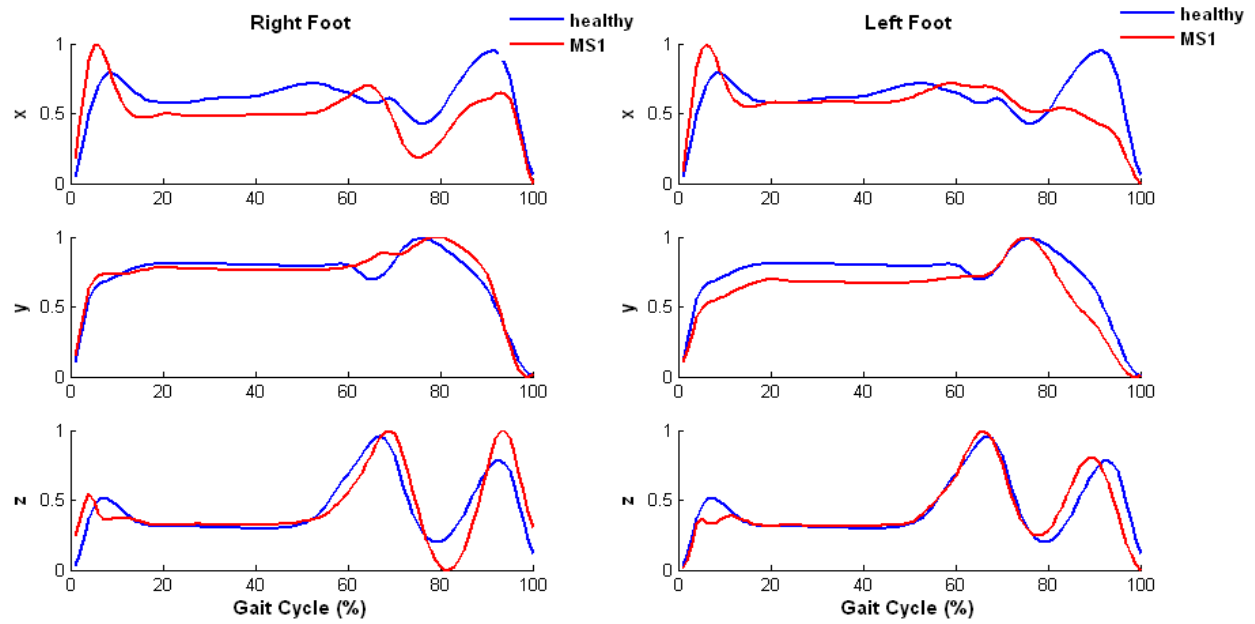


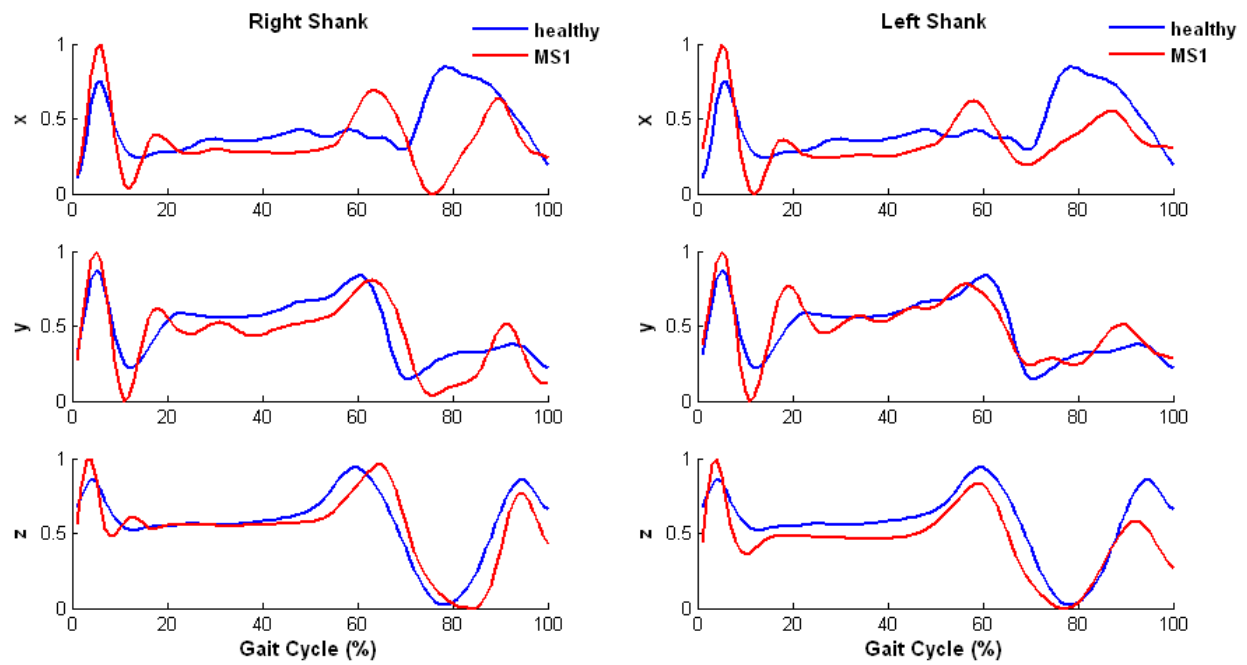
Figure 11-5: Comparison of grade of similarity between right and left EMG in MS-1.

Figure 11-6 shows the acceleration pattern in a gait cycle of the MS1, compare with the averaged acceleration signal pattern in ten healthy female subjects. Both right and left acceleration signals of MS1 subject were shown in this figure. Figure 11-7 shows the fuzzy similarity relationships (the mean values of the acceleration signals during the seven gait phases of the gait cycle) of this female subject with Multiple Sclerosis, for comparison of left and right symmetrical study.

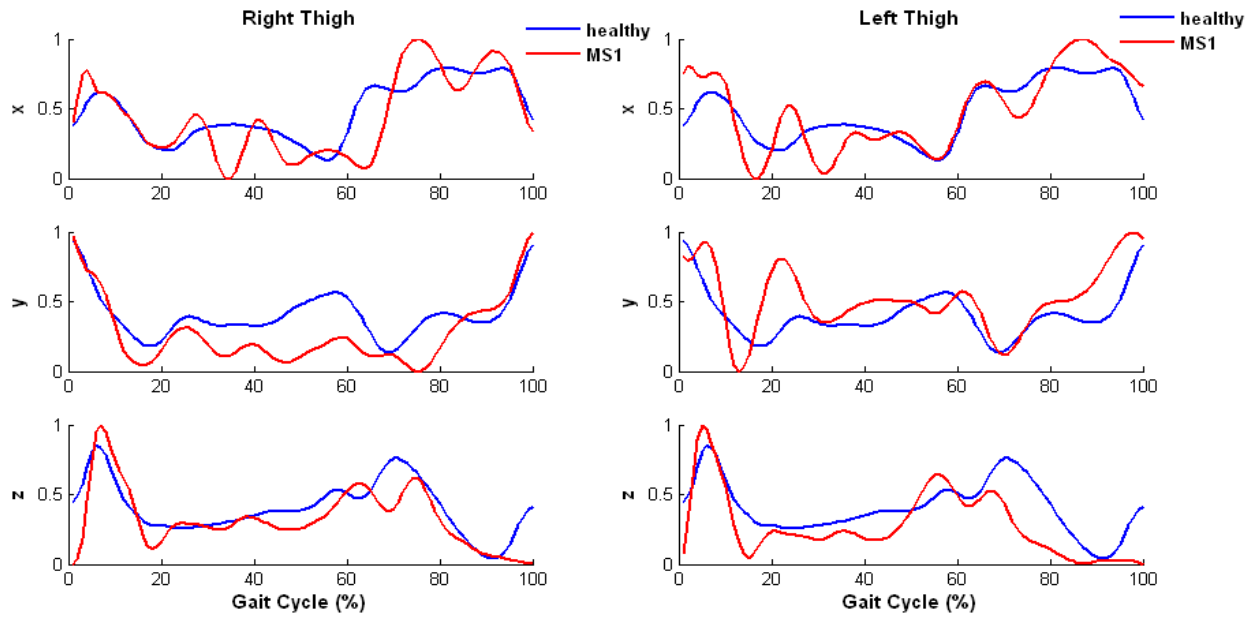
(A)



(B)



(C)



(D)

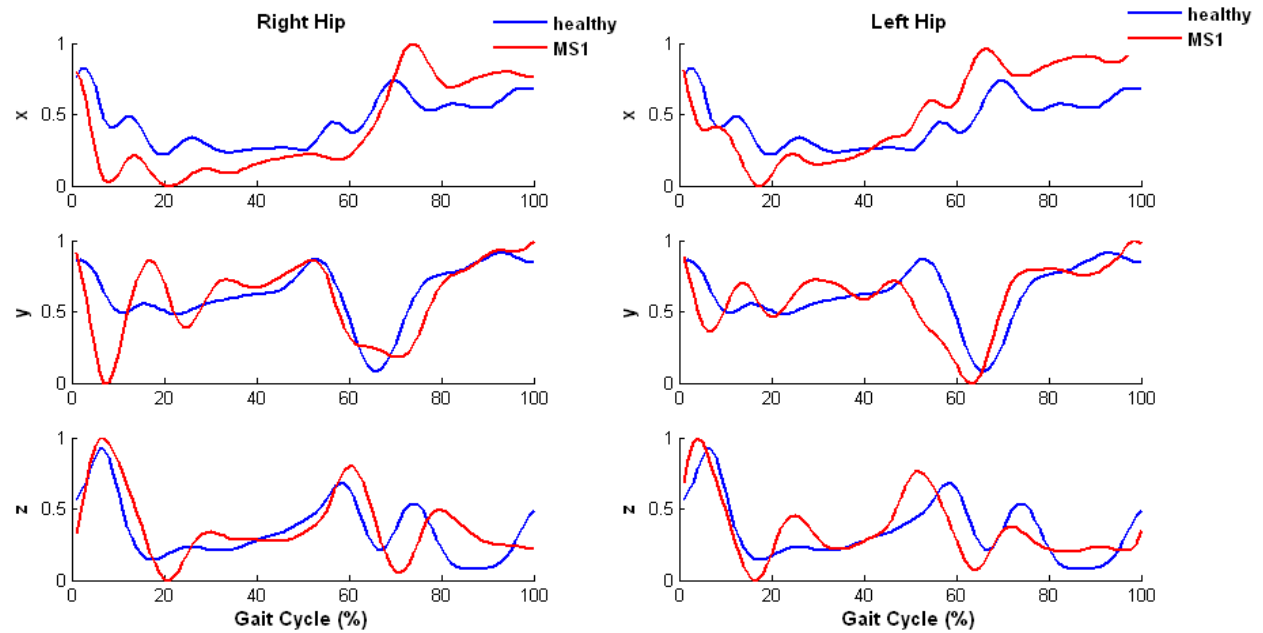


Figure 11-6: Comparison of acceleration signal pattern in a gait cycle between healthy subjects and MS1. (A) right and left foot acceleration pattern; (B) right and left shank acceleration pattern; (C) right and left thigh acceleration pattern; and (D) right and left hip acceleration pattern.

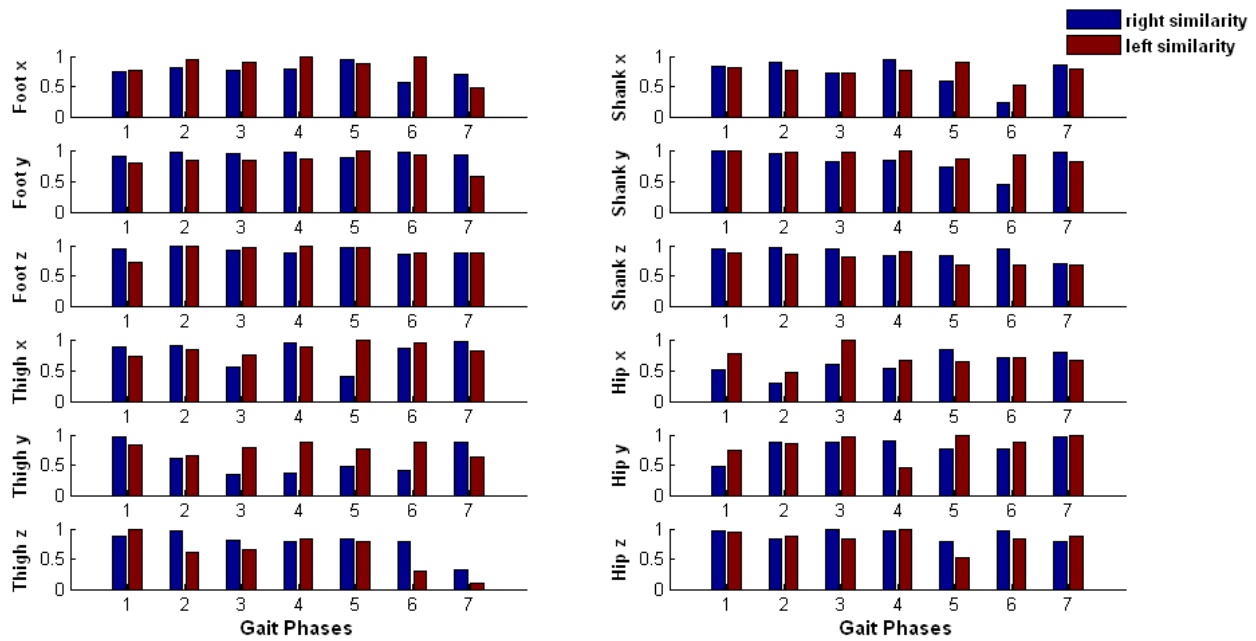


Figure 11-7: Comparison of grade of similarity between right and left acceleration in MS1.

Analysis:

(A) Temporal stride variability

The effects on stride variability are shown in Figure 11-1. Although this multiple sclerosis subject (MS1) has very mild symptoms, the stride-to-stride variability is increased compared with the healthy subject. Both the SD and CV were larger in MS1 compared with all the healthy subjects (Table 11-3 and Table 11-4). In addition, the variability increased dramatically after 60 strides during a three-minute walking trail. This may lead to the suspicion of some indications of occurrence of fatigue to increase variability between 60 to 100 strides. Finally, her gait had higher stance phase (67.33 on right leg) and double stance phase (15.97) than the healthy subjects (range 58.5~63.5% in stance phase, and 10.5~14.0% in double-stance phase), which also indicated some level of instability and/or walking with caution, and the severity of the symptoms on her left leg.

(B) 3-D ground reaction forces

The ground reaction forces of healthy subject and of the female subject with multiple sclerosis (MS1) are shown in 3-D in Figure 11-2. The force curve in the vertical direction, F_z , indicates that the MS1 has a flat foot contact, compared with the healthy subjects with clear first and second peaks forming this typical M-shape force pattern in the vertical direction. The vertical force curve also shows the longer ground contact duration on the right foot (the stance phase) in MS1. The able-bodied subjects depict a clear force curve that illustrates the weight transfer from the heel to the mid-foot and the mid-foot to the ball of the foot for push-off. The MS1 subject shows smaller slope at the end of the stance phase or pre-swing phase which indicates the MS subject has no clear toe-off (foot clearance problems). By comparing the magnitude of the anterior-posterior force of the healthy subjects, the MS1 subject revealed the magnitude of this force was much lower. There was a significant difference between right and left in the mediolateral force that the curve of the right force in the MS1 subject was below the force in the healthy subject, and the curve of the left force in the MS1 subject was above the force in healthy subject.

Figure 11-3 depicts the grade of similarity for the MS1 subject. There were moderate similarities in vertical and mediolateral force, but much lower similarities in the anterior-posterior force, especially the left side force, showing the severe effect on that side of her gait.

(C) EMG activity patterns

Whereas the muscle contraction is very rapid in the able-bodied subjects, the Figure 11-4 shows that the MS1 subject exhibits some long-latency stretch reflex in the soleus muscle. EMG activity was found to be significantly greater in the MS1 subject compared to the healthy group during the initial swing phase of the gait for both right and left lateral gastrocnemius. The tibialis

anterior activity was significantly greater during early double-stance and early swing phase. The increased EMG activity that was apparent in the ankle plantar-flexor muscles in the MS subject is thought to be a mechanism to counteract balance deficits and may have implications for both fatigue and spasticity [109]. The EMG activity of the Erector Spinae was found to be greater in the MS1 than in healthy subjects, which is likely to be a factor in the instability during stance phase, as well as serving to reduce the risk of falling.

Figure 11-5 shows that there is least similarity of right rectus femoris/ biceps femoris in the pre-swing phase, the least similarity of right vastus lateralis in the initial swing phase.

(D) Acceleration pattern analysis

The acceleration curves in figure 11-6 show a gradual smooth progression through consecutive walking cycles for the able-bodied subjects, whereas there is an occurrence of a very sharp turning during transition events of the cycle with MS1 subject. Table 11-5 concludes the characteristics of each segment's accelerations compared with average healthy subjects.

Table 11-5: Characteristics of segment's accelerations in MS-1

	Right	Left
Foot x	Sharp rise in initial contact, much lower acceleration in swing phase.	Sharp rise in initial contact, no acceleration in swing phase.
Foot y	No deceleration phase after toe-off.	Lower magnitude during entire cycle
Foot z	Early sharp rise in initial contact and sharp rise in the terminal swing.	Lower acceleration in initial contact, early acceleration in terminal swing.
Shank x	Sharp rise in initial contact, small rise in mid-stance phase and pre-swing phase, lower and delayed acceleration in swing phase.	Same as right shank + some unstable acceleration in mid-stance phase.
Shank y	Sharp rise in initial contact, early rise in mid-	Sharp rise in initial contact, early

	stance phase and delayed deceleration on toe-off, small rise in terminal swing phase.	rise in mid-stance phase, small rise in terminal swing phase, instable acceleration during the mid- and terminal stance phase.
Shank z	Sharp rise in initial contact, delayed acceleration on toe-off, less acceleration in terminal swing phase.	Sharp rise in initial contact, less acceleration on toe-off, less acceleration in terminal swing phase.
Thigh x	Sharp rise in initial contact, instable during mid- and terminal stance phase, delayed sharp rise on toe-off, sharp rise in terminal swing phase.	Sharp rise in initial contact, instable in mid- and terminal stance phase, sharp rise in terminal swing phase.
Thigh y	Large deceleration in early stance phase, instable during entire stance phase, sharp rise in terminal swing phase.	Sharp deceleration in early stance phase, sharp rise in mid-stance phase, early rise in terminal swing phase.
Thigh z	Sharp rise in initial contact, instable throughout the rest of the stance phase, continue decrease in swing phase without terminal rise which can be seen in healthy subjects.	Sharp rise and decrease in initial contact, instable during the rest of the stance phase, early deceleration in swing phase without terminal rise.
Hip x	Sharp deceleration in initial contact, delayed sharp rise on toe-off.	Sharp deceleration in initial contact, early sharp rise on toe-off.
Hip y	Sharp deceleration in initial contact, instable in stance phase, delayed acceleration in swing phase, there is a rise on the end of terminal swing phase.	Sharp deceleration in initial contact, instable in stance phase, early deceleration in terminal stance phase, and early acceleration after toe-off, rise on end of terminal swing phase.
Hip z	Sharp rise in initial contact, delayed deceleration on toe-off, delayed acceleration in swing phase.	Early sharp acceleration in initial contact, early rise on toe-off.

Figure 11-7 shows the least similarity on both right and left thigh vertical accelerations in terminal swing phase. There are small similarities on right shank x in the mid-swing phase and right hip x in the mid-stance phase. The rest shows moderate to high similarities through entire gait cycle, which indicate the mild symptoms of this female multiple sclerosis patient.

- **Multiple Sclerosis Case #6 (MS6)**

Subject is a 29 year old male, was diagnosed with multiple sclerosis in September 2009. He was a basketball player before diagnosis. He had right leg tremor. Medication was *Naltrexon* 4.5mg per day for the treatment of multiple sclerosis by preventing relapses and reducing the progression of the MS. The temporal stride variability, pattern of GRF, EMG, and acceleration, and their similarity of MS6 are shown in the Appendix IX (Figure AIX-1 to Figure AIX-7, and Table AIX-1).

(A) Summary of Stride variability

In Figure AIX-1, the stride-to-stride variability was greatly increased in all temporal stride variables (stride time, stance phase, swing phase, and double-stance phase) in the MS6 subject, especially after 30 strides during the three-minute walking trail. This shows the higher level of the instability and severity of the symptoms in MS6, compared with the female multiple sclerosis patient (MS1). In addition, the subject's gait has longer stance and double-stance phase, just like that of the MS1.

(B) Summary of GRF

In Figure AIX-2, MS6 subject shows flat foot contact without two peaks in the vertical GRF. In anterior-posterior plane, there are much lower magnitudes of GRF compared with the healthy subjects. In mediolateral plane, GRF of MS6 has a delayed rise at the time of initial contact.

In Figure AIX-3, MS6 subject shows smaller grade of similarities during swing phases in anterior-posterior GRF (caused by lower magnitudes of GRF), and smaller similarities during initial and mid-swing phases in the vertical GRF (caused by longer stance phase) on both right and left legs.

(C) Summary of EMG patterns

Figure AIX-4 shows there is a longer latency stretch reflex in the left soleus, and some levels of spasticity in the right soleus. EMG activity was found to be significantly greater in MS6 during the initial swing phase for both right and left tibialis anterior. There was greater EMG activity in MS6 for both right and left lateral gastrocnemius. There was a greater EMG activity on left vastus lateralis during the single-support stance phase. There was a level of spasticity for both right and left rectus femoris during initial swing. There was greater EMG activity in MS6 for right and left biceps femoris during terminal swing. There was greater EMG activity in on both right and left gluteus medius during stance phase, and greater activity in right gluteus medius during swing phase. The erector spinae muscles show much greater activities compared with the healthy subjects.

Figure AIX-5 shows the grade of similarity of all EMG activities of MS6. The left tibialis anterior, vastus lateralis, and biceps femoris shows significant small similarities during mid- and terminal stance phases, whereas right rectus femoris and gluteus medius shows small similarities during initial swing and mid-swing phases.

(D) Summary of acceleration

The characterization of acceleration in MS6 subject can be found in the Table AIX-1 in Appendix IX. In Figure AIX-7, both right and left thigh and hip show much lower similarities in

the anterior-posterior plane and mediolateral plane, respectively. The rest have moderate to high grades of similarities during seven gait phases.

- **Conclusion of Multiple Sclerosis**

Feature analysis for multiple sclerosis are concluded in Table 11-6, based on all six MS subjects (MS-2, MS-3, MS-4, and MS-5 and shown in Appendix V, VI, VII, VIII, respectively). The table describes the important characteristics of MS found from the results and analysis in this study.

Table 11-6: Characteristics of Multiple Sclerosis

Feature	Characteristics
Stride Variability	MS has increased variability, the more or less depends on the severity of the symptoms. Stride variability dramatically increased from the occurrence of the functional fatigue. This increased temporal variability indicates that the MS subjects have some levels of fall risks or walking with cautious due to common symptoms of foot-drops and tremors. Study of stride variability has the most advantages that it is easy to find out the time of functional fatigue occurring in each individual MS subjects.
Ground Reaction Force (GRF)	In vertical direction, MS subjects have no M-shaped GRF showing in the healthy subject. MS patients showed more or less flat-foot contact the ground with shortened duration of the peak seen in the sever cases. In anterior-posterior direction, MS subjects show lower GRF than

	<p>healthy subjects. This may be due to the slower speed in MS patients, but may also indicate the less force generated from muscles (for example the quadriceps muscle group) and other internal forces.</p> <p>In mediolateral direction, MS also shows some lower force compared with healthy subjects. The mediolateral postural instability has been suggested as a risk factor for falls, the weak GRF in this direction may also be one of the reasons that the stride variability was increased in MS subjects.</p>
Electromyography (EMG)	<p>Soleus and gastrocnemius are ankle plantar flexors, and thought to be stabilizing the foot and knee during the stance phase of the gait. MS subjects show increased EMG activity in the stance phase which may be a mechanism to counteract balance deficits.</p> <p>Tibialis anterior is an ankle dorsiflexor and most active at heel strike and prevent “foot-slap”. There was a delay in maximum tibialis anterior activity at heel strike in MS patients which may be a factor in the instability during stance phase, and there were also weakness of the activity in the single support time as contributing to foot drop.</p> <p>In addition, in most of MS subjects, tibialis anterior activity was significant greater during early swing phase when it supposes to assists the toes in clearing the floor.</p> <p>Vastus lateralis and rectus femoris are extensor muscles of the knee and hip flexor. There was spasticity occurring in the single support time of the stance phase in most of the MS subjects.</p>

	<p>Biceps femoris is flexor of the knee. There was also spasticity in the stance phase in most of the MS subjects.</p> <p>Gluteus medius is hip abductor and stabilizer. There was increased EMG activity in mid-stance phase and early swing phase in some MS subjects.</p> <p>Erector spinae in the lower back is a group of stabilizers. There were higher activities in the loading response and initial swing phase which might due to the compensation mechanism for instable gait in most of the MS subjects.</p>
Segmental Acceleration	<p>A sharp rise in acceleration or deceleration in the initial contact and terminal swing phase appears in most of MS subjects which could be the results of foot-drop and a mechanism to counteract balance deficits.</p> <p>Inconsistent and lower acceleration occurs in affected in particular shank and thigh in anterior-posterior direction, especially with MS tremor subjects.</p> <p>In general, the acceleration pattern is closely associated with the GRF and EMG activity patterns. It is difficult to analyze them separately.</p>

11.5 Study of Cerebral Palsy

- **Cerebral Palsy Case #2 (CP2)**

Subject is a 17 year old male with spastic diplegic cerebral palsy. He had left hip arthritis and bilateral flat feet deformity. He had 5 degrees knee flexion contracture bilateral. Patient walked bare-foot on the treadmill with harness support at speed of 0.5 m/s.

Figure 11-8 illustrates the stride-to-stride fluctuations over 100 strides of this CP2 subject, compared with a healthy male subject. In Figure 11-8, the stride variables change from one stride to the next.

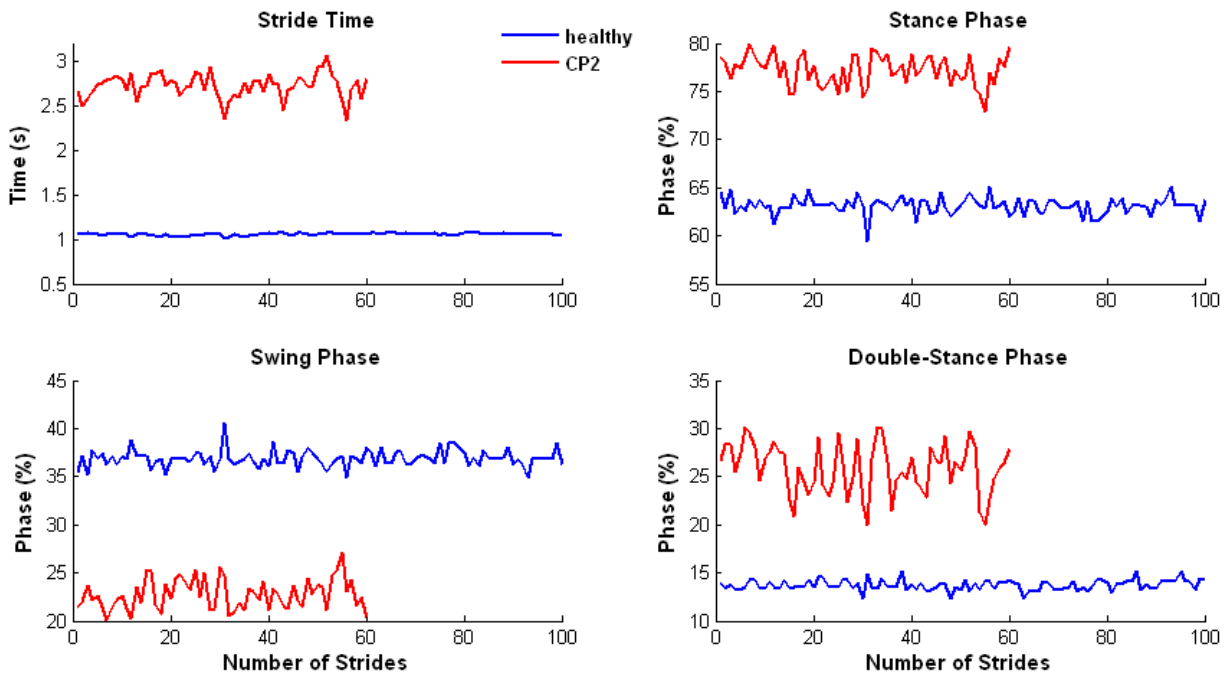


Figure 11-8: Stride variability of healthy subject and a male cerebral palsy case 2 (CP-2).

Figure 11-9 shows the ground reaction force pattern (GRF) in a gait cycle of the CP2 subject, compare with the averaged GRF in twelve healthy male subjects. The magnitudes of the GRF were normalized based on the body mass of each subject (%BW).

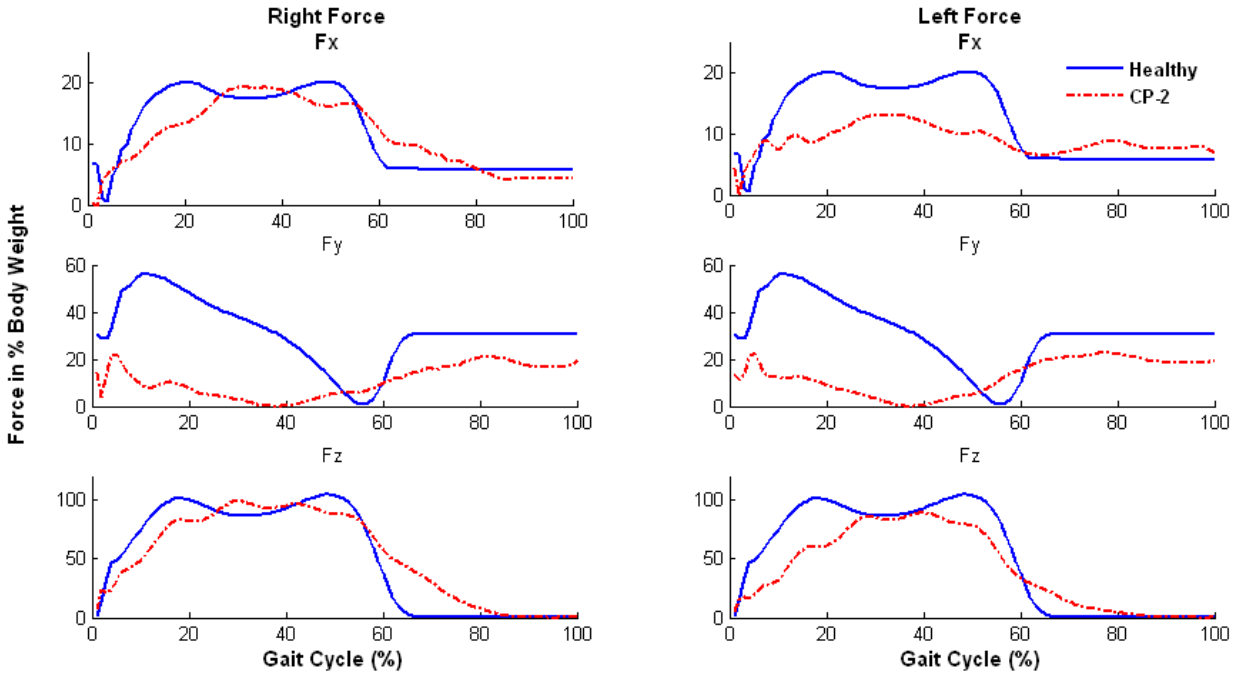


Figure 11-9: Right and left ground reaction forces in 3-D in CP-2: mediolateral (Fx)/anterioposterior (Fy)/vertical (Fz), compared between averaged healthy-male subjects and a male cerebral palsy patient (CP-2). Note: the y axis is the normalization of the magnitudes of force values by body weight of the each subject (%BW), and the x axis is a full gait cycle in %.

Fuzzy similarity relationships were obtained from Equation 8.5 and illustrated in Figure 11-10, which shows the fuzzy similarity relationships (the mean values of the force signals during the seven gait phases of the gait cycle) between healthy subjects and the CP2 subject, for comparison of left and right symmetrical approach.

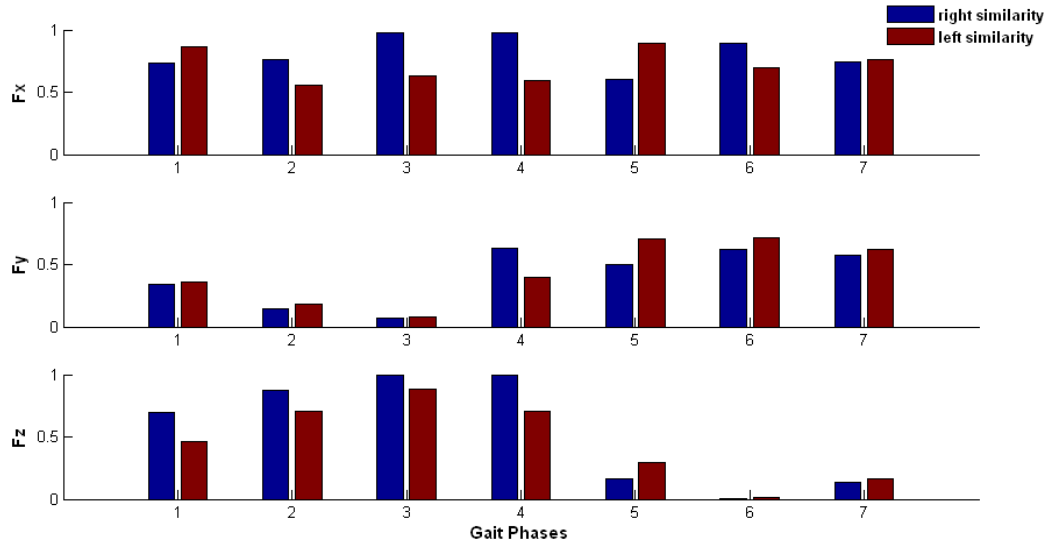


Figure 11-10: Comparison of grade of similarity between right and left GRFs in CP-2.

Figure 11-11 shows the electrical muscle activity pattern in a gait cycle of the CP-2, compare with the averaged muscle activity in twelve healthy male subjects. Both right and left sides EMG signals of CP-2 were shown in this figure.

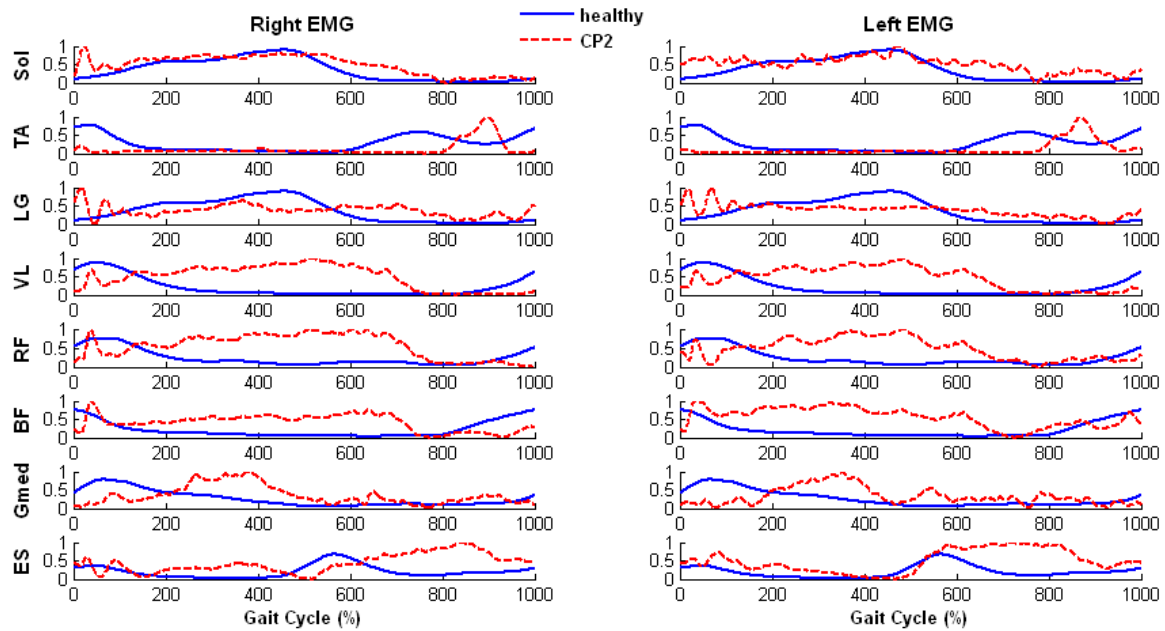


Figure 11-11: Average EMG activity of the eight muscles in a gait cycle in CP-2 compared to averaged healthy control group.

Fuzzy similarity relationships are obtained from Equation 8.5 and illustrated in Figure 11-12, which shows the fuzzy similarity relationships (the mean values of the EMG signals during the seven gait phases of the gait cycle) of CP-2, for comparison of left and right symmetrical approach.

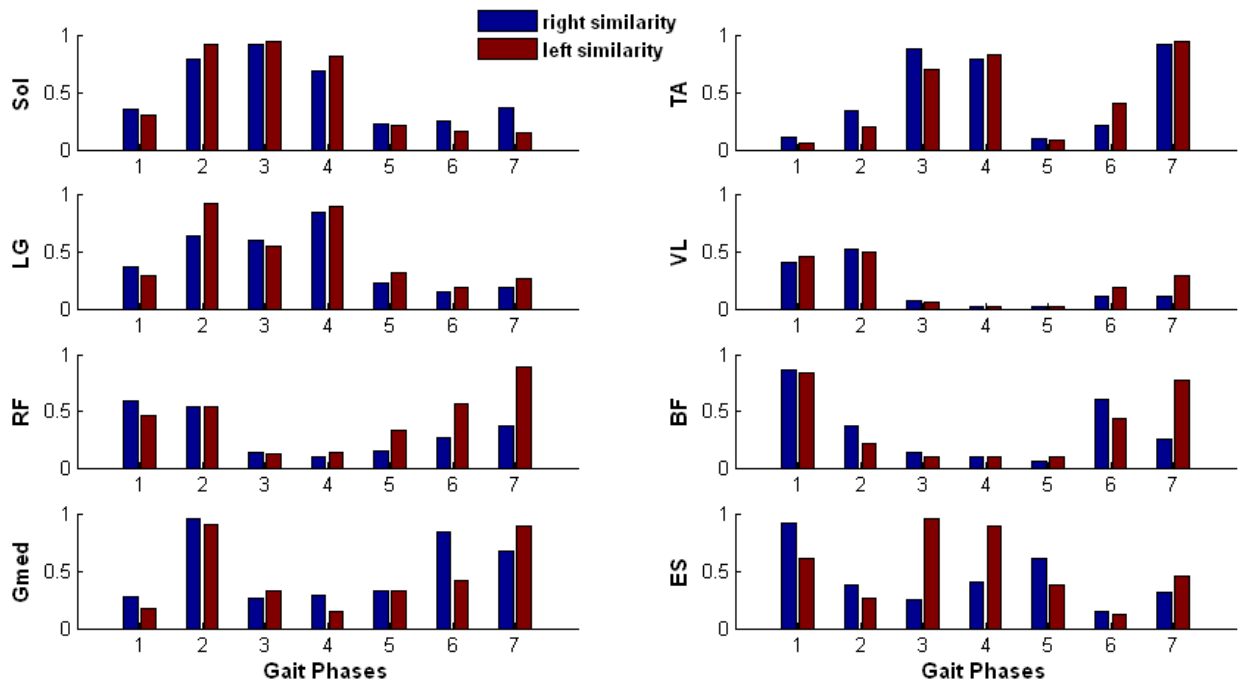
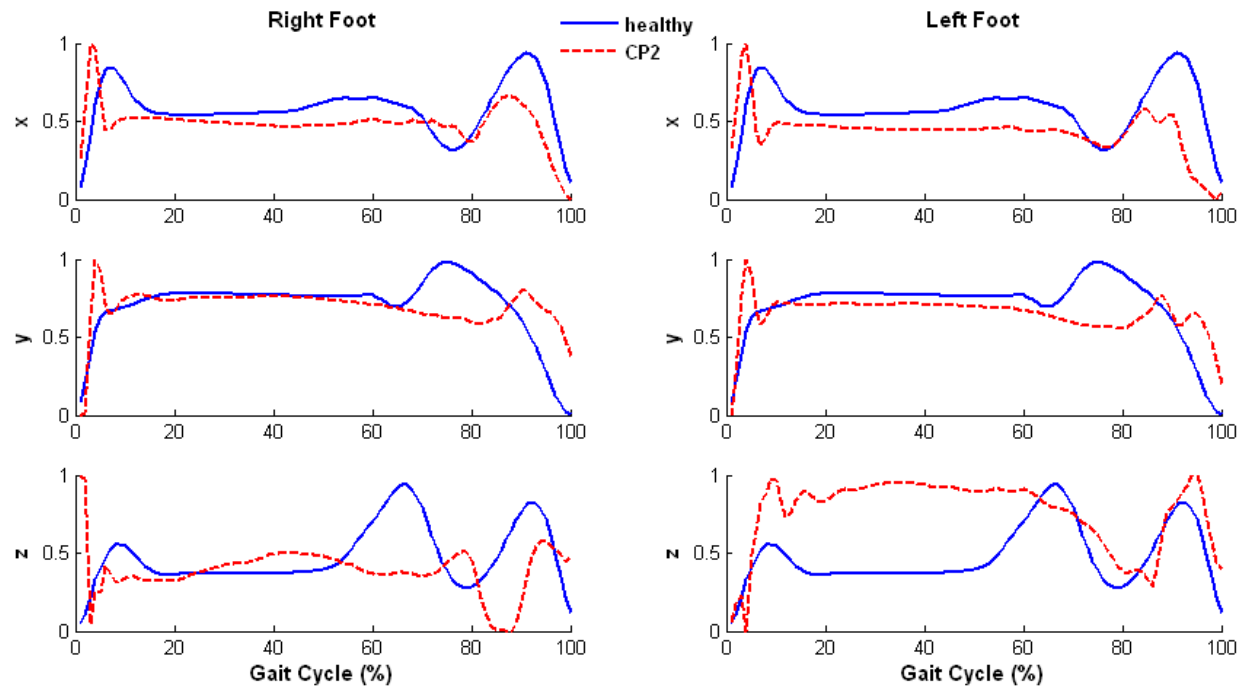


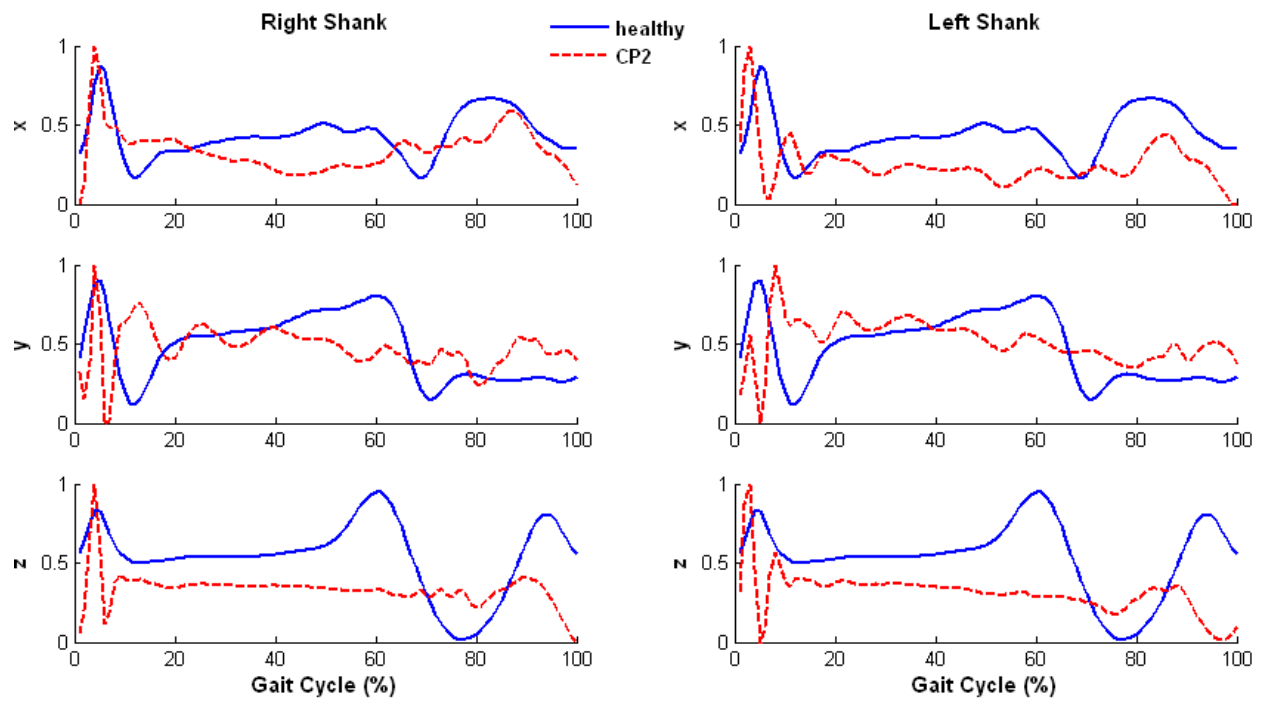
Figure 11-12: Comparison of grade of similarity between right and left EMG in CP-2.

Figure 11-13 shows the acceleration pattern within a gait cycle for the CP-2 subject as compared with the averaged acceleration pattern in twelve healthy female subjects. Both right and left EMG signals of CP-2 subject were shown in this figure. Figure 11-14 shows the fuzzy similarity relationships (the mean values of the acceleration signals during the seven gait phases of the gait cycle) of CP-2 subject for comparison of left and right symmetrical study.

(A)



(B)



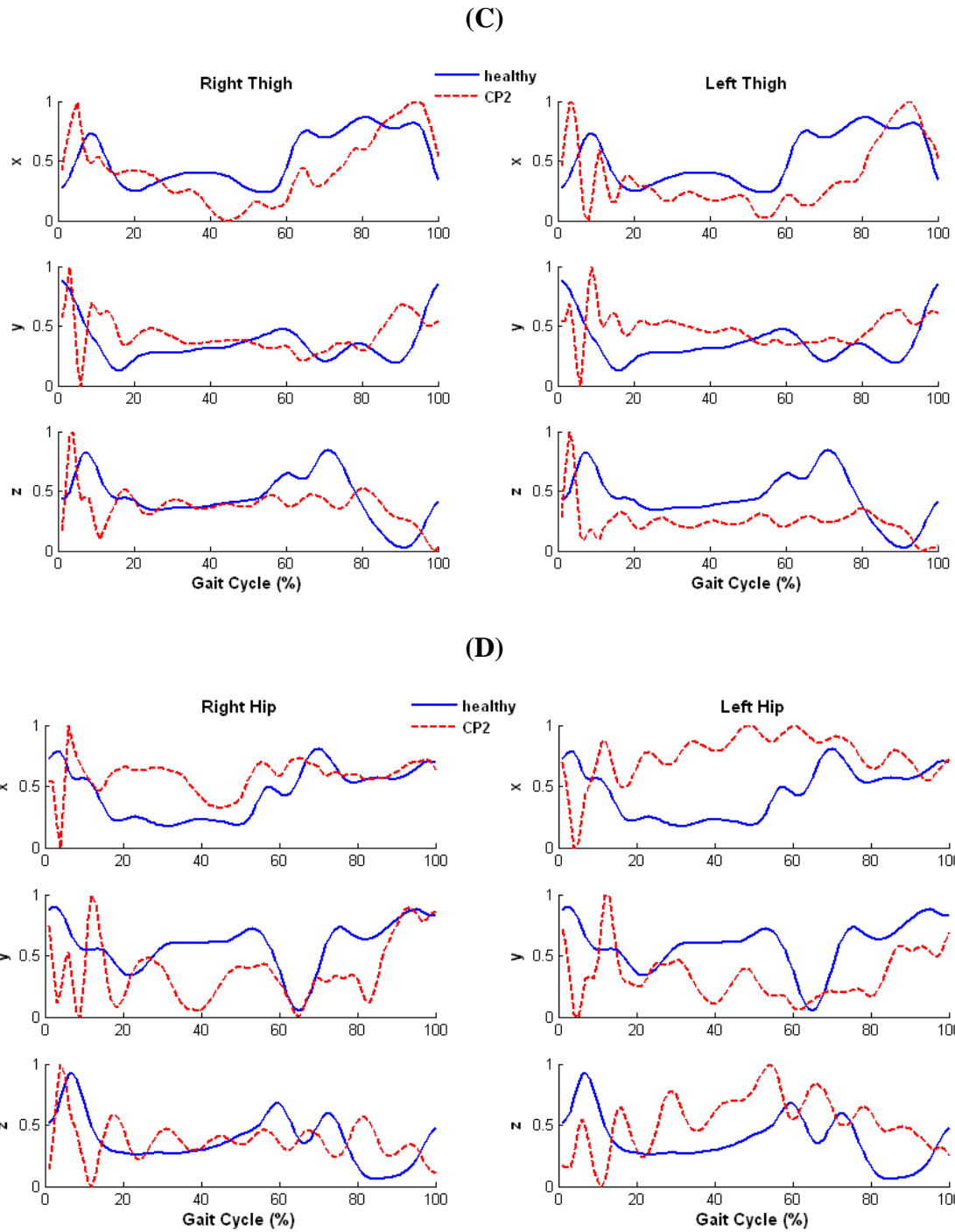


Figure 11-13: Comparison of acceleration signal pattern in a gait cycle between healthy subjects and CP-2. (A) right and left foot acceleration pattern; (B) right and left shank acceleration pattern; (C) right and left thigh acceleration pattern; and (D) right and left hip acceleration pattern.

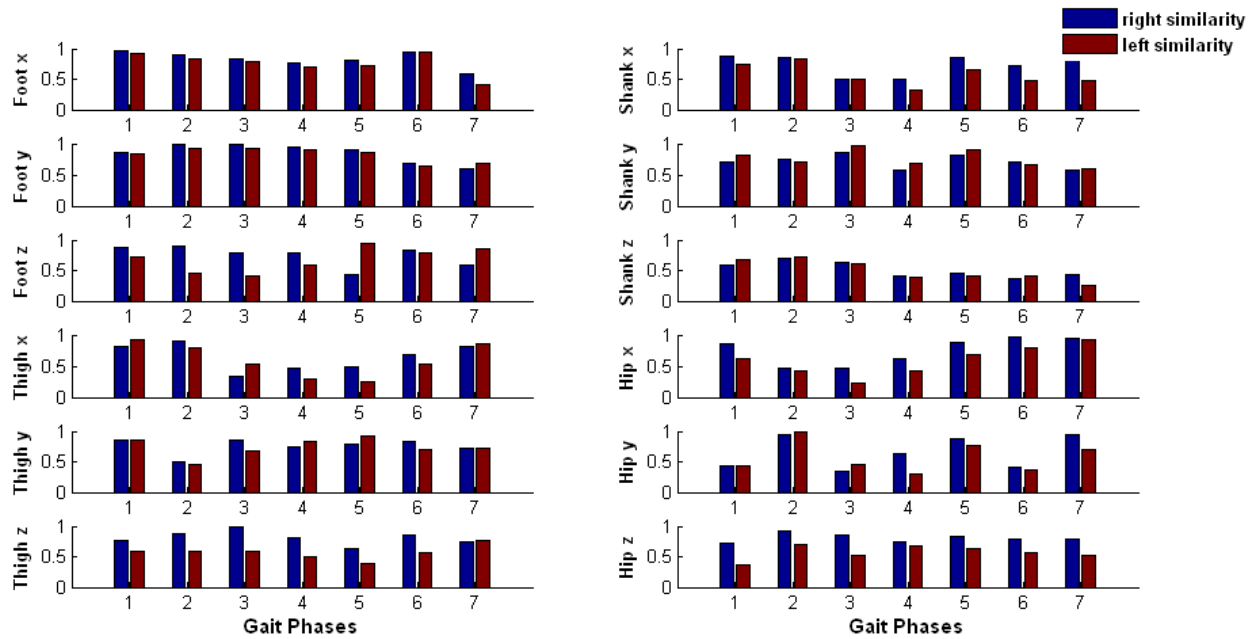


Figure 11-14: Comparison of grade of similarity between right and left acceleration in CP2.

Analysis:

(A) Temporal stride variability

There were only 60 strides found in three-minute walking trail from this cerebral palsy subject (CP2) due to the slow walking speed (0.5 m/s). Figure 11-8 depicts the higher variability of all these stride variables, compared with healthy subject. The subject exhibits much longer stride time, stance phase, and double-stance phase, whereas there were much shortened swing phase. The increased variability indicates the severe instability of this subject's gait even with the support of the harness.

(B) 3-D ground reaction forces

Figure 11-9 depicts the ground reaction force pattern of the CP2 subject as compared with averaged healthy subjects. In the vertical direction, this CP2 subject has much longer stance phase which causes the least grade of similarity in initial and mid-swing phases, and with only

one short-time peak around the time of 30% of the gait cycle, indicates that he has no smooth ground contact from heel to toe. In anterior-posterior direction, the CP2 subject shows much lower forces throughout the full gait cycle. In mediolateral direction, the left leg had much lower force than his right leg, which indicated he had some severity of deformity on his left extremity or pain on the left side (i.e. left hip arthritis refer to the description of CP-2).

(C) EMG activity patterns

Table 11-7: Description of EMG patterns of CP-2

	Right	Left
Soleus	Spasticity appears in the initial contact and continues with higher muscle activity until toe-off. Significant small similarity appears in swing phases due to longer duration of the stance.	Same as right Sol, but with more serious instability EMG signals.
Tibialis Anterior (TA)	Muscle weakness appears from in the initial contact to the end of the stance phase. Spasticity appears immediately after toe-off. This typical EMG pattern causes significant small similarity in initial and initial-swing phases.	Same as right TA.
Gastrocnemius Lateralis (LG)	Spasticity appears initial contact, mid-stance and swing phases, which results in significant small similarity during these phases.	Same as right LG.
Vastus	Weakness appears in the initial contact and terminal	

Lateralis (VL)	swing phase, spasticity appears after single support in the stance phase which results in significant small similarity appears in phase 3,4, and 5.	Same as right VL.
Rectus Femoris (RF)	Same as right VL	Same as right RF.
Biceps Femoris (BF)	Spasticity appears begins in the initial contact, and continues till the end of the stance phase, which results in small grade of similarity in later stance phase. Muscle weakness appears in the terminal swing phase. Note this weakness is more serious than the left leg.	Same as right BF.
Gluteus Medius (Gmed)	Muscle weakness appears in the loading response. Spasticity appears about 20~85% of the gait cycle. Significant small similarity appears in phase 1, 3, and 4.	Same as right Gmed.
Elector Spinae (ES)	Spasticity appears almost the entire gait, especially the last 40% of the gait cycle. Significant small similarity appears in mid-swing phase.	Same as right ES.

(D) Acceleration pattern analysis

Table 11-7 concludes the characteristics of each segment's accelerations of CP-2, compared with average healthy subjects.

Table 11-8: Characteristics of segment's accelerations of CP-2

	Right	Left
Foot x	Sharp rise in initial contact, much lower magnitude in swing phase which results in small similarity in terminal swing phase.	Sharp rise in initial contact, lower acceleration in swing phase. Significant small similarity in terminal swing phase.
Foot y	Sharp rise in initial contact, delayed and lower magnitude in swing phase.	Same as right foot y.
Foot z	Early sharp rise in initial contact and lower magnitude through the rest of the cycle.	Sharp rise and continue with high magnitude in stance phase, causing smaller similarity in mid- and terminal stance phases, sharp rise in terminal swing phase.
Shank x	Sharp rise in initial contact, lower magnitude in the rest of the gait cycle, significant differences from the healthy in the terminal stance and pre-swing phase.	Same as right shank x.
Shank y	Sharp rise in initial contact, lower level of magnitude with instability in the rest of the gait cycle. Most significant differences appear in phase 4.	Same as right shank y.
Shank z	Sharp rise in initial contact, lower magnitude in the rest of gait cycle. Significant small similarity appears in sub-phases in swing.	Same as right shank z.
Thigh x	Sharp rise in initial contact, lower magnitude with some level of instability through the stance phase, rise in terminal swing phase. Significant small similarity appears in terminal stance phase.	Same as right thigh x. Significant small similarity appear in pre-swing and mid-swing phases.
Thigh y	Sharp rise in initial contact, high magnitude in mid-stance phase, early rise in the terminal swing phase. Significant differences appear in mid-stance phase.	Same as right thigh y.
Thigh z	Sharp rise in initial contact, lower magnitude in swing phase. Significant differences appear in initial swing.	Same as right thigh z, note the magnitude is lower than right during stance phase.

Hip x	Sharp rise in initial contact, higher magnitude with instability throughout the rest of the gait cycle. Significant small similarity appears in mid- and terminal stance phases.	Same as right hip x with much more instability might due to the deformity and pain from the arthritis.
Hip y	Instable magnitude in the beginning of stance phase, sharp rise at 15% of the cycle, lower magnitude in the rest of the gait cycle. Significant small similarity appears in initial contact, mid- and terminal stance, and mid-swing phase, which indicates the serious hip problems on this CP patient.	Same as right hip y with much lower magnitude in terminal swing phase, again results from the deformity and pain on the left hip.
Hip z	Sharp rise in initial contact, instable magnitude throughout the rest of the gait cycle.	Much lower magnitude in the initial contact due to the deformity which results in the small similarity in loading response, instable and higher magnitude in the rest of the gait cycle.

- **Conclusion of Cerebral Palsy**

The feature analyses for cerebral palsy subjects are illustrated Table 11-9, based on all four CP subjects (CP-1, CP-3, and CP-4 are shown in Appendix X, XI, XII, respectively). The table describes the important characteristics of CP found from the results and analysis in this study.

Table 11-9: Characteristics of Cerebral Palsy

Feature	Characteristics
Stride Variability	<p>CP has also increased variability, the more or less depends on the severity of the symptoms and with or without the assistance such as harness. This increased temporal variability may due to the joint deformity and abnormality of muscle tones, such as hypertonia and hypotonia. We can further investigate from the pattern analysis of GRF, EMG, and acceleration.</p>
Ground Reaction Force (GRF)	<p>In vertical direction, All CP subjects showed a much shortened peak in the stance phase which indicates the typical toe-walking gait. In anterior-posterior direction, CP subjects showed lower GRF than healthy subjects. This may be due to the slower speed in CP subjects, but may also indicate the less force generated from muscles and other internal forces from the joints in this direction.</p> <p>In mediolateral direction, CP subjects also showed some lower force compared with healthy subjects.</p>
Electromyography (EMG)	<p>Soleus and Tibialis anterior are agonist-antagonist muscle pair for ankle plantarflexation and dorsiflexion, respectively. All CP subjects showed opposite muscle activities of these two muscles to the healthy subjects. This could be the major deforming factor of the ankle in cerebral palsy, which causes toe-walking.</p> <p>Spasticity appears in the initial contact and rest of the stance phase or early swing phase in most of the CP subjects. Gastrocnemius was thought to be the primary equinus deforming factor of the ankle in cerebral palsy.</p> <p>Vastus lateralis and rectus femoris (muscle in the quadriceps) are extensor muscles of the knee and hip flexor. Spasticity of these two muscles occurs in the stance phase and early swing phase in most of the CP subjects.</p> <p>Biceps femoris is flexor of the knee. There was also spasticity in the mid-stance phase and early swing phase in most of the CP subjects.</p>

	<p>Gluteus medius is hip abductor and stabilizer. There was increased EMG activity in swing phase in most of CP subjects.</p> <p>Erector spinae in the lower back is a group of stabilizers. There were higher activities in the loading response and initial swing phase similar to MS subjects.</p>
Segmental Acceleration	<p>A sharp rise in acceleration or deceleration in the initial contact and terminal swing phase appears in most of CP subjects which could be the results of toe-walking (smaller surface contacting ground which results in more force generated in initial contact).</p> <p>Unstable acceleration occurs in particular thigh and hip in most of the CP subjects which indicates some levels of knee and hip contractures in these subjects.</p> <p>In addition, all CP subjects had some levels of foot clearance problems showing particularly in foot y acceleration at toe-off time, which might be result from a pelvic drip due to abductor insufficiency.</p>

Chapter 12: Comparative Analysis and Discussion

In the last chapter, the case studies of multiple sclerosis and cerebral palsy were shown separately. In this chapter, the two mobility-related impairments will analytically be compared. The characteristic of each disorder is categorized and explained in detail.

There will also be the analysis of another stroke subject, hemiparetic stroke subject, who make two visits for testing in an interval of two months (before and after the hydrotherapy).

12.1 Multiple Sclerosis (MS3) vs Cerebral Palsy (CP3)

- Comparison of Ground Reaction Forces

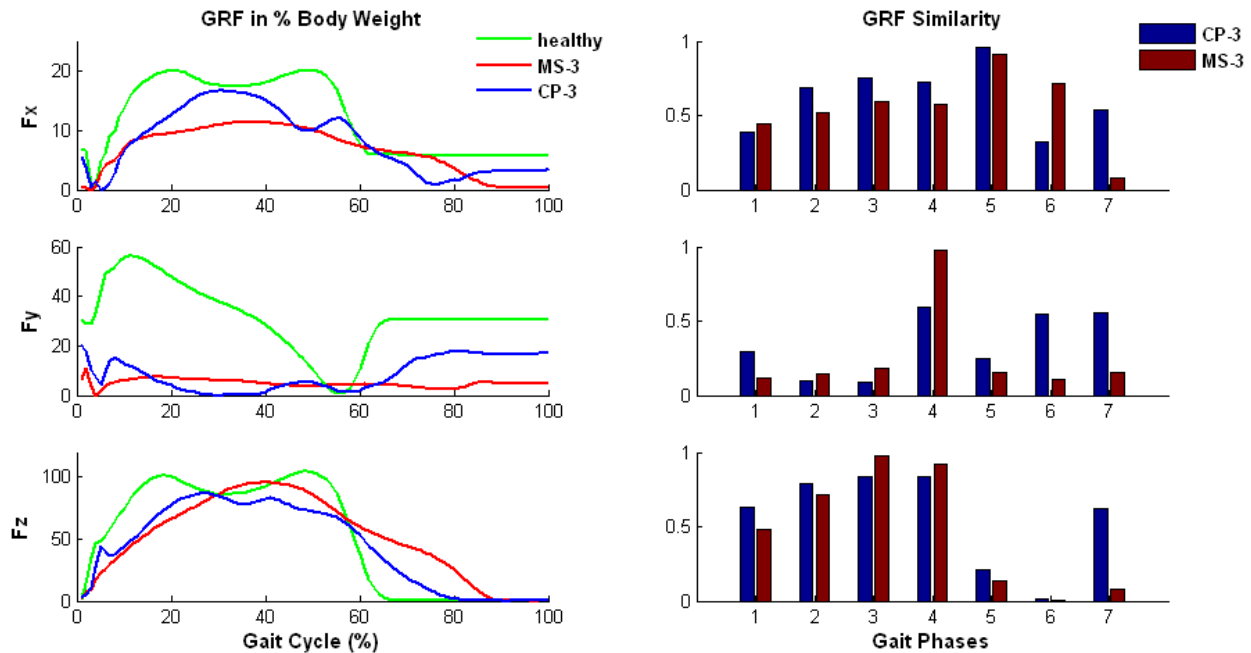


Figure 12-1: Comparison of ground reaction force and grade of similarity between MS-3 and CP-3.

- Comparison of EMG Muscle Activity

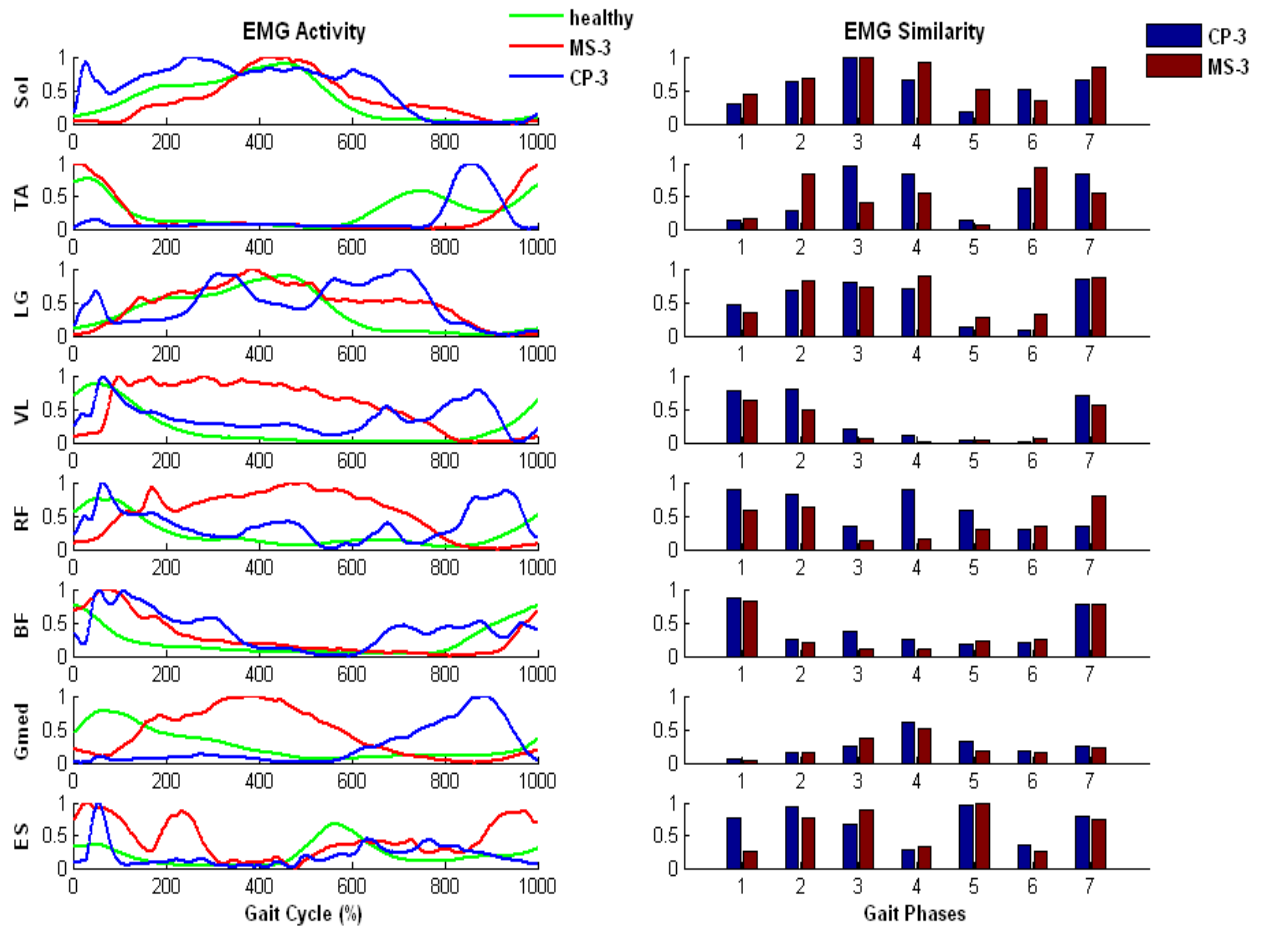
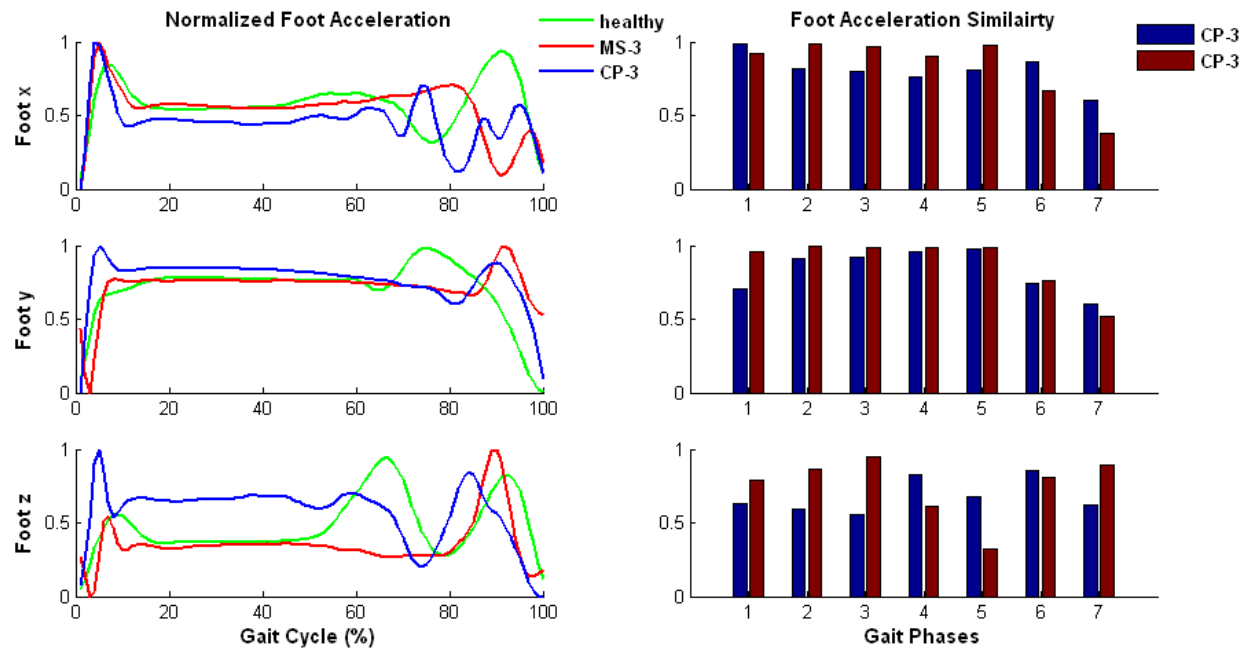


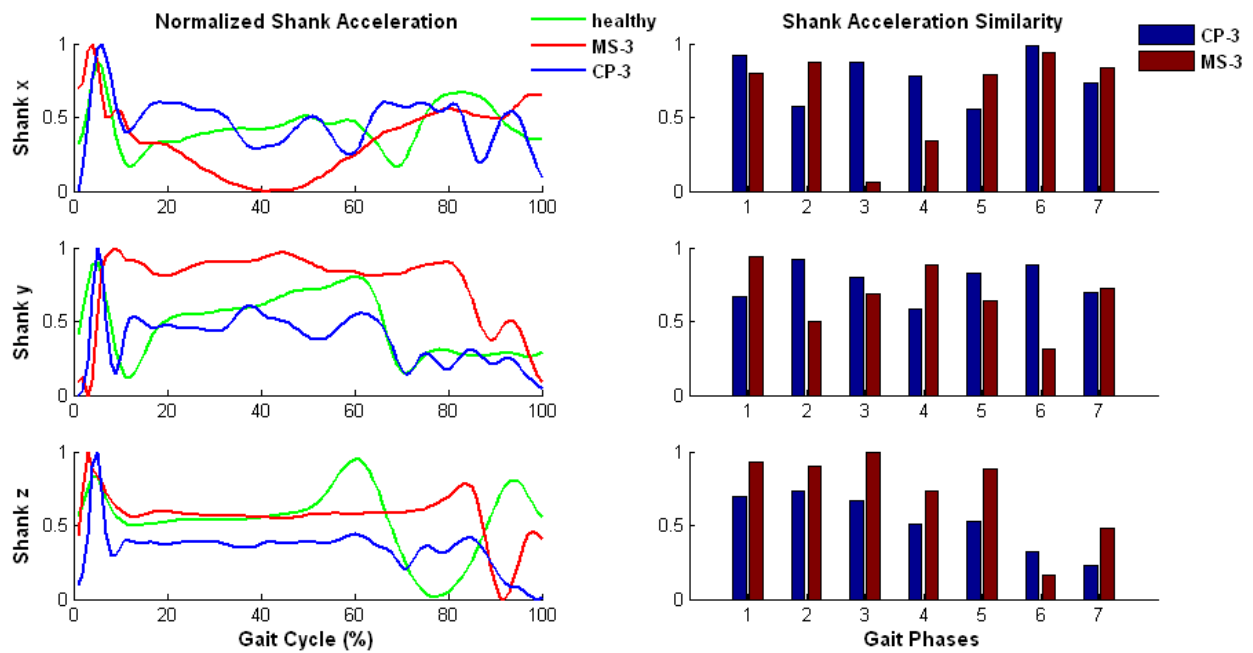
Figure 12-2: Comparison of EMG patterns and grade of similarity between MS-3 and CP-3.

- Comparison of Acceleration Patterns

(A)



(B)



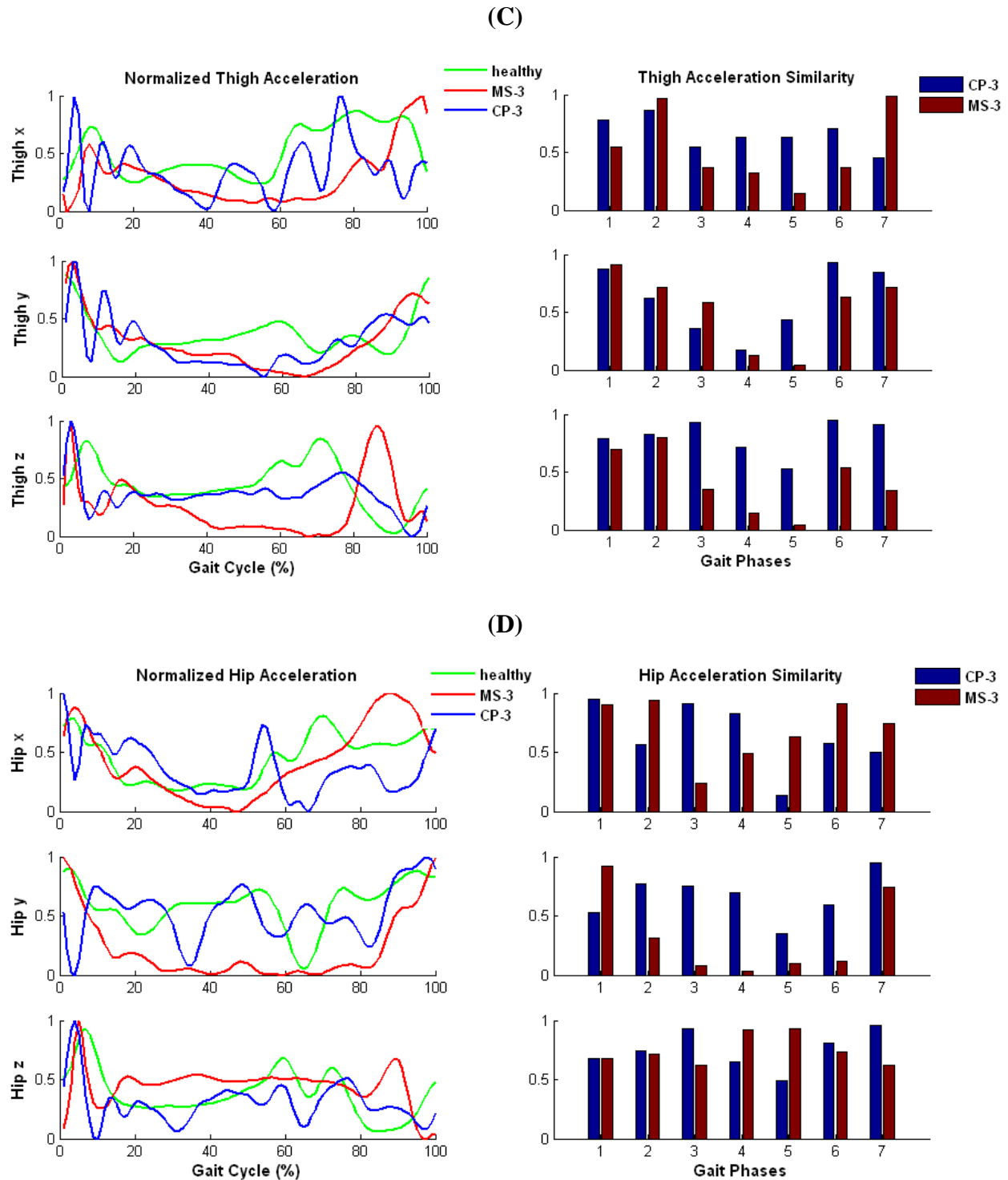


Figure 12-3: Comparison of segment's acceleration and similarity between MS-3 and CP-3. (A) Foot acceleration and similarity; (B) Shank acceleration and similarity; (C) Thigh acceleration and similarity; and (D) Hip acceleration and similarity.

- Analysis in table form

Table 12-1: Comparative Analysis between MS and CP

Feature	Multiple Sclerosis	Cerebral Palsy
GRF	<ul style="list-style-type: none"> • Delayed and single peak ground contact. 	<ul style="list-style-type: none"> • A single peak ground contact, but appears earlier than MS, which shows typical toe-walking gait.
Muscle Activity	<ul style="list-style-type: none"> • Muscle weakness in the stance phase on Soleus. • Slightly higher activities in the initial contact on Tibialis. • Delayed activities in the Gluteus medius. 	<ul style="list-style-type: none"> • Spasticity appears in the stance phase on Soleus and Gastrocnemius, combined with Tibialis muscle weakness in the loading response, results in the toe-walking. • Muscle weakness in the stance phase and spasticity in the swing phase results in the scissoring gait from hip and knee contractures.
Acceleration	<ul style="list-style-type: none"> • There is small deceleration on the foot-clearance in the initial swing phase, showing on foot y. • There are generally lower accelerations on thigh and hip. 	<ul style="list-style-type: none"> • There is little or no deceleration in the initial swing phase on foot y, which shows the CP subject with more foot-clearance problems. • There are very unstable acceleration signals on shank, thigh, and hip due to the scissoring gait patterns.

12.2 A Hemiparetic Stroke Subject (made two times visits for testing)

- Comparison of Ground Reaction Forces

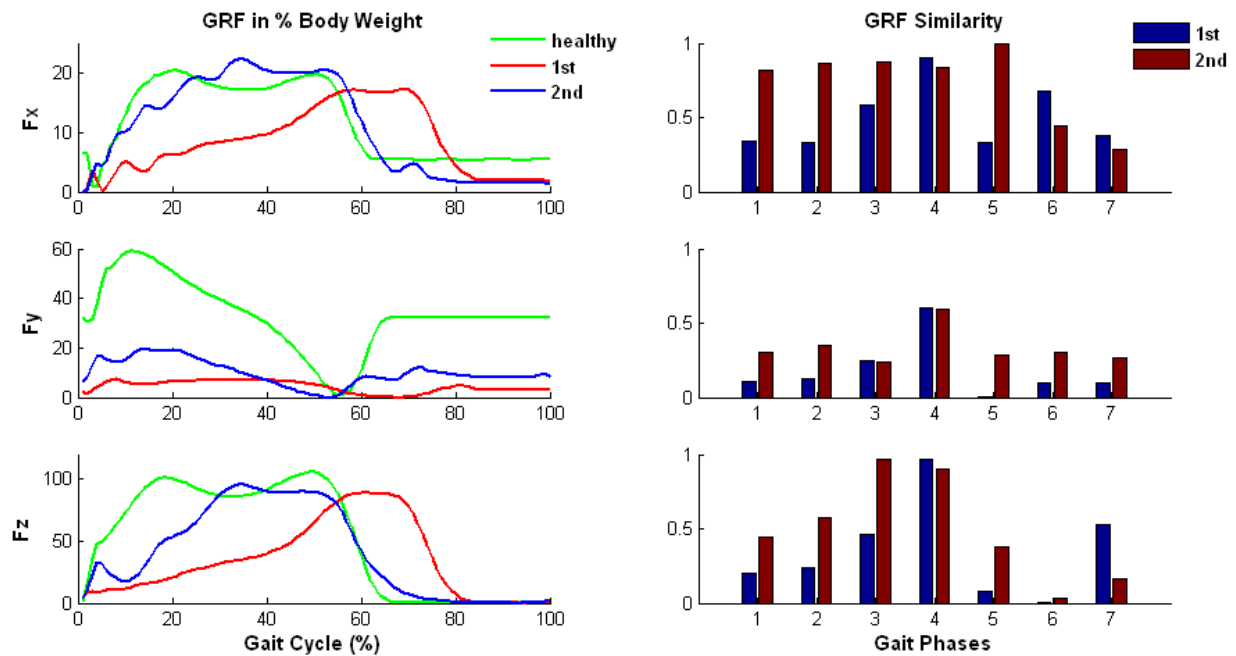


Figure 12-4: GRF and similarity of the stroke subject with two visits in two month interval.

- Comparison of EMG Muscle Activity

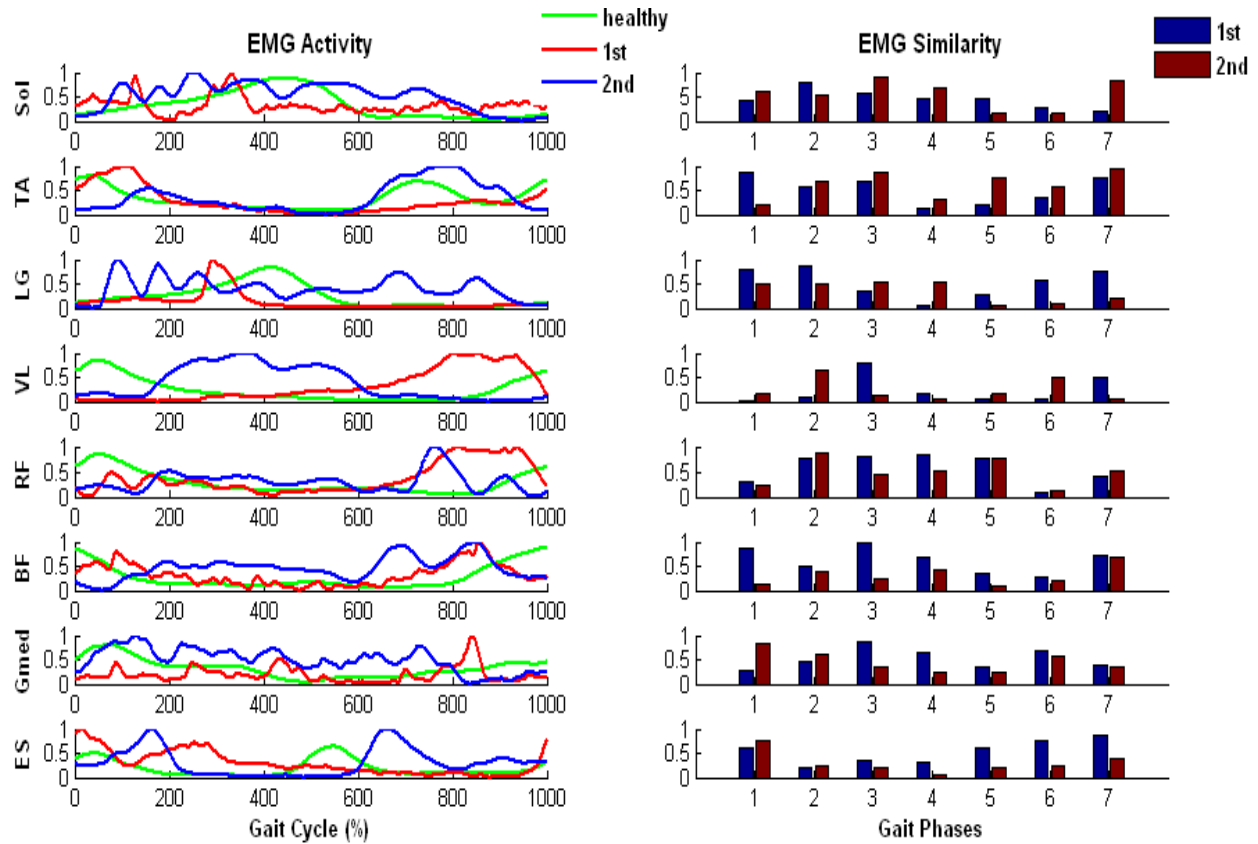
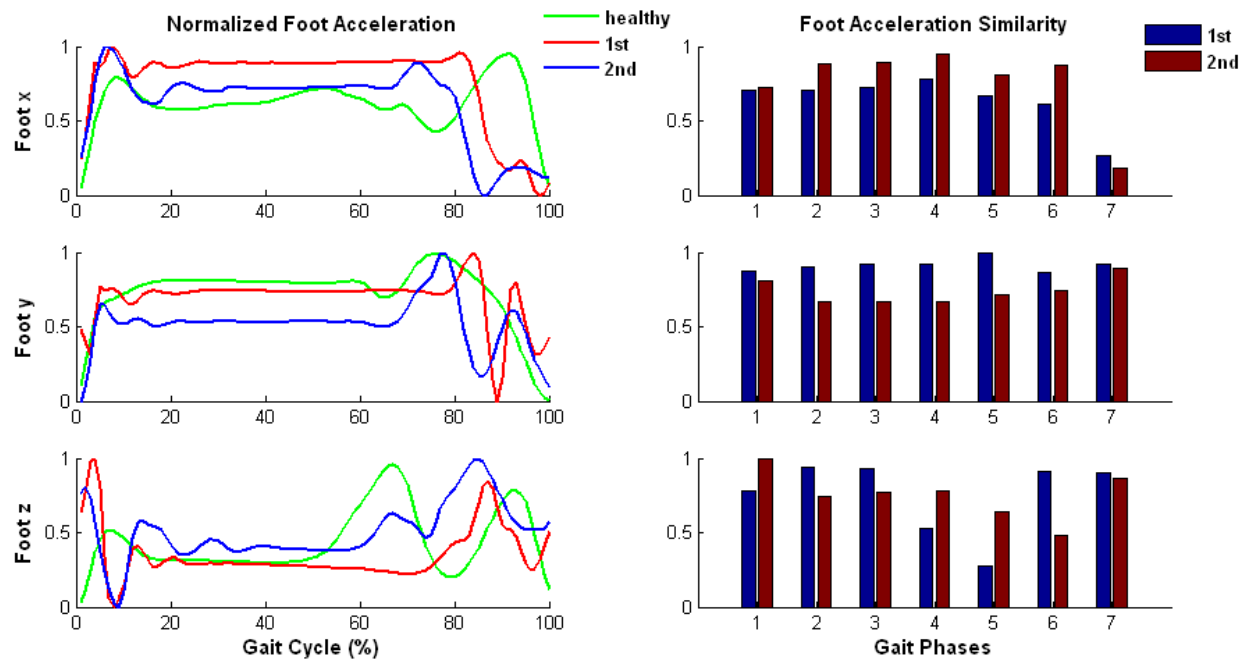


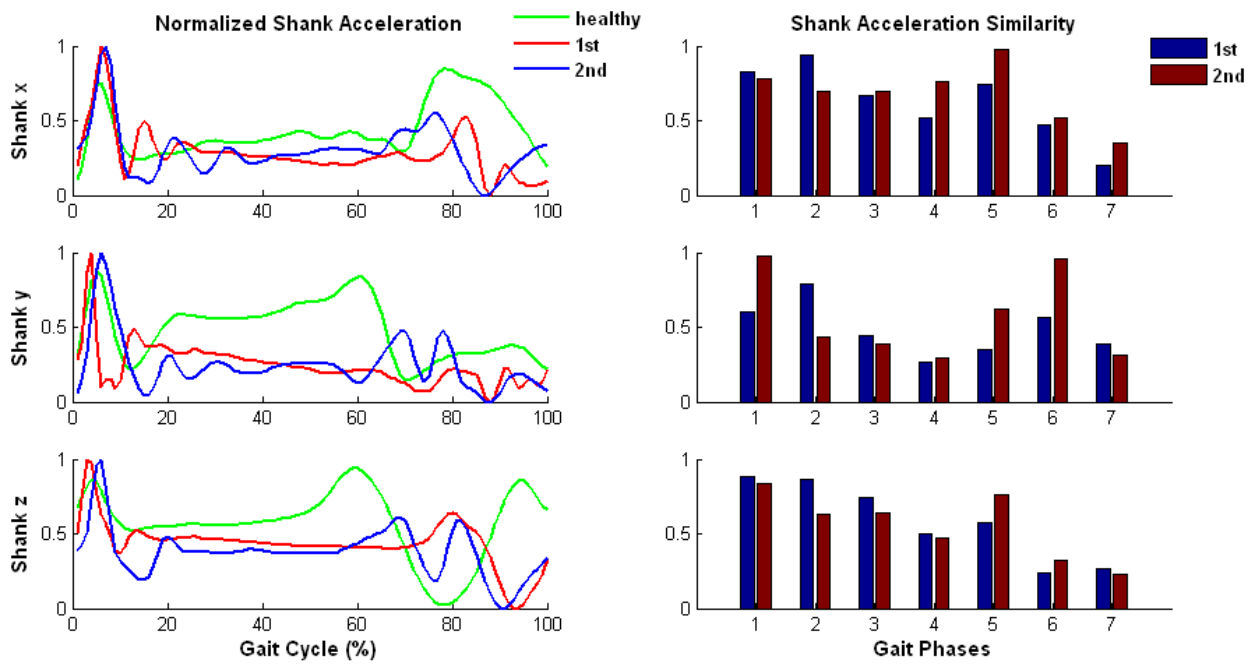
Figure 12-5: Comparison of EMG patterns and similarity between two times of visits with two months interval.

- Comparison of Acceleration Patterns

(A)



(B)



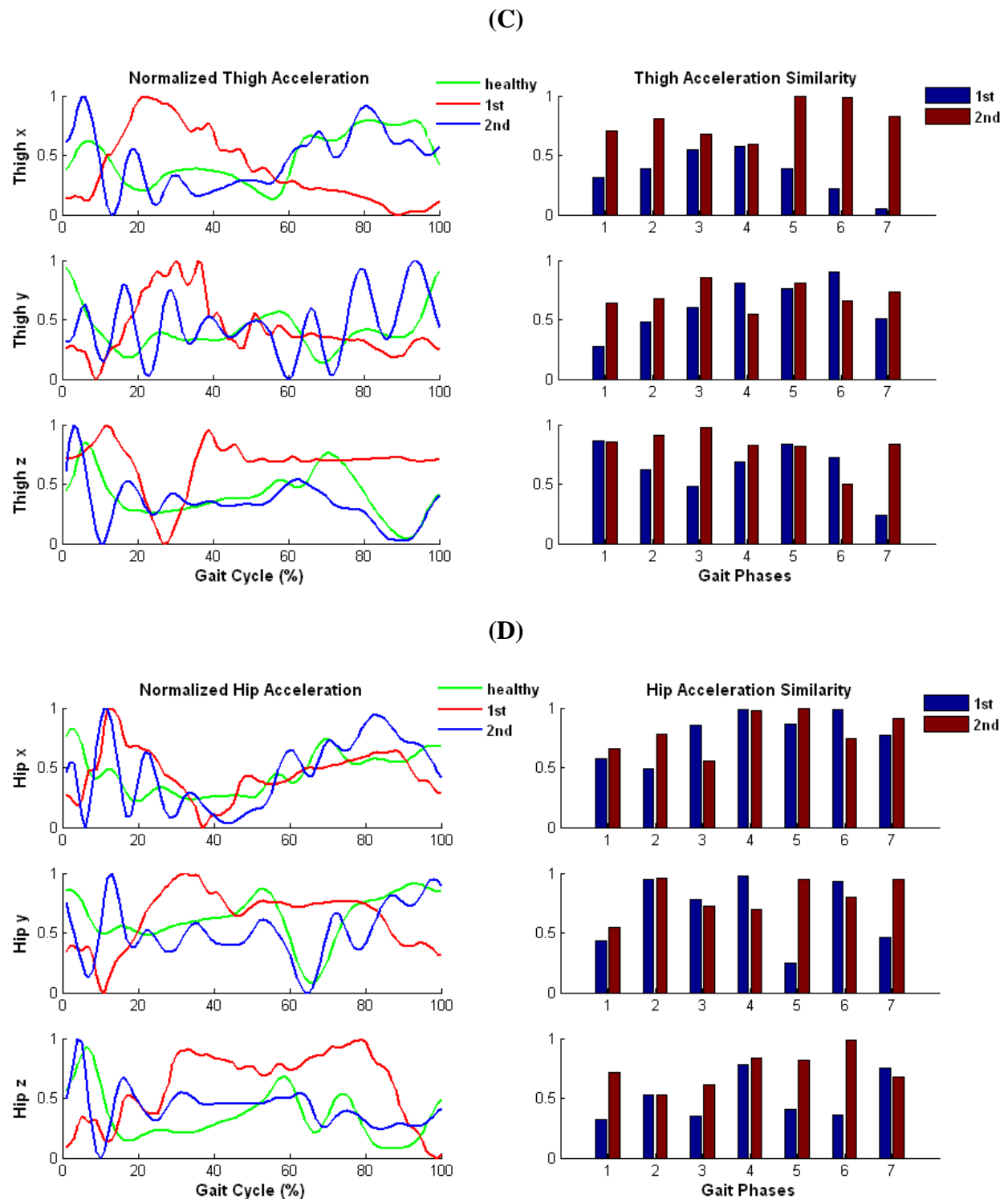


Figure 12-6: Comparison of segment's acceleration and similarity between two visits of a stroke subject. (A) Foot acceleration and similarity; (B) Shank acceleration and similarity; (C) Thigh acceleration and similarity; and (D) Hip acceleration and similarity.

- Analysis in table form

Table 12-2: Comparative Analysis before and after two-month hydrotherapy in Stroke1

Feature	Comparison
Walking Speed	The 1 st visit walking speed was 0.1 m/s, whereas the 2 nd visit walking speed was 0.3 m/s
GRF	The GRFs of the 2 nd visit are much higher than in the 1 st visit on all three planes. The stance phase in the 2 nd visit is much shorter than the 1 st visit.
Muscle Activity	In her 1 st visit, the muscle activities show generally weakness throughout the entire gait cycle. In her 2 nd visit, the muscle activities are improved on most of the muscles.
Acceleration	The subject has improved the grade of similarities on most of the segment's accelerations. There are still problems with the foot-clearing, and instability on the shank, thigh, and hip.

Chapter 13: Conclusions, Outcomes and Claims of the Research

Background

The kinematics, kinetics and electromyographic data of human locomotion were investigated, in order to increase our understanding of the neurophysiology/biomechanics of gait for augmenting objective measurements of mobility and functional status.

Objective

The objective is to develop a measurement methodology for the efficient and reliable analysis of human gait dynamics at a level that quantifies variations from morphometrically adjusted normal in three dimensions.

The methodology makes the recognition, quantification and differentiation of mobility-related impairments possible.

Outcomes of this research

This research work has introduced an innovative system that will represent a next-generation gait recognition, quantification and differentiation device.

The developed system provides three different operating modes: (1) *gait recording*; (2) *gait playback*; and (3) *gait training*. Each mode performs a different function that serves a different therapy purpose. From this perspective, it can be thought of as three machines combined into a single unit. When operating as a “gait recording machine” (Mode 1), the system measures and records the gait characteristics of the individual using the instrumented gait

analysis system. This generates a “data record” of the person’s gait, which is stored in the knowledge base. Some of the benefits of this system when operated in this mode include:

- Using this function with healthy subjects, data records can be captured that characterize the gait patterns of “normal individuals” from a sample population.

Benefit: Statistical analysis of normal gait data is enabled.

- Similarly, data records can be captured that characterize the gait patterns of individuals with a particular type of gait impairment, based on a sample survey population.

Benefit: Statistical analysis of impaired gait data is enabled.

- Using this function with one individual, data records can be captured over a series of therapy sessions and changes in the person’s gait with time, as a result of the prescribed therapy, can be identified and tracked.

Benefit: Measurement of effectiveness (MOE) of therapy is enabled.

- The use of this function allows the characterization and differentiation of gait-related impairment.

When the system is operated as a “gait playback machine” (Mode 2), stored data records from gait recording sessions can be retrieved from the knowledge base and gait characteristics can be reviewed using the data presentation features of the automated system. This allows for the review and understanding of the recorded gait data by the doctor, therapist, and/or patient.

Finally, when the system is operated as a “gait training machine” (Mode 3), the stored data within the knowledge-based instrumented analysis scheme will be used to move the subject’s legs according to a prescribed and programmed gait motion profile.

Claims of this research

- [1] This innovative technology is applicable across the entire spectrum of pathophysiological and biomedical etiologies of mobility impairment.
- [2] It is possible to use computational intelligence methodologies driven by a wearable sensor array system to reliably and effectively monitor gait disability.
- [3] This innovative system provides three-dimensional, real-time analysis of functional impairments in human locomotion.
- [4] This novel technology will revolutionize the quantification and characterization of gait impairments and thus have immediate research applications.
- [5] This new technology increases our understanding of the development of an adaptive compensatory system for human locomotion with the purpose of developing novel technology for efficient and reliable acquisition and analysis of human gait.
- [6] This technology will be capable of direct real-time comparison of any ambulatory subject's gait pattern to a predicted, morphometrically adjusted normal pattern utilizing fuzzy logic systems.
- [7] A new computational intelligence methodology has been developed based on fuzzy inferential reasoning.
- [8] The new technology enables the recognition and differentiation of gait disorders.
- [9] A novel sensor data fusion algorithm has been developed using the methods of fuzzy relational matrices.

Chapter 14: Suggestions for Future Enhancements

The accuracy of the measurement is a critical issue to assure quality and achieve continuous improvement of clinical gait and movement analysis. The future of gait analysis lies in the ability to process data quickly and identify the patient's functional deficits. There are a number of suggestions to improve the measurement, and therefore improve the quality of the analysis.

- Wireless and portable sensor measurement

The future research on clinical gait is seeking to create a system to provide instrumented wireless gait analysis outside of traditional, expensive motion laboratories. Such a system has the potential to be highly informative by allowing data collection throughout the day in a variety of environments, thus providing a vast quantity of long-term data not obtainable with current gait analysis systems. First, the system has to contain the light-weight, miniature inertial sensors for direct measurement and analysis. Second, the system has to be portable which enables the mobile measurement in any environments. Finally, most of the components in the system have to be wireless to reduce the errors from the cable moving effects, and improve for the time consumption during data acquisition.

- Sensor validation

For the reliable monitoring of gait, it is necessary to have accurate sensor information. However, sensors may sometimes be faulty or may even become unavailable due to the limitation or maintenance activities. The problem of sensor validation is therefore a critical part of measurement. A sensor validation scheme fulfills the tasks of detection and estimation. The former task involves the discovery of a malfunction in a sensor while the latter task includes

localization (establishing which sensor has failed); identification (determining the type of failure); and estimation (indicating the effect and extent of the failure).

- Real-time measurement

Once the measurement has been improved in a way to be portable, wireless and easy set-up, a system needs to be developed for real-time acquisition of human locomotion. This system will lead to greater accuracy than the current systems. These enhanced capabilities will eliminate clustering limitations and data reduction, reduce the cost of gait analysis as a clinical treatment planning service, and improve the turnaround and availability of information for clinical decision making. The advantages to be realized include a real-time motion acquisition and display, higher data sample rates, substantially increased work volumes, full body motion acquisition, reduced data loss from occlusion, and a significant time saving for data analysis. Successful development and commercialization of a real-time data acquisition system represents a new paradigm for human motion analysis.

References

- [1] “Clinical Guidelines on the Identification, Evaluation, and Treatment of Overweight and Obesity in Adults” (1998) National Institutes of Health, National Heart, Lung and Blood Institute, June, 1998.
- [2] “Constraint-induced movement therapy”, American Stroke Association.
- [3] “Thames Valley Children’s Centre – Cerebral Palsy – Causes and Prevalence”, Retrieved June 2007.
- [4] Alvaro Pascual-Leone, Amir Amedi, Felipe Fregni, Lotfi B. Merabet, (2005) “The Plastic Brain Cortex,” *Annu. Rev. Neurosci* (28), pp. 377-401.
- [5] American Spinal Injury Association. “International Standards for Neurological Classifications of Spinal Cord Injury”. Revised ed. Chicago, III: American Spinal Injury Association, 2000:1-23.
- [6] Amyotrophic Lateral Sclerosis Fact Sheet (2004) National Institute of Neurological Disorder and Stroke, 9/28/2004.
- [7] Arsenault A.B., Winter D.A., Marteniuk R.G., Hayes K.C. (2001) “How many strides are required for the analysis of electromyographic data in gait?” *Scand J Rehabil Med* 18, pp. 133–135.
- [8] Arvidsson, A., Collin, T., Kirik, D., Kokaia, Z., Lindvall, O., (2002) “Neuronal replacement from endogenous precursors in the adult brain after stroke,” *Nat Med* (8), pp. 963-970.
- [9] Astrup, J., Siesjo, B.K., Symon, L., (1981) “Thresholds in cerebral ischemic- the ischemic penumbra,” *Stroke* (12), pp. 723-725.

- [10] Ayyappa E., "Normal Human Locomotion, Part 1: Basic Concepts and Terminology" *Journal of Prosthetics and Orthotics*, 1997; 9:10-17.
- [11] Backman, L., Dixon, R.A., (1992) "Psychological compensation: A theoretical framework," *Psychological Bulletin*, 112, pp. 259-283.
- [12] Barbeau H, & Rossignol S (1987) "Recovery of locomotion after chronic spinalization in the adult cat." *Brain Res* 1987; 412:84-95.
- [13] Bernier, P.J., Vinet, J., Cossette, M., Parent, A. (2000) "Characterization of the subventricular zone of the adult human brain: evidence for the involvement of bcl-2," *Neurosci Res* (37), pp. 67-78.
- [14] Betancourt, B., Sarkodie-Gyan, T et al. (2007) "Automated Interpretable Membership Functions in Human Gait", *IEEE 10th International Conf. on Rehabilitation Robotics*, pp. 666-671.
- [15] Biernaskie, J., Corbet, D., (2001) "Enriched rehabilitative training promotes improved forelimb motor function and enhanced dendritic growth after focal ischemic injury," *J. Neurosci.* 21 (14), pp. 5272-5280.
- [16] Brown, J.A., Lutsep, H.I., Weinand, M., Cramer, S.C., (2006) "Motor cortex stimulation for the enhancement of recovery from stroke: a prospective, multicenter safety study," *Neurosurgery*; 58, pp. 464-473.
- [17] Buck P., Morrey BF., Chao EY., "The optimum position of arthrodesis of the ankle. A gait study of the knee and ankle" *The Journal of Bone & Joint Surgery*, 1987; 69:1052-1062.

- [18] Cappozzo A., Catani F., Leardini A., Benedetti MG., Croce UD., "Position and orientation in space of bones during movement: experimental artefacts." *Clin Biomech*, 1996; 11(2):90-100.
- [19] Carmichael, S.T., (2003), "Plasticity of cortical projections after stroke," *Neuroscientist* (9), pp. 64-75.
- [20] Carmichael, S.T., Chesset, M.F., (2002) "Synchronous neuronal activity is a signal for axonal sprouting after cortical lesions in the adult," *J. Neurosci.* 22 (14), pp. 6062-6070.
- [21] Center for Disease Control (CDC), "Economic costs associated with mental retardation, cerebral palsy, hearing loss, and vision impairment – United States", 2003.
- [22] Chen J., Kwong K., Chang D., Luk J., Bajcsy R., "Wearable sensors for reliable fall detection" *Proceedings of the 2005 IEEE Engineering in Medicine and Biology 27th Annual Conference*, 2005.
- [23] Chen, P., Goldberg, D.E., Kolb, B., Lanser, M., Benowitz, L.I., (2002) "Inosine induces axonal rewiring and improves behavioral outcome after stroke," *Proc. Natl. Acad. Sci. USA* 99 (13), pp. 9031-9036.
- [24] Cifu, D.X., Stewart, D.G., (1999) "Factors affecting functional outcome after stroke: a critical review of rehabilitation interventions," *Arch Phys Med Rehabil* (80) pp. 35-39.
- [25] Collen, F.M., Wade, D.T., Bradshaw, C.M., (1990) "Mobility after stroke: reliability of measures of impairment and disability," *Int Disabil Stud* 12(1), pp. 6-9.54.
- [26] Collen, F.M., Wade, D.T., Robb, G.F., Bradshaw, C.M., (1991) "The Rivermead Mobility Index: a further development of the Rivermead Motor Assessment," *Int Disabil Stud* 13(2), pp. 50-54

- [27] Craft, S., et al. (1998), "Cerebrospinal fluid and plasma insulin levels in Alzheimer's disease: relationship to severity of dementia and apolipoprotein E genotype," *Neurology* (50), pp. 164-168.
- [28] Craft, S., et al. (1999), "Enhancement of memory in Alzheimer disease with insulin and somatostatin, but not glucose," *Arch Gen Psychiatry* (56), pp. 1135-1140.
- [29] Cram, J.R., Kasman, G.S., and Holtz, J. "Introduction to surface electromyography." Maryland: Aspen Publishers, 1998.
- [30] Crone, C., (1965), "Facilitated transfer of glucose from blood into brain tissue," *J. Physiol.* (181), pp. 103-113.
- [31] Da Cunha, I.T. Jr., Lim, P.A., Qureshy, H., Henson, H., Monga, T., & Protas, E.J., (2002) "Gait outcomes after acute stroke rehabilitation with supported treadmill ambulation training: a randomized controlled pilot study." *Ach Phs Med & Reha*, 2002, 83, 1258-65.
- [32] Davids J.R., Foti T., Dabelstein J., Blackhurst D.W., Bagley A., "Objective assessment of dyskinesia in children with cerebral palsy" *J Pediatr Orthop*, 1999; 19(2):211-214.
- [33] Dawson, M., Sarkodie-Gyan,T., Provincialli, L., Hesse, S., (1996) "Gait initiation, development of a measurement system for use in the clinical environment", *Biomed. Technik*, 41, pp. 213-217.
- [34] De Luca C.J. "The use of surface electromyography in biomechanics" *Journal of Applied Biomechanics*, 1997; 13(2): 135-163.
- [35] Di Lazzaro, V., Dileone, M., Profice, P., Pilato, F., Cioni, B., Meglio, M., Capone, F., Tonali, P.A., Rothwell, J.C., (2006) "Direct demonstration that repetitive transcranial magnetic stimulation can enhance corticospinal excitability in stroke," *Stroke*; 37, pp. 2850-2853.

- [36] Dietz V, Colombo G, Jensen L, et al (1995) "Locomotor capacity of spinal cord in paraplegic patients." *Ann Neurol* 1995; 37:555-556.
- [37] Dijkhuizen, R.M., Singhal, A.B., Mandeville, J.B., Wu, O., Halpern, E.F., Finklestein, S.P., Rosen, B.R., Lo, E.H., (2003) "Correlation between brain reorganization, ischemic damage, and neurologic status after transient focal cerebral ischemia in rats: a functional magnetic resonance imaging study," *J. Neurosci.* 23 (2), pp. 510-517.
- [38] Ditunno J.F., Young W., Donovan W.H., et al., "The international standards booklet for neurological and functional classification of spinal cord injury". American Spinal Injury Association. *Paraplegia*, 1994;32(2):70-80.
- [39] Dobkin, B. H: (1999) "Overview of treadmill locomotor training with partial body weight support: A neurophysiology sound approach whose time has come for randomized clinical trials." *Neurorehabil and Neural Repair* 13: pp. 157-165.
- [40] Dobkin, B.H. (2003) "The clinical science of neurologic rehabilitation," Oxford University Press, New York.
- [41] Downey, C.A., "Pathokinesiology Department, Physical Therapy Department: Observational Gait Analysis Handbook" The Association of Rancho Los Amigos Medical Center, 1989.
- [42] Duysens, D., Duysens, J., Pearson, K., (1998), "From cat to man: basic aspects of locomotion relevant to motor rehabilitation of SCI," *NeuroRehabilitation* (10), pp. 107-118.
- [43] Echols K., DeLuca S.C., Ramey S.L., Taub E., "Constraint-induced movement therapy versus traditional therapeutic services for young children with cerebral palsy: a randomized controlled trial" *Dev Med Child Neurol.* 2002; 91(suppl):29.

- [44] Eicher P.S., Batshaw M.L., Cerebral Palsy, Pediatric Clinics of North America, 1993; 40(3):537-551.
- [45] Feinstein, A.R., (1987) "Clinimetrics," Yale University Press, New Haven.
- [46] Field-Fote E., "Combined use of body weight support, functional electric stimulation, and treadmill training to improve walking ability in individuals with chronic incomplete spinal cord injury" Arch Phys Med Rehabil 2001; 82:818-25.
- [47] Fish D., Nielsen J.P., "Clinical assessment of human gait" American Academy of Orthotists and Prosthetists, 1993; 5:39-48.
- [48] Fitzgerald R.H., Kaufer H., Malkani A.L., et al. (2002) "Orthopaedics" Mosby. Pp 71-107.
- [49] Frenkel-Toledo, S., Giladi, N., Peretz, C., Herman, T., Gruendlinger, L., Hausdorff, J.M., (2005), "Treadmill walking as an external pacemaker to improve gait rhythm and stability in Parkinson's disease," Movement Disorders (20), pp. 1109-1114.
- [50] Frost, S.B., Barbay, S., Friel, K.M., Plautz, E.J., Nudo, R.J., (2003) "Reorganization of remote cortical regions after ischemic brain injury: a potential substrate for stroke recovery," J. Neurophysiol. 89 (6), pp. 3205-3214.
- [51] Fuglevand A.J., Winter D.A., Patla A.E., Stashuk D., "Detection of motor unit action potentials with surface electrodes: influence of electrode size and spacing." Bio Cybern, 1992; 67:143-153.
- [52] Gabell A. and Nayak U.S.L. (1984) "The effect of age on the variability in gait" J. Gerontol., 39:662-666.

- [53] Gardner M.B., Holden M.K., Leikaukas S.M., et al. "Partial body weight support with treadmill locomotion to improve gait after incomplete spinal cord injury: A single-subject experimental design" *Phys Ther* 1998; 78:361-74.
- [54] Gerozissis, K., (2000), "Brain insulin and feeding: a bi-directional communication," *Eur J Pharmacol* (490), pp. 59-70.
- [55] Giangregorio L.M., Hicks A.L., Webber C.E., Phillips S.M., Craven B.C., Bugaresti J.M., McCartney N., "Body weight supported treadmill training in acute spinal cord injury: impact on muscle and bone" *Spinal Cord*, 2005; 43:649-657.
- [56] Giesser B., Beres J., Budovitch A., Herlihy E., Harkema S., "Locomotor training using body weight support on a treadmill improves mobility in persons with multiple sclerosis: a pilot study" *Multiple Sclerosis*, 2007; 13(2):224-231.
- [57] Gispen, W.H., Biessels, G.J., (2000), "Cognition and synaptic plasticity in diabetes mellitus," *Trends Neurosci* (23), pp. 542-549.
- [58] Glenn WW, Brouillette RT, Dentz B, et al. Fundamental considerations in pacing of the diaphragm for chronic ventilatory insufficiency: A multi-center study. *Pacing Clin Electrophysiol.* 1988; 11(2):2121-2127.
- [59] Glenn WW, Hogan JF, Loke JS, et al. Ventilatory support by pacing of the conditioned diaphragm in quadriplegia. *N Engl J Med.* 1984;310(18):1150-1155.
- [60] Goldberger A.L., Amaral L., Hausdorff J.M., Ivanov P.C., Peng C.K., Stanley H.E., "Fractal dynamics in physiology: Alterations with disease and aging" *Proceedings of the National Academy of Sciences of the United States of America*, 2002; 99:2466-2472.
- [61] Grabiner P., Biswas S., Grabiner M., "Age-related changes in spatial and temporal gait variables". *Arch Phys Med Rehabil.* 2001 Jan; 82(1):31-5.

- [62] Granata K.P., Padua D.A., Abel M.F. (2004) "Repeatability of surface EMG during gait in children" *Gait & Posture* 22: 346-350.
- [63] Griffin L., West D.J., West B.J., "Random stride intervals with memory" *Journal of Biological Physics*, 2000; 26:185-202.
- [64] Guimaraes R.M., Isaacs B., "Characteristics of the gait in old people who fall" *Int Rehabil Med*, 1980; 2:177-180.
- [65] Gwatkin D.R., Guillot M., Heuveline P., "The burden of disease among the global poor" *Lancet*, 1999; 354:586-589.
- [66] Hankey, G.J., Warlow, C.P., (1999), "Treatment and secondary prevention of stroke: evidence, costs, and effects on individuals and populations," *Lancet* (354), pp. 1457-1463.
- [67] Harkema SJ, Hurley SL, Patel UK, et al (1997) "Human lumbosacral spinal cord interprets loading during stepping." *J Neurophysiol* 1997; 77:797-811.
- [68] Hausdorff J.M., "Gait variability: methods, modeling and meaning" *Journal of NeuroEngineering and Rehabilitation*, 2005; 2:19-27.
- [69] Hausdorff, J.M., (2007), "Gait dynamics, fractals and falls: Finding meaning in the stride-to-stride fluctuations of human walking," *European Workshop on Movement Science*, Vol 26, Issue 4, pp. 555-589.
- [70] Hausdorff J.M., Edelberg H.K., Mitchell S.L., Goldberger A.L., Wei J.Y., "Increased gait unsteadiness in community-dwelling elderly fallers" *Arch Phys Med Rehabil*, 1997; 78:278-283.

- [71] Hausdorff J.M., Mitchell S.L., Firtion R., Peng C.K., Cudkowicz M.E., Wei J.Y. “Altered fractal dynamics of gait: reduced stride-interval correlations with aging and Huntington's disease” *J Appl Physiol*, 1997; 82:262–269.
- [72] Hausdorff J.M., Peng C.K., Ladin Z. Wei J.Y., Goldberger A.L., “Is walking a random walk? Evidence for long-range correlations in stride interval of human gait” *J Appl Physio*, 1995; 78:349-358.
- [73] Hausdorff J.M., Rios D., Edelberg H.K., “Gait variability and fall risk in community-living older adults: a 1-year prospective study” *Arch Phys Med Rehabil*, 2001; 82:1050-1056.
- [74] Havrankova, J., Schmechel, D., Roth, J., Brownstein, M., (1978) “Identification of insulin in rat brain,” *Proc Natl Acad Sci USA* (75), pp. 5737-5741.
- [75] Henty JR., Ewins DJ., “Applications of gyroscope angular velocity sensors in FES sytems” presented at 6th International Workshop on Functional Electrostimulation, Vienna, Austria, 1998.
- [76] Hesse S., Bertelt C., Schaffrin A., Malezic M., Mauritz K.H., “Restoration of gait in nonambulatory hemiparetic patients by treadmill training with partial body weight support” *Arch Phys Med Rehabil*, 1994; 75:1087-1093.
- [77] Hesse S, Konrad M, Uhlenbrock D, et al. “Treadmill walking with partial body weight support versus floor walking in hemiparetic subjects”. *Arch Phys Med Rehabil*1999; 80:421-427.
- [78] Hesse, S, Uhlenbrock, D, Sarkodie-Gyan, T, (1999) “Gait pattern of severely disabled hemiparetic subjects on a new controlled gait trainer as compared to assisted treadmill walking with partial body weight support, “ *Journal Clinical Rehabil*, 13, pp. 401-410.

- [79] Hesse, S. (2001) "Locomotor therapy in neurorehabilitation," *NeuroRehabilitation* 2001; 16:1-7.
- [80] Hesse, S., Uhlenbrock, D. "First Prototype of a Gait Trainer," German Patent DE 197 25 973 C2.
- [81] Hesse, S., Uhlenbrock, D. "Spring Element for the Insert at Treadmill Training," German Patent DE 197 25 972 C1.
- [82] Hesse, S., Uhlenbrock, D. "Gait Training Machine," German Patent DE 198 05 164.
- [83] Hesse, S., Uhlenbrock, D. (2000) "A mechanized Gait Trainer for restoration of gait," *Journal Rehab Res Dev* 2000; 37(6): 701-708.
- [84] Hesse, S., Uhlenbrock, D., Sarkodie-Gyan, T: (1999) "Development of an advanced mechanized gait-trainer, controlling movement of the center of mass, for restoration of gait in non-ambulatory subjects," *Journal of Biomed. Technik*, Band 44, Heft 7-8, pp. 194-201.
- [85] Hesse, S., Uhlenbrock, D., Werner, C., Bardeleben, A. (2000) "A mechanized gait trainer for restoring gait in non-ambulatory subjects," *Arch Phys Med Rehabil* 2000; 81: 1158-1162.
- [86] Hesse, S., Werner, C., Uhlenbrock, D., v. Frankenberg, S., Bardeleben, A., Brandl-Hesse, B. (2001) "An electromechanical gait trainer for restoration of gait in hemiparetic stroke patients: preliminary results," *Neurorehabilitation and Neural Repair* 2001; 15: 39-50.
- [87] Hesse, S., Werner, C., v. Frankenberg, S., Bardeleben, A. (2003) "Treadmill training with partial weight support after stroke," *Phs Med Rehabil Clin N Am*, 14: 111-123.

- [88] Hill, J.M., Lesniak, M.A., Pert, C.B., Roth, J., (1986) "Autoradiographic localization of insulin receptors in rat brain: prominence in olfactory and limbic areas," *Neuroscience* (17), pp. 1127-1138.
- [89] Hodgson JR, Roy, RR, deLeon R, et al (1994) "Can the mammalian lumbar spinal cord learn a motor task"? *Med Sci Sports Exerc*, 1994; 26:1491-1497.
- [90] Holden, M.K., Gill, K.M., Maglioni, M.R., Nathan, J., Peihl, B.L., (1984) "Clinical gait assessment in the neurologically impaired, Reliability and meaningfulness," *Phys Ther* 64(1), pp. 35-40.
- [91] Hreljac A., Marshall R.N. and Hume P.A., 2000. Evaluation of lower extremity overuse injury potential in runners. *Medicine and Science in Sport and Exercise* 32:1635-1641.
- [92] Hubbard I.J., Parsons M.W., Neilson C., Carey L.M., "Task-specific training: evidence for and translation to clinical practice" *Occupational Therapy International*, 2009; 16:175-189.
- [93] Huiying Yu, Sarkodie-Gyan, T. et al. (2007) "Identification of Human Gait using Fuzzy Inferential Reasoning", *IEEE 10th International Conf. on Rehabilitation Robotics*, pp. 656-660.
- [94] Hummel, F.C., Cohen, L.G., (2006) "Non-invasive brain stimulation: a new strategy to improve neurorehabilitation after stroke?" *Lancet Neurol*; 5, pp.708-712.
- [95] Ian H. Robertson, Jaap M.J. Murre (1999) "Rehabilitation of Brain Damage: Brain Plasticity and Principles of Guided Recover," *Psychological Bulletin*, Vol. 125, No. 5. pp. 544-575.

- [96] Jean, W.C., Spellman, S.R., Nussbaum, E.S., Low, W.C., (1998) "Reperfusion injury after focal cerebral ischemia: the role of inflammation and the therapeutic horizon," *Neurosurgery* (43), pp. 1382-1396; discussion 1396-1397.
- [97] Jensen, K., Sarkodie-Gyan, T. "The Paradigm of a Smart Gait Emulator," *Proceedings of the 2004 Japan-USA Symposium on Flexible Automation*, Denver, CO, July 19-21, 2004.
- [98] Jensen, K.J: (2005) "Diagnostics of Human Locomotion," M.S. Thesis, New Mexico Institute of Mining and Technology, Department of Mechanical Engineering, Mechatronics Program.
- [99] Jensen, Kirt, Sarkodie-Gyan, T. "Experimental Investigations on a Gait Emulator for Neurological Rehabilitation," *World Automatic Control Congress, Proceedings, WAC* Seville, Spain, 2004.
- [100] Jin, K., Minami, M., Lan, J.Q., Mao, X.O., Batteur, S., Somon, R.P., et al (2001) "Neurogenesis in the dentate subgranular zone and rostral subventricular zone after focal cerebral ischemia in the rat," *Proc. Natl. Acad. Sci. USA* (98), pp. 4710-4715.
- [101] Jonas Faijerson, (2007), "Neural Stem/Progenitor Cells in the Post-Ischemic Environment: Proliferation, Differentiation and Neuroprotection," PhD Dissertation, Goetebords University, Sweden.
- [102] Jones, T.A., Greenough, W.T., (1996) "Ultrastructural evidence for increased contact between astrocytes and synapses in rats reared in a complex environment," *Neurobiol. Learn. Mem.* 65 (1), pp. 48-56.
- [103] Jones, T.A., Schallert, T., (1992) "Overgrowth and pruning of dendrites in adult rats recovering from neocortical damage," *Brain Res.* 581 (1), pp. 156-160.

- [104] Jones, T.A., Schallert, T., (1994) "Use-dependent growth of pyramidal neurons after neocortical damage," *J. Neurosci.* 14 (4), pp. 2140-2152.
- [105] Jordan, K., Challis, J.H., Newell, K. M., (2007), "Speed influences on the scaling behavior of gait cycle fluctuations during treadmill running," *Human Movement Science* (26), pp. 87-102.
- [106] Jorgensen H.S., Kammersgaard L.P., Nakayama H., Raaschou H.O., Larsen K., Hubbe P., Olsen T.S., "Treatment and Rehabilitation on a stroke unit improves 5-year survival – A community-based study" *Stroke, Journal of the American Heart Association*, 1999; 30:930-933.
- [107] Kato, H., Kogure, K., (1999), "Biochemical and molecular characteristics of the brain with developing cerebral infarction," *Cell Mol Neurobiol* (19), pp. 93-108.
- [108] Keith R.A., "The comprehensive treatment team in rehabilitation." *Achieves of Physical Medicine and Rehabilitation*, 1991; 72:269-274.
- [109] Kelleher K.J., Spence W.D., Solomonidis S.E., Apatsidis D. "The characterization of gait patterns with multiple sclerosis". *Disabil Rehabil.* 2010; 32(15): 1242-50.
- [110] Kempermann, G., Kuhn, H.G., Gage, F.H., (1997) "More hippocampal neurons in adult mice living in an enriched environment," *Nature*; 386, pp. 493-495.
- [111] Kern, W., et al. (2001), "Improving influence of insulin on cognitive functions in humans," *Neuroendocrinology* (74), pp. 270-280.
- [112] Kesler A., Leibovich G., Herman T., Gruendlinger L., Giladi N., Hausdorff J.M., "Shedding light on walking in the dark: the effects of reduced lighting on the gait of older adults with higher-level gait disorder and controls" *J neuroengineering Rehabil*, 2005; 2:27.

- [113] Kiisa Nishikawa, Andrew A. Biewener, Peter Aerts, et al. (2006) "Neuromechanics: an integrative approach for understanding motor control," Symposium, Biomechanics and Neuromuscular Control of the Society for Integrative and Comparative Biology, Orlando, Florida, pp. 1-39.
- [114] Kirshblum S. Campagnolo D. Delisa J., (2001) "Spinal Cord Medicine" Lippincott Williams & Wilkins.
- [115] Klose K.J., Jacobs P.L., Broton J.G., et al. "Evaluation of a training program for persons with SCI paraplegia using the Parastep I Ambulation System: Part 1, Ambulation Performance and Anthropometric Measures" *Archiv Physical Med Rehabil*, 1997; 78(8):808-814.
- [116] Komitava, M., Mattsson, B., Eriksson, P.S., Johansson, B.B., (2005) "Enriched environment increases neural stem/progenitor cell proliferation and neurogenesis in the subventricular zone of stroke-lesioned adult rats," *Stroke* (36), pp. 1278-1282.
- [117] Komitova, M., Perfilieva, E., Mattsson, B., Ericsson, P.S., Johansson, B.B., (2002) "Effects of cortical ischemia and postischemic environment enrichment on hippocampal cell genesis and differentiation in the adult rat," *J. Cereb Blood Flow Metab* (22), pp. 852-860.
- [118] Komitova, M., Zhao, L.R., Gido, G., Jahansson, B.B., Ericsson, P., (2005) "Postischemic exercise attenuates whereas enriched environment has certain enhancing effects on lesion-induced subventricular zone activation in the adult rat," *Eur J. Neurosci* (21), pp. 2397-2405.

- [119] Kornack, D.R., Rakie, P., (2001) "The generation, migration, and differentiation of olfactory neurons in the adult primate brain," *Proc. Natl. Acad. Sci. USA* (98), pp. 4752-4757.
- [120] Kotila, M., Waltimo, O., Niemi, M.L., Laaksonen, R., Lempinen, M., (1984) "The profile of recovery from stroke and factors influencing outcome," *Stroke* (15), pp. 1039-1044.
- [121] Krakauer, J.W., (2006) "Motor-learning: its relevance to stroke recovery and neurorehabilitation," *Curr Opin Neurol*; 19, pp. 84-90.
- [122] Kumar N., Pankaj D., Mahajan A., Kumar A., Sohi BS., "Evaluation of normal gait using electro-goniometer" *Journal of Scientific & Industrial Research*, 2009; 68:696-698.
- [123] Kwakkel G., Peppen R.V., Wagenaar R.C., et al. "Effects of augmented exercise therapy time after stroke: A meta-analysis" *Stroke*, 2004; 35:2529-2539.
- [124] Kwakkel, G. (1998) "Dynamics in functional recovery after stroke," Ponsen & Looijen BV, The Netherlands.
- [125] Kwakkel, G., Kollen, B.J., Lindeman, E., (2004) "Understanding the pattern of functional recovery after stroke: Facts and theories," *Restorative Neurolo Neurisci* (22), pp. 281-229.
- [126] Kwakkel, G., Kollen, B.J., Wagenaar, R.C., (1999) "Therapy impact on functional recovery in stroke rehabilitation: A critical review of the literature," *Physiotherapy* 85 (7), pp. 377-391.
- [127] Kyriazis V., "Gait analysis techniques" *Journal of Orthopaed Traumatol*, 2001; 1:1-6.
- [128] Lagunju I.A., Fatunde O.J., "The child with cerebral palsy in a developing country – diagnosis and beyond" *Journal of Pediatric Neurology*, 2009; 7:375-379.

- [129] Langhorne, P., Duncan, P., (2001), "Does the organization of postacute stroke care really matter?" *Stroke* (32), pp. 268-274.
- [130] Langhorne, P., Pollock, A., (2002) "What are the components of effective stroke unit care?" *Age Ageing* (31), pp. 365-371.
- [131] Laporte, R. E., Kuller, L. H., Kupfer, D. J. "An objective measure of physical activity for epidemiological research," *Am. J. Epidemiol*, 1979; 109:158–167.
- [132] Lau H., Tong K., "The reliability of using accelerometer and gyroscope for gait event identification on persons with dropped foot" *Gait Posture*, 2008; 27(2):248-257.
- [133] Lee JA., Cho SH., Lee JW., Lee KH., Yang HK., "Wearable accelerometer system for measuring the temporal parameters of gait" in *Proc. 29th Int. Conf. IEEE EMBS*, Lyon, France, 2007; 483-486.
- [134] Lee, C.D., Folsom, A.R., Blair, S.N., (2003) "Physical activity and stroke risk. A meta-analysis," *Stroke* (34), pp. 2475-2482.
- [135] Lefaucher, J.P., (2006) "Stroke recovery can be enhanced by using repetitive transcranial magnetic stimulation (rTMS)," *Neurophysiol Clin*; 36, pp. 105-115.
- [136] Lie, D.C., Colamarino, S.A., Song, H.J., Desire, L., Mira, H., Consiglio, A., Lein, E.S., Jessberger, S., Lansford, H., Dearie, A.R., Gage, F.H., (2005) "Wnt signaling regulates adult hippocampal neurogenesis," *Nature* (437), pp. 1370-1375.
- [137] Liepert, J., Miltner, W. H., Bauder, H., Sommer, M., Dettmers, C., Taub, E., Weiller, C., (1998) "Motor cortex plasticity during constraint-induced movement therapy in stroke patients," *Neurosci. Lett* (250), pp. 5-8.
- [138] Liepert, J., Storch, P., Fritsch, A., Weiller, C., (2000) "Motor cortex disinhibition in acute stroke," *Clin. Neurophysiol* (111), pp. 671-676.

- [139] Lim, D.A., Tramontin, A.D., Trevejo, J.M., Herrera, D.G., Garcia-Verdugo, J.M., Alvarez-Buylla, A., (2000) "Noggin antagonizes bmp signaling to create a niche for adult neurogenesis," *Neuron* (28), pp. 713-726.
- [140] Lin V.W.H., Cardenas D.D., Cutter N.C., Hammond M.C., (2002) "spinal Cord Medicine: Principles and Practice" Demos Medical Publishing.
- [141] Lindvall, O., Kokaia, Z., (2004) "Recovery and rehabilitation in stroke: stem cells," *Stroke* (35), pp. 2691-2694.
- [142] Lledo, P.M., Alonso, M., Grubb, M.S., (2006), "Adult neurogenesis and functional plasticity in neuronal circuits," *Nat Rev Neurosci* (7), pp. 179-193.
- [143] Lovely RG, Gregor RJ, Roy RR, et al. "Effects of training on the recovery of full weight-bearing stepping in the adult spinal cat" *Exp Neuro* (11), 1986; 92:421-435.
- [144] Lovely RG, Gregor RJ, Roy RR, et al (1990) "Weight-bearing hindlimb stepping in treadmill-exercised adult cats". *Brain Res* 1990; 514:206-218.
- [145] Lublin F.D., Reingold S.C., "Defining the clinical course of multiple sclerosis: results of an international survey. National Multiple Sclerosis Society (USA) Advisory Committee on Clinical Trials of New Agents in Multiple Sclerosis" *Neurology*, 1996; 46(4):907-911.
- [146] Ludovic Righetti, Auke Jan Ijspeert, (2006) "Programmable Central Pattern Generators: an application to biped locomotion control," *Proc IEEE Internacional Conf on Robotics and Automation*, Orlando, Florida, pp. 1585-1590.
- [147] Luinge HJ., Veltink PH., "Inclination measurement of human movement using a 3D accelerometer with autocalibration" *IEEE Trans. Neural Syst. Rehabil. Eng.*, 2004; 12:112-121.

- [148] Luo, C.X., Jiang, J., Zhou, Q.G., Zhu, X.J., Wang, W., Zhang, Z.J., et al. (2007) "Voluntary exercise-induced neurogenesis in the postischemic dentate gyrus is associated with spatial memory recovery from stroke," *J. Neurosci. Res* (85), pp. 1637-1646.
- [149] Luria, A. R., (1963) "Restoration of function after brain injury," Oxford, England: Pergamon.
- [150] Luria, A.R., Naydin, V.L., Tsvetkova, L.S., Vinarskaya, E.N. (1975) "Restoration of higher cortical functions following local brain damage," In P.J., Vinken & G.W. Bruyn (Eds), *Handbook of clinical neurology* (Vol. 3, pp. 368-433), New York: Elsevier.
- [151] MacDonald, C. E., Sarkodie-Gyan, T., et al (2007) "Determination of Human Gait Phases using Fuzzy Inference", *IEEE 10th International Conf. on Rehabilitation Robotics*, pp. 661-665.
- [152] Margolis, R.U., Altszuler, N., (1967) "Insulin in the cerebrospinal fluid," *Nature* (215), pp. 1375-1376.
- [153] Markakis, E.A., Gage, F.H., (1999) "Adult-generated neurons in the dentate gyrus send axonal projections to field ca3 and are surrounded by synaptic vesicles," *J. Comp Neurol* (406), pp. 449-460.
- [154] Mayagoitia RE., Nene AV., Veltink PH., "Accelerometer and rate gyroscope measurement of kinematics: an inexpensive alternative to optical motion analysis systems" *J. Biomech*, 2002; 35:537-542.
- [155] Mccubbin J.A., Shasby G.B., "Effects of isokinetic exercise on adolescents with cerebral palsy" *Phys. Act. Q.*, 1985; 2:56-64.

- [156] McIntosh, G.C., Brown, S.H., Rice, R.R., (1997) "Rhythmic auditory-motor facilitation of gait patterns in patients with Parkinson's Disease," J. Neuro., Neurosurg. Psychiatry, Vol 62(1), pp. 22-26.
- [157] McIntosh, G.C., Thaut, M.H., Rice, R.R., (1996) "Rhythmic auditory stimulation (RAS) as entrainment and therapy technique in gait of stroke and Parkinson's Disease patients, MusicMedicine 2, MMB Music, St. Louis, pp.145-152.
- [158] McNevin N.H., Coraci L., Schafer J., "Gait in adolescent cerebral palsy: The effect of partial unweighting" Arch Phys Med Rehabil 2000; 81:525-8.
- [159] Meek, C., Langhorne, P., (2003) "A systematic review of exercise trials post stroke," Clin Rehabil (17), pp. 6-13.
- [160] Meeteren N.L., Brakkee J.H., Hamers F.P., Helders P.J., Gispen W.H., "Exercise training improves functional recovery and motor nerve conduction velocity after sciatic nerve crush lesion in rat" Archives of Physical Medicine and Rehabilitation, 1997; 1:70-77.
- [161] Meeteren N.L., Brakkee J.H., Helders P.J., Gispen W.H., "The effect of exercise training on functional recovery after sciatic nerve crush in the rat" Journal of Periphery Nerve System, 1998; 3(4):277-282.
- [162] Mehrholz J., Werner C., Kugler J., Pohl M., "Electromechanical-assisted training for walking after stroke" Cochrane Database Syst Rev 2007;4:CD006185.
- [163] Memezawa, H., Minamisawa, H., Smith, M.L., Siesjo, B.K., (1992) "Ischemic penumbra in a model of reversible middle cerebral artery occlusion in the rat," Exp Brain Res (89), pp. 67-78.

- [164] Menz H.B., Lord S.R., Fitzpatrick R.C., “Acceleration patterns of the head and pelvis when walking are associated with risk of falling in community-dwelling older people” *J Gerontol A Biol sci Med Sci*, 2003; 58:M446-M452.
- [165] Mila Komitova, Barbro B. Johansson, Peter S. Ericsson (2006) “On neural plasticity, new neurons and the postischemic milieu: An integrated view on experimental rehabilitation,” *Exp. Neurology* 199, pp. 42-55.
- [166] Miller E.W., “Body weight supported treadmill and overground training in a patient post cerebrovascular accident” *Neurorehabilitation*, 2001; 16:155-63.
- [167] Miltner, W.H., Bauder, H., Sommer, M., Dettmers, E., Taub, E., (1999) “Effects of constraint-induced movement therapy on patients with chronic motor deficits after stroke: a replication,” *Stroke* (30), pp. 586-592.
- [168] Miyai I., Fujimoto Y., Ueda Y., Yamamoto H., Nozaki S., Saito T., Kang J., “Treadmill training with body weight support: Its effect on Parkinson’s disease” *Arch Phys Med Rehabil*, 2000; 81:849-852.
- [169] Miyai, I., Fujimoto, Y., Yamamoto, H., Ueda, Y., Saito, T., Nozaki, S., & Kang, J., (2002) “Long-term effect of body weight-supported treadmill training in Parkinson’s disease: A randomized controlled trial,” *Arch Phys Med & Rehab*, 2002, 83, 1370-1373.
- [170] Moe-Nilssen R., “A new method for evaluating motor control in gait under real-life environmental conditions. Part I: The instrument” *Clin. Biomech*, 1998; 13:320-327.
- [171] Moe-Nilssen R., Helbostad J.L., “Estimation of gait cycle characteristics by trunk accelerometry” *J. Biomech*, 2004; 37:121-126.
- [172] Morag E., Cavanagh P.R. “Structural and functional predictors of regional peak pressures under the foot during walking” *J Biomech* 1999; 32:359-370.

- [173] Morris, S.L., Dodd, K.J., Morris, M.E., (2004) "Outcomes of progressive resistance strength training following stroke: a systematic review," *Clin Rehabil* (18), pp. 27-39.
- [174] Muir, G.O., Steeves, J.D., (1998) "Sensorimotor stimulation to improve locomotor recovery after spinal cord injury," *Trends Neurosci* (20), pp. 72-77.
- [175] Mukhiya R., Gangopadhyay S., Guha B., et al. "MEMS Accelerometer driven fuel control system for Automobile applications" *Smart Structures, devices, and system IV*, 2008, Melbourne, Australia.
- [176] Multiple sclerosis: Hope through research. National Institute Neurological Disorder and Stroke (NINDS), 1996. NIH publication No. 96-75.
- [177] Murray C.J.L., Lopez A.D., "Mortality by cause for eight regions of the world: global burden of disease study" *Lancet*, 1997; 349:1269-1276.
- [178] Murray C.J.L., Lopez A.D., "The global burden of disease: a comprehensive assessment of mortality and disability from diseases, injuries and risk factors in 1990 and projected to 2020." Cambridge, MA, Harvard School of Public Health on behalf of the World Health Organization and the World Bank, 1996 (Global Burden of Disease and Injury Series, Vol. 1).
- [179] Napieralski, J.A., Butler, A.K., Chesset, M.F., (1996) "Anatomical and functional evidence for lesion-specific sprouting of corticostriatal input in the adult rat," *J. Comp. Neuro.* 373 (4), pp. 484-497.
- [180] National Spinal Cord Injury Statistical Center (NSCISC), "Facts and Figures at a Glance" April, 2009.
- [181] Nene AV., Mayagoitia RE., Veltink PH., "Assessment of rectus femoris function during initial swing phase" *Gait Posture*, 1999; 9:1-9.

- [182] Niswender, K.D., Baskin, D.G., Schwartz, M.W., (2004) "Insulin and its evolving partnership with leptin in the hypothalamic control of energy homeostasis," Trends Endocrinol Metab (15), pp. 362-369.
- [183] Nudo, R.J., (2007), "Postinfarct cortical plasticity and behavioral recovery," Stroke (38), pp. 840-845.
- [184] O'Byrne J.M., Jenkinson A., O'Brien T.M., "Quantitative Analysis and Classification of Gait Patterns in Cerebral Palsy using a Three-Dimensional Motion Analyzer" J Child Neurol, 1998; 13:101-108.
- [185] Ou Ma, Ziumin Dao, Lucas Martinez, T. Sarkodie-Gyan (2007) "Dynamically removing partial body mass using acceleration feedback for neural training," IEEE 10th International Conf. on Rehabilitation Robotics, pp. 1102-1107.
- [186] Pailhous, J., Bannard, M., (1992), "Steady-state fluctuations of human walking," Behavioral Brain Research (47), pp. 181-189.
- [187] Pappas, I.P.I., Popovic, M.R., Keller, T., Dietz, V., Morari, M., (2001) "A reliable gait phase detection system," IEEE Trans Neural Systems and Rehabilitation Engineering, Vol 9, No. 2, pp. 113-125.
- [188] Parent, J.M., Vexler, Z.S., Gong, C., Derugin, N., Ferriero, D.M., (2002) "Rat forbrain neurogenesis and striatal neuron replacement after focal stroke," Ann Neurol (52), pp. 802-813.
- [189] Peppen Van R., Kwakkel G., Wood-Dauphinee S., et al. "The impact of physical therapy on functional outcome after stroke: What's the evidence?" Clin Rehabil, 2004; 18:833-862.

- [190] Perry J., "Gait Analysis: Normal and Pathological Function" 1992, New Jersey, SLACK Inc.
- [191] Platz, T., van Kaick, S., Moller, L., Freund, S., Winter, T., Kim, I.H., (2005) "Impairment-oriented training and adaptive motor cortex reorganization after stroke: a fTMS study," J. Neurol; 252, pp. 1363-1371
- [192] Plautz, E.J., Barbay, S., Frost, S.B., Friel, K.M., Dancause, N., Zoubina, E.V., Stove, A.M., Quaney, B.M., Nudo, R.J., (2003) "Post-infarct cortical plasticity and behavioral recovery using concurrent cortical stimulation and rehabilitative training: a feasibility study in primates," Neurol. Res. 25 (8), pp. 801-810.
- [193] Plum, L., Schubert, M., Bruning, J.C., (2005), "The role of insulin receptor signaling in the brain," Trends Endocrinol Metab (16) pp. 59-65.
- [194] Pomeroy, V.M., King, L., Pollock, A., Baily-Hallam, A., Langhorne, P., (2006) "Electrostimulation for promoting recovery of movement or functional ability after stroke," Cochrane Database Syst Rev; 19, CD003241.
- [195] Protas E.J., Holmes A., Qureshy H., et al. "Supported treadmill ambulation training after spinal cord injury: A pilot study" Arch Phys Med Rehabil 2001; 82:825-31.
- [196] Pullman SL., Goodin DS., Marquinez AI., Tabbal S., Rubin M., "Clinical utility of surface EMG" Report of the therapeutics and technology assessment subcommittee of the American Academy of Neurology, Neurology, 2000; 55:171-177.
- [197] Recommendations on rehabilitation services for persons with multiple sclerosis in Europe. Brussels, European Multiple Sclerosis Platform and Rehabilitation in Multiple Sclerosis, 2004 (European Code of Good Practice in Multiple Sclerosis).

- [198] Richards CL, Malouin F, Dumas F, et al (1997) "Early and intensive treadmill locomotor training for young children with cerebral palsy: a feasibility study." *Pediatr Phys Ther* 1997; 9:258-265.
- [199] Rients B. Huitema, At L. Hof, Theo Mulder, Wiebo H. Brouwer, Rient Dekker, Klaas Postema, (2004) "Functional Recovery of Gait and Joint Kinematics After Right Hemispheric Stroke," *Arch Phys Med Rehabil*, Vol 85, pp. 1082-1988.
- [200] Robinson J., Kett A., Bolam M. "Spasticity in spinal cord injured patients: Initial measures and long-term effects of electrical stimulation" *Arch Phys Med Rehabil*, 1988; 69:862-868.
- [201] Rodgers M.M., "Dynamic foot biomechanics" *J Orthop Sports Phys Ther* 1995; 21:306-316.
- [202] Romero, J.R., Babikian, V.L., Katz, D.I., Finklestein, S.P., (2006) "Neuroprotection and stroke rehabilitation: modulation and enhancement of recovery," *Behav Neurol* (17), pp. 17-24.
- [203] Rosamond W., Flegal K., Friday G., Heart disease and stroke statistics, 2007 update: a report from the American Heart Association Statistics Committee and Stroke Statistics Subcommittee. *Circulation* 2007;115:e69--e171.
- [204] Rosenbaum P., "The definition and classification of cerebral palsy" *NeoReviews*, 2006; 7:569-574.
- [205] Sackley C.M., Lincoln R.B., "Physiotherapy for stroke patients: a survey of current practice" *Physiotherapy Theory Practice*, 1996; 12:87-96.
- [206] Sarkodie-Gyan, T. (2006) "Neurorehabilitation Devices: Engineering Design, Measurement, and Control, " *McGraw-Hill Publishing Co.*, ISBN:0-07-144830-6.

- [207] Sarkodie-Gyan, T., Jensen, K.J. (2007) "Design of a 3DOF Robotic System for use in Neurorehabilitation", IEEE 10th International Conf. on Rehabilitation Robotics, pp. 650-655.
- [208] Sarti C., et al. "International trends in mortality from stroke, 1968 to 1994" *Stroke*, 2000; 31:1588-1601.
- [209] Sartorius N., "Rehabilitation and quality of life" *Hospital and Community Psychiatry*, 1992; 43:1180-1181.
- [210] Sasaki, Y., Araki, T., Millbrandt, J., (2006) "Stimulation of nicotinamide adenine dinucleotide biosynthetic pathways delays axonal degeneration after axotomy," *J. Neurosci.*, 26, pp. 8484-8491.
- [211] Schaafsma J.D., Giladi N., Balash Y., Bartels A.L., Gurevich T., Hausdorff J.M. "Gait dynamics in Parkinson's disease: relationship to Parkinsonian features, falls, and response to levodopa" *J Neurol Sci*, 2003; 212:47-53.
- [212] Schindl M.R., Forstner C., Kern H., et al. "Treadmill training with partial body weight support in nonambulatory patients with cerebral palsy" *Arch Phys Med Rehabil* 2000; 81:301-6.
- [213] Schmidt H., Werner C., Bernhardt., Hesse S., Kruger J., "Gait rehabilitation machines based on programmable footplates" *Journal of NeuroEngineering and Rehabilitation*, 2007; 4:2.
- [214] Schmidt, R.A., Lee, T., (1999) "Motor control and learning," Champaign, IL. Human kinetics.

- [215] Seung-Hoon Lee, Yun-Hee Kim, Young-Ju Kim, Byung-Woo Yoon (2008) “Enforced physical training promotes neurogenesis in the subgranular zone after focal cerebral ischemia,” *J. Neurosci.* JNS-10434, pp. 1-8.
- [216] Shaw S.E., Morris D.M., Uswatte G., McKay S., Meythaler J.M., Taub E. “Constraint-induced movement therapy for recovery of upper-limb function following traumatic brain injury” *Journal of Rehabil Research & Development*, 2005; 42:769-778.
- [217] Sheridan P., Solomont J., Kowall N., Hausdorff J.M. “Influence of executive function on locomotor function: divided attention increases gait variability in Alzheimer’s disease” *J. Am. Geriatr Soc*, 2003; 51(11):1633-7.
- [218] Shors, T.J., Miesegaes, G., Beylin, A., Zhao, M., Rydel, T., Gould, E., (2001) “Neurogenesis in the adult is involved in the formation of trace memories,” *Nature* (410), pp. 372-376.
- [219] Skinner H.B. (1995, 2nd edition). “Current Diagnosis & Treatment in Orthopedics” McGraw-Hill.
- [220] Soderberg G.L., Cook T.M., “Electromyography in Biomechanics” *Physical Therapy*, 1984; 64 (12):1813-1820.
- [221] Spinal cord injury facts and figures at a glance, updated 2009. Publication of the National Spinal Cord Injury Statistical Center (NSCISC), Birmingham, Alabama.
- [222] Stefan Hesse, Henning Schmidt, Cordula Werner, (2006) “Machines to support motor rehabilitation after stroke: 10 years of experience in Berlin,” *J. Rehabil Res & Dev*, Vol. 43, Number 5, pp. 671-678.

- [223] Stewart, K.C., Cauraugh, J.H., Summers, J.J., (2006) “Bilateral movement training and stroke rehabilitation: a systematic review and meta-analysis,” *J. Neurol Sci*; 244, pp. 89-95.
- [224] Stroke Unit Trialists Collaboration. Organized inpatient (stroke unit) care for stroke., (2002), *Cochrane Database Syst Rev* (1), CD000197.
- [225] Stucki G., Ewert T., Cieza A., “Value and application of the ICF in rehabilitation medicine” *Disability and Rehabilitation*, 2002; 24:932-938.
- [226] Sullivan KJ, Dobkin BH, Tavakol M, et al (2001) Post-stroke cortical plasticity induced by step training. *Society for Neuroscience Proceedings* 2001; 27.
- [227] Sutliff M.H., “Contribution of impaired mobility to patient burden in multiple sclerosis” *Current Medical Research and Opinion*, 2010; 26(1):109-119.
- [228] Talelli, P., Greenwood, R.J., Rothwell, J.C., (2006) “Arm function after stroke: neurophysiological correlates and recovery mechanisms assessed by transcranial magnetic stimulation,” *Clin Neurophysiol*; 117, pp. 1641-1659.
- [229] Tao L. “Development of Wearable Sensor System for Human Dynamic Analysis” PhD Dissertation, Kochi University of Technology, Kochi Japan, Sept. 2006.
- [230] Taub E., Crago J., Burgio L., et al. “An operant approach to overcoming learned nonuse after CNS damage in monkeys and man: the role of shaping” *J Exp Anal Behav*.1994; 61:281 –293.
- [231] Taub E., Miller N.E., Novack T.A., et al. “Technique to improve chronic motor deficit after stroke” *Arch Phys Med Rehabil*.1993; 74:347 –354.
- [232] Taub E., Pidikiti R.D., DeLuca S.C., Crago J.E. “Effects of motor restriction of an unimpaired upper extremity and training on improving functional tasks and altering

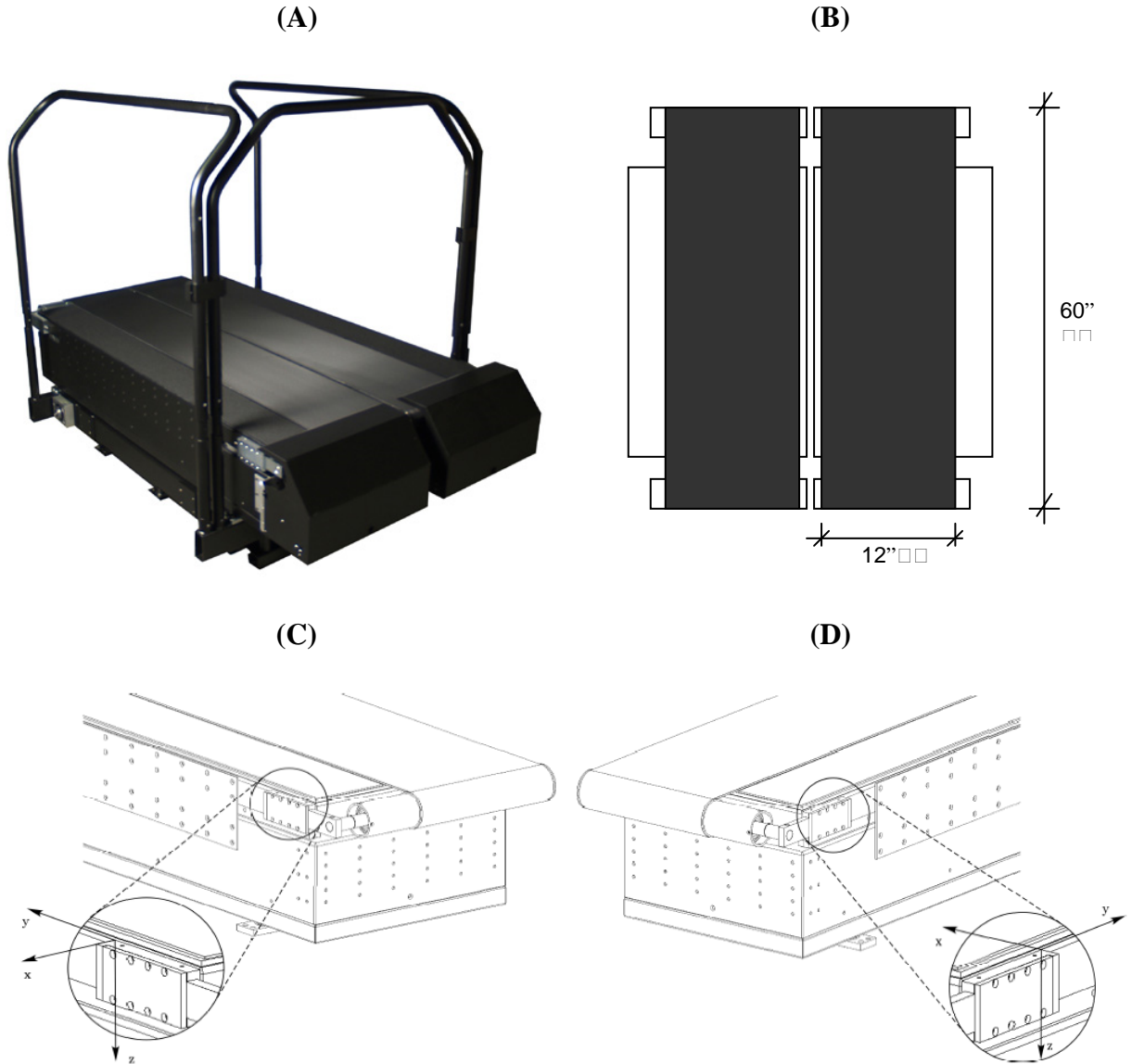
- brain/behaviors” In: Toole J, Ed. Imaging and Neurologic Rehabilitation. New York, NY: Demos; 1996:133–154.
- [233] Taub E., Ramey S.L., Deluca S., Echols K. “Efficacy of constraint-induced movement therapy for children with cerebral palsy with asymmetric motor impairment” *Pediatrics*, 2004; 113:305-312.
- [234] Taub E., Uswatte G., Pidikiti R. “Constraint-Induced Movement therapy: a new family of techniques with broad application to physical rehabilitation—a clinical review” *J Rehabil Res Dev*.1999; 36:237 –251.
- [235] Taupin, P. (2007) “BrdU immunohistochemistry for studying adult neurogenesis: paradigms, pitfalls, limitations, and validation,” *Brain Res Rev* (53), pp. 198-214.
- [236] Taupin, P., Gage, F.H., (2002) “Adult neurogenesis and neural stem cells of the central nervous system in mammals,” *J. Neurosci Res* (69), pp. 745-749.
- [237] Teixeira da Cunha I., Lim P.A., Qureshy H., et al. “Gait outcomes after acute stroke rehabilitation with supported treadmill ambulation training: A randomized controlled pilot study” *Arch Phys Med Rehabil* 2002; 83:1258-65.
- [238] Terrier P., Turner V., Schutz Y., “GPS analysis of human locomotion: Further evidence for long-range correlations in stride-to-stride fluctuations of gait parameters” *Hum Mov Sci*, 2005; 24:97-115.
- [239] Thaut M.H., McIntosh G.C., Rice R.R., “Rhythmic facilitation of gait training in hemiparetic stroke rehabilitation” *J Neurol Sci*, 1997; 151:207–212.
- [240] The Stroke Unit Trial Lists’ Collaboration. Organized inpatient (stroke unit) care for stroke (Cochrane Review). *Cochrane Database of Systematic Reviews*, 2002; 1:CD000197.

- [241] The world health report 2004 – Changing history. Geneva, World Health Organization, 2004 (Statistical Annex).
- [242] Twisk, J.W.R., (2003) “Applied Longitudinal Data Analysis for Epidemiology,” Cambridge University Press.
- [243] Uhlenbrock D., Sarkodie-Gyan T., Reiter F., Konrad M. “Development of a servo-controlled Gait Trainer for the rehabilitation of non-ambulatory patients” Biomed. Technik 1997; 42:196-202.
- [244] Uhlenbrock, D: (1997) “Construction and evaluation of a servo-controlled gait trainer for early gait rehabilitation in non-ambulatory stroke patients” M.S. Thesis University of Teesside, UK.
- [245] Uhlenbrock, D; (1999) “An advanced biomedical gait training machine for the rehabilitation of non-ambulatory stroke patients based on computer-aided human motion analysis,” Ph.D. Thesis, University of Teesside, UK.
- [246] United Cerebral Palsy Research and Education Foundation (U.S.), “Cerebral Palsy Fact Sheet”, Retrieved August 2007.
- [247] Van Peppen, R.P., Kortsmit, M., Lindeman, E., Kwakkel, G., Langhorne, P., (2006) “Effects of visual feedback therapy on postural control in bilateral standing after stroke: a systematic review,” J. Rehabil Med; 38, pp. 3-9.
- [248] Vaughn C.L., Davis B.L., O’Connor J.C. “Dynamics of Human Gait” Western Cape, South Africa: Kiboho Publishers, 1999.
- [249] Visintin M, Barbeau H, Korner-Bitensky N, et al (1998) “A new approach to retain gait in stroke patients through body weight support and treadmill stimulation”. Stroke, 1998; 28:1122-1128.

- [250] Ward, N.S. (2005) “Mechanisms underlying recovery of motor function after stroke,” *Postgrad Med J.* 81, pp. 510-514.
- [251] Warlow, C., Sudlow, C., Dennis, M., Wardlaw, J., Sandercock, P., (2003), “Stroke,” *Lancet* (362), pp. 1211-1224.
- [252] Webster, J. B., Messin, S., Mullaney, D. J., Kripke, D. F. “Transducer design and placement for activity recording,” *Med. Biol. Eng. Comp*, 1982; 20:741–744.
- [253] Werner, C., v. Frankenberg, S., Treig, T., Konrad, M., Hesse, S. (2002) “Treadmill Training with partial body weight support and an electromechanical gait trainer for restoration of gait in subacute stroke patients,” *Stroke* 2002; 33: 2895-2901.
- [254] Wernig A, Muller S, Nanassy A, et al (1995) Laufband therapy based on rules of spinal locomotion is effective in spinal cord injured persons. *Eur J Neurosci* 1995; 7:823-829.
- [255] Wernig A, Nanassy A, Muller S (1999) Laufband (treadmill) therapy in incomplete paraplegia and tetraplegia. *J Neurotrauma* 1999; 16:719-726.
- [256] Wernig A., Muller S., “Laufband locomotion with body weight support improved walking in persons with severe spinal cord injuries” *Paraplegia* 1992; 30:229-38.
- [257] West B.J., Griffin L., “Allometric control, inverse power laws and human gait” *Chaos Solitons & Fractals*, 1999; 10:1519-1527.
- [258] Winter D.A. (1991). “Biomechanics and Motor control of Human Gait: Normal, Elderly and Pathological”. Waterloo Biomechanics Press, Waterloo, Ontario.
- [259] Winter, D.A. (1979). *Biomechanics of human movement*. New York: John Wiley & Sons.
- [260] Winter, D.A., (1990) “Biomechanics and motor control of human movement” (2nd Ed.), 1990, New York, John Wiley and Sons.

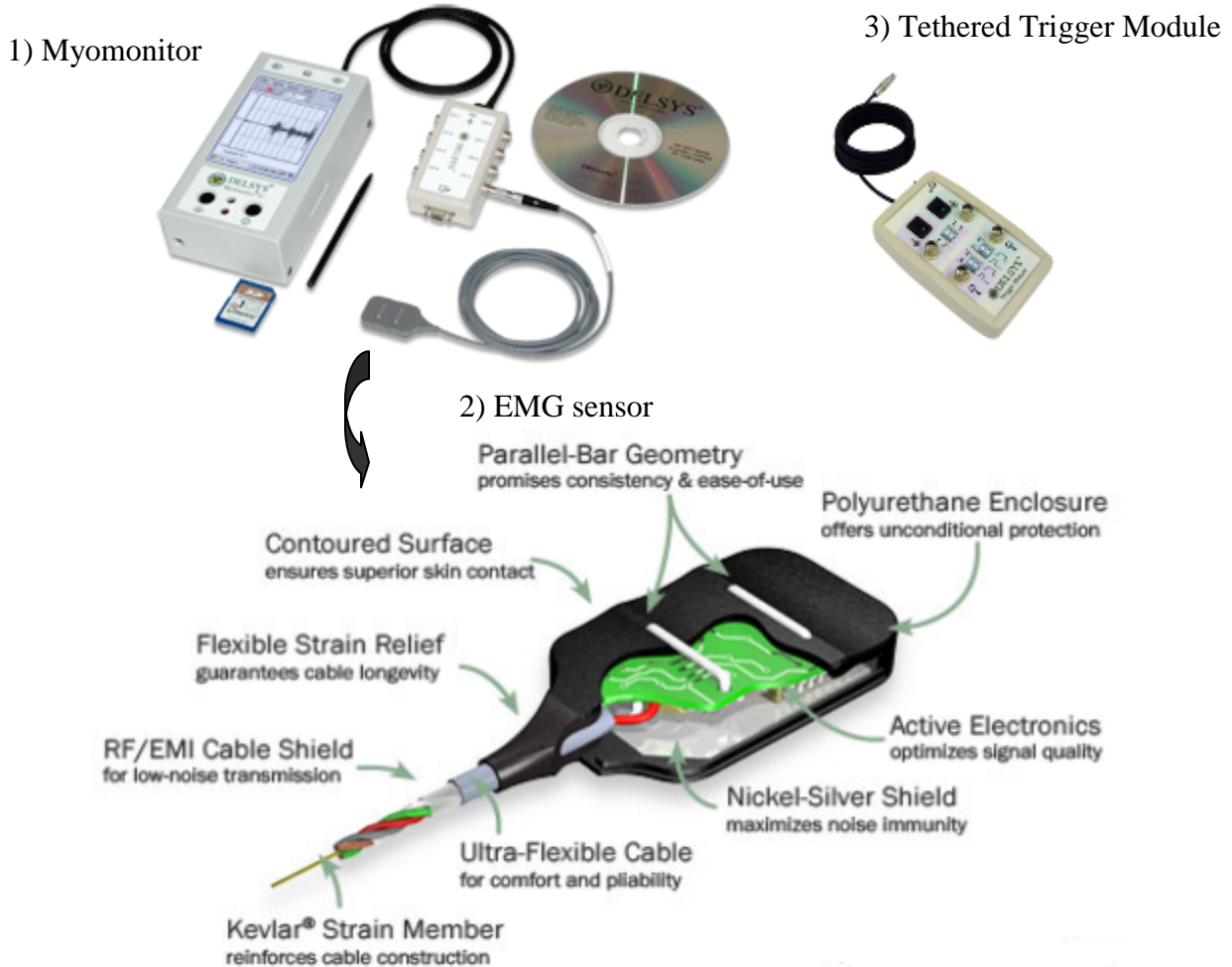
- [261] Woodburn J., Helliwell P.S., “Observations on the F-Scan in-shoe pressure measuring system” *Clinical Biomechanics*, 1996; 11(5):301-304.
- [262] Wu G., Liu W., Hitt J., Millon D. “Spatial, temporal and muscle action patterns of Tai Chi Gait” *Journal of Electromyography and Kinesiology* 2004; 14: 343-354.
- [263] Yarcony M., Jaeger J., Roth E., Krajly R., Quintern J., “Functional neuromuscular stimulation for standing after spinal cord injury” *Arch Phys Med Rehabil*, 1999; 71:201-206.
- [264] Yardimci A., “Fuzzy logic based gait classification for hemiplegic patients” *Proceedings of the 7th International Symposium on Intelligent Data Analysis*, 2007.
- [265] Zadeh L.A. "Fuzzy sets" *Information and Control* 8, 1965; 3: 338-353.
- [266] Zimmermann H.J., (1991, 2nd Edition) “Fuzzy Sets Theory – and Its Applications” Kluwer Academic, Boston.

Appendix I: Structure of Bertec Treadmill



The instrumented treadmill (*Bertec Corporation* in USA). **(A)**: The split-belt treadmill consists of two treads running side by side. Each tread has a 6-component force plate underneath to measure loads exerted on the tread belts. Each tread is driven and controlled separately. **(B)**: Two independent surfaces, 60 inches long and 12 inches wide per belt. Note picture is not to scale. **(C)**: Coordinate system for load measurements on left half of the treadmill. The center of the coordinate system is at the inner corner of the arm block with y-axis forward, x-axis to the left outwards, and z-axis downward. **(D)**: Coordinate system for load measurements on right half of treadmill. The center of the coordinate system is at the inner corner of the arm block with y-axis forward, x-axis to the left, and z-axis downward.

Appendix II: Delsys EMG system components



Delsys Myomonitor® Wireless EMG systems (www.delsys.com).

The goal with EMG measurements is to maximize the signal to noise ratio. Technological developments have decreased the level of noise in the EMG signal. One of the most important developments was the introduction of the bipolar recording technique. Bipolar electrode arrangements are used with a differential amplifier, which functions to suppress signals common to both electrodes. Essentially, differential amplification subtracts the potential at one electrode from that at the other electrode and then amplifies the difference. Delsys EMG electrode with its unique parallel bar geometry ensures consistency across measurements. 1cm spacing is spatially optimal for full-bandwidth signal detection. Fixed inter-sensor distance minimizes amplitude and temporal variability across measurements.

Appendix III: Description of the ADXL330



Small, Low Power, 3-Axis $\pm 3 g$ iMEMS® Accelerometer

ADXL330

FEATURES

3-axis sensing

Small, low-profile package

4 mm × 4 mm × 1.45 mm LFCSP

Low power

180 μA at $V_S = 1.8 V$ (typical)

Single-supply operation

1.8 V to 3.6 V

10,000 g shock survival

Excellent temperature stability

BW adjustment with a single capacitor per axis

RoHS/WEEE lead-free compliant

APPLICATIONS

Cost-sensitive, low power, motion- and tilt-sensing applications

Mobile devices

Gaming systems

Disk drive protection

Image stabilization

Sports and health devices

GENERAL DESCRIPTION

The ADXL330 is a small, thin, low power, complete 3-axis accelerometer with signal conditioned voltage outputs, all on a single monolithic IC. The product measures acceleration with a minimum full-scale range of $\pm 3 g$. It can measure the static acceleration of gravity in tilt-sensing applications, as well as dynamic acceleration resulting from motion, shock, or vibration.

The user selects the bandwidth of the accelerometer using the C_X , C_Y , and C_Z capacitors at the X_{OUT} , Y_{OUT} , and Z_{OUT} pins. Bandwidths can be selected to suit the application, with a range of 0.5 Hz to 1600 Hz for X and Y axes, and a range of 0.5 Hz to 550 Hz for the Z axis.

The ADXL330 is available in a small, low profile, 4 mm × 4 mm × 1.45 mm, 16-lead, plastic lead frame chip scale package (LFCSP_LQ).

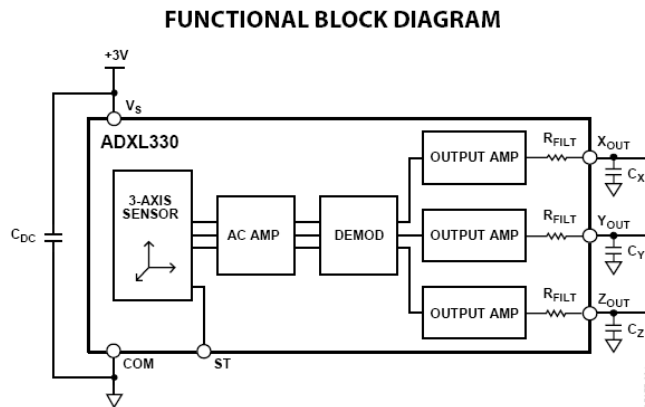


Figure 1.

Rev. A

Information furnished by Analog Devices is believed to be accurate and reliable. However, no responsibility is assumed by Analog Devices for its use, nor for any infringements of patents or other rights of third parties that may result from its use. Specifications subject to change without notice. No license is granted by implication or otherwise under any patent or patent rights of Analog Devices. Trademarks and registered trademarks are the property of their respective owners.

One Technology Way, P.O. Box 9106, Norwood, MA 02062-9106, U.S.A.
Tel: 781.329.4700 www.analog.com
Fax: 781.461.3113 ©2007 Analog Devices, Inc. All rights reserved.

SPECIFICATIONS

$T_A = 25^\circ\text{C}$, $V_S = 3\text{ V}$, $C_X = C_Y = C_Z = 0.1\text{ }\mu\text{F}$, acceleration = 0 g, unless otherwise noted. All minimum and maximum specifications are guaranteed. Typical specifications are not guaranteed.

Table 1.

Parameter	Conditions	Min	Typ	Max	Unit
SENSOR INPUT	Each axis				
Measurement Range		± 3	± 3.6		g
Nonlinearity	% of full scale		± 0.3		%
Package Alignment Error			± 1		Degrees
Interaxis Alignment Error			± 0.1		Degrees
Cross Axis Sensitivity ¹			± 1		%
SENSITIVITY (RATIOMETRIC) ²	Each axis				
Sensitivity at X_{OUT} , Y_{OUT} , Z_{OUT}	$V_S = 3\text{ V}$	270	300	330	mV/g
Sensitivity Change Due to Temperature ³	$V_S = 3\text{ V}$		± 0.015		%/ $^\circ\text{C}$
ZERO g BIAS LEVEL (RATIOMETRIC)	Each axis				
0 g Voltage at X_{OUT} , Y_{OUT} , Z_{OUT}	$V_S = 3\text{ V}$	1.2	1.5	1.8	V
0 g Offset vs. Temperature			± 1		mg/ $^\circ\text{C}$
NOISE PERFORMANCE					
Noise Density X_{OUT} , Y_{OUT}			280		$\mu\text{g}/\sqrt{\text{Hz}}$ rms
Noise Density Z_{OUT}			350		$\mu\text{g}/\sqrt{\text{Hz}}$ rms
FREQUENCY RESPONSE ⁴					
Bandwidth X_{OUT} , Y_{OUT} ⁵	No external filter		1600		Hz
Bandwidth Z_{OUT} ⁵	No external filter		550		Hz
R_{FILT} Tolerance			$32 \pm 15\%$		k Ω
Sensor Resonant Frequency			5.5		kHz
SELF TEST ⁶					
Logic Input Low			+0.6		V
Logic Input High			+2.4		V
ST Actuation Current			+60		μA
Output Change at X_{OUT}	Self test 0 to 1		-150		mV
Output Change at Y_{OUT}	Self test 0 to 1		+150		mV
Output Change at Z_{OUT}	Self test 0 to 1		-60		mV
OUTPUT AMPLIFIER					
Output Swing Low	No load		0.1		V
Output Swing High	No load		2.8		V
POWER SUPPLY					
Operating Voltage Range		1.8		3.6	V
Supply Current	$V_S = 3\text{ V}$		320		μA
Turn-On Time ⁷	No external filter		1		ms
TEMPERATURE					
Operating Temperature Range		-25		+70	$^\circ\text{C}$

¹ Defined as coupling between any two axes.

² Sensitivity is essentially ratiometric to V_S .

³ Defined as the output change from ambient-to-maximum temperature or ambient-to-minimum temperature.

⁴ Actual frequency response controlled by user-supplied external filter capacitors (C_X , C_Y , C_Z).

⁵ Bandwidth with external capacitors = $1/(2 \times \pi \times 32\text{ k}\Omega \times C)$. For C_X , $C_Y = 0.003\text{ }\mu\text{F}$, bandwidth = 1.6 kHz. For $C_Z = 0.01\text{ }\mu\text{F}$, bandwidth = 500 Hz. For C_X , C_Y , $C_Z = 10\text{ }\mu\text{F}$, bandwidth = 0.5 Hz.

⁶ Self-test response changes cubically with V_S .

⁷ Turn-on time is dependent on C_X , C_Y , C_Z and is approximately $160 \times C_X$ or C_Y or $C_Z + 1\text{ ms}$, where C_X , C_Y , C_Z are in μF .

ADXL330

ABSOLUTE MAXIMUM RATINGS

Table 2.

Parameter	Rating
Acceleration (Any Axis, Unpowered)	10,000 g
Acceleration (Any Axis, Powered)	10,000 g
V_S	-0.3 V to +7.0 V
All Other Pins	(COM - 0.3 V) to ($V_S + 0.3$ V)
Output Short-Circuit Duration (Any Pin to Common)	Indefinite
Temperature Range (Powered)	-55°C to +125°C
Temperature Range (Storage)	-65°C to +150°C

Stresses above those listed under Absolute Maximum Ratings may cause permanent damage to the device. This is a stress rating only; functional operation of the device at these or any other conditions above those indicated in the operational section of this specification is not implied. Exposure to absolute maximum rating conditions for extended periods may affect device reliability.

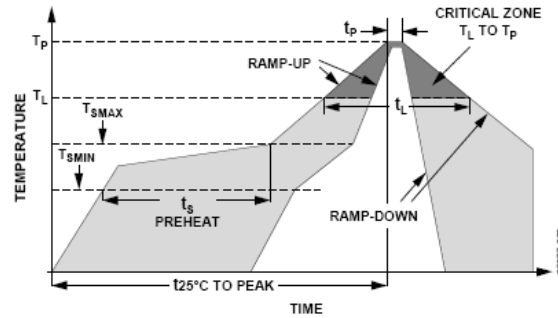


Figure 2. Recommended Soldering Profile

Table 3. Recommended Soldering Profile

Profile Feature	Sn63/Pb37	Pb-Free
Average Ramp Rate (T_L to T_P)	3°C/s max	3°C/s max
Preheat		
Minimum Temperature (T_{SMIN})	100°C	150°C
Maximum Temperature (T_{SMAX})	150°C	200°C
Time (T_{SMIN} to T_{SMAX}), t_s	60 s to 120 s	60 s to 180 s
T_{SMAX} to T_L		
Ramp-Up Rate	3°C/s max	3°C/s max
Time Maintained Above Liquidous (T_L)		
Liquidous Temperature (T_L)	183°C	217°C
Time (t_L)	60 s to 150 s	60 s to 150 s
Peak Temperature (T_P)	240°C + 0°C/-5°C	260°C + 0°C/-5°C
Time within 5°C of Actual Peak Temperature (t_p)	10 s to 30 s	20 s to 40 s
Ramp-Down Rate	6°C/s max	6°C/s max
Time 25°C to Peak Temperature	6 minutes max	8 minutes max

ESD CAUTION

ESD (electrostatic discharge) sensitive device. Electrostatic charges as high as 4000 V readily accumulate on the human body and test equipment and can discharge without detection. Although this product features proprietary ESD protection circuitry, permanent damage may occur on devices subjected to high energy electrostatic discharges. Therefore, proper ESD precautions are recommended to avoid performance degradation or loss of functionality.



ADXL330

ABSOLUTE MAXIMUM RATINGS

Table 2.

Parameter	Rating
Acceleration (Any Axis, Unpowered)	10,000 g
Acceleration (Any Axis, Powered)	10,000 g
V_S	-0.3 V to +7.0 V
All Other Pins	(COM - 0.3 V) to ($V_S + 0.3$ V)
Output Short-Circuit Duration (Any Pin to Common)	Indefinite
Temperature Range (Powered)	-55°C to +125°C
Temperature Range (Storage)	-65°C to +150°C

Stresses above those listed under Absolute Maximum Ratings may cause permanent damage to the device. This is a stress rating only; functional operation of the device at these or any other conditions above those indicated in the operational section of this specification is not implied. Exposure to absolute maximum rating conditions for extended periods may affect device reliability.

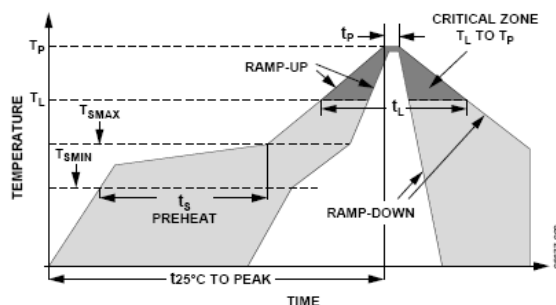


Figure 2. Recommended Soldering Profile

Table 3. Recommended Soldering Profile

Profile Feature	Sn63/Pb37	Pb-Free
Average Ramp Rate (T_L to T_P)	3°C/s max	3°C/s max
Preheat		
Minimum Temperature (T_{SMIN})	100°C	150°C
Maximum Temperature (T_{SMAX})	150°C	200°C
Time (T_{SMIN} to T_{SMAX}), t_s	60 s to 120 s	60 s to 180 s
T_{SMAX} to T_L		
Ramp-Up Rate	3°C/s max	3°C/s max
Time Maintained Above Liquidous (T_L)		
Liquidous Temperature (T_L)	183°C	217°C
Time (t_L)	60 s to 150 s	60 s to 150 s
Peak Temperature (T_P)	240°C + 0°C/-5°C	260°C + 0°C/-5°C
Time within 5°C of Actual Peak Temperature (t_P)	10 s to 30 s	20 s to 40 s
Ramp-Down Rate	6°C/s max	6°C/s max
Time 25°C to Peak Temperature	6 minutes max	8 minutes max

ESD CAUTION

ESD (electrostatic discharge) sensitive device. Electrostatic charges as high as 4000 V readily accumulate on the human body and test equipment and can discharge without detection. Although this product features proprietary ESD protection circuitry, permanent damage may occur on devices subjected to high energy electrostatic discharges. Therefore, proper ESD precautions are recommended to avoid performance degradation or loss of functionality.



PIN CONFIGURATION AND FUNCTION DESCRIPTIONS

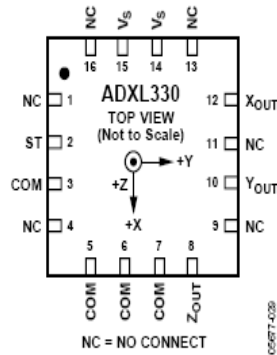


Figure 3. Pin Configuration

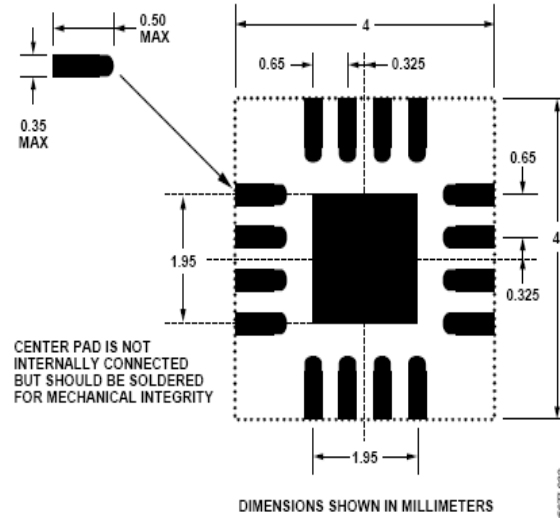


Figure 4. Recommended PCB Layout

Table 4. Pin Function Descriptions

Pin No.	Mnemonic	Description
1	NC	No Connect
2	ST	Self Test
3	COM	Common
4	NC	No Connect
5	COM	Common
6	COM	Common
7	COM	Common
8	Z _{OUT}	Z Channel Output
9	NC	No Connect
10	Y _{OUT}	Y Channel Output
11	NC	No Connect
12	X _{OUT}	X Channel Output
13	NC	No Connect
14	V _S	Supply Voltage (1.8 V to 3.6 V)
15	V _S	Supply Voltage (1.8 V to 3.6 V)
16	NC	No Connect

TYPICAL PERFORMANCE CHARACTERISTICS

N > 1000 for all typical performance plots, unless otherwise noted.

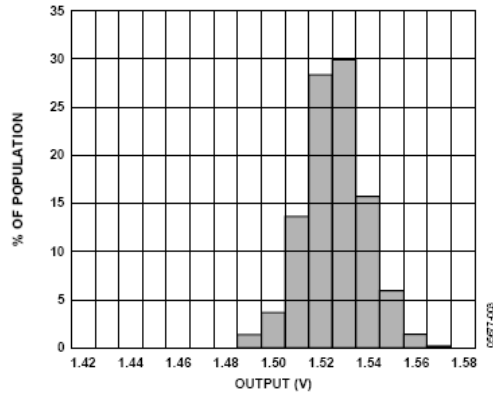


Figure 5. X-Axis Zero g Bias at 25°C, $V_s = 3$ V

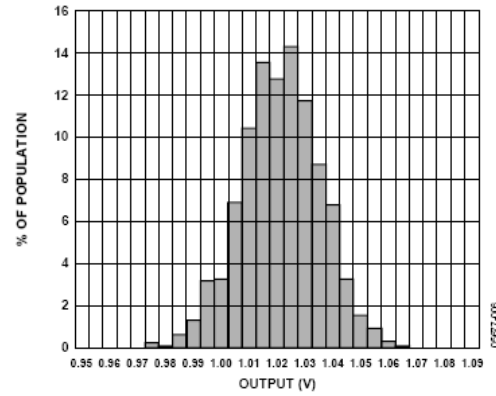


Figure 8. X-Axis Zero g Bias at 25°C, $V_s = 2$ V

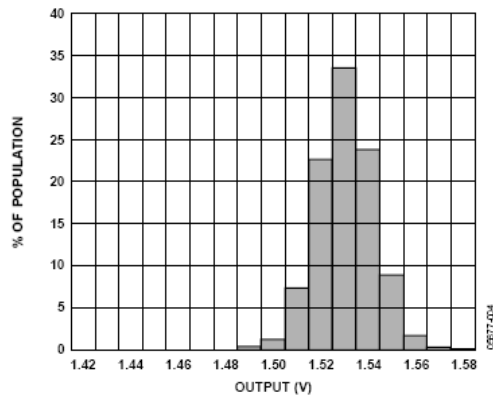


Figure 6. Y-Axis Zero g Bias at 25°C, $V_s = 3$ V

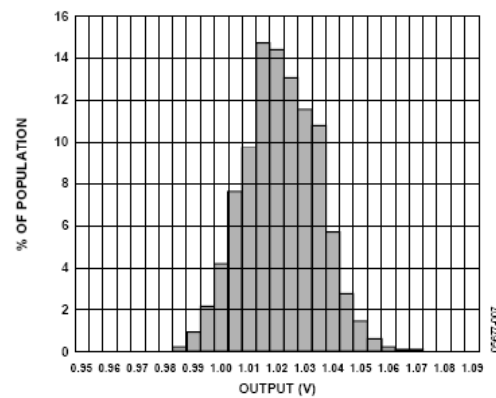


Figure 9. Y-Axis Zero g Bias at 25°C, $V_s = 2$ V

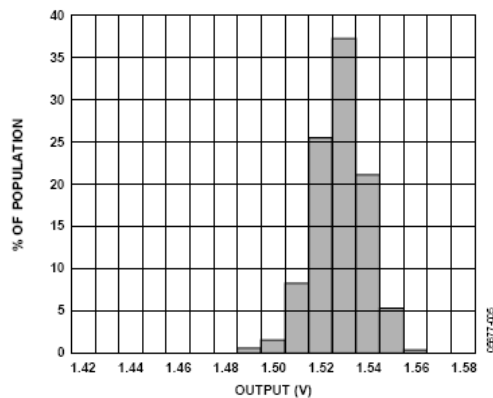


Figure 7. Z-Axis Zero g Bias at 25°C, $V_s = 3$ V

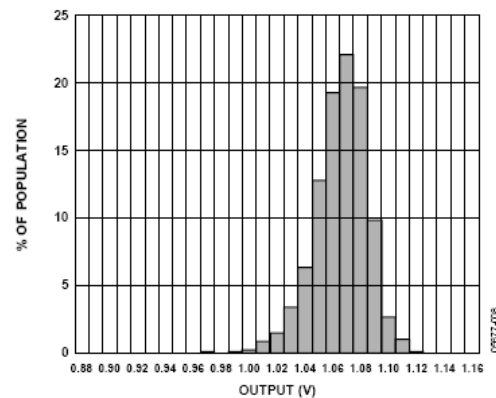


Figure 10. Z-Axis Zero g Bias at 25°C, $V_s = 2$ V

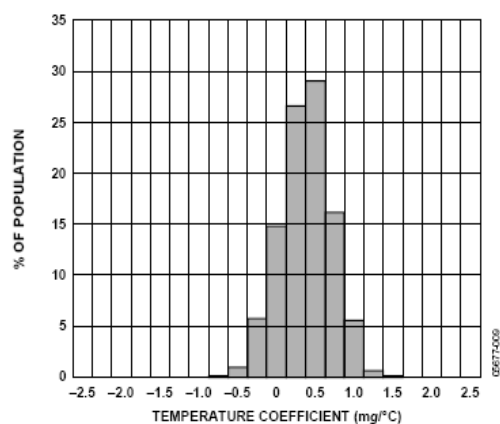


Figure 11. X-Axis Zero g Bias Temperature Coefficient, $V_S = 3\text{ V}$

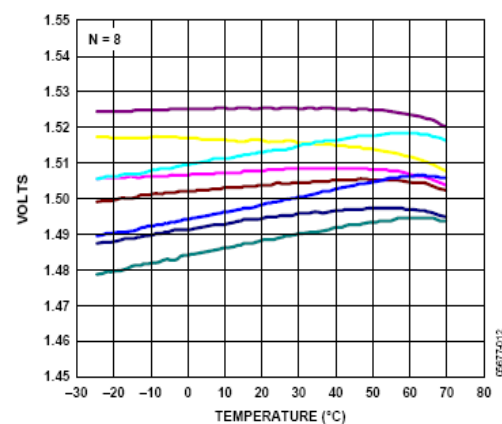


Figure 14. X-Axis Zero g Bias vs. Temperature—8 Parts Soldered to PCB

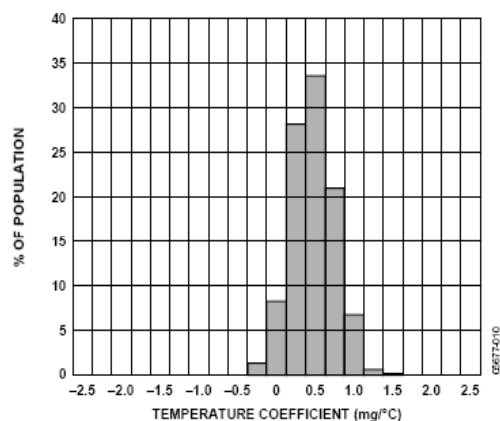


Figure 12. Y-Axis Zero g Bias Temperature Coefficient, $V_S = 3\text{ V}$

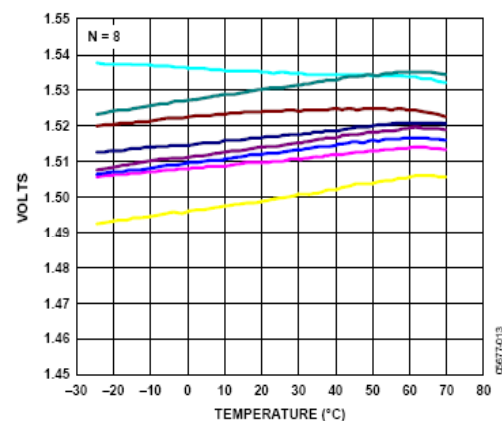


Figure 15. Y-Axis Zero g Bias vs. Temperature—8 Parts Soldered to PCB

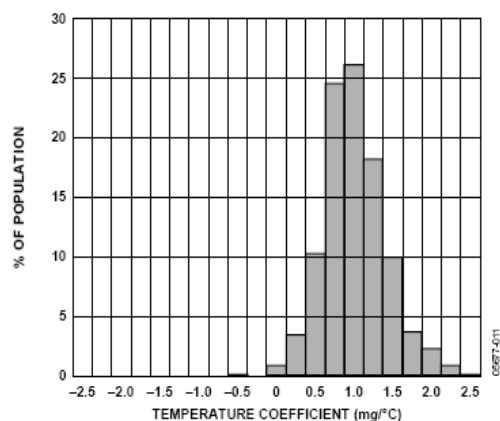


Figure 13. Z-Axis Zero g Bias Temperature Coefficient, $V_S = 3\text{ V}$

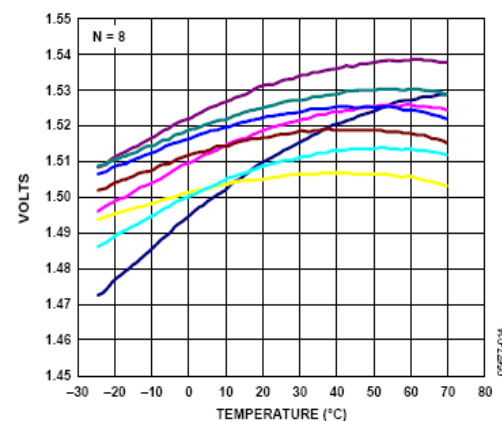


Figure 16. Z-Axis Zero g Bias vs. Temperature—8 Parts Soldered to PCB

ADXL330

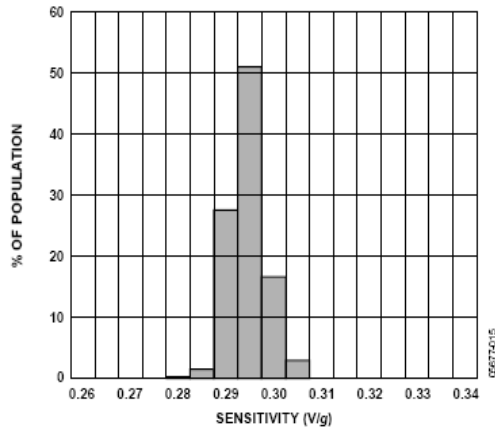


Figure 17. X-Axis Sensitivity at 25°C, $V_S = 3\text{ V}$

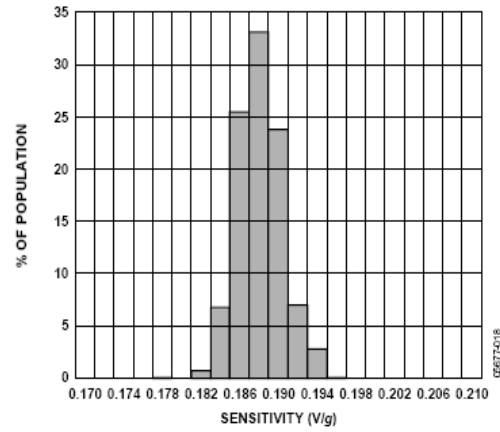


Figure 20. X-Axis Sensitivity at 25°C, $V_S = 2\text{ V}$

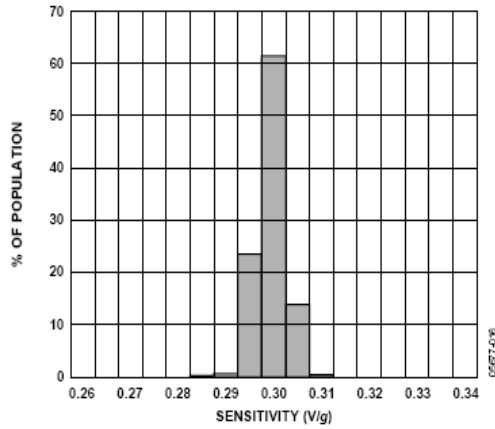


Figure 18. Y-Axis Sensitivity at 25°C, $V_S = 3\text{ V}$

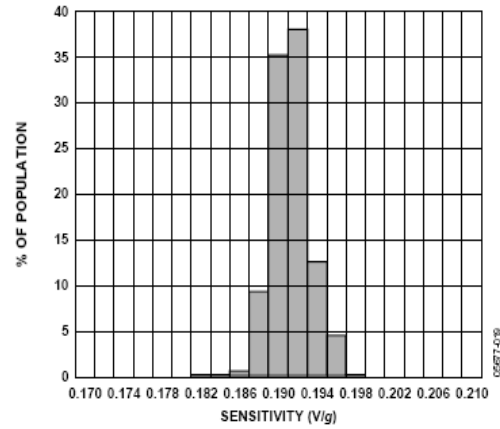


Figure 21. Y-Axis Sensitivity at 25°C, $V_S = 2\text{ V}$

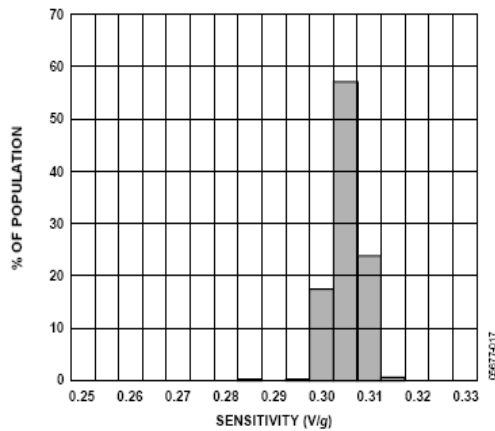


Figure 19. Z-Axis Sensitivity at 25°C, $V_S = 3\text{ V}$

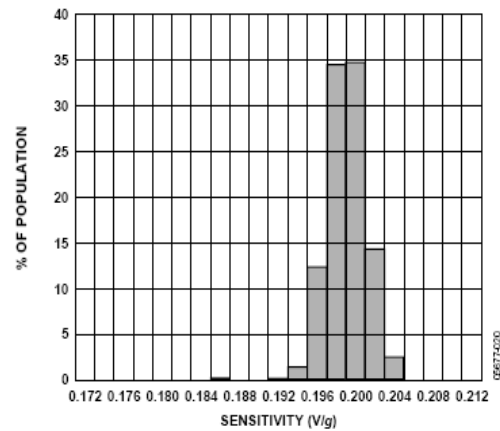


Figure 22. Z-Axis Sensitivity at 25°C, $V_S = 2\text{ V}$

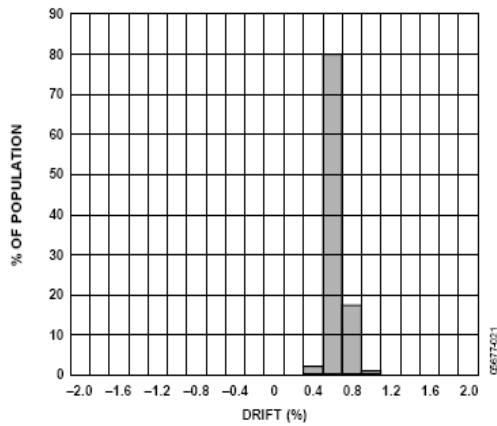


Figure 23. X-Axis Sensitivity Drift Over Temperature, $V_s = 3\text{ V}$

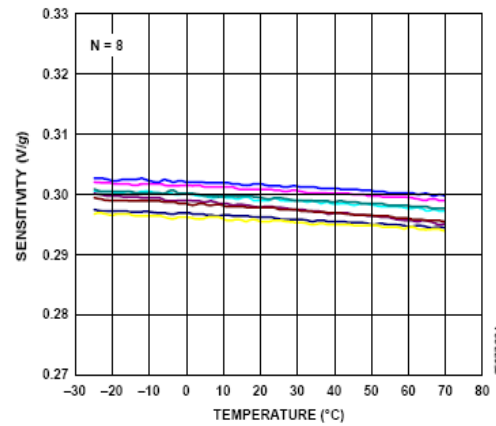


Figure 26. X-Axis Sensitivity vs. Temperature
8 Parts Soldered to PCB, $V_s = 3\text{ V}$

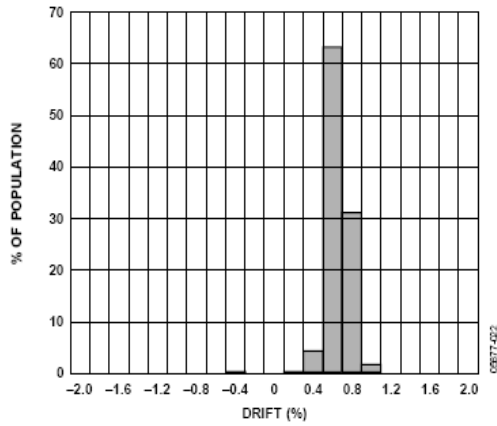


Figure 24. Y-Axis Sensitivity Drift Over Temperature, $V_s = 3\text{ V}$

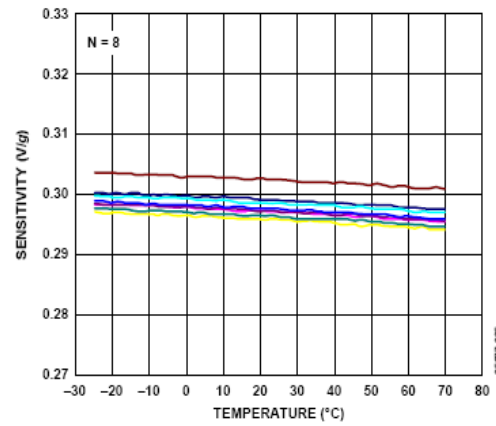


Figure 27. Y-Axis Sensitivity vs. Temperature
8 Parts Soldered to PCB, $V_s = 3\text{ V}$

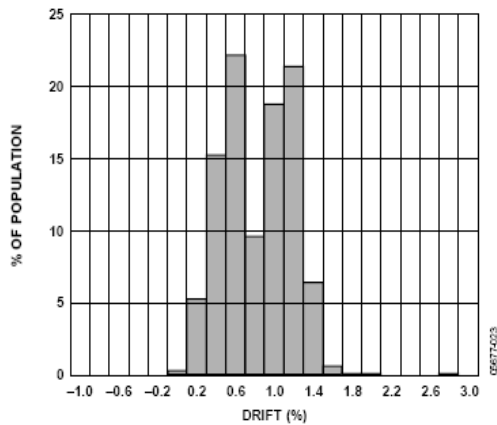


Figure 25. Z-Axis Sensitivity Drift Over Temperature, $V_s = 3\text{ V}$

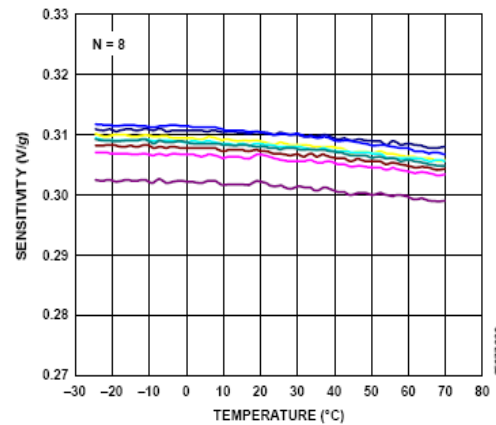


Figure 28. Z-Axis Sensitivity vs. Temperature
8 Parts Soldered to PCB, $V_s = 3\text{ V}$

ADXL330

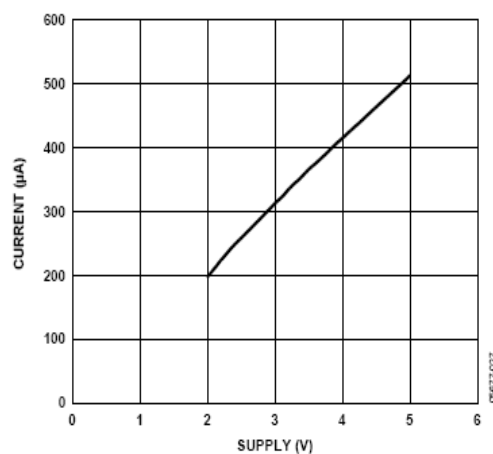


Figure 29. Typical Current Consumption vs. Supply Voltage

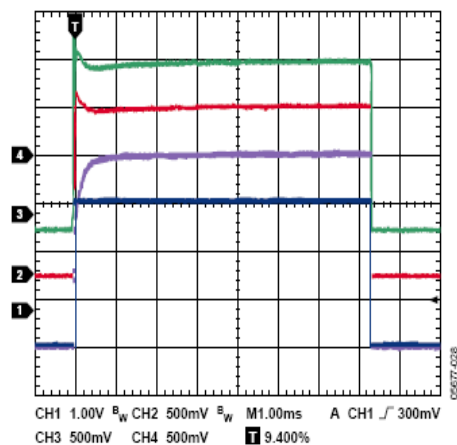


Figure 30. Typical Turn-On Time— $C_X, C_Y, C_Z = 0.0047 \mu F, V_S = 3 V$

THEORY OF OPERATION

The ADXL330 is a complete 3-axis acceleration measurement system on a single monolithic IC. The ADXL330 has a measurement range of ± 3 g minimum. It contains a polysilicon surface micromachined sensor and signal conditioning circuitry to implement an open-loop acceleration measurement architecture. The output signals are analog voltages that are proportional to acceleration. The accelerometer can measure the static acceleration of gravity in tilt sensing applications as well as dynamic acceleration resulting from motion, shock, or vibration.

The sensor is a polysilicon surface micromachined structure built on top of a silicon wafer. Polysilicon springs suspend the structure over the surface of the wafer and provide a resistance against acceleration forces. Deflection of the structure is measured using a differential capacitor that consists of independent fixed plates and plates attached to the moving mass. The fixed plates are driven by 180° out-of-phase square waves. Acceleration deflects the moving mass and unbalances the differential capacitor resulting in a sensor output whose amplitude is proportional to acceleration. Phase-sensitive demodulation techniques are then used to determine the magnitude and direction of the acceleration.

The demodulator output is amplified and brought off-chip through a 32 k Ω resistor. The user then sets the signal bandwidth of the device by adding a capacitor. This filtering improves measurement resolution and helps prevent aliasing.

MECHANICAL SENSOR

The ADXL330 uses a single structure for sensing the X, Y, and Z axes. As a result, the three axes sense directions are highly orthogonal with little cross axis sensitivity. Mechanical misalignment of the sensor die to the package is the chief source of cross axis sensitivity. Mechanical misalignment can, of course, be calibrated out at the system level.

PERFORMANCE

Rather than using additional temperature compensation circuitry, innovative design techniques ensure high performance is built-in to the ADXL330. As a result, there is neither quantization error nor nonmonotonic behavior, and temperature hysteresis is very low (typically less than 3 mg over the -25°C to $+70^{\circ}\text{C}$ temperature range).

Figure 14, Figure 15, and Figure 16 show the zero g output performance of eight parts (X-, Y-, and Z-axis) soldered to a PCB over a -25°C to $+70^{\circ}\text{C}$ temperature range.

Figure 26, Figure 27, and Figure 28 demonstrate the typical sensitivity shift over temperature for supply voltages of 3 V. This is typically better than $\pm 1\%$ over the -25°C to $+70^{\circ}\text{C}$ temperature range.

ADXL330

APPLICATIONS

POWER SUPPLY DECOUPLING

For most applications, a single 0.1 μF capacitor, C_{DC} , placed close to the ADXL330 supply pins adequately decouples the accelerometer from noise on the power supply. However, in applications where noise is present at the 50 kHz internal clock frequency (or any harmonic thereof), additional care in power supply bypassing is required as this noise can cause errors in acceleration measurement. If additional decoupling is needed, a 100 Ω (or smaller) resistor or ferrite bead can be inserted in the supply line. Additionally, a larger bulk bypass capacitor (1 μF or greater) can be added in parallel to C_{DC} . Ensure that the connection from the ADXL330 ground to the power supply ground is low impedance because noise transmitted through ground has a similar effect as noise transmitted through V_S .

SETTING THE BANDWIDTH USING C_X , C_Y , AND C_Z

The ADXL330 has provisions for band limiting the X_{OUT} , Y_{OUT} , and Z_{OUT} pins. Capacitors must be added at these pins to implement low-pass filtering for antialiasing and noise reduction. The equation for the 3 dB bandwidth is

$$F_{-3\text{dB}} = 1/(2\pi(32 \text{ k}\Omega) \times C_{(X,Y,Z)})$$

or more simply

$$F_{-3\text{dB}} = 5 \mu\text{F}/C_{(X,Y,Z)}$$

The tolerance of the internal resistor (R_{FILT}) typically varies as much as $\pm 15\%$ of its nominal value (32 k Ω), and the bandwidth varies accordingly. A minimum capacitance of 0.0047 μF for C_X , C_Y , and C_Z is recommended in all cases.

Table 5. Filter Capacitor Selection, C_X , C_Y , and C_Z

Bandwidth (Hz)	Capacitor (μF)
1	4.7
10	0.47
50	0.10
100	0.05
200	0.027
500	0.01

SELF TEST

The ST pin controls the self test feature. When this pin is set to V_S , an electrostatic force is exerted on the accelerometer beam. The resulting movement of the beam allows the user to test if the accelerometer is functional. The typical change in output is -500 mg (corresponding to -150 mV) in the X-axis, 500 mg (or 150 mV) on the Y-axis, and -200 mg (or -60 mV) on the Z-axis. This ST pin may be left open circuit or connected to common (COM) in normal use.

Never expose the ST pin to voltages greater than $V_S + 0.3 \text{ V}$. If this cannot be guaranteed due to the system design (for instance, if there are multiple supply voltages), then a low V_F clamping diode between ST and V_S is recommended.

DESIGN TRADE-OFFS FOR SELECTING FILTER CHARACTERISTICS: THE NOISE/BW TRADE-OFF

The selected accelerometer bandwidth ultimately determines the measurement resolution (smallest detectable acceleration). Filtering can be used to lower the noise floor to improve the resolution of the accelerometer. Resolution is dependent on the analog filter bandwidth at X_{OUT} , Y_{OUT} , and Z_{OUT} .

The output of the ADXL330 has a typical bandwidth of greater than 500 Hz. The user must filter the signal at this point to limit aliasing errors. The analog bandwidth must be no more than half the analog-to-digital sampling frequency to minimize aliasing. The analog bandwidth can be further decreased to reduce noise and improve resolution.

The ADXL330 noise has the characteristics of white Gaussian noise, which contributes equally at all frequencies and is described in terms of $\mu\text{g}/\sqrt{\text{Hz}}$ (the noise is proportional to the square root of the accelerometer bandwidth). The user should limit bandwidth to the lowest frequency needed by the application to maximize the resolution and dynamic range of the accelerometer.

With the single-pole, roll-off characteristic, the typical noise of the ADXL330 is determined by

$$\text{rms Noise} = \text{Noise Density} \times (\sqrt{BW} \times 1.6)$$

Often, the peak value of the noise is desired. Peak-to-peak noise can only be estimated by statistical methods. Table 6 is useful for estimating the probabilities of exceeding various peak values, given the rms value.

Table 6. Estimation of Peak-to-Peak Noise

Peak-to-Peak Value	% of Time that Noise Exceeds Nominal Peak-to-Peak Value
$2 \times \text{rms}$	32
$4 \times \text{rms}$	4.6
$6 \times \text{rms}$	0.27
$8 \times \text{rms}$	0.006

USE WITH OPERATING VOLTAGES OTHER THAN 3 V

The ADXL330 is tested and specified at $V_S = 3 \text{ V}$; however, it can be powered with V_S as low as 1.8 V or as high as 3.6 V. Note that some performance parameters change as the supply voltage is varied.

The ADXL330 output is ratiometric, therefore, the output sensitivity (or scale factor) varies proportionally to the supply voltage. At $V_S = 3.6$ V, the output sensitivity is typically 360 mV/g. At $V_S = 2$ V, the output sensitivity is typically 195 mV/g.

The zero g bias output is also ratiometric, so the zero g output is nominally equal to $V_S/2$ at all supply voltages.

The output noise is not ratiometric but is absolute in volts; therefore, the noise density decreases as the supply voltage increases. This is because the scale factor (mV/g) increases while the noise voltage remains constant. At $V_S = 3.6$ V, the X- and Y-axis noise density is typically $230 \mu\text{g}/\sqrt{\text{Hz}}$, while at $V_S = 2$ V, the X- and Y-axis noise density is typically $350 \mu\text{g}/\sqrt{\text{Hz}}$.

Self test response in g is roughly proportional to the square of the supply voltage. However, when ratiometricity of sensitivity is factored in with supply voltage, the self test response in volts is roughly proportional to the cube of the supply voltage. For example, at $V_S = 3.6$ V, the self test response for the ADXL330 is approximately -275 mV for the X-axis, +275 mV for the Y-axis, and -100 mV for the Z-axis.

At $V_S = 2$ V, the self test response is approximately -60 mV for the X-axis, +60 mV for the Y-axis, and -25 mV for the Z-axis.

The supply current decreases as the supply voltage decreases. Typical current consumption at $V_S = 3.6$ V is 375 μA , and typical current consumption at $V_S = 2$ V is 200 μA .

AXES OF ACCELERATION SENSITIVITY

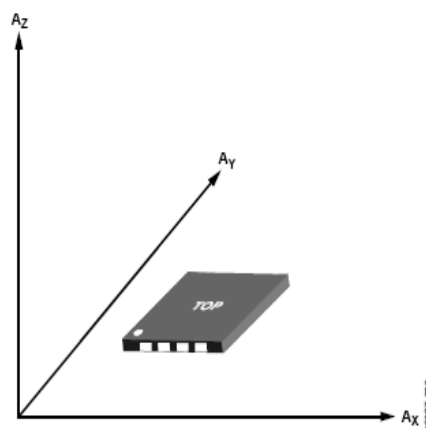


Figure 31. Axes of Acceleration Sensitivity, Corresponding Output Voltage Increases When Accelerated Along the Sensitive Axis

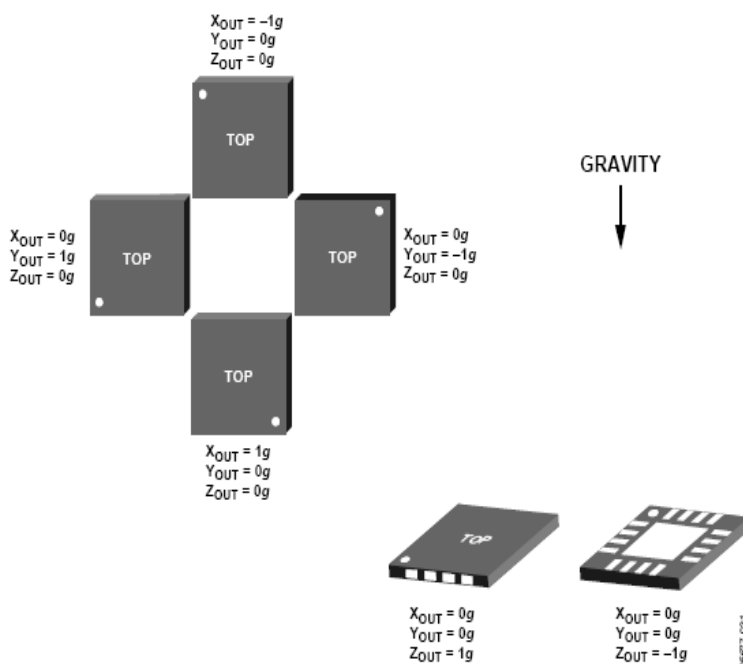
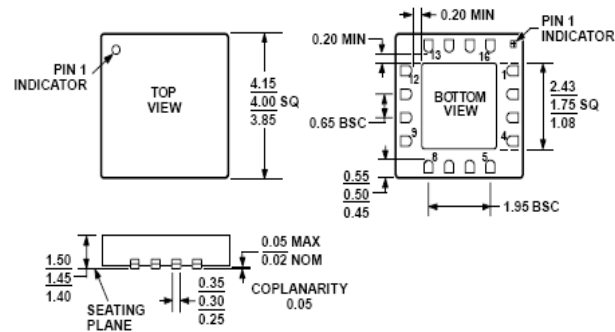


Figure 32. Output Response vs. Orientation to Gravity

ADXL330

OUTLINE DIMENSIONS



*STACKED DIE WITH GLASS SEAL.

Figure 33. 16-Lead Lead Frame Chip Scale Package (LFCSP_LQ)
4 mm × 4 mm Body, Thick Quad
(CP-16-5a*)
Dimensions shown in millimeters

ORDERING GUIDE

Model	Measurement Range	Specified Voltage	Temperature Range	Package Description	Package Option
ADXL330KCPZ ¹	±3 g	3 V	–25°C to +70°C	16-Lead LFCSP_LQ	CP-16-5a
ADXL330KCPZ-RL ¹	±3 g	3 V	–25°C to +70°C	16-Lead LFCSP_LQ	CP-16-5a
EVAL-ADXL330Z ¹				Evaluation Board	

¹ Z = Pb-free part.

Appendix IV: Subjects anthropometric measurement form

Anthropometric Measurement

Name		ID #	
Male/Female		Date of Birth (mm/dd/yy)	
Weight (kg)		Standing Height (cm)	
Upper Body	(cm)	Lower Body	(cm)
Right Shoulder Ht		Right Knee Ht Seated	
Left Shoulder Ht		Left Knee Ht Seated	
Right Armpit Ht		Right Thigh Circum.	
Left Armpit Ht		Left Thigh Circum.	
Waist Height		Right Upper Leg Circum.	
Seated Height		Left Upper Leg Circum.	
Head Length		Right Knee Circum.	
Head Breadth		Left Knee Circum.	
Head to Chin Ht		Right Calf Circum.	
Neck Circum.		Left Calf Circum.	
Shoulder Breadth		Right Ankle Circum.	
Chest Depth		Left Ankle Circum.	
Chest Breadth		Right Ankle Ht Outside	
Waist Depth		Left Ankle Ht Outside	
Waist Breadth		Right Foot Breadth	
Buttock Depth		Left Foot Breadth	
Hip Breadth Standing		Right Foot Length	
Right Shoulder to Elbow Ln.		Left Foot Length	
Left Shoulder to Elbow Ln.		Right Ankle Width	
Right Forearm Hand Ln.		Left Ankle Width	
Left Forearm Hand Ln.		Right Knee Width	
Right Biceps Circum.		Left Knee Width	
Left Biceps Circum.		Chest Circum.	
Right Elbow Circum.		Right Thigh Length	
Left Elbow Circum.		Left Thigh Length	
Right Forearm Circum.		Right Mid-thigh Circum.	
Left Forearm Circum.		Left Mid-thigh Circum.	
Right Wrist Circum.		Right Calf Length	
Left Wrist Circum.		Left Calf Length	
		% Fat	
Have you ever had injury on our lower limb? Or have you suffered from mental problem? Are you taking any medications? If yes, please indicate. How long have you been diagnosed?			

Appendix V: Results of Multiple Sclerosis Patient 2 (MS2)

- **Description**

Subject is a 40 year old female, was diagnosed with mild symptoms of multiple sclerosis in June 2009. She complained having left foot drop during walking. Medication includes *Avonex (Interferon beta)* for relapsing remitting multiple sclerosis (RRMS). She was test bare-footed, walking on the instrumented treadmill with the harness support for three minute continually, at speed of 0.65 m/s.

- **Temporal Stride Variability**

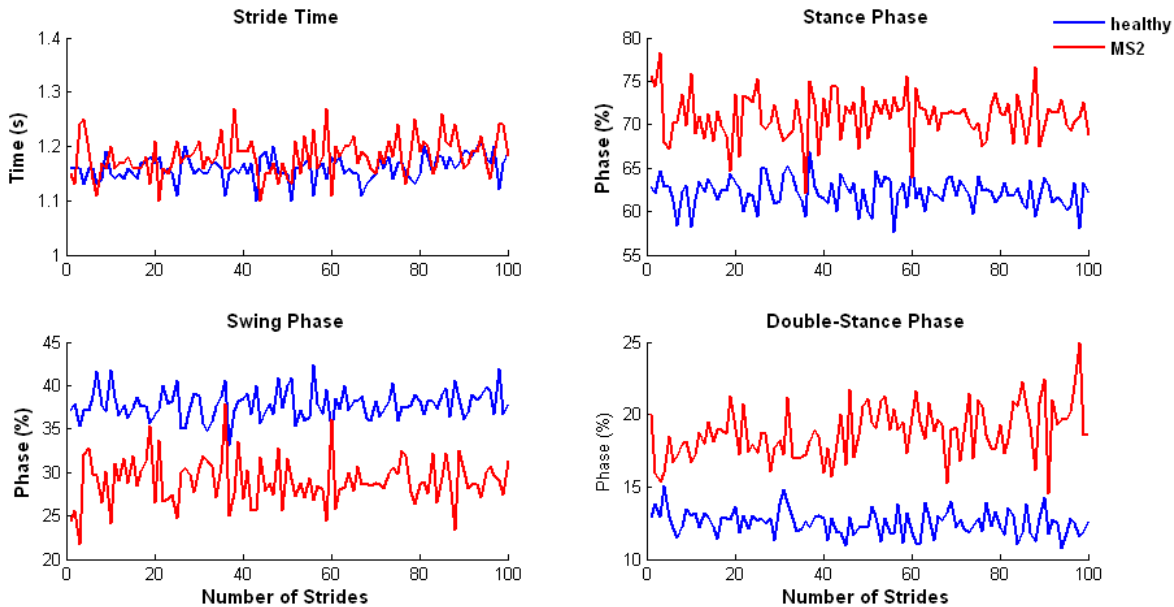


Figure AV-1: Stride variability of a healthy female and female multiple sclerosis subject case 2 (MS-2).

Summary: The MS2 subject has greater temporal variability, especially shown in stance/swing/double-stance phases, compared with the healthy female subject. She has shorter swing phase, and longer stance/double-stance phases. The duration of the double-stance phase

gradually increased with greater variability which indicates some levels of functional fatigue appearing in the walking trial.

- **Ground Reaction Forces**

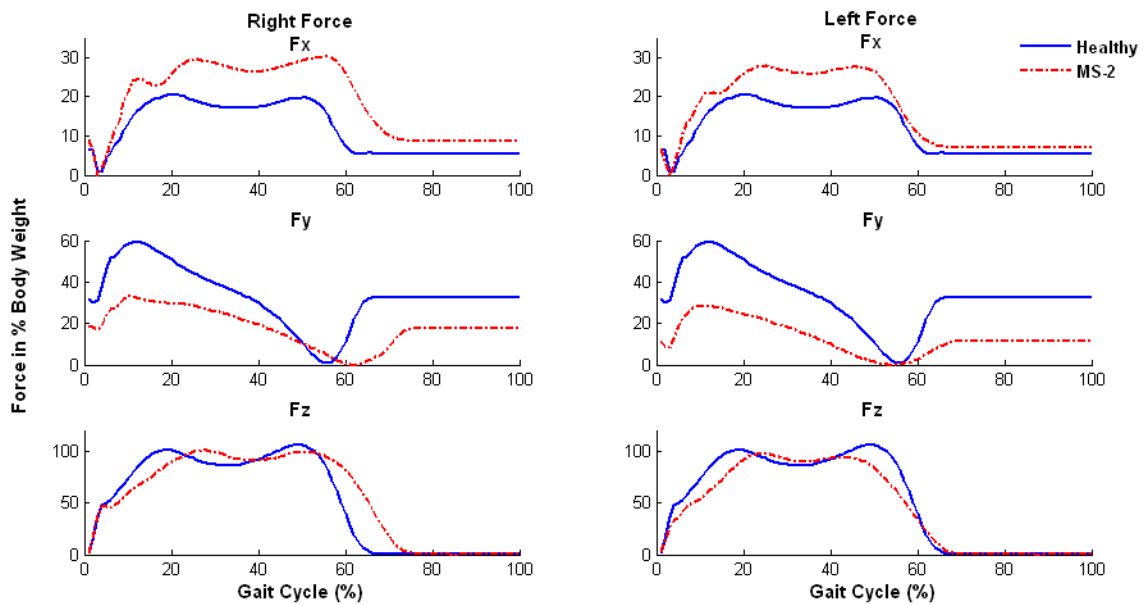


Figure AV-2: Right and left GRF in 3-D in multiple sclerosis subject case 2 (MS-2).

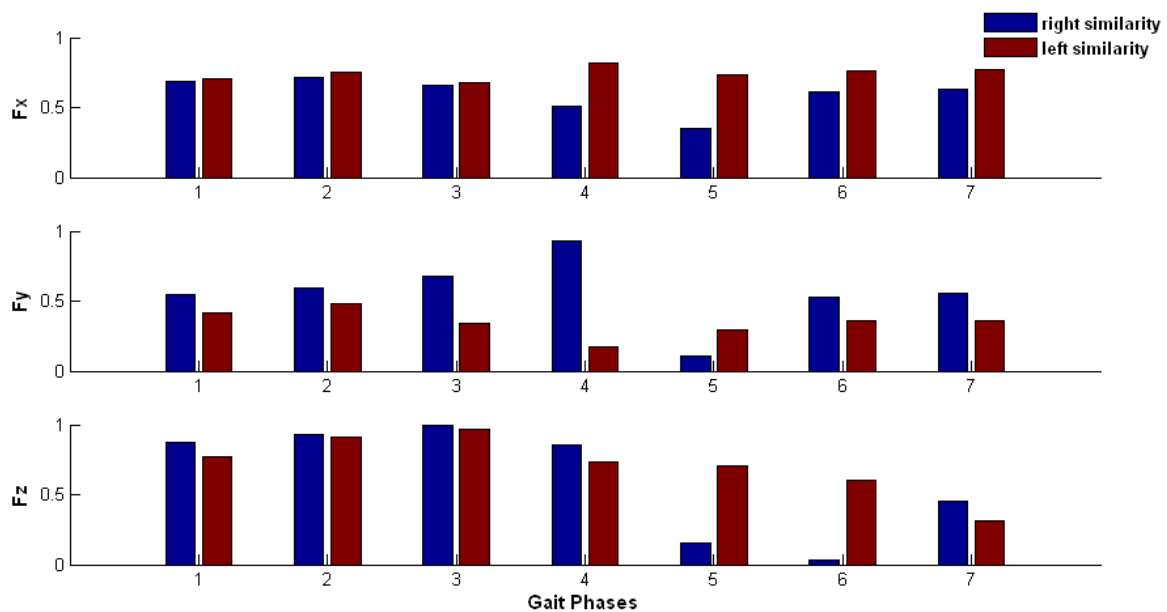


Figure AV-3: Grade of similarity on right and left GRF in MS-2.

Summary:

The force curve in the vertical direction (Fz) shows a longer stance phase than the healthy subjects on right foot of the MS2, which indicates the affected leg was on the left (with reference to her description). The foot drop on the left side also caused much shortened interval of two peaks in the stance phases. In anterior-posterior direction (Fy), MS2 has lower magnitude of force than healthy subjects for both right and left feet (left Fy < right Fy). In mediolateral direction (Fx), MS2 has higher GRF than healthy subjects (right Fx > left Fx). The right force has the significant small similarity on all three planes during initial swing and mid-swing phases due to the longer loading times in the stance phase. She has quite high similarity for the rest of the forces which indicate she has fresh and mild multiple sclerosis or in her remission stage of RRMS.

• EMG Muscle Activity Patterns

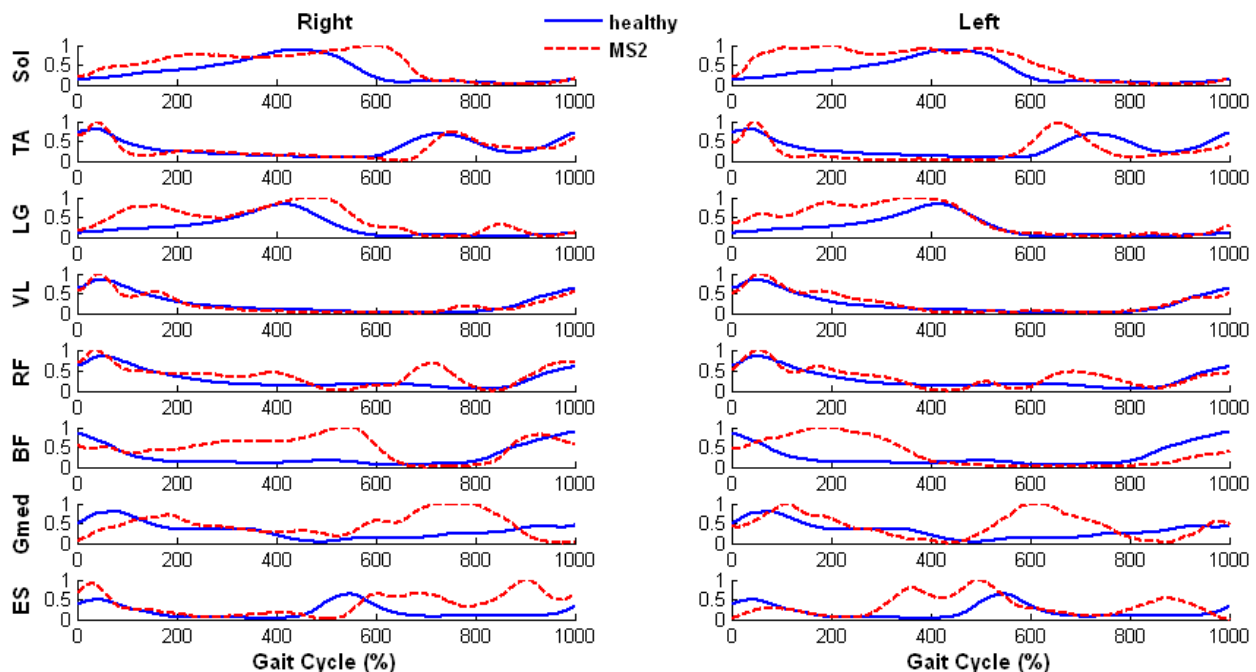


Figure AV-4: Comparison of EMG pattern in a full gait cycle between able-bodied subjects and MS-2 subject.

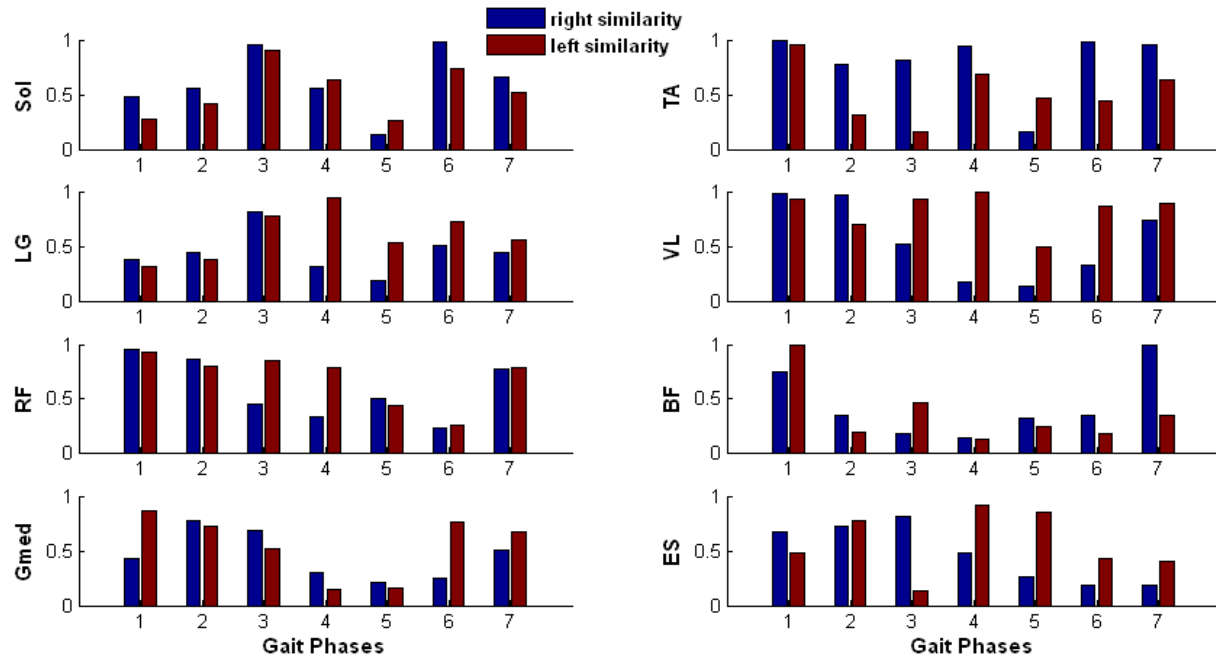


Figure AV-5: Grade of similarity on right and left EMG in MS-2.

Summary:

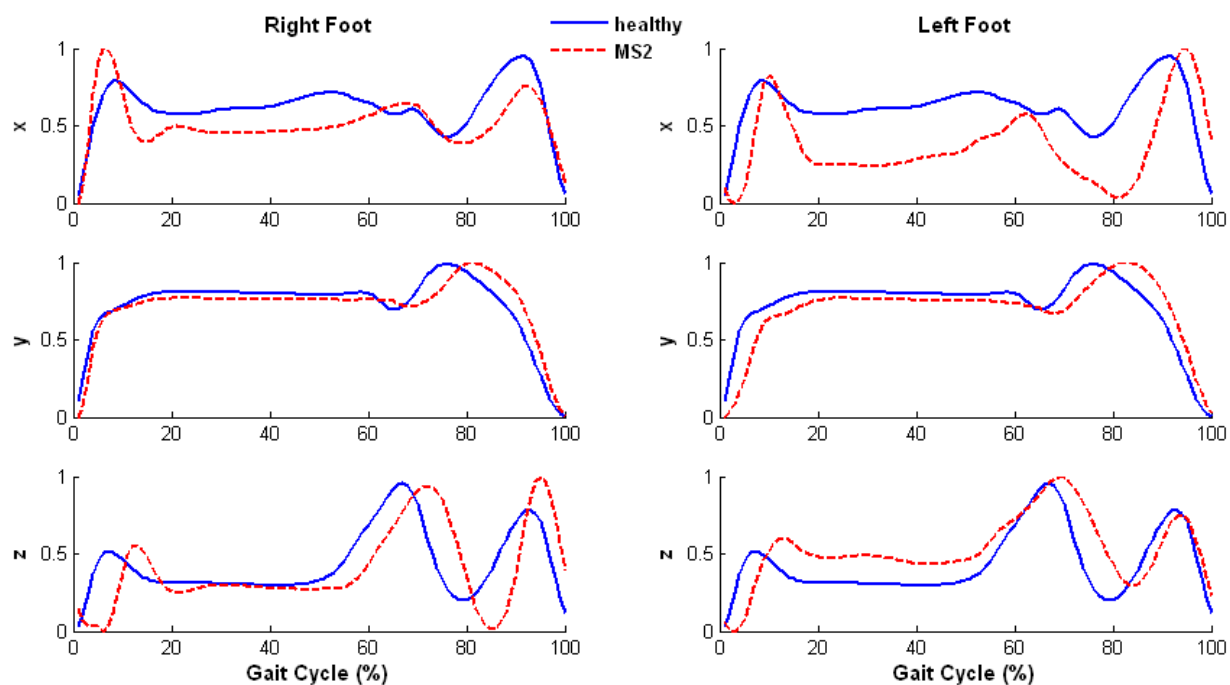
Table AV-1: Summary of EMG activity in MS-2

	Right	Left
Soleus	Higher muscle activities appear in stance phase. Significant small similarity appears in the initial swing.	Same as right Sol.
Tibialis Anterior (TA)	Spasticity appears the initial contact. Significant small similarity appears in initial swing due to longer loading time in right.	Spasticity at initial contact and initial swing phase. Significant small similarity appears in mid-stance.
Gastrocnemius Lateralis (LG)	Higher muscle activities appear entire stance phase and mid-stance. Significant small similarity appears in initial swing.	Spasticity appears from initial contact until the mid-stance phase. Significant small similarity appears in the loading response.
Vastus Lateralis (VL)	Sharp rise in the initial contact. Least similarity in pre- and initial swing.	Sharp rise in the initial contact. Moderate to high similarity for all gait phases
Rectus Femoris (RF)	Spasticity appears in the initial contact and initial swing phase. The least similarity appears in mid-swing.	Same as right RF.

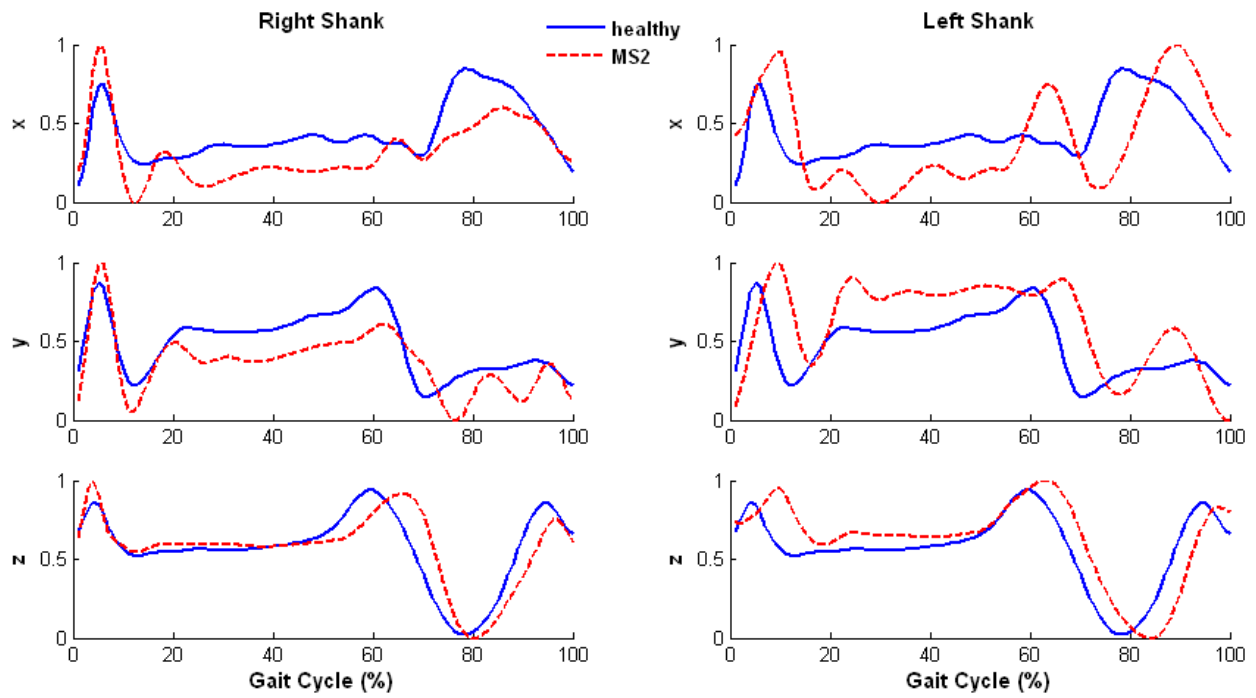
Biceps Femoris (BF)	Muscle weakness appears in the initial contact and terminal swing phase. Spasticity appears in the stance phase up to 60% of full gait cycle. Significant small similarity starts from mid-stance to mid-swing phases.	Muscle weakness appears in the initial contact and terminal swing phase. Spasticity appears in the stance phase up to 40% of full gait cycle. Significant small similarity starts from mid-stance to mid-swing phases.
Gluteus Medius (Gmed)	Muscle weakness appears in the loading response and terminal swing phase. Spasticity appears in initial and mid-swing phase. Significant small similarity appears in pre- and initial swing.	Same as right Gmed.
Erector Spinae (ES)	Sharp rise in the initial contact. Spasticity appears after 60% of the gait cycle. Significant small similarity in entire swing phase.	Muscle weakness appears in the initial contact, spasticity appears in the mid-stance and terminal swing phase. Significant small similarity in the terminal stance phase.

- **Acceleration Patterns**

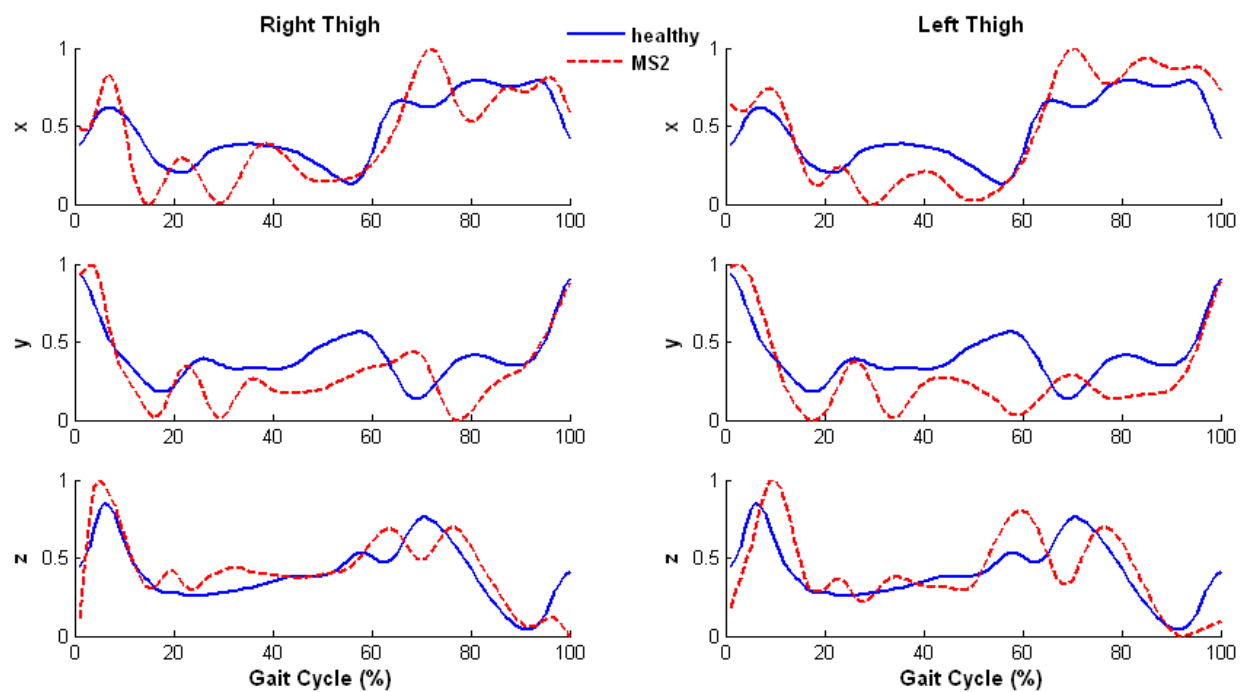
(A)



(B)



(C)



(D)

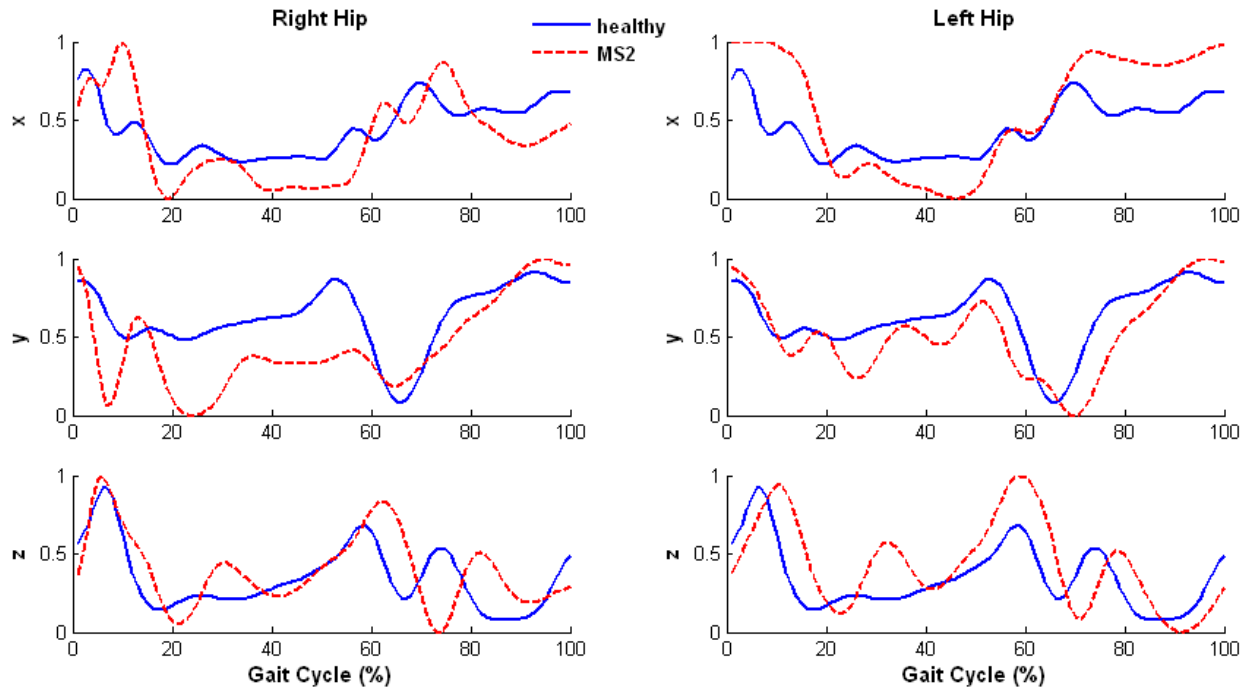


Figure AV-6: Comparison of acceleration pattern in a gait cycle between able-bodied subjects and MS-2. (A) Foot (B) Shank (C) Thigh and (D) Hip accelerations

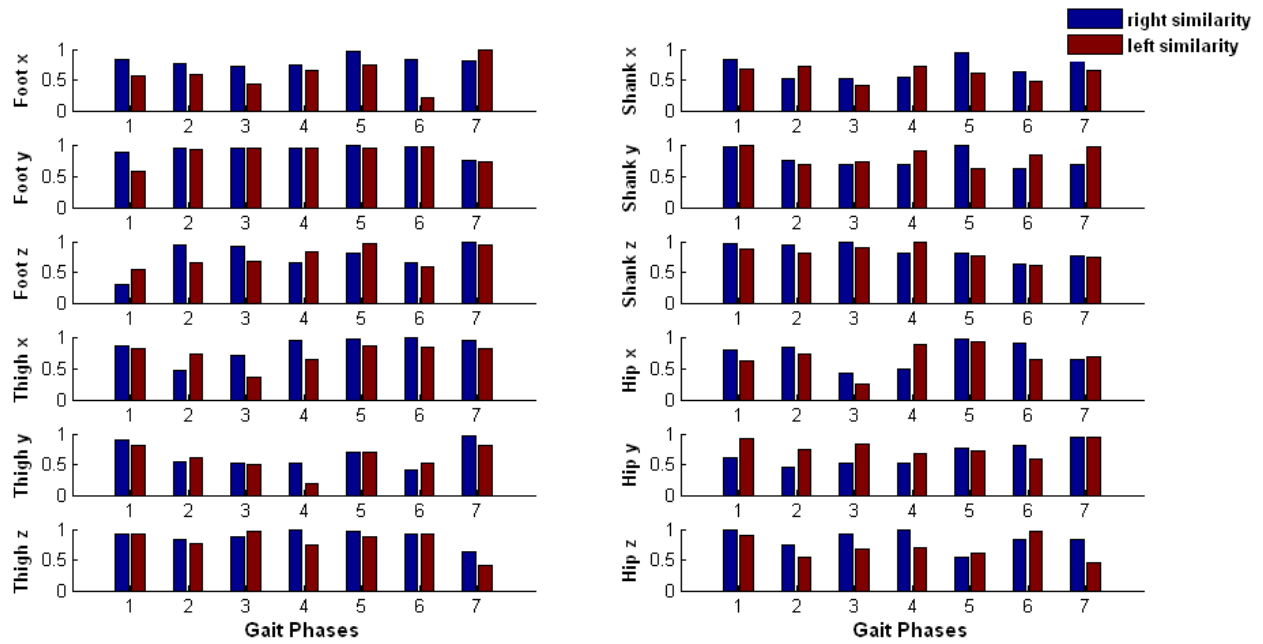


Figure AV-7: Grade of similarity on right and left acceleration in MS-2.

Summary:**Table AV-2: Characterization of acceleration in MS-2**

	Right	Left
Foot x	Sharp rise in the initial contact, lower magnitude throughout the rest of the stance phase, delayed and reduced acceleration in swing phase.	Sharp and delayed rise in initial contact, lower magnitude than right foot in stance phase, deceleration sharply after toe-off, delayed and sharp acceleration in terminal swing (which cause significant small similarity in mid-swing).
Foot y	Delayed acceleration after toe-off during the initial swing.	Delayed and lower acceleration in the initial contact and delayed acceleration in initial swing.
Foot z	Much delayed acceleration in loading response which causes significant small similarity at that time. Delayed acceleration in pre-swing and terminal swing.	Delayed but sharp rise in initial contact, high magnitude during stance phase, delayed deceleration in initial swing.
Shank x	Sharp rise in initial contact, lower magnitude in stance phase, delayed and reduced acceleration in swing phase.	Sharp rise in initial contact, level of instability showing in stance phase on this affected leg, delayed but sharp rise in acceleration in swing phase.
Shank y	Sharp rise in initial contact, lower magnitude during stance phase, instable and reduced acceleration in swing phase.	Sharp and delayed rise in initial contact, instable acceleration during the stance phase, delayed deceleration before toe-off which causes significant small similarity in pre-swing.
Shank z	Sharp rise in acceleration in initial contact, delayed acceleration on toe-off.	Sharp and delayed acceleration in initial contact, remaining high magnitude during stance phase, delayed deceleration before toe-off.
Thigh x	Sharp rise in initial contact, instable magnitude throughout the stance phase, sharp rise in initial swing phase	Sharp and delayed rise in initial contact, lower and instable magnitude in stance phase, sharp rise and high acceleration in swing phase.

Thigh y	Sharp and delayed deceleration in early stance phase, instable and lower magnitude during stance phase, early rise in terminal swing.	Sharp and delayed deceleration in initial contact, instable and lower magnitude throughout the rest of the gait cycle.
Thigh z	Sharp rise in initial contact, lower magnitude in terminal swing.	Sharp and delayed rise in initial contact, instable magnitude in stance phase, early sharp rise in pre-swing phase.
Hip x	Sharp and delayed deceleration in early stance phase, dramatically decreased throughout the stance phase, sharp rise in initial swing phase, lower magnitude in terminal swing phase.	Much delayed deceleration in early stance phase, and lower magnitude through the rest of the stance phase, early sharp rise around toe-off time, high magnitude in mid- and terminal swing phases.
Hip y	Sharp deceleration in initial contact, lower magnitude in stance phase, sharp rise in swing phase, lower magnitude in terminal swing phase.	Delayed rise in initial contact, rise in single support time, sharp delayed rise in pre-swing phase, and lower magnitude in terminal swing phase.
Hip z	Sharp rise in initial contact, rise in single support time, sharp rise in pre-swing phase.	Sharp and delayed rise in initial contact, sharp rise in single support, sharp rise in pre-swing phase.

Appendix VI: Results of Multiple Sclerosis Patient 3 (MS3)

- **Description**

Subject is a 62 year old male, was diagnosed with relapsing remitting multiple sclerosis and type II diabetes three years ago. He started with gait instability and fell in the summer of 2006. This MS subject had more serious gait problems. From observation of this subject, he had quite slow walking speed, and walking with left hand touching the wall occasionally along the long corridor, and walking with left limp. He is on *Rebif (interferon beta 1a)* 44mcg, 3 times per week. He apparently has moderate to severe spinal canal stenosis (narrowing of the spaces in the spine, resulting in compression of the nerve roots or spinal cord by bony spurs or soft tissues, such as disks, in the spinal canal) at L4-5. He has multiple white matter foci on his brain MRI, the largest is within the right frontal lobe, in deep white matter near the convexity with a bulls-eye configuration, measuring 1.78×1.09×1.2 cm. His spinal fluid was positive for oligoclonal bands (indicates that immunoglobulins are produced in central nervous system which is an important indicator in the diagnosis of multiple sclerosis). The patient was tested with bare-foot walking on the instrumented treadmill with harness support for stabilization at patient acceptable speed of 0.15 m/s.

- **Temporal Stride Variability**

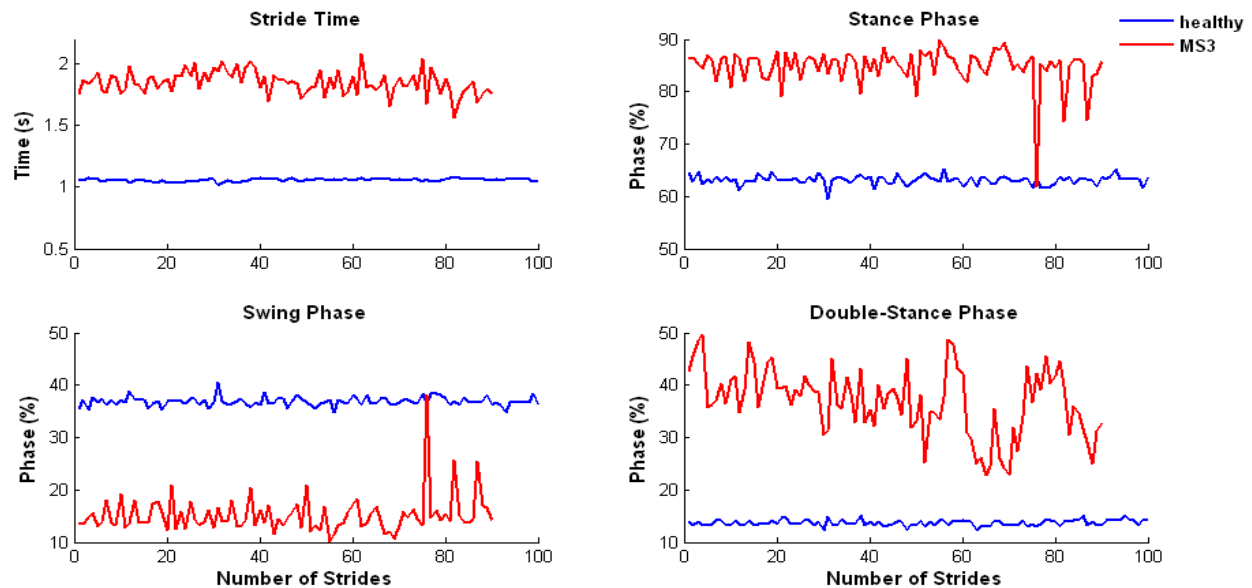


Figure AVI-1: Stride variability of a healthy subject compared with multiple sclerosis case 3 (MS-3).

Summary: With this lower walking speed, there were only 90 strides extracted during three-minute walking trial in MS-3 subject. The subject has greater temporal variability for all variables compared with a healthy male subject. He has much longer stride time due to the slower walking speed, much shorter swing phase, and longer stance/double-stance phases. The variability increased dramatically after 55 strides during the three-minute walking which indicates the fatigue around that time. In addition, there was a reduction in the stance phase and a peak increment in the swing phase, around 75 strides which indicate a falling risk happening at that time.

- **Ground Reaction Forces**

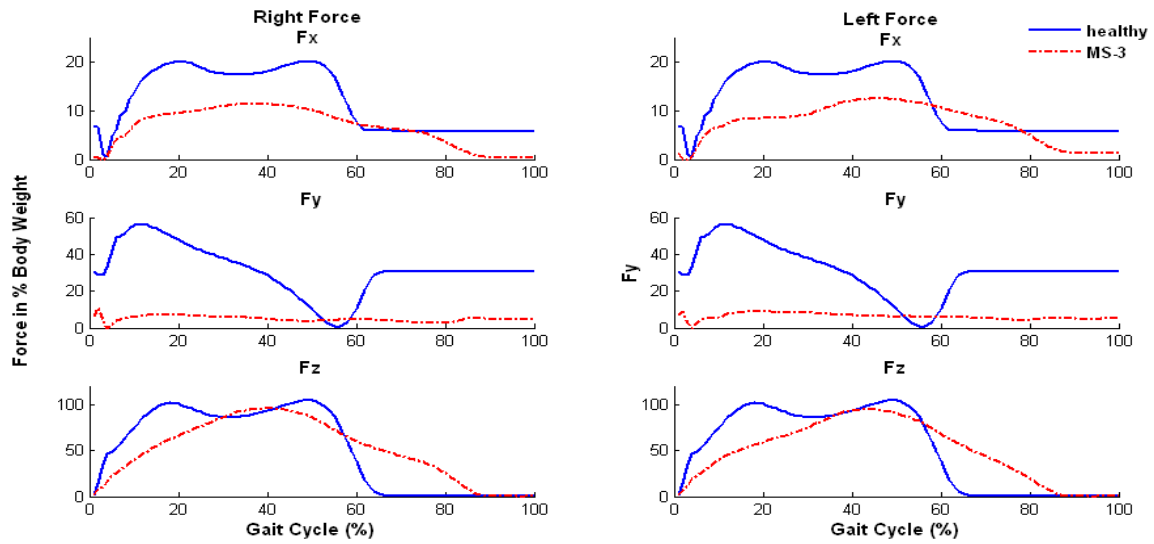


Figure AVI-2: Right and left GRF in 3-D in MS3.

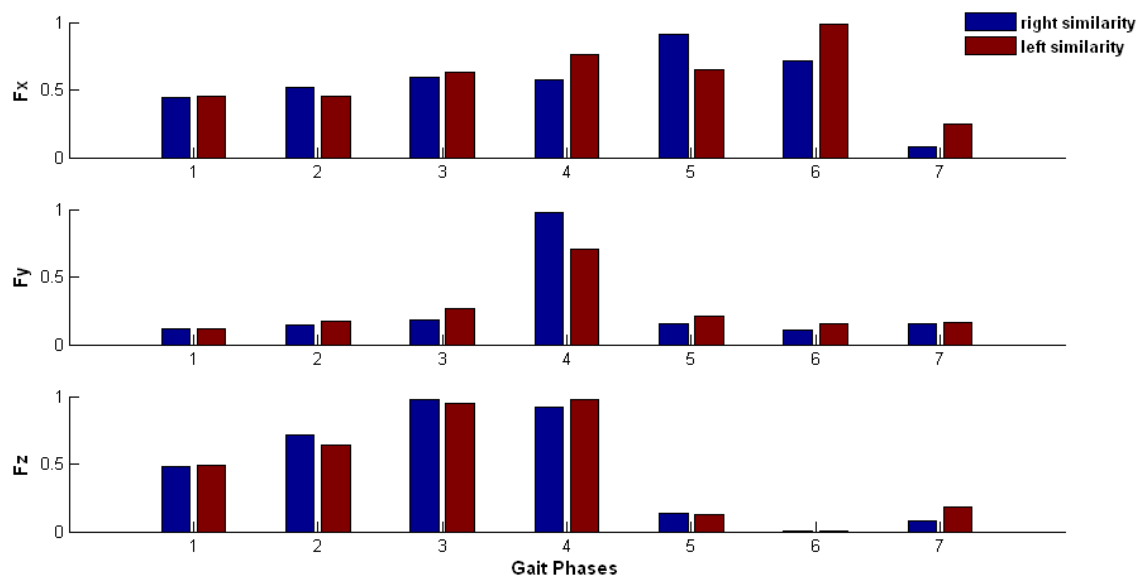


Figure AVI-3: Grade of similarity on right and left GRF in MS-3.

Summary:

The force curve in the vertical direction (F_z) shows a much longer stance phase (approximately 85% of the full gait cycle) in MS-3 subject than the healthy subjects on both right and left feet, which indicates his gait has serious problems on both legs. There was only one

shortened peak time during stance phase showing that his gait had no smooth force transition events from heel to toe which forms the ‘M’ shape with two peaks in Fz. In anterior-posterior direction (Fy), MS-3 has much lower magnitudes of force than healthy subjects for both right and left feet, this might due to very low walking speed with weak GRF. In mediolateral direction (Fx), MS-3 has also constant plateau-wise form of GRF. There are significant small similarity in anterior-posterior force and mid-swing in vertical force. This indicates the serious gait problem with MS3.

- **EMG Muscle Activity Patterns**

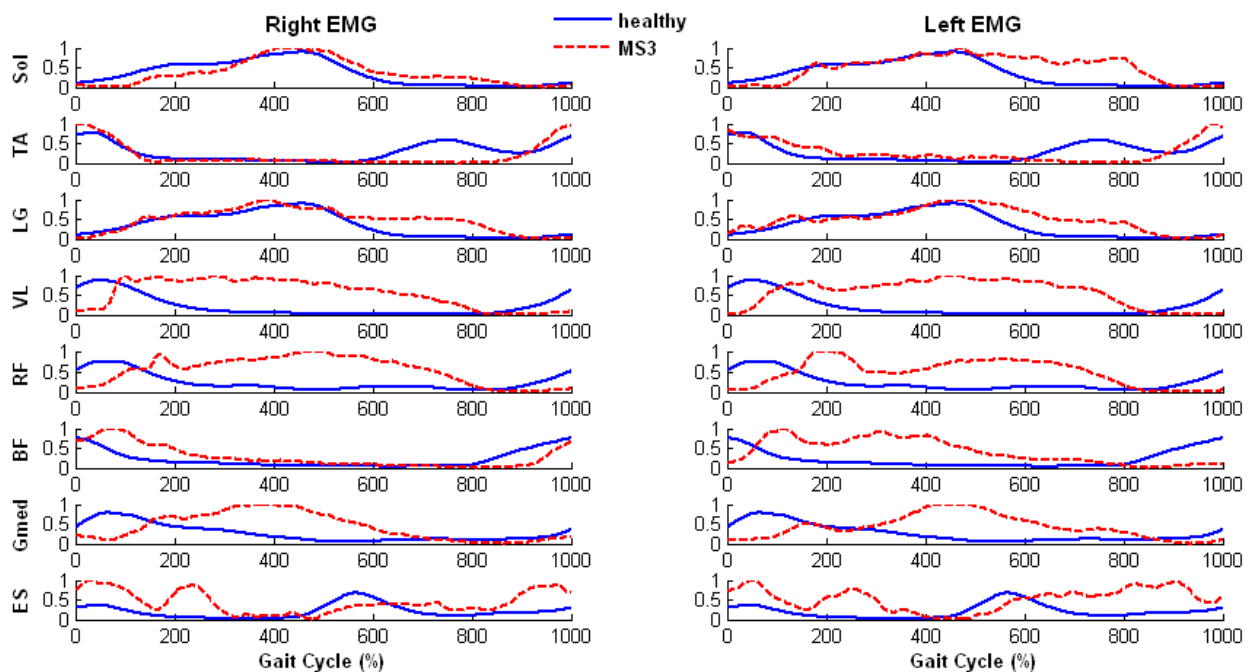


Figure AVI-4: Comparison of EMG pattern in a gait cycle between able-bodied subjects and MS-3.

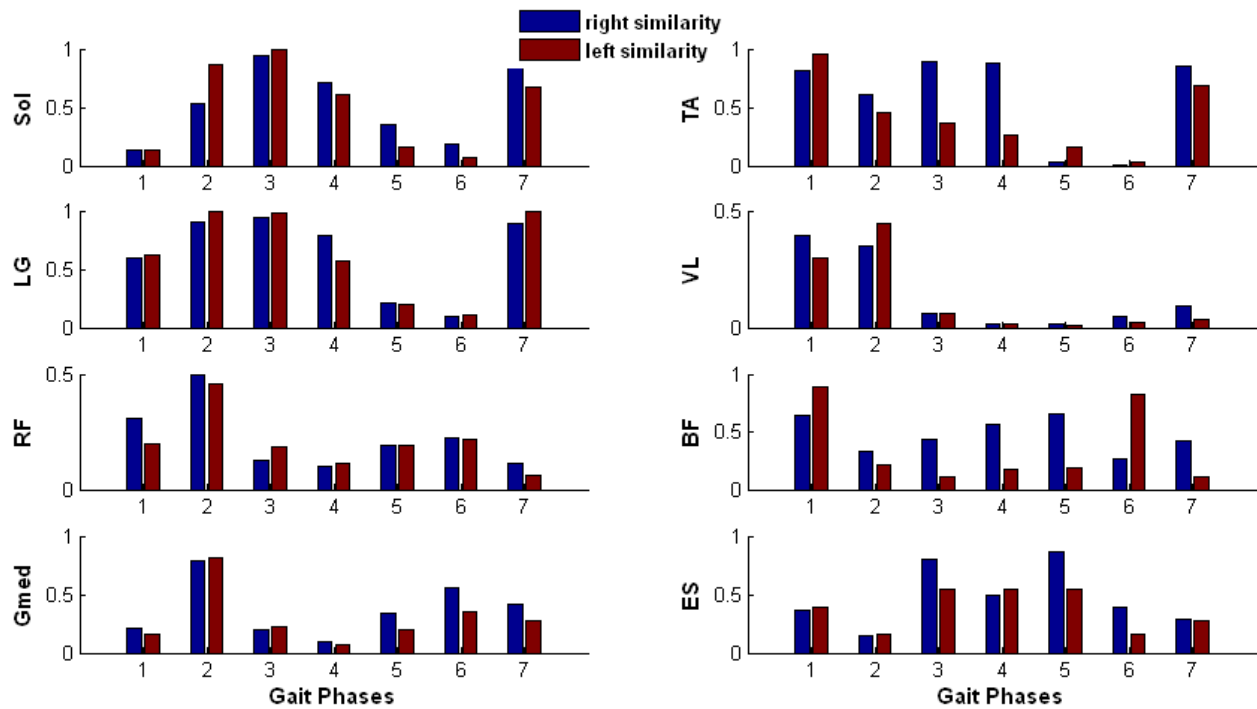


Figure AVI-5: Grade of similarity on right and left EMG in MS-3.

Summary:

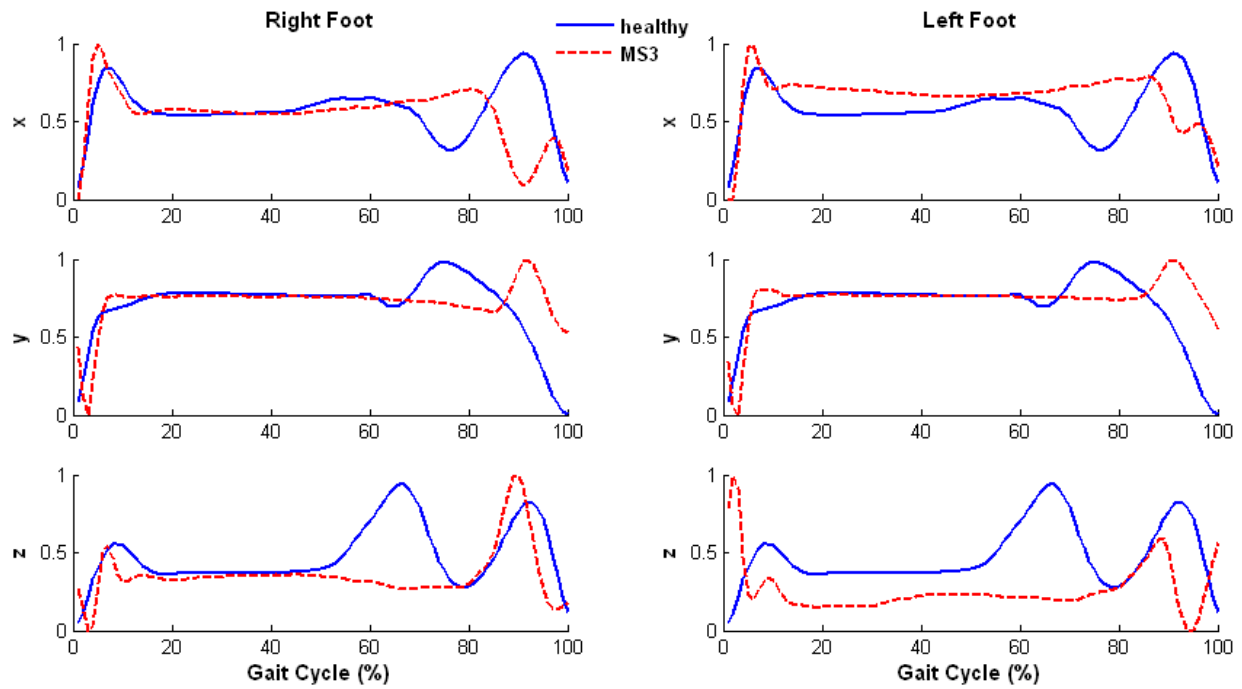
Table AVI-1: Summary of EMG activity in MS-3

	Right	Left
Soleus	Weakness in the beginning of the stance and small spasticity appears at the end of stance phase. Significant small similarity appears in loading response and mid-swing.	Same as right Sol but higher spasticity appears at the end of stance phase. Significant small similarity appears in loading response, initial and mid-swing phases.
Tibialis Anterior (TA)	Muscle weakness appears in the late stance phase. Significant small similarity in initial and mid-swing phases.	Same as right TA.
Gastrocnemius Lateralis (LG)	Spasticity appears in the late stance phase. Significant small similarity in initial and mid-swing phases.	Same as right LG.

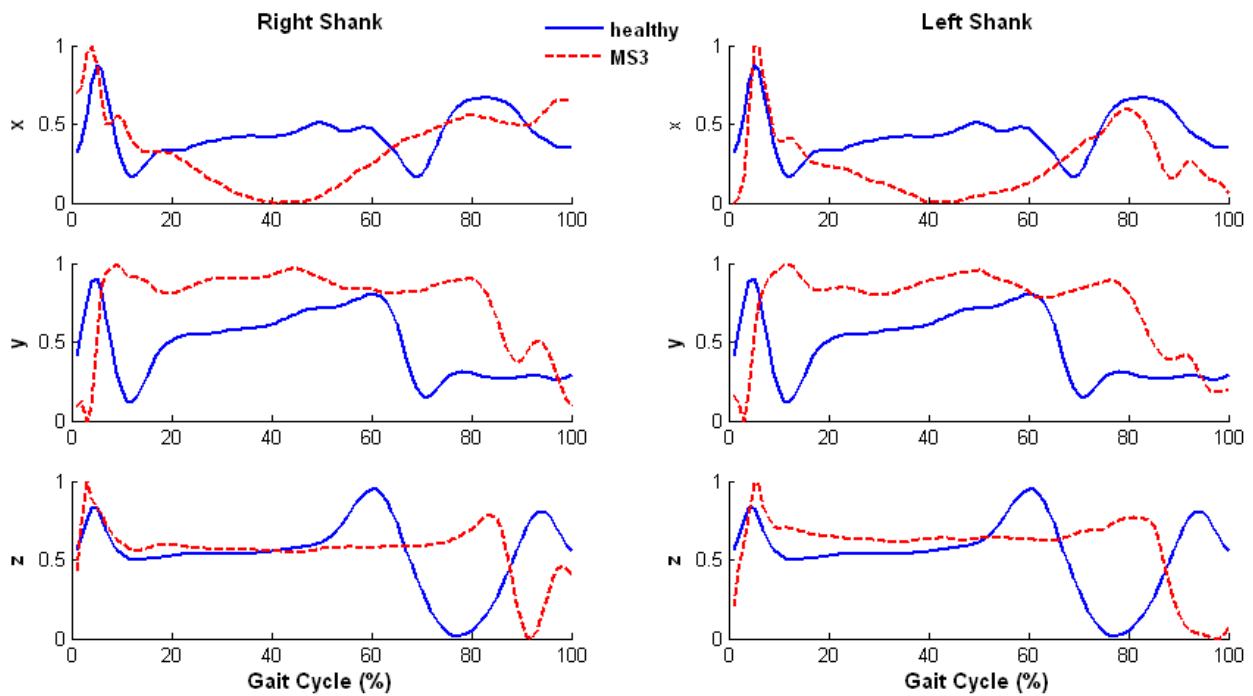
Vastus Lateralis (VL)	Weakness appears in the initial contact and terminal swing, spasticity appears after single support in the stance phase. Significant small similarity appears in phase 3~7.	Same as right VL.
Rectus Femoris (RF)	Weakness appears in the loading response, spasticity appears after single support and continue until end of the stance phase. Significant small similarity appears pre-and terminal swing phases.	Same as right RF.
Biceps Femoris (BF)	Spasticity appears in the stance phase up to 30% of full gait cycle, weakness appears in the terminal swing phase. Significant small similarity appears in mid-swing phase.	Muscle weakness appears in the initial contact and terminal swing phase. Spasticity appears in the stance phase up to 60% of full gait cycle. Significant small similarity appears from mid-stance to terminal-swing phases.
Gluteus Medius (Gmed)	Muscle weakness appears in the loading response. Spasticity appears about 20~60% of the gait cycle. Significant small similarity appears through entire gait cycle.	Same as right Gmed.
Erector Spinae (ES)	Spasticity appears in loading response, and up to 30% of the gait cycle. Spasticity also appears in the terminal swing phase. Significant small similarity appears in mid-stance phase.	Same as right ES.

- Acceleration Patterns

(A)



(B)



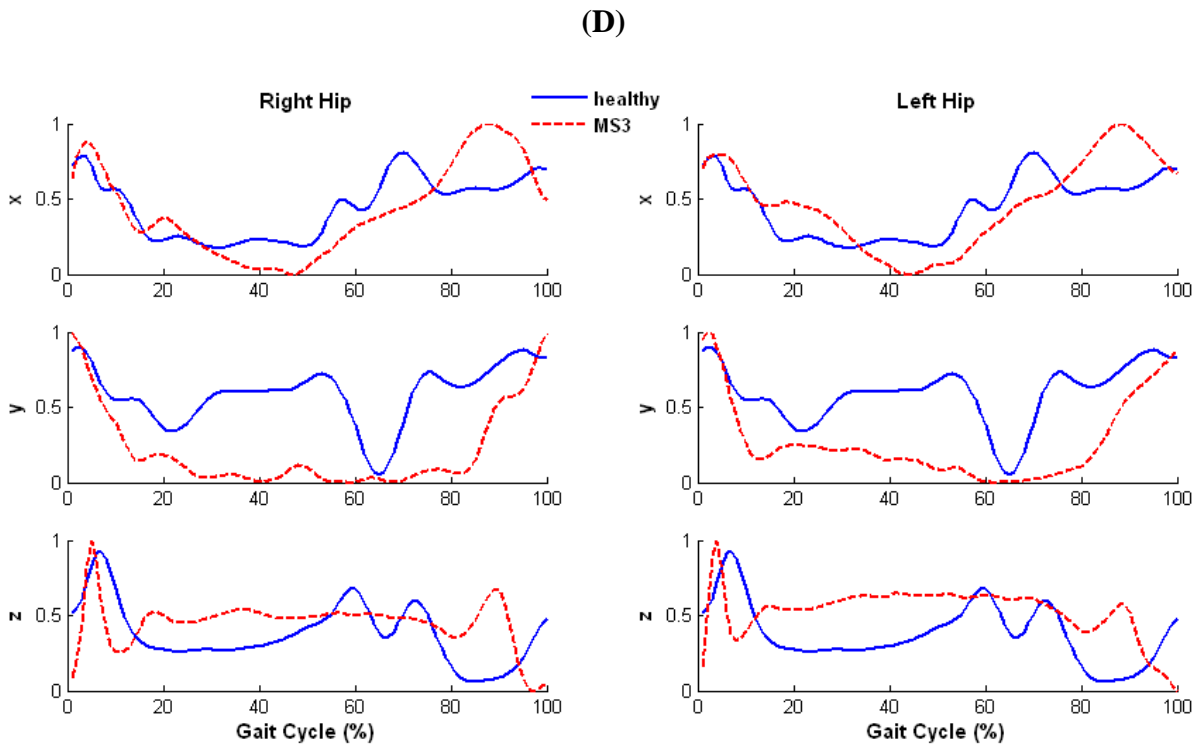
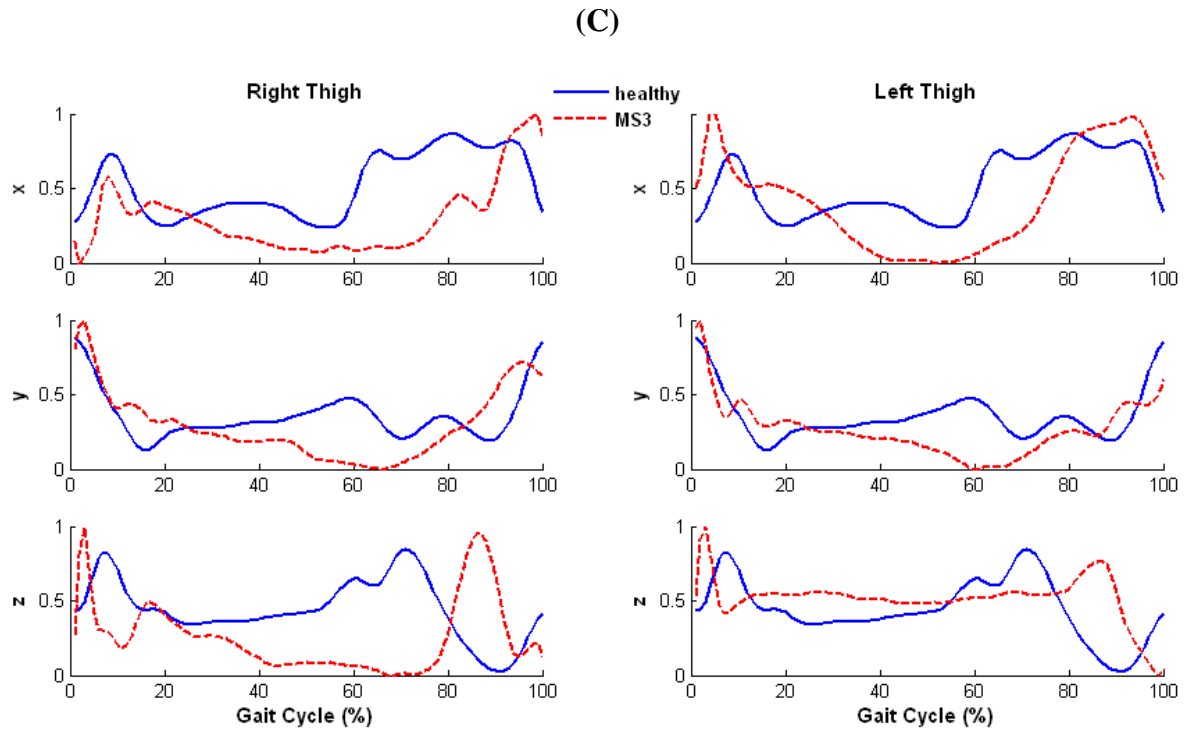


Figure AVI-6: Comparison of acceleration pattern in a gait cycle between able-bodied subjects and MS-3. (A) Foot (B) Shank (C) Thigh and (D) Hip acceleration

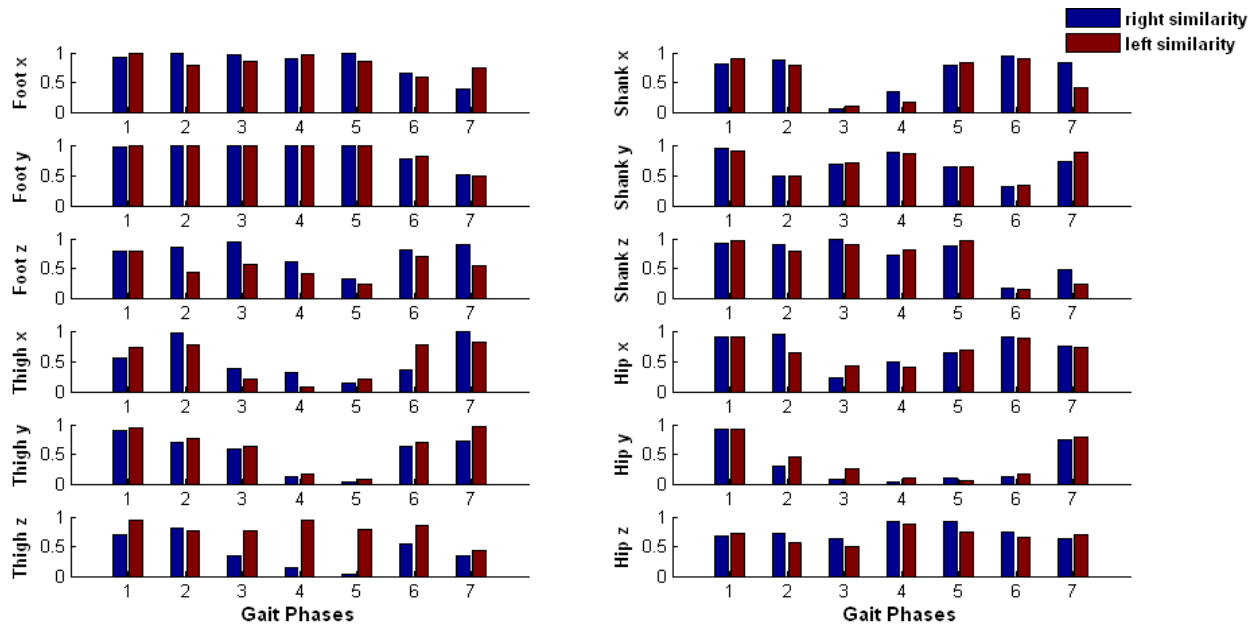


Figure AVI-7: Grade of similarity on right and left acceleration in MS-3.

Summary:

Table AVI-2: Characterization of acceleration in MS-3

	Right	Left
Foot x	Sharp rise in the initial contact, lower and delayed acceleration in swing phase which results in a significant small similarity in terminal swing phase.	Sharp rise in initial contact, higher magnitude in stance phase, lower acceleration in swing which causes significant small similarity in mid-swing phase.
Foot y	Delayed and sharp rise in acceleration in initial contact and swing phase.	Same as right foot y. Significant small similarity appears in the terminal swing phase.
Foot z	Lower and shortened acceleration in loading response, delayed but sharp rise in acceleration after toe-off. Significant small similarity appears in initial swing phase.	Sharp rise in initial contact, lower magnitude during the rest of stance phase, lower acceleration in swing phase. Significant small similarity appears in the initial swing phase.
Shank x	Sharp rise in initial contact, and then dramatically decreased below the baseline of the healthy pattern in the stance phase which results in significant small similarity in terminal stance and pre-swing phases.	Same as right shank x.

Shank y	Sharp and delayed rise in initial contact and continues with higher magnitude for the entire gait cycle. Significant small similarity appears in mid-swing phase.	Same as right shank y.
Shank z	Sharp rise in acceleration in initial contact, delayed and lower acceleration in swing phase which causes significant small similarity in mid- and terminal swing phases.	Same as right shank z.
Thigh x	Lower magnitude appears entire gait cycle which results in small similarity for the most of the phases.	Sharp rise in initial contact, lower magnitude in stance phase, sharp rise in acceleration in swing phase. Significant small similarity appears in terminal stance, pre- and initial swing phases.
Thigh y	Sharp rise in initial contact and higher magnitude in early stance phase, instable and lower magnitude during the later stance phase, early rise with lower magnitude in swing phase. Significant small similarity appears in pre- and mid-swing phases.	Same as right thigh y.
Thigh z	Sharp rise in initial contact, dramatically decreased throughout the stance phase, sharp rise in swing phase. Significant small similarity appears in terminal stance, pre- and initial swing phases.	Sharp rise in initial contact, higher magnitude in stance phase, delayed rise in swing phase. Significant small similarity appears in terminal swing phase.
Hip x	Sharp rise in initial contact, lower magnitude in stance phase, and increased acceleration in swing phase. Significant small similarity appears in terminal stance and pre-swing phases.	Same as right hip x.
Hip y	Sharp deceleration in initial contact, lower magnitude in stance phase, sharp rise after toe-off. Significant small similarity appears in entire gait cycle except the loading response.	Same as right hip y.
Hip z	Sharp rise in initial contact, higher magnitude throughout the rest of the gait cycle. Significant small similarity appears in terminal stance phase.	Same as right hip z.

Appendix VII: Results of Multiple Sclerosis Patient 4 (MS4)

- **Description**

Subject is a 37 year old man, was diagnosed with multiple sclerosis ten years ago. From observation of this MS subject, he walked with instable and limp gait. Medication includes *Desyrel* for conditions of depression and MS tremor. He was tested with bare-foot walking on the instrumented treadmill for three minutes without harness support, at speed of 0.35 m/s. There were two time fall risks during continue walking trail, patient used treadmill hand bars occasionally as partial support.

- **Temporal Stride Variability**

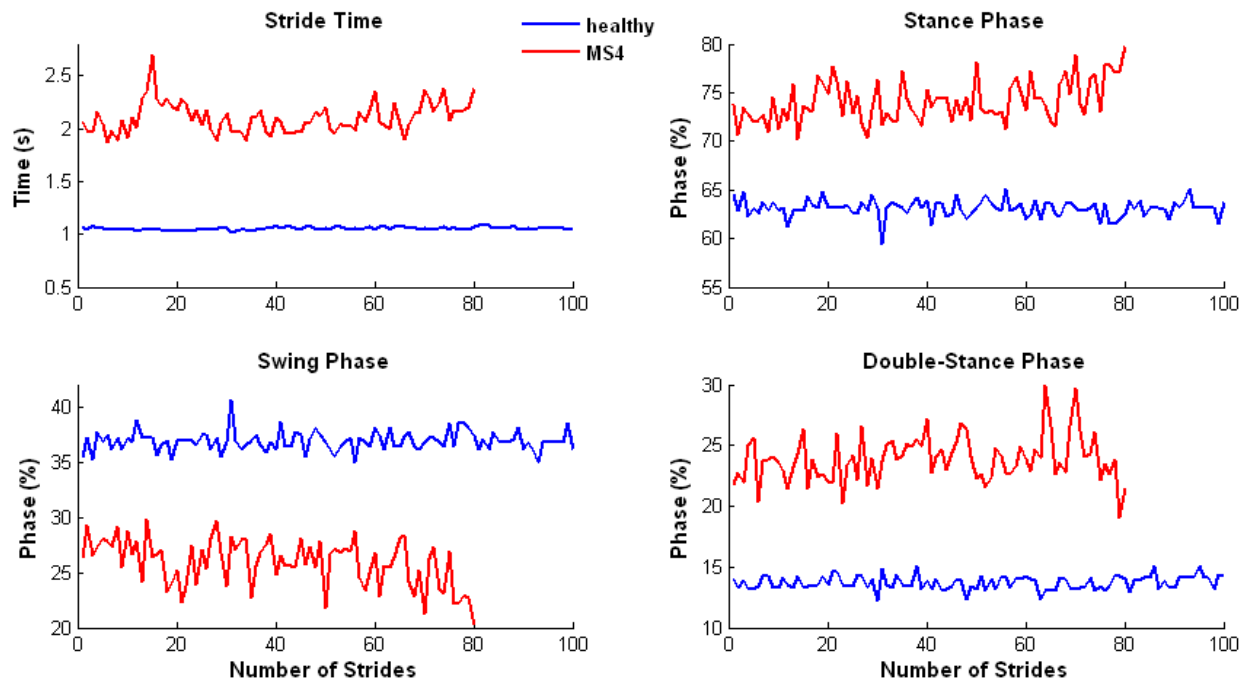


Figure AVII-1: Stride variability of a healthy subject and multiple sclerosis patient case 4 (MS-4).

Summary: there were only 80 strides found from three-minute walking trial in MS-4. The subject has increased variability in all four temporal stride variables, compared with a healthy subject. There was a clear greater increased stride time at 15 strides when the first fall risk appeared. There are gradually increased stance and double-stances phases, and gradually decreased swing phase during the walking trial due to functional fatigue in MS-4. In addition, there was a sharp increase in double-stance phase at around 70 strides when the second fall risk happened.

- **Ground Reaction Forces**

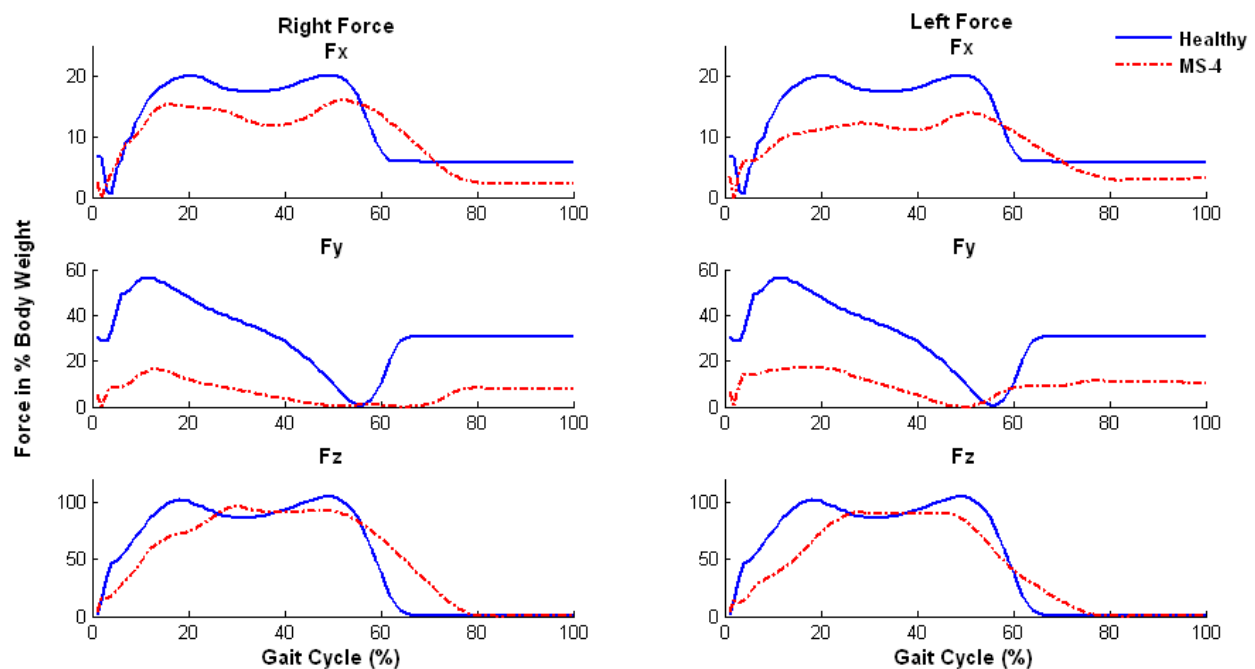


Figure AVII-2: Right and left GRF in 3-D in MS-4.

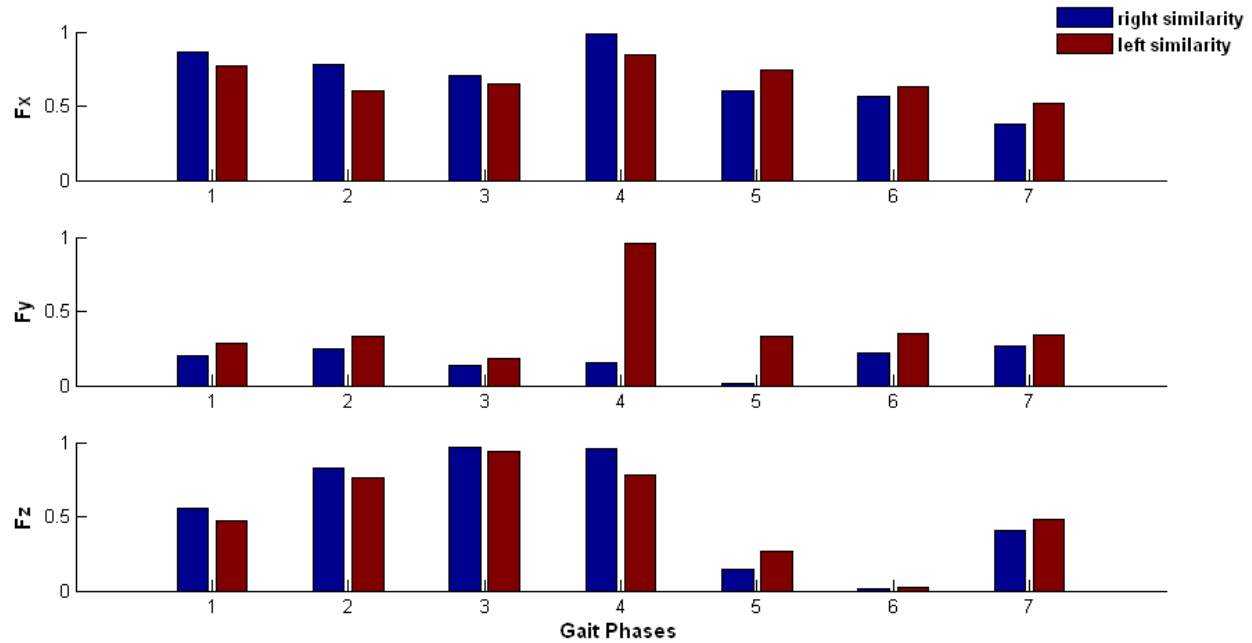


Figure AVII-3: Grade of similarity on right and left GRF in MS-4.

Summary:

In the vertical direction of GRF (F_z), MS-4 subject shows a much longer stance phase (approximately 80% of the full gait cycle) than the healthy subjects on both right and left feet, which indicates his gait has serious problems on both legs, time of right F_z is slightly longer than left F_z . This indicates the base support side was right leg, and the more server effective side was left. There was a flat-foot with short contacting ground duration in stance phase, especially on the left foot. In anterior-posterior direction (F_y), MS-4 has lower magnitudes of GRF than healthy subjects for both right and left feet. In mediolateral direction (F_x), MS-4 has lower and delayed magnitude of GRF (left $F_x < \text{right } F_x$). There is significant small similarity in anterior-posterior GRF and swing phase in vertical force.

- **EMG Muscle Activity Patterns**

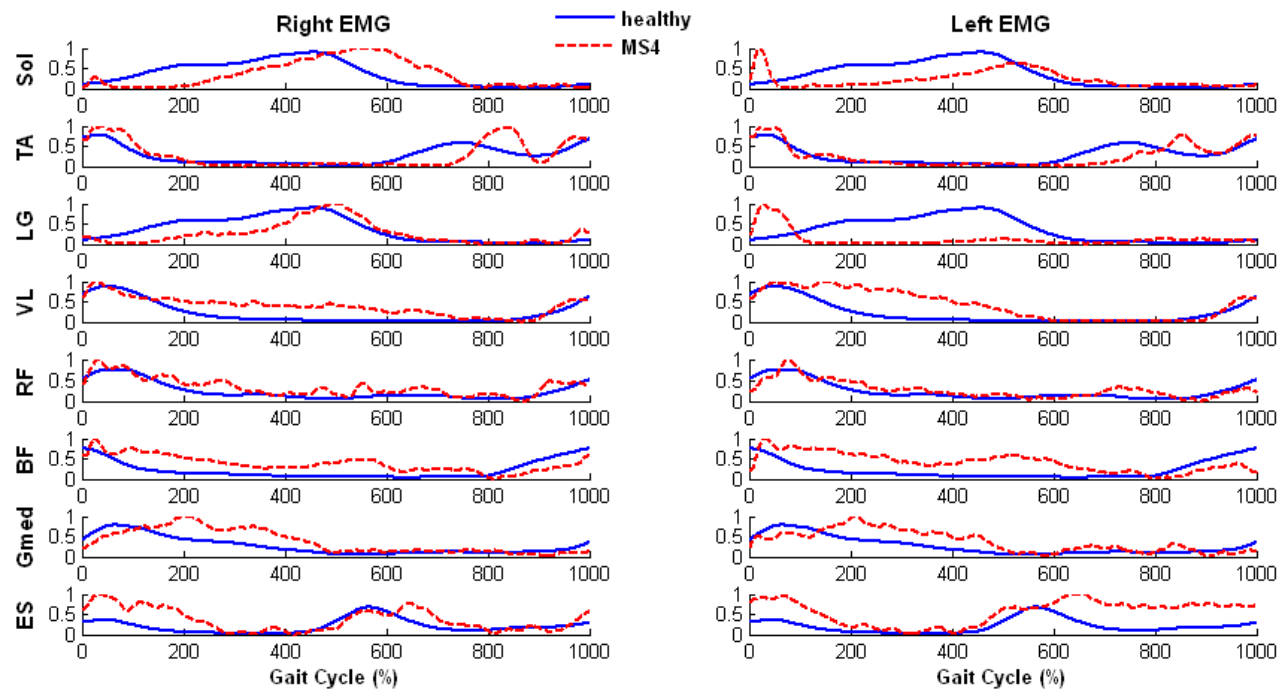


Figure AVII-4: Comparison of EMG in a gait cycle between able-bodied subjects and MS-4.

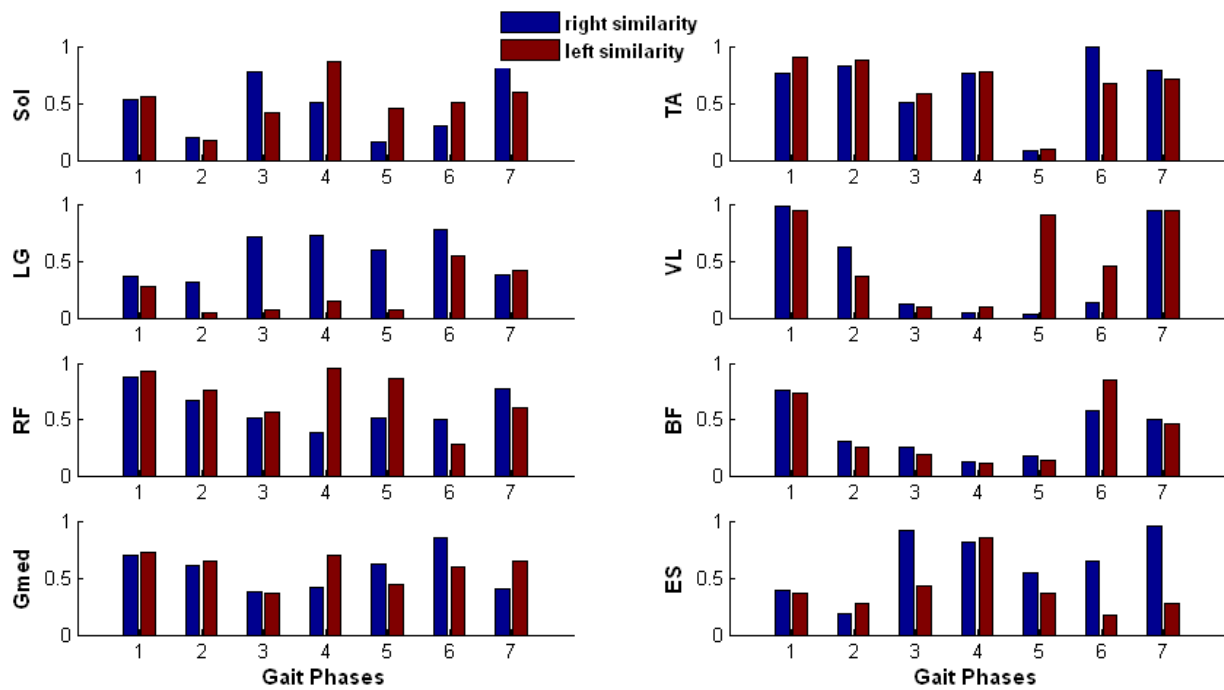


Figure AVII-5: Grade of similarity on right and left EMG in MS-4.

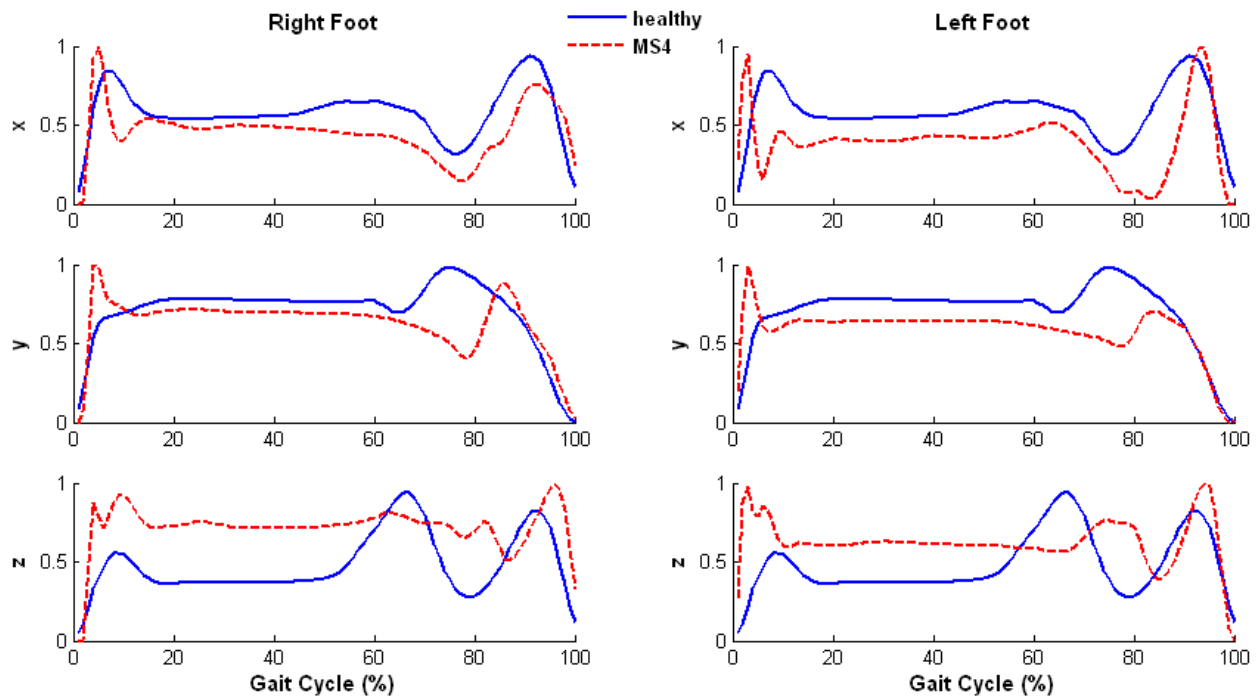
Summary:**Table AVII-1: Summary of EMG activity in MS-4**

	Right	Left
Soleus	Muscle weakness in the beginning of the stance and delayed muscle activity in the late stance phase. Significant small similarity appears in mid-stance phase and initial swing phase.	A peak activity appears in the initial contact, and weakened activity in the rest of stance phase. Significant small similarity appears in mid-stance phase and initial swing phase.
Tibialis Anterior (TA)	Spasticity appears in the loading response, and delayed but increased muscle activity in the swing phase. Significant small similarity in initial swing phase.	Same as right TA.
Gastrocnemius Lateralis (LG)	Weakness appears in the early stance phase and peak activity in the late stance phase. Significant small similarity appears in mid-stance phase.	Spasticity appears in the initial contact and then the muscle weakness appears in the rest of the gait cycle which results in the significant small similarity of this muscle in a full gait cycle.
Vastus Lateralis (VL)	Higher muscle activity appears in stance phase. Significant small similarity appears in phase 3~6.	Even higher muscle activity than right VL in the stance phase. Significant small similarity appears in terminal stance phase and pre-swing phase.
Rectus Femoris (RF)	Instable spasticity appears the entire gait cycle. Significant small similarity appears in pre-swing phase.	Similar to right RF, significant small similarity appears in mid-swing phase.
Biceps Femoris (BF)	Spasticity appears in the stance phase and the muscle weakness appears in the swing phase. Significant small similarity appears in pre- and mid-swing phase.	Same as right BF.
Gluteus Medius (Gmed)	Muscle weakness appears in the initial contact. Spasticity appears in the mid-stance phase which results in the significant small	Same as right Gmed.

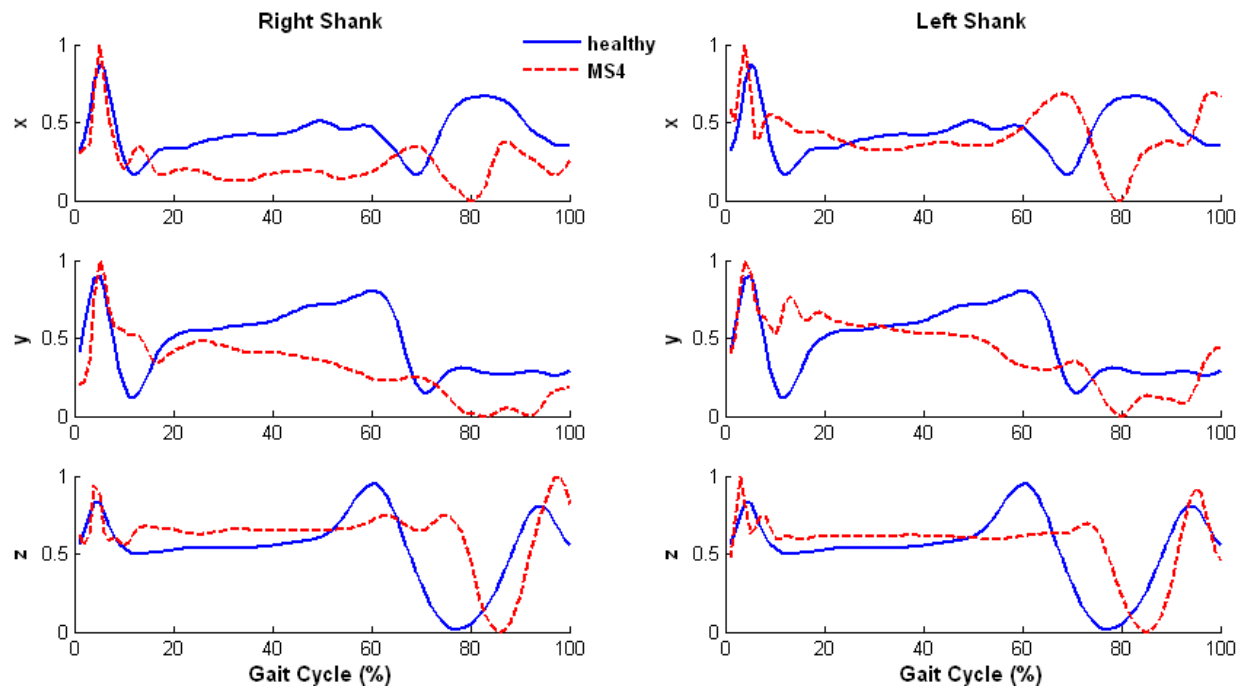
	similarity in the phase.	
Erector Spinae (ES)	Spasticity appears in early stance phase, and up to 30% of the gait cycle which results in significant small similarity appears in mid-stance phase.	Same as right ES. Significant small similarity appears in mid-stance phase and mid-swing phase.

- Acceleration Patterns

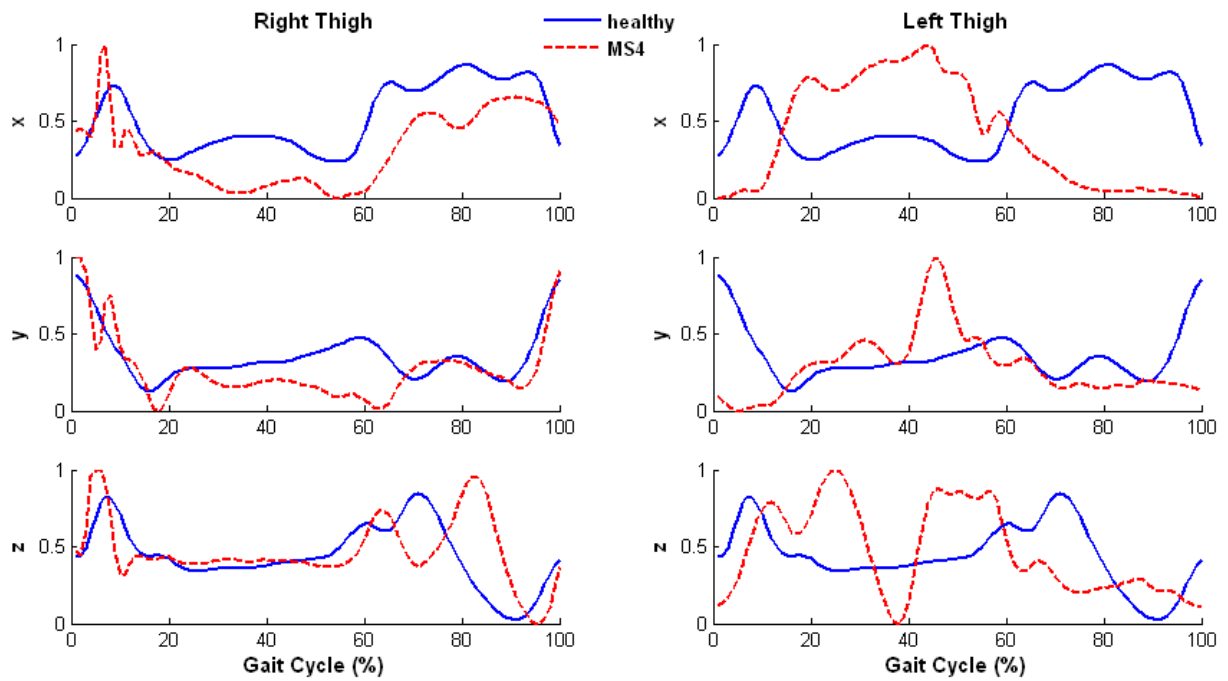
(A)



(B)



(C)



(D)

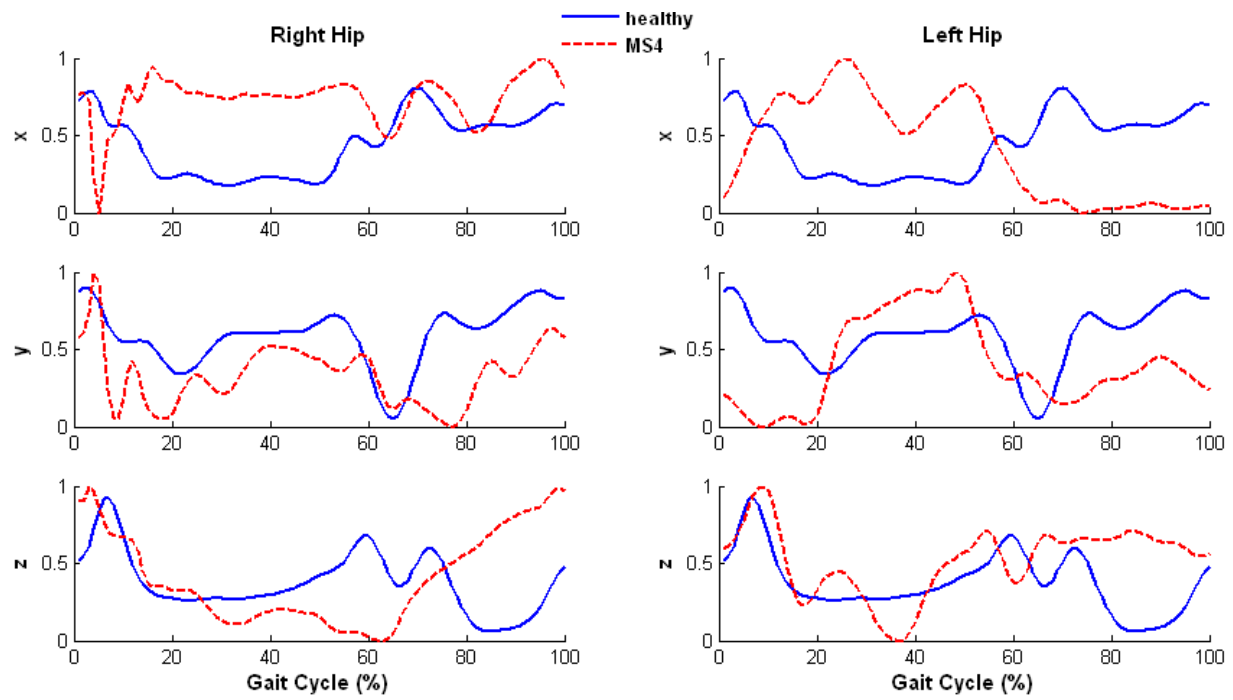


Figure AVII-6: Comparison of acceleration pattern in a gait cycle between able-bodied subjects and MS-4.

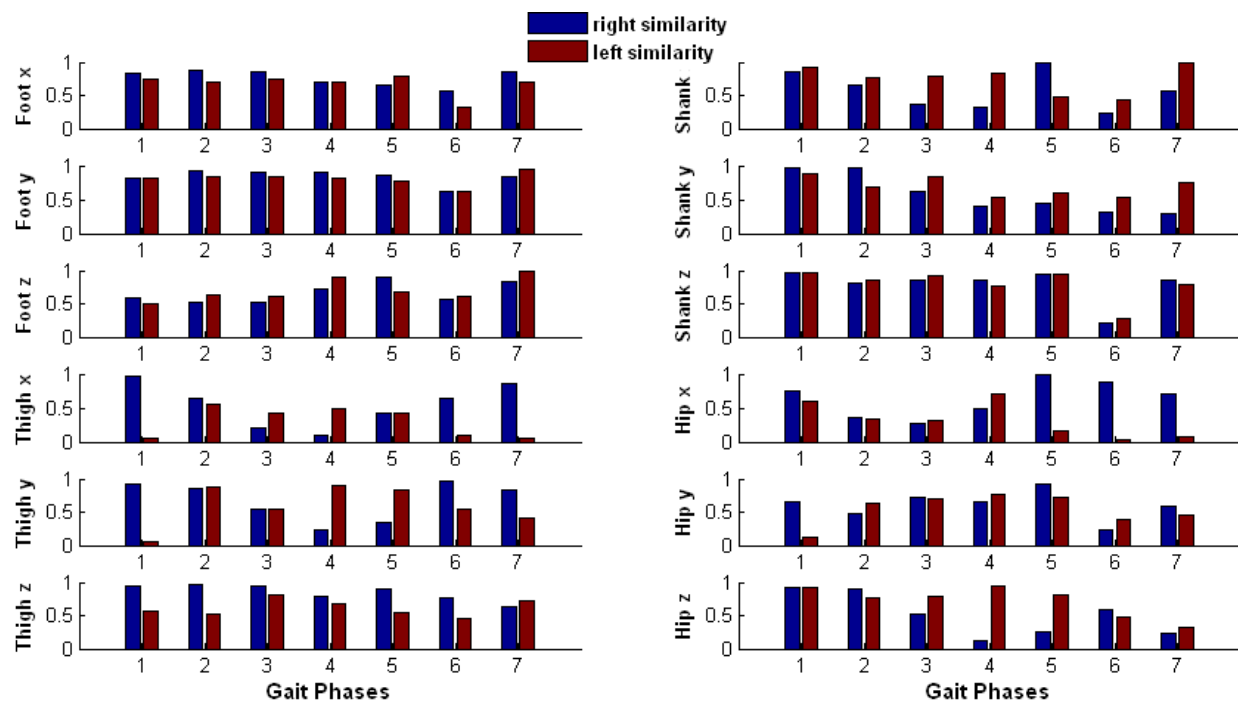


Figure AVII-7: Grade of similarity on right and left acceleration in MS-4.

Summary:

Table AVII-2: Characterization of acceleration in MS-4

	Right	Left
Foot x	Sharp rise in the initial contact, lower magnitude throughout the rest of the stance phase, delayed and reduced acceleration in swing phase. Significant small similarity appears in the mid-swing phase.	Sharp rise in initial contact, much lower magnitude in stance phase, sharp rise in acceleration in swing phase which causes significant small similarity in mid-swing phase.
Foot y	Sharp rise in acceleration in initial contact, lower magnitude in the rest of the stance phase, delayed and reduced acceleration in swing phase which results in the small similarity in mid-swing phase.	Same as right foot y.
Foot z	Much higher magnitude appears entire gait cycle, which causes significant small similarity.	Same as right foot z.

Shank x	Sharp rise in initial contact, lower magnitude in stance phase, delayed and reduced acceleration in swing phase. Significant small similarity appears in the pre-, initial, and mid-swing phases.	Sharp rise in initial contact, sharp rise in the pre-swing phase, and lower acceleration in swing phase. Significant small similarity appears in the initial and mid-swing phases.
Shank y	Sharp rise in initial contact, lower magnitude during stance phase, instable and reduced acceleration in swing phase. Significant small similarity appears in the mid- and terminal swing phases.	Same as right shank y. Significant similarity appears in the mid-swing phase.
Shank z	Sharp rise in acceleration in initial contact, lower magnitude appears in the stance phase, delayed and reduced acceleration in swing phase. Significant small similarity appears in terminal stance phase and pre-swing phase.	Same as right shank z.
Thigh x	Sharp rise in initial contact, instable magnitude throughout the stance phase, sharp rise in initial swing phase	Delayed but higher acceleration in the stance phase and much lower magnitude appears in the swing phase. Significant small similarity appears almost entire gait cycle.
Thigh y	Sharp and delayed deceleration in early stance phase, instable and lower magnitude during stance phase. Significant small similarity appears in the pre- and initial swing phases.	Much lower magnitude in the initial contact, increased acceleration in the late stance phase, much lower magnitude appears in the swing phase. Significant small similarity appears in the loading response and terminal swing phase.
Thigh z	Sharp rise in initial contact, delayed acceleration appears in the later phases of the cycle.	Delayed but higher rise in early stance phase, rise in pre-swing phase, and lower magnitude in the

		swing phase. Significant small similarity appears in mid-swing.
Hip x	Sharp deceleration with immediate acceleration in initial contact, continuing with high magnitude in the stance, rise in acceleration in terminal swing phase. Significant small similarity appears in mid- and terminal stance.	Similar pattern to left thigh x.
Hip y	Sharp acceleration and immediate deceleration in initial contact, lower and instable magnitude in stance phase, lower and delayed acceleration in swing phase which causes small similarity in the mid-swing phase.	Similar pattern to left thigh y.
Hip z	Sharp rise in initial contact, lower magnitude in the stance phase, sharp rise in pre-swing phase before toe-off. Significant small similarity appears in pre- and entire swing phases.	Sharp and delayed rise in initial contact, lower magnitude in the stance phase, higher magnitude in the swing phase. Significant small similarity appears in the terminal swing phase.

Appendix VIII: Results of Multiple Sclerosis Patient 5 (MS5)

- **Description**

Subject is a 45 year old male, was diagnosed with fairly mild multiple sclerosis in 2002. He is on *Copaxone* for Relapsing-Remitting MS. The subject walked bare-foot on the instrumented treadmill at speed of 0.75 m/s.

- **Temporal Stride Variability**

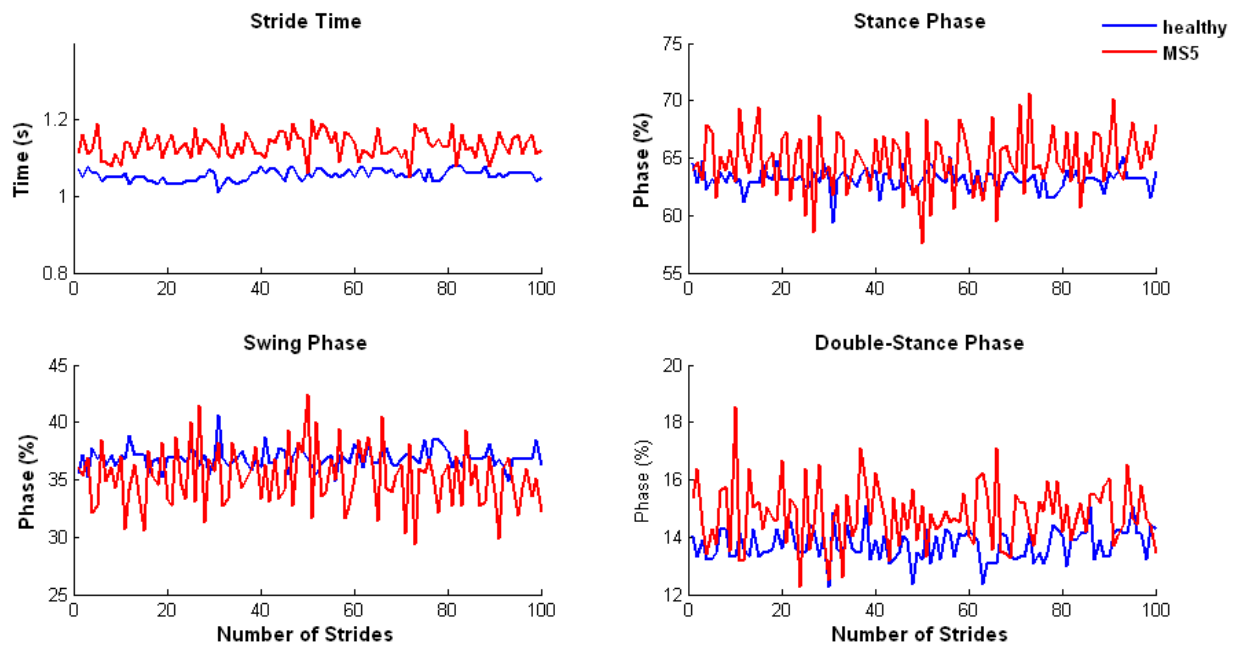


Figure AVIII-1: Stride variability of a healthy subject and multiple sclerosis patient case 5 (MS-5).

Summary: Although the MS5 had higher variability in all temporal stride variables compared with healthy subject, the time during are very similar to the healthy which indicates the mild symptoms of MS5. The increased variability appears constant throughout the three-minute walking trial which also indicates the non- or mild symptom of functional fatigue in MS5 subject.

- **Ground Reaction Forces**

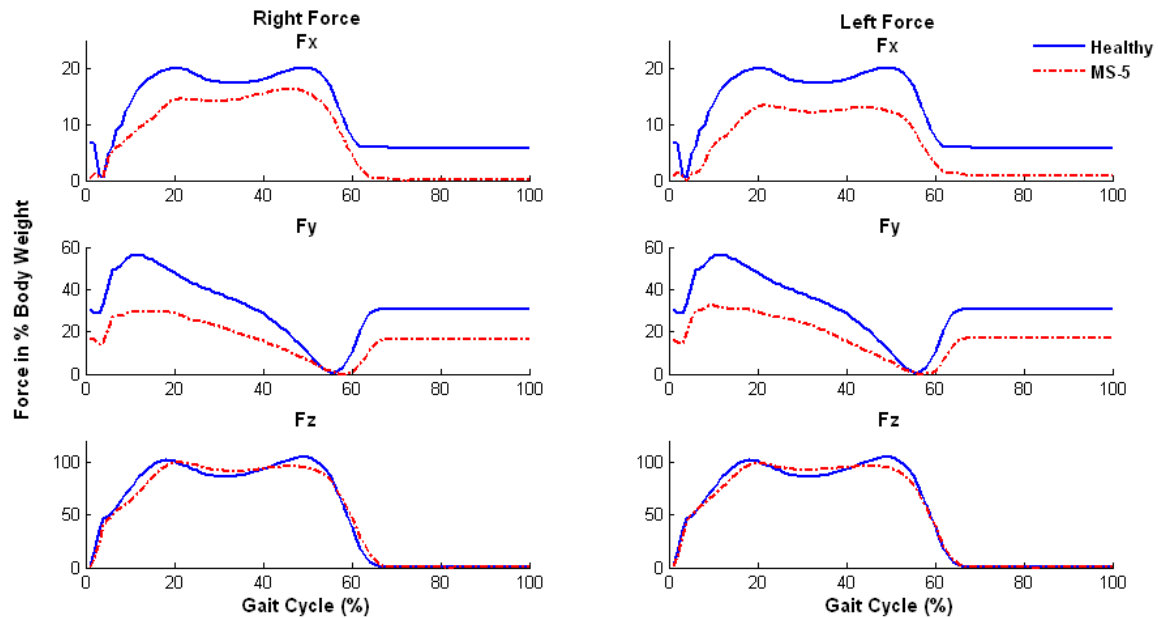


Figure AVIII-2: Right and left GRF in 3-D in MS-5.

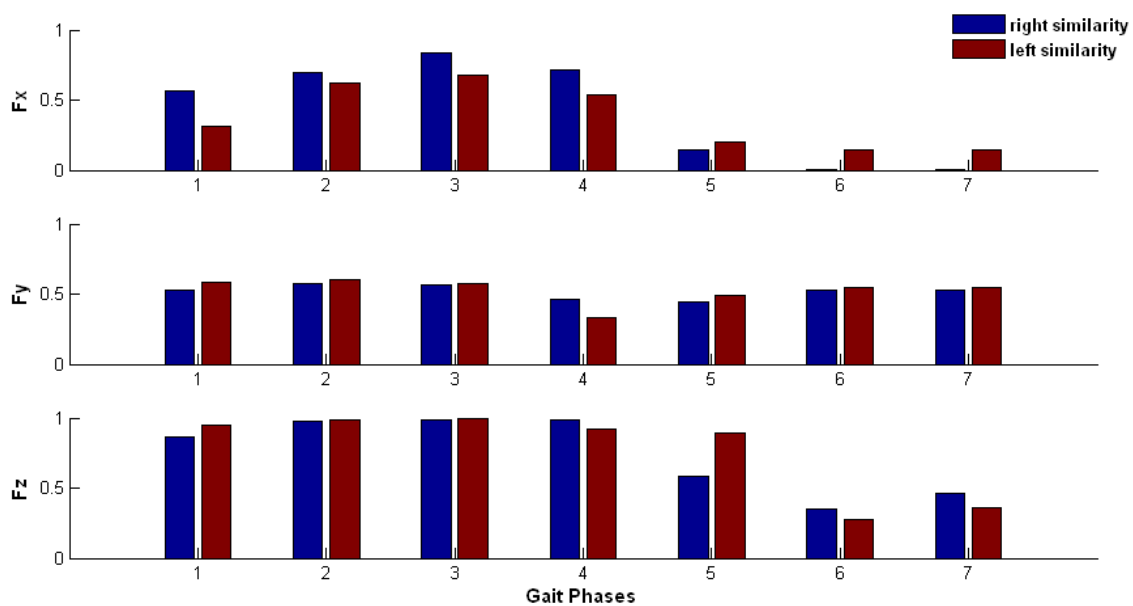


Figure AVIII-3: Grade of similarity between right and left GRF in MS-5.

Summary: In the vertical direction, the GRF appears slightly smaller M shape of the ground contact. There are smaller magnitudes of GRF in the anterior-posterior and mediolateral directions in MS5 subject.

- **EMG Muscle Activity Patterns**

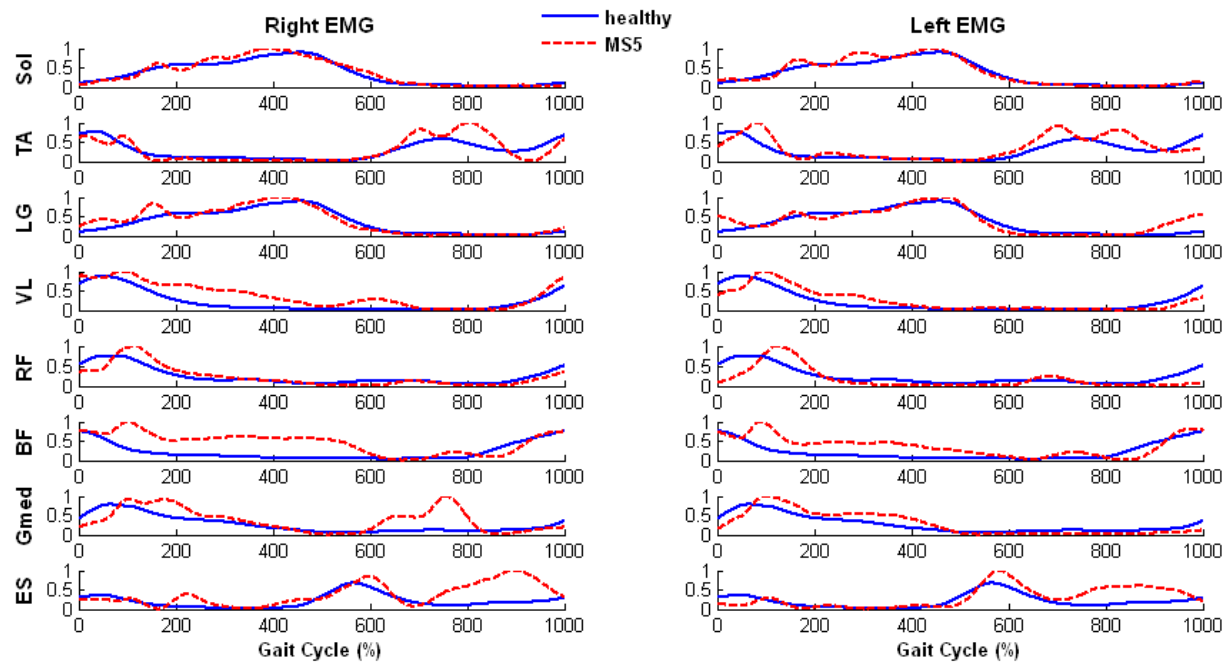


Figure AVIII-4: Comparison of EMG pattern in a gait cycle between able-bodied subjects and MS-5.

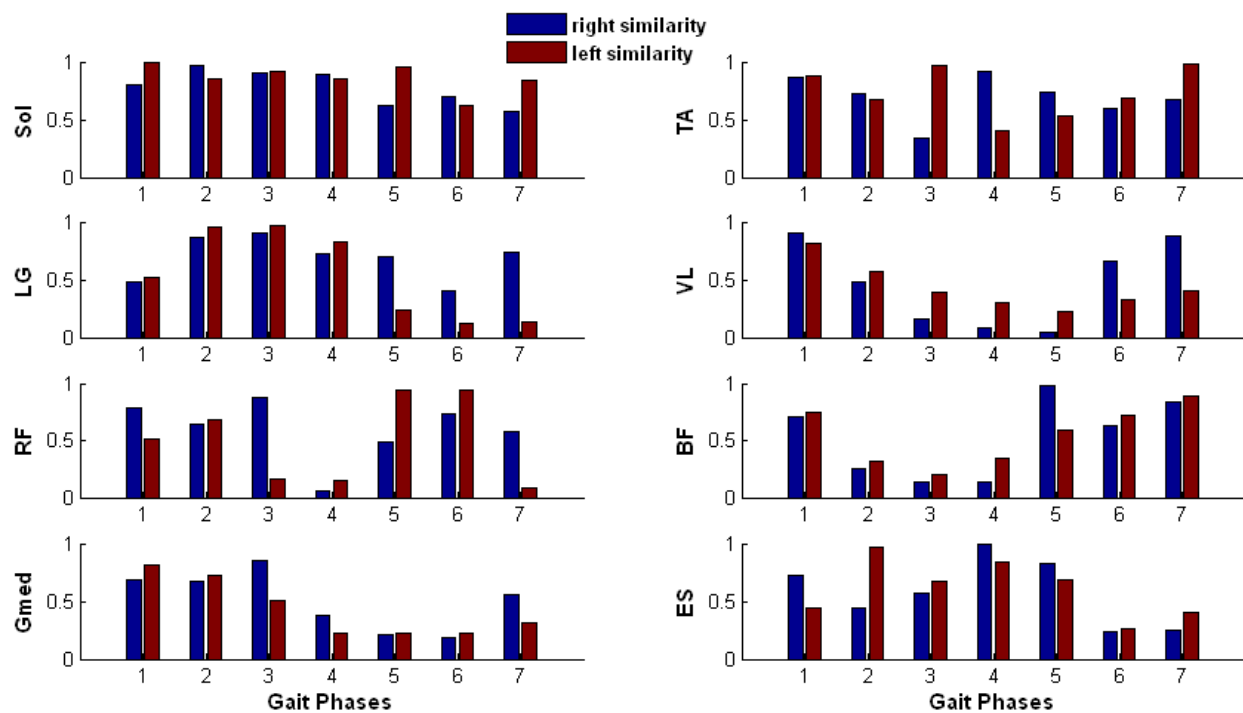


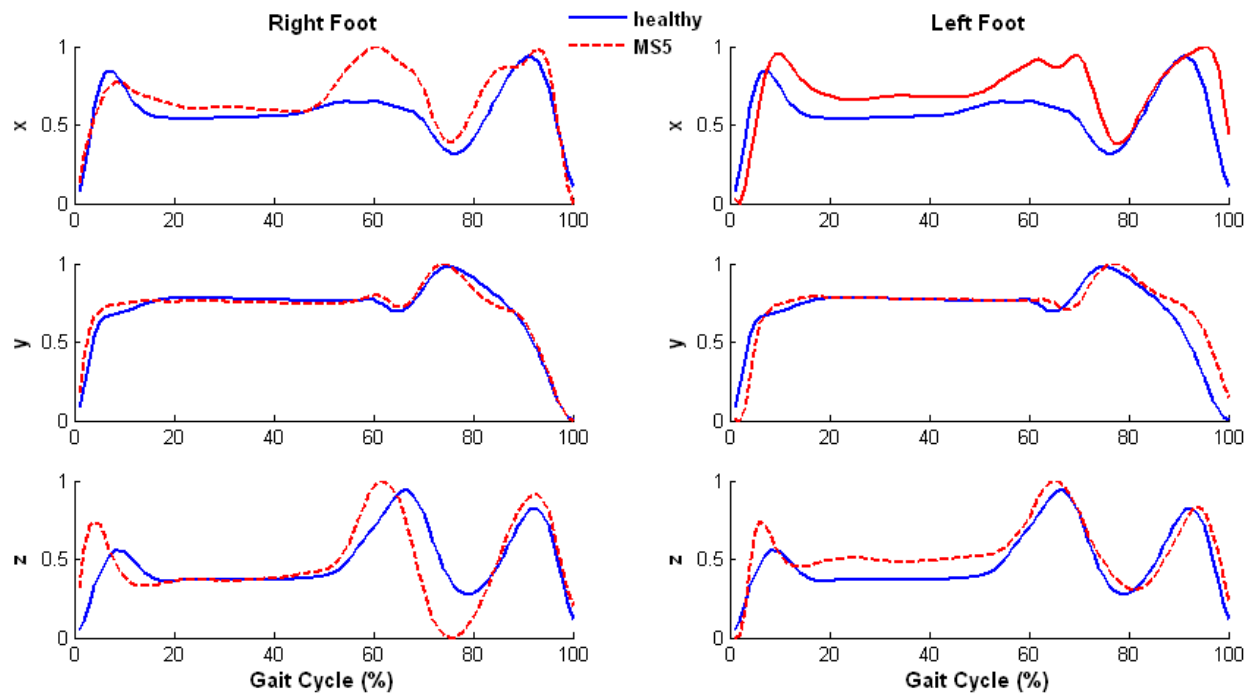
Figure AVIII-5: Grade of similarity on right and left EMG in MS-5.

Summary:**Table AVIII-1: Summary of EMG activity in MS-5**

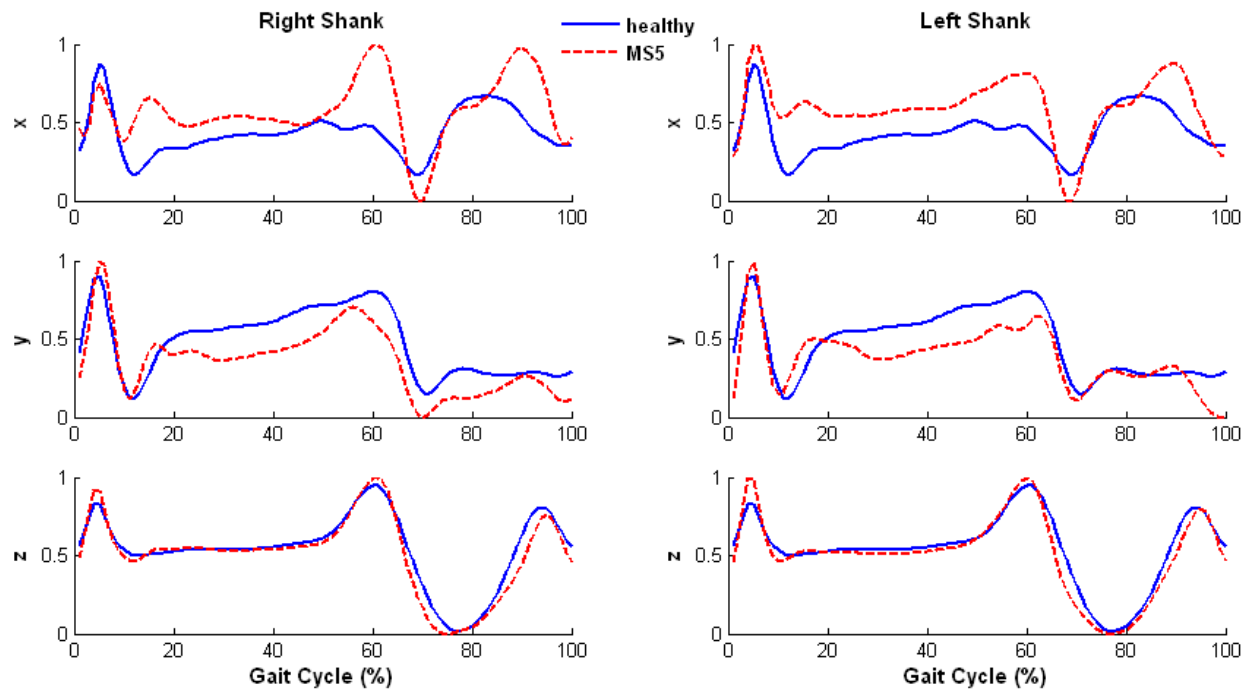
	Right	Left
Soleus	Similar EMG pattern as the healthy subjects with higher similarity levels in all gait phases.	Same as right soleus.
Tibialis Anterior (TA)	Small spasticity appears in the loading response and mid-swing phase. Small similarity appears in the terminal stance phase.	Similar to right TA, small similarity appears in the pre-swing phase.
Gastrocnemius Lateralis (LG)	Spasticity appears in the early stance phase.	Spasticity appears in the initial contact and terminal swing phase. Significant small similarity appears in mid- and terminal swing phases.
Vastus Lateralis (VL)	Higher muscle activity appears in the stance phase and terminal swing phase. Significant small similarity appears in pre- and initial swing phases.	Same as right VL.
Rectus Femoris (RF)	Weakness appears in the initial contact, spasticity appears late stance phase. Significant small similarity appears pre-swing phase.	Same as right RF with muscle weakness in the terminal swing phase. Significant small similarity also appears in the terminal swing.
Biceps Femoris (BF)	Spasticity appears in the stance phase. Significant small similarity appears in the terminal stance and pre-swing phases.	Same as right BF.
Gluteus Medius (Gmed)	Muscle weakness appears in the initial contact. Spasticity appears in the mid-stance and initial swing phases. Significant small similarity appears in the initial and mid-swing phases.	Muscle weakness appears in the initial contact. Spasticity appears in the mid-stance phase. Significant small similarity appears in the initial and mid-swing phases.
Erector Spinae (ES)	Higher muscle activity appear in the transition event from stance to swing phase, and late swing phase which indicates some levels of adaptation for instability gait.	Same as right ES, significant small similarity appears in the mid- and terminal swing phases.

- **Acceleration Patterns**

(A)



(B)



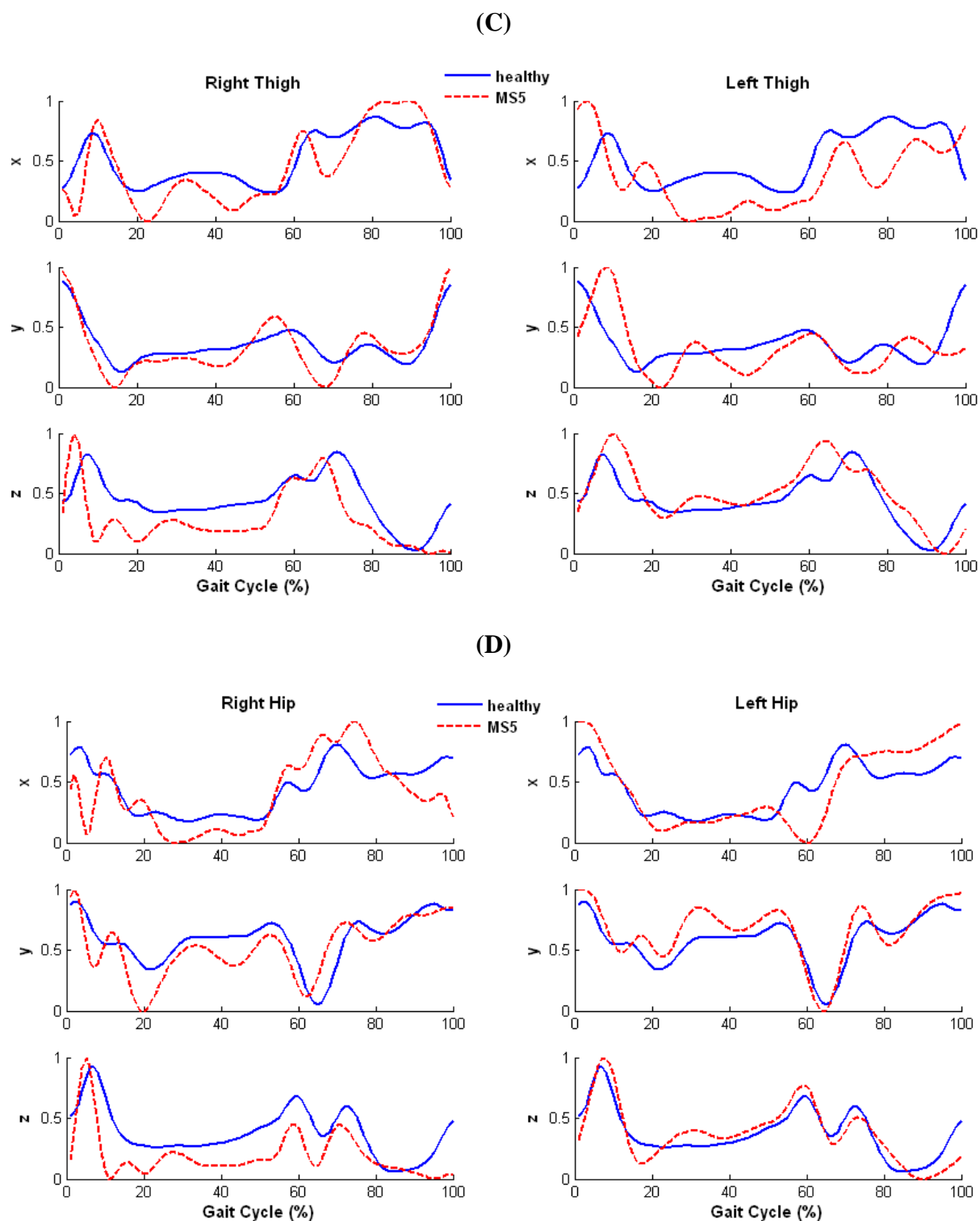


Figure AVIII-6: Comparison of acceleration pattern in a gait cycle between able-bodied subjects and MS-5.

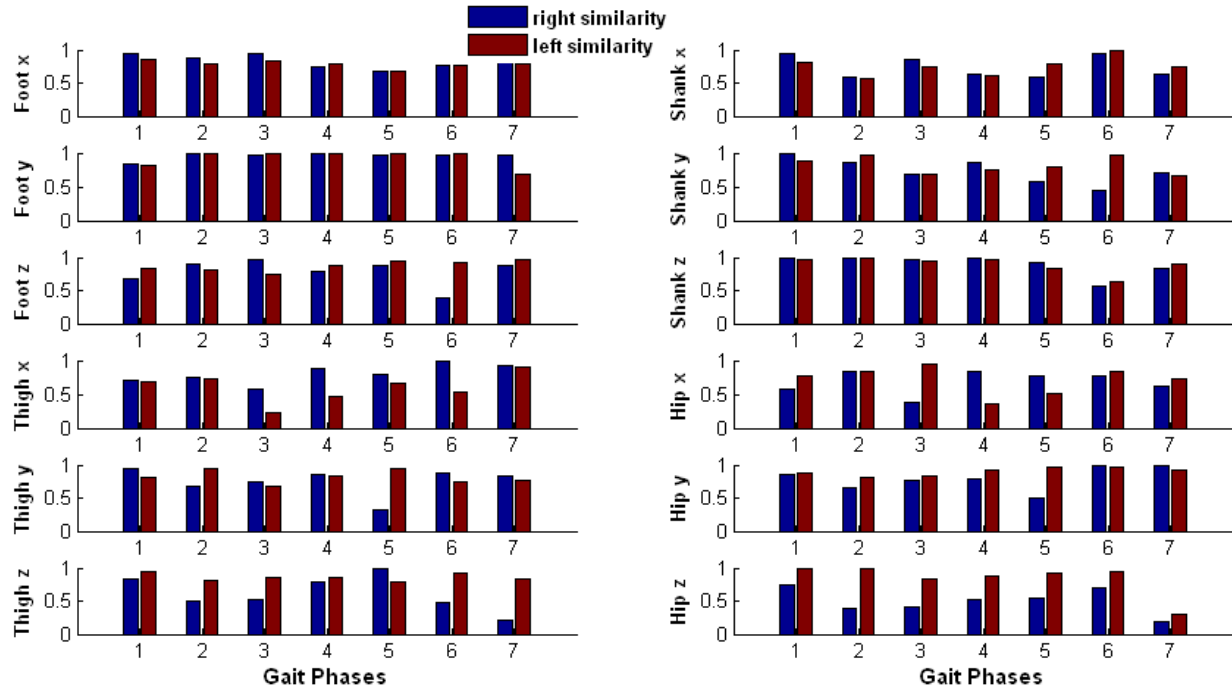


Figure AVIII-7: Grade of similarity on right and left acceleration in MS-5.

Summary:

Table AVIII-2: Characterization of acceleration in MS-5

	Right	Left
Foot x	There was an increased acceleration in swing phase. Relatively small similarity appears in initial swing phase.	There were general increased magnitudes during the full gait cycle. Relatively smaller similarity appears in initial swing phase.
Foot y	The pattern of Fy was very similar to the healthy subjects with high similarity through the walking cycle.	Similar to right foot y except that there was a little delayed deceleration in terminal swing phase which cause relatively small similarity in that phase.
Foot z	A sharp early rise occurs in the initial contact, early and sharp rise also appears in the swing phase. Smaller similarity appears in the mid-swing phase.	Similar to the right foot z. In addition, there was a constant high magnitude in the stance phase than the right foot z and healthy

		subjects.
Shank x	A lower acceleration appears in the initial contact, following with a constant higher magnitude in the rest of the stance phase, and then the higher acceleration occurs in the swing phase. Relatively small similarity appears in mid-stance and initial swing phases.	Similar pattern to shank x, except that there was a sharp rise in the initial contact. The smallest similarity appears in the mid-stance phase.
Shank y	Sharp rise in initial contact, following with lower magnitude during stance phase and the most of the swing phase. Significant small similarity appears in the mid-swing phase.	Similar pattern to shank y, except there was a normal magnitude in the mid-swing phase same as healthy subjects compared with right side, but much lower magnitude in the terminal swing phase.
Shank z	Perfect matched pattern with healthy subjects, there was only a little increased acceleration in the initial contact.	Same as right shank z.
Thigh x	There was a sharp and delayed rise in initial contact, instable magnitude throughout the stance phase, following with an increased but delayed acceleration in swing phase. Significant small similarity appears in the terminal stance phase.	There was a very early sharp rise in the initial contact, following with much lower magnitudes in mid- and terminal stance phases, and swing phase. Significant small similarity appears in the terminal stance phase.
Thigh y	Sharp deceleration in initial contact, early increased acceleration in the pre-swing and an early sharp deceleration in initial swing phase, a slightly higher magnitude in swing phase. Significant small similarity appears in initial swing phase.	There was a sharp increased acceleration in early stance phase, following with inconstant and relatively low magnitudes in the rest of the cycle.
Thigh z	Sharp rise in initial contact, lower and instable magnitude in the following gait cycle. Significant small similarity appears in the terminal swing phase.	Sharp rise in the early stance phase, following with a instable and slightly higher magnitude.
Hip x	There was instable and lower magnitude in the	There was a sharp deceleration in

	stance phase, following with early increased acceleration in early swing phase, and then lower magnitude in the terminal swing phase. Significant small similarity appears in the mid-stance phase.	the early stance phase, lower magnitude in the pre-swing phase, and higher magnitude in the late swing phase. Significant small similarity appears in the pre-swing phase.
Hip y	Sharp deceleration in initial contact, following the lower and instable magnitude in stance phase. Relatively small similarity appears in the initial swing phase.	There were relatively higher magnitudes in the stance phase, and a sharp rise in the initial swing phase. There were modulate to high similarity compared with right hip y.
Hip z	Sharp rise in initial contact, following with instable lower magnitudes in the rest of the cycle. Significant small similarity appears in the terminal swing phase.	There was a sharp rise in the initial contact following with a slightly higher magnitude in the rest of the stance phase.

Appendix IX: Results of Multiple Sclerosis Patient 6 (MS6)

- **Description**

Subject is a 29 year old male, a basketball player, was diagnosed with multiple sclerosis in September 2009. He could walk without any assistive devices. By talking to this MS subject, he complained that he was always feeling tired and having right leg tremor. Medication for RRMS was *Naltrexon*, 4.5mg/day. Subject was tested with bare-foot walking on the instrumented treadmill without any assistants continuing for three-minutes, at self-selective speed of 0.5 m/s.

- **Temporal Stride Variability**

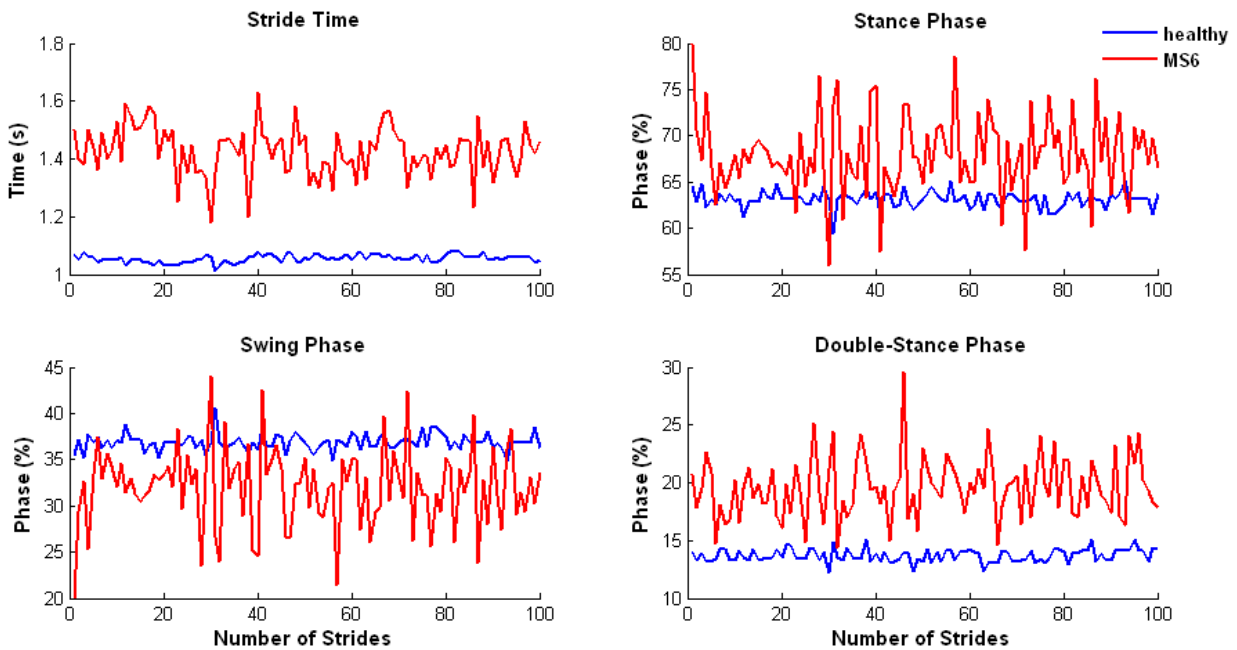


Figure AIX-1: Stride variability of a healthy subject and multiple sclerosis patient case 6 (MS-6).

- **Ground Reaction Forces**

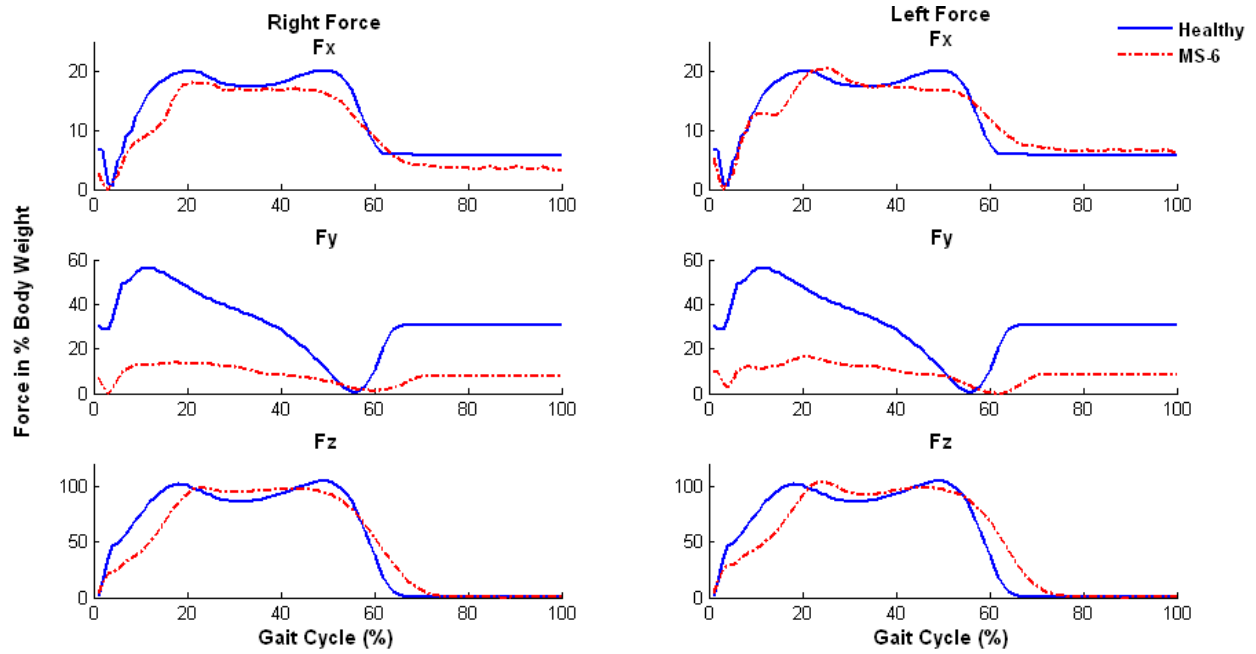


Figure AIX-2: Right and left GRF in 3-D in MS-6.

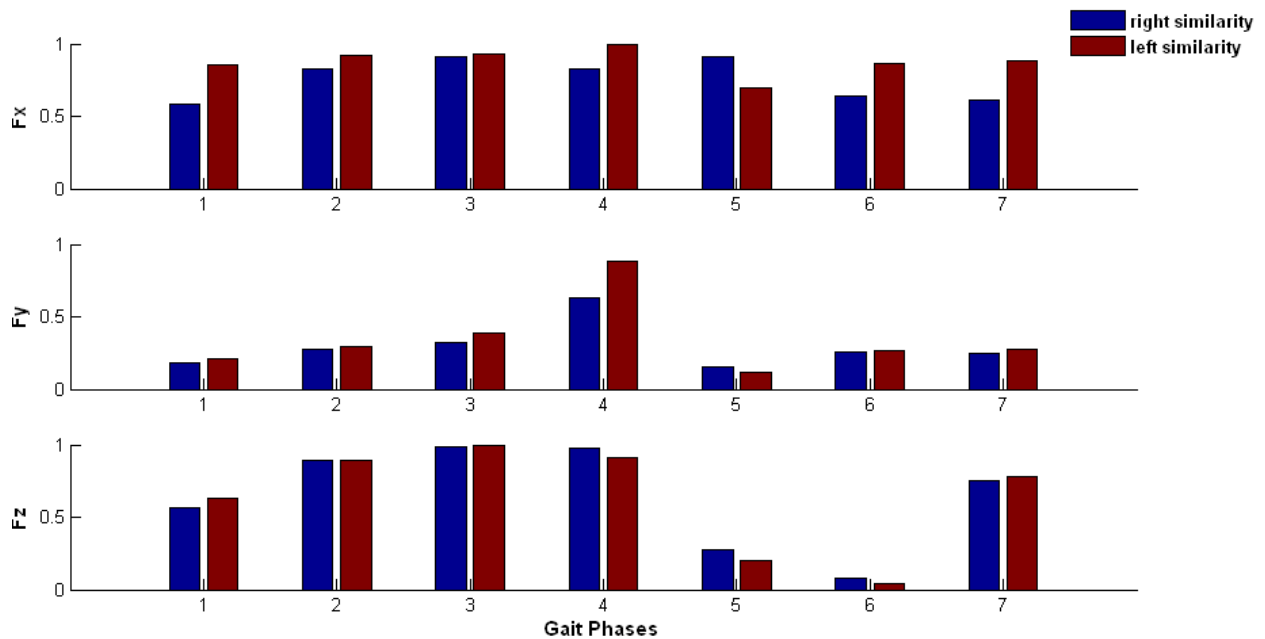


Figure AIX-3: Grade of similarity on right and left GRF in MS-6.

- **EMG Muscle Activity Patterns**

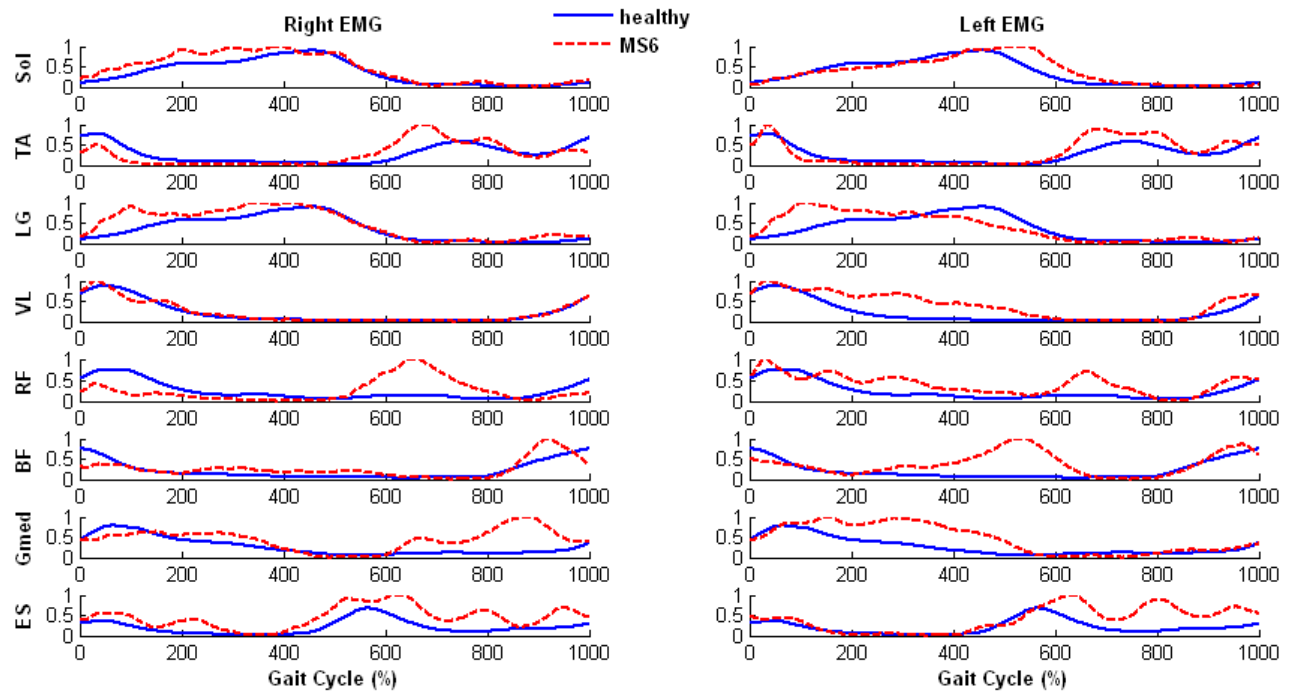


Figure AIX-4: Comparison of EMG pattern in a gait cycle between able-bodied subjects and MS-6.

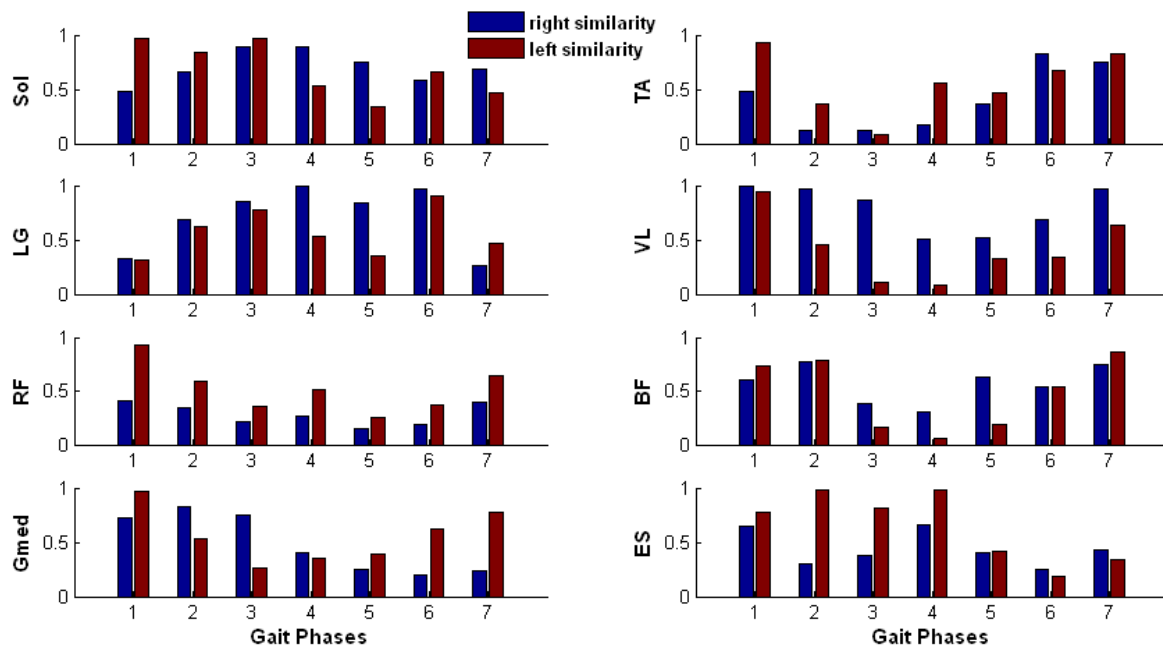
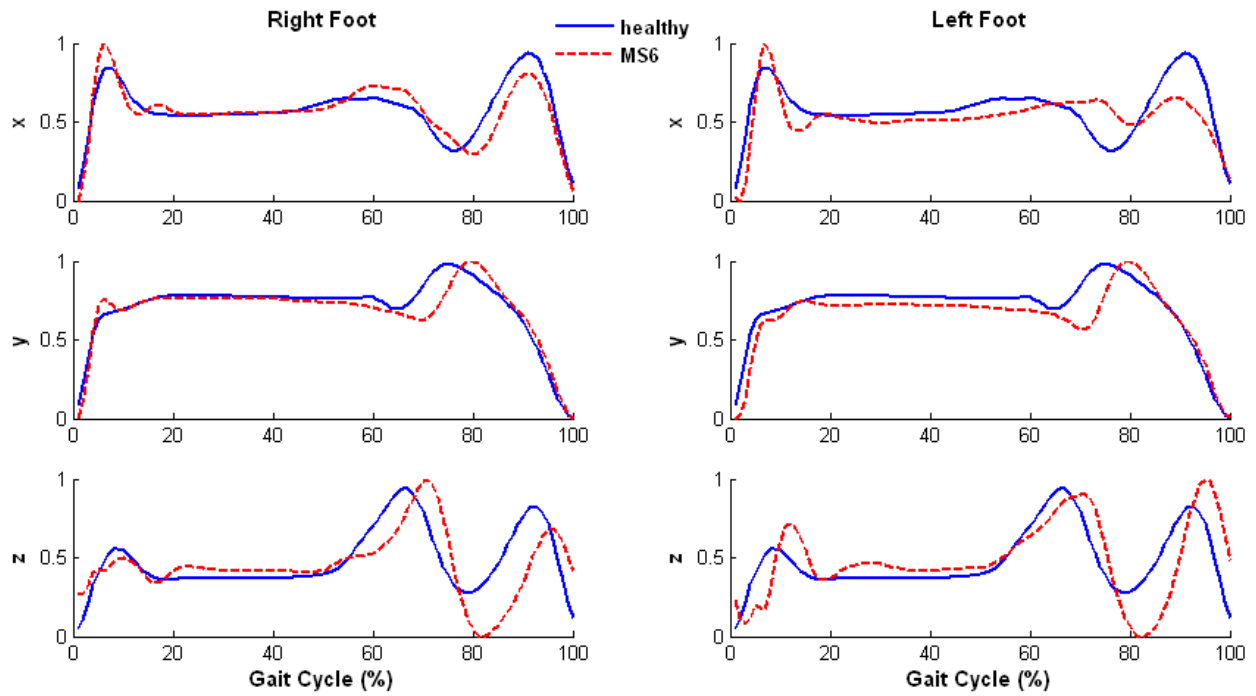


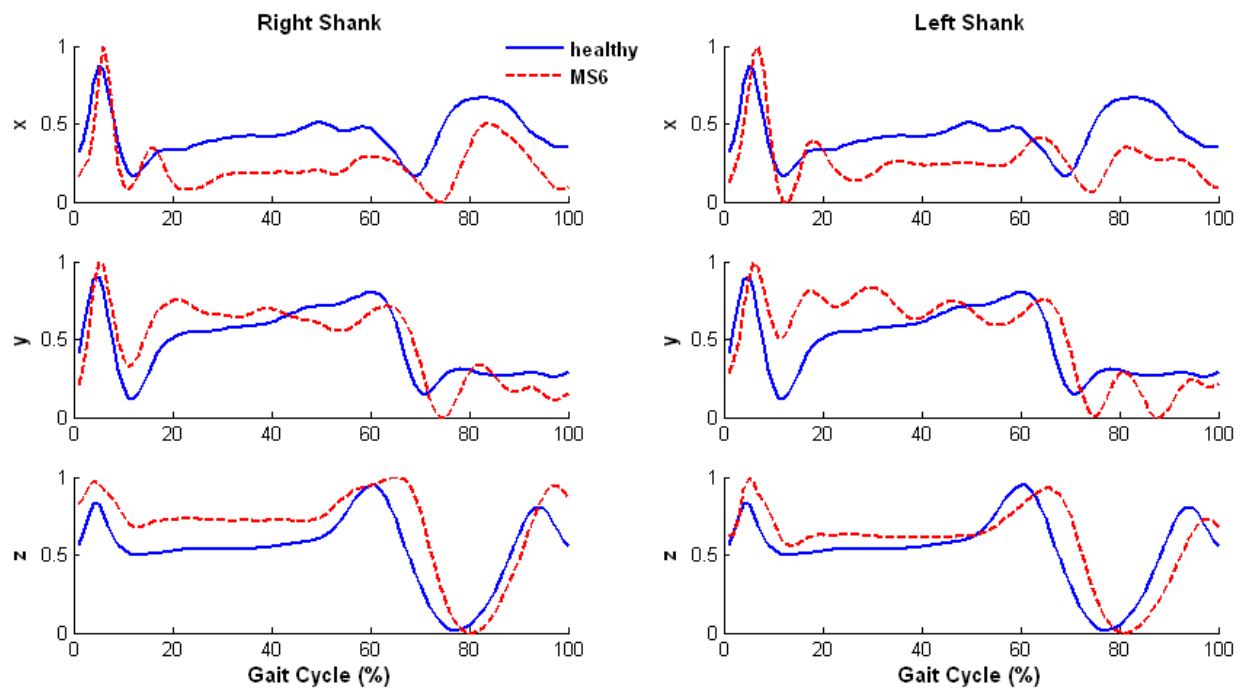
Figure AIX-5: Grade of similarity on right and left EMG in MS-6.

- Acceleration Patterns

(A)



(B)



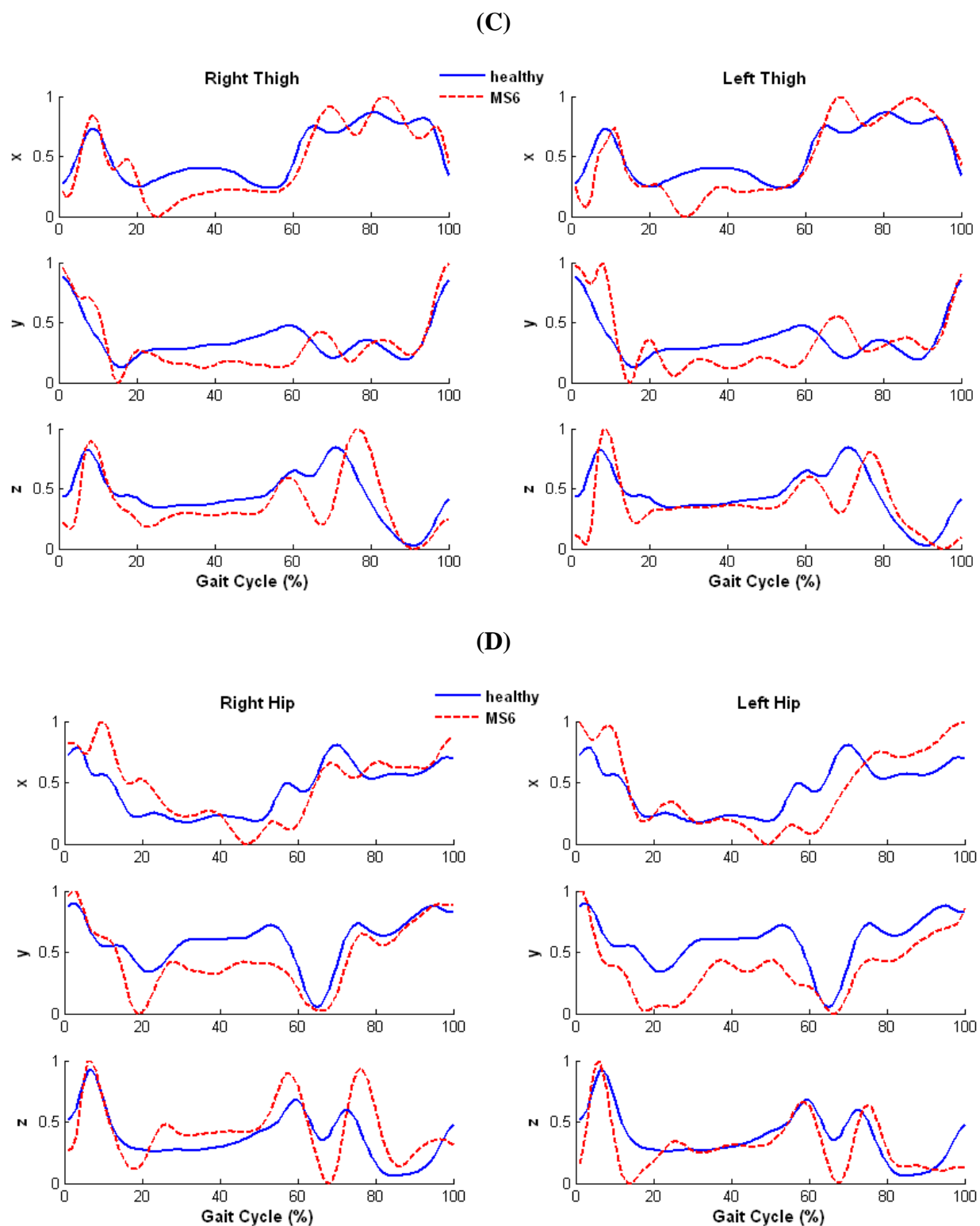


Figure AIX-6: Comparison of acceleration pattern in a gait cycle between able-bodied subjects and MS-6.

Table AIX-1: Characterization of acceleration in MS-6

	Right	Left
Foot x	There was a sharp rise in the initial contact, delayed and reduced acceleration in swing phase. Similarity was relatively high.	Same as right foot x.
Foot y	Slightly increased acceleration in the initial contact, delayed acceleration in the swing phase. Similarity was relatively high.	Delayed acceleration after toe-off. Similarity was relatively high.
Foot z	Delayed acceleration in initial swing phase, and smaller acceleration in terminal swing phase. Similarity was relatively high.	Delayed and sharp rise in acceleration in initial contact, and sharp rise in acceleration in terminal swing phase. Similarity was relatively high.
Shank x	Sharp rise in initial contact, delayed and reduced magnitude in the rest of the cycle. Relatively small similarity appears almost every phases.	Same as right shank x.
Shank y	Sharp rise in initial contact, instable acceleration during the stance phase. Relatively small similarity appears in the terminal swing phase.	Same as right shank y.
Shank z	Sharp and increased acceleration in initial contact, continue high level of acceleration during stance phase, delayed deceleration on toe-off and higher acceleration in terminal swing. Relatively small similarity appears in the mid-swing phase.	Same as right shank z.
Thigh x	Sharp rise in initial contact, slightly lower acceleration throughout the stance phase, higher acceleration in swing phase. Relatively small similarity appears in the mid-stance phase.	Same as right thigh x.
Thigh y	Sharp and delayed deceleration in early stance phase, lower acceleration during rest of the stance phase, sharp increased acceleration in	Same as right thigh y.

	terminal swing. Significant small similarity appears in the pre-swing phase.	
Thigh z	Sharp and delayed rise in initial contact, lower acceleration in the rest of the stance phase, sharp deceleration on toe-off, and sharp increased in mid-swing phase. Significant small similarity appears in the initial swing phase.	Sharp and delayed rise in the initial contact, sharp deceleration after toe-off, and a sharp rise acceleration in the swing phase. Significant small similarity appears in the terminal swing.
Hip x	Sharp and delayed rise in early stance phase, dramatically decreased throughout the stance phase, early lower acceleration in swing phase, increased acceleration in terminal swing. Significant small similarity appears in the pre-swing phase.	Same as right hip x.
Hip y	Sharp deceleration appears in early stance phase, following with the lower magnitude in the rest of the stance phase, delayed rise in swing phase. Significant small similarity appears in the initial swing phase.	Same as right hip y. Significant small similarity appears in the mid-stance phase.
Hip z	Sharp rise in initial contact, sharp reduction in early single support, higher acceleration in rest of the stance phase, much sharp acceleration and deceleration in swing phase. Significant small similarity appears in the initial swing phase.	Sharp rise in the initial contact, sharp deceleration in after toe-off. Significant small similarity appears in the initial swing phase.

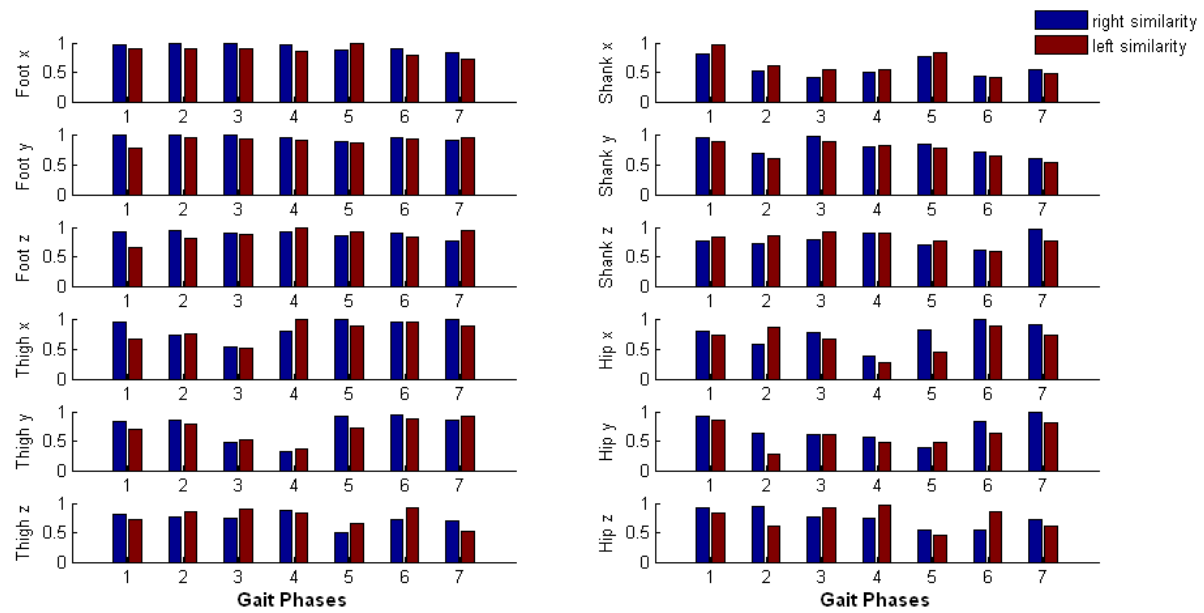


Figure AIX-7: Grade of similarity on right and left acceleration in MS-6.

Appendix X: Results of Cerebral Palsy Patient 1 (CP1)

- **Description**

Subject is a 26 year old female with diplegic (both lower extremity) cerebral palsy, community ambulatory. From the observation, she could walk without any assistant devices with slower speed. Her gait is typically characterized by toe walking, a crouched gait with flexed knees. She was tested during bare-foot walking on the instrumented treadmill for continuing three minutes, at speed of 0.5 m/s.

- **Temporal Stride Variability**

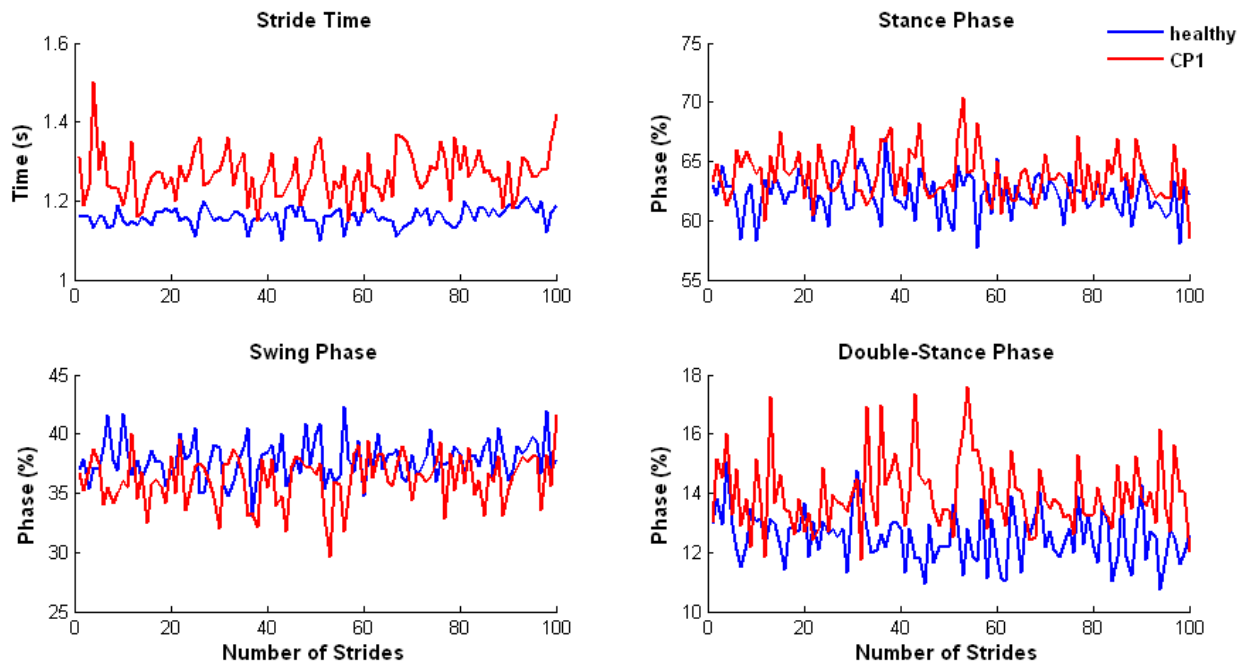


Figure AX-1: Stride variability of a healthy subject and female cerebral palsy patient case 1 (CP-1).

Analysis: CP-1 subject had increased variability in all temporal stride variables compared with healthy subject. The increased variability appears constant throughout the three-minute walking trial which also indicates the mild symptom of this patient. In addition, duration of her stance

phase and swing phase were similar to healthy subject, only slightly increased stride time and double stance phase in her gait.

- **Ground Reaction Forces**

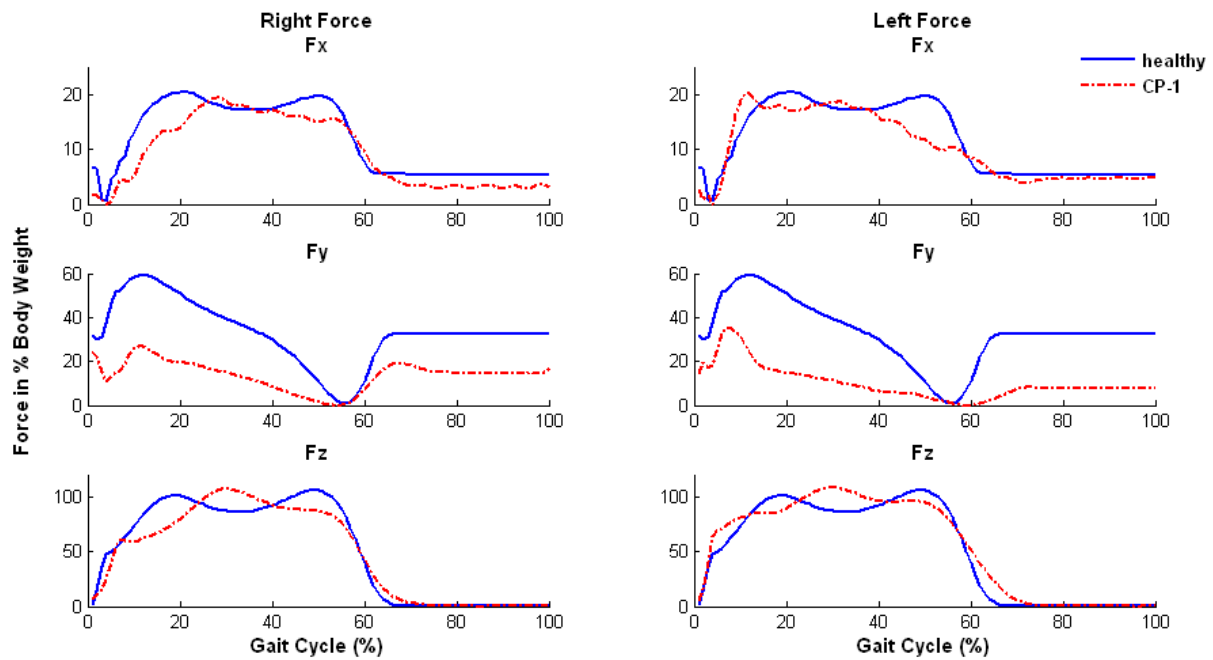


Figure AX-2: Right and left GRF in 3-D in CP-1.

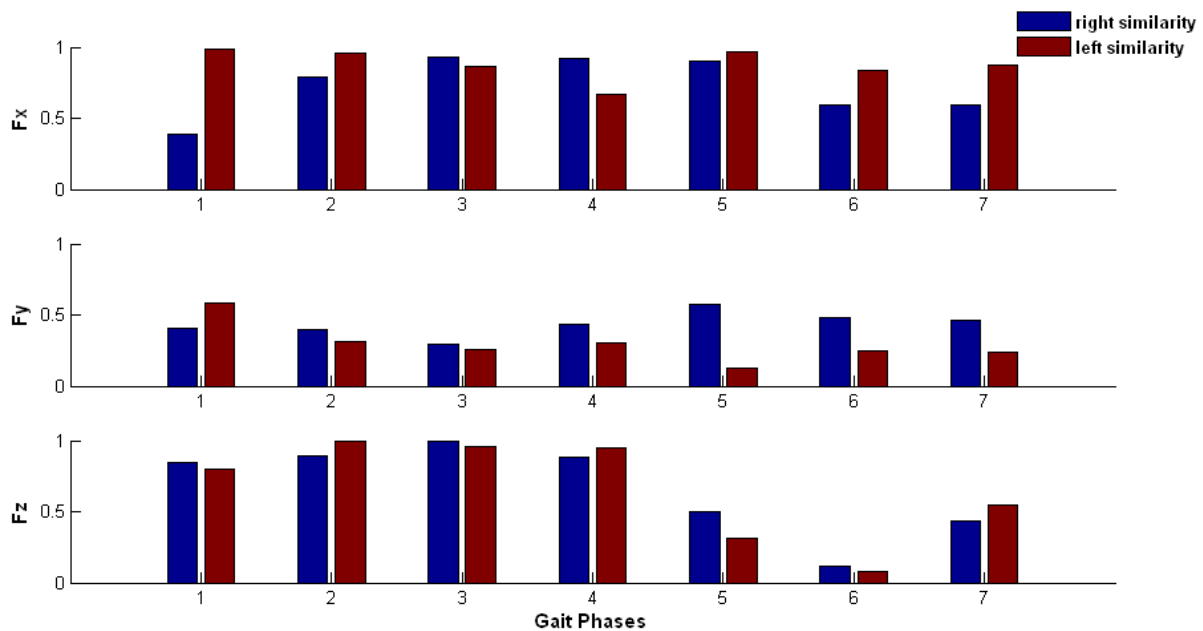


Figure AX-3: Grade of similarity on right and left GRF in CP-1.

Summary:

In vertical direction, CP-1 had slightly longer stance phase (left foot was slightly longer than the right foot) than healthy subjects. She had only one shortened peak at the time around 30% of the gait cycle which was about half time of the stance phase. In anterior-posterior direction, CP-1 shows lower GRF than healthy subjects. In the mediolateral direction, CP-1 had delayed rise of GRF on right foot, but early sharp rise of GRF on left foot during the loading response.

- **EMG Muscle Activity Patterns**

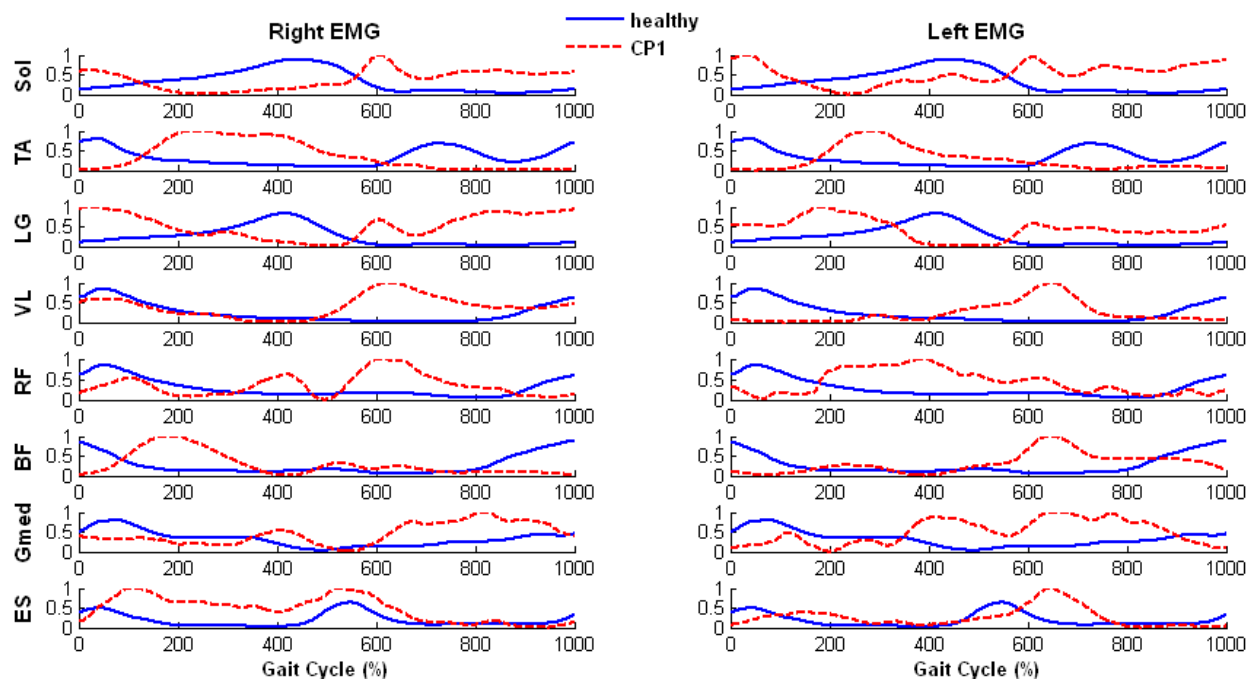


Figure AX-4: Comparison of EMG pattern in a gait cycle between able-bodied subjects and CP-

1.

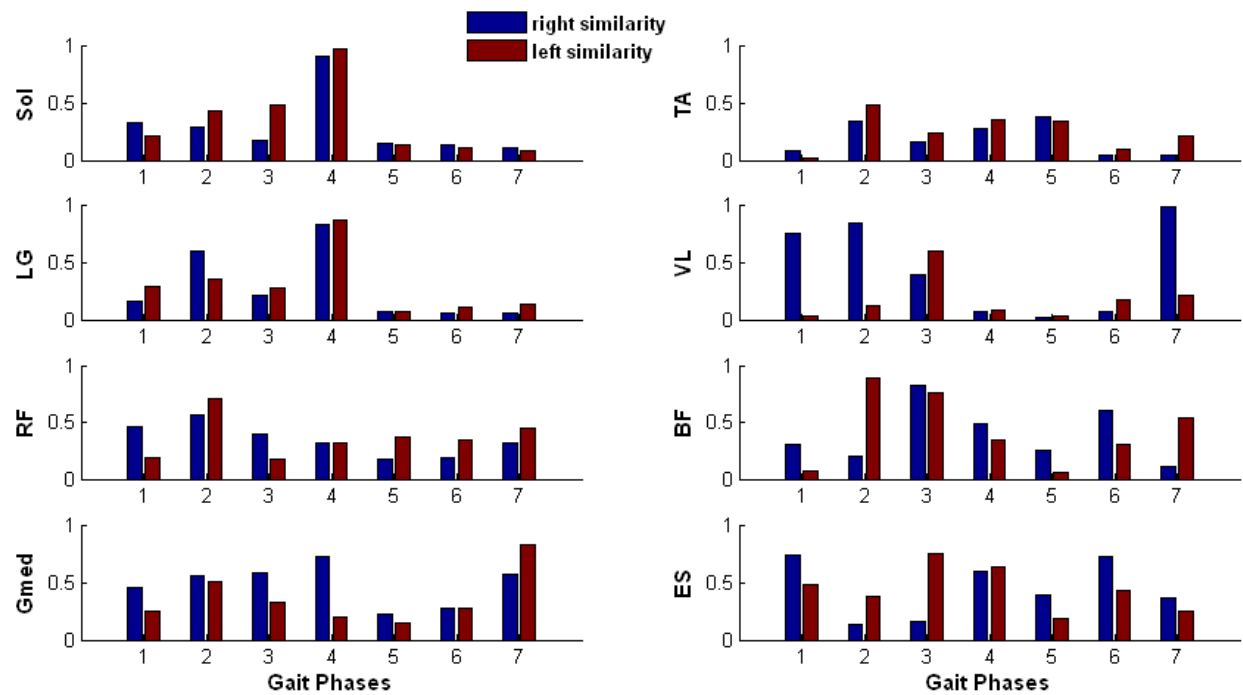


Figure AX-5: Grade of similarity on right and left EMG in CP-1.

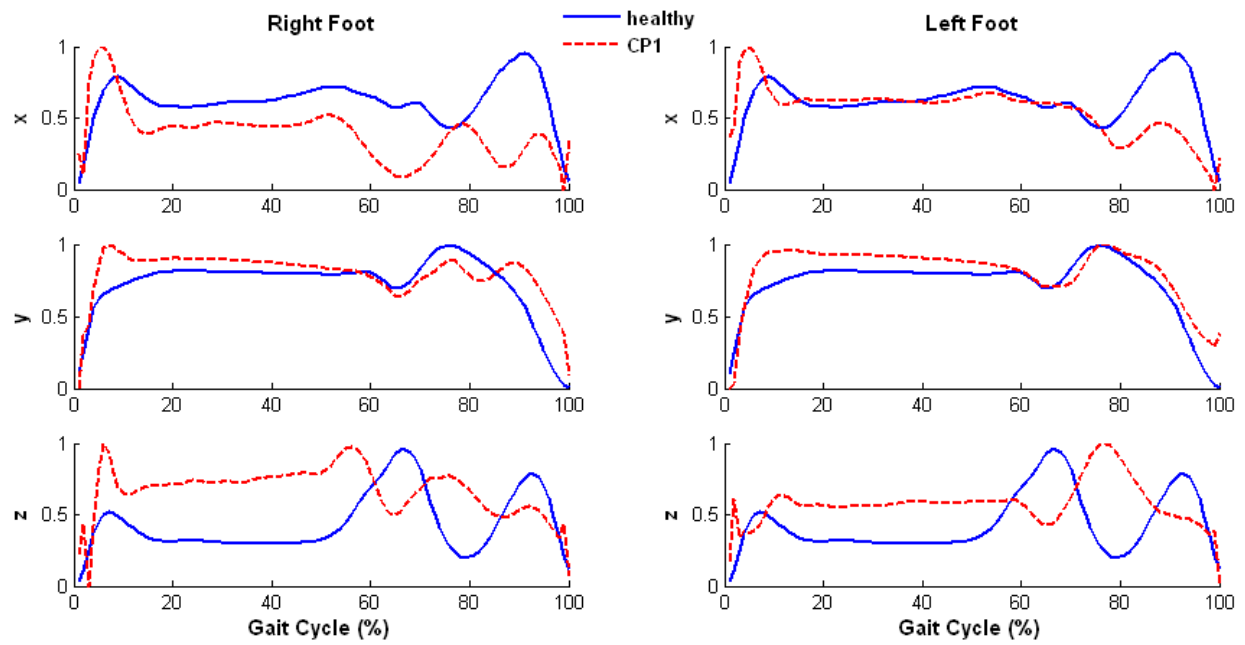
Summary:**Table AX-1: Summary of EMG activity in CP-1**

	Right	Left
Soleus	Spasticity appears in the initial contact until the end of loading response. Muscle weakness starts from the single support until the end of stance phase. Spasticity occurs on toe-off time until the cycle ends. This shows a completely opposite EMG pattern of healthy subjects. Significant small similarity occurs almost in every phase in the cycle.	Same as right Soleus.
Tibialis Anterior (TA)	Muscle weakness appears in the initial contact to the end of loading response. Spasticity appears immediately when the single limb support starts, until toe-off. Muscle weakness appears in the entire swing phase. Again, this pattern shows completely opposite EMG activity in healthy patient. In addition, TA and Soleus are clear agonist-antagonist muscle pair which can be seen in this CP-1 patient's EMG pattern, however, they activated at wrong time compared with the healthy subject, which can be explained why CP patients has no heel contact, but toe-walk instead. This complete wrong activities result in very low similarity in CP-1.	Same as right TA.
Gastrocnemius Lateralis (LG)	There were similar pattern showing in Soleus.	Same as right LG.
Vastus Lateralis (VL)	Weakness appears in the initial contact and terminal swing, spasticity appears in the pre-swing phase until the end of mid-swing phase. Significant small similarity appears in phase 4, 5, and 6.	Same as right VL with much smaller similarity in all gait phases.
Rectus Femoris	Weakness appears in the loading response, spasticity appears after single support and	Same as right RF. Significant small

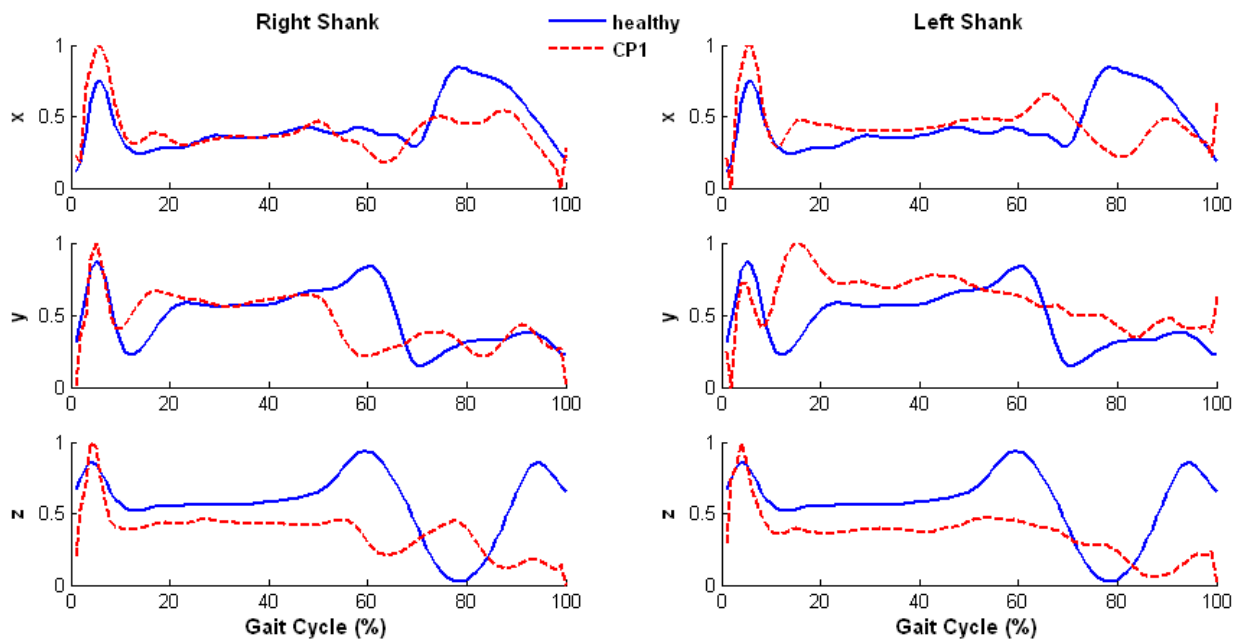
(RF)	continue until the end of mid-swing phase. Weakness appears in the terminal swing phase. Significant small similarity appears pre-and mid-swing phases.	similarity appears in loading response and terminal stance.
Biceps Femoris (BF)	Muscle weakness appears in the initial contact, following with spasticity in the mid-stance phase. Weakness appears again in the terminal swing phase. Significant small similarity appears in the mid-stance and terminal swing phases.	Weakness appears in the initial contact, and terminal swing phase which causes smaller similarity in those phases. Spasticity appears in the initial swing phase.
Gluteus Medius (Gmed)	Muscle weakness appears in the loading response until end of mid-stance phase. Spasticity appears in terminal stance and entire swing phase. Significant small similarity appears in initial and mid-swing phases.	Same as right Gmed. Significant small similarity appears in pre- and initial swing phases.
Elector Spinae (ES)	Spasticity appears in the stance phase. Significant small similarity appears in mid-stance and terminal stance phases.	Spasticity appears in the stance phase, and much higher activity in initial swing phase. Significant small similarity appears in the initial swing phase.

- **Acceleration Patterns**

(A)



(B)



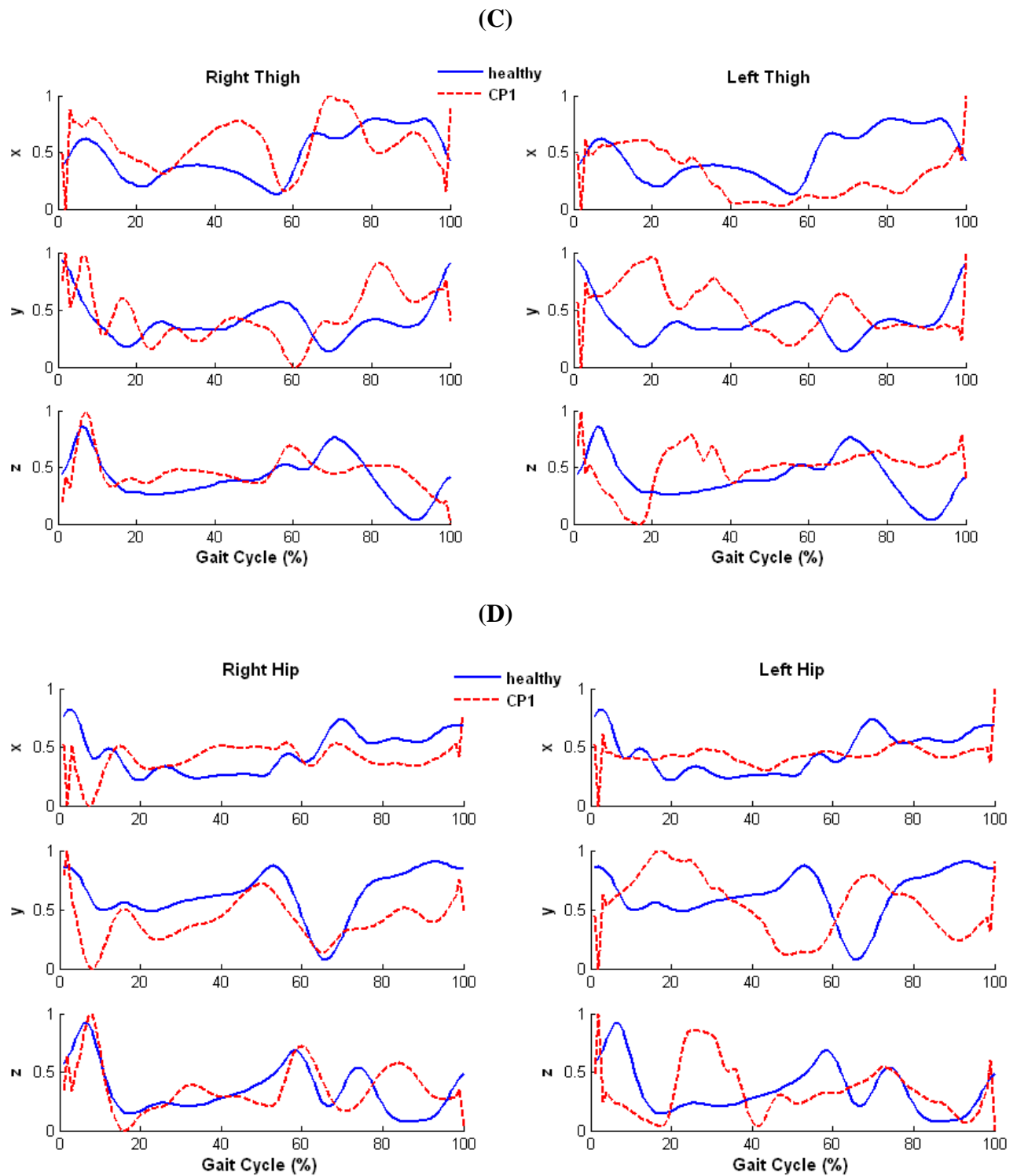


Figure AX-6: Comparison of acceleration pattern in a gait cycle between able-bodied subjects and CP-1.

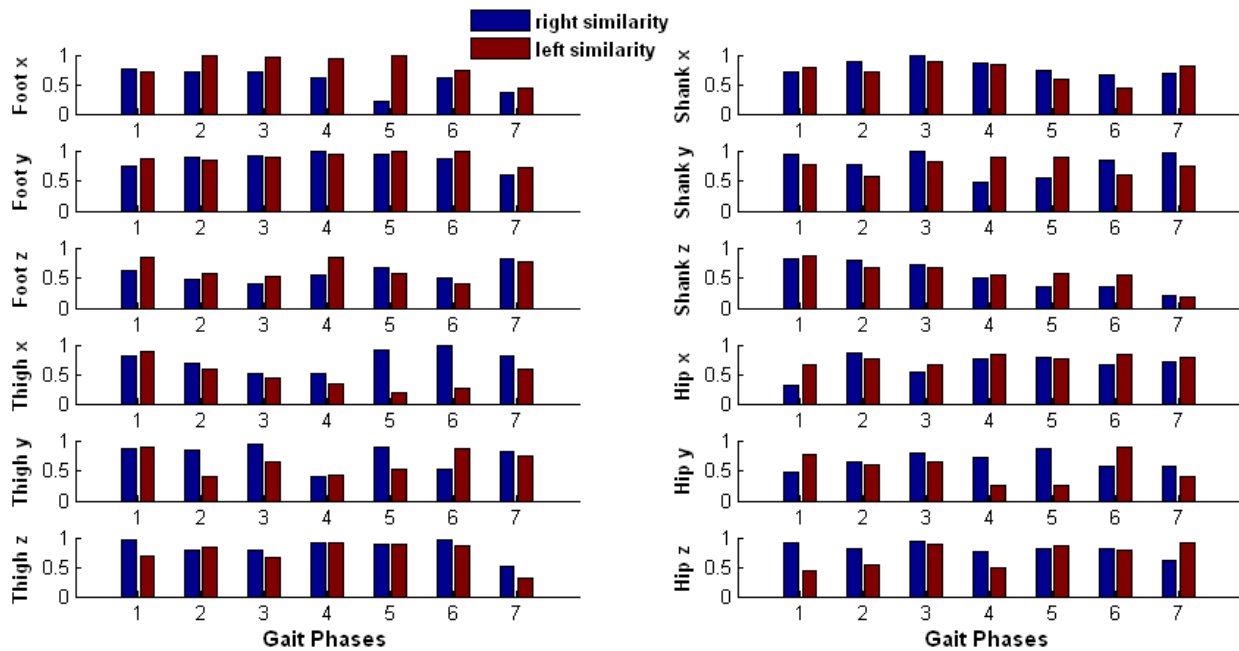


Figure AX-7: Grade of similarity on right and left acceleration in CP-1.

Summary:

Table AX-2: Characterization of acceleration in CP-1

	Right	Left
Foot x	Sharp rise in the initial contact, following with the lower magnitude throughout the rest of the cycle. Significant small similarity appears in the initial swing phase.	Sharp rise in the initial contact, lower acceleration in the terminal swing phase. Significant small similarity appears in terminal swing phase.
Foot y	Sharp rise in initial contact, continuing with the high acceleration until toe-off. Lower magnitude in the swing phase. Significant small similarity appears in terminal swing.	Same as right foot y.
Foot z	Sharp rise in the initial contact, following with the high acceleration before toe-off. Lower and delayed acceleration in the swing phase. Significant small similarity	Same as right foot z, significant small similarity appears in the mid-swing phase.

	appears in the terminal stance phase.	
Shank x	Sharp rise in initial contact, early deceleration appears in the end of the stance phase, lower acceleration in the swing phase. Small similarity appears in the mid-swing phase.	Sharp rise in initial contact, following with the high magnitude in the stance phase, there was a small acceleration at toe-off, lower acceleration appears in the swing phase. Significant small similarity appears in the mid-swing phase.
Shank y	Sharp rise in initial contact, following with high magnitude in the stance phase, early deceleration in the pre-swing phase which results in the small similarity at that time.	High acceleration appears most of the time in the full gait cycle. Small similarity appears in the mid-stance and mid-swing phases.
Shank z	Sharp rise in acceleration in initial contact, following with the lower magnitude throughout the rest of the cycle. Significant small similarity appears in the terminal swing phase.	Same as right shank z.
Thigh x	Sharp rise in initial contact, continuing with higher magnitude in the rest of stance phase, a sharp rise in the initial swing phase following with lower magnitude in the late swing phase. Significant small similarity appears in the terminal stance and pre-swing phases.	Sharp rise in the initial contact, continuing with high magnitude in the mid-stance phase. There were lower magnitudes from the terminal swing until the end of the cycle. Significant small similarity appears in initial swing and mid-swing phases.
Thigh y	Unstable but higher magnitudes throughout the entire cycle. Significant small similarity appears in the pre-swing phase.	Same as right thigh y.
Thigh z	Sharp rise in initial contact, high acceleration in stance phase, early acceleration before toe-off. Significant small similarity appears in the terminal swing phase.	Sharp and early rise in the initial contact, higher acceleration in the stance phase and terminal swing phase. Significant small similarity appears in the terminal swing phase.
	Lower acceleration in the initial contact,	

Hip x	following with slightly higher acceleration in the stance phase, lower magnitude in the swing phase. Significant small similarity appears in the loading response.	Same as right hip x.
Hip y	Sharp deceleration in the initial contact, following with the lower magnitude in the rest of stance phase and entire swing phase. Small similarity appears in loading response.	Lower magnitude in the initial contact, following with high acceleration in the single limb support, and then decelerates in the terminal stance phase, lower magnitude in the late swing phase. Significant small similarity appears in the pre- and initial swing phases.
Hip z	Sharp rise in initial contact, unstable acceleration through the rest of the cycle. Significant small similarity appears in the terminal swing phase.	Same as right hip z. Significant small similarity appears in the pre-swing phase. This unstable pattern might be the result from the hip deformity (flexion contracture).

Appendix XI: Results of Cerebral Palsy Patient 3 (CP3)

- **Description**

Subject is 18 year old male with diplegic cerebral palsy (lower extremity). He had bilateral knee flexion contracture (30 degrees on the right and 25 degrees on the left). Medication was *Botox* (muscle relaxant) injection every six months. Subject walked bare-footed on the instrumented treadmill with harness support, at speed of 0.3 m/s.

- **Temporal Stride Variability**

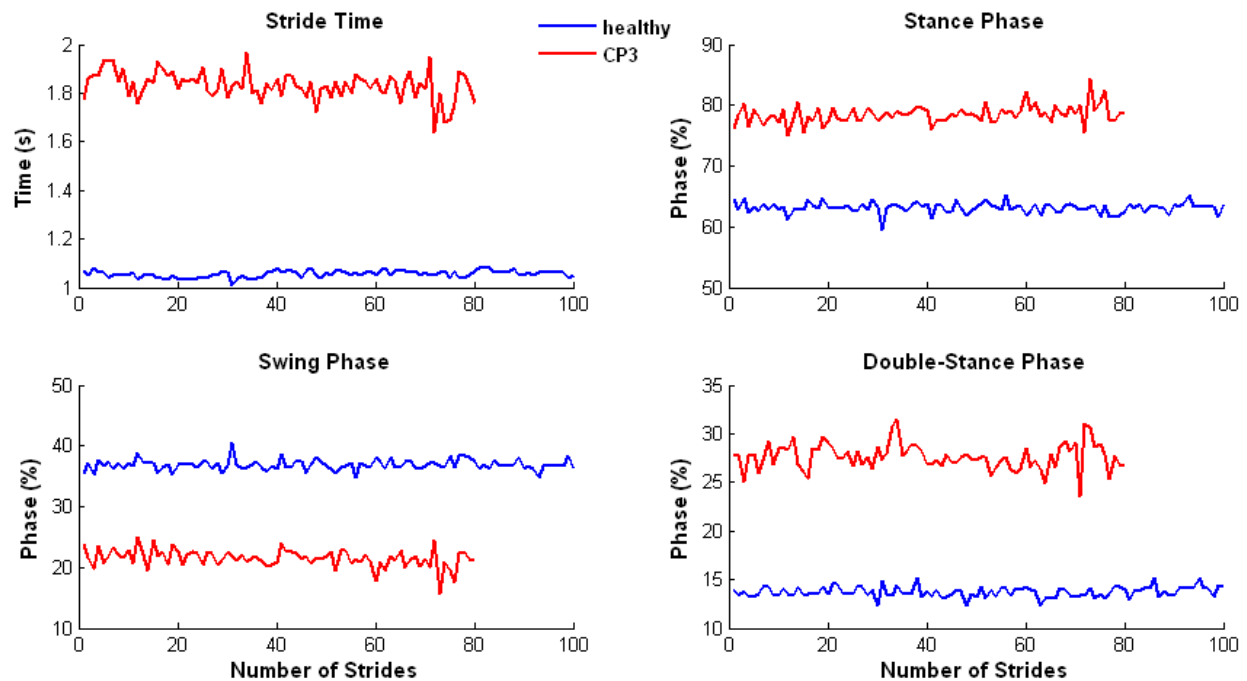


Figure AXI-1: Stride variability of a healthy subject and a male cerebral palsy case 3 (CP-3).

Summary: Due to the slower walking speed of this CP-3 subject, there were only 80 strides found within three-minute walking trial. The stride variability was increased slightly compared with the healthy subject, this might be the effect of the harness support. The stance phase and double-stance phase of this patient were much longer than the healthy, and his swing phase was much shorter than the healthy.

- **Ground Reaction Forces**

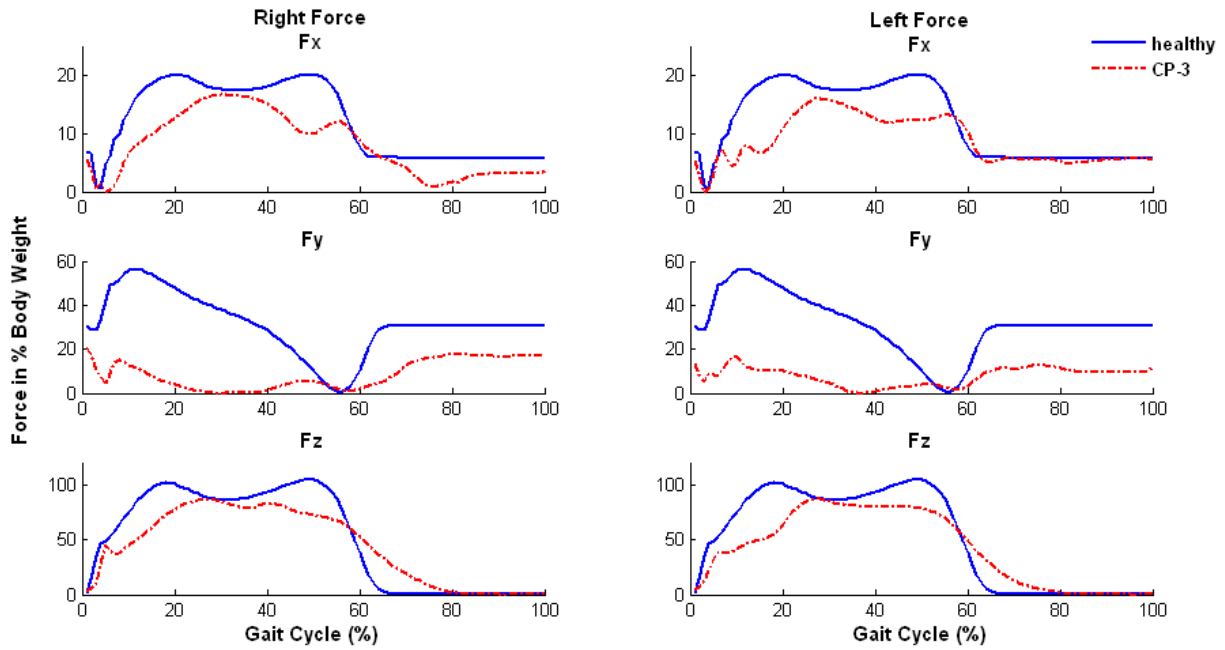


Figure AXI-2: Right and left GRF in 3-D in CP-3.

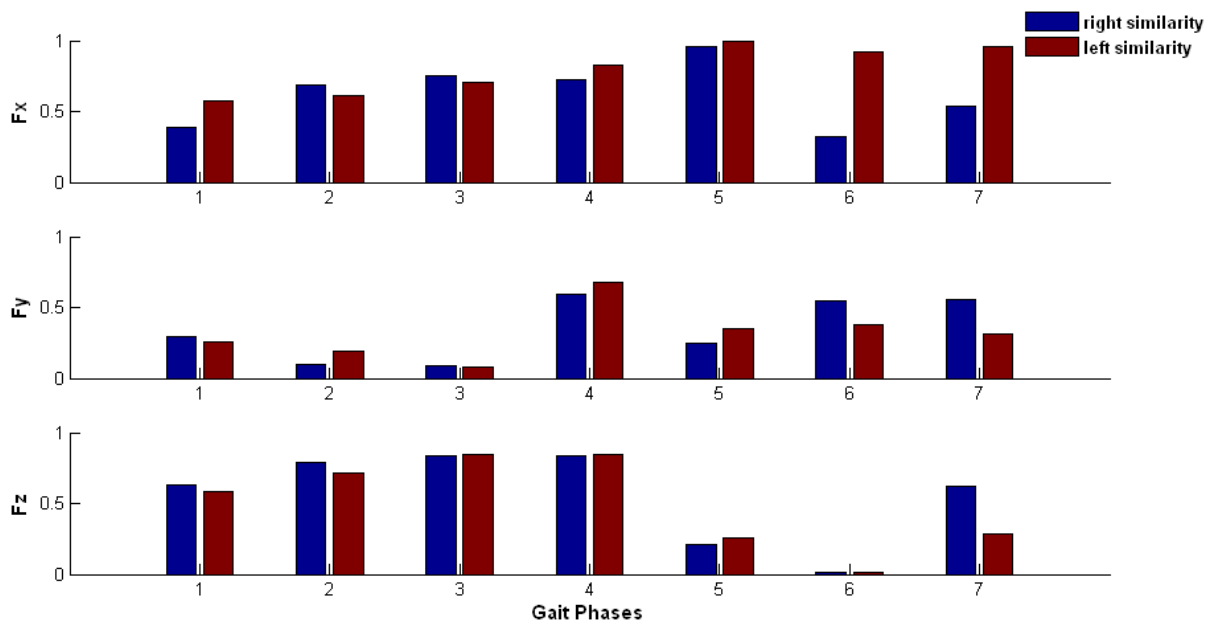


Figure AXI-3: Grade of similarity between right and left GRF in CP-3.

Summary:

In the vertical direction, the stance phase of CP-3 on both feet were much longer (80% of the gait cycle) than healthy subjects. There was a typical shortened one peak in the stance phase which was also shown in other CP patients. In anterior-posterior direction, there was much lower GRF than healthy subjects, and same as in the mediolateral direction. Significant small similarity appears in the mid-swing phase in vertical direction, and the entire cycle in the anterior-posterior direction.

• EMG Muscle Activity Patterns

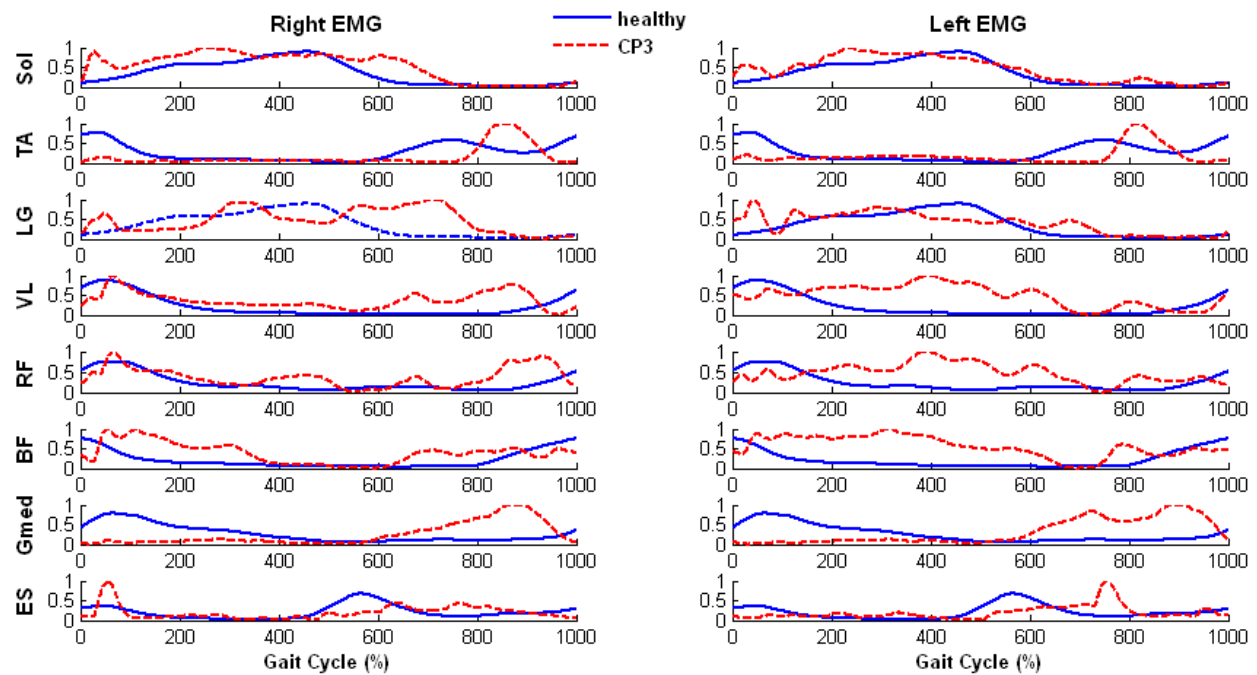


Figure AXI-4: Comparison of EMG pattern in a gait cycle between able-bodied subjects and CP-3.

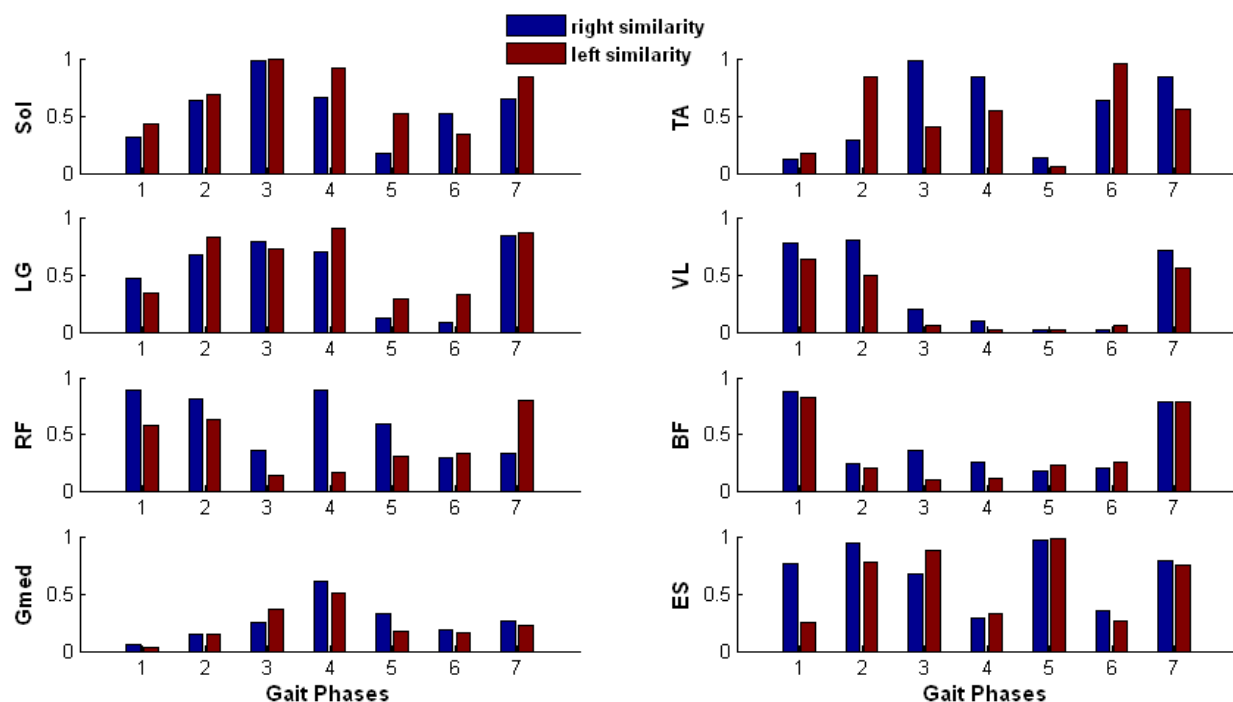


Figure AXI-5: Grade of similarity on right and left EMG in CP-3.

Summary:

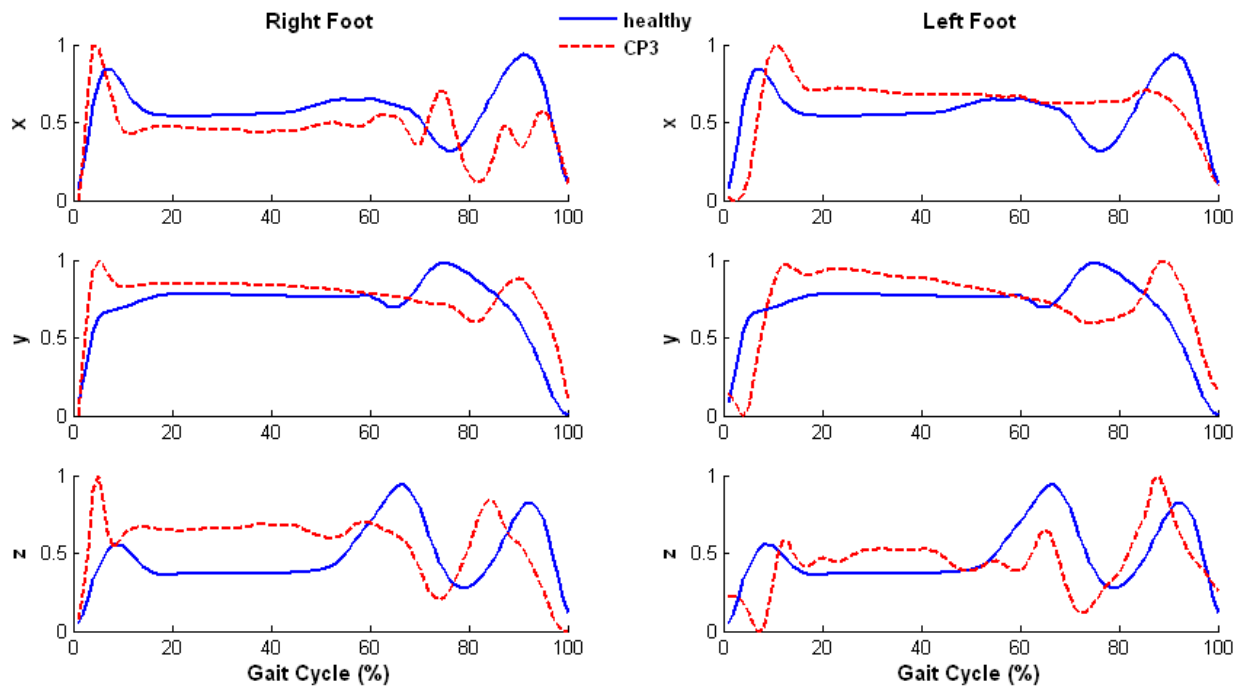
Table AXI-1: Summary of EMG activity in CP-3

	Right	Left
Soleus	Spasticity appears in the initial contact, and continuing until end of the stance phase. Significant small similarity appears in the initial swing phase.	Same as right Soleus, significant small similarity appears in the mid-swing phase.
Tibialis Anterior (TA)	Muscle weakness appears in the entire stance phase, spasticity occurs in the early swing phase. Significant small similarity appears in the loading response and initial swing phase.	Same as right TA.
Gastrocnemius Lateralis (LG)	Spasticity appears in the initial contact, and continuing in the rest of the stance phase. Significant small similarity in initial and mid-swing phases.	Same as right LG.
Vastus Lateralis	Weakness appears in the initial contact and terminal swing, spasticity appears after single	

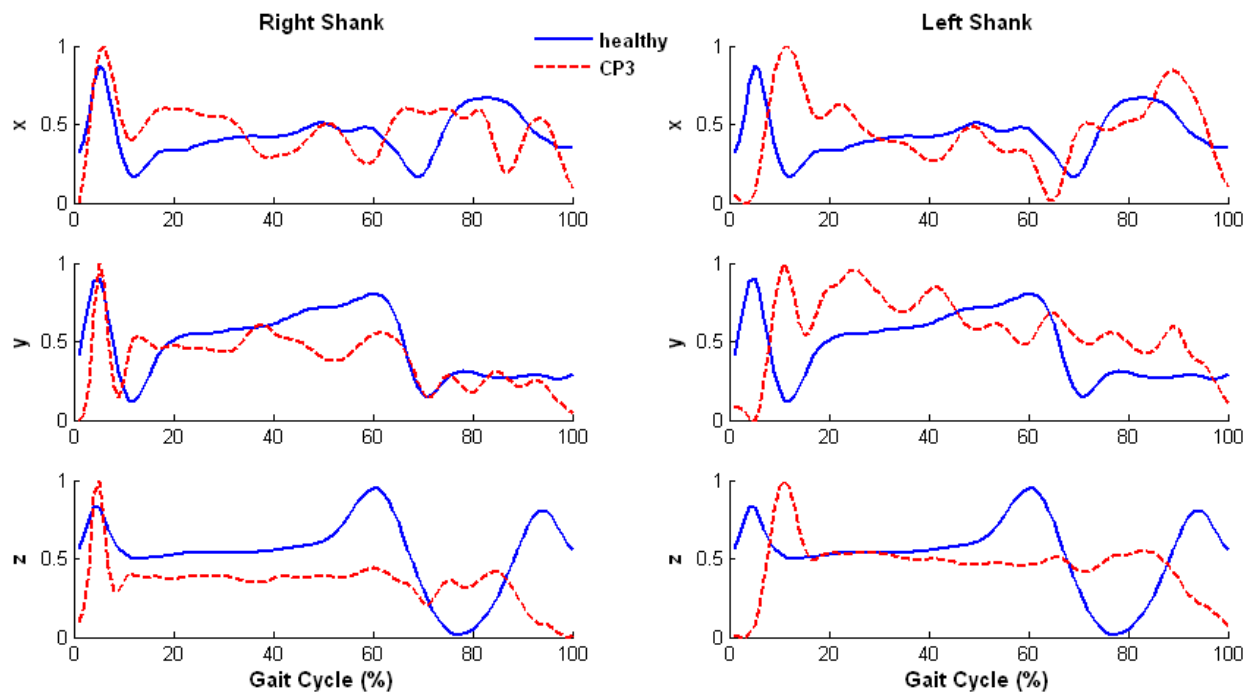
(VL)	support in the stance phase and early swing phase. Significant small similarity appears in phase 3~6.	Same as right VL.
Rectus Femoris (RF)	Weakness appears in the initial contact, spasticity appears after single support and continue until the terminal swing. Significant small similarity appears mid-swing phases.	Same as right RF. Significant small similarity appears pre-and initial swing phases.
Biceps Femoris (BF)	Muscle weakness appears in the initial contact, following with the spasticity until 40% of the gait cycle. Spasticity appears again in the initial and mid-swing phases. Significant small similarity appears in the phase 2~6.	Muscle weakness appears in the initial contact, following with the spasticity until 65% of the gait cycle.
Gluteus Medius (Gmed)	Muscle weakness appears in the early stance phase. Spasticity appears in the late swing phase. This entire opposite pattern of healthy subjects causes the significant small similarity appearing in all phases in the gait cycle.	Same as right Gmed.
Elector Spinae (ES)	Spasticity appears in loading response. Significant small similarity appears in pre- and mid-swing phases.	Muscle weakness appears in the initial contact.

- **Acceleration Patterns**

(A)



(B)



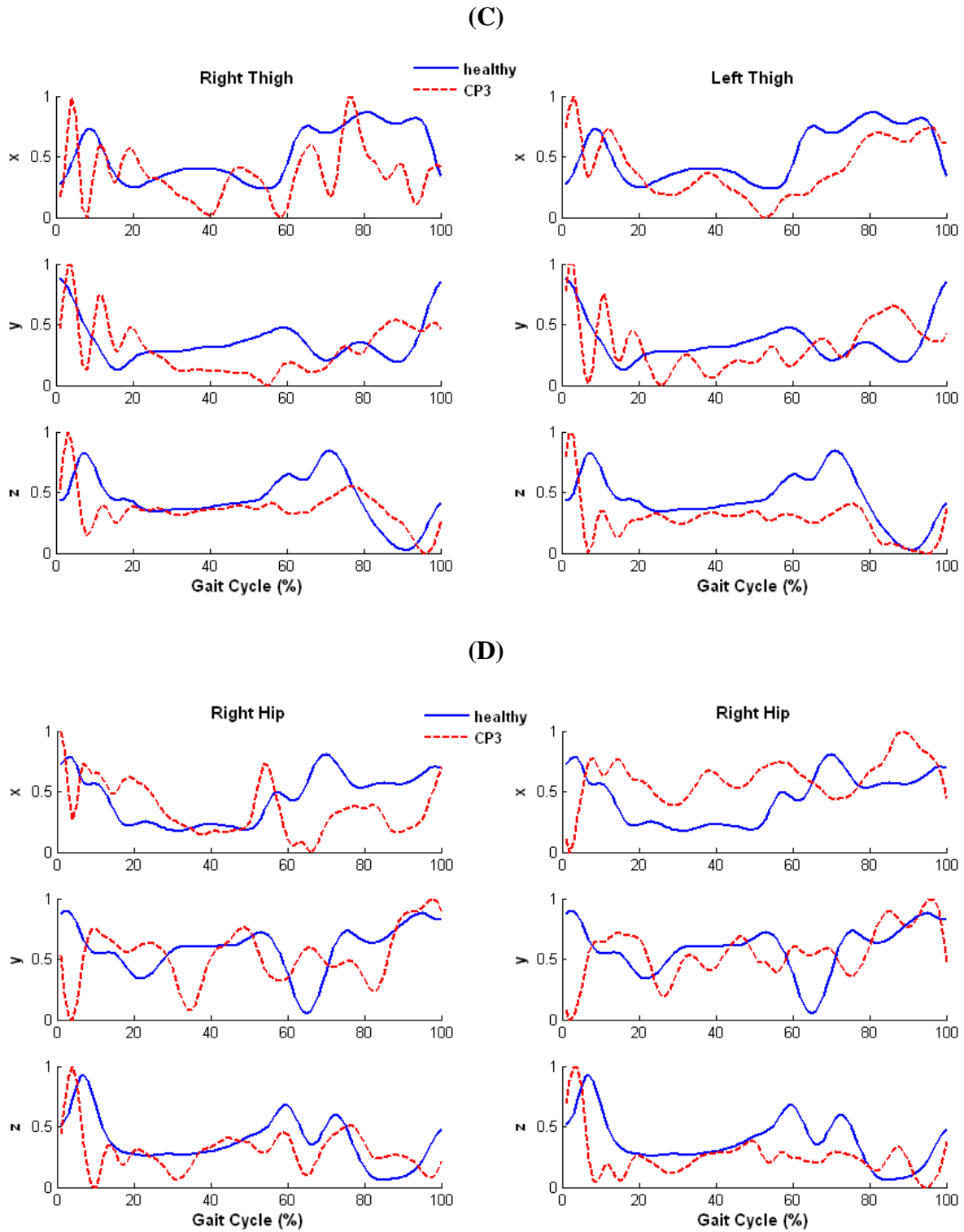


Figure AXI-6: Comparison of acceleration pattern in a gait cycle between able-bodied subjects and CP-3.

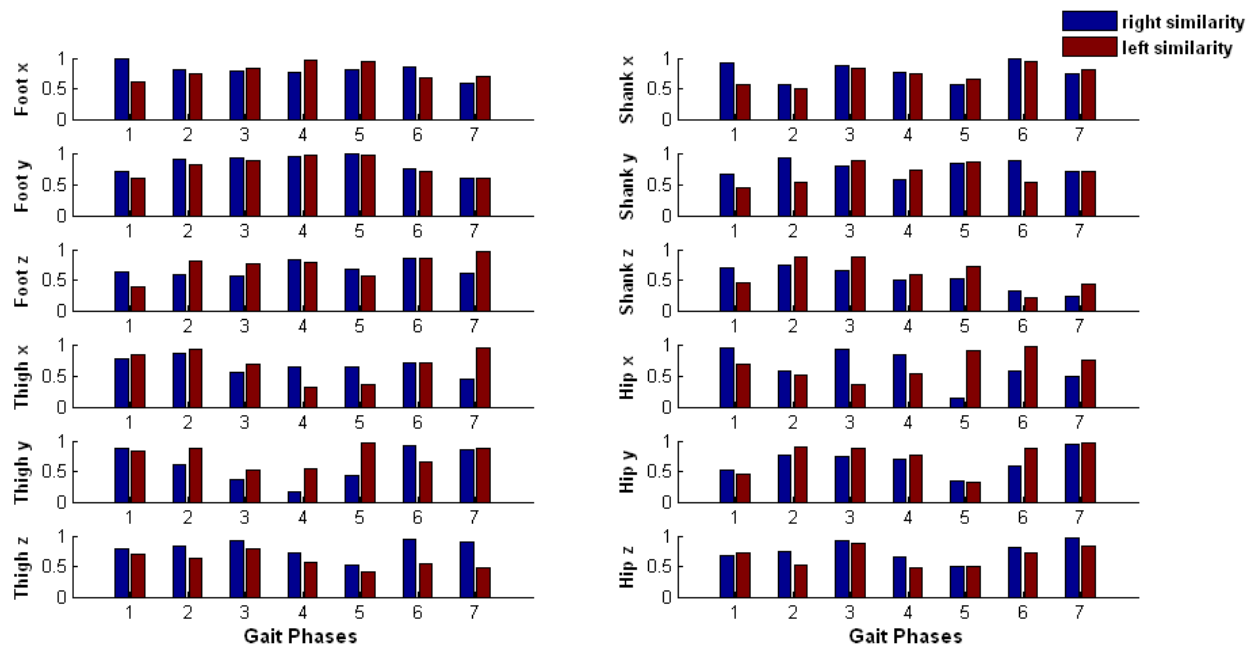


Figure AXI-7: Grade of similarity on right and left acceleration in CP-3.

Summary:

Table AXI-2: Characterization of acceleration in CP-3

	Right	Left
Foot x	Sharp rise in the initial contact, following with lower acceleration in the rest of the cycle. Small similarity appears in the terminal swing phase.	Sharp and delayed rise in the initial contact, following with the higher acceleration in the stance phase, and lower acceleration in the swing phase.
Foot y	Sharp rise in initial contact, delayed acceleration after toe-off. Small similarity appears in the terminal swing phase.	Same as right foot y.
Foot z	Sharp rise in the initial contact, following with the higher acceleration in the stance phase. Significant small similarity appears in the loading response.	Much delayed rise in the initial contact following with high acceleration in the stance phase. Sharp rise in the terminal swing phase.

Shank x	Sharp rise in initial contact, unstable acceleration in the rest of the cycle, might due to the bilateral knee flexion contracture. Small similarity appears in the mid-stance phase.	Delayed and sharp rise in initial contact, following with unstable acceleration in the rest of the cycle. Small similarity appears in the mid-stance phase.
Shank y	Sharp rise in initial contact, unstable acceleration in the rest of the cycle.	Same as right shank y.
Shank z	Sharp rise in acceleration in initial contact, following with lower acceleration in the rest of the cycle. Significant small similarity appears in the mid- and terminal swing phases.	Same as right shank z.
Thigh x	Sharp rise in initial contact, very unstable acceleration pattern in the gait cycle. Significant small similarity appears in the pre- and initial swing phases.	Sharp rise in the initial contact, following with lower acceleration in the rest of the cycle. Significant small similarity appears in the pre- and initial swing phases.
Thigh y	Sharp and unstable acceleration in the loading response, following with lower magnitude in the rest of the stance phase. Small similarity appears in pre-swing phase.	Unstable acceleration appears in a full gait cycle. Small similarity appears in the pre-swing phase.
Thigh z	Sharp rise in initial contact, followed with lower acceleration in the rest of the cycle. Small similarity appears in the initial swing phase.	Same as right thigh z.
Hip x	Sharp deceleration in the initial contact, followed with high acceleration in early stance phase, and lower acceleration in the swing phase. Significant small similarity appears in the initial swing phase.	Sharp increased acceleration in the initial contact, followed with high acceleration in the stance phase, and high acceleration in the terminal swing phase. Small similarity appears in the mid-stance phase.
Hip y	Lower acceleration in the initial contact, following with unstable magnitudes in the rest of the cycle, which indicate some	Same as right hip y.

	levels of hip contractures.	
Hip z	Sharp rise in initial contact, following with unstable magnitude in the rest of the cycle. Small similarity appears in initial swing phase.	Same as right hip z.

Appendix XII: Results of Cerebral Palsy Patient 4 (CP4)

- **Description**

Subject is 55 year old male with right spastic hemiplegia due to cerebral palsy. He was also diagnosed with epilepsy in 1966. Medication includes muscle relaxant *Dantrolene sodium*, 5mg per day. Subject was tested with bare-foot walking on the instrumented treadmill for continuing three minutes, at speed of 0.45 m/s.

- **Temporal Stride Variability**

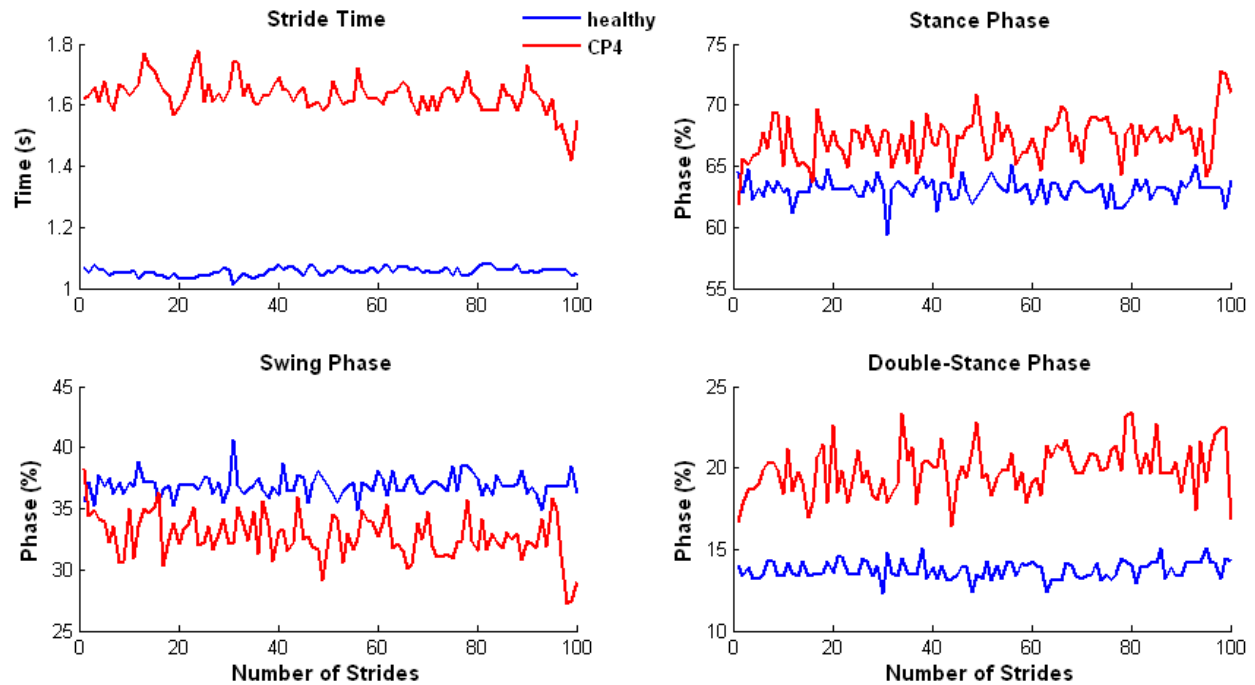


Figure AXII-1: Stride variability of a healthy male subject and a cerebral palsy case 4 (CP-4).

Summary: Stride variability of CP-4 was increased compared with a healthy male subject. The stance phase and double-stance phase were longer than healthy subject with much greater fluctuations. The stride time was much longer than healthy subject, but gradually reduced which showing some levels of fatigue.

- **Ground Reaction Forces**

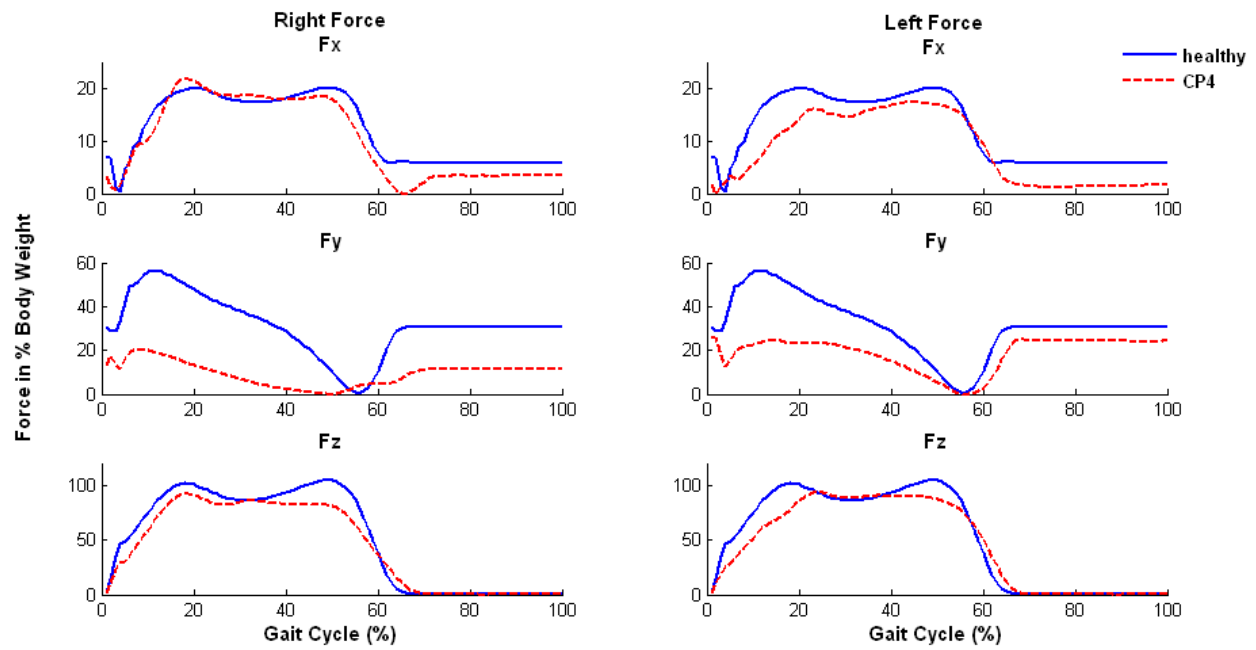


Figure AXII-2: Right and left GRF in 3-D in CP-4.

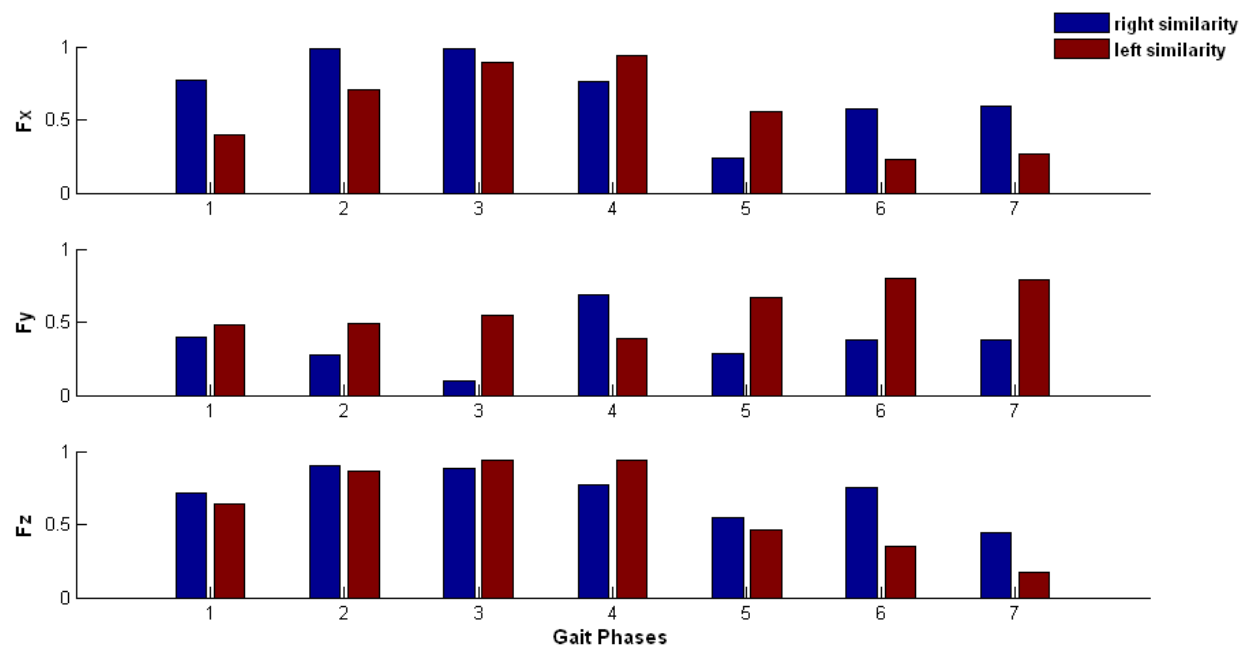


Figure AXII-3: Grade of similarity on right and left GRF in CP-4.

Summary: In vertical direction, CP-4 had slightly lower GRF with first peak higher than the second peak pattern. The longer duration of the ground contact of CP-4 indicates the mild symptoms of this subject compared with other three CP subjects. In anterior-posterior direction, CP-4 had much lower GRF than healthy, but right leg showed more sever symptom than the left leg which indicates the right leg was mostly affected. In mediolateral direction, there was a sharp rise in GRF on the first peak on the right, whereas the lower GRF appeared in the full gait cycle on the left.

- **EMG Muscle Activity Patterns**

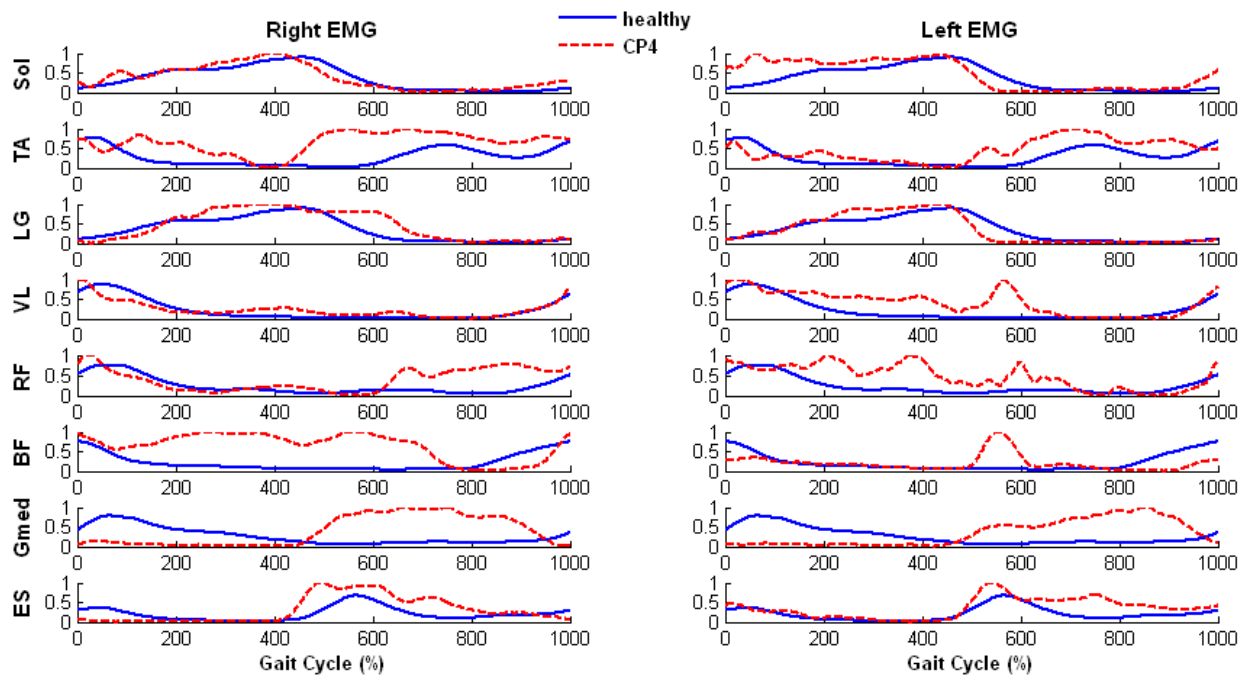


Figure AXII-4: Comparison of EMG pattern in a gait cycle between healthy subjects and CP-4.

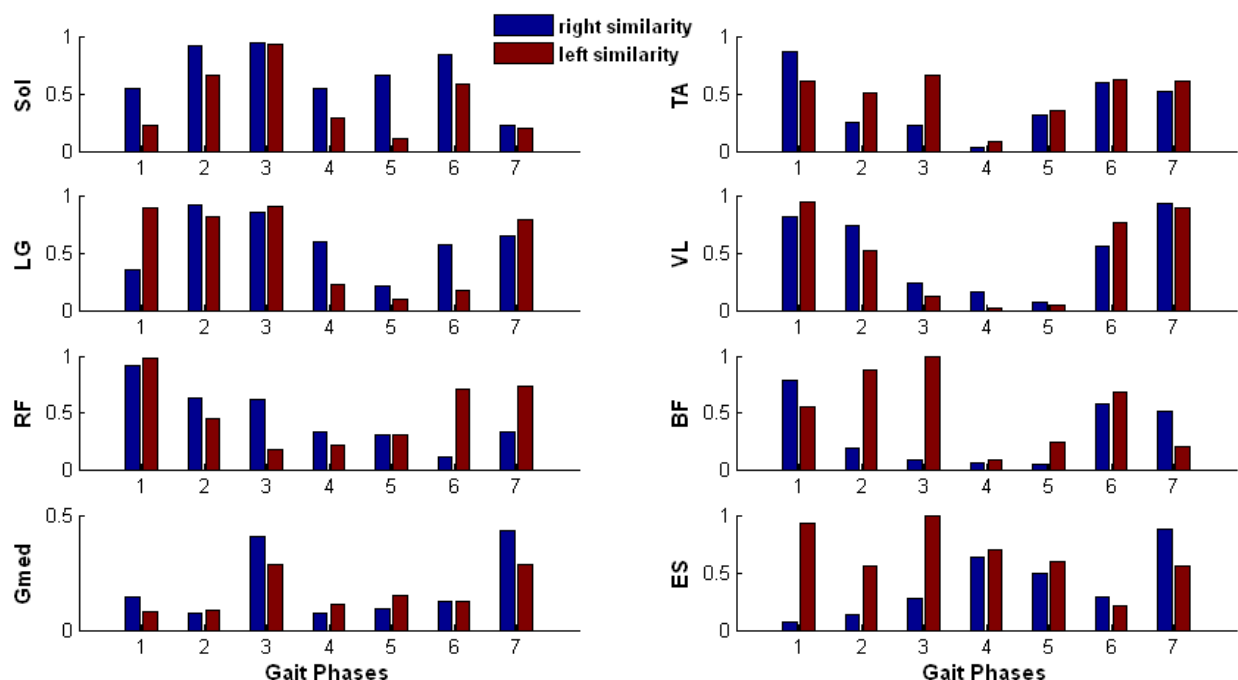


Figure AXII-5: Grade of similarity of right and left EMG in CP-4.

Summary:

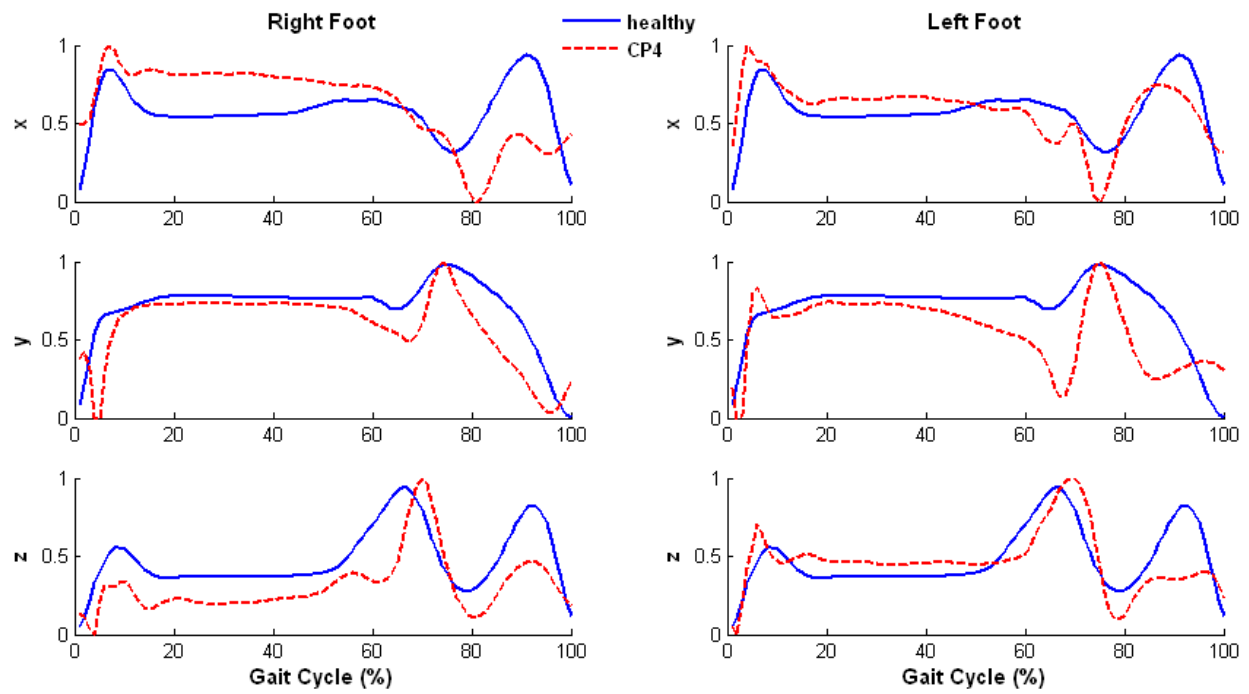
Table AXII-1: Summary of EMG activity in CP-4

	Right	Left
Soleus	Spasticity appears in the stance phase and terminal swing phase. Significant small similarity appears in loading response and terminal swing phase.	Same as right Sol. Significant small similarity appears in initial and terminal swing phases.
Tibialis Anterior (TA)	Muscle weakness appears in the initial contact, following with spasticity for the rest of the cycle. Significant small similarity appears in pre-swing phase.	Same as right TA.
Gastrocnemius Lateralis (LG)	Spasticity appears in the late stance phase. Significant small similarity in initial swing phase.	Same as right LG.
Vastus	Slight spasticity appears in the terminal stance and pre-swing phases. Significant	Similar to right VL, but with much higher and elongated

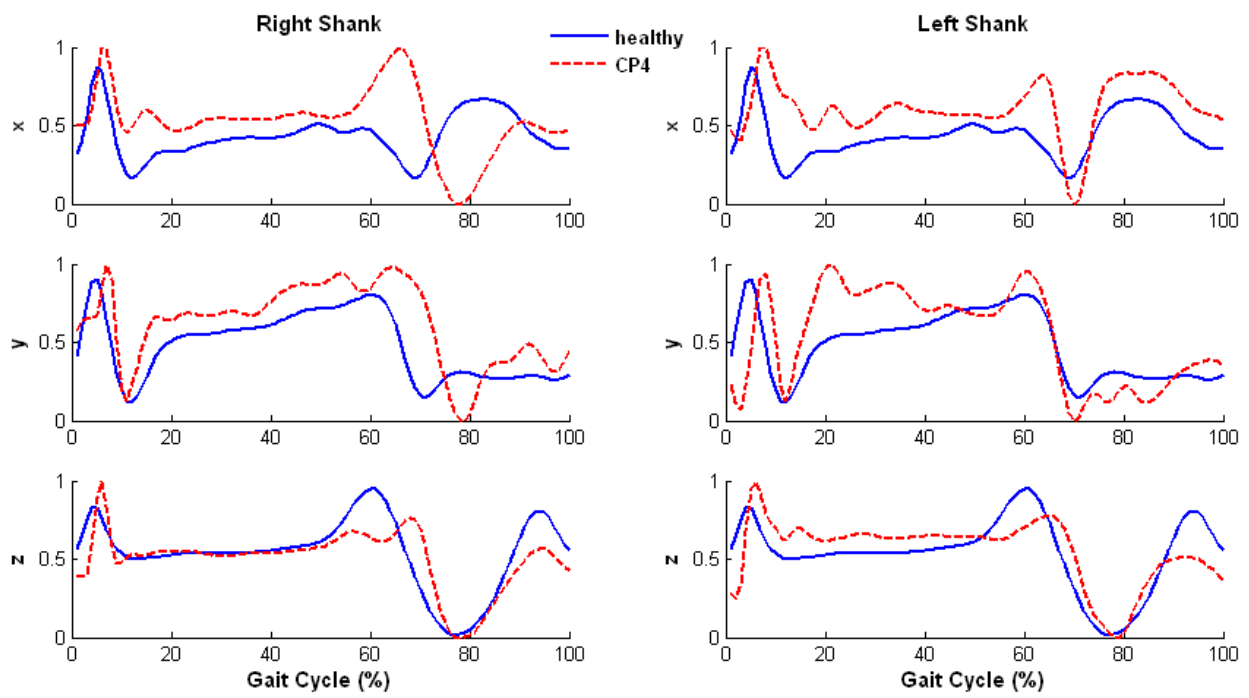
Lateralis (VL)	small similarity appears in pre-swing and initial swing phases.	muscle activities in stance phase. Significant small similarity appears in phase 3, 4, and 5.
Rectus Femoris (RF)	Spasticity appears in the initial contact and swing phase. Significant small similarity appears mid-swing phase.	Spasticity appears all the way of the gait cycle. Significant small similarity appears in pre-swing phase.
Biceps Femoris (BF)	Spasticity appears in the stance phase, following with muscle weakness in swing. Significant small similarity appears in pre- and initial swing phases.	Muscle weakness appears in the initial contact, and spasticity appears in about 55% of the gait cycle, muscle weakness appears in the late swing phase.
Gluteus Medius (Gmed)	Muscle weakness appears in the early stance phase following with spasticity for the most of the rest gait cycle. Significant small similarity appears almost entire gait cycle.	Same as right Gmed.
Elector Spinae (ES)	Muscle weakness appears in initial contact, spasticity appears in the terminal stance and pre-swing phase. Significant small similarity appears in the loading response and mid-stance.	Spasticity appears from the terminal stance to the end of the gait cycle. Significant small similarity appears in mid-swing phase.

- **Acceleration Patterns**

(A)



(B)



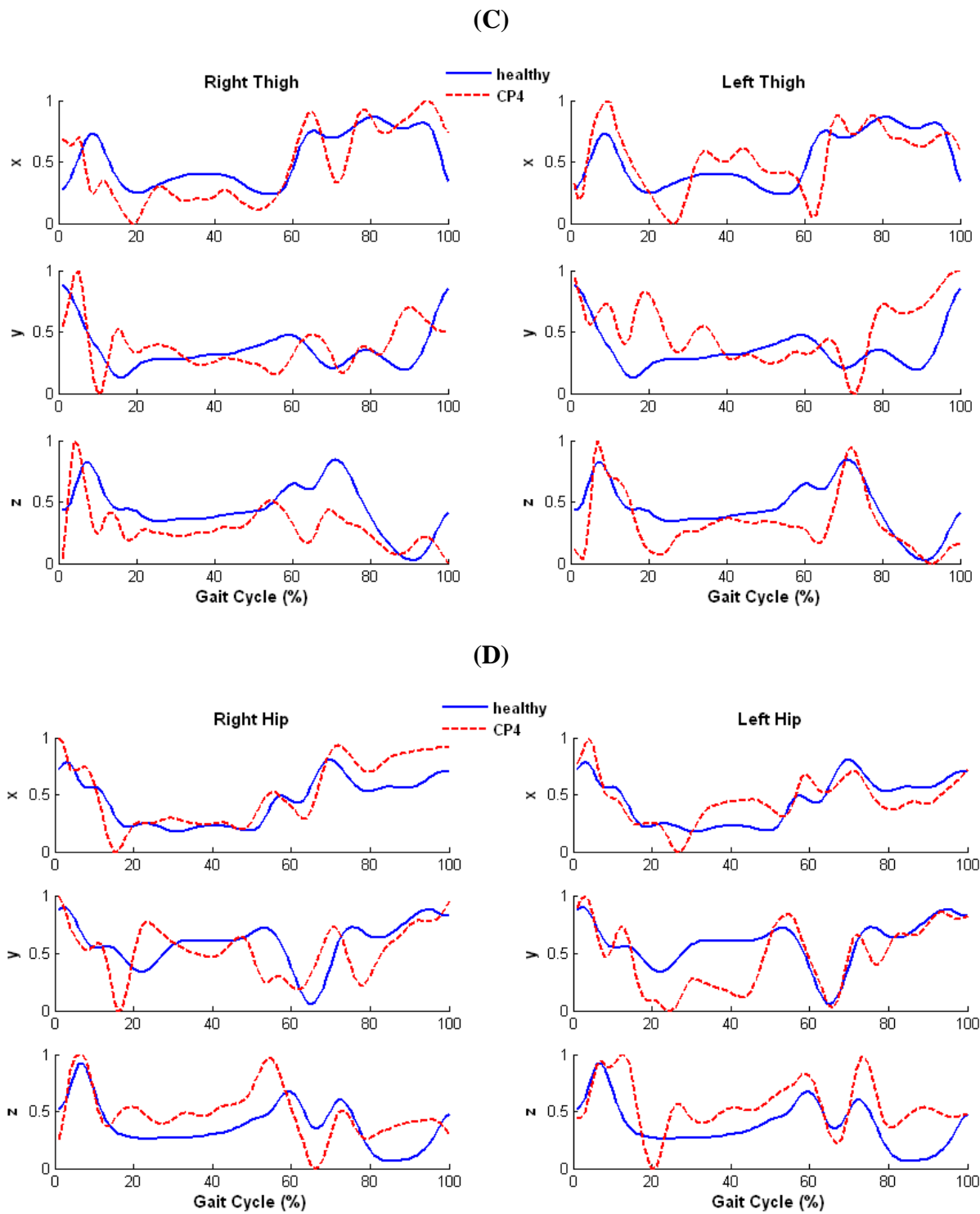


Figure AXII-6: Comparison of acceleration pattern in a gait cycle between healthy subjects and CP-4.

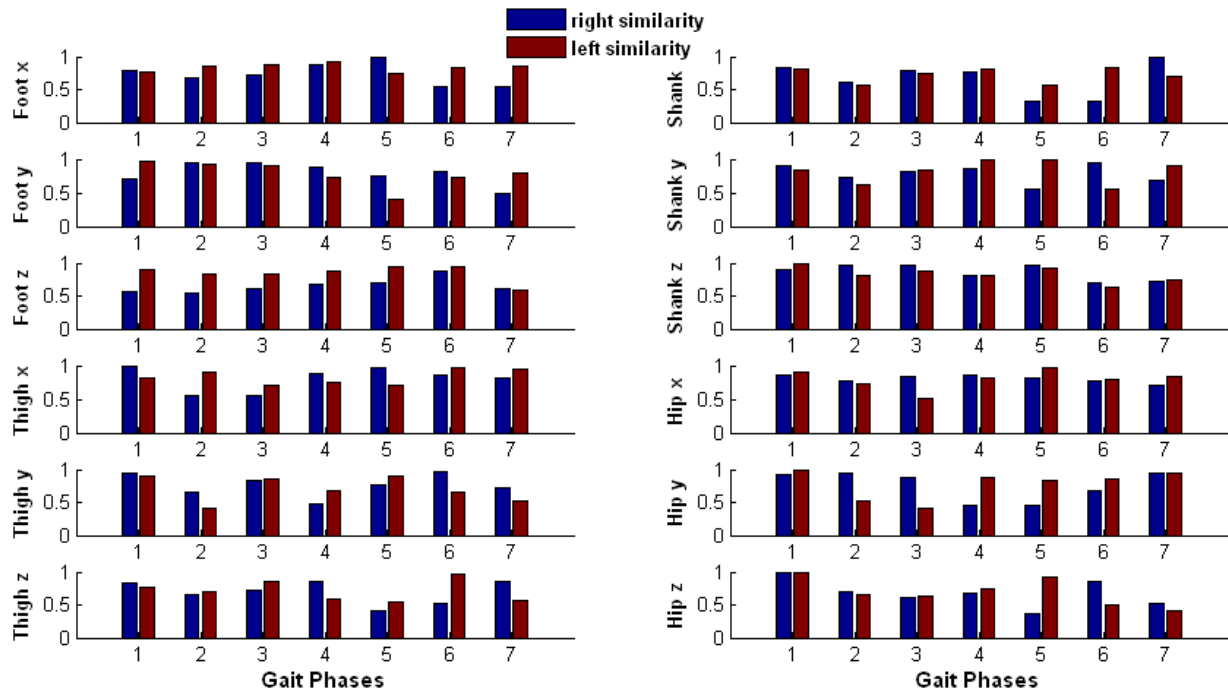


Figure AXII-7: Grade of similarity of right and left acceleration in CP-4.

Summary:

Table AXII-2: Characterization of acceleration in CP-4

	Right	Left
Foot x	Sharp rise in the initial contact, following with high acceleration in stance phase, and then much sharp deceleration on toe-off, following with lower acceleration in swing phase. Small similarity appears in the mid-swing phase.	Sharp rise in the initial contact, following with slightly higher acceleration in stance phase, and sharp deceleration on toe-off, following with slightly lower acceleration in swing.
Foot y	Lower acceleration in stance and toe-off, sharp rise in early swing and sharp deceleration in the late swing.	Sharp rise in the initial contact, following with gradually reduced magnitude in stance, and a sharp rise in swing.
Foot z	Lower magnitude in stance and sharp rise	A sharp rise in initial contact,

	in early swing and lower magnitude in late swing.	following with slight higher magnitude in the stance, a sharp rise in early swing and lower magnitude in late swing.
Shank x	Sharp rise in initial contact, following with higher magnitude in stance, a sharp rise in pre-swing. Significant small similarity appears in initial and mid-swing.	Same as right shank x, in addition with higher acceleration in swing phase.
Shank y	Sharp and delayed rise in initial contact, following with unstable high acceleration during the stance phase.	Same as right shank y.
Shank z	Sharp rise in initial contact, lower acceleration on toe-off and terminal swing.	Same as right shank z.
Thigh x	Sharp rise in initial contact, slightly lower and unstable acceleration throughout the stance phase, unstable acceleration in swing phase.	Sharp rise in initial contact, unstable acceleration in stance phase and swing phase.
Thigh y	Sharp rise in initial contact, following with lower acceleration for the rest of the cycle.	Unstable with increased acceleration in stance phase, higher acceleration in swing phase.
Thigh z	Sharp rise in initial contact, lower acceleration in stance and swing phase.	Sharp rise in initial contact, lower acceleration in stance, a sharp rise in swing.
Hip x	Sharp rise in initial contact, dramatically decreased in early stance, an increased acceleration in swing.	Sharp rise in initial contact, an increased acceleration in terminal stance and pre-swing phase, lower magnitude in swing phase.
Hip y	Much unstable pattern appears in the gait cycle.	Same as right hip y. Significant small similarity appears in terminal stance.
Hip z	Sharp rise in initial contact, following with higher acceleration in stance, and a sharp rise in pre-swing phase, and an increased acceleration in late swing phase. Significant small similarity appears in	Sharp and delayed rise in initial contact, sharp reduction in early single support, higher acceleration during rest of the stance phase, and a sharp rise in mid-swing. Significant

	initial swing phase.	small similarity appears in terminal swing.
--	----------------------	---

Note the CP-4 was diagnosed with diplegic cerebral palsy, the patterns of the acceleration shows some levels of unsymmetrical with right leg sever affected.

Appendix XIII: Results of Stroke Subject 1 with her 1st Visit (Stroke1_1)

- **Description**

Subject is 37 year old female, was diagnosed as right hemiparetic stroke after her second child was born. From the observation of her first visit to our lab, she was walking with right side paralysis, including walking with left leg as base of support, wearing right ankle brace to protect the foot-drop, dragging right foot gait, having difficulty with right hand activities such as lifting, grasping, extending outward and lifting up the right arm. She also had speed problem. She was tested with bare-foot walking on the instrumented treadmill with harness support at very slow speed (0.1 m/s), continuing with three minutes trial.

- **Temporal Stride Variability**

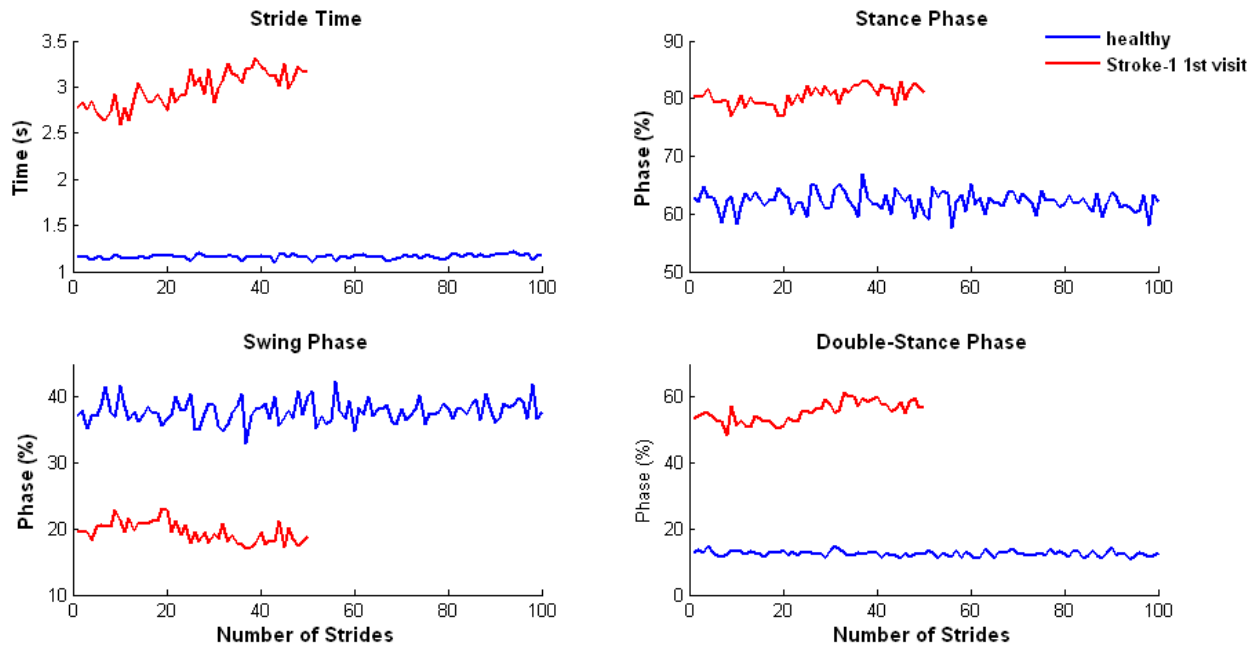


Figure AXIII-1: Stride variability of a healthy female subject and a female hemiparetic stroke patient case 1 with her first visit.

Summary: There were only 50 strides extracted from the Stroke-1 subject at her first visit due to very slow speed of walking. She has slightly increased fluctuation, this might be the results of partial body weight support by harness assistance. The stride time increased during the walking which may indicate some fatigue. The double-stance phase was almost three-time greater than healthy subject. The stance phase and swing phase were almost twice greater than the healthy subject.

- **Ground Reaction Forces**

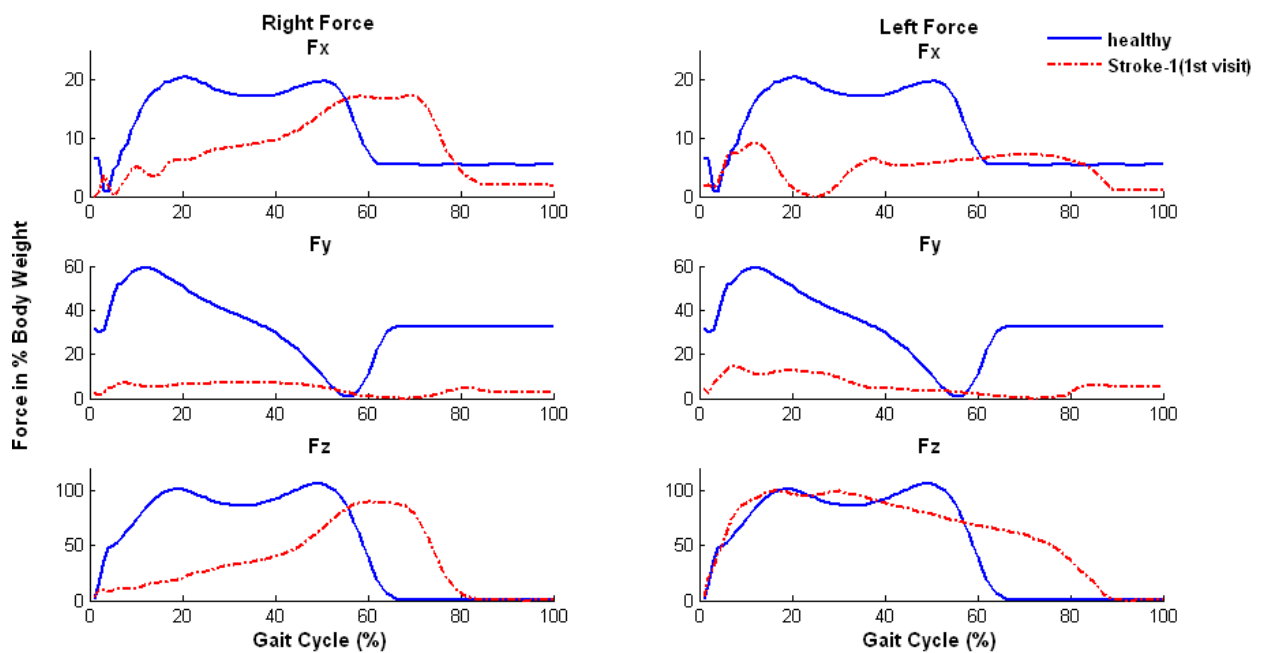


Figure AXIII-2: Right and left GRF in 3-D in stroke patient 1 with her 1st visit.

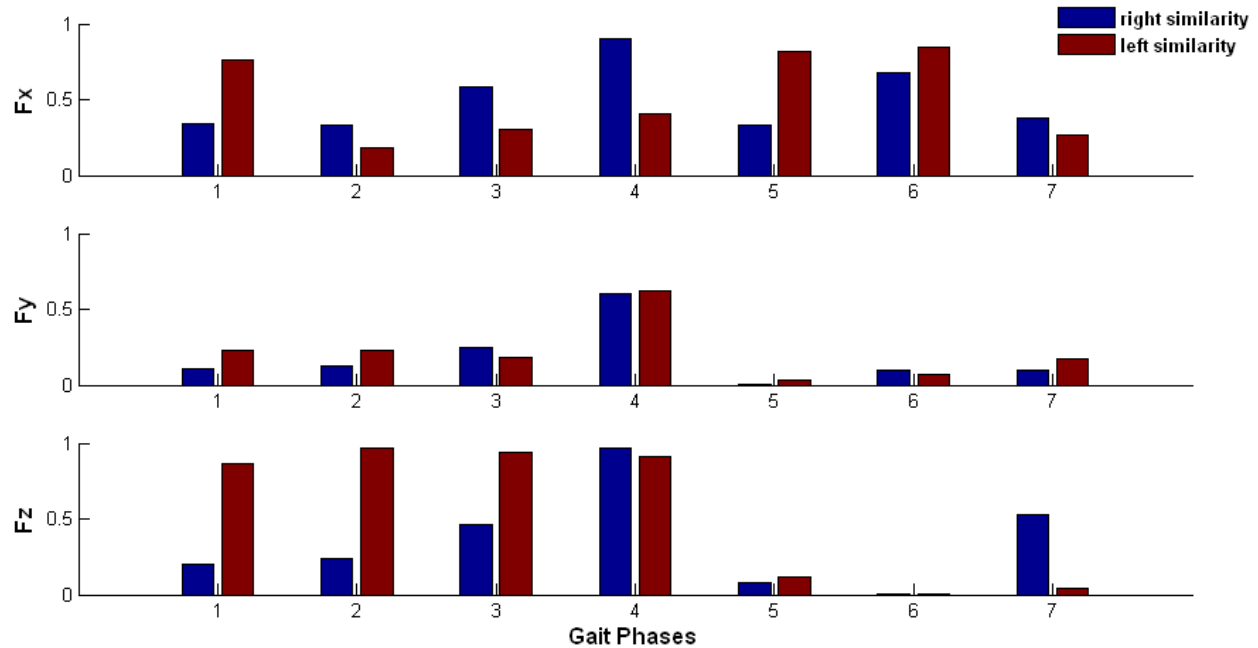


Figure AXIII-3: Grade of similarity between right and left GRF in stroke-1 with her 1st visit.

- EMG Muscle Activity Patterns**

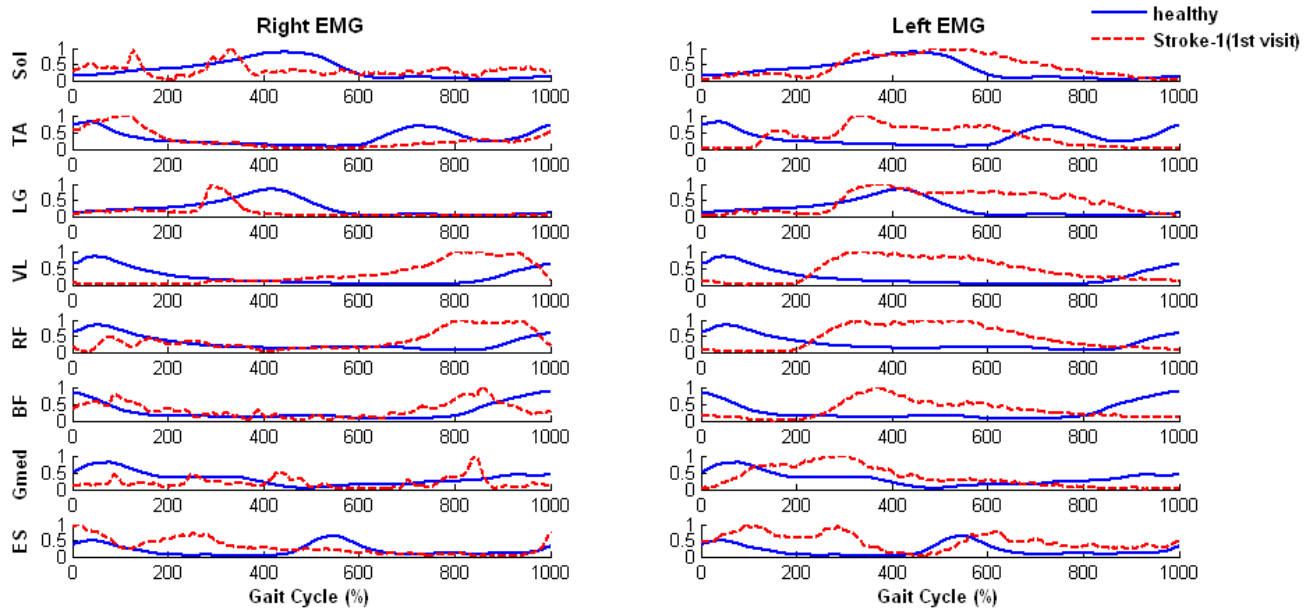


Figure AXIII-4: Comparison of EMG activity in a gait cycle between healthy subjects and stroke-1 with her 1st visit.

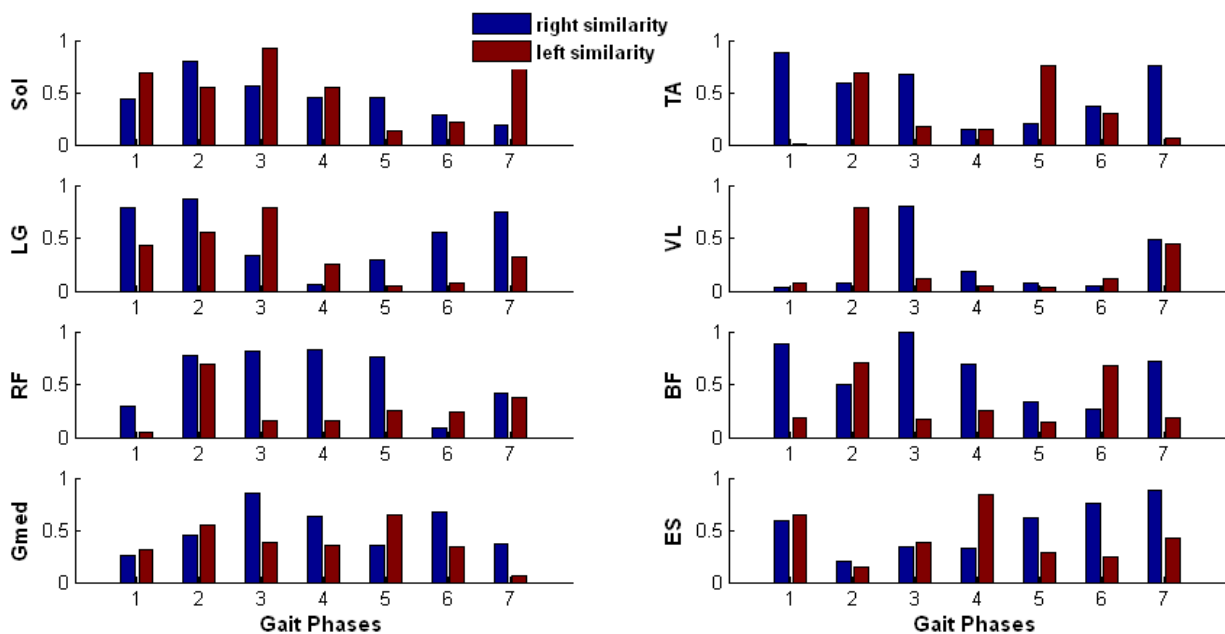
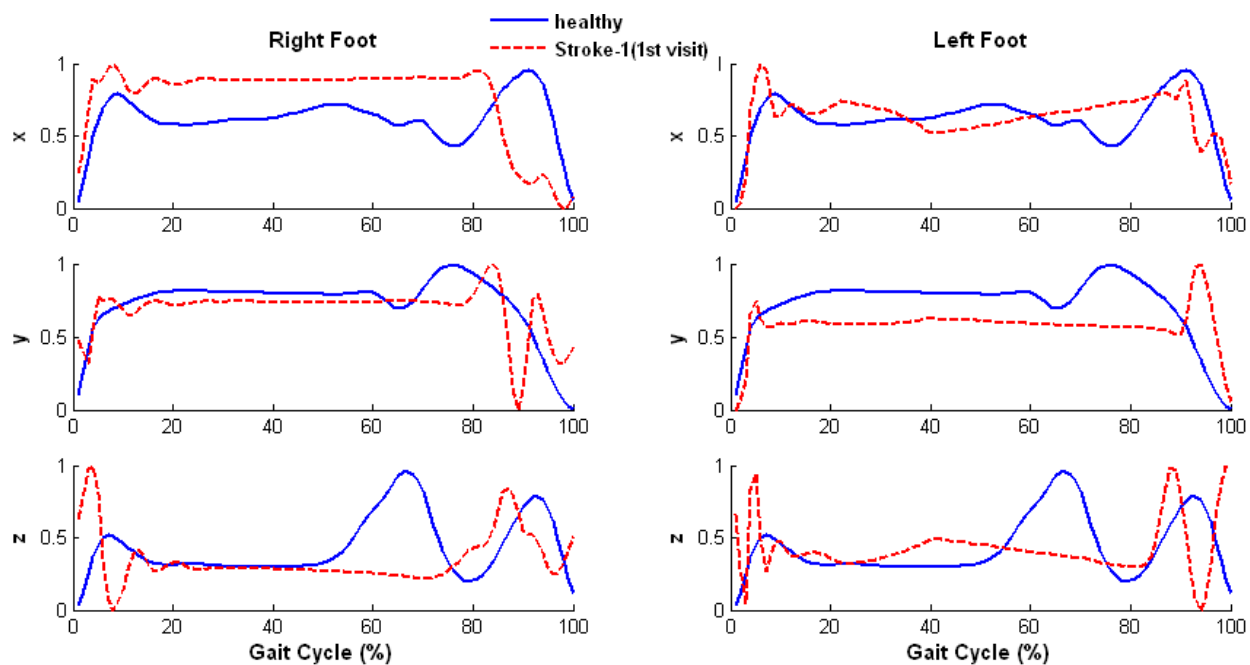


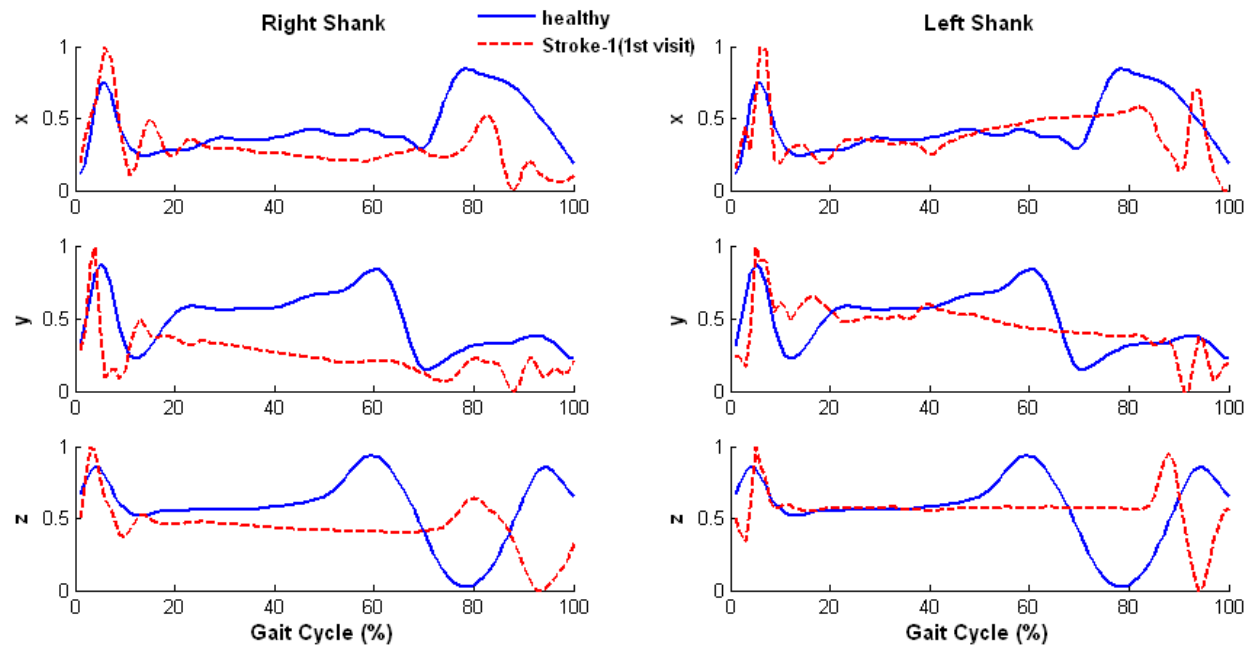
Figure AXIII-5: Grade of similarity of right and left EMG in stroke-1 with her 1st visit.

- **Acceleration Patterns**

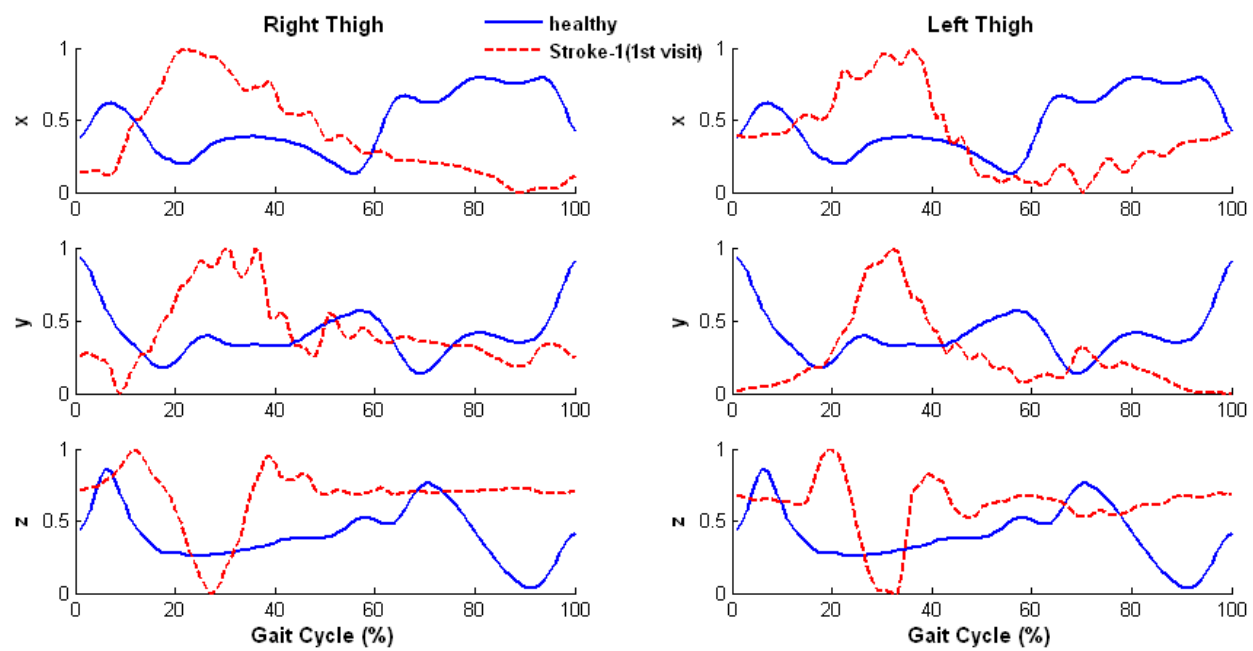
(A)



(B)



(C)



(D)

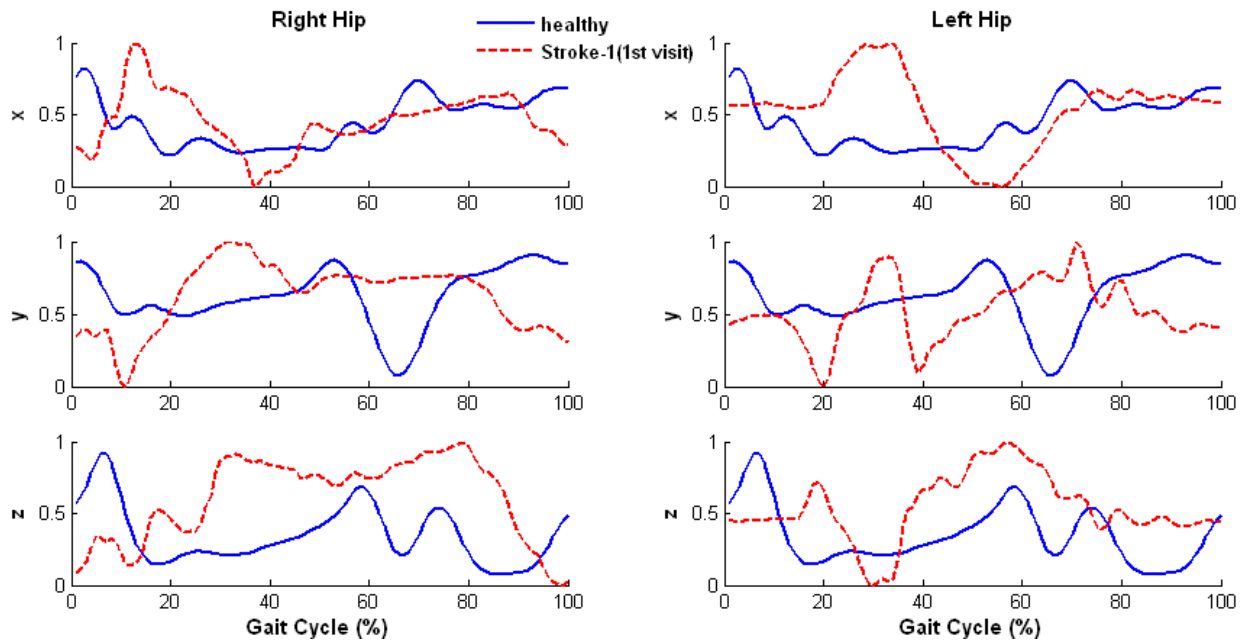


Figure AXIII-6: Comparison of acceleration pattern in a gait cycle between healthy subjects and stroke-1 subject with her 1st visit.

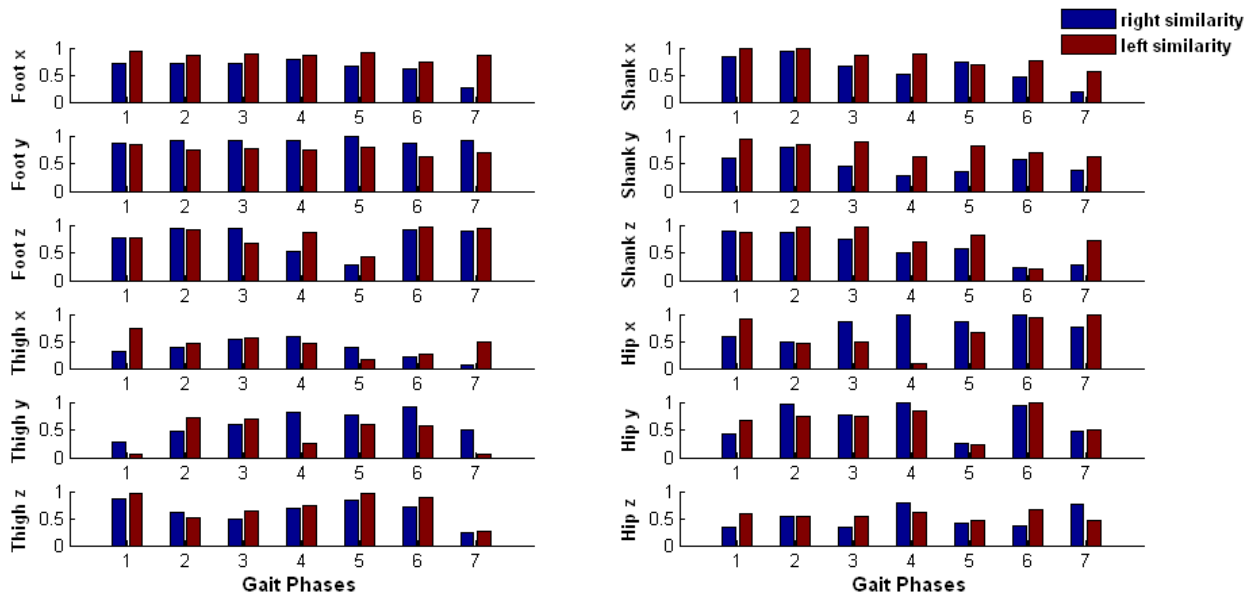


Figure AXIII-7: Grade of similarity of right and left acceleration in stroke-1 subject with her 1st visit.

Appendix XIV: Results of Stroke Subject 1 with her 2nd Visit (Stroke1_2)

- **Description**

This is the same subject in appendix XI, but with her second visit after two months. By talking to the subject, she had been through the hydro-physical therapy, three times a week, one hour each time. She also did walking exercise overground without brace at home, 30 minutes per day. From the observation of her overground walking, her gait has been improved dramatically. Subject was walking bare-foot on the treadmill for continuing three-minute at speed of 0.5 m/s, which was much faster than the first visit.

- **Temporal Stride Variability**

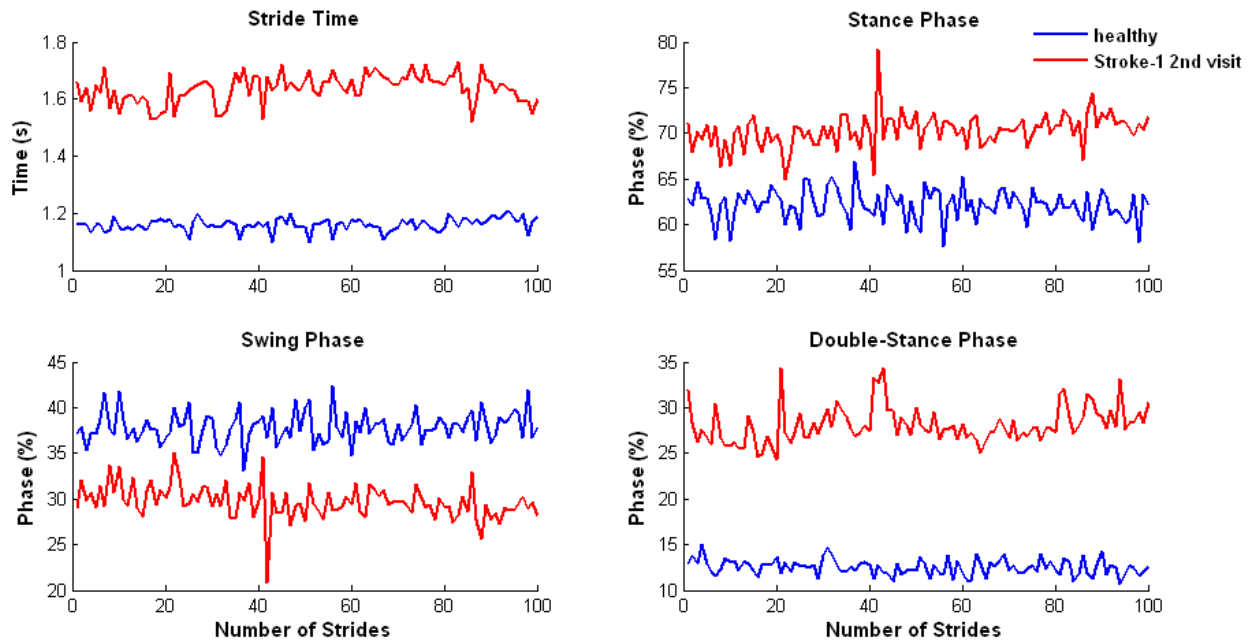


Figure AXIV-1: Stride variability of a healthy female subject with a female stroke subject at her second visit.

Summary: Stroke-1 subject at her second visit after two month of hydrotherapy treatment, has showed much better gait dynamic. The walking speed was greatly increase, therefore, there were 100 strides found in her three-minute walking trial. The stride variability was slightly increased

compared with the healthy subject. There was a sharp increased stance phase and a sharp decreased swing phase at time around 42 strides, which the fall risk might occur at that time. The double-stance phase was still greater than healthy subject almost twice of the length.

- **Ground Reaction Forces**

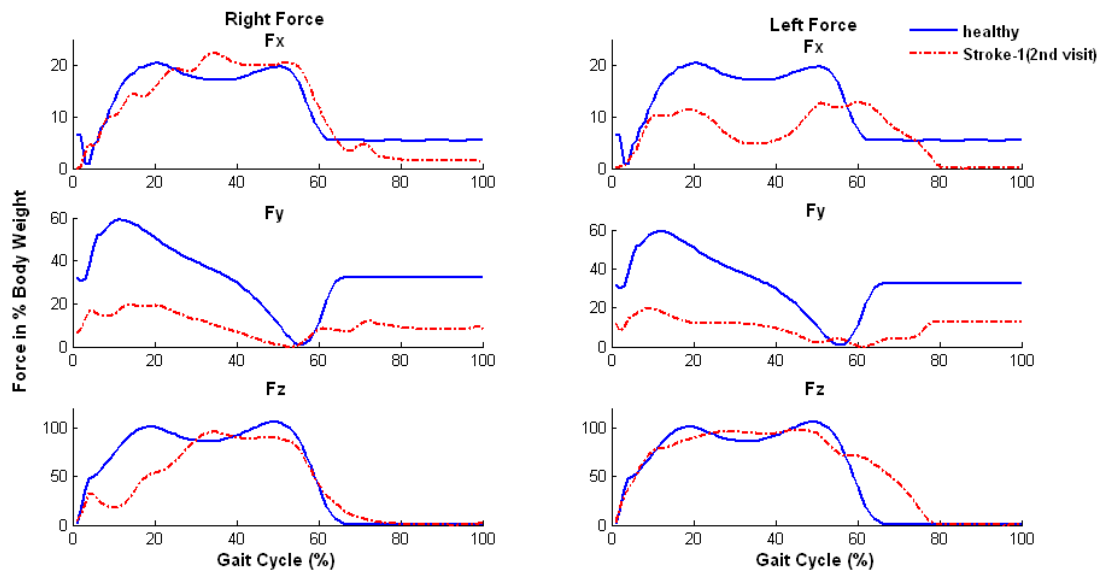


Figure AXIV-2: Right and left GRF in 3-D in stroke-1 subject with her 2nd visit.

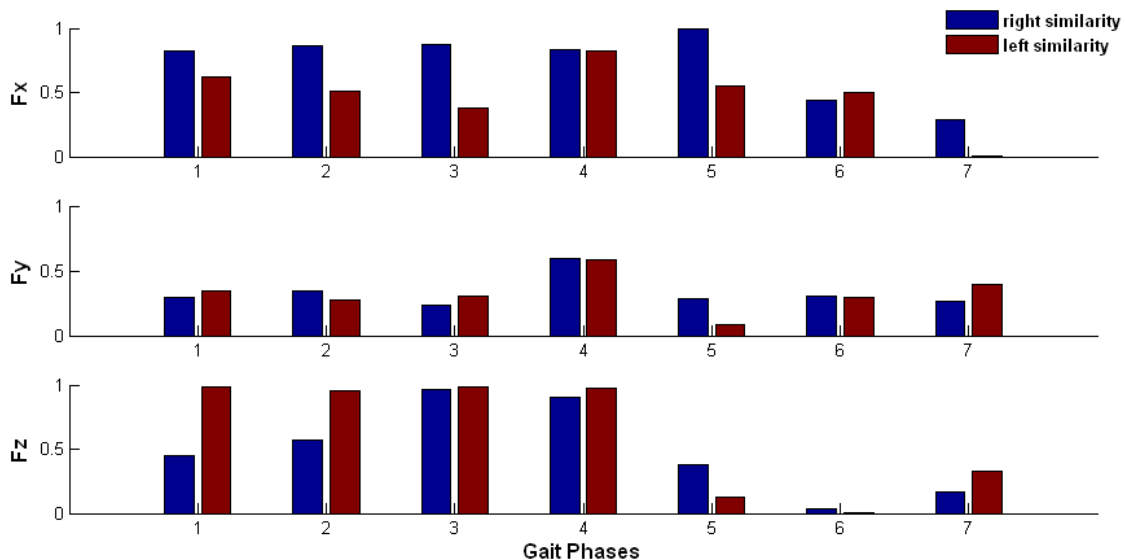


Figure AXIV-3: Grade of similarity between right and left GRF in stroke-1 subject at her 2nd visit.

- **EMG Muscle Activity Patterns**

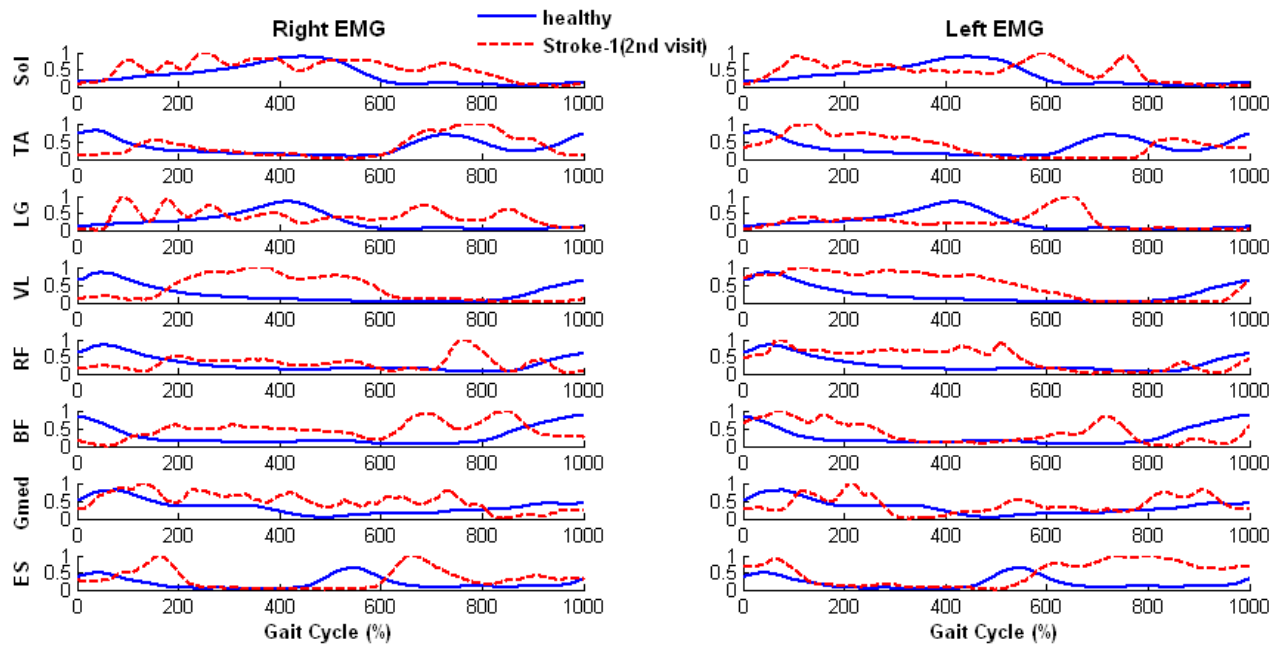


Figure AXIV-4: Comparison of EMG activity in a gait cycle between healthy subjects and stroke-1 subject at her 2nd visit.

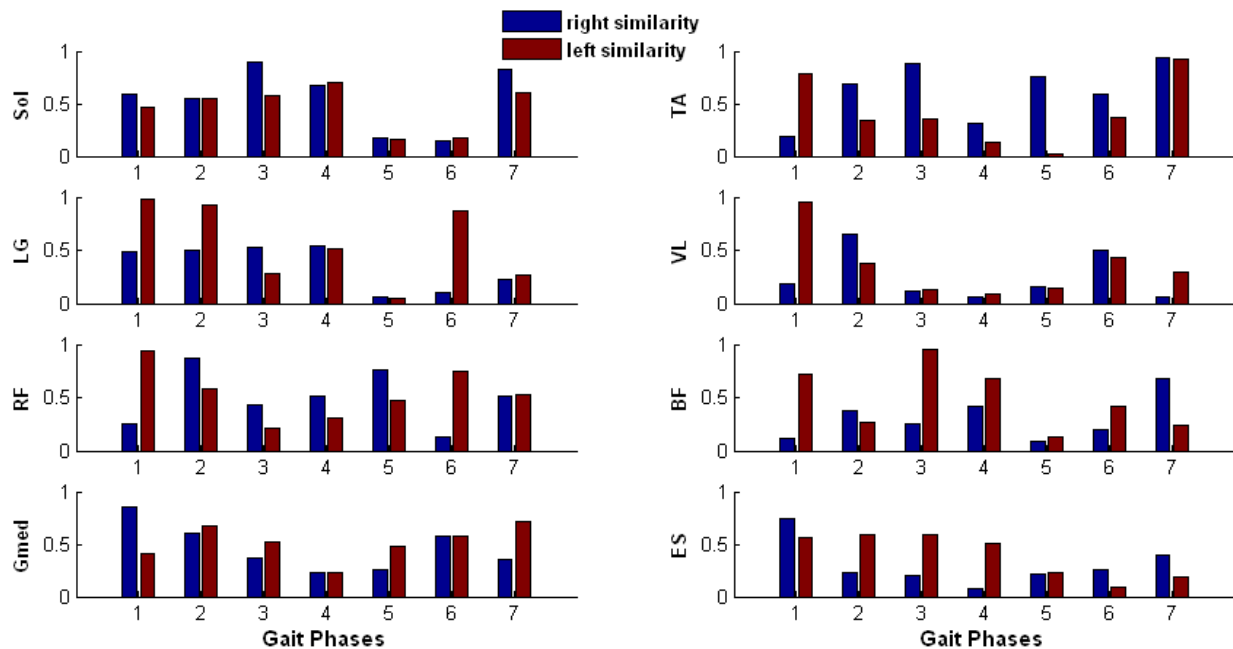
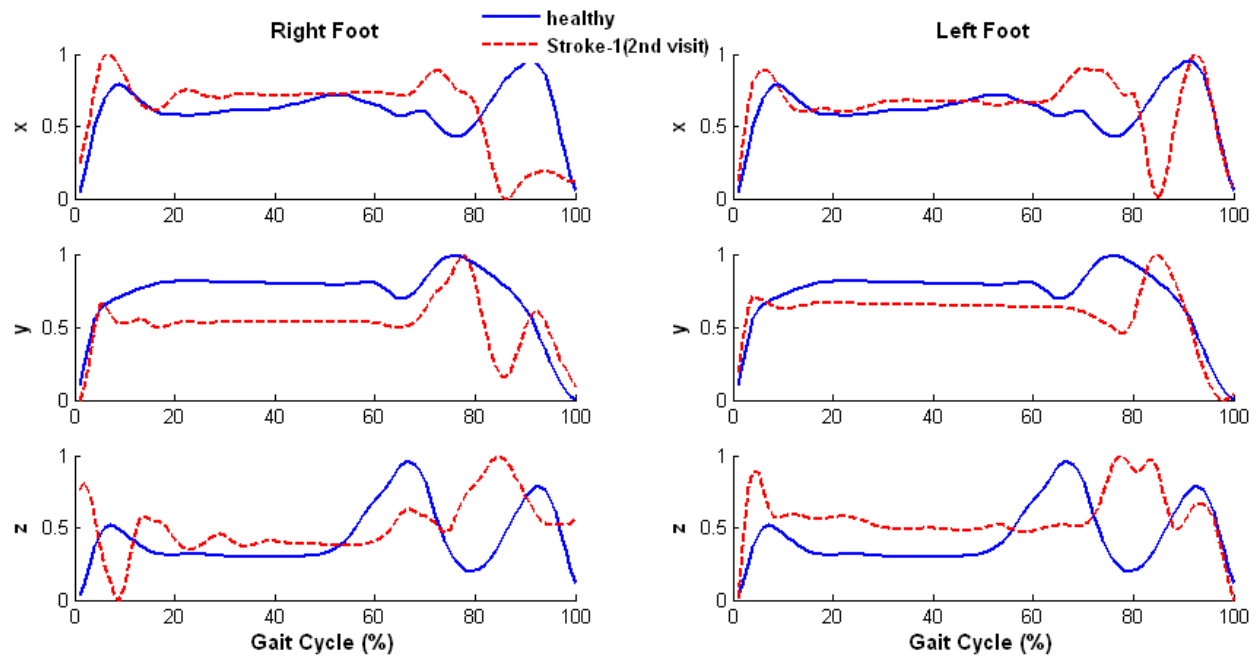


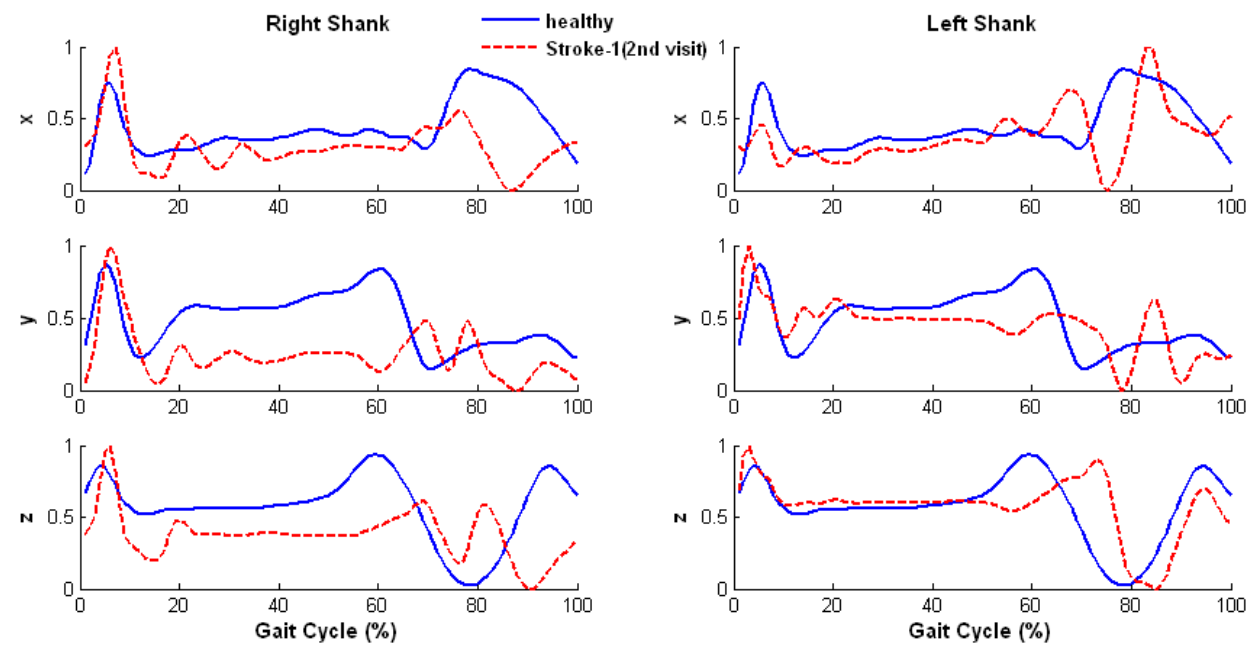
Figure AXIV-5: Grade of similarity of right and left EMG in stroke-1 with her 2nd visit.

- **Acceleration Patterns**

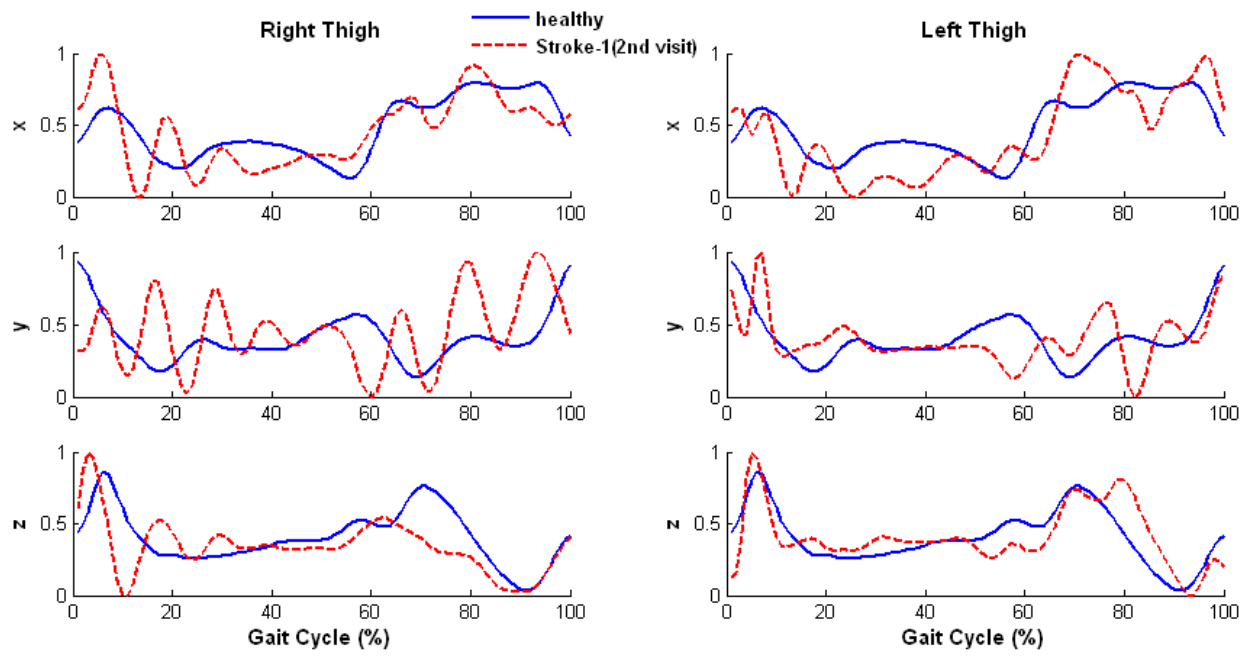
(A)



(B)



(C)



(D)

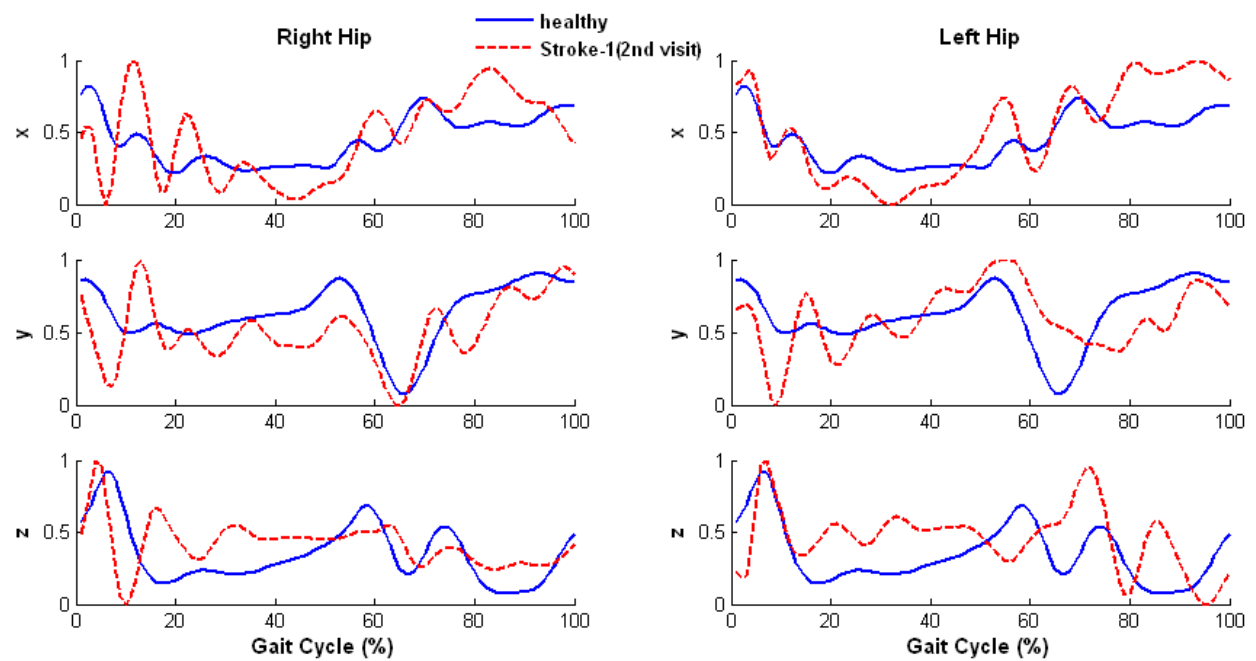


Figure AXIV-6: Comparison of acceleration pattern in a gait cycle between healthy subjects and stroke-1 at her 2nd visit.

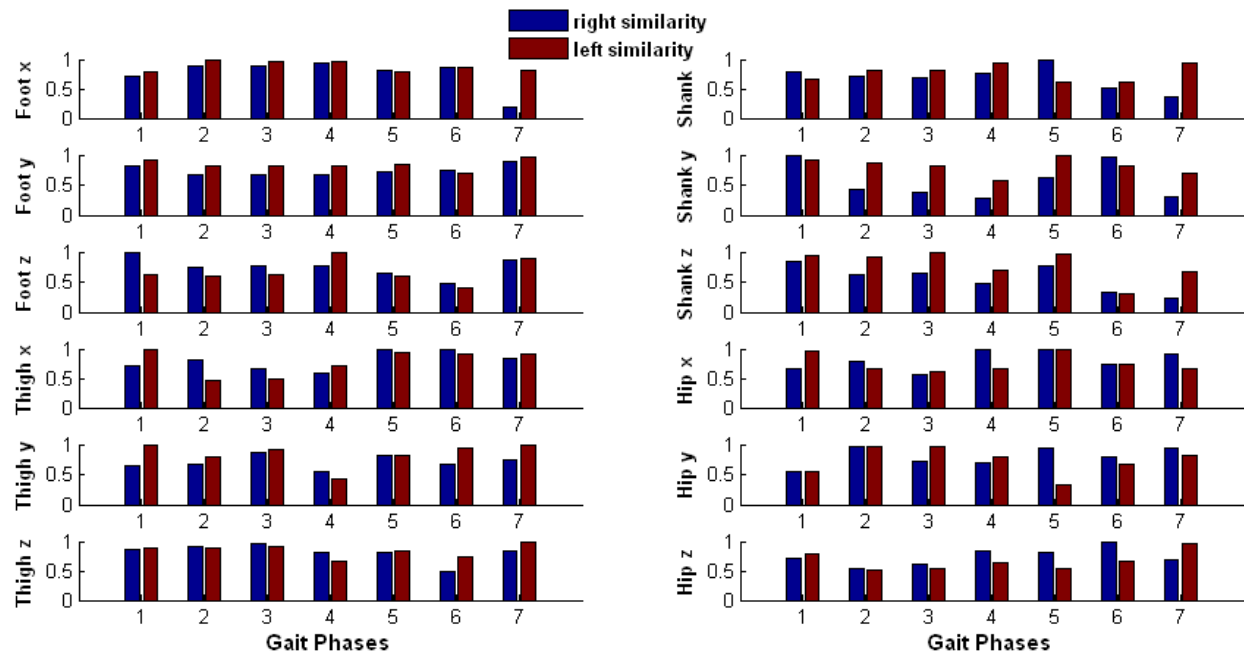


Figure AXIV-7: Grade of similarity of right and left acceleration in stroke-1 at her 2nd visit.

Appendix XV: Results of Stroke Patient 2 (Stroke2)

- **Description**

Subject is a 53 year old female, was diagnosed with left-side hemiplegic stroke on November 18, 2009. She was on physical therapy (walking over-ground and on the treadmill) at the time point of the experiment, three times per week and one hour per time. By observation, she had fairly mild symptom with left side hemiplegia. She did walk bare-footed on the treadmill without any assistant devices at speed of 0.6 m/s. The ground reaction forces, EMG activities and segment accelerations were recorded continually for three-minutes.

- **Temporal Stride Variability**

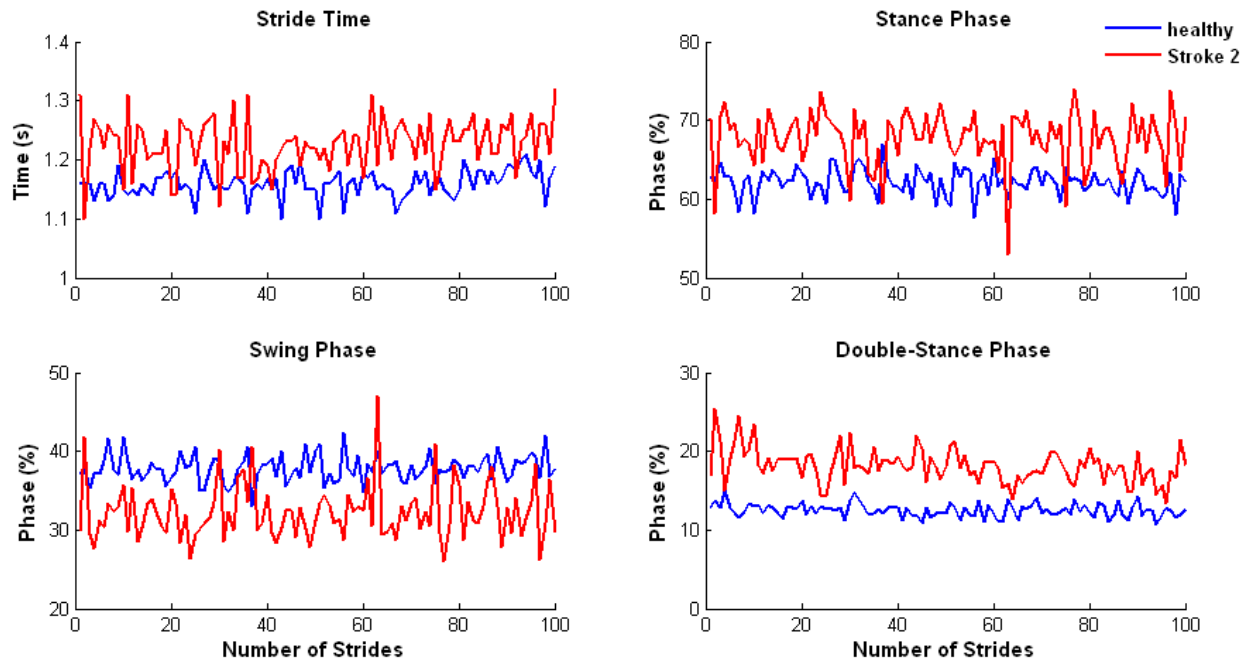


Figure AXV-1: Stride variability of a healthy female and a female stroke subject case 2 (Stroke-2).

Summary: The Stroke-2 subject showed quite consistent dynamic gait through the entire gait cycle, with slightly increased fluctuation of stride variables. This indicates the stroke-2 had mild

symptoms of the stroke compared with the stroke-1. There were slightly increased stance phase and double-stance phase, and slightly decreased swing phase in stroke-2.

- **Ground Reaction Forces**

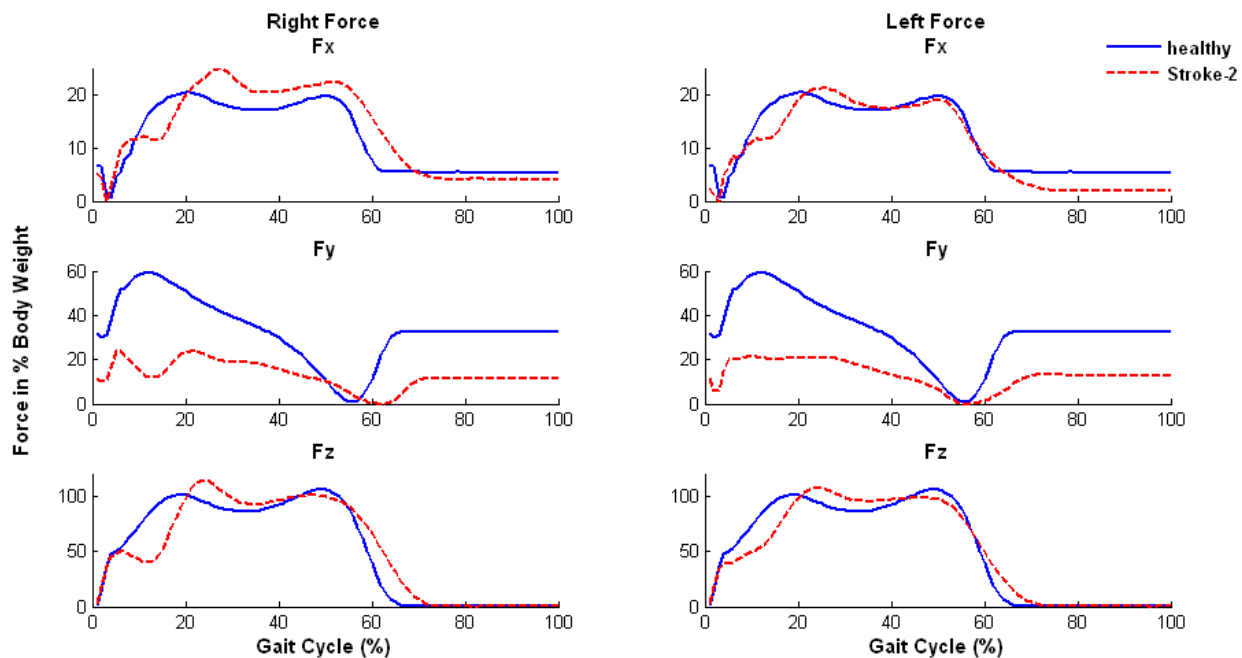


Figure AXV-2: Right and left GRF in 3-D in Stroke-2.

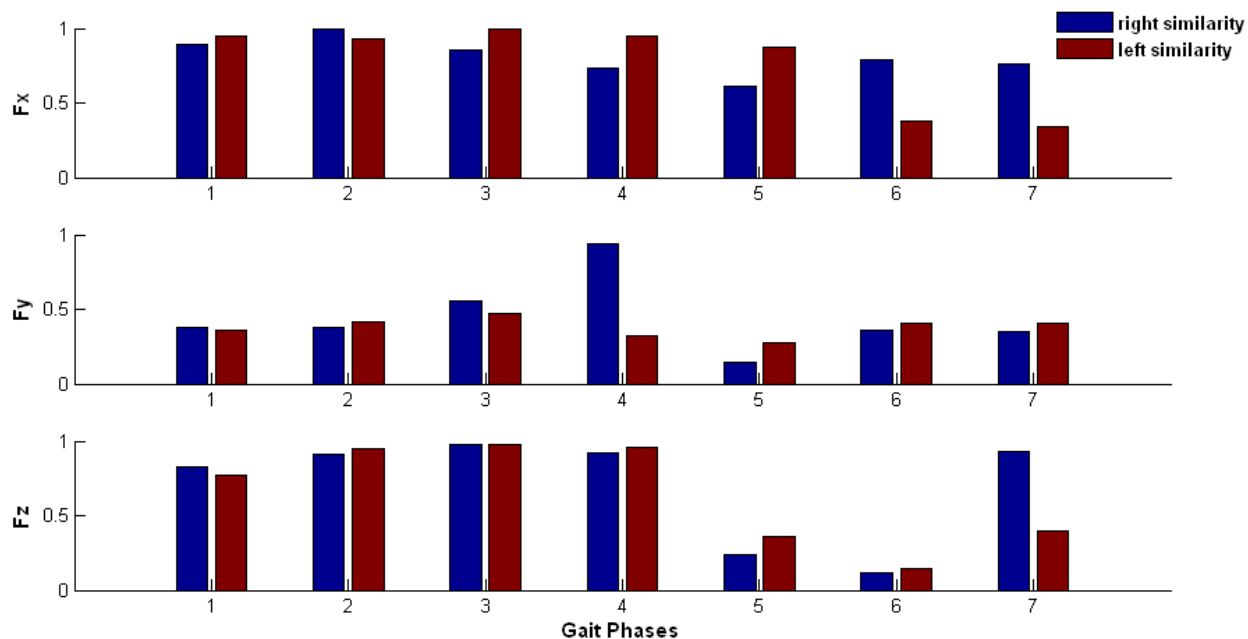


Figure AXV-3: Grade of similarity between right and left GRF in Stroke-2.

Summary:

In vertical direction, there was a sharp delayed first peak GRF in stroke-2, right foot was apparent than the left. Her stance phase was slightly longer than the healthy subject, around 70 % of the gait cycle. In anterior-posterior direction, there was lower GRF on both sides. In mediolateral direction, there was much greater GRF on right side than the left side.

- **EMG Muscle Activity Patterns**

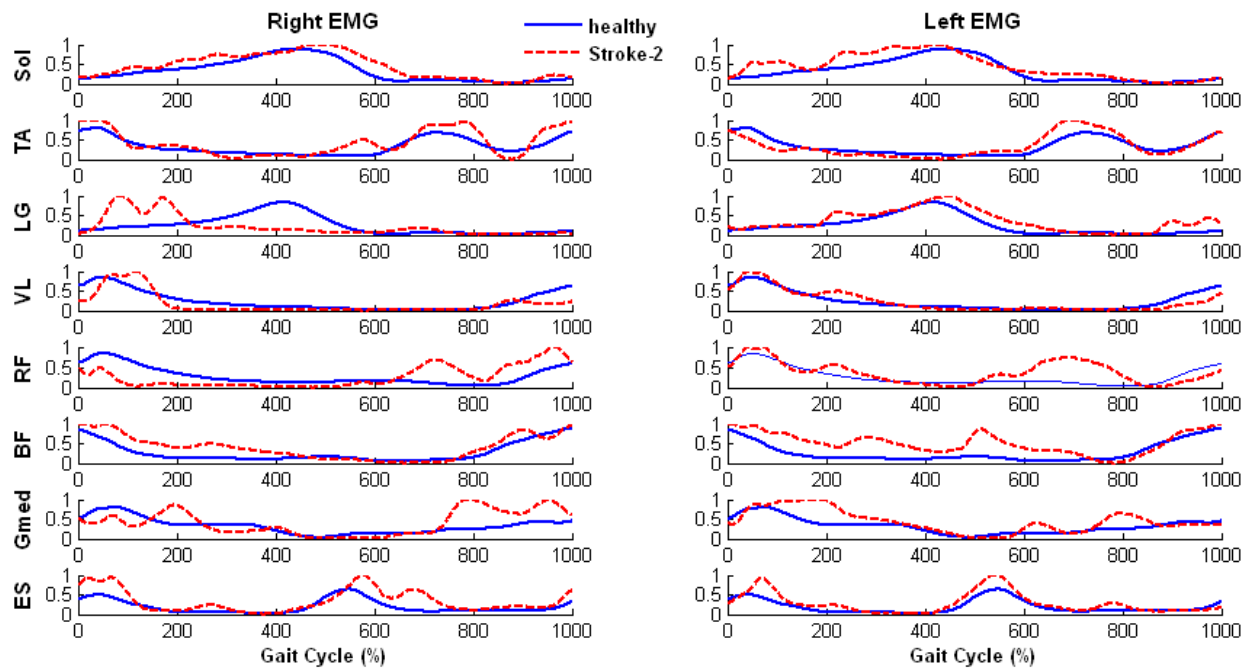


Figure AXV-4: Comparison of EMG activity in a gait cycle between healthy subjects and Stroke-2.

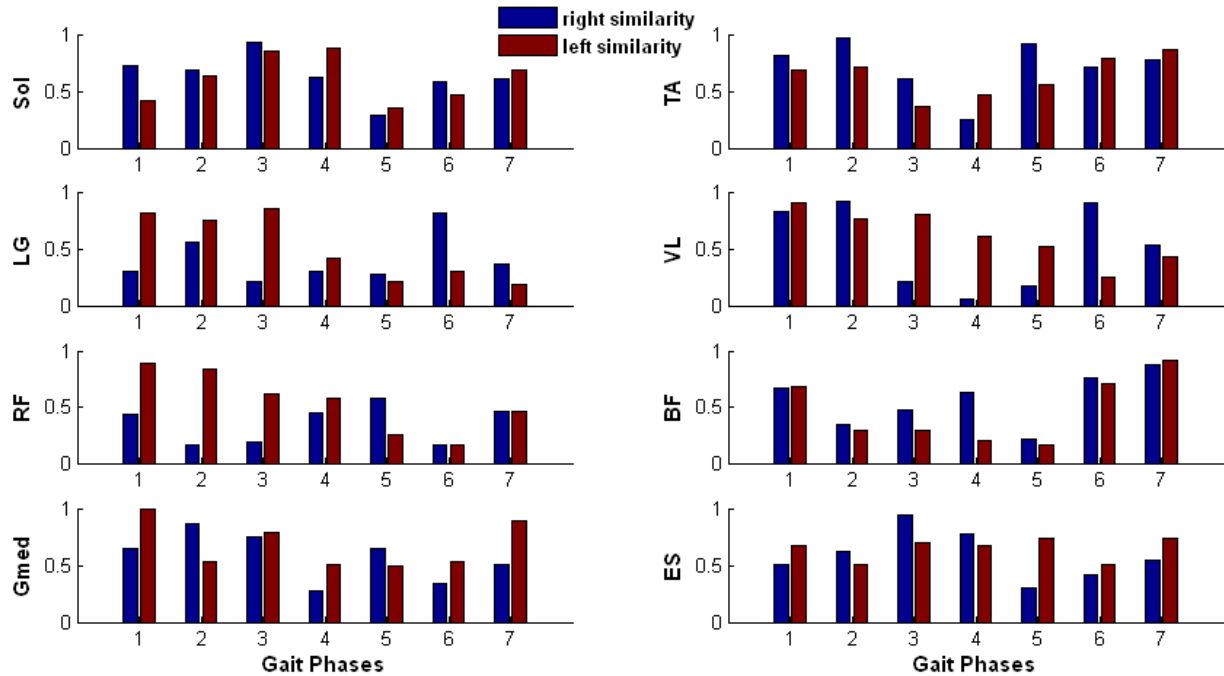


Figure AXV-5: Grade of similarity of right and left EMG in Stroke-2.

Summary:

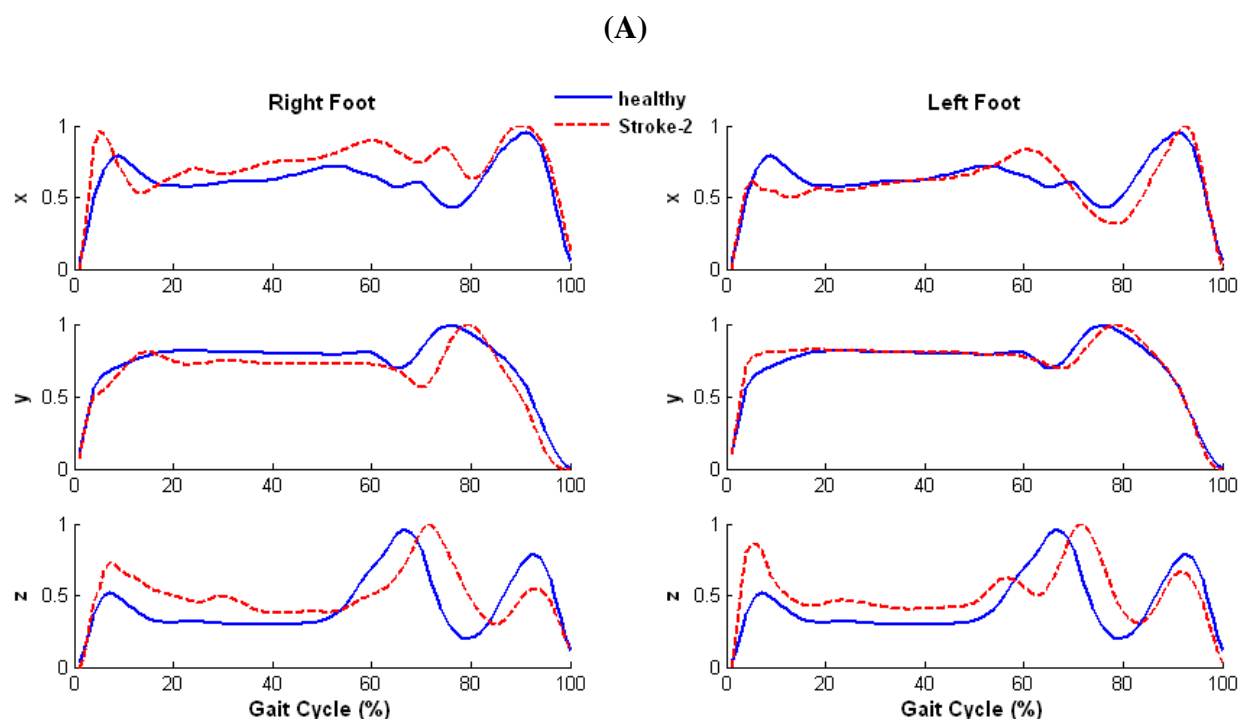
Table AXV-1: Summary of EMG activity in Stroke-2

	Right	Left
Soleus	Slightly delayed activity results in the smaller grade of similarity in initial swing.	Higher and unstable muscle activity in the stance phase, smaller similarity appears in the initial swing.
Tibialis Anterior (TA)	Higher activity appears in the initial contact and swing phase, smaller similarity appears in the pre-swing phase.	Muscle weakness appears in the initial contact, but higher activity occurs in the early swing phase.
Gastrocnemius Lateralis (LG)	Spasticity appears in the early stance phase, but with muscle weakness in the late stance phase. Significant small similarity occurs in the initial contact, terminal stance, pre- and initial swing, and terminal swing phases.	Latten muscle activity in the stance phase. Smaller similarity appears in the initial and terminal swing phases.
Vastus Lateralis (VL)	Delayed but longer muscle activity in the initial contact following with the lower muscle activity along the rest of the cycle. Significant small similarity appears in the pre-swing phase.	Similar to right VL, smaller similarity appears in the mid-swing phase.

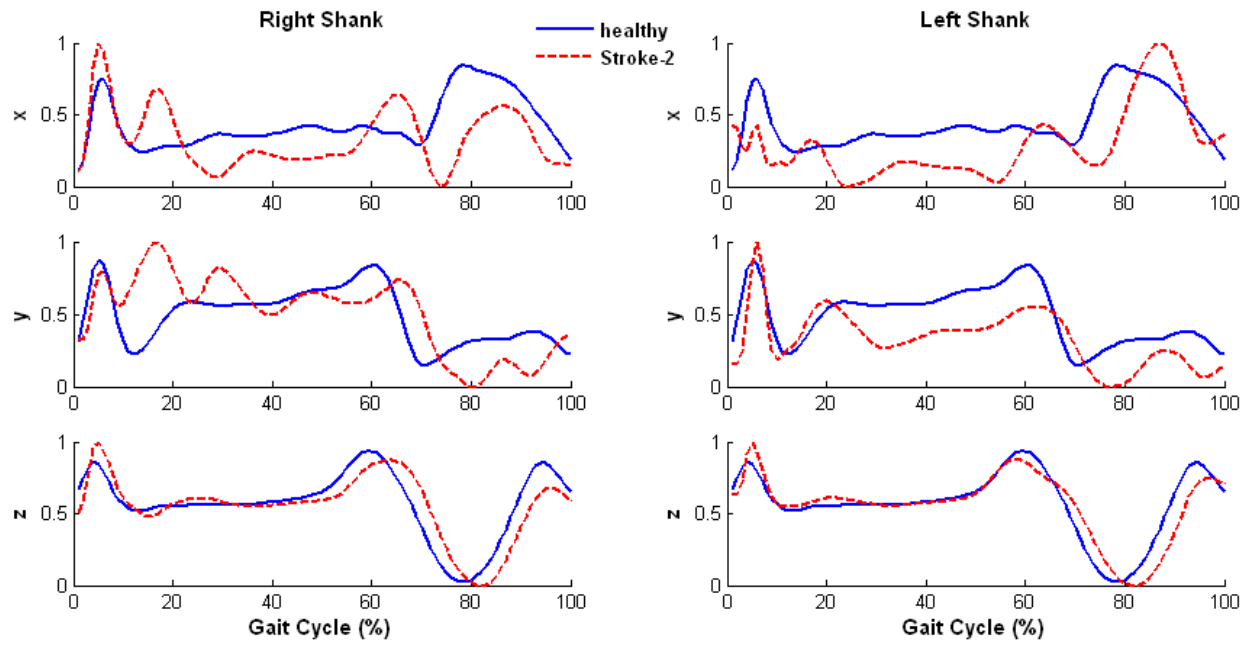
Rectus Femoris (RF)	Muscle weakness occurs in the early stance phase, spasticity appears in the swing phase. Significant small similarity appears in the mid-stance, terminal stance, and mid-swing phases.	Muscle spasticity appears in the initial contact and early swing phase. Significant small similarity appears in the pre- and mid-swing phases.
Biceps Femoris (BF)	Spasticity appears in the early stance phase. Significant small similarity appears in the initial swing phase.	Similar to right BF, significant small similarity appears in the pre- and initial swing phases.
Gluteus Medius (Gmed)	Muscle weakness occurs in the initial contact, following with spasticity in the mid-stance phase and late swing phase. Smaller similarity appears in the pre-swing phase.	Muscle spasticity appears in the mid-stance phase and early swing phase.
Elector Spinae (ES)	Spasticity appears in the initial contact and initial swing phase. Smaller similarity appears in the initial swing phase.	Similar to right ES.

Note: Different muscle activities between right and left show typical hemiplegic symptoms of the stroke.

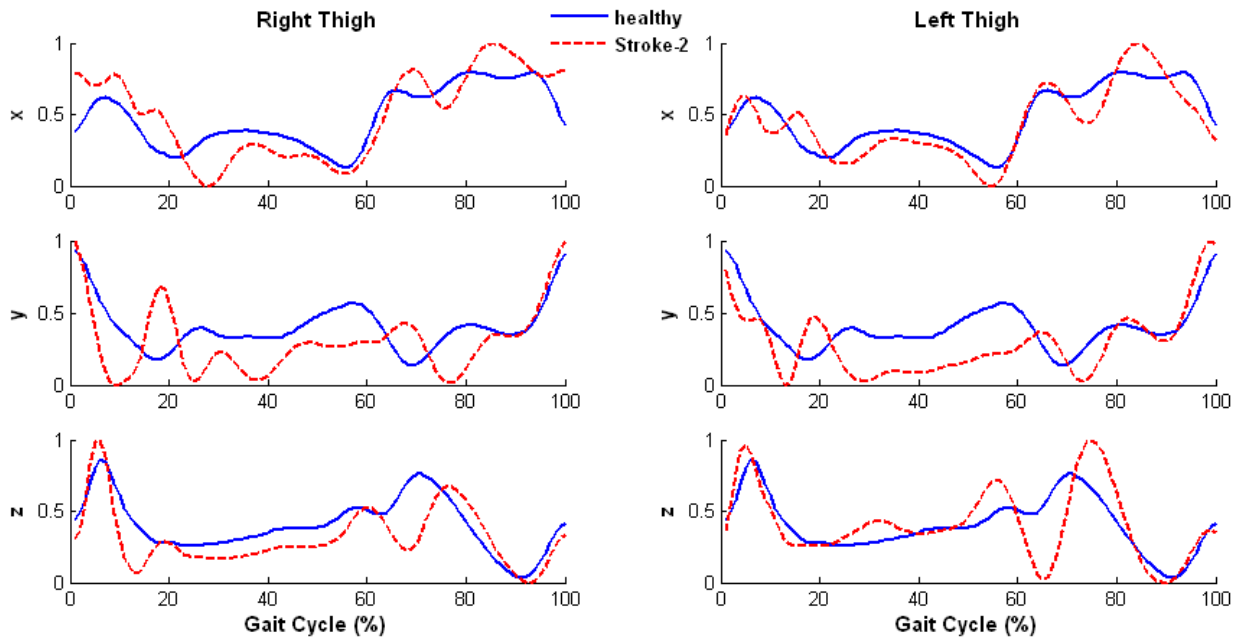
- **Acceleration Patterns**



(B)



(C)



(D)

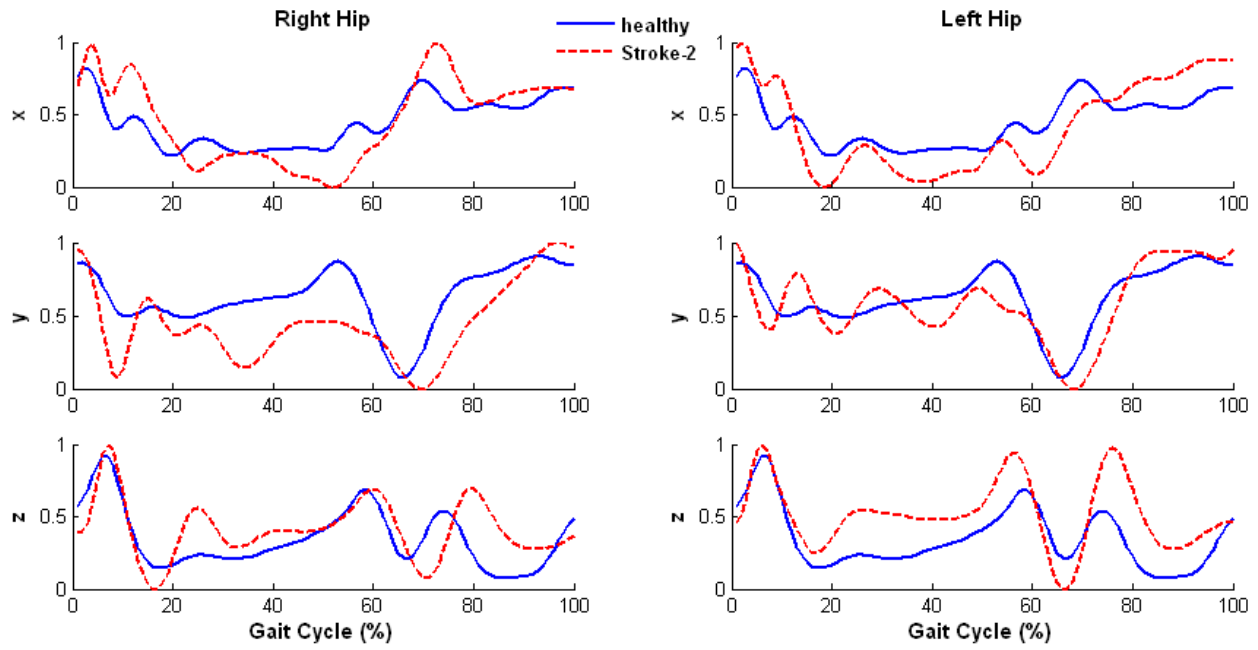


Figure AXV-6: Comparison of acceleration pattern in the gait cycle between healthy subjects and Stroke-2.

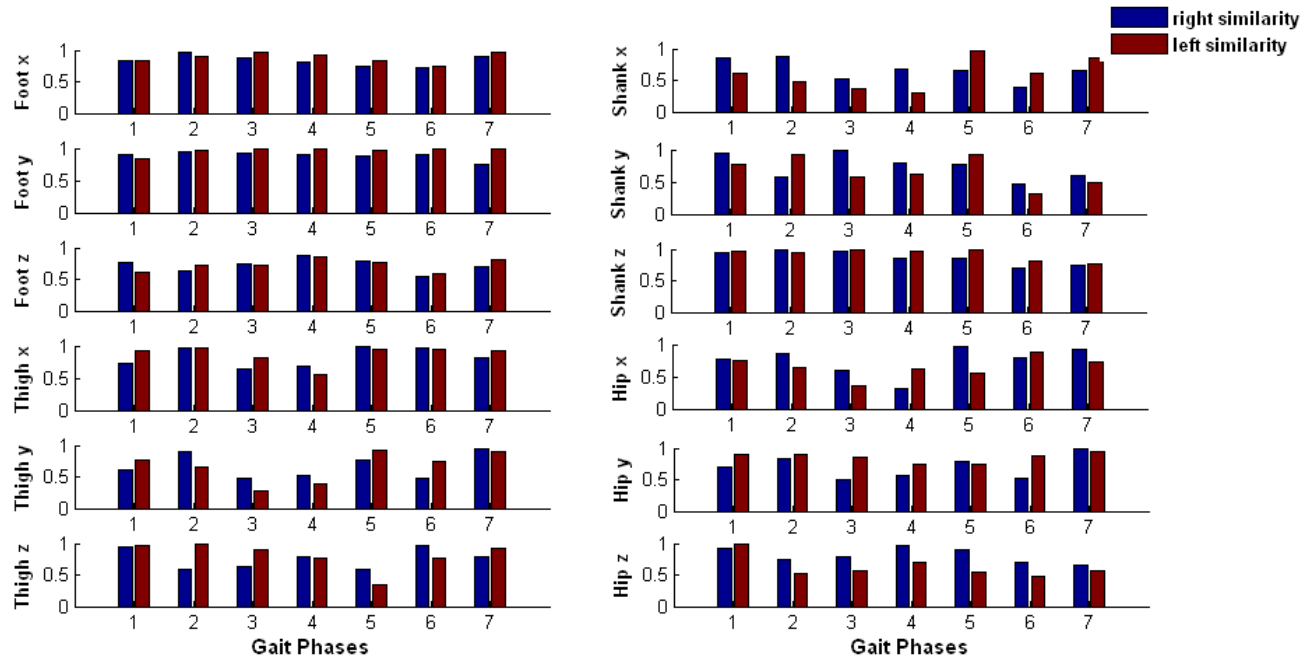


Figure AXV-7: Grade of similarity of right and left acceleration in Stroke-2.

Summary:**Table AXV-2: Characterization of acceleration in Stroke-2**

	Right	Left
Foot x	Peak rise in the initial contact following with higher magnitude in the entire gait cycle. There are modulate and high similarity within the gait cycle.	Lower acceleration in the early stance phase, and there is a sharp rise in the pre-swing phase.
Foot y	There is a delayed foot clearance in the pre-swing phase. High similarity appears in the entire gait cycle.	Sharp acceleration appears in the initial contact, delayed acceleration in the initial swing phase.
Foot z	Sharp acceleration appears in the initial contact following with the high magnitude in the stance phase, delayed acceleration in the swing phase. Modulate similarities appear in the entire gait cycle.	Similar to foot z.
Shank x	Sharp acceleration appears in the initial contact following with the unstable magnitude in the rest of the stance phase, delayed and lower acceleration appears in the mid-swing phase. Significant small similarity appears in the mid-swing phase.	Lower acceleration appears in initial contact and continues to the pre-swing phase. There is a sharp increased acceleration in the late swing phase. Significant small similarity appears in the pre-swing phase.
Shank y	Higher unstable acceleration appears in the stance phase, lower acceleration occurs in the swing phase. Significant small similarity appears in the mid-swing phase.	Similar to right shank y, but with lower magnitude in late stance phase.
Shank z	Sharp rise in acceleration appears in the initial contact, delayed and lower acceleration in the swing phase. Modulate and high similarities occur in the entire gait cycle.	Similar to right shank z.
Thigh x	Higher magnitude appears in the early stance phase, following with lower magnitude in the late stance phase. There are sharp rise in acceleration in the swing phase.	Similar patterns to right thigh x.
Thigh y	There is very unstable pattern of acceleration in this direction results in	Similar to right thigh y.

	significant small similarity appears in the terminal stance and pre-swing phases.	
Thigh z	A sharp rise in acceleration appears in the initial contact, following with lower acceleration in the rest of the gait cycle.	A sharp rise in acceleration appears in the initial contact, following with unstable accelerations in the rest of the stance phase, there is a sharp deceleration in the pre-swing phase and a sharp acceleration in the mid-swing phase. Significant small similarity appears in the initial swing phase.
Hip x	Higher magnitude in the early stance phase following with the lower magnitude in the late stance, there is a sharp rise in the acceleration in the early swing phase. Significant small similarity appears in the pre-swing phase.	Similar to right hip x.
Hip y	A sharp deceleration appears in the loading response, following with the lower magnitude in the stance phase. There is a delayed acceleration in the swing phase. Smaller similarity appears in the terminal stance phase.	There is a very unstable pattern of acceleration in the stance phase, and a sharp rise in acceleration in the swing phase.
Hip z	A sharp rise in acceleration appears in the initial contact, following with higher magnitude in the rest of the stance phase, there is a sharp rise in acceleration in the swing phase.	Similar to the right hip z. Significant small similarity appears in the swing phase.

Appendix XVI: Results of Spinal Cord Injury (SCI)

- **Description**

Subject is 48 year old male with a long history of intractable partial epilepsy. Several years ago he fell as a result of a sudden seizure and fractured his cervical spine. With this he sustained a so called Brown-Sequard syndrome (partial hemisection of the spinal cord). From the observation of his gait, he was walking with right leg dragging and using the left leg as base of the support and pushing away to the right.

- **Temporal Stride Variability**

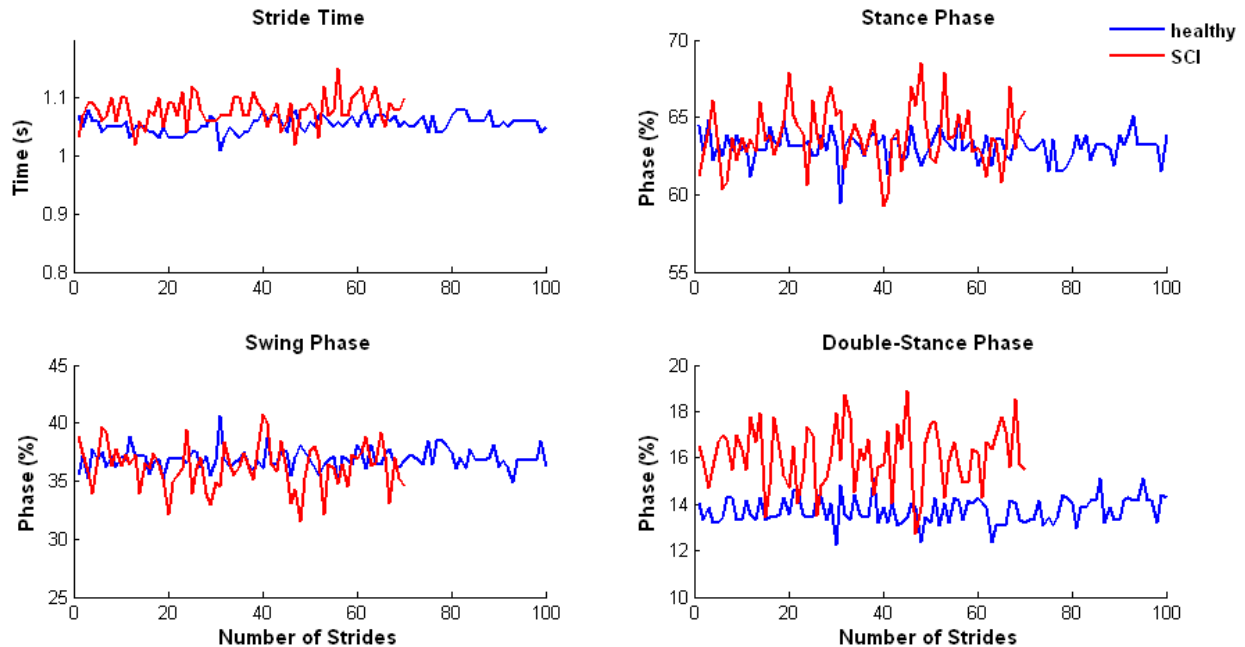


Figure AXVI-1: Stride variability of a healthy male subject and a male patient with spinal cord injury (SCI).

Summary: There is increased stride variability in all stride variables, compared with the healthy subject. There is a significant large fluctuation in stance phase and double-stance phase in SCI.

- **Ground Reaction Forces**

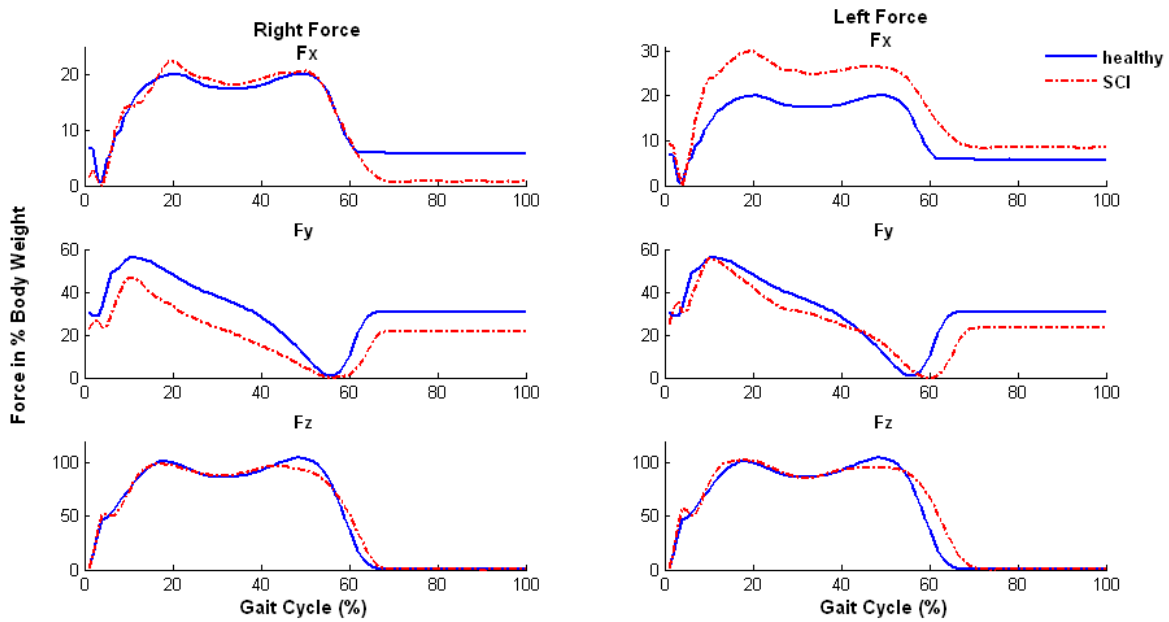


Figure AXVI-2: Right and left GRF in 3-D in Spinal Cord Injury subject.

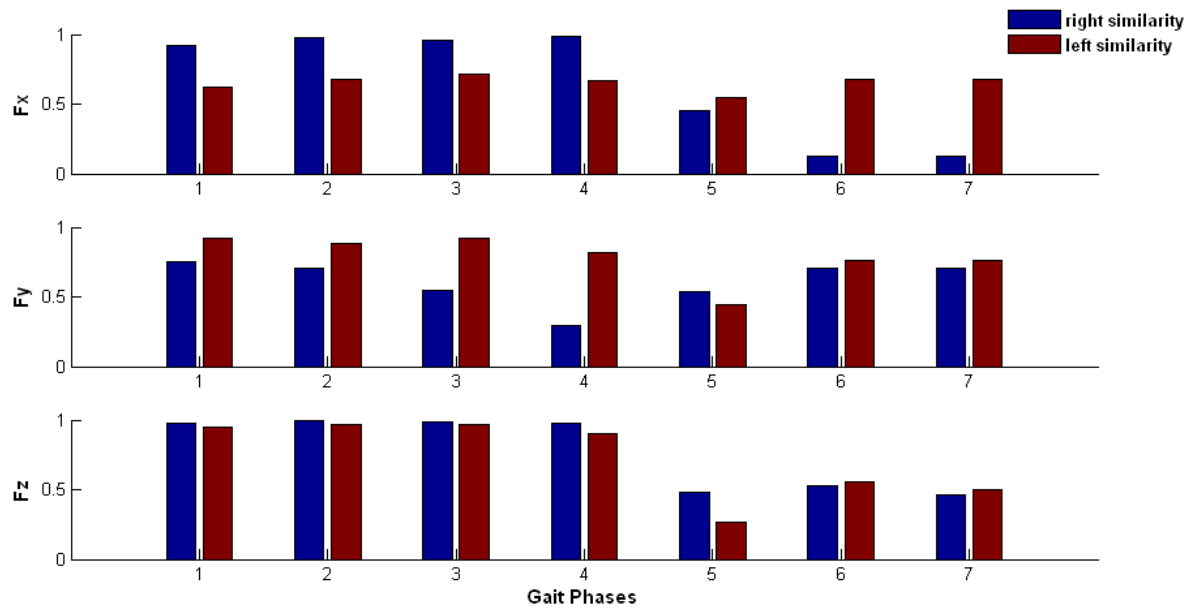


Figure AXVI-3: Grade of similarity of right and left GRF in Spinal Cord Injury subject.

Summary: In the vertical direction, the behavior of the grand reaction force of SCI subject is perfectly matched to averaged healthy subjects, having those smooth ‘M-shape’ pattern, which indicates the mild symptoms of this subject. The left foot GRF has slightly longer ground

contacting time than the right foot, which tells us the more severe symptoms on the right side. In the anterior-posterior direction, there is lower GRF on the right side. In the mediolateral direction, there is higher GRF on the left side which indicates some levels of compensation mechanisms. The similarity analysis shows this SCI subject has very mild gait problems.

- **EMG Muscle Activity Patterns**

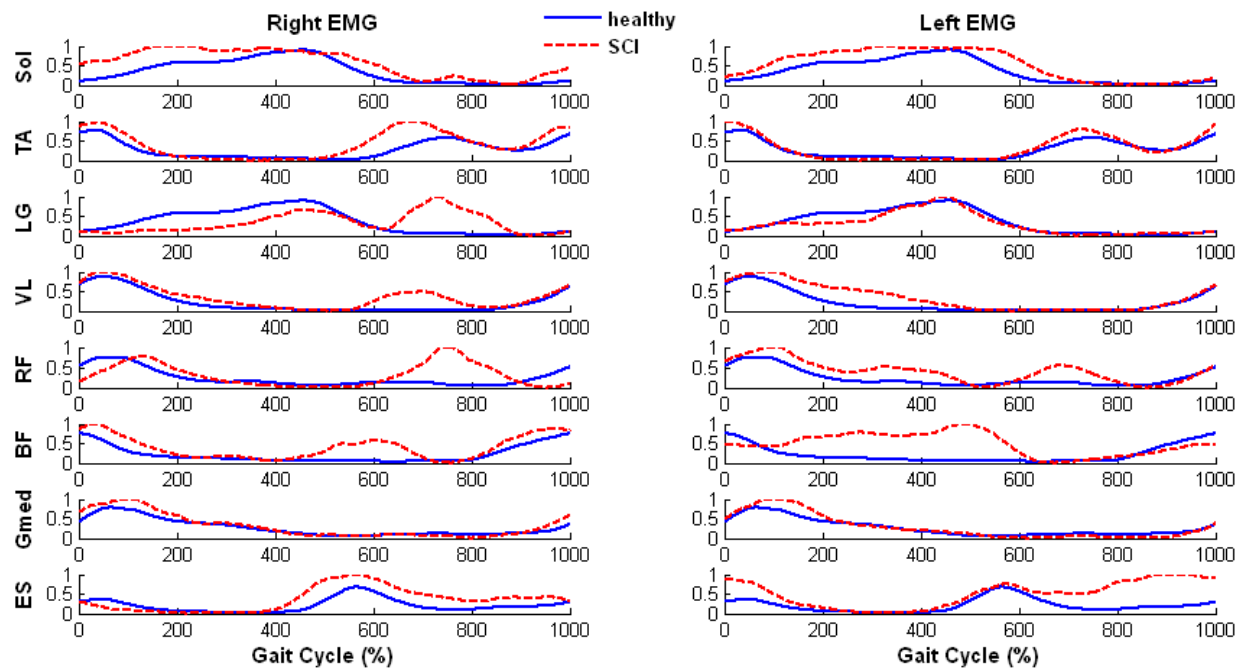


Figure AXVI-4: Comparison of EMG activity in a full gait cycle between healthy subjects and Spinal Cord Injury subject.

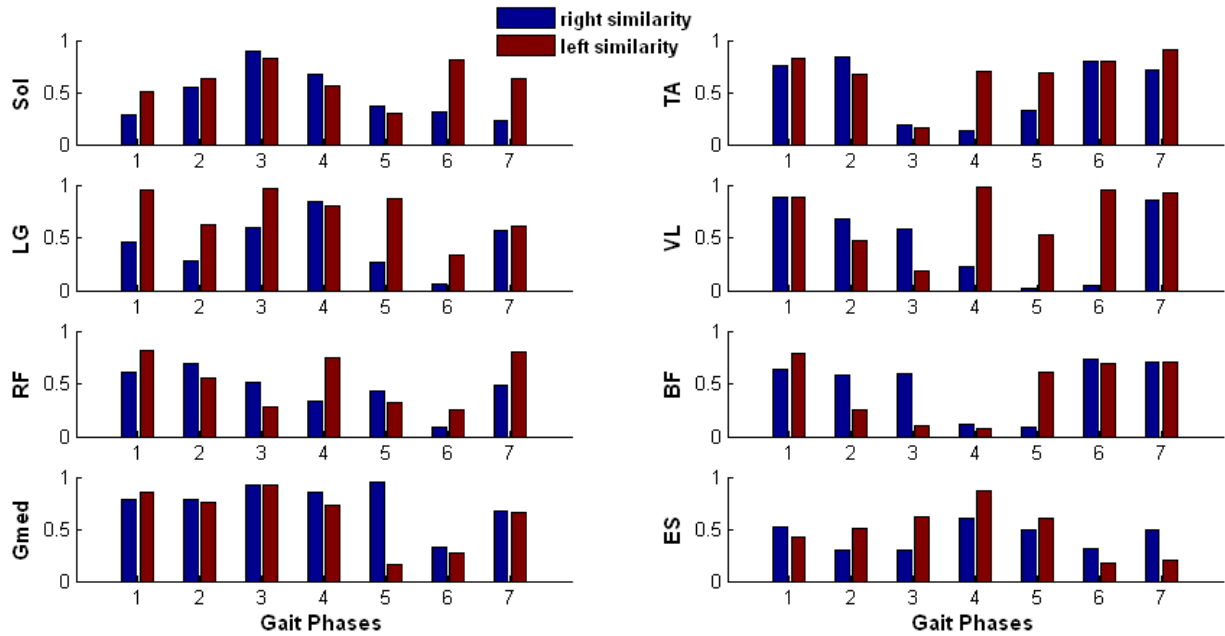


Figure AXVI-5: Grade of similarity of right and left EMG activity in Spinal Cord Injury subject.

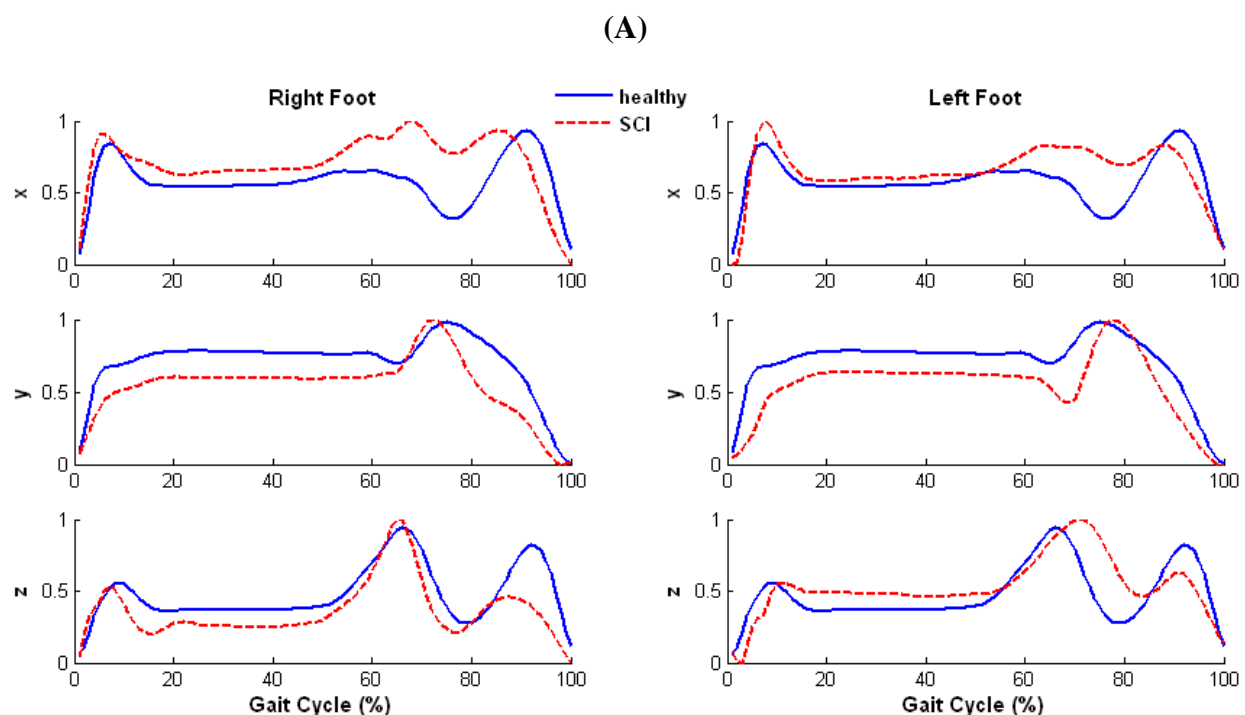
Summary:

Table AXVI-1: Summary of EMG Activity in Spinal Cord Injury Case Study

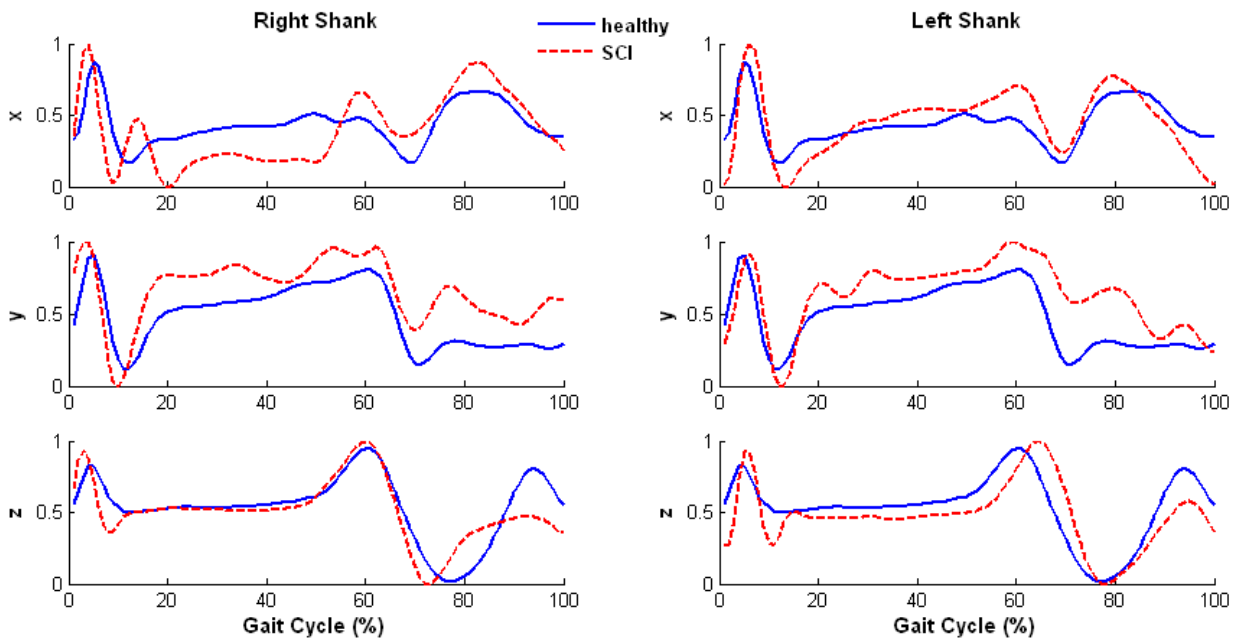
	Right	Left
Soleus	Spasticity appears in the entire stance phase. Significant small similarity appears in the initial contact and terminal swing phase.	Similar to right soleus, significant small similarity appears in the initial swing phase.
Tibialis Anterior (TA)	Spasticity appears in the initial contact and early swing phase. Significant small similarity appears in the terminal stance and pre-swing phases.	Similar to right TA. Significant small similarity appears in the terminal stance phase.
Gastrocnemius Lateralis (LG)	Muscle weakness appears in the stance phase, spasticity occurs in the early swing phase. Significant small similarity appears in the mid-swing phase.	Muscle weakness appears in the mid-stance phase.
Vastus Lateralis (VL)	Spasticity appears in the early swing phase. Significant small similarity appears in the initial and mid-swing phases.	Spasticity appears in the mid-stance phase.
Rectus Femoris	Delayed muscle activity occurs in the loading response, and muscle spasticity occurs in the	Spasticity appears in the entire stance phase and early swing

(RF)	mid-swing phase. Significant small similarity appears in the mid-swing phase.	phase. Significant small similarity appears in the mid-swing phase.
Biceps Femoris (BF)	Spasticity appears in the loading response, pre-swing, and terminal swing phases. Significant small similarity appears in the terminal stance, pre-swing and initial swing phases.	Spasticity appears in the entire stance phase. Significant small similarity appears in the terminal stance and pre-swing phases.
Gluteus Medius (Gmed)	Spasticity appears in the loading response.	Similar to right Gmed.
Elector Spinae (ES)	Muscle weakness appears in the loading response, spasticity appears in the pre-swing and entire swing phases.	Spasticity appears in the initial contact, spasticity appears in the swing phase.

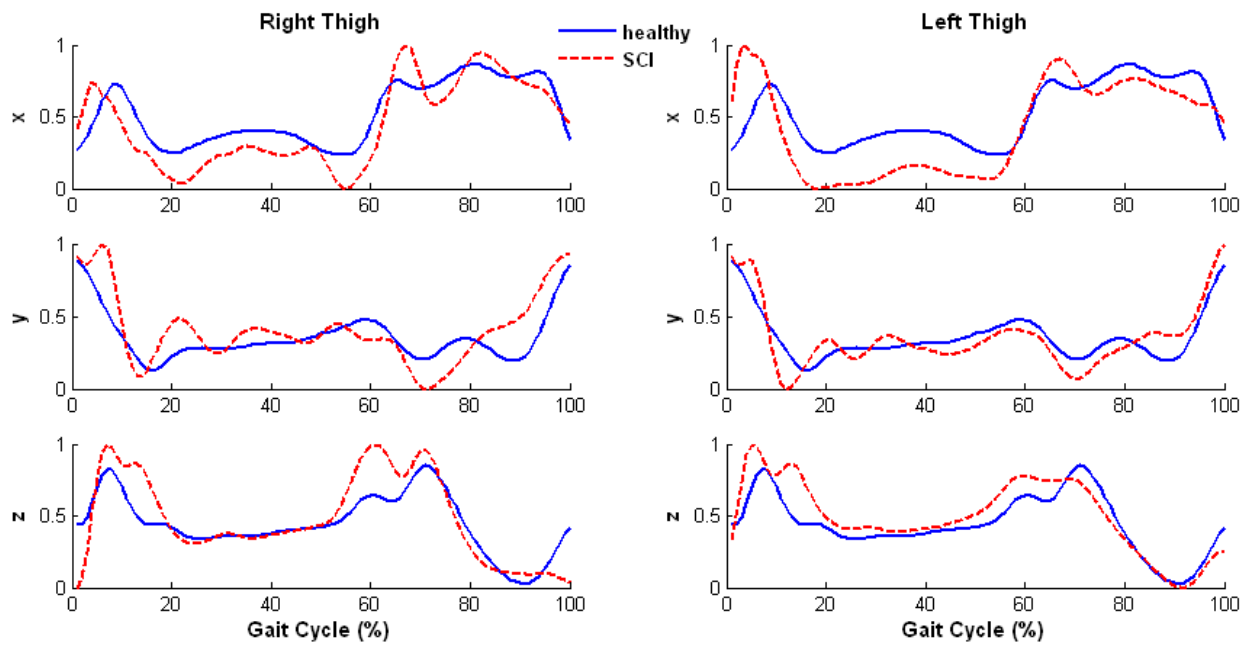
- **Acceleration Patterns**



(B)



(C)



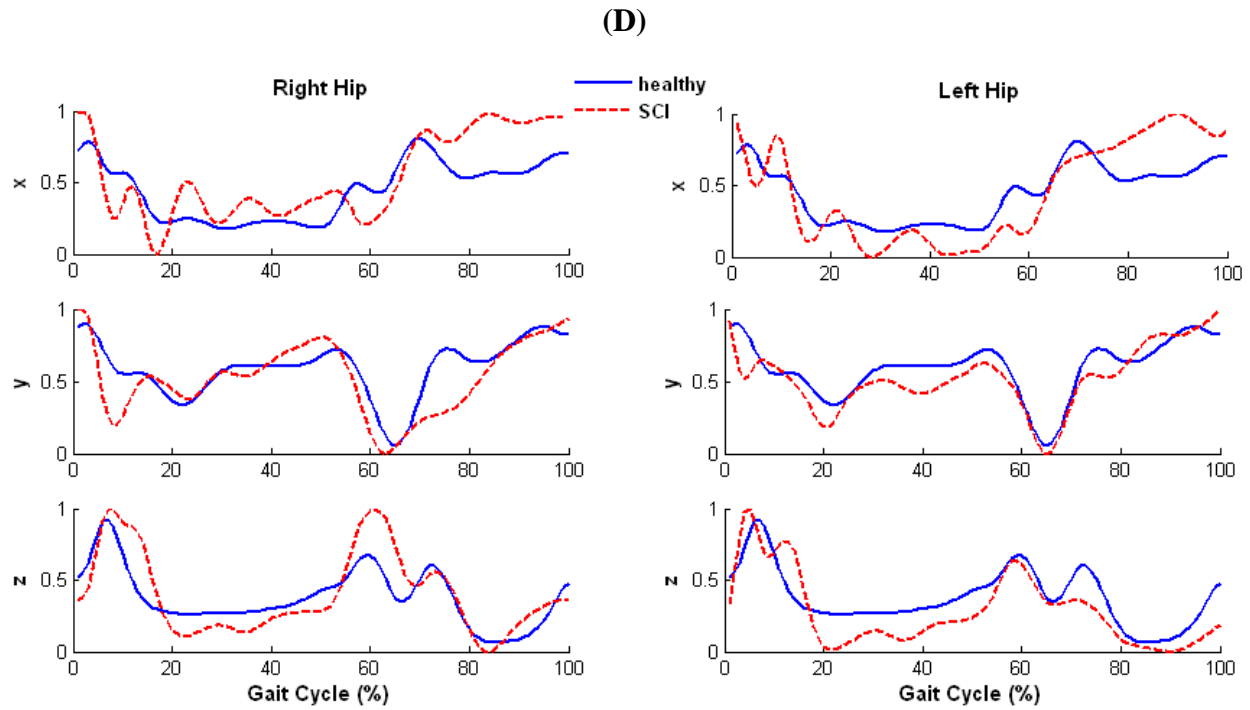


Figure AXVI-6: Comparison of acceleration pattern in a full gait cycle between healthy subjects and Spinal Cord Injury subject.

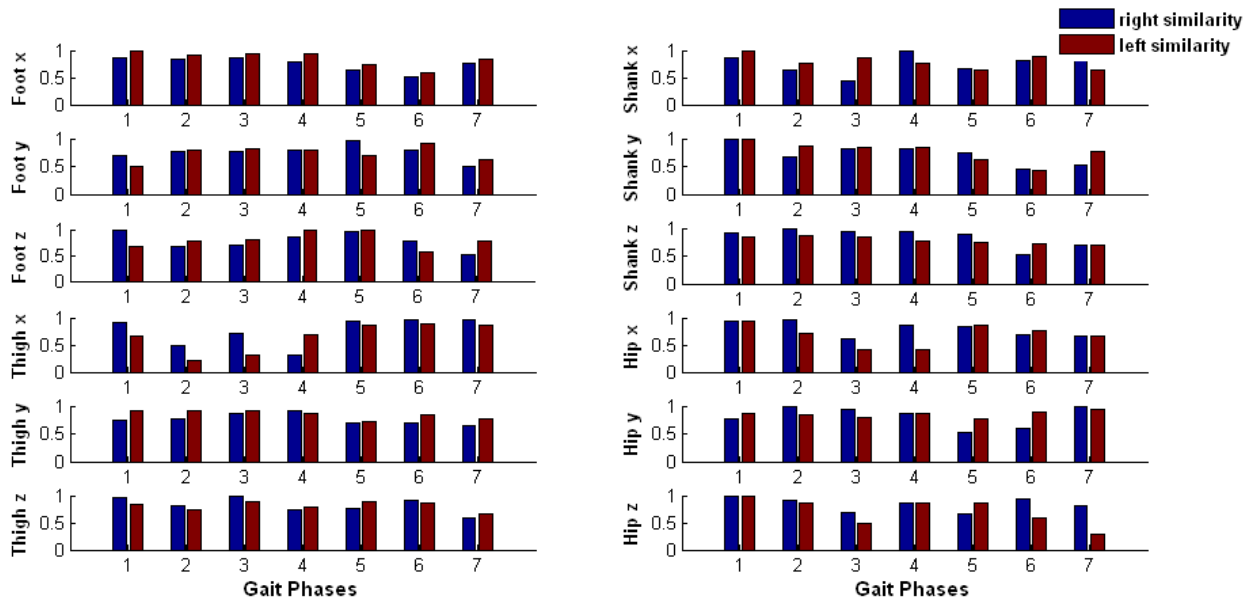


Figure AXVI-7: Grade of similarity of right and left acceleration in Spinal Cord Injury subject.

Summary:

Table AXVI-2: Characterization of acceleration in Spinal Cord Injury Case Study

	Right	Left
Foot x	A sharp rise in acceleration in the initial contact, following with high magnitude in the rest of the gait cycle. Smaller similarity appears in the mid-swing phase.	Similar to foot x.
Foot y	Lower acceleration occurs in the loading response and the rest of the stance phase. There is no deceleration at foot clearance which indicates the gait problems on the right foot. Smaller similarity appears in the terminal swing phase.	Lower acceleration occurs in the loading response and lower magnitude in the stance phase, slightly delayed acceleration appears in the initial swing phase.
Foot z	Early deceleration appears in the early stance phase, following with lower magnitude in the rest of the stance, a sharp rise in acceleration in the initial swing phase, and a lower acceleration appears in the terminal swing phase. Smaller similarity appears in the terminal swing phase.	Delayed acceleration appears in the loading response, following with the higher magnitude in the rest of the stance phase, a sharp rise in acceleration in early swing phase, and lower acceleration in the terminal swing phase.
Shank x	A sharp rise in acceleration appears in the initial contact, following with the lower magnitude in mid-stance phase, higher acceleration appears in the swing phase. Smaller similarity appears in the terminal stance phase.	A sharp rise in acceleration in the initial contact, following with a sharp deceleration, an increased acceleration appears in the stance phase, and a sharp rise in acceleration appears in the swing phase.
Shank y	A sharp deceleration appears in the loading response, following with a sharp rise in the acceleration, and continues with higher magnitude in the rest of the gait cycle. Significant small similarity appears in the mid-swing phase.	Same as right shank y.
Shank z	A sharp rise in acceleration in the initial contact, following with a sharp deceleration, lower acceleration appears in the swing phase. Smaller similarity appears in the mid-swing phase.	Similar to right shank z.

Thigh x	Lower acceleration appears in the stance phase, a sharp rise in acceleration in initial swing phase. Smaller similarity appears in the pre-swing phase.	A sharp rise in acceleration in the initial contact, following with a sharp deceleration, and continues with lower magnitude in the stance phase, a sharp rise in the initial swing phase. Significant small similarity appears in the mid-stance phase.
Thigh y	A delayed deceleration in the loading response, following with unstable behavior of acceleration pattern.	Similar to right thigh y.
Thigh z	A sharp rise in acceleration in the loading response and pre-swing phase.	Similar pattern to right thigh z.
Hip x	A sharp deceleration appears in the initial contact, following with very unstable pattern of signal, and an increased acceleration in the swing phase. Smaller similarity appears in the terminal stance phase.	Same as right hip x.
Hip y	A sharp deceleration in the initial contact, and lower acceleration in the initial swing phase. Smaller similarity appears in the initial swing phase.	Same as right hip y.
Hip z	A sharp rise in acceleration appears in the initial contact, following with a large deceleration, and a sharp acceleration appears in the pre-swing phase. Smaller similarity appears in the terminal stance phase.	A sharp rise in acceleration appears in the initial contact, following with a large deceleration in the stance phase. Significant small similarity appears in the terminal swing phase.

Appendix XVII: Results of Traumatic Brain Injury (TBI)

- **Description**

Subject is 35 year old male who had a car accident in December 23, 2009. He was in coma for three weeks in the hospital. He was on physical rehabilitation eight hours everyday. Medication includes *abilify* (*aripiprazole*) for depression and anxious. He was tested at the free-walking speed (0.75 m/s) on the instrumented treadmill without any assistant devices.

- **Temporal Stride Variability**

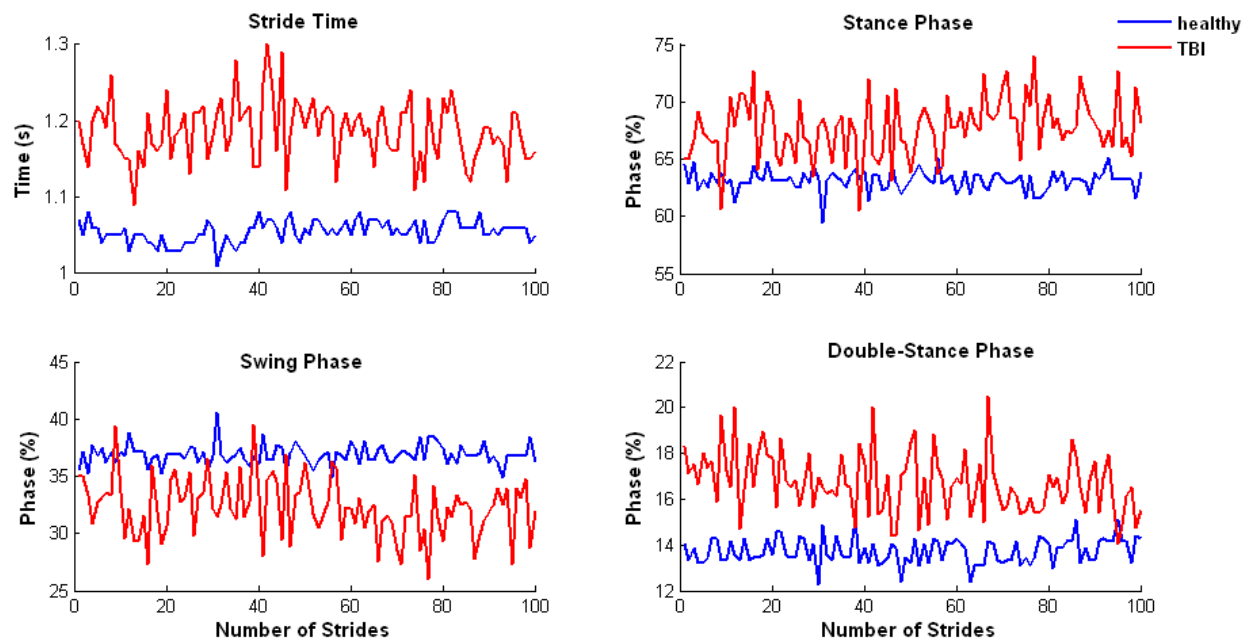


Figure AXVII-1: Comparison of stride variability between a healthy male subject and a male with Traumatic Brain Injury (TBI).

Summary: TBI subject has much increased stride variability in all stride variables. There is an increase in the stride time, stance phase, and double-stance phase, and a decrease in swing phase.

- **Ground Reaction Forces**

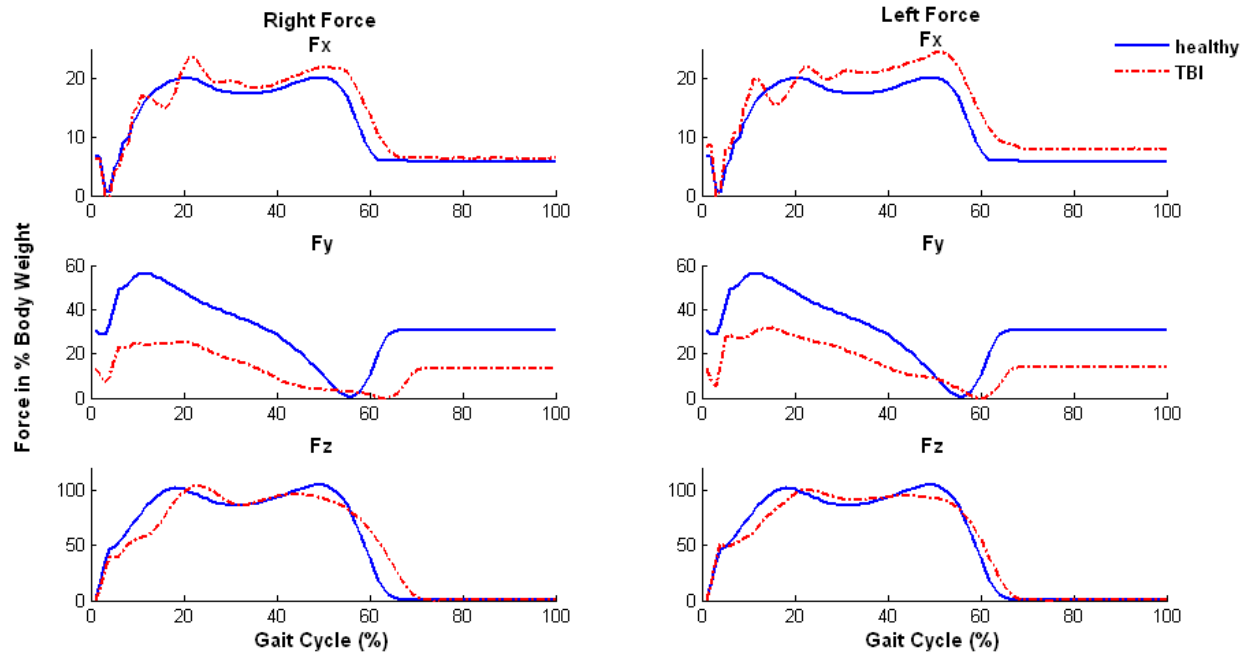


Figure AXVII-2: Right and left GRF in 3-D in Traumatic Brain Injury subject.

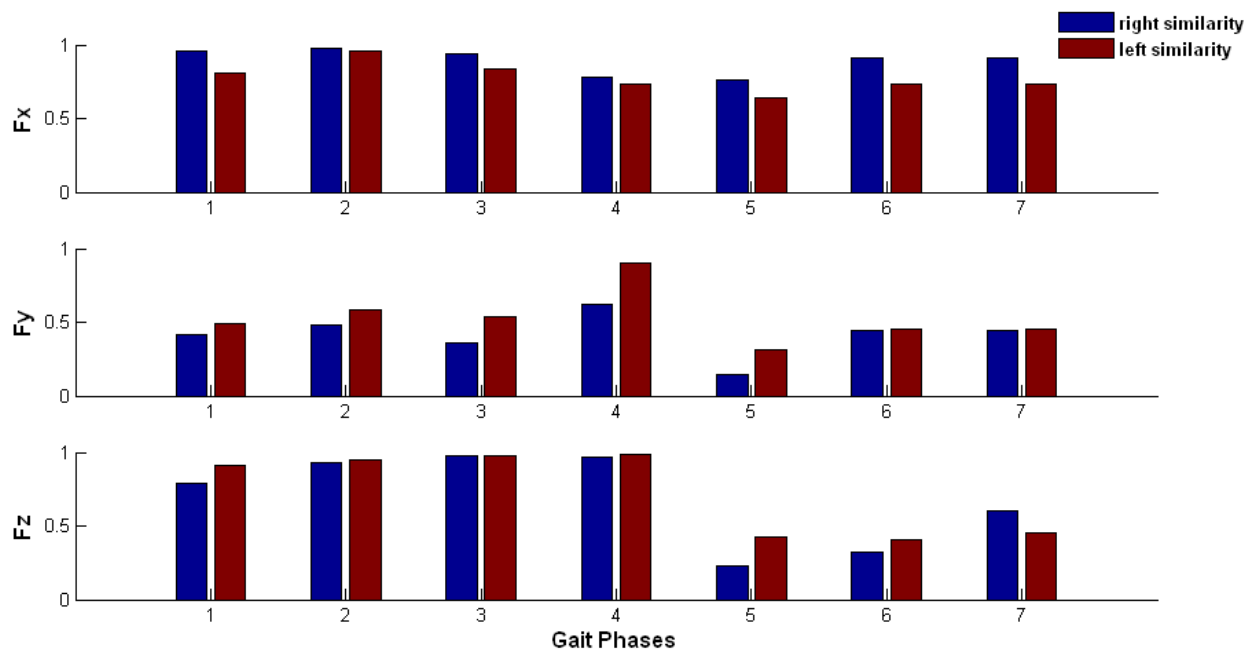


Figure AXVII-3: Grade of similarity between right and left GRF in TBI subject.

Summary: In the vertical direction, the TBI has slightly longer stance phase with delayed for the first peak and lower GRF in the second peak. In the anteroposterior direction, there is lower

GRF with TBI. In the mediolateral direction, there is unstable GRF signal in TBI. Smaller similarity appears mostly in the pre- and mid-swing phases in the vertical and anterioposterior directions.

- **EMG Muscle Activity Patterns**

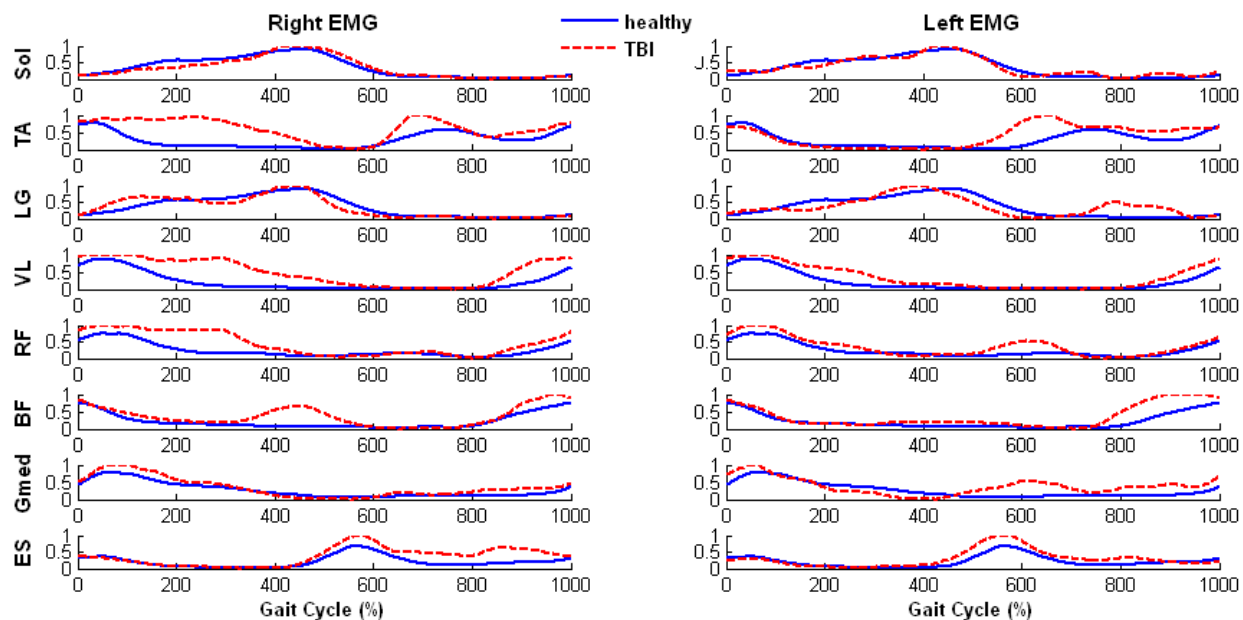


Figure AXVII-4: Comparison of EMG activity in a gait cycle between healthy subjects and TBI.

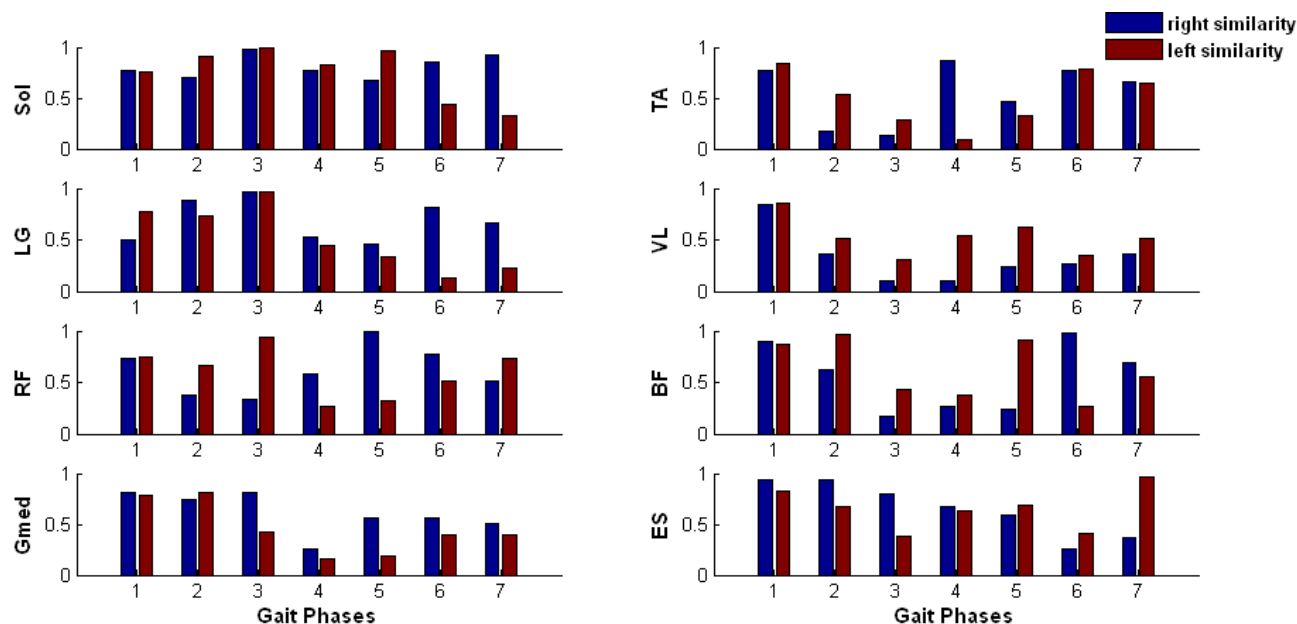


Figure AXVII-5: Grade of similarity of right and left EMG in TBI.

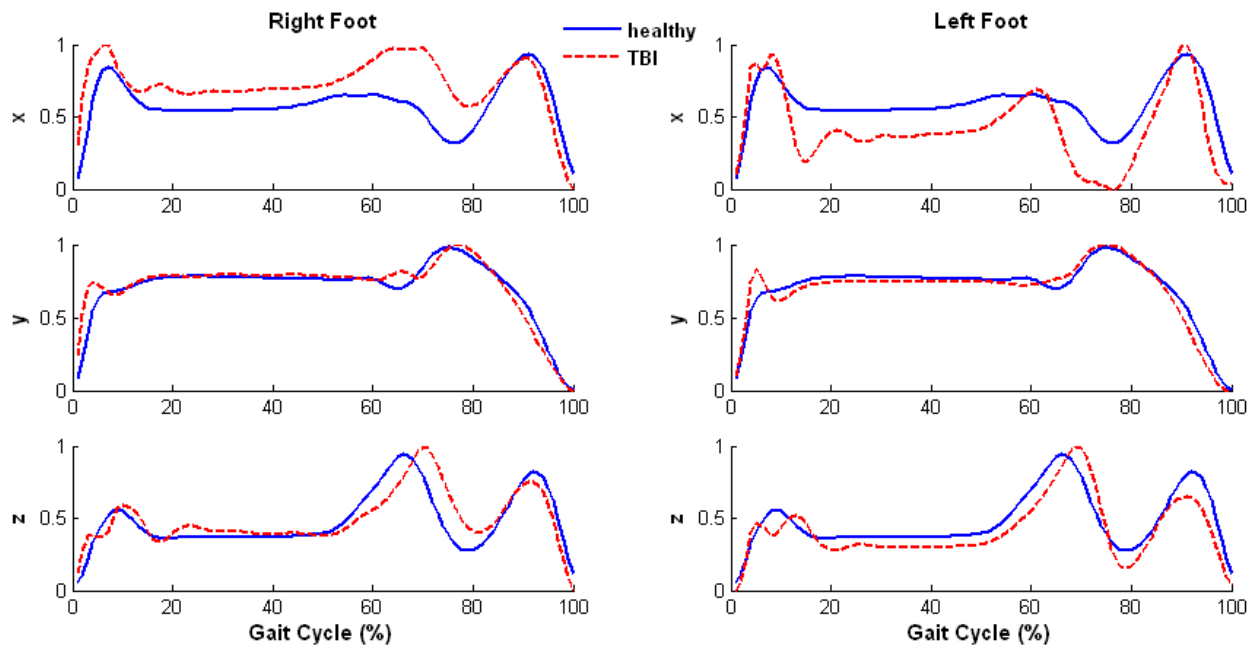
Summary:

Table AXVII-1: Summary of EMG Activity in Traumatic Brain Injury Case Study

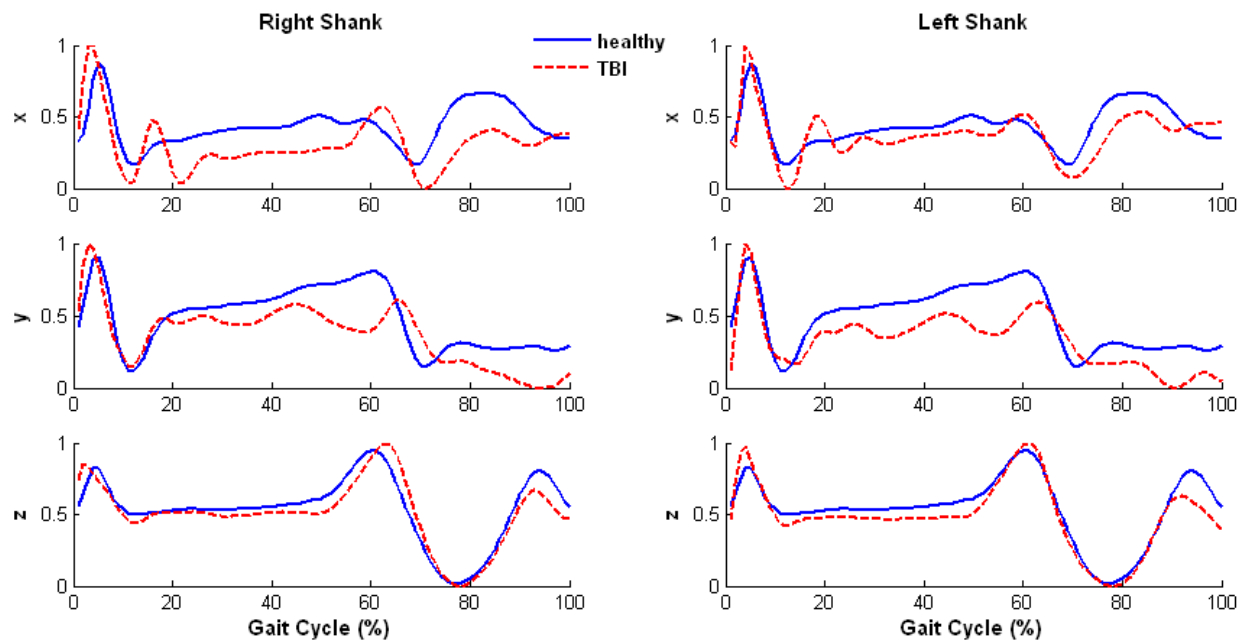
	Right	Left
Soleus	Muscle activities almost follow the pattern of the healthy. Moderate and high grade of similarity appear in the entire gait cycle.	Same as right Soleus.
Tibialis Anterior (TA)	Spasticity occurs in the most of the stance phase and early swing phase. Significant small similarity appears in the mid- and terminal stance phases.	Early activity appears in the pre-swing phase. Significant small similarity appears in the pre-swing phase.
Gastrocnemius Lateralis (LG)	There are some higher muscle activities in the early stance phase.	There are some higher muscle activities in the stance phase and mid-swing phase. Significant small similarity appears in the mid-swing.
Vastus Lateralis (VL)	Spasticity occurs the entire stance phase, and terminal swing phase. Significant small similarity appears in the terminal stance and pre-swing phases.	Similar to right VL.
Rectus Femoris (RF)	Spasticity occurs in the early stance phase up to 40% of the gait cycle, and slightly higher activity in the terminal swing phase. Smaller similarity appears in the terminal stance phase.	Spasticity occurs in the early stance phase up to 30% of the gait cycle, and spasticity occurs again in the pre-swing phase. Smaller similarity appears in the pre-swing phase.
Biceps Femoris (BF)	Spasticity occurs in the mid-stance and terminal swing phases. Significant small similarity appears in the terminal stance, pre- and initial swing phases.	Spasticity occurs in the late swing phase. Smaller similarity appears in the mid-swing phase.
Gluteus Medius (Gmed)	Spasticity occurs in the early stance and late swing phases. Smaller similarity appears in the initial swing phase.	Spasticity occurs in the initial contact and most of the swing phase. Significant small similarity appears in the pre- and initial swing phases.
Erector Spinae (ES)	Higher muscle activities occur after mid-stance phase to the end of the gait cycle. Significant small similarity appears in the mid-swing phase.	Spasticity occurs in the pre-swing phase.

- **Acceleration Patterns**

(A)



(B)



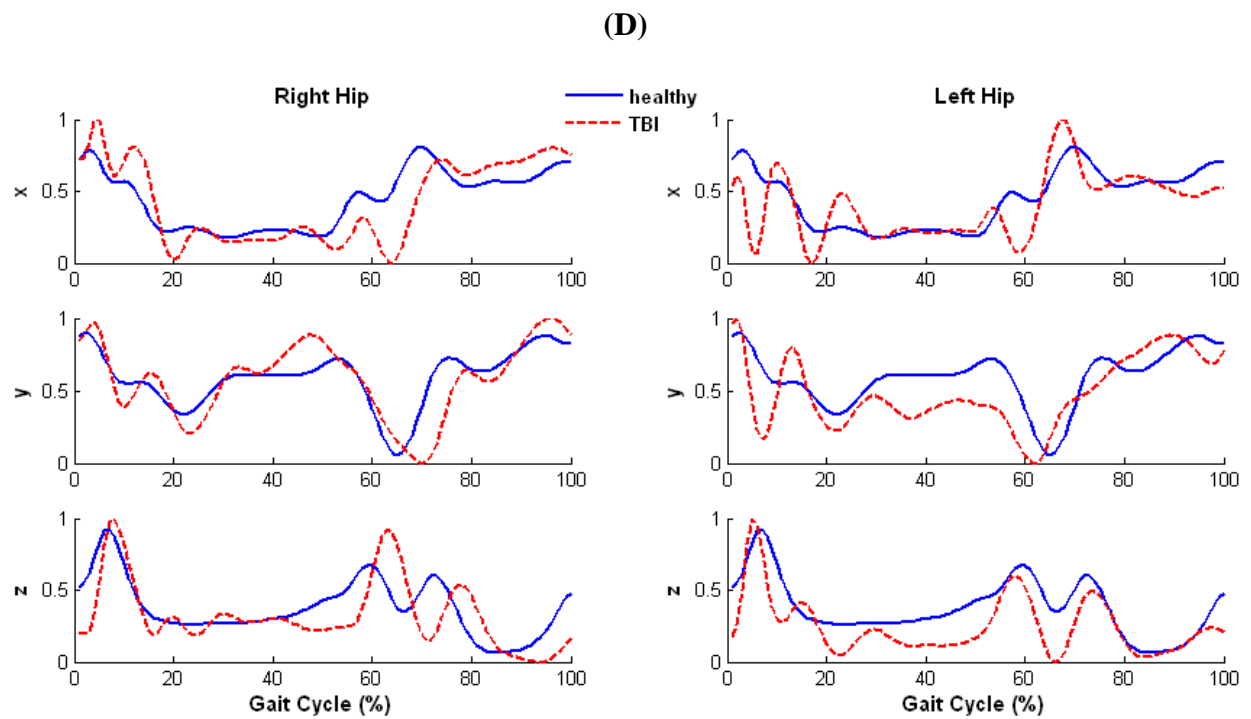
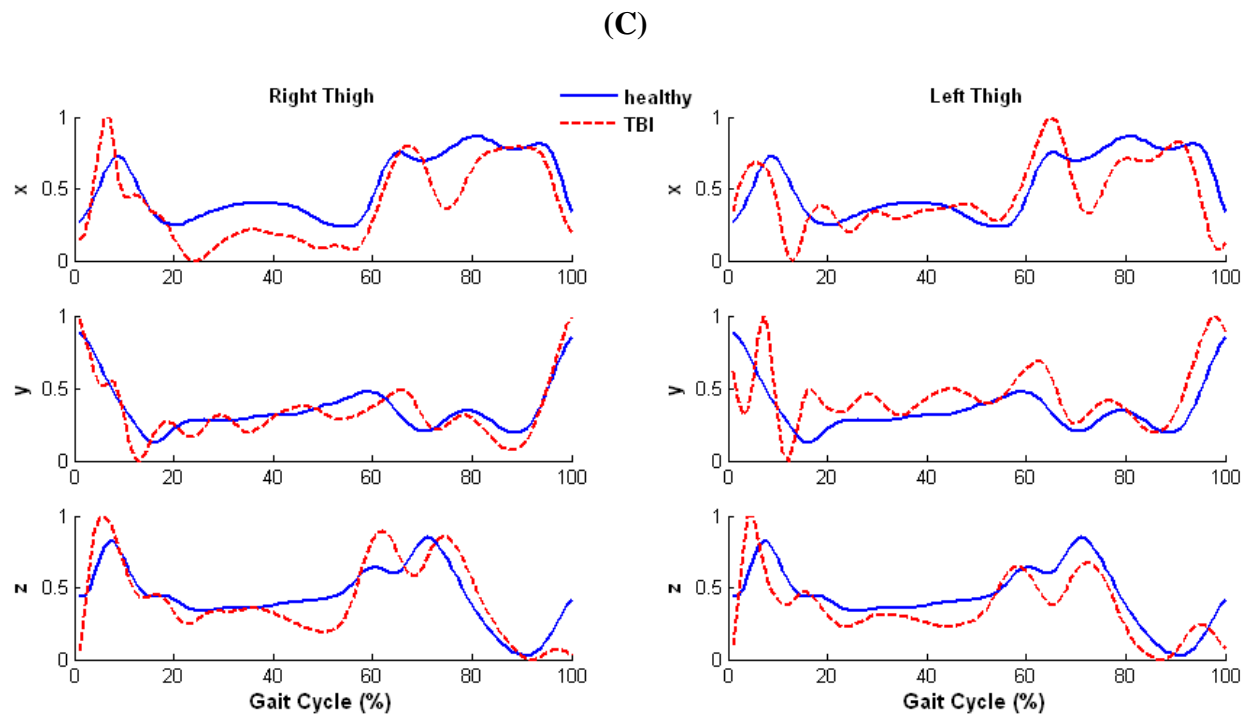


Figure AXVII-6: Comparison of acceleration pattern in a gait cycle between healthy subjects and TBI subject.

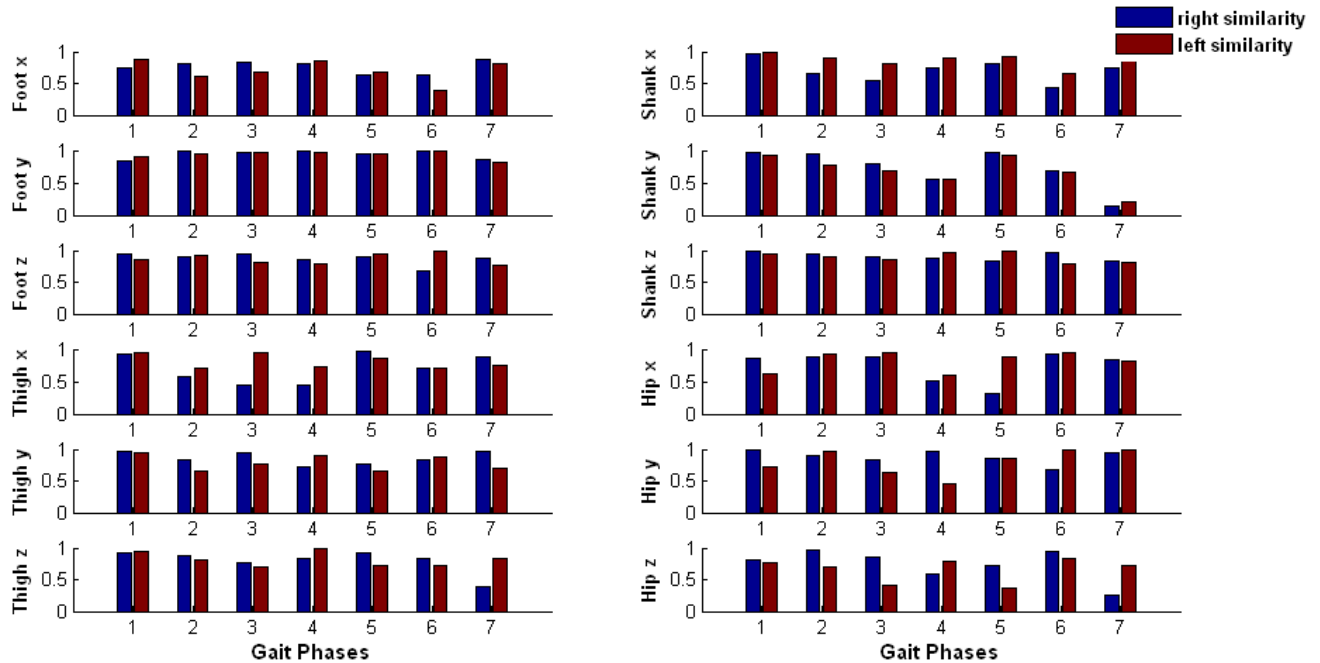


Figure AXVII-7: Grade of similarity of right and left acceleration in TBI.

Summary:

Table AXVII-2: Characterization of acceleration in Traumatic Brain Injury Case Study

	Right	Left
Foot x	A sharp rise in acceleration in the initial contact, following with higher magnitude in the rest of the stance phase and early swing phase.	A sharp rise in acceleration in the initial contact, following with a large deceleration, and continues with lower magnitude in the rest of the stance, a large deceleration occurs in the initial swing phase, following with a sharp rise in acceleration in the mid-swing phase. Smaller similarity appears in the mid-swing phase.
Foot y	A sharp rise in acceleration in the initial contact, foot clearance problem in the initial swing phase.	Same as right foot y.
Foot z	Unstable behavior occurs in the early stance phase.	Same as right foot z.
Shank x	A sharp rise in acceleration in the initial contact, following with lower magnitude in the stance phase. There is a sharp turning	Same as right shank x.

Shank y	<p>pattern in the initial swing, following with a lower acceleration in the swing phase. Smaller similarity appears in the mid-swing phase.</p> <p>A sharp rise in acceleration in the initial contact, following with unstable lower magnitude in the stance phase, a lower acceleration occurs in the swing phase. Significant small similarity appears in the terminal swing phase.</p>	Same as right shank y.
Shank z	<p>There is a very much matched pattern to healthy subjects, results in the high grade of similarity among the full gait cycle.</p>	Same as right shank z.
Thigh x	<p>A sharp rise in acceleration occurs in the initial contact, lower magnitude in the rest of the stance phase, unstable magnitude in the swing phase. Smaller similarity appears in the terminal stance and pre-swing.</p>	Very unstable pattern in the stance phase, a sharp rise in acceleration in initial swing phase, following with unstable magnitude in the rest of the swing phase.
Thigh y	<p>Some levels of unstable pattern appear in the entire gait cycle.</p>	A sharp rise in acceleration occurs in the loading response, following with unstable signals in the rest of the cycle.
Thigh z	<p>A sharp rise in acceleration in the initial contact, lower magnitude in the stance phase, an increased acceleration occurs in the swing initial swing phase. Smaller similarity appears in the terminal swing.</p>	Similar to right thigh z.
Hip x	<p>Higher acceleration appears in the early stance phase, lower acceleration occurs in the initial swing phase. Significant small similarity appears in the initial swing.</p>	Unstable pattern appears in the early stance phase, a sharp rise in acceleration occurs in the pre-swing phase.
Hip y	<p>Higher deceleration appears in the stance phase and initial swing phase.</p>	Similar to right hip y. Smaller similarity appears in the pre-swing phase.
Hip z	<p>A sharp rise in acceleration appears in the initial contact, following with unstable magnitude in the stance phase, a sharp rise in the initial swing phase. Significant small similarity appears in the terminal swing phase.</p>	A sharp rise in acceleration appears in the initial contact, following with low and unstable magnitude in the rest of the gait cycle. Smaller similarity appears in the initial swing phase.

Appendix XVIII: Results of Elderly Faller

- **Description**

Subject is 76 year old elderly male, had a slow moderately disorganized gait related to probable fat embolism after a fall from a roof several years ago with hip/femur fractures. He also had very strong diabetes. Subject was tested with bare-foot walking on the treadmill with harness support at speed of 0.3 m/s.

- **Temporal Stride Variability**

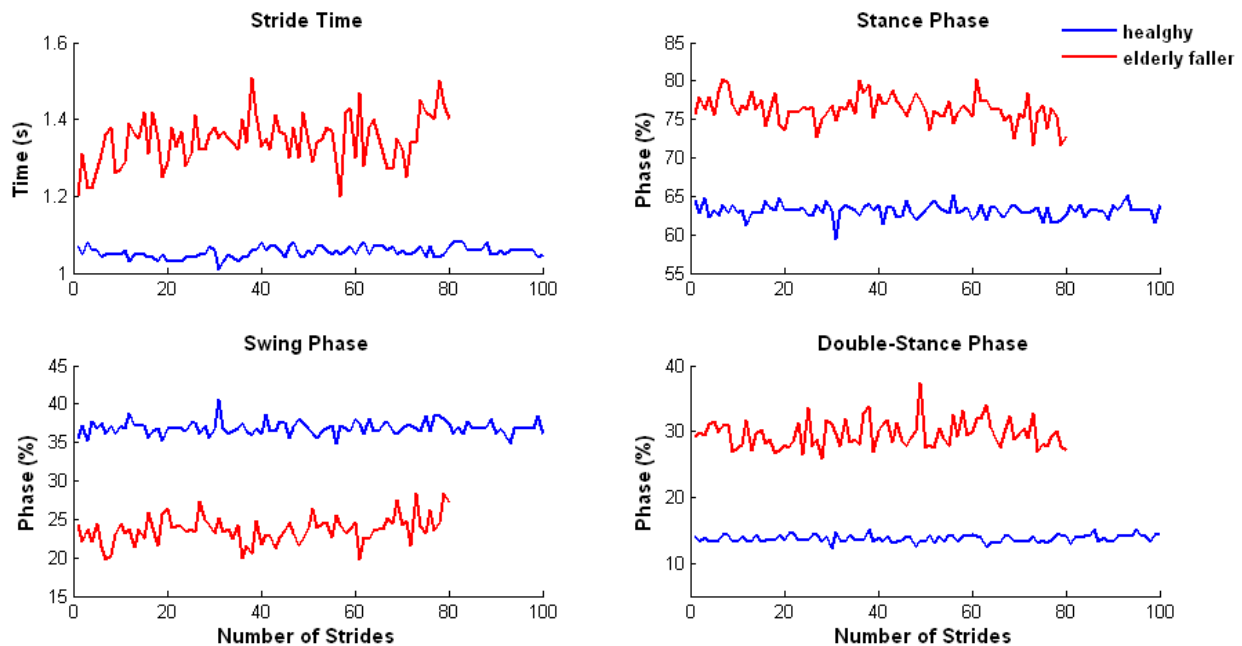


Figure AXVIII-1: Stride variability of a healthy male subject and an elderly faller subject.

Summary: Due to the slower treadmill walking speed, there were only 80 strides extracted from this elderly faller subject. The subject has increased both in magnitude and variability, in stride time, stance phase, and double-stance phase; and decreased magnitude in swing phase.

- **Ground Reaction Forces**

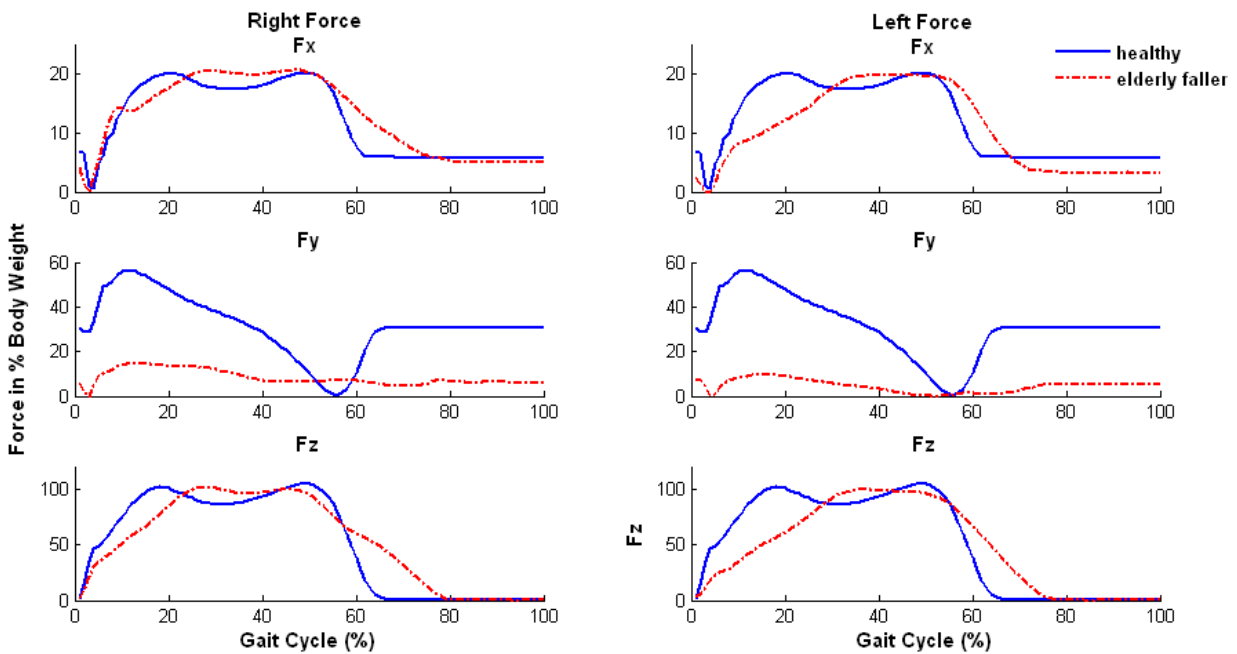


Figure AXVIII-2: Right and left GRF in 3-D in an elderly faller patient.

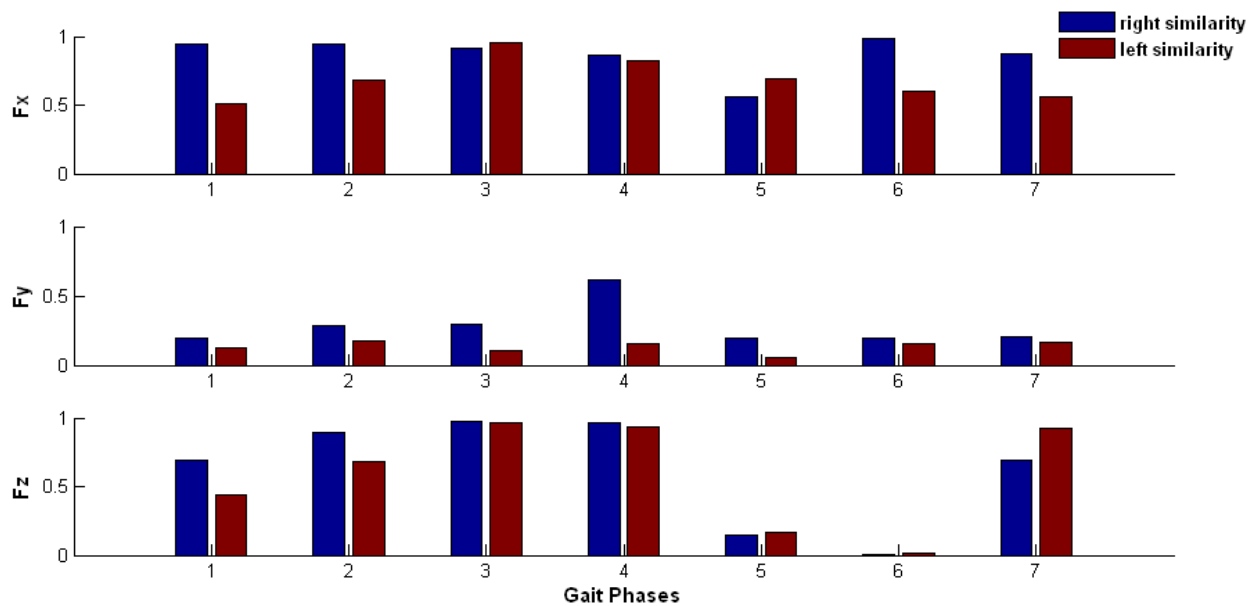


Figure AXVIII-3: Grade of similarity between right and left GRF in elderly faller patient.

Summary: In the vertical direction, there is a longer stance phase on both side (right foot is longer than left foot, suggest that the affected side was left); there is also shortened peak time

duration in the elderly faller subject. In the anterioposterior direction, there is much lower GRF compared with healthy subject. In the mediolateral direction, there is delayed and lower gradient in the early stance phase, especially showing on left foot. The grade similarity analysis showing the most gait problems in GRF appear in the anteioposterior direction.

- **EMG Muscle Activity Patterns**

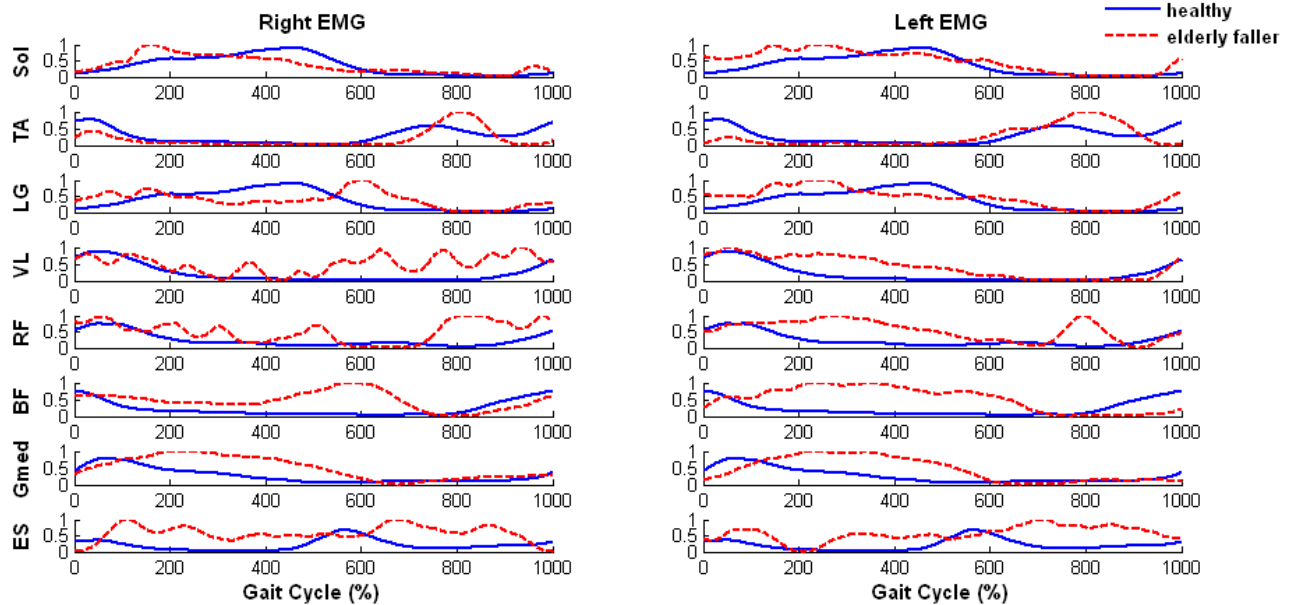


Figure AXVIII-4: Comparison of EMG activity in a gait cycle between healthy subjects and an elderly faller.

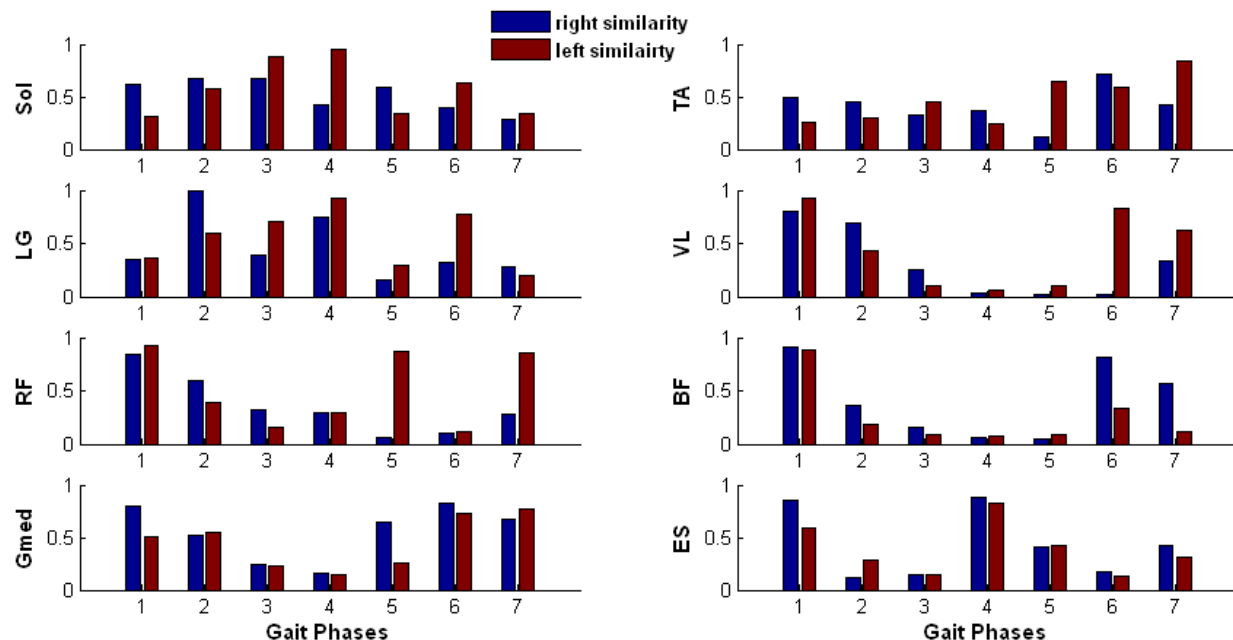


Figure AXVIII-5: Grade of similarity of right and left EMG in an elderly faller subject.

Summary:

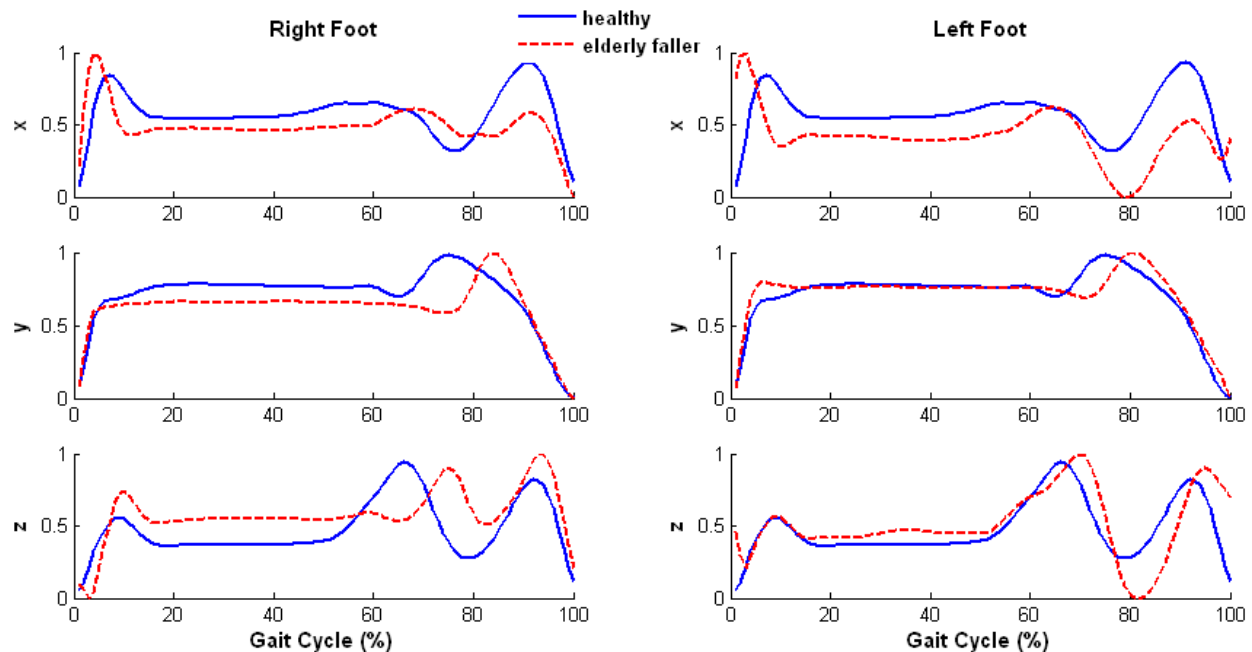
Table AXVIII-1: Summary of EMG Activity in Elderly Faller Case Study

	Right	Left
Soleus	Spasticity occurs in the mid-stance phase and terminal swing phase. Smaller similarity occurs in the terminal swing phase.	Higher and latency muscle activity in the stance phase, and spasticity occurs in the terminal swing phase.
Tibialis Anterior (TA)	Muscle weakness appears in the initial contact, and spasticity appears in swing phase. Significant small similarity appears in the initial swing phase.	Similar to right TA. Smaller similarity appears in the pre-swing phase.
Gastrocnemius Lateralis (LG)	Spasticity occurs in the early stance, following with muscle weakness in the late stance, spasticity occurs in the pre-swing phase. Significant small similarity occurs in the initial swing phase.	Spasticity appears in the stance phase up to 30% of the gait cycle. Muscle weakness occurs in the rest of the stance phase. Spasticity occurs in the terminal swing phase. Significant small similarity appears in the terminal swing phase.
Vastus Lateralis (VL)	There is very unstable muscle activity pattern throughout the gait cycle. Significant small similarity appears in the pre- and initial swing phases.	Spasticity occurs from mid-stance phase to the end of the stance which results in the significant small similarity in the pre- and initial swing phases.

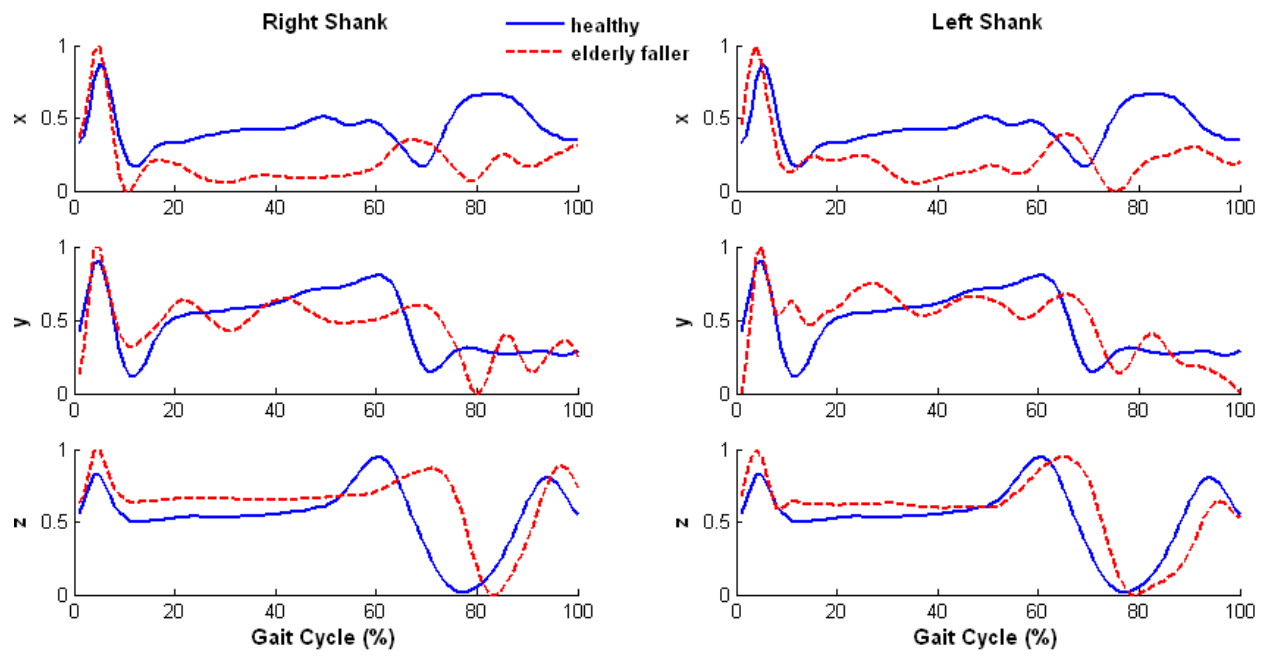
Rectus Femoris (RF)	Unstable muscle activity pattern throughout the entire gait cycle. Spasticity occurs in the late stance and swing phases. Significant small similarity appears in the initial and mid-swing phases.	Spasticity occurs from mid-stance to the end of the stance phase. Spasticity occurs in the mid-swing phase. Significant small similarity appears in the mid-stance and mid-swing phases.
Biceps Femoris (BF)	Spasticity occurs in the entire stance phase. Significant small similarity appears in the terminal stance, pre- and initial swing phases.	Same as right BF.
Gluteus Medius (Gmed)	Spasticity occurs in the stance phase. Significant small similarity appears in the pre-swing phase.	Delayed muscle activity in the initial contact, following with spasticity in the stance phase. Significant small similarity appears in the pre-swing phase.
Elector Spinae (ES)	Spasticity appears in the entire gait cycle. Significant small similarity appears in the mid- and terminal stance phases, and mid-swing phase.	Same as right ES.

- Acceleration Patterns

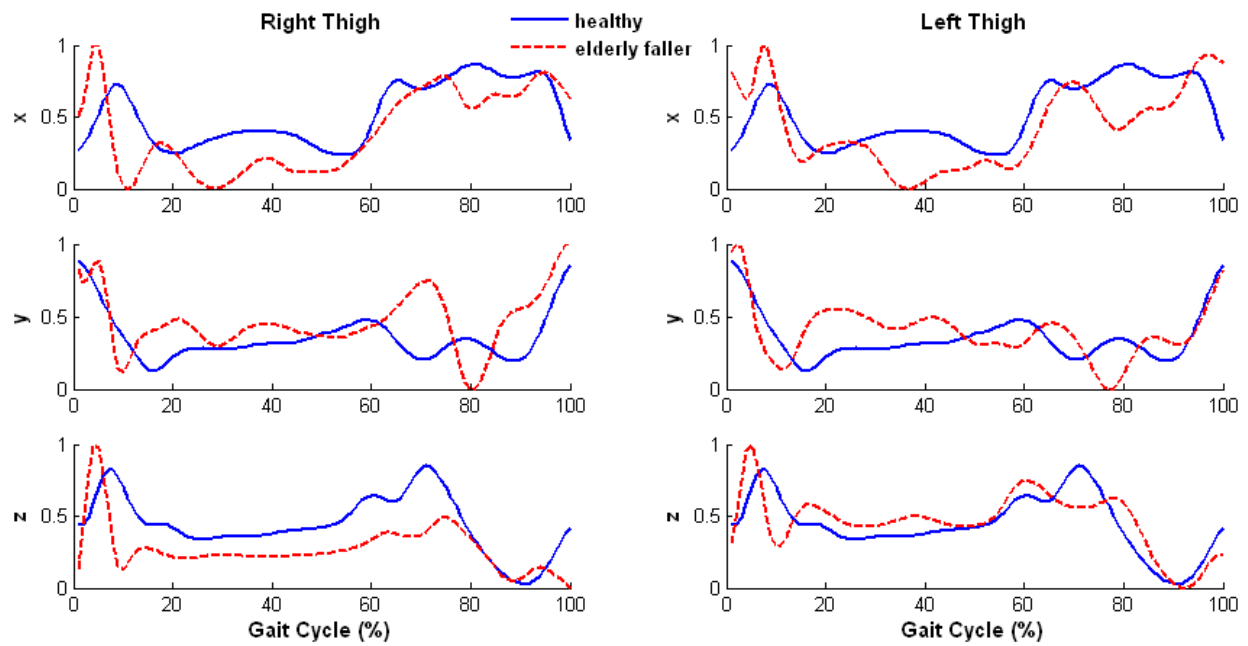
(A)



(B)



(C)



(D)

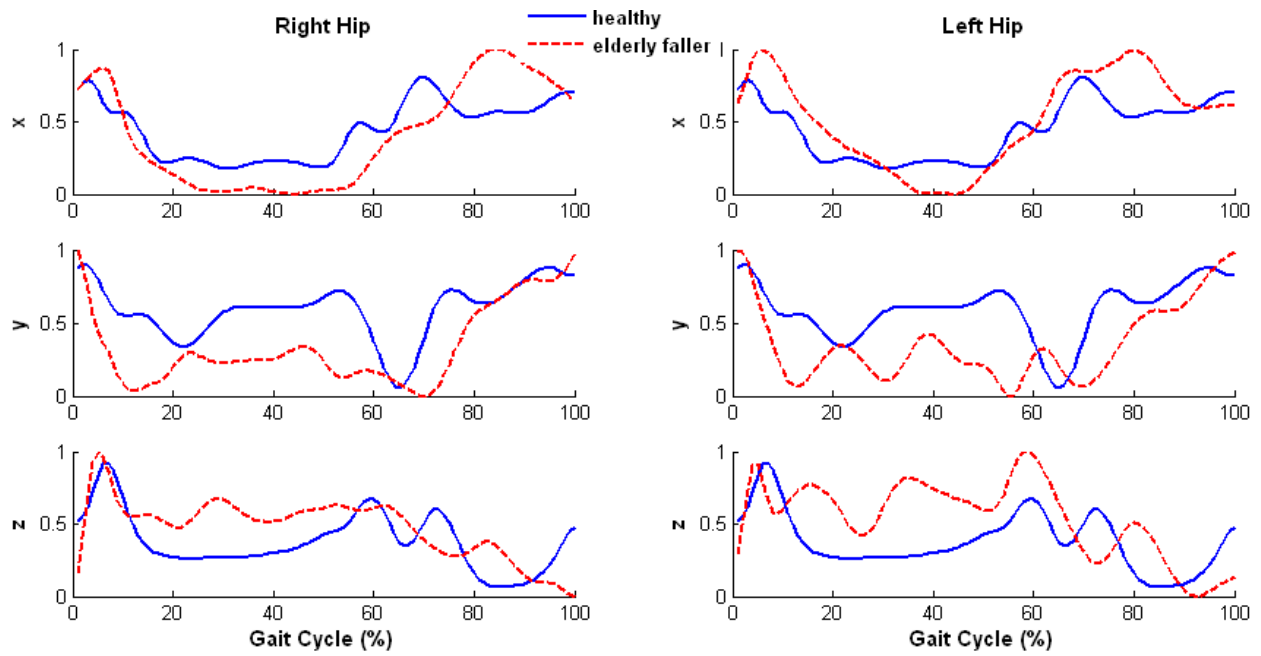


Figure AXVIII-6: Comparison of acceleration pattern in a gait cycle between healthy subjects and an elderly faller subject.

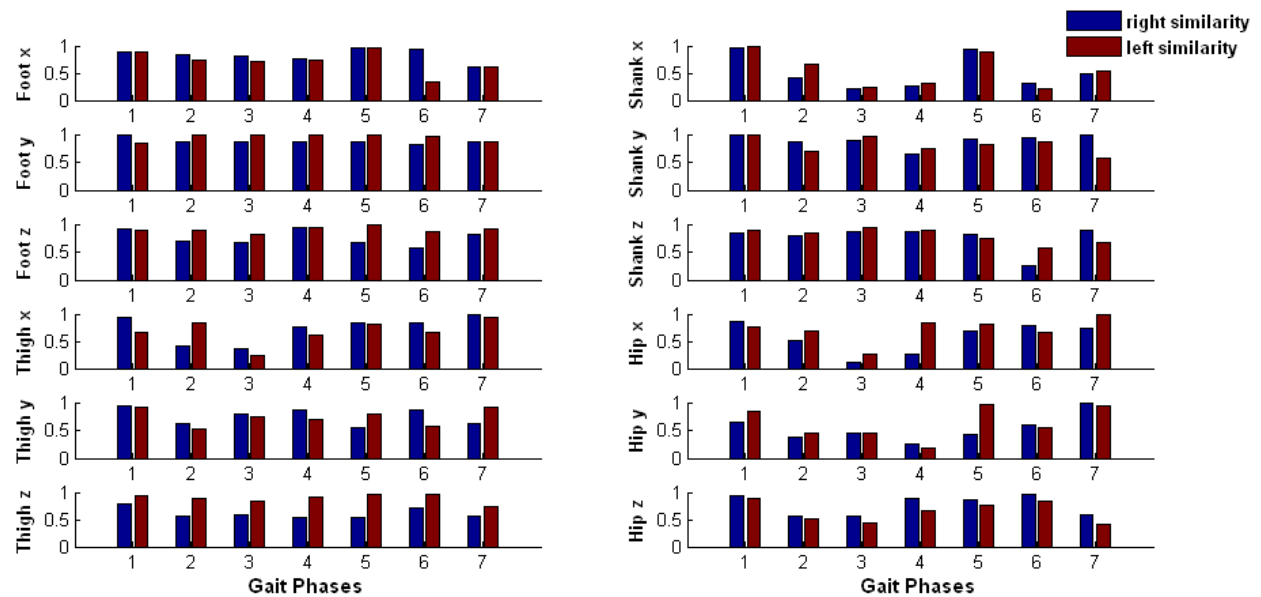


Figure AXVIII-7: Grade of similarity of right and left acceleration in elderly faller subject.

Summary:

Table AXVIII-2: Characterization of acceleration in Elderly Faller Case Study

	Right	Left
Foot x	A sharp rise in acceleration in the initial contact, lower magnitude in the stance phase, lower acceleration in the swing phase.	Same as right foot x. Significant small similarity appears in the mid-swing phase.
Foot y	Lower acceleration occurs in the initial contact following with lower magnitude in the rest of the stance phase, a delayed rise in acceleration in the swing phase.	A sharp rise in acceleration occurs in the initial contact, delayed acceleration in the swing phase.
Foot z	A sharp rise in acceleration in the loading response following with higher magnitude in the rest of the stance phase, delayed acceleration occurs in the initial swing phase.	A sharp deceleration in the initial swing phase following with a sharp rise in acceleration in the mid-swing phase.
Shank x	A sharp rise in acceleration in initial contact, following with lower magnitude in the rest of the stance phase, lower acceleration occurs in the swing phase. Significant small similarity appears almost the entire gait cycle.	Same as right shank x.
Shank y	A sharp rise in acceleration in initial contact, following with unstable magnitude in the rest of the stance phase, a delayed and sharp deceleration occurs in the swing phase	Same as right shank y.
Shank z	A sharp rise in acceleration in the initial contact following with higher magnitude in the stance phase, delayed deceleration and acceleration in the swing phase. Significant small similarity appears in the mid-swing phase.	Similar to right shank z.
Thigh x	A sharp rise in acceleration in initial contact, following with unstable magnitude in the rest of stance phase. Unstable signals appear in swing phase. Significant small similarity appears in terminal stance phase.	Same as right thigh x.

Thigh y	A sharp deceleration occurs in the loading response, following with very unstable magnitude in the rest of the gait cycle. Smaller similarity appears in the initial swing phase.	Similar to right thigh y.
Thigh z	A sharp rise in acceleration occurs in initial contact, lower magnitude in the rest of the gait cycle.	A sharp rise in acceleration occurs in initial contact, following with unstable magnitude in the stance phase, lower acceleration in initial swing phase.
Hip x	A delayed deceleration occurs in the loading response, following with lower magnitude in the stance phase, a sharp rise in acceleration in the swing phase. Significant small similarity appears in terminal stance phase.	Similar to right hip x.
Hip y	A sharp deceleration occurs in the initial contact, following with lower magnitude in the rest of the stance phase. A delayed acceleration in the initial swing phase. Significant small similarity appears in the pre-swing phase.	Similar to right hip y, with unstable magnitude in the stance phase.
Hip z	A sharp rise in acceleration occurs in the initial contact, following with higher magnitude in the rest of the stance phase, lower acceleration occurs in the swing phase.	Similar to right hip z, with more unstable magnitude in the stance phase. Smaller similarity appears in the terminal swing phase.

Appendix XIX: Results of Idiopathic Neurological Disorder (IND)

- **Description**

Subject is 58 year old female with idiopathic neurologic disorder for almost twenty years. Since then she sits in a wheelchair. She was tested by walking bare-footed on the instrumented treadmill with harness support at speed of 0.1 m/s, continuing three minutes.

- **Temporal Stride Variability**

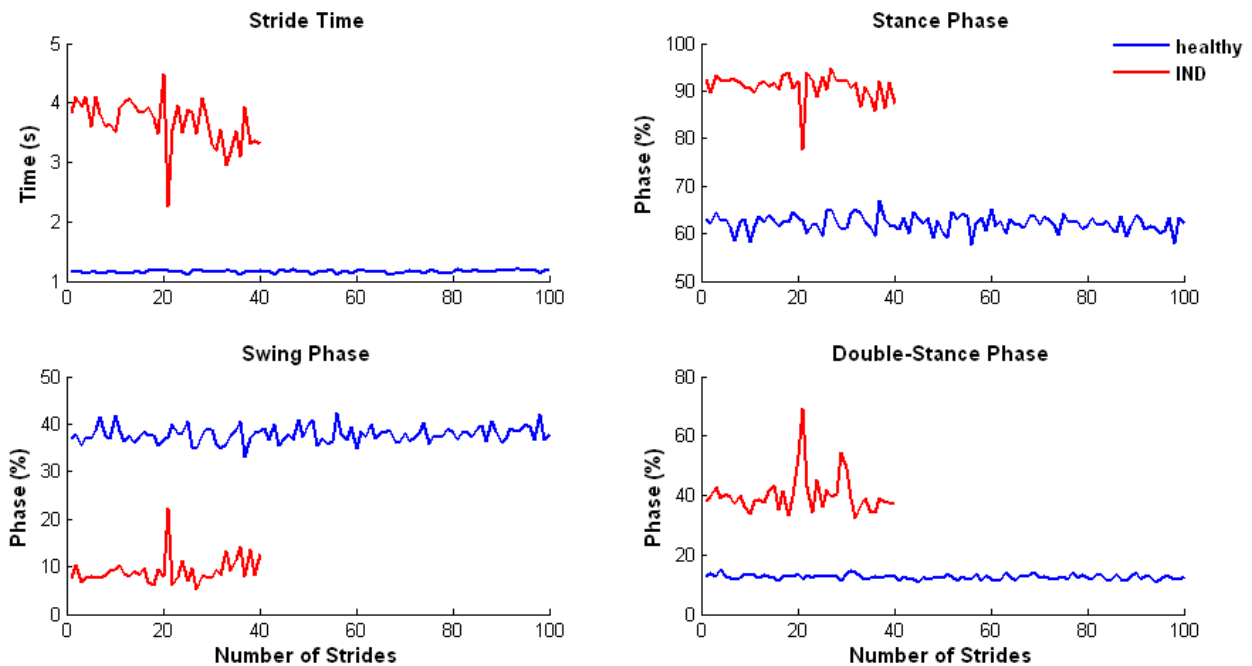


Figure AXIX-1: Stride variability of a healthy female subject and a female patient with idiopathic neurologic disorder (IND).

Summary: Due to very slow walking speed of this IND subject, there were only 40 strides extracted from three-minute walking trial. The subject has greater variability at the time of 20 strides, which indicates there might be some fall risk at that time. The stride time, stance phase, and double-stance phase are much longer than healthy subject, whereas the swing phase is much shorter.

- **Ground Reaction Forces**

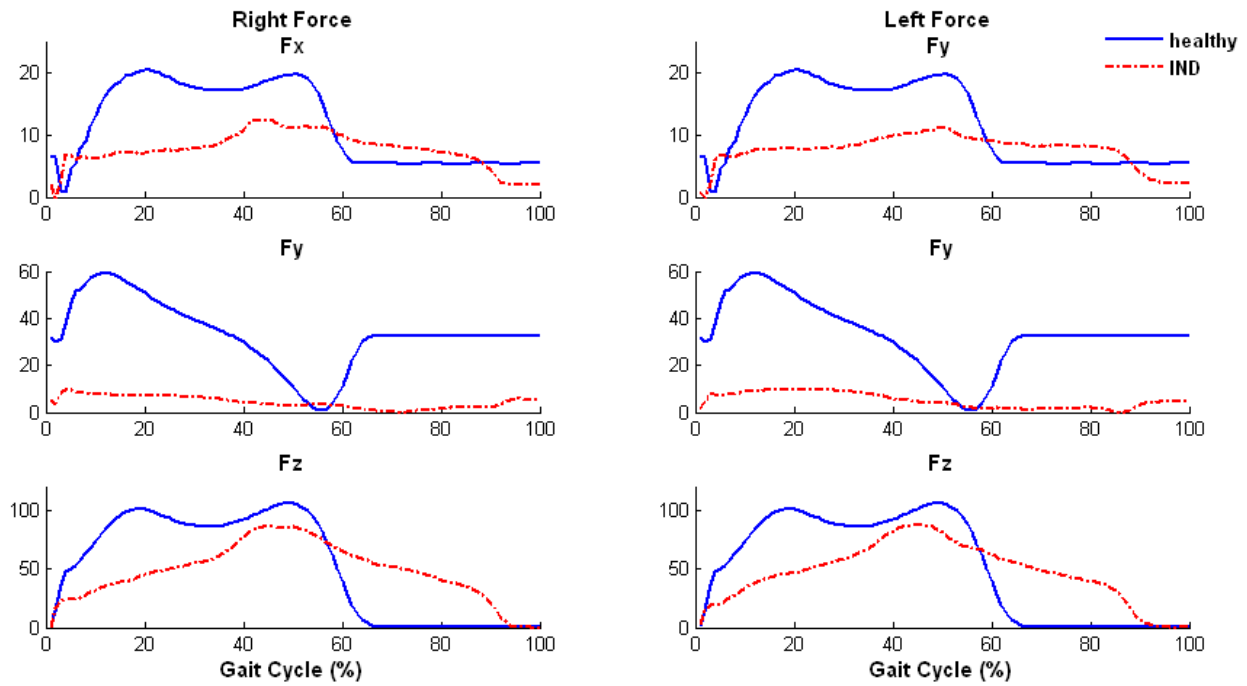


Figure AXIX-2: Right and left GRF in 3-D in female patient with idiopathic neurologic disorder (IND).

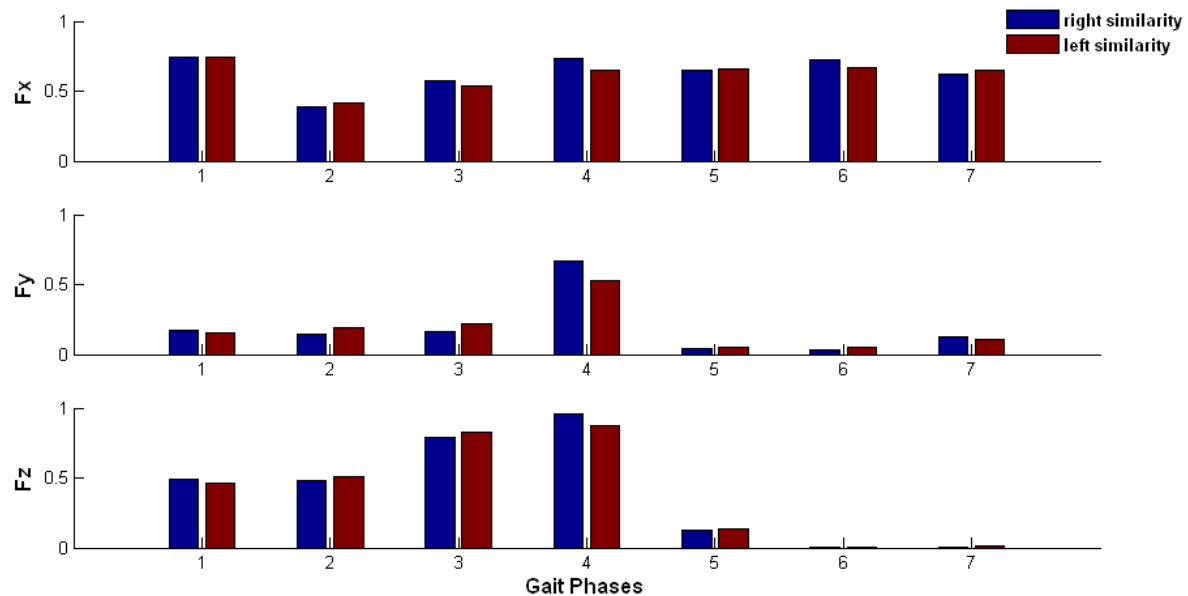


Figure AXIX-3: Grade of similarity between right and left GRF in idiopathic neurologic disorder case study.

Summary: In the vertical direction, the subject has much longer stance phase (more than 90% of the full gait cycle) on both sides, compared with the healthy subject. The magnitudes of the GRF in this direction are also quite low with shorten peak contact. In the anterioposterior and mediolateral directions, the GRF was very low. The behavior of her GRF in three dimensions shows the sever gait problems which results in the low to very low grade of similarity.

- **EMG Muscle Activity Patterns**

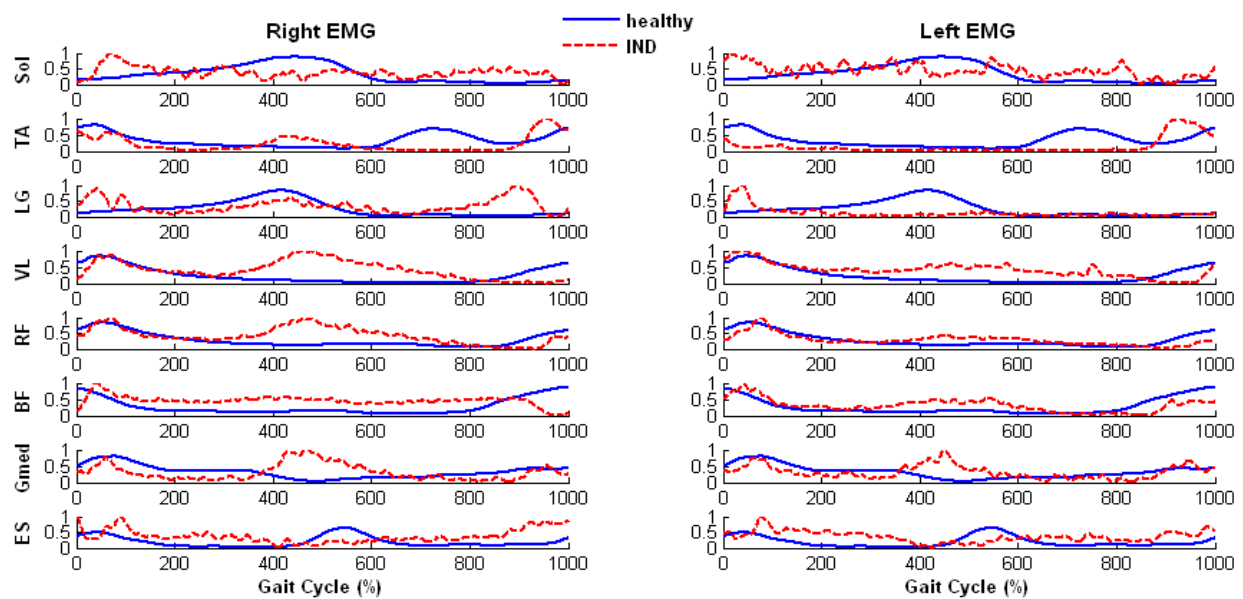


Figure AXIX-4: Comparison of EMG activity in a gait cycle between healthy subjects and IND.

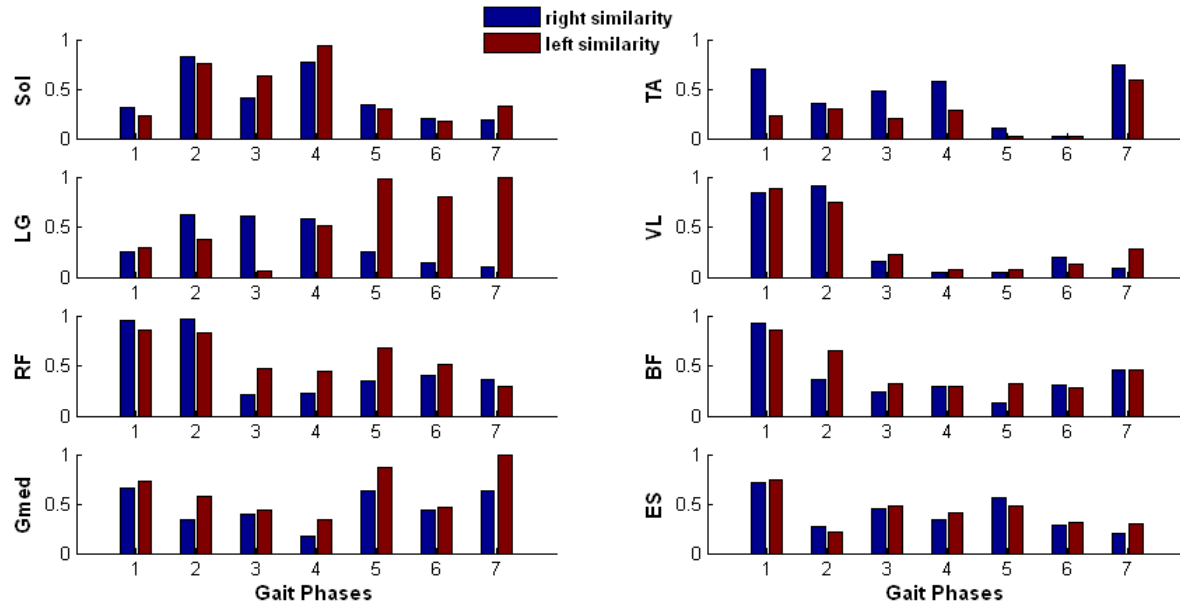


Figure AXIX-5: Grade of similarity of right and left EMG in IND subject.

Summary:

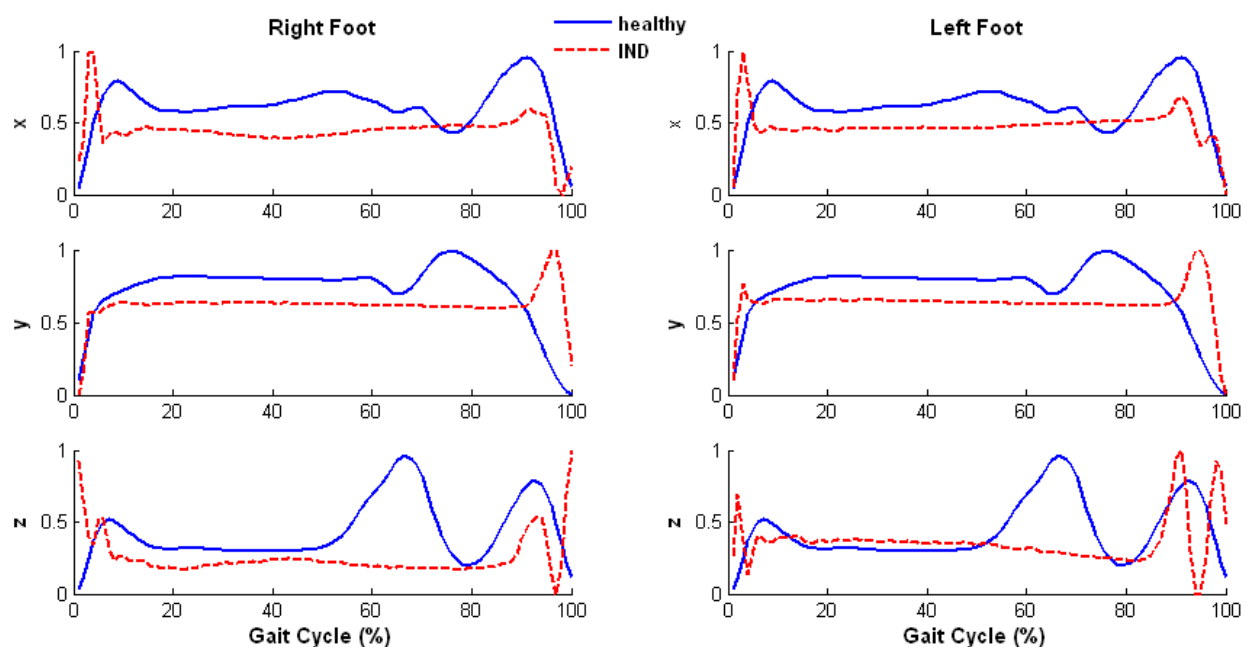
Table AXIX-1: Summary of EMG Activity in Idiopathic Neurologic Disorder Case Study

	Right	Left
Soleus	Spasticity occurs in the loading response, following with very unstable muscle activities in the rest of the gait cycle. Significant small similarity appears in the initial contact, mid- and terminal swing phases.	Same as right Soleus.
Tibialis Anterior (TA)	Muscle weakness occurs in the early stance phase and early swing phase, there is spasticity in the terminal swing phase. Significant small similarity appears in the initial and mid-swing phases.	Same as right TA.
Gastrocnemius Lateralis (LG)	Spasticity occurs in the loading response, following with very unstable muscle activities in the rest of the gait cycle. There is spasticity in the late swing phase. Significant small similarity appears in the terminal stance and terminal swing phases.	Spasticity occurs in the loading response, following with muscle weakness in the rest of the stance phase.
Vastus Lateralis (VL)	Spasticity occurs in the late stance phase, muscle weakness occurs in the terminal swing phase. Significant small similarity appears from mid-stance to the end of the gait cycle.	Same as right VL.

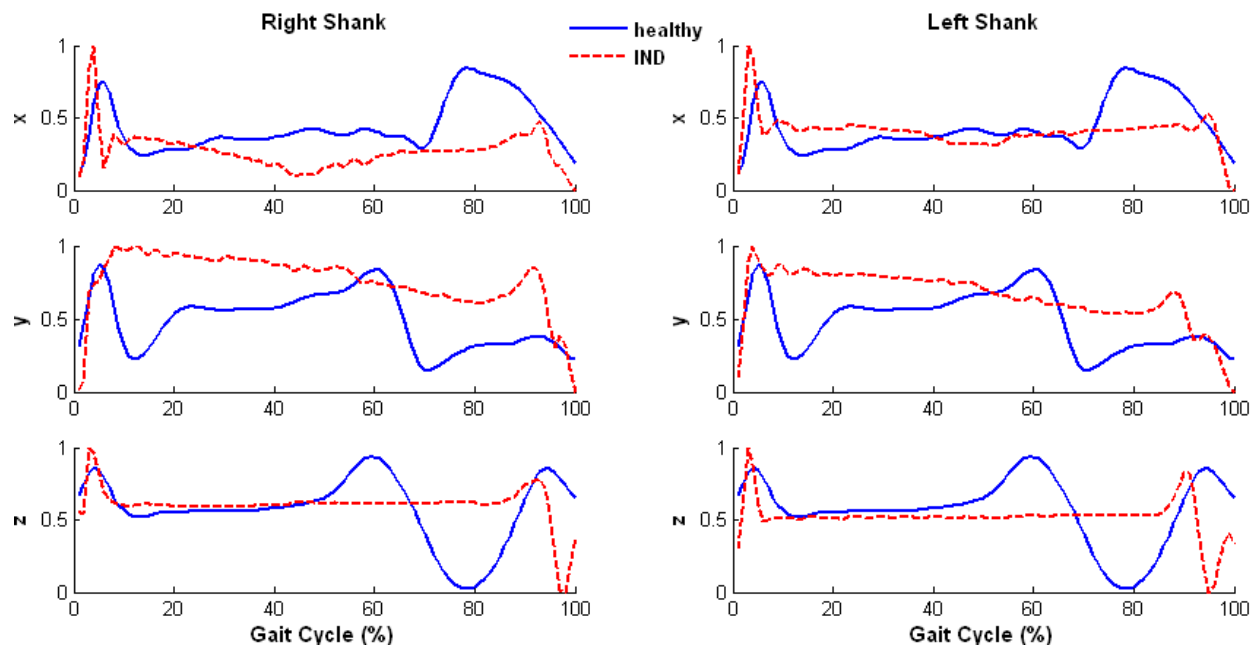
Rectus Femoris (RF)	Spasticity occurs in the stance phase, muscle weakness occurs in the terminal swing phase. Significant small similarity appears in the terminal stance and pre-swing phases.	Same as right RF.
Biceps Femoris (BF)	Spasticity occurs from loading response to mid-swing phases. Muscle weakness appears in the terminal swing phase, which in fact was the entire swing phase in this subject. Significant small similarity appears in the initial swing phase.	Same as right BF.
Gluteus Medius (Gmed)	Muscle weakness occurs in the early stance phase, spasticity occurs in the terminal stance phase with very unstable muscle activities. Significant small similarity appears in the pre-swing phase.	Same as right Gmed.
Elector Spinae (ES)	Spasticity occurs in the early stance phase and late swing phase. The very unstable muscle activities occur in the entire gait cycle.	Same as right ES.

- **Acceleration Patterns**

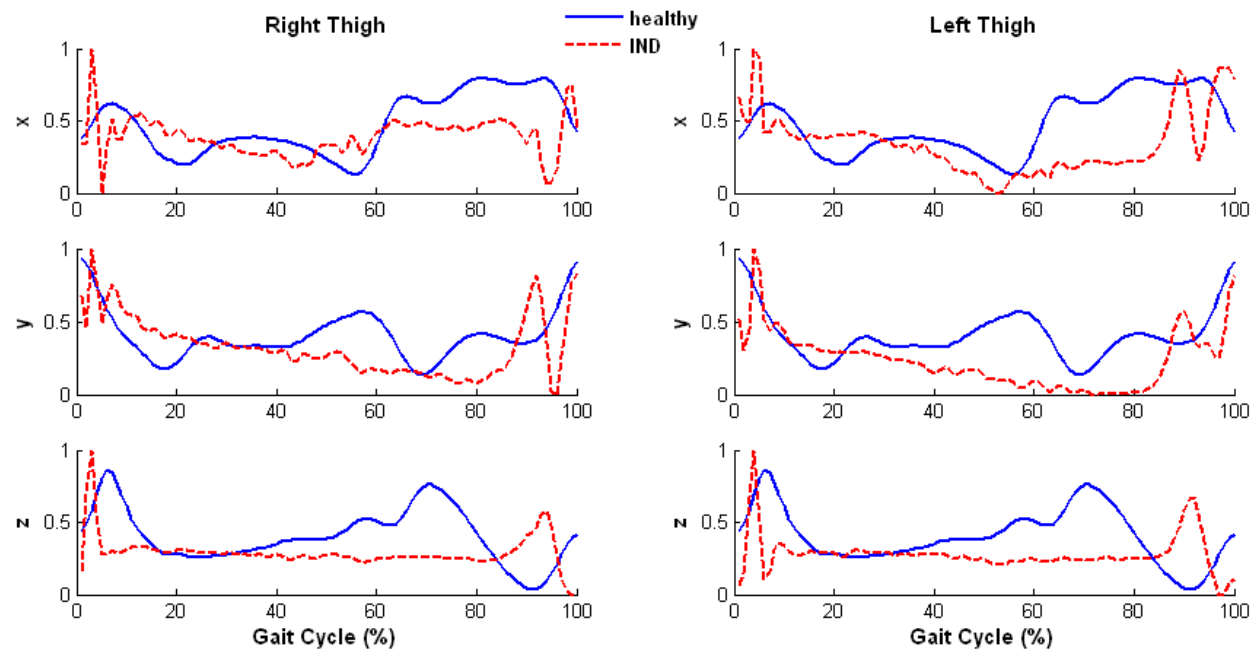
(A)



(B)



(C)



(D)

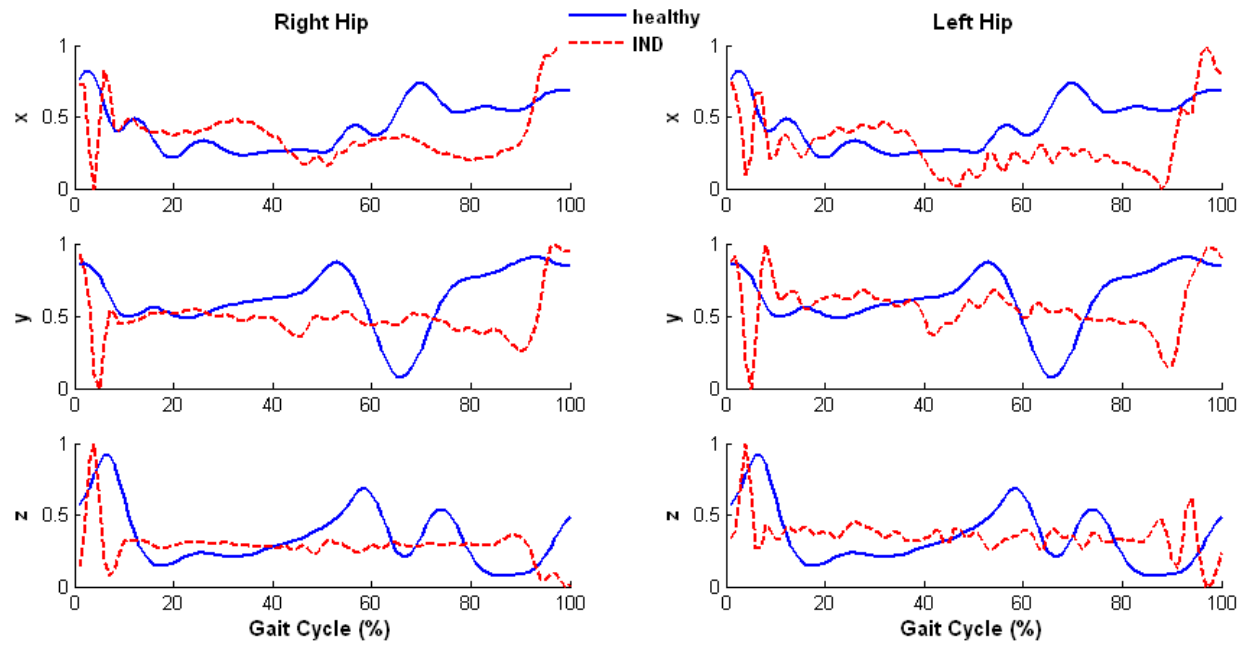


Figure AXIX-6: Comparison of acceleration pattern in a gait cycle between healthy subjects and idiopathic neurologic disorder patient (IND).

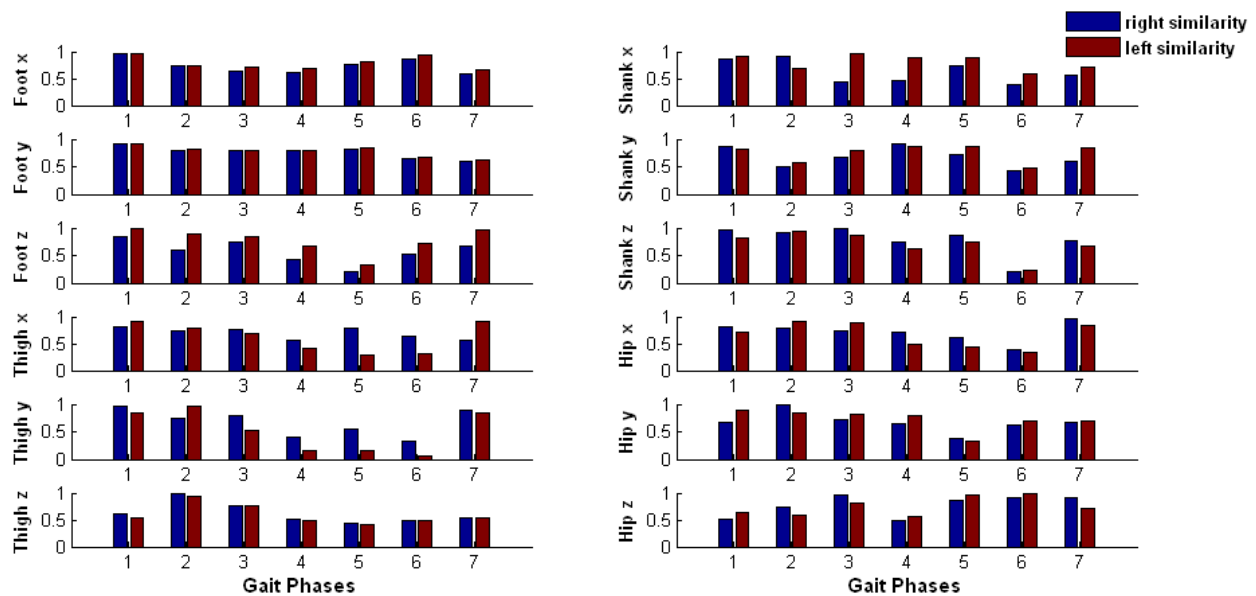


Figure AXIX-7: Grade of similarity of right and left acceleration in idiopathic neurologic disorder (IND).

Summary:**Table AXIX-2: Characterization of acceleration in Idiopathic Neurologic Disorder Patient**

	Right	Left
Foot x	A sharp rise in acceleration occurs in the initial contact, following with a very low magnitude in the rest of the gait cycle.	Same as right foot x.
Foot y	Lower acceleration occurs in the initial contact following with the lower magnitude in the rest of the stance phase, there is a sharp rise in acceleration in the swing phase.	Same as right foot y.
Foot z	There are low to very low acceleration in the entire gait cycle. Significant small similarity appear sin the initial swing phase.	A sharp rise in acceleration in the initial contact, a much delayed and sharp rise in acceleration in the swing phase.
Shank x	A sharp rise in acceleration in the initial contact following with lower magnitude in the rest of stance and swing phases. Significant small similarity appears in the mid-swing phase.	Same as right shank x.
Shank y	A sharp rise in acceleration in the initial contact, following with very high magnitude in the stance phase, there is a much delayed deceleration in the swing phase. Significant small similarity appears in the mid-swing phase.	Same as right shank y.
Shank z	A sharp rise in acceleration occurs in the initial contact, a much delayed deceleration occurs in the swing phase. Significant small similarity appears in the mid-swing phase.	Same as right shank z.
Thigh x	A sharp rise in acceleration occurs in the initial contact, following with very unstable magnitude in the rest of the gait cycle.	Same as right thigh x, significant small similarity appears in the initial and mid-swing phases.
Thigh y	A sharp rise in acceleration occurs in the initial contact, following with low and unstable magnitude in the stance phase. A	Same as right thigh y.

Thigh z	<p>sharp rise in acceleration in swing phase. Significant small similarity appears in the pre-, initial, and mid-swing phases.</p> <p>A sharp rise in acceleration occurs in the initial contact, following with lower and unstable magnitude in the rest of the gait cycle. A much delayed and lower acceleration occurs in the swing phase.</p>	Same as right thigh z.
Hip x	<p>A sharp deceleration occurs in the initial contact following with unstable magnitude in the stance phase, a much delayed and higher acceleration occurs in the swing phase. Significant small similarity appears in the mid-swing phase.</p> <p>A sharp deceleration occurs in the initial contact, following with unstable magnitude in the rest of the stance phase. A much delayed acceleration occurs in the swing phase. Significant small similarity appears in the initial swing phase.</p>	Similar to right hip x, with more unstable magnitude in the entire gait cycle.
Hip y	<p>A sharp deceleration occurs in the initial contact, following with unstable magnitude in the rest of the stance phase. A much delayed acceleration occurs in the swing phase. Significant small similarity appears in the initial swing phase.</p>	Same as right hip y.
Hip z	<p>A sharp rise in acceleration occurs in the initial contact, following with unstable magnitude in the rest of the gait cycle.</p>	Similar to right hip z.

Curriculum Vita

Huiying Yu was born in Tianjin, China, the first daughter of Ruichang Yu and Jianping Liu. Huiying Yu earned her Bachelor of Sciences degree in Biomedical Sciences from the University of Durham, United Kingdom in 2004. She received her Master of Philosophy degree in Computational Biology in 2005 from the University of Cambridge, United Kingdom. In 2006 she joined the doctoral program at University of Texas at El Paso.

Huiying Yu has been the recipient of numerous honors and awards such as the University of Texas at El Paso Graduate School Research Award, National Science Foundation Advance Award, and NASA Fellowship Award. While pursuing her PhD degree, she worked as a research assistant and teaching assistant for the department of Electrical and Computer Engineering. She was the research leader in the Laboratory for Human Motion Analysis and Neurorehabilitation. She was also the president of Neuroscience Research Association Organization.

Huiying Yu has presented her research works at numbers of international conferences and workshops. She presented the 10th and 11th Proceeding of international conferences of Rehabilitation and Robotics (ICORR) in 2007 and 2009. She has also a published journal paper on Measurement in Elsevier in April 2010.

Huiying Yu's dissertation entitled, "Categorization of Functional Impairments in Human Locomotion using the Methods of the Fusion of Multiple Sensors and Computational Intelligence," was supervised by Dr. Thompson Sarkodie-Gyan.

Permanent address: 500 Rubin Drive, Apartment 1213
El Paso, Texas, 79912

This dissertation was typed by Huiying Yu.